

5-16-2003

A Theory and Analysis of Planing Catamarans in Calm and Rough Water

Zhengquan Zhou
University of New Orleans

Follow this and additional works at: <https://scholarworks.uno.edu/td>

Recommended Citation

Zhou, Zhengquan, "A Theory and Analysis of Planing Catamarans in Calm and Rough Water" (2003).
University of New Orleans Theses and Dissertations. 28.
<https://scholarworks.uno.edu/td/28>

This Dissertation is protected by copyright and/or related rights. It has been brought to you by ScholarWorks@UNO with permission from the rights-holder(s). You are free to use this Dissertation in any way that is permitted by the copyright and related rights legislation that applies to your use. For other uses you need to obtain permission from the rights-holder(s) directly, unless additional rights are indicated by a Creative Commons license in the record and/or on the work itself.

This Dissertation has been accepted for inclusion in University of New Orleans Theses and Dissertations by an authorized administrator of ScholarWorks@UNO. For more information, please contact scholarworks@uno.edu.

**A THEORY AND ANALYSIS OF PLANING CATAMARANS
IN CALM AND ROUGH WATER**

A Dissertation

Submitted to the Graduate Faculty of the
University of New Orleans
in partial fulfillment of the
requirements for the degree of

Doctor of Philosophy
in
Engineering and Applied Science

by

Zhengquan Zhou

B.S., Harbin Engineering University, 1982
M.S., China Ship Research and Development Academy, 1985
M.S., University of New Orleans, 2000

May 2003

Copyright 2003, Zhengquan Zhou

DEDICATION

To my wife Yang Qing and my daughter YinYin,

Thank you for your love and support.

ACKNOWLEDGEMENTS

I am very grateful to Dr. William S. Vorus, who is my dissertation advisor. Without his support, encouragement, and continuous guidance throughout my graduate study years at the University of New Orleans, the accomplishment of this dissertation work would be impossible.

I also wish to thank Dr. Russell E. Trahan for his support during the dissertation project research.

A “thank you” also goes to Dr. Jeffrey M. Falzarano, Dr. Kazim M. Akyuzlu, Dr. Martin Guillot and Dr. Dongming Wei for their encouragement and for serving on my dissertation committee.

During my study in UNO, many of my friends and classmates provided their generous help to me. I would like to express my appreciation to Mr. Larry DeCan, Mr. Paul Sorensen and Mr. Shawn Wilber. Special thanks to Mr. Larry DeCan and Ms. Sacha Wichers for their help in polishing my English.

I also acknowledge the faculty and staff of the School of Naval Architecture and Marine Engineering for their support in the many years. Special thanks to Mr. George Morrissey and Ms. Cheryl Johnson for their help and assistances.

Finally, many thanks go to my family members and friends, especially my wife and my daughter for their support, encouragement, and understanding during the years of my graduate study.

TABLE OF CONTENTS

ACKNOWLEDGEMENTS.....	iv
TABLE OF CONTENTS.....	v
ABSTRACT.....	xi
Chapter 1: INTRODUCTION.....	1
1.1 Planing craft.....	1
1.2 Background on theoretical planing research.....	3
1.3 Vorus'(1996) planing monohull model and its derivatives	6
1.4 Present research and objectives	14
Chapter 2: CATAMARAN FLOW PHYSICS	16
2.1 Problem description	16
2.2 Coordinate systems	17
2.3 Method of solution: slender-body theory, solution domain transformation, and time marching.....	19
2.4 Sectional flow physics	24
2.5 Vortex distribution model.....	29
2.6 Sectional boundary value problem.....	31

2.7 Steady planing problem	34
2.8 Seakeeping problem of a planing catamaran	35

Chapter 3: FIRST ORDER NONLINEAR CATAMARAN

HYDRODYNAMIC THEORY	37
3.1 Steady planing in calm water	38
3.1.1 First order kinematic boundary condition.....	38
3.1.2 First order displacement continuity condition	46
3.1.3 First order pressure continuity condition	51
3.2 Planing dynamics in seaway	57
3.2.1 Pressure continuity condition in seakeeping.....	57
3.2.2 Water wave model	64
3.2.3 Vessel motion model.....	67
3.2.4 Wetted length and the transient draft.....	70
3.2.5 Impact velocity in waves	72

Chapter 4: SECOND ORDER NONLINEAR CATAMARAN

HYDRODYNAMIC THEORY	75
4.1 Second order calm water steady planing theory	75
4.1.1 Second order velocity continuity equations.....	76
4.1.1.1 Kinematic boundary condition and its integral equation	76
4.1.1.2 Kernel function $\chi(\zeta)$	82
4.1.1.3 Bound vortex $\gamma_c(\zeta, \tau)$	84

4.1.1.4 Velocity continuity condition.	87
4.1.2 Displacement continuity condition	91
4.1.2.1 Water surface elevation.....	91
4.1.2.2 Kernel function $\chi^*(\zeta)$	94
4.1.2.3 Displacement continuity equation.....	96
4.1.3 Pressure continuity condition for steady planing.....	98
4.2 Second order nonlinear seakeeping theory	102
4.2.1 Pressure distribution model.....	102
4.2.1.1 Pressure continuity condition.....	103
4.2.1.2 Burger's equation and location of free vortex	107
4.2.1.3 Pressure distribution formulae	110
4.2.2 Water wave model	111
4.2.3 Vessel motion model.....	112
4.2.4 Boat impact velocity in waves	113
Chapter 5: NUMERICAL MODELS.....	115
5.1 First order numerical model.....	116
5.1.1 Numerical analysis of 1 st order velocity continuity equations.....	116
5.1.2 Numerical model of 1 st order displacement continuity condition.....	122
5.1.3 Numerical model of 1 st order pressure continuity condition	126
5.1.4 Numerical model of the 1 st order bounded vortex strength distribution.....	130
5.2 Second order numerical model	132
5.2.1 Numerical analysis of 2nd order velocity continuity equations.....	132

5.2.2 Numerical model of displacement continuity equation	141
5.2.3 Numerical model of pressure continuity equations	143
5.2.4 Numerical model of bound vortex strength distribution $\gamma_c(\zeta, \tau)$	143
5.2.4.1 Computation of the γ_{normal} term.....	144
5.2.4.2 Computation of the $\gamma_{dis-singular}$ term.....	145
Chapter 6: TIME DOMAIN NUMERICAL SOLUTION.....	149
6.1 Solution procedures	149
6.2 Non-null and null hydrodynamics in the impact or extraction phase	159
6.3 Solution procedure for CUW and CW phases	160
6.3.1 Solution procedure for CUW phase.....	161
6.3.2 Solution procedure for CW phase.....	164
Chapter 7: VALIDATION OF THE NUMERICAL ANALYSIS IN THE 2 ND	
ORDER THEORY	167
7.1 Three fundamental integrals	167
7.1.1 Validation of the elemental integral I_1 and I_2	168
7.1.2 Numerical comparison and numerical accuracy of the I_3 integral	171
7.1.2.1 Deadrise angle $\beta = 0$ case	173
7.1.2.2 Deadrise angle $\beta \neq 0$ case	178
7.2 Comparison of the numerical results for γ_c computation.....	180

Chapter 8: NUMERICAL COMPARISONS FOR STEADY PLANING	183
8.1 30FT high speed planing catamaran with steps	183
8.2 Steady planing computations	194
Chapter 9: HIGH SPEED CATAMARAN PLANING IN WAVES	208
9.1 Numerical results of 2 nd order model.....	209
9.2 Comparisons for the regular wave case	216
9.3 Comparison for the random wave case.....	224
Chapter 10: DISCUSSION ON PLANING DYNAMICS: INFLUENCE OF	
THE TEMPORAL DERIVATIVE TERM $\frac{\partial}{\partial \tau} \Big _{\xi=const}$	236
10.1 The temporal derivative terms	237
10.2 The computation of the temporal derivatives	240
10.3 Physical explanation for Euler's equation	
of the free vortex distribution	249
10.4 Free vortex location on the sheet	251
10.4.1 Second order condition for the free vortex location	255
10.4.2 First order condition for the free vortex location.....	258
10.4.3 An alternative of the first order condition for the free vortex location.....	260
10.5 Numerical result comparison	263
Chapter 11: CONCLUSIONS AND SUGGESTIONS FOR FURTHER WORK	
.....	272

11.1 Summary and conclusions	272
11.2 Suggestions to further works	275
REFERENCES	276
Appendix A: KINEMATICAL BOUNDARY CONDITION AND VELOCITY CONTINUITY CONDITION.....	280
Appendix B: DISPLACEMENT CONTINUITY CONDITION.....	295
Appendix C: PRESSURE CONTINUITY CONDITION FOR STEADY PLANING	309
Appendix D: PRESSURE DISTRIBUTION AND EULER'S EQUATION IN SEAKEEPING.....	319
Appendix E: COMPUTATION OF BOUND VORTEX DISTRIBUTION.....	331
Appendix F: KERNEL FUNCTION $\chi(\zeta)$	337
Appendix G: KERNEL FUNCTION $\chi^*(\zeta)$	348
Appendix H: FUNDAMENTAL INTEGRALS IN VELOCITY CONTINUITY FORMULATION	351
Appendix I: TIME MARCHING ALGORITHM.....	377
Appendix J: FUNDAMENTAL INTEGRALS IN THE FIRST ORDER MODEL	383
Appendix K: INPUT FILES FOR THE REGULAR WAVE EXAMPLE.....	398
Appendix L: ELLIPTIC INTEGRALS	402
VITA.....	408

ABSTRACT

A planing catamaran is a high-powered, twin-hull water craft that develops the lift which supports its weight, primarily through hydrodynamic water pressure. Presently, there is increasing demand to further develop the catamaran's planing and seakeeping characteristics so that it is more effectively applied in today's modern military and pleasure craft, and offshore industry supply vessels.

Over the course of the past ten years, Vorus (1994,1996,1998,2000) has systematically conducted a series of research works on planing craft hydrodynamics. Based on Vorus' planing monohull theory, he has developed and implemented a first order nonlinear model for planing catamarans, embodied in the computer code CatSea. This model is currently applied in planing catamaran design. However, due to the greater complexity of the catamaran flow physics relative to the monohull, Vorus's (first order) catamaran model implemented some important approximations and simplifications which were not considered necessary in the monohull work.

The research of this thesis is for relieving the initially implemented approximations in Vorus's first order planing catamaran theory, and further developing and extending the theory and application beyond that currently in use in CatSea. This has been achieved through a detailed theoretical analysis, algorithm development, and careful coding.

The research result is a new, complete second order nonlinear hydrodynamic theory for planing catamarans. A detailed numerical comparison of the Vorus's first order nonlinear theory and the second order nonlinear theory developed here is carried out. The second order nonlinear theory and algorithms have been incorporated into a new catamaran design code (NewCat). A detailed mathematical formulation of the base first order CatSea theory, followed by the extended second order theory, is completely documented in this thesis.

CHAPTER 1

INTRODUCTION

1.1 Planing Craft

A planing boat, typically either a monohull or catamaran, is a high powered water-craft that develops the necessary lifting forces which support its weight primarily through hydrodynamic water pressure. This hydrodynamic lifting of a planing craft is different from that of a displacement type of vessel, which is supported primarily by hydrostatic pressure.

In order for the planing craft to develop the necessary dynamic lift, its speed must be high, and the geometric shape of the wetted regions of the hull must be properly configured. When properly configured the hull geometry has a declining deadrise angle from bow to stern. A typical planing craft has a hard chine, and may have both longitudinal and transverse steps at intermediate positions over the wetted region. The planing craft is typically run with a small bow-up trim or attack angle. This attack angle, along with the hull geometry, results in the development of high pressure on the bottom surface, which lifts the hull, thereby reducing the wetted surface, and hence reducing the vessel resistance.

For a displacement-type vessel, there is no significant difference between the drafts at the running state ($U \neq 0$) and at the static state ($U = 0$). However, there is a large difference for planing craft. The change in the planing craft's draft, trim angle, and wetted length, are directly related to the craft's forward velocity and hull geometry. This relationship is highly nonlinear.

As the planing craft speed increases the hydrodynamic pressure on the bottom increases. The high-pressured water in the displaced volume is forced from under the boat in the form of a high-speed jet of water. The pressure differential at the water boundary creates what is commonly known as a spray jet. The water in the jet-head region, with its high pressure p , generates the spray when it meets the air at the nominal atmospheric pressure p_a . Associated with it is a loss of energy, and hence a drag or resistance. The jet processes are special processes associated with planing crafts. The typical characteristics of a planing craft can be characterized as "small volume, light displacement, and high speed". Thus there are many application areas for planing craft.

Presently there is an increasing demand for planing monohulls and catamarans within the offshore industry. They offer important commercial applications, such as high speed and low cost support to the supply operations of the oil industry. This low cost but high-speed support is becoming increasingly important as oil production moves into the deep-sea area where the high cost of large-scale helicopter operations becomes prohibitive.

The military's need for high-speed craft is also increasing. In many cases, in spite of bad sea conditions, military craft must run at maximum attainable speed to meet mission requirements. Therefore, the quantification of seakeeping performance of a

planing craft in a seaway is a new challenge that is being pressed on to the Naval Architects of today.

1.2 Background on Theoretical Planing Research

Steady, calm water, planing and seakeeping dynamics are the primary performance modes that planing craft designers need to consider. However, until very recently, the development of the hydrodynamic theory that will support design studies has been virtually nonexistent.

The planing hydrodynamics problem can be classified into three categories according to the physics of interest as

- (1) cylinder impact (as in a drop-test);
- (2) steady forward speed in calm water;
- (3) impact with forward speed in a seaway.

Each of these problems has its unique characteristics. In the cylinder impact problem, there only exists a vertical downward impact velocity. In the steady planing problem, there exists a forward speed without a downward impact velocity. In the seakeeping case, there exists a forward ship speed and also a downward impact velocity. Since in a non-dimensional form the spatial variable \bar{x} and the time variable τ are identical (refer to Eq.(1.2)), the solution to the impact problem can be simply used to deal with the steady planing problem via slender body theory.

Planing hydrodynamic research can also be classified according to craft geometry as:

- (1) Monohull planing hydrodynamics;
- (2) Catamaran planing hydrodynamics.

The theoretical and numerical difficulties in solving planing hydrodynamics problems are listed as the following:

(1) Physical flow complexity via the extreme nonlinearity makes the hydrodynamic processes difficult to model. For example, the processes of impact into the water, extraction from the water, and the jet head detachment as well as reattachment, etc., are all complications for modeling;

(2) The high-speed jet, or water spray, generated in planing is a limiting difficulty. For example, in a typical mono-hull steady planing problem, the jet head length may be on the order of $\Delta b = z_b - z_c = 0.00063 - 0.0079$ as fractions of half-beam (Vorus, 1996), depending largely on section deadrise angle. The length is so small and the flow speed is so high in this region that it requires small element lengths and extremely high numerical accuracy. For instance, Zhao & Faltinsen (1993,1996), in an example of water impact with a simple symmetrical semi-infinite wedge-cylinder section, used an element length on the order of 10^{-18} of half beam for their numerical computation.

(3) Another difficult issue is that the location of the jet-head in the chine-unwetted flow is not known in advance; the unknown flow boundary developing with time makes the problem virtually impossible to compute using available CFD methods.

Theoretical research on steady planing dates back to the early of 1930's. The pioneering work was von Karman's (1929) impact analysis of seaplane landing, and

Wagner's (1932) flat-plate model for investigation of water-entry problems. Over the past seventy years, there has been a large amount of published research, not all of which can be cited herein due to the limitations of this thesis. Instead, only those papers that relate directly to the focus of this research will be cited.

In the majority of the past research efforts, due to the inherent difficulties in flow physics cited above, planing problems have been approximately solved by applying the basic assumptions of zero-gravity, zero-viscosity and zero-compressibility. Some examples of these approaches via 2-D impact solution and slender body theory are Tulin(1957), Cointe (1989,1991), Zhao & Faltinsen (1993,1996), Vorus (1996), Kim, Vorus, and Troesch (1996), Zhao et al (1997), Savander(1997), Royce and Vorus(1998), Xu, Troesch, and Vorus (1998), Breslin (2000), Vorus & Royce (2000), Judge (2001), and Royce (2001). Lai & Troesch (1995,1996), performed a 3-D lifting surface solution for planing but it relied on 2-D/SBT predictions (Vorus(1996)) for the position of the jet-head boundary.

The papers cited above all deal with the steady planing of monohulls. Theoretical research on catamaran steady planing hydrodynamics, and on the seakeeping performance of planing, in general, is nearly blank, existing only a few rather crude methods (Zarnick(1978), Payne(1990), Payne(1995), and Akers et al (2000)) which are found not to be sensitive enough to geometric detail to provide reliable design guidance.

The first work leading to the modern approach to planing, beyond that of von Karman(1929) and Wagner(1932), was Tulin (1957). Here "strip theory", in the context of slender body theory, was applied to steady, calm-water mono-hull planing. Tulin's success was due to the use of slender body theory to study three-dimensional planing in

terms of two-dimensional (impact) flow in cross-flow planes. He gives the jet velocity and spray area length ε , the pattern of stream lines, dynamic lift, spray drag and induced drag expressions. The drawback of this paper is that his model is too highly simplified to use in practical design. Tulin's development is for a delta-plan form and the jet-head is assumed to lie along its edges, or the chine. Thus, it is a fully "chine-wetted" flow, which ignores the very important "chine-unwetted" flow phase, where the jet-head is not known in advance.

A fully non-linear two-dimensional water entry problem has been computed with reasonable numerical accuracy for a special simplified ideal section by Zhao & Faltinsen (1993, 1996). However, the requirement of the high resolution of element length up to 10^{-18} of half beam makes its use impractical. This method has not been applied in a planing application, and if it was it could predict only calm-water planing of prismatic hulls.

Savitsky (1964) presented a semi-empirical method for the hydrodynamic design of planing monohulls. Savitsky's method allows designers to estimate hull resistance and trim angle using the two equations of equilibrium with coefficients regressed from empirical data from towing tank tests of prismatic planing hulls. Savitsky's method has been very popular with planing boat designers over the years in providing the foundation for the majority of the preliminary resistance predictions of planing mono-hulls. However, Savitsky's method is clearly not sensitive enough to geometric detail to be of use to designers in evaluating even today's planing monohull configurations.

1.3 Vorus(1996) Planing Monohull Model and Its Derivatives

Although many methods have been published in the last seventy years, most of them are theoretically simplified to the point that they are not practical for use in a design environment. Presently, there is believed to be only one theoretical model with enough potential resolution of the physical issues to be practically applied in planing monohull hydrodynamic design studies. That is the Vorus'(1996) monohull impact and planing model .

For the prediction of impact loads and steady planing resistance, Vorus (1996) introduced a "flat" cylinder theory for impact of cylinders with arbitrary sectional contour, which was later generalized to temporal cylinder geometry variation for planing analysis of hulls with geometry variation longitudinally (under the slender body transformation $x = Ut$). Vorus' method represents a physically consistent approximation via ordering of the variables in the exact formulation to lowest order. His work has been proved to provide a practical method and a useful tool (a mono-hull hydrodynamic design code acronymed VsSea) for analysis of lift and resistance of planing monohulls of rather general configuration. It is considered by this writer to be a milestone in planing craft hydrodynamic research and development.

The Vorus' (1996) monohull theory has provided the basis for the extended catamaran work developed in this thesis. The monohull theory is explained with the aid of Fig. 1.1, Fig. 1.2 and Fig. 1.3. In these figures, the body geometry is prescribed and deadrise angle, $\beta(z)$, is assumed to be small.

Assume a planing craft advancing in water with a constant forward speed U , in the coordinate system of Figure 1.1, where $O_0 - x_0 y_0 z_0$ is a space-fixed coordinate system.

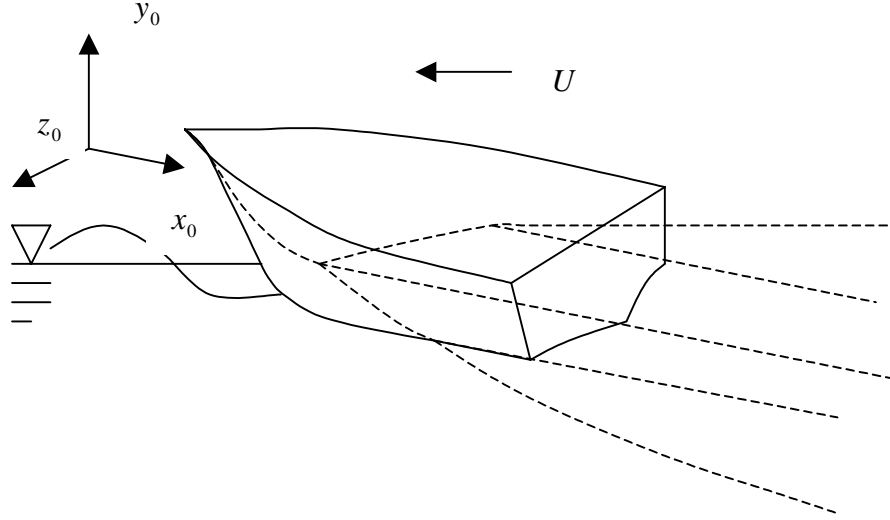


Fig. 1.1 A planing monohull

Defining x as a distance variable in the boat-fixed system (Refer to Chapter 2), there is a relation between the spatial variable x and the time variable t ,

$$x = U \cdot t \quad (1.1)$$

Defining the non-dimensional variables \bar{x} , τ and using (1.1),

$$\bar{x} = \frac{x}{z_{CH}} = \frac{U \cdot t}{z_{CH}}, \quad \tau = \frac{U \cdot t}{z_{CH}} \quad (1.2)$$

where z_{CH} is the offset of the hard chine.

The non-dimension variables, \bar{x} and τ , are therefore identical, such that the velocity distribution in the hull section at \bar{x} corresponds to an impacting cylinder solution at time τ .

To this end there exists a velocity transformation between the 2-D impact velocity $V(t)$ and the forward speed U :

$$V(t) = U \cdot \tan \alpha(t) \quad (1.3)$$

where $\alpha(t)$ is the attack angle of the keel relative to the stream speed U .

By the above relations, a 2-D impact theory can be used as the theoretical basis for both steady and unsteady planing. Thus, the impact problem is the theoretical basis for the 3-D development.

1.3.1 Vorus' 2-D impact theory

In Vorus' 2-D impact theory, on impact, the free-surface is turned back under the contour, forming an initially attached jet with velocity $V_j(t)$ (Figure 1.2). $z_b(t)$ and $z_c(t)$ are called the "jet spray-root," or "jet-head" and "zero-pressure offset," or "separation point," respectively. Initially, the zero-pressure point $z_c(t)$ closely follows the jet spray-root, $z_b(t)$, with both advancing rapidly together outward along the bottom contour. The dynamic pressure distribution shows a sharp spike and large negative

gradient into the point $z_c(t)$. This process is referred to as the "chine-unwetted" (CUW) flow phase, which is depicted in Fig. 1.2.

With advancing time, when the zero-pressure point $z_c(t)$ reaches the chine, it comes to an abrupt halt. The jet-head $z_b(t)$ continues moving outward from under the chine and across the free-surface. This is the "chine-wetted" flow phase depicted in Fig. 1.3. With the jet now separating at the physical hard chine $Z_{CH}(x)$, the pressure peak near $z_c(t)$ is reduced.

In the Vorus (1996) model, the essential step of exploiting the flatness of the cylinder and collapsing the cylinder and free-surface contours to the z -axis for the purpose of satisfying (nonlinear) boundary conditions, was a dramatic simplification of the mathematical model. In Fig. 1.2 and 1.3, the non-dimensional horizontal axis variable is defined as $\zeta = \zeta(\tau) = z/z_c(t)$.

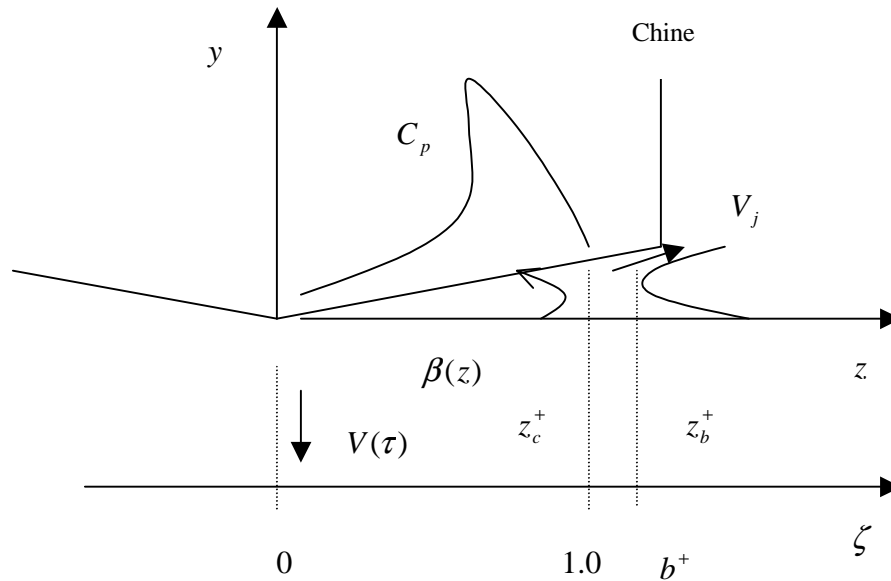


Fig. 1.2 Planing monohull sectional model for "chine un-wetted" phase

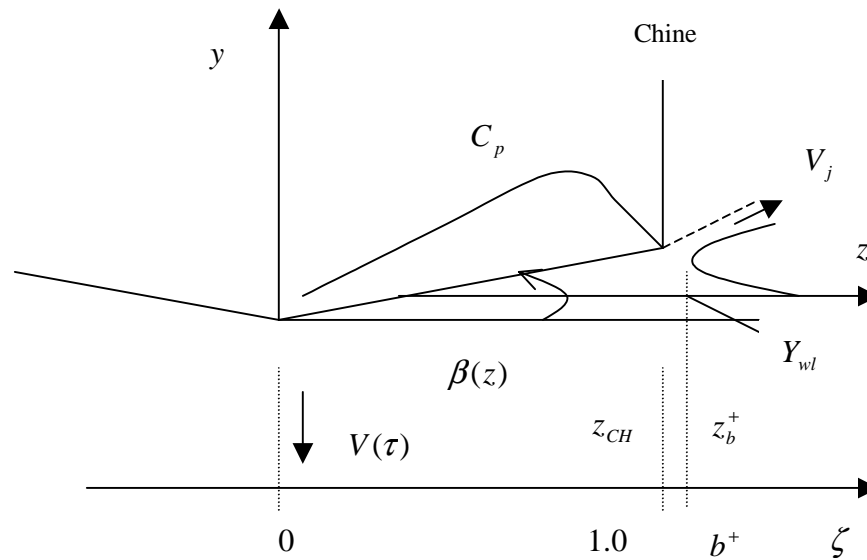


Fig. 1.3 Planing monohull sectional model for the "chine wetted" phase

A monohull planing in calm water has a symmetric jet of velocity $V_j(t)$, a jet separation point $z_c(t)$, as well as a jet head position $z_b(t)$, the same as in the symmetric impact problem.

In the chine un-wetted problem (Figure 1.2), there are three unknowns:

- jet velocity: $V_j(\tau)$;
- jet separation point or zero dynamic pressure point on contour: $z_c(\tau)$
- jet head location or spray-root truncation point: $z_b(\tau)$;

Based on Vorus(1996), there are three equations from which to determine these three unknowns:

- Velocity continuity (Kutta) condition;

- Displacement continuity condition;
- Pressure continuity condition;

In the chine-wetted problem, depicted in Figure 1.3, the jet separation point z_c is known and fixed at the hard chine $Z_{CH}(\tau)$, so that there are only two unknowns:

- jet velocity: $V_j(\tau)$;
- jet head location or spray-root truncation point: $z_b(\tau)$;

This requires,

- Velocity continuity condition;
- Pressure continuity condition;

Since z_c is fixed at the chine and z_b lies outside the hull, the free-surface displacement continuity condition is not needed in the chine-wetted (CW) phase.

The solution of the monohull planing problem is in terms of hyper-geometric functions (refer to equation (47), (55) and (56) in Vorus(1996) for detail).

1.3.2 Development of Vorus'96 model

Vorus' 96 model was extended to a time-dependent hydro-elastic impact model by Kim et al. (1996) to solve for the elastic response and coupled dynamics of a vessel at impact environment. Savander(1997) applied the Vorus(1996) two-dimensional impact model with a "correction" technique to develop a second iteration of the three-dimensional solution for steady planing. As an extension to Vorus' 96 symmetrical impact theory, Xu et al (1998) modeled asymmetrical monohull impact. In Xu's work, two possible types of flows with the asymmetric model are studied. Type A model

simulates a small asymmetry impact, and Type B model simulates a large asymmetry impact. In type A model, CUW and CW flows can be developed at the two sides of the contour, but not symmetrically. In type B model, the CUW flow can only be developed on one side, the other side always in CW flow phase, refer to Fig.1 in Xu et al (1998). The symmetric monohull flow necessarily exhibits Type A flow where the jet heads are attached symmetrically on both sides from keel to chine, and both separate together. The symmetric catamaran treated here is assumed to exhibit Type B flow on each of the demihulls because of the assumed large asymmetry of each; the jet-heads are both attached to the outside, but separate immediately from the keels to the inside (refer to chapter 2). The Type B flow characteristics are addressed further in the catamaran theoretical development.

The experimental work for verifying the Vorus' theory was via the full-scale experiments reported in Royce and Vorus (1998), as well as the laboratory impact experiments of Judge (2001). Royce (2001) has made efforts to extend Vorus' 96 theory to include the reattachment of separated flow for two-dimensional impact.

In the last ten years, Vorus has performed a series of research works on planing hydrodynamics, structure impact reduction and sea-keeping prediction of planing craft, including both planing mono-hulls and planing catamarans (Vorus 1992, Vorus 1996, Kim, Vorus, Troesch, and Gollwitzer 1996, Royce 1996, Royce and Vorus 1998, Xu, Troesch, Vorus 1998, Vorus 1999, Vorus and Royce 2000). The foundation of all of above is the Vorus'96 theory.

1.4 Present Research and Objectives

A catamaran is a twin-hull planing craft composed of two demi-hulls connected by a cross-over structure. The cross-over structure forms the ceiling of an interior air tunnel which complicates the mathematical modeling of the catamaran. The planing catamaran cross section is depicted in Fig. 1.4.

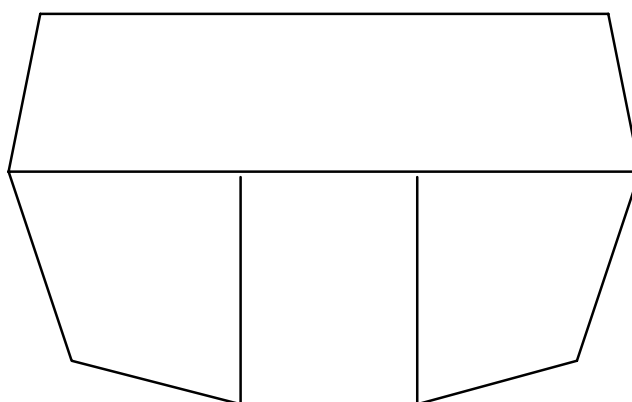


Fig. 1.4 Cross section of a planing catamaran viewed from behind transom

Because of the difference in the structure with mono-hulls, there are differences in the mathematical modeling of a planing mono-hull verse a planing catamaran.

Based on the Vorus' 96 theory described above, Vorus has developed and implemented a first order nonlinear model for the catamaran hydrodynamic analysis, embodied in the computer code CatSea. This model has been applied in planing catamaran design. However, due to the greater complexity of the catamaran flow physics

relative to the mono-hull, Vorus's model has made some approximations and simplifications which were not considered necessary in the monohull work.

The present research is for relieving the initially implemented approximations by Vorus, and further developing and extending the planing catamaran hydrodynamics theory and application beyond that currently in use in CatSea. The subject approximations and the simplifications are specifically:

- 1) A linearized form of the kinematic conditions which does not reflect the orders of magnitude of the variables established in Vorus(1996), and
- 2) Discard of a part of the temporal derivatives appearing in the pressure continuity conditions and in the pressure distribution formulation.

These two main approximations, particularly, in the simplified first order nonlinear CatSea model will be relieved through careful analysis, development, and coding.

In the present work, a new complete second order nonlinear hydrodynamic theory for planing catamarans is developed. A detail numerical comparison of the first order nonlinear theory and the second order nonlinear theory is carried out. The second order nonlinear theory and algorithms have been incorporated into a new catamaran design code (NewCat). A detail mathematical formulation of the base 1st order CatSea theory, followed by the extended 2nd order theory, is completely documented in this thesis.

CHAPTER 2
CATAMARAN FLOW PHYSICS

2.1 Problem Description

The problem addressed is a slender three-dimensional planing catamaran running on the surface of water at a high constant forward speed U , with or without ambient head or following waves (Fig. 2.1).

With ambient waves, this is a planing catamaran sea-keeping dynamics problem. Without waves, the problem is a steady planing problem. Both cases are treated in this thesis.

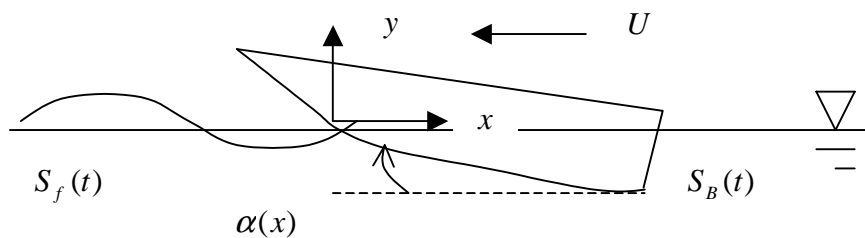


Figure 2.1 Definition of the problem

In Fig. 2.1, the x, y coordinate system is the boat-fixed bow coordinate system which has been described more detail in the following section. U is the forward speed, $S_f(t)$ is the wave surface, $S_B(t)$ is the wetted body surface, $\alpha(x)$ is the attack angle measured from the baseline.

The following traditional assumptions are made:

- (1) The flow is incompressible, irrotational and homogeneous over the whole fluid region;
- (2) Gravity is ignorable, because of the high speed (zero gravity);
- (3) The fluid behaves as ideal (zero viscosity).

Therefore, the problem can be modeled as a potential flow problem described by a 3-D Laplace equation:

$$\frac{\partial^2 \phi(x, y, z; t)}{\partial x^2} + \frac{\partial^2 \phi(x, y, z; t)}{\partial y^2} + \frac{\partial^2 \phi(x, y, z; t)}{\partial z^2} = 0 \quad (x, y, z) \in \Omega \quad (2.1)$$

where $\Omega(x, y, z)$ is the fluid domain.

2. 2 Coordinate Systems

Four coordinate systems are employed to describe the flow of a planing catamaran in waves with general three-degree-of-freedom motion.

- a) Earth-fixed Coordinate System $O_0 - x_0 y_0 z_0$

Coordinate system $O_0 - x_0 y_0 z_0$ is fixed in space. The (x_0, z_0) plane lies on the calm water surface, with x_0 positive toward the stern. y_0 is positive upward, as depicted in Fig. 2.2.

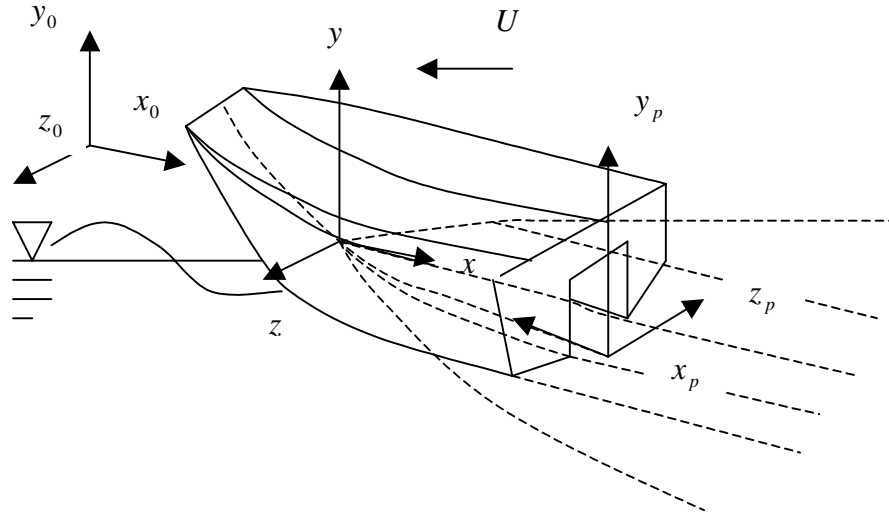


Figure 2.2 Coordinate Systems

b) Boat-fixed Bow Coordinate System $O - xyz$

Let $O - xyz$ be a right-handed coordinate system with the origin located on the undisturbed free surface and vertical centerplane at the forward end of the waterline. The (x, z) plane coincides with the undisturbed free surface, with y positive upwards, and x from the forward keel intersection to the transom. This coordinate system translates with the forward speed U , see Fig. 2.2. At the initial time, the $O - xyz$ system coincides with the $O_0 - x_0 y_0 z_0$ system.

- c) Boat-fixed Transom Coordinate System $O_p - x_p y_p z_p$

Define a right-handed coordinate system $O_p - x_p y_p z_p$ located at the transom on the vertical centerplane in the undisturbed water surface, y_p is positive upwards, but x_p is directed from the transom forward against the x -axis direction. This coordinate system translates with the boat with the forward speed U , but no rotation, see Fig. 2.2.

- d) Boat-fixed Transom Coordinate System $O_T - x_T y_T z_T$

Define the vessel motion coordinate system $O_T - x_T y_T z_T$ to be a body-fixed coordinate system, with the origin located at the transom section (refer to Figure 3.7). This body-fixed $O_T - x_T y_T z_T$ system moves and rotates with the boat together. The x_T - axis is along the longitudinal centerline, from stern to bow and the y_T - axis is upwards. The $O_T - x_T y_T z_T$ system is initially superimposed on the translation coordinate system $O_p - x_p y_p z_p$.

2. 3 Method of Solution: Slender-body Theory, Solution Domain Transformation, and Time Marching

In the $O - xyz$ system, the motion of the cross sectional contour of the planing catamaran at x , as viewed from transom, appears to be a 2-D "flat" cylinder contour "impacting" through the free surface with velocity $V(x) = U \tan \alpha(x)$, just as with the

description of the monohull case in Chapter 1. This is shown in Fig. 2.3a and 2.3b. In these figures, $\beta(x, z)$ is the deadrise angle, $V(x)$ is the impact velocity. The relation between the spatial variable x and the time variable t is defined in Eq.(2.2) and (2.3).

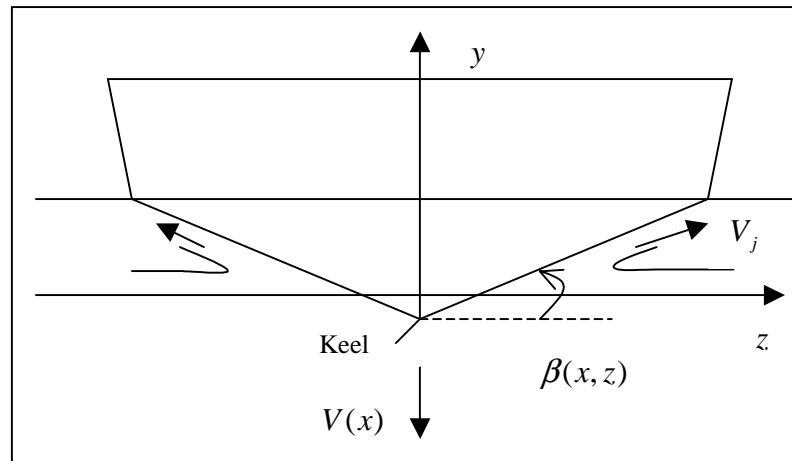


Fig. 2.3a 2-D cylinder impacting as section of planing monohull

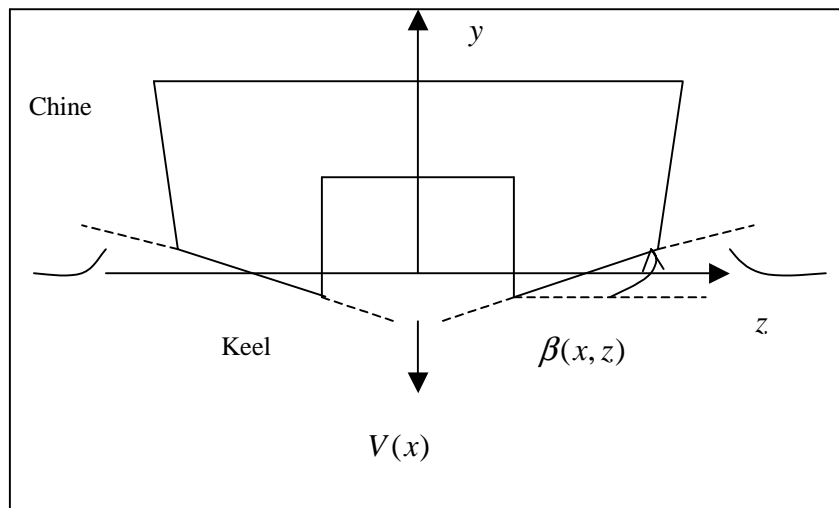


Fig. 2.3b 2-D cylinder impacting as section of planing catamaran

Using the similar non-dimensional expression as in the mono-hull case in Eq. (1.2), but with the normalizing variable being the keel offset $z_K(x)$ (instead of the chine offset z_{CH} with the monohull), we have,

$$\bar{x} = \frac{x}{z_K} = \frac{U \cdot t}{z_K}, \quad \tau = \frac{U \cdot t}{z_K} \quad (2.2)$$

Therefore,

$$\bar{x} = \tau \quad (2.3)$$

The non-dimensional variables \bar{x} and τ are again identical in the catamaran case. Thus it again allows the use of the time dependent impact theory to predict the cross sectional flow at any x – section along the catamaran length.

Assuming the wetted demi-hulls of the planing catamaran to be slender (Slender body assumption), the cross sectional geometry varies slowly in the longitudinal direction. Thus, the following relationships between the gradients may be assumed:

$$\frac{\partial}{\partial x} \ll \frac{\partial}{\partial y} \quad (2.4)$$

$$\frac{\partial}{\partial x} \ll \frac{\partial}{\partial z} \quad (2.5)$$

Substituting the above approximation into Eq.(2.1), the 3-D flow problem can be approximated using a slender body model:

$$\frac{\partial^2 \phi(x, y, z; t)}{\partial y^2} + \frac{\partial^2 \phi(x, y, z; t)}{\partial z^2} = 0 \quad (y, z; x) \in \Omega \quad (2.6)$$

This transformation means that at any specified time t , the three dimensional flow solution of the slender vessel can be obtained approximately by a slender body theory as a series of two dimensional cross sectional flow solutions. However, it is worth to note that, the solution here is different from the traditional 2-D strip theory, for the connection of the upstream solution to the downstream solution through the x -derivative terms in the system equations and in the initial conditions. In the traditional 2-D strip theory, the solution of upstream section is independent of the downstream solution.

This series of 2-D cross sectional flow along the boat length then can be obtained using the identical transformation between the spatial domain and the time domain in Eq.(2.3). In the $y-z$ plane of the $O-xyz$ system, the cross-sectional flows would be a series of different 2-D "flat" cylinder contours with local relative vertical velocity "impacting" into, or "extracting" from, the free surface continuously in time, from one cylinder to the next based on the variation of geometry axially. The solution of the upstream station will be needed in the x -derivative term computation of the down-stream station. The 2-D cylinders are changing shape with time and the temporal gradients in

the $y - z$ plane are important. Thus, this sequential solution of 2-D cross sectional flows will be found by solving different 2-D "flat" cylinder contours continuously impacting.

Let $\beta(x, z)$ be the local deadrise angle (Fig. 2.3b), and $\alpha(x)$ the local trim angle (Fig. 2.1). With $y_c(x, z)$ denoting the hull surface, the above transformation of the 3-D problem to the 2-D problem must satisfy the following geometrical constrains:

$$\frac{\partial y_c(x, z)}{\partial z} = \tan \beta(x, z) \quad (2.7)$$

and

$$\frac{\partial}{\partial t} = U \frac{\partial}{\partial x} \quad (2.8)$$

The sectional downward impact velocity $V(x)$ in the steady planing case can be found using Eq.(2.8):

$$V(x) = U \tan \alpha(x) \quad (2.9)$$

where $\alpha(x)$ is a small angle of attack. This sectional impact velocity at x is for the calm-water planing only. In the seakeeping case, the sectional impact velocity will have additional components. The detail expression may refer to (3.105).

With the sectional flow fields solved, the hydrodynamic forces and the moments can be found by integration of the pressure distribution over each cross section. The motion of a planing catamaran in waves can then be found by a forward integration of

Newton's second law. Continuing time steps with the updated wave and ship motion conditions gives the motion and load time history of the planing catamaran.

2.4 Sectional Flow Physics

In catamaran case, the chine-unwetted phase may be depicted in Fig. 2.4a and the chine-wetted phase may be depicted in Fig. 2.4b.

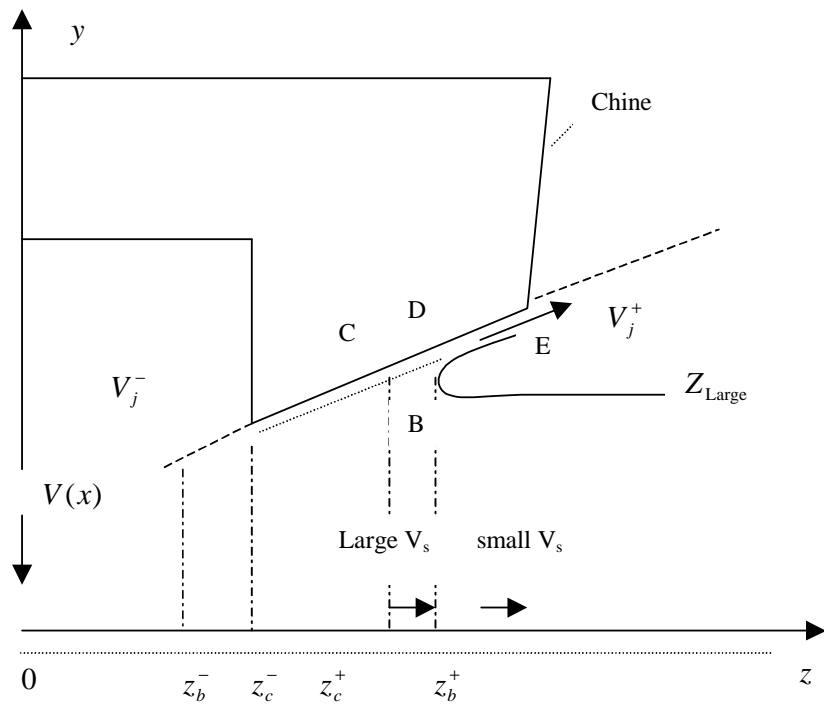


Figure 2.4a Chine unwetted phase of a conventional type catamaran

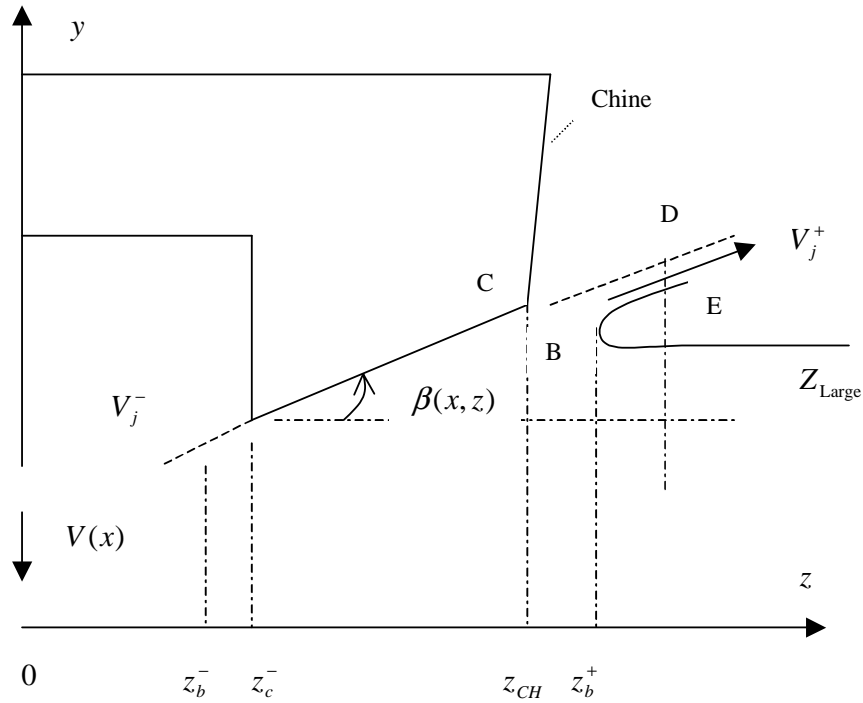


Figure 2.4b Chine wetted phase of a conventional catamaran

In Fig. 2.4, the body geometry of the catamaran consists of two symmetrical single hulls with the assumption of small deadrise angle $\beta(x, z)$. The bottom contour starts from a knuckle, or the keel, denoted as z_k (it is denoted as z_c^- in Fig. 2.4). A hard chine exists on the outside, at Z_{CH} . $V(x)$ is the downward impact velocity of the section. z_b^- and z_b^+ are the inner and outer jet spray-roots. V_j^- and V_j^+ are the jet velocity respectively.

Analogous to Vorus's description of the planing mono-hull (Vorus, 1996), for conventional catamarans, in the CUW impact phase, the water surface is forced to turn back under the bottom of the contour (Fig. 2.4a). Part of the flow near the keel forms an

inner jet with a jet velocity V_j^- , separated at the keel due to the sharp angle of the keel, and part of the flow forms the outer jet attached to the contour.

Point B, in Figure 2.4, with coordinate $z_b^+(t)$, is called the outer jet-head offset, where the jet is truncated. Point C, with the coordinate $z_c^+(t)$, called the jet separation point offset, is the zero dynamic pressure point on the body contour. The inner jet separates at the keel z_k , which denoted as z_c^- , the inner jet-head is truncated at $z_b^-(t)$. Point D, E and Z_{Large} are reference points.

The jet head point $z_b^+(t)$ separates the outer flow into branches. The upper branch is bounded by lines $\overline{C-D}$ and $\overline{B-E}$, and the lower branch is bounded by the line $\overline{B-Z_{Large}}$ located on the free-surface contour bounding the lower flow domain.

Let $V_s(z,t)$ be the cylinder and free surface contour tangential velocity. In the chine-unwetted flow phase (Fig. 2.4a), the flow velocity $V_s(z,t)$ in the jet head region ($z_b^+ - z_c^+$) and on the upper branch is much higher than the impact velocity:

$$V_s(z,t) \gg V(x,t) \quad \text{on the upper branch} \quad (2.10)$$

Conversely, on the lower branch, the flow velocity is much lower than the impact velocity, due to the large volume of the lower flow domain relative to the jet dimensions:

$$V_s(z,t) \ll V(x,t) \quad \text{on the lower branch} \quad (2.11)$$

In the chine-wetted flow phase (Fig. 2.4b), the separation point has reached the hard chine, $z_c^+(t) = Z_{CH}$. The line $\overline{C-D}$ is now on the water surface contour, and the flow velocity in the upper branch drops to a lower order. The jet-head moves out across the free surface.

The description of the outer flow in CW phase is applicable to the inner flow of catamarans. However, there is a difference for the inner flow of the catamaran. The inner flow does not exist as a chine-unwetted flow, only as a chine-wetted flow. The inner separation point $z_c^-(t)$ is the keel point $z_k(x)$.

The flow characteristic that, the CUW flow can only be developed on one side, the other side always in CW flow phase, described above for catamarans is the same as the "type B" flow in the asymmetric impact model for planing mono-hulls (Xu et al, 1998). For the catamaran, the outer jet flow is attached to the outside, but the inner flow separates from the keel. The characteristic of large asymmetry, manifest in steep deadrise to the inside, clearly make the catamaran flow a "type B" flow (refer to Fig. 1 in Xu et al, 1998).

Following Vorus(1996), the flatness of the bottom contour of the catamaran is exploited by collapsing the bottom contour and the free surface to the $z-$ axis for the purpose of satisfying boundary conditions.

The $z-$ axis of Figs. 2.4a and 2.4b shows the boundary segments where different boundary conditions are satisfied (refer to Fig. 2.6). The boundary switches from the upper branch at point B to the lower branch with a discontinuity in jet tangential velocity $V_s(z, t)$ (but with continuous potential) (Vorus 1996), which is depicted in Fig. 2.4a.

Fig. 2.4c shows a conventional catamaran with a transverse step. In modern catamaran design, the downstream shoulder of the step will generally return to approximately the original hull lines, thereby separating the hull into different regions, as depicted in Fig. 2.4c. The concept of the step is to eliminate the relatively ineffective chine-wetted region of the hull. Since that part of the hull, aft of the chine wetting point, has a very small contribution to the useful dynamic lift, but a substantial contribution to unwanted frictional resistance, its operational efficiency is very low. In today's new design concepts, a step produces a trip which changes the low-pressure chine-wetted region to a high-pressure chine-unwetted region, thereby allowing the after part of the craft to increase its operational efficiency. In essence, the chine-wetted flow is interrupted and detached by the step and then starts over on re-attachment as a chine-unwetted flow. The step shown on Figure 2.4c is exaggerated in size for conceptual clarity.

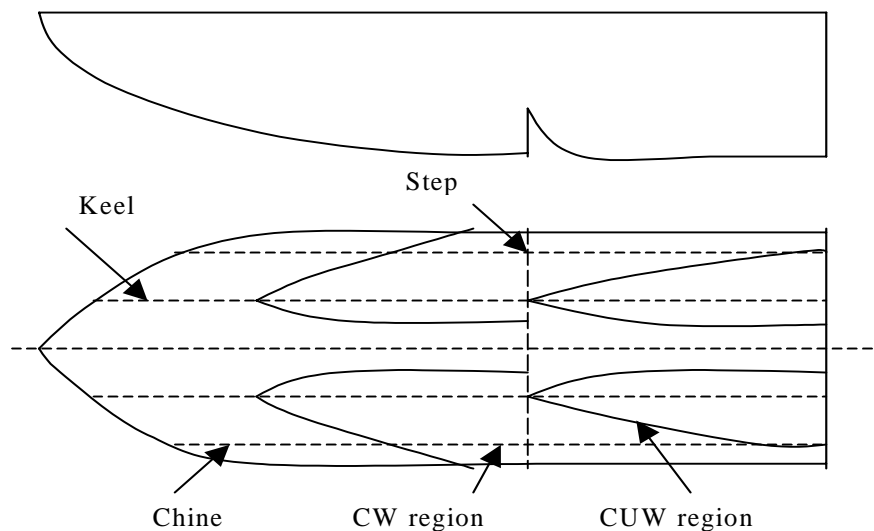


Fig.2.4c A transverse step and CUW , CW regions

2.5 Vortex Distribution Model

A vortex distribution theory has been applied in modeling the catamaran sectional hydrodynamics problem.

With every variable normalized on the keel offset $z_k(x)$, we have:

$$\zeta = \frac{z}{z_k(x)} \quad (2.12)$$

The normalized physical model is depicted in Fig. 2.5, where

$$b^+ = z_b^+ / z_k, \quad b^- = z_b^- / z_k, \quad z_c = z_c^+ / z_k, \quad z_c^- = z_k / z_k = 1 \quad (2.13)$$

A vortex distribution model with boundary conditions on the z -axis, based on the normalized physical model of Fig. 2.5, is shown in Fig. 2.6. Since the scale of Fig. 2.6 is so small, it is very difficult to show the hull segment in the same figure, the reader may refer to Fig. 2.5 when reading Fig. 2.6.

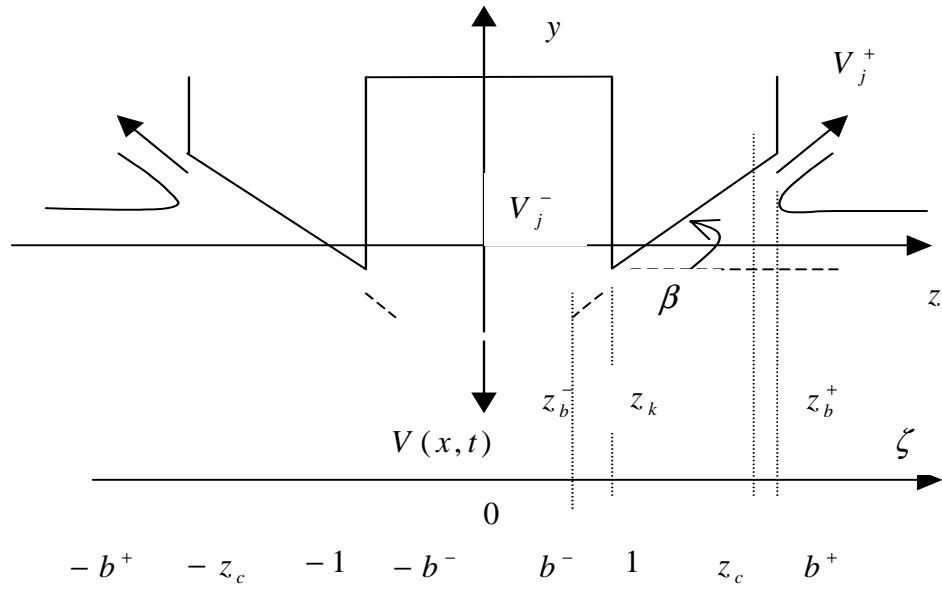


Figure 2.5 Normalized physical model

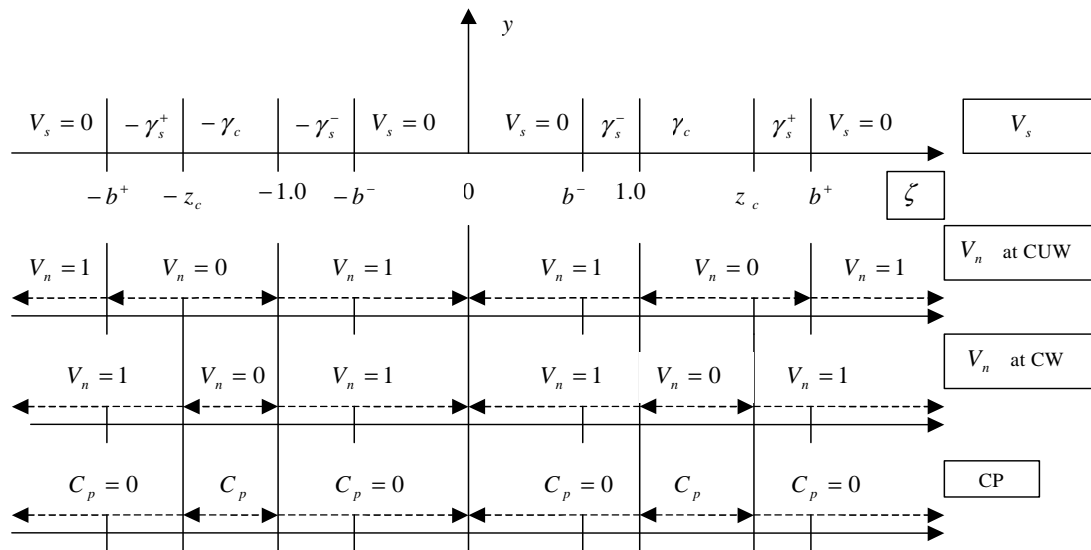


Fig. 2.6 Vortex distribution model

In Fig. 2.6, $V_s(\zeta, \tau)$ and $V_n(\zeta, \tau)$ are the tangential and normal velocities on the boundary, which are normalized on the impact velocity $V(x)$. Vortex sheets are arranged along the contour to satisfy the boundary conditions.

The bound vortex $\gamma_c(\zeta, \tau)$ is located on the body contour, the free vortex $\gamma_s^+(\zeta, \tau)$ is located on the outer jet head region, and the free vortex $\gamma_s^-(\zeta, \tau)$ is located on the inner jet head region.

$$\gamma(\zeta, \tau) = \gamma_c(\zeta, \tau) \quad 1 \leq \zeta \leq z_c \quad (2.14)$$

$$\gamma(\zeta, \tau) = \gamma_s^+(\zeta, \tau) \quad z_c \leq \zeta \leq b^+(\tau) \quad (2.15)$$

$$\gamma(\zeta, \tau) = \gamma_s^-(\zeta, \tau) \quad b^- \leq \zeta \leq 1 \quad (2.16)$$

2.6 Sectional Boundary Value Problem

Based on the physical model in Fig. 2.6, the sectional boundary value problem can be solved by using the proper boundary conditions and a group of constraint conditions as follows:

(1) Governing Equation:

$$\frac{\partial^2 \phi(x, y, z; t)}{\partial y^2} + \frac{\partial^2 \phi(x, y, z; t)}{\partial z^2} = 0 \quad (y, z; x) \in \Omega \quad (2.17)$$

(2) Kinematic boundary condition:

On the body wetted surface, the flow must satisfy the zero normal velocity kinematic boundary condition (refer to Fig. 2.6):

$$\left. \frac{\partial \phi}{\partial n} \right|_{\zeta = \zeta(\tau)} = V_n \quad \zeta = \zeta(\tau) \quad (2.18)$$

In the body-fixed coordinate system $O - xyz$, the kinematic boundary condition can be expressed as (Fig. 2.6):

$$V_n = 0 \quad 1 \leq \zeta \leq b^+ \quad \text{CUW} \quad (2.19)$$

$$V_n = 0 \quad 1 \leq \zeta \leq z_c \quad \text{CW} \quad (2.20)$$

(3) The pressure condition (dynamic boundary condition)

The pressure on the free surface and the body surface beyond the wetted points is equal to atmospheric pressure, which is appropriately defined as zero (Fig. 2.6):

$$C_p(\zeta, \tau) = 0 \quad b^- \leq \zeta \leq 1 \text{ and } z_c \leq \zeta \leq b^+ \quad (2.21)$$

$$C_p(\zeta, \tau) = 0 \quad \text{on the FS sheet: } 0 \leq \zeta < b^- \text{ and } \zeta > b^+ \quad (2.22)$$

(4) The Kutta constraint condition

The Kutta condition should be satisfied at the separation points, i.e. $\zeta = 1$ and $\zeta = z_c$, which requires the vortex strength to be continuous across these points (Fig. 2.6).

$$|\gamma_c(\zeta, \tau)| < \infty \quad \text{at } \zeta = 1 \text{ and } \zeta = z_c \quad (2.23)$$

(5) Displacement continuity constraint condition (mass conservation condition)

This constraint requires a continuous body-free-surface contour at the jet-head point b^+ in CUW flow.

$$y_c(b^+, \tau) = y_s(b^+, \tau) \quad \text{when } \zeta = b^+ \quad (2.24)$$

Here, y_s is the elevation of free surface.

Let γ_c^* represent the time-integrated displacement vortex strength (refer to Chapter 3 for γ_c^* definition), the Kutta condition on the displacement vortex strength requires:

$$|\gamma_c^*(\zeta, \tau)| < \infty \quad \text{when } \zeta \rightarrow b^+ \quad (2.25)$$

The above formulation states the mathematical foundation to solve the boundary value problem in this thesis.

2.7 Steady Planing Problem

The first problem to be studied in this thesis is the steady planing of a catamaran in calm water.

In the steady planing problem, there are two essential variables: (z, x) , where z variable is the transverse coordinate and x is the coordinate along the vessel length (refer to Fig. 2.2). The equivalent nondimensional form is (ζ, \bar{x}) for convenience. Since \bar{x} is identical with τ according to Eq.(2.3), thus variable pair (ζ, τ) will be used in the steady planing model.

In the steady planing problem, refer to Fig. 2.5, there are two symmetrical jet velocities $V_j^+(\tau)$ and $V_j^-(\tau)$, two jet heads $z_b^+(\tau)$ and $z_b^-(\tau)$, two jet separation points, $z_c^+(\tau)$ and $z_c^-(\tau)$ for a catamaran. Since the inner flow separates at the keel z_k at any time, $z_c^-(\tau) = z_k$, this leaves one unknown jet separation point $z_c^+(\tau) = z_c^-(\tau)$.

In the chine un-wetted flow phase, there are therefore five unknowns:

- Two jet velocities $V_j^+(\tau)$ and $V_j^-(\tau)$;
- Two jet head locations $z_b^+(\tau)$ and $z_b^-(\tau)$;
- One jet separation point or zero dynamic pressure point on contour, $z_c^+(\tau)$

And there are five equations according to the description in Section 2.6:

- Two velocity continuity conditions (Kutta conditions) when $z \rightarrow z_k$ and $z \rightarrow z_c^+$;
- Two pressure continuity conditions at $z = z_b^+(\tau)$, $z = z_b^-(\tau)$;
- One free-surface displacement continuity condition when $z \rightarrow z_b^+(\tau)$;

In the chine-wetted flow phase, on the other hand, since the jet separation point z_c^+ is known and fixed at the chine Z_{CH} , there are four unknowns:

- Two jet velocities $V_j^+(\tau)$ and $V_j^-(\tau)$;
- Two jet head locations $z_b^+(\tau)$ and $z_b^-(\tau)$;

As in the case of the mono-hull, since z_c^+ is known, the free-surface displacement condition is not needed in this case. This leaves the four equations for the CW phase:

- Two velocity continuity conditions (Kutta condition) at $z \rightarrow z_k$ and $z \rightarrow z_c^+$;
- Two pressure continuity conditions;

2.8 Seakeeping Problem of a Planing Catamaran

The second problem to be studied in this thesis will be the sea-keeping problem, or an unsteady planing problem, of a planing catamaran in waves.

In the sea-keeping problem, there are three essential independent coordinates: (z, x, t) , the equivalent nondimensional form is (ζ, ξ, τ) . But by using the time marching method, the seakeeping problem can be transformed into a series of two dimensional

cross-section cylinder impact problems at each time step, but with a complete x -flow problem solved for each time.

In seakeeping, at each time step, for the complete x - flow problem, there are same number of unknowns and same number of equations as in the mathematical model of the steady planing. Comparing with the steady planing, the difference is that, the solution process in the steady planing is only one-time-step process, but it is a multi-time-step process in seakeeping. The wetted surface and the water line of the catamaran vary at each time step in seakeeping.

The velocity continuity condition and the displacement continuity condition in seakeeping at each time step are the same as those in the steady planing. However, the pressure continuity condition in seakeeping is different from the pressure condition in the steady planing since the pressure $p(x, z; t)$ involves the time variable t .

In seakeeping, an unsteady planing model, wave model, and the vessel motion model will each need to be developed.

CHAPTER 3

FIRST ORDER NONLINEAR CATAMARAN HYDRODYNAMIC THEORY

William Vorus has developed a first order nonlinear hydrodynamic theory to support his research and engineering activities for catamaran craft design. CatSea is a catamaran design code based on the first order theory developed by Vorus. The basis of the first order theory is a non-linear slender-body theory, with the near-field being the nonlinear sectional impact flow adapted from the theory of Vorus (1996) for the twin hull case. In the time domain, the near-field section cylinders effectively change shape in time according to the variation of geometry axially as they impact with the local relative vertical velocity between the water surface and the keel. The effects of the jet formed by the large transversely squeeze-flow (both out and in) under the relatively flat hull sections is rationally included in the first order nonlinear theory (refer to Fig. 2.3b and Fig. 2.4). CatSea has been successfully applied in planing catamaran design. However, due to the complexity of the problem itself, Vorus' first order model has made some significant approximations and simplifications. This chapter briefly reviews Vorus' first order nonlinear theory as the basis of the second order nonlinear extension developed as the central contribution of this thesis.

We first review Vorus' first order model for steady planing in calm water, and then his first order model for dynamics in a seaway.

3.1 Steady Planing in Calm Water

3.1.1 First order kinematic boundary condition

As discussed in Chapter 2, in the chine un-wetted flow phase of both the first and second order models, there are five unknowns, thus we need five equations for a unique solution. Let us first review the velocity continuity equations.

A downward moving coordinate system $\zeta - o_{keel} - \eta$ on the body boundary is depicted in Fig. 3.1. In Fig. 3.1, $V_s(\zeta)$ and $V_n(\zeta)$ are the total tangential and normal flow velocities on the bottom contour, and $v(\zeta)$, $w(\zeta)$ are the respective perturbations. β is a small deadrise angle, and V is the section impact velocity.

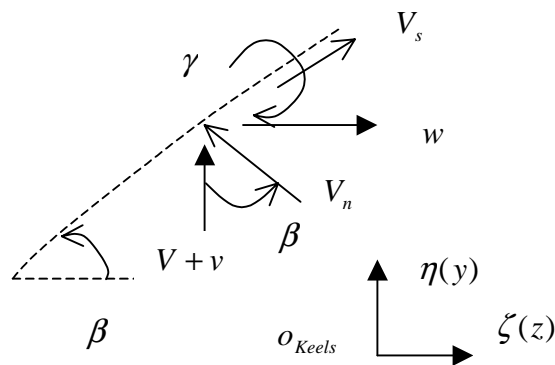


Fig. 3.1 Kinematic boundary condition

In Fig. 3.1, the kinematic boundary condition requires a solid wall non-penetration condition (refer to Fig. 2.5 and Fig. 2.6),

$$V_n(\zeta, \tau) = 0 \quad \text{for } 1 \leq \zeta \leq z_c \quad (3.1)$$

By applying the above condition, we can find the following equation on the hull, the detailed derivation of which can be found in Appendix A:

$$v(\zeta, \tau) = -V(\tau) \quad \text{for } 1 \leq \zeta \leq z_c \quad (3.2)$$

By the Biot-Savart law, an integral equation can be derived from the kinematic boundary condition in (3.2) (refer to the derivation of (21) in Vorus (1996)).

$$\frac{1}{2\pi} \int_{b^-}^{b^+} \gamma(\zeta_0, \tau) \left[\frac{1}{\zeta_0 - \zeta} + \frac{1}{\zeta_0 + \zeta} \right] d\zeta_0 = -V(\tau) \quad \text{on } 1 \leq \zeta \leq z_c \quad (3.3)$$

The vortex strength γ is distributed on the axis as described in Fig. 2.6. The unknown bound vortex $\gamma_c(\zeta, \tau)$ in (3.3) over the hull segment can be expressed in terms of the free vortex $\gamma_s^+(\zeta, \tau)$ and $\gamma_s^-(\zeta, \tau)$ over the free surface segments; refer to Figure 2.6. Considering the fact that on $-1 \leq \zeta_0 \leq 1$, $\gamma_c(\zeta_0, \tau) = 0$, the integral equation in (3.3) can be expressed as (refer to Appendix A):

$$\frac{1}{2\pi} \int_{-z_c}^{z_c} \frac{\gamma_c(\zeta_0, \tau)}{\zeta_0 - \zeta} d\zeta_0 = f(\zeta, \tau) \quad 1 \leq \zeta \leq z_c \quad (3.4)$$

where,

$$f(\zeta, \tau) = -V(\tau) - \frac{1}{\pi} \int_{b^-}^1 \gamma_s^-(\zeta_0, \tau) \frac{\zeta_0}{\zeta_0^2 - \zeta^2} d\zeta_0 - \frac{1}{\pi} \int_{z_c}^{b^+} \gamma_s^+(\zeta_0, \tau) \frac{\zeta_0}{\zeta_0^2 - \zeta^2} d\zeta_0 \quad (3.5)$$

with the integration region as defined in Fig. 2.5.

(3.4) is a standard Hilbert type integral equation to be solved for the vortex distribution $\gamma_c(\zeta, \tau)$. It can be inverted semi-analytically using the Hilbert integral transform at time τ for the contour vortex strength $\gamma_c(\zeta, \tau)$.

The solution to the above singular integral equation applied in CatSea is:

$$\gamma_c(\zeta, \tau) = -\frac{2}{\pi} \cdot \chi(\zeta) \int_{-z_c}^{z_c} \frac{f(\zeta_0)}{\chi(\zeta_0)} \frac{d\zeta_0}{\zeta_0 - \zeta} \quad \text{on } 1 \leq \zeta \leq z_c \quad (3.6)$$

where $\chi(\zeta)$ is the kernel function.

The integral kernel function introduced in (3.6) has the following form, the detail derivation of which is in the Appendix F.

$$\chi(\zeta) = \frac{1}{\sqrt{(\zeta^2 - 1)(z_c^2 - \zeta^2)}} \quad (3.7)$$

Expand equation (3.6) considering the symmetry of $\chi(\zeta)$ and $f(\zeta, \tau)$. After substituting the kernel function $\chi(\zeta)$, and the right-hand-side $f(\zeta)$ of (3.5) into (3.6), the bound vortex strength $\gamma_c(\zeta, \tau)$ is the following:

$$\begin{aligned}
\gamma_c(\zeta) = & \frac{4\zeta}{\pi} \chi(\zeta) \{V(\tau) \cdot \int_{\zeta_1=1}^{z_c} \frac{d\zeta_1}{\chi(\zeta_1)(\zeta_1^2 - \zeta^2)} \\
& + \frac{1}{\pi} \int_{b^-}^1 \gamma_S^-(\zeta_0, \tau) \cdot \zeta_0 \cdot \int_{\zeta_1=1}^{z_c} \frac{d\zeta_1}{\chi(\zeta_1)(\zeta_1^2 - \zeta^2)(\zeta_0^2 - \zeta_1^2)} d\zeta_0 \\
& + \frac{1}{\pi} \int_{z_c}^{b^+} \gamma_S^+(\zeta_0, \tau) \cdot \zeta_0 \cdot \int_{\zeta_1=1}^{z_c} \frac{d\zeta_1}{\chi(\zeta_1)(\zeta_1^2 - \zeta^2)(\zeta_0^2 - \zeta_1^2)} d\zeta_0 \}
\end{aligned} \tag{3.8}$$

To simplify (3.8), introduce a useful partial fraction reduction identity (Vorus 1996):

$$\frac{1}{(\zeta_1^2 - \zeta^2)(\zeta_0^2 - \zeta_1^2)} = \frac{1}{\zeta_0^2 - \zeta^2} \left\{ \frac{1}{\zeta_0^2 - \zeta_1^2} + \frac{1}{\zeta_1^2 - \zeta^2} \right\} \tag{3.9}$$

The bound vortex strength $\gamma_c(\zeta, \tau)$ becomes:

$$\begin{aligned}
\gamma_c(\zeta, \tau) = & \frac{4\zeta}{\pi} \chi(\zeta) \{V(\tau) \cdot [-\Lambda(\zeta)] \\
& + \frac{1}{\pi} \int_{b^-}^1 \gamma_S^-(\zeta_0, \tau) \frac{\zeta_0}{\zeta_0^2 - \zeta^2} d\zeta_0 [\Lambda^-(\zeta_0) - \Lambda(\zeta)] \quad \text{on } 1 \leq \zeta \leq z_c \\
& + \frac{1}{\pi} \int_{z_c}^{b^+} \gamma_S^+(\zeta_0, \tau) \frac{\zeta_0}{\zeta_0^2 - \zeta^2} d\zeta_0 [\Lambda^+(\zeta_0) - \Lambda(\zeta)] \}
\end{aligned} \tag{3.10}$$

where $\Lambda(\zeta)$, $\Lambda^-(\zeta_0)$ and $\Lambda^+(\zeta_0)$ in (3.10) are the parameter integral terms defined as:

$$\Lambda(\zeta) = \int_{\zeta_1=1}^{z_c} \frac{d\zeta_1}{\chi(\zeta_1)(\zeta^2 - \zeta_1^2)} \quad 1 \leq \zeta \leq z_c \tag{3.11}$$

$$\Lambda^-(\zeta_0) = \int_{\zeta_1=1}^{\zeta_1=z_c} \frac{d\zeta_1}{\chi(\zeta_1)(\zeta_0^2 - \zeta_1^2)} \quad b^- \leq \zeta_0 \leq 1 \quad (3.12)$$

$$\Lambda^+(\zeta_0) = \int_{\zeta_1=1}^{\zeta_1=z_c} \frac{d\zeta_1}{\chi(\zeta_1)(\zeta_0^2 - \zeta_1^2)} \quad z_c \leq \zeta_0 \leq b^+ \quad (3.13)$$

(3.10) has singularity points in its solution domain when $\zeta \rightarrow 1$ and $\zeta \rightarrow z_c$. The Kutta condition in (2.23) requires the vortex strength to be continuous across these points. By non-singularization in (3.10), two velocity continuity conditions could be derived from (3.10) (refer to Appendix A), which will provide the two of five equations for solving the five unknowns in CUW phase:

$$0 = \left\{ -\Lambda(1) + \frac{1}{\pi} \int_{b^-}^1 \gamma_s^-(\zeta_0, \tau) \frac{\zeta_0}{\zeta_0^2 - 1} [\Lambda^-(\zeta_0) - \Lambda(1)] d\zeta_0 \right. \\ \left. + \frac{1}{\pi} \int_{z_c}^{b^+} \gamma_s^+(\zeta_0, \tau) \frac{\zeta_0}{\zeta_0^2 - 1} [\Lambda^+(\zeta_0) - \Lambda(1)] d\zeta_0 \right\} \quad \text{when } \zeta \rightarrow 1^+ \quad (3.14)$$

$$0 = \left\{ -\Lambda(z_c) + \frac{1}{\pi} \int_{b^-}^1 \gamma_s^-(\zeta_0, \tau) \frac{\zeta_0}{\zeta_0^2 - z_c^2} [\Lambda^-(\zeta_0) - \Lambda(z_c)] d\zeta_0 \right. \\ \left. + \frac{1}{\pi} \int_{z_c}^{b^+} \gamma_s^+(\zeta_0, \tau) \frac{\zeta_0}{\zeta_0^2 - z_c^2} [\Lambda^+(\zeta_0) - \Lambda(z_c)] d\zeta_0 \right\} \quad \text{when } \zeta \rightarrow z_c \quad (3.15)$$

Therefore, with the first order KBC (3.4), the solutions of (3.10), (3.14) and (3.15) obtained by Vorus consist of the Elliptic integrals of the first kind, second kind and third kind. For example, the singular integral term in (3.11) will be in the following form,

$$\Lambda(\zeta) = I_1 + I_2(\zeta) + I_3(\zeta) \quad 1 \leq \zeta \leq z_c \quad (3.16)$$

where,

$$I_1 = \int_{\zeta_1=1}^{z_c} \frac{\zeta_1^2}{\sqrt{(\zeta_1^2-1)(z_c^2-\zeta_1^2)}} d\zeta_1 = z_c E\left(\frac{\pi}{2}, \sqrt{1-1/z_c^2}\right) \quad (3.17)$$

$$\begin{aligned} I_2(\zeta) &= (\zeta^2 - z_c^2 - 1) \cdot \int_{\zeta_1=1}^{z_c} \frac{1}{\sqrt{(\zeta_1^2-1)(z_c^2-\zeta_1^2)}} d\zeta_1 \\ &= (\zeta^2 - z_c^2 - 1) \cdot \frac{1}{z_c} F\left(\frac{\pi}{2}, \sqrt{1-1/z_c^2}\right) \end{aligned} \quad (3.18)$$

$$\begin{aligned} I_3(\zeta) &= (\zeta^2 - 1)(z_c^2 - \zeta^2) \cdot \int_{\zeta_1=1}^{z_c} \frac{1}{(\zeta^2 - \zeta_1^2) \cdot \sqrt{(\zeta_1^2-1)(z_c^2-\zeta_1^2)}} d\zeta_1 \\ &= \frac{z_c^2 - \zeta^2}{z_c \zeta^2} \left\{ \Pi\left[\frac{\pi}{2}, \frac{\zeta^2(z_c^2-1)}{z_c^2(\zeta^2-1)}, \sqrt{1-1/z_c^2}\right] + (\zeta^2 - 1) F\left(\frac{\pi}{2}, \sqrt{1-1/z_c^2}\right) \right\} \end{aligned} \quad (3.19)$$

where $F\left(\frac{\pi}{2}, \sqrt{1-1/z_c^2}\right)$, $E\left(\frac{\pi}{2}, \sqrt{1-1/z_c^2}\right)$, and $\Pi\left(\frac{\pi}{2}, \frac{\zeta^2(z_c^2-1)}{z_c^2(\zeta^2-1)}, \sqrt{1-1/z_c^2}\right)$ are the

Elliptic integrals of the first, second and third kind respectively (refer to Gradshteyn and Ryzhik, 1965).

After mathematical reduction, the semi-analytical expression of the integral terms in (3.14) have the form,

$$\Lambda(1) = \frac{1}{z_c} \{z_c [E(k) - F(k)]\} \quad (3.20)$$

$$\Lambda^-(\zeta) - \Lambda(1) = \frac{1}{z_c} \left\{ \frac{\pi}{2\zeta} \sqrt{(z_c^2 - \zeta^2)(1 - \zeta^2)} [1 - \Lambda_0(\varepsilon_2 \setminus k)] \right\} \quad b^- \leq \zeta \leq 1 \quad (3.21)$$

$$\Lambda^+(\zeta) - \Lambda(1) = \frac{1}{z_c^2} \left\{ \frac{z_c^2 - 1}{z_c} F(k) - \frac{\pi}{2\zeta} \sqrt{(\zeta^2 - 1)(\zeta^2 - z_c^2)} [1 - \Lambda_0(\varepsilon_3 \setminus k)] \right\}$$

$$z_c \leq \zeta \leq b^+ \quad (3.22)$$

where,

$$\Lambda_0(\varepsilon \setminus k) = \frac{2}{\pi} \{ F(k)E(\varepsilon \setminus k') - [F(k) - E(k)]F(\varepsilon \setminus k') \} \quad (3.23)$$

$$k = \sqrt{1 - \frac{1}{z_c^2}} \quad (3.24)$$

$$k' = \frac{1}{z_c} \quad (3.25)$$

$$\varepsilon_2 = \arcsin \left(z_c \sqrt{\frac{1 - \zeta^2}{z_c^2 - \zeta^2}} \right) \quad (3.26)$$

$$\varepsilon_3 = \arcsin \sqrt{\frac{\zeta^2 - z_c^2}{\zeta^2 - 1}} \quad (3.27)$$

In above expressions, $F(k) = F(\frac{\pi}{2}, k)$, $E(k) = E(\frac{\pi}{2}, k)$ are the first kind, second kind elliptic integrals respectively.

With the integral terms $\Lambda(\zeta)$, $\Lambda^-(\zeta_0)$ and $\Lambda^+(\zeta_0)$ in terms of the Elliptic integral functions, the reduced form of the velocity continuity condition in Eq.(3.14) becomes:

$$\begin{aligned}
0 = & \{-z_c[E(k) - F(k)] - \frac{1}{2} \int_{b^-}^1 \gamma_s^-(\zeta_0, \tau) \sqrt{\frac{z_c^2 - \zeta_0^2}{1 - \zeta_0^2}} [1 - \Lambda_0(\varepsilon_2 \setminus k)] d\zeta_0 \\
& + \frac{1}{\pi} \frac{z_c^2 - 1}{z_c} F(k) \int_{z_c}^{b^+} \gamma_s^+(\zeta_0, \tau) \frac{\zeta_0}{\zeta_0^2 - 1} d\zeta_0 \\
& - \frac{1}{2} \int_{z_c}^{b^+} \gamma_s^+(\zeta_0, \tau) \sqrt{\frac{\zeta_0^2 - z_c^2}{\zeta_0^2 - 1}} [1 - \Lambda_0(\varepsilon_3 \setminus k)] d\zeta_0 \}
\end{aligned} \tag{3.28}$$

Similarly, the semi-analytical form of the integral terms in (3.15) is obtained by the similar evaluations in terms of elliptic integrals:

$$\Lambda(z_c) = \frac{1}{z_c^2} \left\{ z_c E(k) - \frac{1}{z_c} F(k) \right\} \tag{3.29}$$

$$\Lambda^-(\zeta) - \Lambda(z_c) = \frac{1}{z_c^2} \left\{ \frac{1 - z_c^2}{z_c} F(k) + \frac{\pi}{2\zeta} \sqrt{(z_c^2 - \zeta^2)(1 - \zeta^2)} [1 - \Lambda_0(\varepsilon_2 \setminus k)] \right\}$$

$$b^- \leq \zeta \leq 1 \tag{3.30}$$

$$\Lambda^+(\zeta) - \Lambda(z_c) = \frac{1}{z_c^2} \left\{ -\frac{\pi}{2\zeta} \sqrt{(\zeta^2 - 1)(\zeta^2 - z_c^2)} [1 - \Lambda_0(\varepsilon_3 \setminus k)] \right\}$$

$$z_c \leq \zeta \leq b^+ \tag{3.31}$$

Substituting the above integrals into (3.15), the semi-analytical form of the velocity continuity equation at $\zeta \rightarrow z_c$ is:

$$\begin{aligned}
0 = & -z_c E(k) + \frac{1}{z_c} F(k) \\
& + \frac{1}{\pi} \frac{1-z_c^2}{z_c} F(k) \int_{b^-}^1 \gamma_s^-(\zeta_0, \tau) \frac{\zeta_0}{\zeta_0^2 - z_c^2} d\zeta_0 \\
& - \frac{1}{2} \int_{b^-}^1 \gamma_s^-(\zeta_0, \tau) \sqrt{\frac{1-\zeta_0^2}{z_c^2 - \zeta_0^2}} [1 - \Lambda_0(\varepsilon_2 \setminus k)] d\zeta_0 \\
& - \frac{1}{2} \int_{z_c}^{b^+} \gamma_s^+(\zeta_0, \tau) \sqrt{\frac{\zeta_0^2 - 1}{\zeta_0^2 - z_c^2}} [1 - \Lambda_0(\varepsilon_3 \setminus k)] d\zeta_0
\end{aligned} \tag{3.32}$$

(3.28) and (3.32) are two of the five equations needed for a unique solution.

3.1.2 First order displacement continuity condition

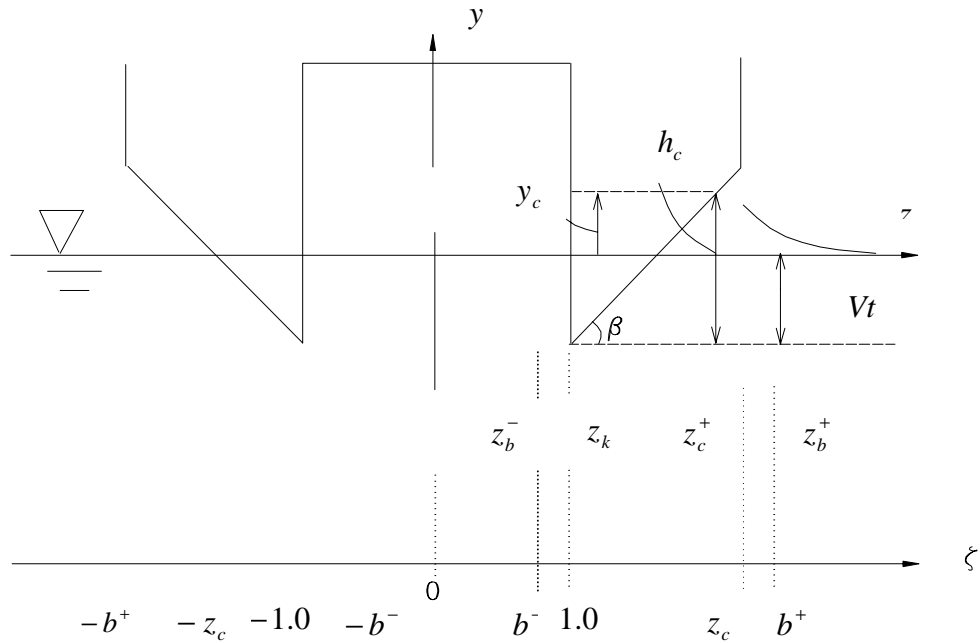


Fig. 3.2 Displacement continuity condition model

Revert temporarily back into the time domain of the equivalent impact problem, $[0, t]$. In the chine-unwetted phase, the dimensional body bottom contour $y_c(z, t)$ can be expressed from Fig. 3.2 as:

$$y_c(z, t) = h_c(z, t) - Vt \quad z_k \leq z \leq z_b^+ \quad (3.33)$$

where $h_c(z, t)$ is the water surface elevation above the keel.

$$h_c(z, t) = \begin{cases} (z - z_k) \tan \beta(z) & z_k \leq z \leq z_b^+(t) \\ 0 & z_b^-(t) \leq z < z_k \end{cases} \quad (3.34)$$

The second branch of h_c is an approximation, assuming that the fluid surface is first order undeflected as the fluid separates at the keel.

Define the net vertical fluid velocity of the contour, from (3.2) as:

$$\frac{\partial y_c(z, t)}{\partial t} = -V(t) = v(z, t) \quad \text{on } z_k \leq z \leq z_b^+ \quad (3.35)$$

Integration of the above equation in time and nondimensionalization of the results yield the following equation (refer to Appendix B):

$$v^*(\zeta, \tau) = f_1(\zeta, \tau) \quad 1 \leq \zeta \leq b^+ \quad (3.36)$$

where, the "asterisk" superscript denotes the time integrated variables:

$$v^*(z, t) = \int_{\tau=0}^t v(z, \tau) d\tau \quad (3.37)$$

and,

$$f_1(\zeta, \tau) = \begin{cases} -\tilde{Y}_{wl} + \tilde{h}_c(\zeta, \tau) & 1 \leq \zeta \leq b^+(\tau) \\ -\tilde{Y}_{wl} & b^- \leq \zeta < 1 \end{cases} \quad (3.38)$$

where \tilde{Y}_{wl} is the nondimensionalized water-line transient draft and,

$$\tilde{h}_c(\zeta, \tau) = \begin{cases} (\zeta - 1) \tan \beta(\zeta) & 1 < \zeta \leq b^+(\tau) \\ 0 & b^-(\tau) \leq \zeta \leq 1 \end{cases} \quad (3.39)$$

The vertical velocity time integral, $v^*(\zeta, \tau)$ in Eq. (3.36), is expressible in terms of the time-integrated displacement vortex strength, $\gamma_c^*(\zeta, \tau)$, by the Biot-Savart law. By replacing $v^*(\zeta, \tau)$ in terms of the integral of $\gamma_c^*(\zeta, \tau)$ in (3.36), Vorus has derived an integral equation for the displacement continuity condition (refer to Appendix B) as:

$$\frac{1}{2\pi} \int_{-b^+}^{-b^-} \gamma_c^*(\zeta_0, \tau) \frac{1}{\zeta_0 - \zeta} d\zeta_0 + \frac{1}{2\pi} \int_{b^-}^{b^+} \gamma_c^*(\zeta_0, \tau) \frac{1}{\zeta_0 - \zeta} d\zeta_0 = -\tilde{Y}_{wl} + \tilde{h}_c(\zeta, \tau) \quad (3.40)$$

where $\gamma_c^*(\zeta_0) = \int_{\tau=0}^t \gamma_c(\zeta_0, \tau) d\tau$ is the time-integral of the vortex strength.

Using the standard Hilbert type singular integral equation transform as in (3.6), the solution to $\gamma_c^*(\zeta, \tau)$ of (3.40) is,

$$\gamma_c^*(\zeta, \tau) = -\frac{2}{\pi} \chi^*(\zeta) \left[\int_{\zeta=-b^+}^{-b^-} \frac{f(\zeta_0, \tau)}{\chi^*(\zeta_0)} \frac{d\zeta_0}{(\zeta_0 - \zeta)} + \int_{\zeta=b^-}^{b^+} \frac{f(\zeta_0, \tau)}{\chi^*(\zeta_0)} \frac{d\zeta_0}{(\zeta_0 - \zeta)} \right] \quad (3.41)$$

The corresponding kernel function $\chi^*(\zeta)$ (refer to Appendix G) in (3.41) is:

$$\chi^*(\zeta) = \frac{1}{\sqrt{(\zeta^2 - (b^-)^2)((b^+)^2 - \zeta^2)}} \quad (3.42)$$

The difference of $\chi^*(\zeta)$ from the kernel function $\chi(\zeta)$ in (3.7) is that its solution domain is now on the arcs of $-b^+ \leq \zeta \leq -b^-$ and $b^- \leq \zeta \leq b^+$, versus $\chi(\zeta)$ in (3.7) on $-z_c \leq \zeta \leq 1$ and $1 \leq \zeta \leq z_c$.

Substituting (3.42) into (3.41) and grouping the singular terms together, the vortex strength $\gamma_c^*(\zeta, \tau)$ will have the following form:

$$\begin{aligned}
\gamma_c^*(\zeta, \tau) = & -\frac{4\zeta}{\pi} \chi^*(\zeta) \cdot \{ -(\tilde{Y}_{wl} + \tan \beta) \cdot \left[-\int_{\zeta_0=1}^{b^+} \frac{1}{\chi^*(\zeta_0)(b^{+2} - \zeta_0^2)} d\zeta_0 \right. \right. \\
& + (b^{+2} - \zeta^2) \int_{\zeta_0=1}^{b^+} \frac{1}{\chi^*(\zeta_0)(b^{+2} - \zeta_0^2)(\zeta_0^2 - \zeta^2)} d\zeta_0 \left. \right] \\
& + \tan \beta \cdot \left[-\int_{\zeta_0=1}^{b^+} \frac{\zeta_0}{\chi^*(\zeta_0)(b^{+2} - \zeta_0^2)} d\zeta_0 \right. \\
& \left. \left. + (b^{+2} - \zeta^2) \int_{\zeta_0=1}^{b^+} \frac{\zeta_0}{\chi^*(\zeta_0)(b^{+2} - \zeta_0^2)(\zeta_0^2 - \zeta^2)} d\zeta_0 \right] \right\}
\end{aligned} \tag{3.43}$$

When $\zeta \rightarrow b^+$, a continuous displacement from the section contour onto the free-surface contour at $\zeta = b^+$ requires that the $\gamma_c^*(\zeta, \tau)$ be bounded (refer to (2.25) when in the chine-unwetted flow phase, this requirement results in the displacement continuity condition:

$$0 = (\tilde{Y}_{wl} + \tan \beta) \cdot I_1 - \tan \beta \cdot I_2 \tag{3.44}$$

where,

$$I_1 = \int_{\zeta_1=1}^{b^+} \frac{1}{\chi^*(\zeta_1)(b^{+2} - \zeta_1^2)} d\zeta_1 \tag{3.45}$$

$$I_2 = \int_{\zeta_1=1}^{b^+} \frac{\zeta}{\chi^*(\zeta_1)(b^{+2} - \zeta_1^2)} d\zeta_1 \tag{3.46}$$

The numerical model for evaluating the integral (3.45) and (3.46) will be given in chapter 5.

3.1.3 First order pressure continuity condition

The pressure continuity condition is the dynamic boundary condition of atmospheric pressure on the jet and free-surface. Referring to Fig. 2.6, zero pressure is required on the free contour and the free surface beyond $\zeta = z_c$ ((2.21) and (2.22)).

The pressure coefficient can be obtained from the unsteady Bernoulli equation as:

$$C_p(\zeta, \tau) = \frac{P - P_\infty}{1/2 \rho V^2} = 1 - V_n^2 - V_s^2 - 2 \frac{\partial \phi}{\partial \tau}(\zeta, \tau) \quad b^- \leq \zeta \leq b^+ \quad (3.47)$$

Define the following coordinate transformations (refer to Fig. 3.3):

$$s(\tau) = \frac{\zeta - 1}{z_c(\tau) - 1}, \quad s^-(\tau) = \frac{b^- - 1}{z_c(\tau) - 1}, \quad s^+(\tau) = \frac{b^+ - 1}{z_c(\tau) - 1} \quad (3.48)$$

In this coordinate transform, $z_c(\tau) - 1$ is the wetted contour length in the ζ -coordinate, $(b^+ - 1)$ and $(b^- - 1)$ are the distances to the ends of the outer and inner jet heads relative to the keel.

In terms of these transformations, the solution domain has a new coordinate system, shown in Fig. 3.3; and the body wetted contour is normalized into the $[0,1]$ region at all times.

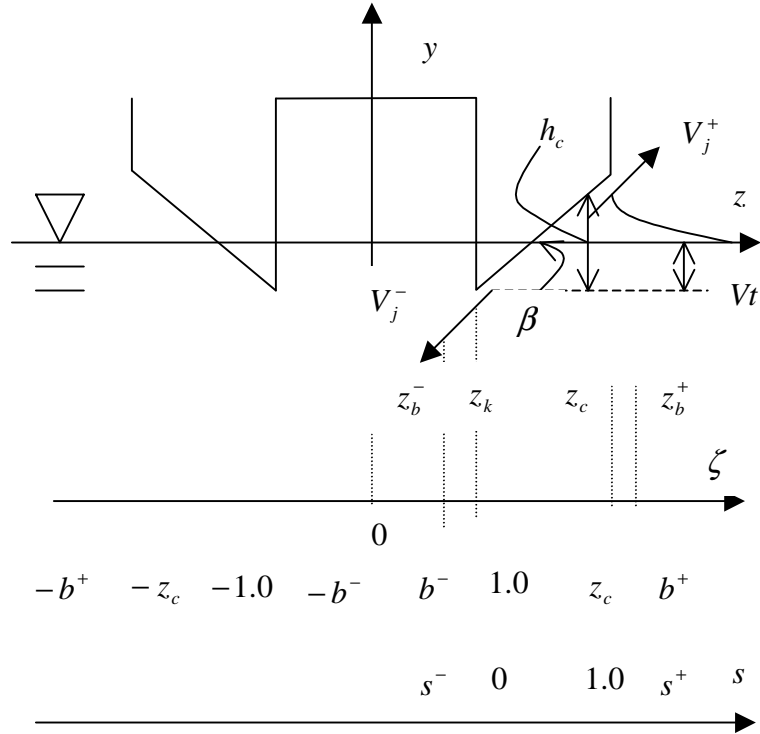


Fig. 3.3 s coordinate system

In the new coordinate system, the pressure distribution in the outer-jet region of $0 \leq s \leq s^+$ is (refer to Appendix C):

$$\begin{aligned}
 C_p(s, \tau) = & 1 - V_n^2(s, \tau) - V_s^2(s, \tau) \\
 & + 2 \frac{\partial z_c}{\partial \tau} \left[\int_{s(\tau)}^{s^+(\tau)} V_s(s_0, \tau) ds_0 + V_s(s, \tau) \cdot s \right] \\
 & + 2(z_c - 1) \left[V_s(s^+, \tau) \frac{ds^+}{d\tau} + \int_{s(\tau)}^{s^+(\tau)} \frac{\partial V_s}{\partial \tau}(s_0, \tau) ds_0 \right]
 \end{aligned} \quad 0 \leq s \leq s^+ \quad (3.49)$$

Similarly, in the inner-jet region of $s^- \leq s \leq 0$,

$$\begin{aligned}
C_p(s, \tau) &= 1 - V_n^2(s, \tau) - V_s^2(s, \tau) \\
&+ 2 \frac{\partial z_c}{\partial \tau} \left[\int_{s(\tau)}^{s^-(\tau)} V_s(s_0, \tau) ds_0 + V_s(s, \tau) \cdot s \right] \\
&+ 2(z_c - 1) \left[V_s(s^-, \tau) \frac{ds^-}{d\tau} + \int_{s(\tau)}^{s^-(\tau)} \frac{\partial V_s}{\partial \tau}(s_0, \tau) ds_0 \right]
\end{aligned} \quad s^- \leq s \leq 0 \quad (3.50)$$

At the jet head z_b^+ , apply the dynamic boundary condition: $C_p(s^+, \tau) = 0$. Eq.

(3.49) gives (refer to Appendix C),

$$\begin{aligned}
&1 - V_n^2(s^+, \tau) - V_s^2(s^+, \tau) \\
&- 2V_s(s^+, \tau) \frac{\partial}{\partial \tau} [s^+ (1 - z_c)] = 0
\end{aligned} \quad (3.51)$$

Using the coordinate transform relation in (3.48),

$$\begin{aligned}
&1 - V_n^2(s^+, \tau) - V_s^2(s^+, \tau) \\
&- 2V_s(s^+, \tau) \frac{\partial}{\partial \tau} [1 - b^+(\tau)] = 0
\end{aligned} \quad (3.52)$$

Expansion of (3.52) gives the spray root velocity:

$$b_\tau^+(\tau) = \frac{V_s^2(s^+, \tau) + V_n^2(s^+, \tau) - 1}{2V_s(s^+, \tau)} \quad (3.53)$$

Recall that in the chine un-wetted flow $V_n(s^+, \tau) = 0$ on the attached free sheet segment, and in the chine wetted flow $V_n(s^+, \tau) = 1$ (Fig. 2.6). Therefore, the pressure continuity condition at $s = s^+$ developed in first order model is, from (3.53), as follows:

- In the chine un-wetted flow

$$b_\tau^+(\tau) = \frac{V_s^2(s^+, \tau) - 1}{2V_s(s^+, \tau)} \quad \text{at } s = s^+ \quad (3.54)$$

- In the chine wetted flow

$$b_\tau^+(\tau) = \frac{1}{2}V_s(s^+, \tau) \quad \text{at } s = s^+ \quad (3.55)$$

At the jet head z_b^- , the keel at z_k is always chine-wetted (Fig. 2.6). By the dynamic boundary condition, similarly the pressure continuity condition at $s = s^-$ is therefore:

$$b_\tau^-(\tau) = \frac{1}{2}V_s(s^-, \tau) \quad \text{at } s = s^- \quad (3.56)$$

The two pressure continuity conditions, in addition to the two velocity continuity and one displacement continuity conditions, sum to the five equations needed to match the five unknowns (four in the chine-wetted case). However, the vortex sheet

distributions on the free sheets in the CUW and CW cases need to be specified. On the free jet-head sheets of $s^- \leq s \leq 0$ and $1 \leq s \leq s^+$ (Fig. 3.3), a constant pressure is required (Fig. 2.6). To solve for the vortex sheet distribution, differentiation of the pressure distribution on the free sheets,

$$\frac{\partial C_p(s, \tau)}{\partial s} = 0 \quad \text{in} \quad s^- \leq s \leq 0 \text{ and } 1 \leq s \leq s^+ \quad (3.57)$$

gives the following Euler equation (Appendix C):

$$\left[V_s(s, \tau) - \frac{\partial z_c}{\partial \tau} s \right] \frac{\partial V_s}{\partial s} - (1 - z_c) \frac{\partial V_s}{\partial \tau}(s, \tau) = 0 \quad 1 \leq s \leq s^+ \quad (3.58)$$

This is a one-dimensional inviscid Burger's differential equation (Vorus, 1996) that the vortex distribution on the free jet-head sheet must satisfy.

Similarly, in the region of $s^- \leq s \leq 0$, the Burger's equation is of the same form,

$$\left[V_s(s, \tau) - \frac{\partial z_c}{\partial \tau} s \right] \frac{\partial V_s}{\partial s} - (1 - z_c) \frac{\partial V_s}{\partial \tau}(s, \tau) = 0 \quad s^- \leq s \leq 0 \quad (3.59)$$

These two equations simply state that there is no particle acceleration once the particles separate at the jet heads. The correspondent numerical analysis is covered in Chapter 5.

The pressure distribution on the contour can be obtained from Eq.(3.49). After the mathematical reduction (details refer to Appendix C), the pressure distribution has the following form:

$$\begin{aligned}
C_p(s, \tau) = & -V_n^2 - V_s^2(s, \tau) + 2 \frac{\partial z_c}{\partial \tau} \left[-\int_1^s V_s(s_0, \tau) ds_0 + s \cdot V_s(s, \tau) \right] \\
& + 2(1 - z_c) \int_1^s \frac{\partial V_s}{\partial \tau}(s_0, \tau) ds_0 + V_s^2(1, \tau) - 2 \frac{\partial z_c}{\partial \tau} V_s(1, \tau) \quad 0 \leq s \leq 1 \quad (3.60) \\
& + V_n^2(s^+, \tau)
\end{aligned}$$

- **In chine wetted case, $V_n(s^+, \tau) = 1$:**

$$\begin{aligned}
C_p(s, \tau) = & 1 - V_s^2(s, \tau) + V_s^2(1, \tau) \\
& - 2 \frac{\partial z_c}{\partial \tau} \left[\int_1^s V_s(s_0, \tau) ds_0 + V_s(1, \tau) - s \cdot V_s(s, \tau) \right] \quad 0 \leq s \leq 1 \quad (3.61) \\
& + 2(1 - z_c) \int_1^s \frac{\partial V_s}{\partial \tau}(s_0, \tau) ds_0
\end{aligned}$$

- **In chine un-wetted case, $V_n(s^+, \tau) = 0$:**

$$\begin{aligned}
C_p(s, \tau) = & V_s^2(1, \tau) - V_s^2(s, \tau) \\
& - 2 \frac{\partial z_c}{\partial \tau} \left[\int_1^s V_s(s_0, \tau) ds_0 + V_s(1, \tau) - s \cdot V_s(s, \tau) \right] \quad 0 \leq s \leq 1 \quad (3.62) \\
& + 2(1 - z_c) \int_1^s \frac{\partial V_s}{\partial \tau}(s_0, \tau) ds_0
\end{aligned}$$

3.2 Planing Dynamics in Seaway

As described in Chapter 2, in steady planing (the calm water case), the nondimensional variables x and τ are identical, thus the steady planing solution (or the x – problem solution) can be predicted by using the time dependent impact solution. However in the seakeeping case, the time variable τ and the distance variable x are now no longer dependent. In seakeeping, at each time step, given the specified position and velocity of the hull at this time step, we solve a complete x – problem. Then the motion equations are applied to update the position and motion of the boat at the beginning of the next time step. Continuing the time marching, step by step, with the updated wave and hull position at each step, the time histories of the coupled boat motions and forces are evaluated by Newton's Law. In the seakeeping computation, the first run is a steady planing (calm water) case, to determine the calm-water equilibrium transom draft and trim angle. This prediction is used as the initial condition in the seakeeping computation.

In this section, we first review the equations for a unique solution in the seakeeping case, then review the vessel motion model and the impact velocity model.

3.2.1 Pressure continuity condition in seakeeping

The velocity continuity condition and the displacement continuity condition in seakeeping at each time step are the same as those in the steady planing. However, the pressure continuity condition in seakeeping is different from the condition in steady planing.

Vorus gives the pressure continuity conditions based on the unsteady Bernoulli equation in the seakeeping case:

$$C_p(x, s; \tau) = V^2(x, \tau) - V_n^2(x, s, \tau) - V_s^2(x, s, \tau) - 2\left[\frac{\partial\phi(x, s; \tau)}{\partial\tau} + \frac{\partial\phi(x, s; \tau)}{\partial x}\right] - \left(\frac{\partial\phi(x, s; \tau)}{\partial x}\right)^2$$

$$0 \leq x \leq L(\tau), \quad 0 \leq s \leq s^+(x, \tau) \quad \text{or} \quad s^- \leq s \leq 0 \quad (3.63)$$

As discussed in Section 2.8, in the seakeeping case there are three independent coordinates (x, z, t) (refer to Chapter 2). The correspondent nondimensional variables are (ξ, ζ, τ) , where the nondimensional longitudinal variable ξ is defined as,

$$\xi(\tau) = \frac{x}{L(\tau)} \quad (3.64)$$

where $L(\tau)$ is the transient wetted length of the vessel in waves. The correspondent transverse variables in seakeeping case are:

$$\zeta = \frac{z}{z_k(x)}, \quad b^+ = b^+(\xi, \tau), \quad b^- = b^-(\xi, \tau), \quad z_c = z_c^+(\xi, \tau) \quad (3.65)$$

The real-time solution domain is shown in Fig. 3.4. By the catamaran variable transformations in Eq. (3.48), the solution domain in Fig. 3.4 can be transformed into a regular computation domain depicted in Fig. 3.5.

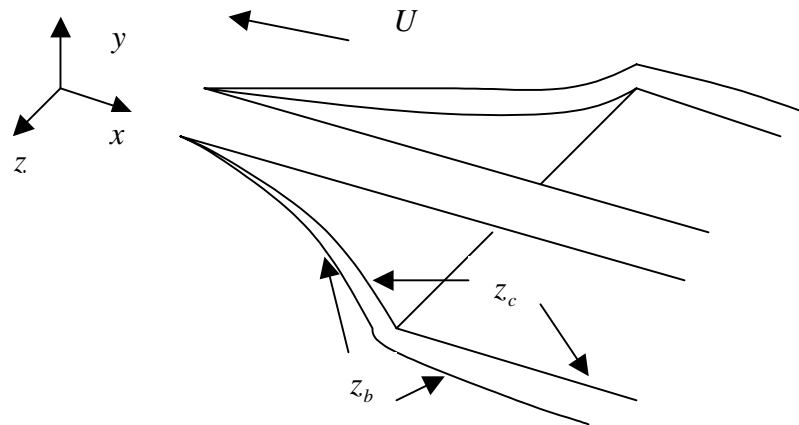


Fig. 3.4 Real solution domain in chine wetted and chine un-wetted phases

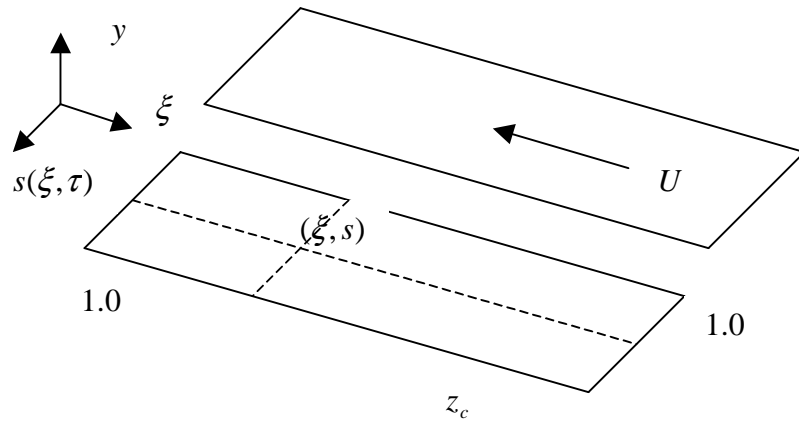


Fig. 3.5 Transformed solution domain

Following the same procedure as in Section 3.1.3, the pressure distribution can be obtained as following; the details are developed in Appendix D:

$$\begin{aligned}
C_p(x, s; \tau) &= V^2(x, \tau) - V_n^2(x, s, \tau) - V_s^2(x, s, \tau) \\
&+ 2z_k(z_c - 1) \left\{ \int_{s(\xi; \tau)}^{s^+(\xi; \tau)} \left[\frac{\partial V_s}{\partial \tau}(\xi, s_0, \tau) + (1 - x \frac{L_\tau}{L}) \frac{\partial V_s(\xi, s_0, \tau)}{\partial x} \right] ds_0 \right. \\
&+ V_s(\xi, s^+, \tau) \left[\frac{\partial s^+}{\partial \tau} + (1 - x \frac{L_\tau}{L}) \frac{\partial s^+}{\partial x} \right] \\
&+ 2z_k z_{c, \tau} \left[\int_{s(\xi; \tau)}^{s^+(\xi; \tau)} V_s(\xi, s_0, \tau) ds_0 + s \cdot V_s(\xi, s, \tau) \right] \\
&+ 2z_k(\xi) z_{c, x} \left[(1 - x \frac{L_\tau}{L}) \int_{s(\xi; \tau)}^{s^+(\xi; \tau)} V_s(\xi, s_0, \tau) ds_0 + (1 - x \frac{L_\tau}{L}) s \cdot V_s(\xi, s; \tau) \right] \\
&+ 2z_{k, x}(\xi) \left[(z_c - 1) \int_{s(\xi; \tau)}^{s^+(\xi; \tau)} V_s(\xi, s_0, \tau) ds_0 \right] \\
&\qquad\qquad\qquad 0 \leq x \leq L(\tau), \quad 0 \leq s \leq s^+(x, \tau) \quad (3.66)
\end{aligned}$$

Similarly, in the region of $s^- \leq s \leq 0$ or $b^- \leq \zeta \leq 1$,

$$\begin{aligned}
C_p(x, s; \tau) &= V^2(x, \tau) - V_n^2(x, s, \tau) - V_s^2(x, s, \tau) \\
&+ 2z_k(z_c - 1) \left\{ \int_{s(\xi; \tau)}^{s^-(\xi; \tau)} \left[\frac{\partial V_s}{\partial \tau}(\xi, s_0, \tau) + (1 - x \frac{L_\tau}{L}) \frac{\partial V_s(\xi, s_0, \tau)}{\partial x} \right] ds_0 \right. \\
&+ V_s(\xi, s^-, \tau) \left[\frac{\partial s^-}{\partial \tau} + (1 - x \frac{L_\tau}{L}) \frac{\partial s^-}{\partial x} \right] \\
&+ 2z_k z_{c, \tau} \left[\int_{s(\xi; \tau)}^{s^-(\xi; \tau)} V_s(\xi, s_0, \tau) ds_0 + s \cdot V_s(\xi, s, \tau) \right] \\
&+ 2z_k(\xi) z_{c, x} \left[(1 - x \frac{L_\tau}{L}) \int_{s(\xi; \tau)}^{s^-(\xi; \tau)} V_s(\xi, s_0, \tau) ds_0 + (1 - x \frac{L_\tau}{L}) s \cdot V_s(\xi, s; \tau) \right] \\
&+ 2z_{k, x}(\xi) \left[(z_c - 1) \int_{s(\xi; \tau)}^{s^-(\xi; \tau)} V_s(\xi, s_0, \tau) ds_0 \right] \\
&\qquad\qquad\qquad s^- \leq s \leq 0 \text{ or } b^- \leq \zeta \leq 1 \quad (3.67)
\end{aligned}$$

In the numerical model of the unsteady hydrodynamics, pressure via the Bernoulli equation requires computation of the $\frac{\partial \phi}{\partial \tau}(x, \tau)$ term in (3.63). The formulation involves computation in a moving coordinate system in the time domain. Therefore, the $\frac{\partial \phi}{\partial \tau}(x, \tau)$ term will be:

$$\frac{\partial \phi}{\partial \tau}[\xi(\tau), \tau] = \frac{\partial \phi}{\partial \tau} \Big|_{\xi=const} + \frac{\partial \phi}{\partial \xi} \frac{\partial \xi}{\partial \tau} = \frac{\partial \phi}{\partial \tau} \Big|_{\xi=const} - x \frac{L_\tau}{L} \frac{\partial \phi}{\partial x} \quad (3.68)$$

where $\xi(\tau)$ is defined in (3.64), $L = L(\tau)$.

The second term in (3.68) is readily incorporated in the dynamic boundary conditions and in the pressure calculation. However, the first term requires differentiation across the time step, which is implied to be numerical. And there are problems in differentiating in time on the fixed ξ – grid. This is most notably at the position of chine wetting, which changes with time such that the time gradients can become very large. Vorus simplified Eq.(3.68) in the 1st order model by assuming that the time derivatives were dominated by temporal wetted length and that the 1st term in Eq. (3.68) was higher order. That is, Vorus used the $x \frac{L_\tau}{L} \frac{\partial \phi}{\partial x}$ term in (3.68), ignoring the $\frac{\partial \phi}{\partial \tau} \Big|_{\xi=const}$ term. This made the numerical computation of the 1st order seakeeping model well behaved.

With the one-term reduction of (3.68), two pressure continuity conditions can be derived from (3.66) and (3.67). At the jet head z_b^+ , $C_p(x, s^+, \tau) = 0$ (see Fig. 2.6). Apply this condition and recall that in the chine un-wetted case $V_n(s^+, \tau) = 0$, and in the chine

wetted case $V_n(s^+, \tau) = V$ (refer to Fig. 2.6), and assuming constant $z_k(x) = z_k$ along the ship length thus $z_k(\xi) = 1$ in the $\zeta - \eta$ system. Therefore the pressure continuity condition (ignoring the time variation $\left. \frac{\partial}{\partial \tau} \right|_{\xi=\text{fixed}}$ term) in the 1st order seakeeping model at

$s = s^+$ is,

- At the jet head z_b^+ , in the chine un-wetted phase

$$\left(1 - x \frac{L_\tau}{L}\right) b_x^+ = \frac{V_s^2(\xi, s^+, \tau) - V^2(\xi, \tau)}{2V_s(\xi, s^+, \tau)} \quad \text{at } s = s^+ \quad (3.69)$$

- At the jet head z_b^+ , in the chine wetted phase

$$\left(1 - x \frac{L_\tau}{L}\right) b_x^+ = \frac{1}{2} V_s(\xi, s^+, \tau) \quad \text{at } s = s^+ \quad (3.70)$$

- At the jet head z_b^- , in the chine wetted phase

$$\left(1 - x \frac{L_\tau}{L}\right) b_x^- = \frac{1}{2} V_s(\xi, s^-, \tau) \quad \text{at } s = s^- \quad (3.71)$$

The Euler differential equation similar to (3.58) and (3.59) implemented in the first order seakeeping model, again dropping the time variation $\left. \frac{\partial}{\partial \tau} \right|_{\xi=\text{fixed}}$ term, is:

$$\{[V_s(\xi, s, \tau) - [\frac{\partial z_c}{\partial x} s(1 - x \frac{L_\tau}{L})]]\} \frac{\partial V_s}{\partial s} - (1 - z_c)(1 - x \frac{L_\tau}{L}) \frac{\partial V_s(\xi, s, \tau)}{\partial x} = 0$$

$$1 \leq s \leq s^+ \quad (3.72)$$

$$\{[V_s(\xi, s, \tau) - [\frac{\partial z_c}{\partial x} s(1 - x \frac{L_\tau}{L})]]\} \frac{\partial V_s}{\partial s} - (1 - z_c)(1 - x \frac{L_\tau}{L}) \frac{\partial V_s(\xi, s, \tau)}{\partial x} = 0$$

$$s^- \leq s \leq 0 \quad (3.73)$$

On the hull contour, the pressure distribution can be derived directly from Bernoulli's equation (refer to (3.63)); the mathematical reduction process is found in Appendix D, with the time variation $\left. \frac{\partial}{\partial \tau} \right|_{\xi=fixed}$ term discarded, the contour pressure distribution is,

- **In the chine wetted case:**

$$C_p(\xi, s; \tau) = V^2(\xi, \tau) - V_s^2(\xi, s, \tau) + V_s^2(\xi, 1, \tau)$$

$$+ 2(z_c - 1) \left\{ \int_{s(\xi, \tau)}^1 (1 - x \frac{L_\tau}{L}) \frac{\partial V_s(\xi, s_0, \tau)}{\partial x} ds_0 \right\}$$

$$+ 2[z_{c,x}(1 - x \frac{L_\tau}{L})] \left[\int_{s(\xi, \tau)}^1 V_s(\xi, s_0, \tau) ds_0 + s \cdot V_s(\xi, s, \tau) - V_s(\xi, 1, \tau) \right]$$

$$0 \leq x \leq L(\tau), 0 \leq s \leq 1 \quad (3.74)$$

- **In the chine un-wetted case:**

$$\begin{aligned}
C_p(\xi, s; \tau) &= V_s^2(\xi, 1, \tau) - V_s^2(\xi, s, \tau) \\
&+ 2(z_c - 1) \left\{ \int_{s(\xi, \tau)}^1 \left(1 - x \frac{L_\tau}{L}\right) \frac{\partial V_s(\xi, s_0, \tau)}{\partial x} ds_0 \right\} \\
&+ 2 \left[z_{c,x} \left(1 - x \frac{L_\tau}{L}\right) \right] \left[\int_{s(\xi, \tau)}^1 V_s(\xi, s_0, \tau) ds_0 + s \cdot V_s(\xi, s, \tau) - V_s(\xi, 1, \tau) \right]
\end{aligned}$$

$$0 \leq x \leq L(\tau), \quad 0 \leq s \leq 1 \quad (3.75)$$

Therefore the pressure continuity condition (3.69) - (3.71) together with the previous velocity continuity condition (3.14) - (3.15) and the displacement continuity condition (3.44) provide enough equations to solve for the unknowns in sea-keeping problem. However, since the solution proceeds in the time domain, the vessel motion equilibrium model is needed, as discussed at the beginning of this section.

3.2.2 Water wave model

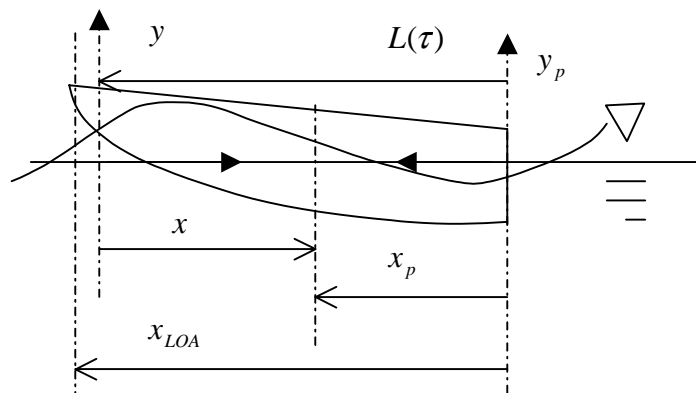


Fig. 3.6 Definition of wave system

The incoming water wave is defined in the transom coordinate system $O_p - x_p y_p z_p$, but the input parameters of the wave system are defined in the bow coordinate system $O - xyz$. Fig. 3.6 depicts the definition of the wave system. In Fig. 3.6, $L(\tau)$ is the transient wetted length, measured from the transom section forward to the instantaneous intersection of the keel and the surface of the wave;

x_p : the distance of x section, measured from the transom section forward;

x : measured from the bow coordinate system xoy which is located on the calm water surface, from the entry point to the stern, with origin right under the intersection point;

x_{LOA} : L_{PP} , the total boat length.

Assuming the wave length λ is much longer than the boat length,

$$\lambda \gg L_{PP} \quad (3.76)$$

Thus, the disturbance (diffraction) of the incoming waves by the hull can be ignored. The non-dimensional regular wave expression is:

$$\zeta(x; \tau) = \zeta_a \sin[\Omega_e \tau + k(L(\tau) - x) + \theta_0] \quad (3.77)$$

Where $\zeta(x, \tau)$ is the wave elevation non-dimensionalized on the maximum keel offset z_k , the non-dimensional wave number $k = 2\pi/\lambda$, λ is the wave length, and $\zeta_a = \zeta_0(1 - e^{-\alpha})$ is a transient wave front where $\alpha: 0 \rightarrow \infty$, ζ_0 is non-dimensional wave

amplitude, θ_0 is the initial phase. The non-dimensional encounter frequency Ω_e is defined as,

$$\Omega_e = \Omega_0 - k \cos \alpha_w \quad (3.78)$$

where Ω_0 is the non-dimensional wave natural frequency $\Omega_0 = \frac{\omega_0 \cdot z_k}{U}$, α_w is the incoming wave angle. In the present code, wave angle is set to be either head sea or following waves ($\alpha_w =$ zero or 180 deg).

The random waves are defined as,

$$\zeta(x; \tau) = \sum_{i=1}^N \zeta_i \sin[\Omega_{e,i} \tau + k_i (L(\tau) - x) + \theta_i] \quad (3.79)$$

where the non-dimensional wave amplitude is:

$$\zeta_i = \frac{1}{2} h_i (1 - e^{-\alpha}) / z_k \quad (3.80)$$

with the wave height h_i defined according to the specified wave spectrum. For example, for the JONSWAP spectrum (Chakrabarti, 1994), characteristic of littoral-zone seas:

$$h_i(\omega) = 2.0 \cdot \sqrt{2.0 \cdot S_{\zeta\zeta}(\omega) \cdot \Delta\omega} \quad (3.81)$$

$$S_{\zeta\zeta}(\omega) = \alpha g^2 \omega^{-5} \exp[-1.25(\omega/\omega_0)^{-4}] \cdot \gamma^{\exp[-\frac{(\omega-\omega_0)^2}{2\tau^2\omega_0^2}]} \quad (3.82)$$

The parameter in (3.81) and (3.82) may refer to Chakrabarti (1994).

3.2.3 Vessel motion model

The vessel motion model is defined with the help of the boat-fixed coordinate system $O_T - x_T y_T z_T$ (refer to section 2.2) (see Figure 3.7).

Let η_3 and η_5 be the heave and pitch angle, respectively, defined at the transom section relative to the translation coordinate system $O_p - x_p y_p z_p$.

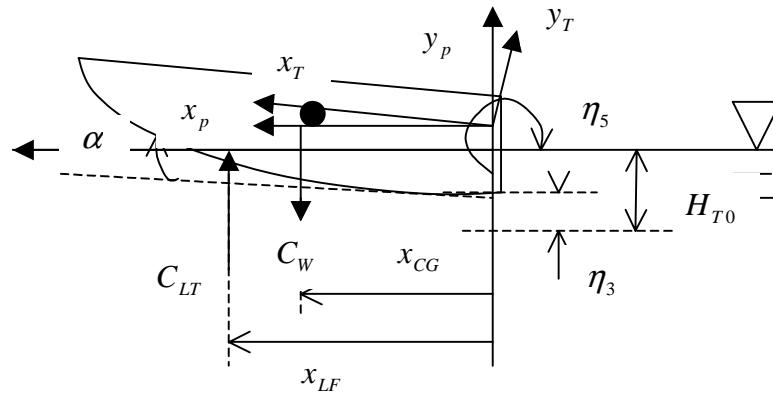


Fig. 3.7 Vessel motion definition

Assume that the boat's non-dimensional weight, denoted by C_W , is located at x_{CG} measured from the transom section. The total lift acting on the boat is C_{LT} , located at x_{LF} , measured from the transom section (Fig. 3.7). Define the Froude number,

$$F_n = \frac{U}{\sqrt{g \cdot z_K}} \quad (3.83)$$

where z_K is the transom keel offset, U is the forward speed of the boat.

The hydrodynamic lift is represented by C_L integrated from the sectional lift coefficient $C_{f,i}$ (refer to Vorus, 1996),

$$C_{f,i} = \frac{f_i}{\frac{1}{2} \rho U^2 z_K} = 2(z_c - 1) \int_0^1 \Delta C_p(s) ds \quad (3.84)$$

where the nondimensional pressure coefficient $\Delta C_p(s)$ is defined as:

$$\Delta C_p(s) = \frac{\Delta p}{\frac{1}{2} \rho U^2} \quad (3.84a)$$

where Δp is the dynamic pressure.

The static buoyancy (relative to the calm water planing waterline) is represented by C_{LB} ,

$$C_{LB} = \frac{L_b}{\frac{1}{2} \rho U^2 z_K^2} = \frac{2\bar{V}}{F_n^2} \quad (3.85)$$

where \bar{V} is the static nondimensional displacement volume of the boat.

Then the total lift is defined as,

$$C_{LT} = C_L + C_{LB} + C_{L,air} \quad (3.86)$$

where $C_{L,air}$ is the aerodynamic lift. The lift moment relative to the transom origin is:

$$C_{MT} = C_{LT} \times x_{LF} \quad (3.87)$$

The total lift center is defined as:

$$x_{LF} = \frac{C_L \times x_L + C_{LB} \times x_B + C_{L,air} \times x_{air}}{C_L + C_{LB} + C_{L,air}} \quad (3.88)$$

where x_L is the hydrodynamic lift center, x_B is the buoyancy center, and x_{air} is the aerodynamic lift center.

Based on the Newton's second law, taking the mass coupling effect into account, the boat heave and pitch accelerations are the solution to:

$$\begin{bmatrix} m & mx_{CG} \\ mx_{CG} & J \end{bmatrix} \cdot \begin{bmatrix} \ddot{\eta}_3 \\ \ddot{\eta}_5 \end{bmatrix} = \begin{bmatrix} C_{LT} - C_W \\ C_{MT} - C_W \times x_{CG} \end{bmatrix} \quad (3.89)$$

where x_{CG} is the longitudinal center of gravity defined in Fig. 3.7, m is the non-dimensional mass of the boat, and the inertia moment J is defined as:

$$J = m\bar{r}^2 \quad (3.90)$$

where \bar{r} is the non-dimensional radius of gyration from the transom. The non-dimensional boat weight C_w in (3.89) is defined as,

$$C_w = \frac{W}{1/2 \rho U^2 z_K^2} \quad (3.91)$$

Denote the determinant of the coefficients in (3.89) as:

$$\Delta = mJ - m^2 x_{CG}^2 = m^2 [\bar{r}^2 - x_{CG}^2] \quad (3.92)$$

The solution gives the boat's accelerations at the time τ as:

$$\ddot{\eta}_3(\tau) = \frac{J(C_{LT} - C_w) - mx_{CG}(C_{MT} - C_w \times x_{CG})}{\Delta} \quad (3.93)$$

$$\ddot{\eta}_5(\tau) = \frac{m(C_{MT} - C_w \times x_{CG}) - mx_{CG}(C_{LT} - C_w)}{\Delta} \quad (3.94)$$

Thus, the time trace of the heave and pitch of the catamaran can be readily obtained by the numerical integration of above equations numerically in time, step by step.

3.2.4 Wetted length and the transient draft

The vertical transient draft of the catamaran can be described by using Fig. 3.8.

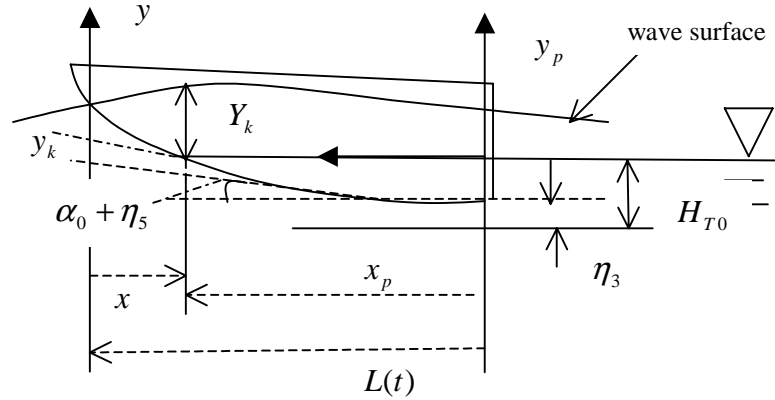


Fig. 3.8 Definition of transient draft

The vertical transient draft Y_k , measured from keel to the transient wave surface, is defined as:

$$Y_k(x, t) = H_{T0} + \zeta_w(L-x, t) - \eta_3(t) - (\alpha_0 + \eta_5(t)) \cdot (L-x) - y_k(x) \quad (3.95)$$

where H_{T0} is the initial draft at the transom, $\zeta_w(L-x, t)$ is wave elevation defined at transom coordinate system, $\alpha_0(x)$ is the initial local keel camber trim angle, and $y_k(x)$ is the keel upset.

To find the transient wetted length $L(t)$ in the transom coordinate system $x_p O_p y_p$, we define the draft $Y_k(0)$ as zero at the entry point $x = 0$:

$$0 = H_{T0} + \zeta_w(L, t) - \eta_3(t) - (\alpha_0 + \eta_5(t)) \cdot L - y_k(0) \quad (3.96)$$

Solve Eq.(3.96) for the wetted length $L(t)$ (refer to Fig. 3.8):

$$H_{T0} - \eta_3(t) = (\alpha_0 + \eta_5(t)) \cdot L(t) + y_k(0) - \zeta_w(L, t) \quad (3.97)$$

This equation serves as the condition to iterate to find the wetted length $L(t)$ at each time step. Substitute Eq.(3.97) back into Eq.(3.95), the new expression of the transient draft at any time step is given by:

$$Y_k(x, t) = (\alpha_0 + \eta_5) \cdot x + y_k(0) - y_k(x) + \zeta_w(L - x, t) - \zeta_w(L, t) \quad (3.98)$$

3.2.5 Impact velocity in waves

The sectional impact velocity in waves will be needed for solving the x -problem in each time step. The vertical impact velocity in the seakeeping problem can be determined from the transient draft equation in Eq.(3.95).

Defined the transient wetted surface as,

$$F(x, t) = y - Y_k(x, t) = 0 \quad (3.99)$$

From the material derivative,

$$\frac{\partial F}{\partial t} + \vec{V} \cdot \nabla F = 0 \quad \text{on } F = 0 \quad (3.100)$$

where $\vec{V} = U\vec{i} + v_k\vec{j}$, $\nabla F = \frac{\partial F}{\partial x}\vec{i} + \frac{\partial F}{\partial y}\vec{j}$, $v_k(x,t)$ is the impact velocity. Since

$$\frac{\partial F}{\partial x} = -\frac{\partial Y_k}{\partial x}, \quad \frac{\partial F}{\partial y} = 1, \quad \frac{\partial F}{\partial t} = -\frac{\partial Y_k}{\partial t}, \quad U = 1 \text{ (the non-dimension form), from Eq.(3.100),}$$

the impact velocity is:

$$v_k(x,t) = \frac{\partial Y_k}{\partial t} + \frac{\partial Y_k}{\partial x} \quad (3.101)$$

Recall the normalized variable $\xi = \frac{x}{L(t)}$ (refer to (3.64)), then the derivatives of $Y_k(x,t)$

implemented in CatSea are,

$$\begin{aligned} \frac{\partial Y_k}{\partial t} = & \dot{\zeta}'_w(L-x,t) + \zeta'_w(L-x,t) \cdot (1-\xi)\dot{l}(t) - \dot{\eta}_3(t) \\ & - (\alpha_0 + \eta_5(t)) \cdot (1-\xi)\dot{l}(t) - \dot{\eta}_5 \cdot (1-\xi)l(t) - y'_k(x)\xi \cdot \dot{l}(t) \end{aligned} \quad (3.102)$$

$$\frac{\partial Y_k}{\partial x} = -\zeta'_w(l-x,t) + (\alpha_0 + \eta_5(t)) - y'_k(x) \quad (3.103)$$

Thus the impact velocity is:

$$\begin{aligned} v_k(x,t) = & \alpha_0 - y'_{k0} \\ & - (y'_k(x) - y'_{k0}) + \eta_5(t) - \dot{\eta}_3(t) - \dot{\eta}_5 \cdot (1-\xi)l(t) \\ & - (\alpha_0 + \eta_5(t)) \cdot (1-\xi)\dot{l}(t) - y'_k(x)\xi \cdot \dot{l}(t) \\ & + \dot{\zeta}'_w(l-x,t) - \zeta'_w(l-x,t) + \zeta'_w(l-x,t) \cdot (1-\xi)\dot{l}(t) \end{aligned} \quad (3.104)$$

Since in CatSea, the input parameters of the wave system are defined in the translating bow system, considering the sign of x - derivatives of $\zeta_w(l-x, t)$ taken in the bow coordinate system, the impact velocity has following form:

$$\begin{aligned}
 v_k(x, t) = & \alpha_0 - y'_{k0} \\
 & - (y'_k(x) - y'_{k0}) + \eta_5(t) - \dot{\eta}_3(t) - \dot{\eta}_5 \cdot (1 - \xi)l(t) \\
 & - (\alpha_0 + \eta_5(t)) \cdot (1 - \xi)\dot{l}(t) - y'_k(x)\xi \cdot \dot{l}(t) \\
 & + \dot{\zeta}_w(l-x, t) + \zeta'_w(l-x, t)[1 - (1 - \xi)\dot{l}(t)]
 \end{aligned} \tag{3.105}$$

In this chapter, we have systematically reviewed the first order theory developed by Vorus. In the next chapter, the second order extension to the first order theory is developed.

CHAPTER 4

SECOND ORDER NONLINEAR CATAMARAN HYDRODYNAMIC THEORY

The first order catamaran theory outlined in the preceding chapter is useful in catamaran design and analysis as it stands. However, due to the complexity of the problem itself, some significant approximations and simplifications have been made in the first order theory. This chapter presents a complete nonlinear catamaran hydrodynamic theory which relieves the major approximations and simplifications in the first order theory. This extended theory is referred to as the “second order nonlinear theory”.

Keeping the same order as in Chapter 3, we first introduce the second order theory on steady planing in calm water, followed by the second order seakeeping theory of catamarans.

4.1 2nd Order Calm Water Steady Planing Theory

In the second order model, we have same number of unknowns (five in the chine un-wetted flow phase and four in the chine wetted phase) as in the 1st order model. In this section, we follow the solution procedure in Chapter 3, where it differs, to develop the same number of equations for the unique solution.

4.1.1 Second order velocity continuity equations

4.1.1.1 Kinematic boundary condition and its integral equation

Use the same downward moving coordinate system $\zeta - o_{keel} - \eta$ as depicted in the Fig. 3.1 to construct the kinematic boundary condition.

The normal and tangential velocities on the hull contour, in terms of the perturbation velocities v and w in Fig. 3.1, are derived in Vorus (1996), and can be expressed as,

$$V_n = (1 + v) \cos \beta - w \sin \beta \quad (4.1)$$

$$V_s = (1 + v) \sin \beta + w \cos \beta \quad (4.2)$$

where $V_s(\zeta)$ and $V_n(\zeta)$ are the total tangential and normal flow velocities on the bottom contour, β is a small deadrise angle.

According to the physical model in Fig. 3.1, the tangential velocity $V_s(\zeta)$ associated with the vortex strength distribution $\gamma(\zeta, \tau)$, can be written:

$$V_s(\zeta, \tau) = -\frac{1}{2} \gamma(\zeta, \tau) + V(\tau) \sin \beta(\zeta, \tau) \quad (4.3)$$

where V is the section impact velocity, $V(\tau) \sin \beta(\zeta, \tau)$ is the stream component along the contour.

In the downward moving coordinate system $\zeta - o_{keel} - \eta$ on the hull boundary, the kinematic boundary condition requires (refer to Fig. 2.6 and (3.1)):

$$V_n(\zeta, \tau) = 0 \quad \text{for } 1 \leq \zeta \leq z_c \quad (4.4)$$

By applying the above condition with (4.1) - (4.4), the following kinematic condition on the hull results. This condition is the same as developed by (Vorus, 1996) for the monohull case, refer to (3.2) for comparison with the first order case. The detailed derivation is in Appendix A:

$$v(\zeta, \tau) + \frac{1}{2} \gamma(\zeta, \tau) \sin \beta(\zeta, \tau) = -V(\tau) \cos^2 \beta(\zeta, \tau) \quad \text{for } 1 \leq \zeta \leq z_c \quad (4.5)$$

Assuming the deadrise angle $\beta(\zeta, \tau)$ of the section contour to be small for order-of-magnitude argument, that is $\beta(\zeta, \tau) = o(\varepsilon)$, the relative orders of magnitude of the variables in (4.5) are assigned in Table 4.1 on the basis of the impact physics (refer to Vorus 1996).

Table 4.1 Order-of-magnitude of variables

Variables	$0 \leq \zeta < b^-$	$b^- \leq \zeta < 1$	$1 \leq \zeta \leq z_c$		$z_c < \zeta \leq b^+$		$\zeta > b^+$
	(CW)	(CW)	(CUW)	(CW)	(CUW)	(CW)	(CUW& CW)
$v(\zeta, \tau)$	$O(\beta)$	$O(\beta)$	$O(1)$	$O(1)$	$O(1)$	$O(\beta)$	$O(\beta)$
$V_s(\zeta, \tau)$	$O(\beta)$	$O(1)$	$O(1/\beta)$	$O(1/\beta)$	$O(1/\beta)$	$O(1)$	$O(\beta)$
$\gamma(\zeta, \tau)$	$O(\beta)$	$O(1)$	$O(1/\beta)$	$O(1/\beta)$	$O(1/\beta)$	$O(1)$	$O(\beta)$
$V_n(\zeta, \tau)$	$V+ O(\beta)$	$V+ O(\beta)$	0	0	$O(\beta)$	$V+$ $O(\beta)$	$V+ O(\beta)$
$V(\tau)$	$O(1)$						

Based on the orders-of-magnitude in Table 4.1, it is easy to see that all terms in Eq. (4.5) are $O(1)$.

Comparing Eq. (4.5) to the Eq. (3.2) in the first order model, an additional leading term $\frac{1}{2}\gamma(\zeta, \tau)\sin\beta(\zeta, \tau)$ has arisen. For simplification of the analysis in the case of the 1st order model, Vorus used a simplified relation in Eq. (3.2) for the KBC by considering this leading term in Eq.(4.5) as a product of perturbations and higher order: $o(\beta)$. In the present second order theory, the deadrise angle $\beta(\zeta, \tau)$ is still the small parameter, of order ε . But the order of the vortex strength $\gamma(\zeta, \tau)$ is assigned as order of $O(\frac{1}{\beta})$, consistent with the increasing "squeeze" flow transversely from under the hull as β

decreases. Therefore, the product term $\frac{1}{2}\gamma(\zeta, \tau) \sin \beta(\zeta, \tau)$ in (4.5) is $O(1)$ and therefore retained in the boundary condition. This is a basis for the name “second order nonlinear theory.” Although the theory in this regard is actually only a consistent first order theory. It is also still a linear boundary condition in the unknowns since β on the hull contour in (4.5) is known. (The solution is, however, nonlinear in the dynamic boundary condition, just as it was in Chapter 3.)

Comparing Eq. (4.5) to the Eq. (3.2), it is clear that the deadrise angle $\beta(\zeta, \tau)$ appears explicitly in the KBC of the 2nd order model, but not in the 1st order.

Express the perturbation velocity $v(\zeta, \tau)$ in (4.5) in terms of vortex strength distribution $\gamma(\zeta, \tau)$ (Fig. 2.6) by the Biot-Savart law, just as with the 1st order theory in Chapter 3, Eq. (3.3):

$$v(\zeta, \tau) = \frac{1}{2\pi} \int_{\zeta_0=-b^+}^{b^+} \frac{\gamma(\zeta_0, \tau)}{(\zeta_0 - \zeta)} d\zeta_0 \quad (4.6)$$

Therefore a singular integral equation representing the kinematic boundary condition (4.5) is:

$$\frac{1}{2}\gamma(\zeta, \tau) \sin \beta(\zeta, \tau) + \frac{1}{2\pi} \int_{b^-}^{b^+} \gamma(\zeta_0, \tau) \left[\frac{1}{\zeta_0 - \zeta} + \frac{1}{\zeta_0 + \zeta} \right] d\zeta_0 = -V(\tau) \cos^2 \beta(\zeta, \tau) \quad \text{on } 1 \leq \zeta \leq z_c \quad (4.7)$$

In (4.7), comparing with (3.3) of the first order model, the added leading term appears.

Eq.(4.7) again can be expressed in terms of the free -sheet vortex strengths $\gamma_s^+(\zeta, \tau)$ and $\gamma_s^-(\zeta, \tau)$ as follows (refer to Eq. (3.4)); refer to Appendix A for the details.

$$\frac{1}{2} \gamma_c(\zeta, \tau) \sin \beta(\zeta, \tau) + \frac{1}{2\pi} \int_{-z_c}^{z_c} \frac{\gamma_c(\zeta_0, \tau)}{\zeta_0 - \zeta} d\zeta_0 = f(\zeta, \tau) \quad 1 \leq \zeta \leq z_c \quad (4.8)$$

where:

$$\gamma_c(\zeta_0, \tau) = 0 \quad \text{on } -1 \leq \zeta_0 \leq 1 \quad (4.9)$$

With non-dimensionalization on the keel offset, z_k , the region $-1 \leq \zeta_0 \leq 1$ in (4.8) is the free space between the demi-hulls (refer to Fig. 2.5). The right hand side of (4.8) is (compare to Eq. (3.5)):

$$f(\zeta, \tau) \equiv -\cos^2 \beta \cdot V(\tau) - \frac{1}{\pi} \int_{b^-}^1 \gamma_s^-(\zeta_0, \tau) \frac{\zeta_0}{\zeta_0^2 - \zeta^2} d\zeta_0 - \frac{1}{\pi} \int_{z_c}^{b^+} \gamma_s^+(\zeta_0, \tau) \frac{\zeta_0}{\zeta_0^2 - \zeta^2} d\zeta_0 \quad (4.10)$$

Note the new terms in (4.8) and (4.10) due to the reordering discussed at (4.5).

Eq.(4.8) is the Carleman-type singular integration equation (Muskhelishvili 1958, Vorus 1996), instead of the Hilbert-type of Chapter 3. Solution of (4.8) is the first theoretical extension of the 1st order theory. Following the same procedure as with Eq.

(3.4), an inversion procedure exists for developing a semi-analytic solution to (4.8). Muskhelishvili(1958) and Tricomi(1957) give the general solution of the Carleman singular integral equation. Following the derivation of Vorus (1996), which was adapted from Muskhelishvili(1958), a solution for (4.8) is developed in Appendix A as (refer to (3.6)),

$$\gamma_c(\zeta, \tau) = 2 \sin \tilde{\beta} \cos \tilde{\beta} f(\zeta, \tau) - \frac{2 \cos \tilde{\beta} \cdot \chi(\zeta, \tau)}{\pi} \int_{-z_c}^{z_c} \frac{\cos \tilde{\beta} f(s)}{\chi(s, \tau)} \frac{ds}{s - \zeta}$$

on $1 \leq \zeta \leq z_c$ (4.11)

where $\chi(\zeta, \tau)$ is the kernel function defined below, and,

$$\tilde{\beta} = \tilde{\beta}(\zeta, \tau) = \tan^{-1}[\sin \beta(\zeta, \tau)] \quad (4.12)$$

The function $\gamma_c(\zeta, \tau)$ satisfies the Hölder condition¹ (Muskhelishvili 1958) on $-z_c \leq \zeta \leq -1$ and $1 \leq \zeta \leq z_c$, as required for the solution procedure outlined by Muskhelishvili.

Comparing with the 1st order solution in Eq. (3.6), an additional term has appeared in the 2nd order solution, (4.11).

¹ Hölder condition: A function $\phi(s)$ is said to satisfy a Hölder condition on L , if for any two points, $s_1 \in L$, $s_2 \in L$,

$$|\phi(s_2) - \phi(s_1)| \leq A \cdot (s_2 - s_1)^\mu$$

4.1.1.2 Kernel function $\chi(\zeta, \tau)$

The kernel function for the Carleman integral equation (4.11) is developed in Appendix F. It has been expressed in following (4.13) and (4.16). It is different from the kernel function in the monohull case (Vorus, 1996). It has two singular points, one located at the keel and the other at the z_c point for the catamaran, versus one for the monohull, at z_c only. It is also different from the kernel function of the 1st order model in Eq.(3.7), with an additional singular product function term $k(\zeta, \tau)$ (see (4.13) to reflect the effect of the variation of the deadrise angle $\beta(\zeta, \tau)$.

(1) the case of a general $\beta(\zeta, \tau)$ in (4.11):

$$\chi(\zeta, \tau) = \frac{\kappa(\zeta, \tau)}{\sqrt{(\zeta^2 - 1)(z_c^2 - \zeta^2)}} \quad (4.13)$$

where the function $k(\zeta, \tau)$ is defined as a product function involves the J-element piecewise linear discretization of the contour in $1 \leq \zeta \leq z_c$ (the contour discretization detail refer to Fig. 5 in Vorus(1996)).

$$\kappa(\zeta, \tau) = \prod_{j=1}^J \left| \frac{t_{j+1} + \zeta}{t_j + \zeta} \right|^{\frac{\tilde{\beta}_j(\tau)}{\pi}} \cdot \left| \frac{\zeta - t_{j+1}}{\zeta - t_j} \right|^{\frac{\tilde{\beta}_j(\tau)}{\pi}} \quad (4.14)$$

where A and μ are positive constants. A is called the Hölder constant and μ is the Hölder index.

In (4.14) the t_j and $\tilde{\beta}_j(\tau)$ are the end offsets and angles of the j th element.

In general, the deadrise angle $\beta = \beta(\zeta, \tau)$ varies in both ζ and time τ as the jet-head advances. For simplifying the computation, the contour will be specialized to be constant deadrise, without transverse camber, so that $\beta = \beta(\tau)$. However, this theory applies to the general case as well.

(2) the case of $\beta(\zeta, \tau)$ constant in ζ :

For deadrise contours $\beta(\zeta, \tau) = \beta(\tau)$ is constant in ζ direction, defining $\kappa(\zeta, \tau) = \kappa_0(\zeta, \tau)$ in this case, then:

$$\kappa_0(\zeta, \tau) = \left| \frac{z_c + \zeta}{1 + \zeta} \right|^{\frac{\tilde{\beta}(\tau)}{\pi}} \cdot \left| \frac{\zeta - z_c}{\zeta - 1} \right|^{\frac{\tilde{\beta}(\tau)}{\pi}} = \left| \frac{z_c + \zeta}{\zeta + 1} \right|^{\frac{\tilde{\beta}(\tau)}{\pi}} \cdot \left| \frac{z_c - \zeta}{\zeta - 1} \right|^{\frac{\tilde{\beta}(\tau)}{\pi}} = \left(\frac{z_c^2 - \zeta^2}{\zeta^2 - 1} \right)^{\frac{\tilde{\beta}(\tau)}{\pi}} \quad (4.15)$$

Such that (4.13) becomes:

$$\chi(\zeta, \tau) = \frac{\kappa_0(\zeta, \tau)}{\sqrt{(\zeta^2 - 1)(z_c^2 - \zeta^2)}} = \frac{1}{\sqrt{(\zeta^2 - 1)(z_c^2 - \zeta^2)}} \cdot \left(\frac{z_c^2 - \zeta^2}{\zeta^2 - 1} \right)^{\frac{\tilde{\beta}(\tau)}{\pi}} \quad (4.16)$$

4.1.1.3 Bound vortex $\gamma_c(\zeta, \tau)$

Expanding the equation (4.11) and considering the symmetry of $\chi(\zeta, \tau)$ and $f(\zeta, \tau)$, the bound vortex strength $\gamma_c(\zeta, \tau)$ is the following:

$$\begin{aligned}
\gamma_c(\zeta, \tau) &= 2 \sin \tilde{\beta} \cos \tilde{\beta} f(\zeta, \tau) \\
&\quad - \frac{2}{\pi} \cos \tilde{\beta} \cdot \chi(\zeta, \tau) \int_{\zeta_1=1}^{\zeta_c} \frac{f(\zeta_1, \tau) \cos \tilde{\beta}}{\chi(\zeta_1, \tau)} \left[\frac{1}{(\zeta_1 - \zeta)} - \frac{1}{(\zeta_1 + \zeta)} \right] d\zeta_1 \\
&= 2 \sin \tilde{\beta} \cos \tilde{\beta} f(\zeta, \tau) \\
&\quad - \frac{4\zeta}{\pi} \cos \tilde{\beta} \cdot \chi(\zeta, \tau) \int_{\zeta_1=1}^{\zeta_c} \frac{f(\zeta_1, \tau) \cos \tilde{\beta}}{\chi(\zeta_1, \tau)} \frac{1}{(\zeta_1^2 - \zeta^2)} d\zeta_1
\end{aligned} \tag{4.17}$$

Substitution of $f(\zeta, t)$ from (4.10) into (4.17) yields:

$$\begin{aligned}
\gamma_c(\zeta, \tau) &= -2 \sin \tilde{\beta} \cos \tilde{\beta} \cos^2 \beta \cdot V(\tau) \\
&\quad - 2 \sin \tilde{\beta} \cos \tilde{\beta} \frac{1}{\pi} \int_{\zeta_0=b^-}^1 \gamma_S^-(\zeta_0, \tau) \frac{\zeta_0}{\zeta_0^2 - \zeta^2} d\zeta_0 \\
&\quad - 2 \sin \tilde{\beta} \cos \tilde{\beta} \frac{1}{\pi} \int_{\zeta_0=z_c}^{b^+} \gamma_S^+(\zeta_0, \tau) \frac{\zeta_0}{\zeta_0^2 - \zeta^2} d\zeta_0 \\
&\quad + \frac{4\zeta}{\pi} \cos \tilde{\beta} \cdot \chi(\zeta, \tau) [\cos^2 \beta \cdot V(\tau) \cdot \cos \tilde{\beta} \cdot \int_{\zeta_1=1}^{\zeta_c} \frac{d\zeta_1}{\chi(\zeta_1, \tau)(\zeta_1^2 - \zeta^2)}] \\
&\quad + \frac{4\zeta}{\pi} \cos \tilde{\beta} \cdot \chi(\zeta, \tau) \left[\frac{1}{\pi} \int_{\zeta_0=b^-}^1 \gamma_S^-(\zeta_0, \tau) \cdot \zeta_0 \cdot \int_{\zeta_1=1}^{\zeta_c} \frac{\cos \tilde{\beta} \cdot d\zeta_1}{\chi(\zeta_1, \tau)(\zeta_1^2 - \zeta^2)(\zeta_0^2 - \zeta_1^2)} \cdot d\zeta_0 \right] \\
&\quad + \frac{4\zeta}{\pi} \cos \tilde{\beta} \cdot \chi(\zeta, \tau) \left[\frac{1}{\pi} \int_{\zeta_0=z_c}^{b^+} \gamma_S^+(\zeta_0, \tau) \cdot \zeta_0 \cdot \int_{\zeta_1=1}^{\zeta_c} \frac{\cos \tilde{\beta} \cdot d\zeta_1}{\chi(\zeta_1, \tau)(\zeta_1^2 - \zeta^2)(\zeta_0^2 - \zeta_1^2)} \cdot d\zeta_0 \right]
\end{aligned} \tag{4.18}$$

Introduce the same partial fraction reduction identity as in Chapter 3 (refer to

(3.9)):

$$\frac{1}{(\zeta_1^2 - \zeta^2)(\zeta_0^2 - \zeta^2)} = \frac{1}{\zeta_0^2 - \zeta^2} \left\{ \frac{1}{\zeta_0^2 - \zeta_1^2} + \frac{1}{\zeta_1^2 - \zeta^2} \right\} \quad (4.19)$$

Substitute the (4.19) into the solution (4.18). Manipulation of that result yields the same convenient form for the bound vortex $\gamma_c(\zeta, \tau)$ as with the 1st order solution (3.10); refer to Appendix E for details. The solution is conveniently written, via (4.19), as the superposition of groups singular and non-singular terms:

$$\gamma_c(\zeta, \tau) = \gamma_{normal}(\zeta, \tau) + \gamma_{singular}(\zeta, \tau) \quad (4.20)$$

Here the normal component is the non-singular part of the solution,

$$\begin{aligned} \gamma_{c,normal}(\zeta, \tau) = & -2 \sin \tilde{\beta} \cos \tilde{\beta} \cos^2 \beta \cdot V(\tau) \\ & - 2 \sin \tilde{\beta} \cos \tilde{\beta} \frac{1}{\pi} \int_{\zeta_0=b^-}^1 \gamma_s^-(\zeta_0, \tau) \frac{\zeta_0}{\zeta_0^2 - \zeta^2} d\zeta_0 \\ & - 2 \sin \tilde{\beta} \cos \tilde{\beta} \frac{1}{\pi} \int_{\zeta_0=z_c}^{b^+} \gamma_s^+(\zeta_0, \tau) \frac{\zeta_0}{\zeta_0^2 - \zeta^2} d\zeta_0 \end{aligned} \quad (4.21)$$

The singular component, from the singular part of the kernel function (refer to (3.10)), is:

$$\begin{aligned}
\gamma_{c,\text{sin gular}}(\zeta, \tau) = & \frac{4\zeta}{\pi} \chi(\zeta, \tau) \cos \tilde{\beta} \{V(\tau) \cos^2 \beta \cos \tilde{\beta} \cdot [-\Lambda(\zeta)] \\
& + \frac{1}{\pi} \cos \tilde{\beta} \int_{\zeta_0=b^-}^1 \gamma_s^-(\zeta_0, \tau) \frac{\zeta_0}{\zeta_0^2 - \zeta^2} d\zeta_0 [\Lambda^-(\zeta_0) - \Lambda(\zeta)] \\
& + \frac{1}{\pi} \cos \tilde{\beta} \cdot \int_{\zeta_0=z_c}^{b^+} \gamma_s^+(\zeta_0, \tau) \frac{\zeta_0}{\zeta_0^2 - \zeta^2} d\zeta_0 [\Lambda^+(\zeta_0) - \Lambda(\zeta)] \}
\end{aligned} \tag{4.22}$$

where ζ is the independent variable ; ζ_0, ζ_1 are the dummy integration variables, with (refer to (3.11) ~ (3.13)) :

$$\Lambda(\zeta) = \int_{\zeta_1=1}^{z_c} \frac{d\zeta_1}{\chi(\zeta_1, \tau)(\zeta^2 - \zeta_1^2)} \quad 1 \leq \zeta \leq z_c \tag{4.23}$$

$$\Lambda^-(\zeta_0) = \int_{\zeta_1=1}^{z_c} \frac{d\zeta_1}{\chi(\zeta_1, \tau)(\zeta_0^2 - \zeta_1^2)} \quad b^- \leq \zeta_0 \leq 1 \tag{4.24}$$

$$\Lambda^+(\zeta_0) = \int_{\zeta_1=1}^{z_c} \frac{d\zeta_1}{\chi(\zeta_1, \tau)(\zeta_0^2 - \zeta_1^2)} \quad z_c \leq \zeta_0 \leq b^+ \tag{4.25}$$

Comparing (4.20), (4.21) and (4.22) with the hull contour bound vortex expression of the 1st order model in (3.10), it is seen that the simplification of the 1st order model has led to the existence of only the similar term of (4.22) in γ_c , without the term of (4.21). Eq. (4.20) represents the second significant difference from 1st order theory.

The numerical analysis for the bound vortex distribution $\gamma_c(\zeta, \tau)$ in Eq.(4.21) and Eq.(4.22) can be found in Chapter 5 and Appendix E .

The velocity continuity condition, which is from the singular component of the vortex distribution, (4.22), is now derived.

4.1.1.4 Velocity continuity condition

Equation (4.22) has two singular points in its solution domain, at $\zeta = 1$ and $\zeta = z_c$. This is when $\zeta \rightarrow 1$ or $\zeta \rightarrow z_c$, where $\chi(\zeta, \tau) \rightarrow \infty$. However, in real (high Reynold's number) flow, the velocities at these points must be finite and continuous.

Following the 1st order development, when $\zeta \rightarrow 1^+$, the requirement that γ_c be bounded results in the following velocity continuity equation (or Kutta condition). This is same as Eq. (3.14) of 1st order model. (For detailed derivations refer to Appendix A):

$$0 = \left\{ -\cos^2 \beta \cdot V(\tau) \cdot \Lambda(1) + \frac{1}{\pi} \int_{b^-}^1 \gamma_s^-(\zeta_0, \tau) \frac{\zeta_0}{\zeta_0^2 - 1} [\Lambda^-(\zeta_0) - \Lambda(1)] d\zeta_0 \right. \\ \left. + \frac{1}{\pi} \int_{z_c}^{b^+} \gamma_s^+(\zeta_0, \tau) \frac{\zeta_0}{\zeta_0^2 - 1} [\Lambda^+(\zeta_0) - \Lambda(1)] d\zeta_0 \right\} \\ \zeta \rightarrow 1^+ \quad (4.26)$$

When $\zeta \rightarrow z_c$, the requirement for boundedness similarly results in the second velocity continuity equation; this is the parallel of (3.15):

$$0 = \left\{ \cos^2 \beta \cdot V(\tau) [-\Lambda(z_c)] + \frac{1}{\pi} \int_{b^-}^1 \gamma_s^-(\zeta_0, \tau) \frac{\zeta_0}{\zeta_0^2 - z_c^2} [\Lambda^-(\zeta_0) - \Lambda(z_c)] d\zeta_0 \right. \\ \left. + \frac{1}{\pi} \int_{z_c}^{b^+} \gamma_s^+(\zeta_0, \tau) \frac{\zeta_0}{\zeta_0^2 - z_c^2} [\Lambda^+(\zeta_0) - \Lambda(z_c)] d\zeta_0 \right\} \\ \zeta \rightarrow (z_c)^- \quad (4.27)$$

The two velocity continuity equations have the same form as the velocity continuity equations in Eq. (3.14) and Eq. (3.15) of 1st order model. But the integrations of Eq. (4.26) and Eq. (4.27) are in terms of the hyper-geometric functions and Beta functions, which are different than the elliptic integral functions of the 1st order model. For example, the singular integral in Eq. (4.23) has the following form (refer to Eq. (3.16) - Eq. (3.19)):

$$\Lambda(\zeta) = I_1 + I_2(\zeta) + I_3(\zeta) \quad 1 \leq \zeta \leq z_c \quad (4.28)$$

where,

$$\begin{aligned} I_1 &= \int_{\zeta_1=1}^{z_c} \frac{\zeta_1^2}{\kappa_0(\zeta_1) \cdot \sqrt{(\zeta_1^2 - 1)(z_c^2 - \zeta_1^2)}} d\zeta_1 \\ &= \frac{1}{2} z_c \cdot B\left(\frac{1}{2} - \frac{\tilde{\beta}}{\pi}, \frac{1}{2} + \frac{\tilde{\beta}}{\pi}\right) \cdot F\left(-\frac{1}{2}, \frac{1}{2} - \frac{\tilde{\beta}}{\pi}; 1; \frac{z_c^2 - 1}{z_c^2}\right) \end{aligned} \quad (4.29)$$

$$\begin{aligned} I_2(\zeta) &= (\zeta^2 - z_c^2 - 1) \cdot \int_{\zeta_1=1}^{z_c} \frac{1}{\kappa_0(\zeta_1) \cdot \sqrt{(\zeta_1^2 - 1)(z_c^2 - \zeta_1^2)}} d\zeta_1 \\ &= \frac{1}{2} (\zeta^2 - z_c^2 - 1) \frac{1}{z_c} \cdot B\left(\frac{1}{2} - \frac{\tilde{\beta}}{\pi}, \frac{1}{2} + \frac{\tilde{\beta}}{\pi}\right) \cdot F\left(\frac{1}{2}, \frac{1}{2} - \frac{\tilde{\beta}}{\pi}; 1; \frac{z_c^2 - 1}{z_c^2}\right) \end{aligned} \quad (4.30)$$

$$\begin{aligned} I_3(\zeta) &= (\zeta^2 - 1)(z_c^2 - \zeta^2) \cdot \frac{1}{2} \int_{t=1}^{z_c^2} t^{\frac{1}{2}} (\zeta^2 - t)^{-1} (t - 1)^{-\frac{1}{2} + \frac{\tilde{\beta}}{\pi}} (z_c^2 - t)^{\frac{1}{2} - \frac{\tilde{\beta}}{\pi}} dt \\ &= -\frac{1}{2} (\zeta^2 - 1)(z_c^2 - \zeta^2) \times \sum_{j=1}^N \frac{1}{\sqrt{t_j}} \cdot \Delta I_{3,j}(\zeta) \end{aligned} \quad (4.31)$$

In (4.31) since the integral $I_3(\zeta)$ in the 2nd order model can not be expressed in a semi-analytical form as I_1 and $I_2(\zeta)$ did, this author thus has modeled the $I_3(\zeta)$ integral as a piecewise constant function discretization integral. The whole integral domain $z_c^2 - 1$ has been discretized into N elements, \bar{t}_j is mean value of the discretized integral element (t_j, t_{j+1}) . The detail derivations can be found in Chapter 7 and in Appendix H. When, in (4.31),

- **Case 1:** $\zeta^2 > t_{j+1}$

$$\Delta I_{3,j}(\zeta) = I_{3,j+1}^- - I_{3,j}^- \quad (4.32)$$

where,

$$I_{3,j}^-(\zeta^2) = -\frac{1}{\zeta^2 - 1} \frac{(t_j - 1)^{\frac{1+\tilde{\beta}}{2}}}{(z_c^2 - t_j)^{\frac{1+\tilde{\beta}}{2}}} \times \frac{1}{\lambda^-} \cdot F\left(\frac{1}{2} + \frac{\tilde{\beta}}{\pi}, 1, \frac{3}{2} + \frac{\tilde{\beta}}{\pi}; \frac{t_j - 1}{\zeta^2 - 1} \cdot \frac{z_c^2 - \zeta^2}{z_c^2 - t_j}\right) \quad (4.33)$$

- **Case 2:** $\zeta^2 < t_j$

$$\Delta I_{3,j}(\zeta) = I_{3,j}^+ - I_{3,j+1}^+ \quad (4.34)$$

where,

$$I_{3,j}^+(\zeta^2) = \frac{1}{z_c^2 - \zeta^2} \cdot \frac{(z_c^2 - t_j)^{\frac{1}{2} + \frac{\tilde{\beta}}{\pi}}}{(t_j - 1)^{\frac{1}{2} + \frac{\tilde{\beta}}{\pi}}} \times \frac{1}{\lambda^+} \cdot F(\lambda^+, 1, \lambda^+ + 1; \frac{z_c^2 - t_j}{z_c^2 - \zeta^2}, \frac{\zeta^2 - 1}{t_j - 1}) \quad (4.35)$$

- **Case 3:** $t_j < \zeta^2 < t_{j+1}$

$$\Delta I_{3,j}(\zeta) = I_{3,0} - I_{3,j}^- - I_{3,j+1}^+ \quad (4.36)$$

where,

$$I_{3,0}(\zeta^2) = \frac{\pi(\zeta^2 - 1)^{\frac{1}{2} + \frac{\tilde{\beta}}{\pi}}}{(z_c^2 - \zeta^2)^{\frac{1}{2} + \frac{\tilde{\beta}}{\pi}}} \times \tan \tilde{\beta} \quad (4.37)$$

In (4.29) to (4.35), $F(\alpha, \beta; \gamma; z)$ is Gauss' hypergeometric function, and $B(x, y)$ is the Beta function (refer to Gradshteyn and Ryzhik, 1965).

The semi-analytical forms of the velocity continuity equations in Eq. (4.26) and Eq. (4.27), which are comparable to the 1st order equations (3.28) and (3.32), are expressed in Chapter 5.

As covered in Chapter 3, the catamaran calm water steady planing case has five unknowns (in CUW case): $V_j^+(\tau)$, $V_j^-(\tau)$, $z_b^+(\tau)$, $z_b^-(\tau)$, and $z_c(\tau)$. The Kutta (velocity continuity) conditions of the kinematic boundary condition provide two out of the five equations (Eq.(4.26) and Eq. (4.27)) needed for the uniqueness. In the following sections, the remaining three required conditions are developed.

4.1.2 Displacement continuity condition

4.1.2.1 Water surface elevation

Again, like in the 1st order case, revert back into the time domain of the equivalent impact problem, $[0, t]$. In the chine-unwetted phase, the dimensional body bottom contour $y_c(z, t)$ can be expressed as (refer to Fig. 3.2):

$$y_c(z, t) = h_c(z, t) - Vt \quad z_k \leq z \leq z_b^+ \quad (4.38)$$

where again $h_c(z, t)$ is the water elevation above the keel:

$$h_c(z, t) = \begin{cases} (z - z_k) \tan \beta & z_k \leq z \leq z_b^+(t) \\ 0 & z_b^-(t) \leq z < z_k \end{cases} \quad (4.39)$$

Define the net vertical fluid velocity of the contour, from (4.5) as:

$$\frac{\partial y_c(z, t)}{\partial t} = -V(t) = v(z, t) + \frac{1}{2} \gamma(z, t) \sin \beta(z) \quad \text{on } z_k \leq z \leq z_b^+ \quad (4.40)$$

It is clear that Eq. (4.40) is just another form of the expression of the KBC with $V(t) = -\partial y_c / \partial t$. Comparing with the definition in (3.35) of the 1st order model, an addition term has been added in (4.40).

Following the same process as in Chapter 3, integration of the above equation in time domain and nondimensionalization of the results yield the following equation (refer to Appendix B):

$$v^*(\zeta, \tau) + \frac{1}{2} \gamma^*(\zeta, \tau) \sin \beta(\zeta) = f_1(\zeta, \tau) \quad 1 \leq \zeta \leq b^+ \quad (4.41)$$

where, again, the "asterisk" superscript denotes the time integrated variables:

$$v^*(z, t) = \int_{\tau=0}^t v(z, \tau) d\tau \quad \text{and} \quad \gamma^*(z, t) = \int_{\tau=0}^t \gamma(z, \tau) d\tau \quad (4.42)$$

and, in (4.41):

$$f_1(\zeta, \tau) = \begin{cases} -\tilde{Y}_{wl} + \tilde{h}_c(\zeta, \tau) & 1 \leq \zeta \leq b^+(\tau) \\ -\tilde{Y}_{wl} & b^- \leq \zeta < 1 \end{cases} \quad (4.43)$$

where \tilde{Y}_{wl} is the non-dimensional water-line transient draft, $\tilde{h}_c(\zeta, \tau)$ may be a general contour or may be a deadrise contour, of the form:

$$\tilde{h}_c(\zeta, \tau) = \begin{cases} (\zeta - 1) \tan \beta & 1 < \zeta \leq b^+(\tau) \\ 0 & b^-(\tau) \leq \zeta \leq 1 \end{cases} \quad (4.44)$$

For simplifying the analysis, a simple deadrise contour form is again adapted here.

The vertical velocity time integral, $v^*(\zeta, \tau)$ in Eq. (4.41), is again expressible in terms of the time-integrated displacement vortex strength, $\gamma_c^*(\zeta, \tau)$, by the Biot-Savart law. Thus the integral equation resulting from the displacement condition is essentially the same form as the KBC velocity condition in (4.7), (also refer to the DC condition in (3.40):

$$\begin{aligned} & \frac{1}{2} \gamma_c^*(\zeta, \tau) \sin \beta(\zeta) + \frac{1}{2\pi} \int_{-b^+}^{-b^-} \gamma_c^*(\zeta_0, \tau) \frac{1}{\zeta_0 - \zeta} d\zeta_0 + \frac{1}{2\pi} \int_{b^-}^{b^+} \gamma_c^*(\zeta_0, \tau) \frac{1}{\zeta_0 - \zeta} d\zeta_0 \\ & = f_1(\zeta, \tau) \end{aligned} \quad 1 \leq \zeta \leq b^+ \quad (4.45)$$

where

$$\gamma_c^*(\zeta_0, \tau) = 0 \quad \text{on } -1 \leq \zeta_0 \leq 1 \quad (4.46)$$

by the definition of (4.44).

Comparing Eq. (4.45) with Eq. (3.40), it is shown that the integral equation of the displacement condition in the 2nd order model has an additional leading term. Again, Eq.(4.45) is of the Carleman-type singular integral equation. Using the same solution

approach as in Eq.(4.11), the solution of Eq.(4.45) is found to be the following (refer to (3.41)); for details refer to Appendix B:

$$\begin{aligned} \gamma_c^*(\zeta, \tau) = & 2 \sin \tilde{\beta} \cos \tilde{\beta} f(\zeta, \tau) \\ & - \frac{2 \cos \tilde{\beta} \cdot \chi^*(\zeta, \tau)}{\pi} \left[\int_{-b^+}^{-b^-} \frac{\cos \tilde{\beta} f(\zeta_0)}{\chi^*(\zeta_0, \tau)} \frac{d\zeta_0}{\zeta_0 - \zeta} + \int_{b^-}^{b^+} \frac{\cos \tilde{\beta} f(\zeta_0)}{\chi^*(\zeta_0, \tau)} \frac{d\zeta_0}{\zeta_0 - \zeta} \right] \end{aligned}$$

on $1 \leq \zeta \leq b^+$ (4.47)

where $\chi^*(\zeta, \tau)$ is the kernel function.

Note again in (4.47) the additional leading term in the 2nd order solution.

4.1.2.2 Kernel function $\chi^*(\zeta, \tau)$

The kernel function $\chi^*(\zeta, \tau)$ for the integral in Eq.(4.47) is developed in Appendix G. The difference of $\chi^*(\zeta, \tau)$ from the kernel function $\chi(\zeta, \tau)$ in (4.13) and (4.16) is that its solution domain is now on the arcs of $-b^+ \leq \zeta \leq -b^-$ and $b^- \leq \zeta \leq b^+$, the ends of which are where the free vortex sheets separate. This is the same as in the first order solution at (3.42).

(1) The same discussion as for the kernel function $\chi(\zeta, \tau)$ before, in general $\beta = \beta(\zeta, \tau)$ case, the kernel function in (4.47) is of the form (refer to (3.42)):

$$\chi^*(\zeta, \tau) = \frac{\kappa(\zeta, \tau)}{\sqrt{(\zeta^2 - (b^-)^2)((b^+)^2 - \zeta^2)}} \quad (4.48)$$

where the function $k(\zeta, \tau)$ has the same definition as in (4.14),

$$\kappa(\zeta, \tau) = \prod_{j=1}^J \left| \frac{t_{j+1} + \zeta}{t_j + \zeta} \right|^{\frac{\beta_j(\tau)}{\pi}} \cdot \left| \frac{\zeta - t_{j+1}}{\zeta - t_j} \right|^{\frac{\beta_j(\tau)}{\pi}} \quad (4.49)$$

where the t_j and $\tilde{\beta}_j(\tau)$ in above formula are the end offsets and angles the same as defined in (4.14).

(2) In the case of $\beta = \beta(\tau)$ independent of ζ , the kernel function is

$$\chi^*(\zeta, \tau) = \frac{\kappa_0(\zeta, \tau)}{\sqrt{(\zeta^2 - (b^-)^2)((b^+)^2 - \zeta^2)}} = \frac{1}{\sqrt{(\zeta^2 - (b^-)^2)((b^+)^2 - \zeta^2)}} \cdot \left(\frac{(b^+)^2 - \zeta^2}{\zeta^2 - (b^-)^2} \right)^{\frac{\tilde{\beta}(\tau)}{\pi}} \quad (4.50)$$

where,

$$\kappa_0(\zeta, \tau) = \left| \frac{b^+ + \zeta}{b^- + \zeta} \right|^{\frac{\tilde{\beta}(\tau)}{\pi}} \cdot \left| \frac{b^+ - \zeta}{b^- - \zeta} \right|^{\frac{\tilde{\beta}(\tau)}{\pi}} = \left| \frac{b^+ + \zeta}{\zeta + b^-} \right|^{\frac{\tilde{\beta}(\tau)}{\pi}} \cdot \left| \frac{b^+ - \zeta}{\zeta - b^-} \right|^{\frac{\tilde{\beta}(\tau)}{\pi}} = \left(\frac{(b^+)^2 - \zeta^2}{\zeta^2 - (b^-)^2} \right)^{\frac{\tilde{\beta}(\tau)}{\pi}} \quad (4.51)$$

The kernel function $\chi^*(\zeta, \tau)$ in (4.48) or (4.50) in the 2nd order theory is different than the kernel function $\chi^*(\zeta, \tau)$ of the 1st order model in (3.42), with additional product term $\kappa(\zeta, \tau)$ to represent the variation of the deadrise angle, $\beta(\zeta, \tau)$. See (4.13) to (4.16) for the similar form in $\chi(\zeta, \tau)$ of the 2nd order velocity boundary condition.

4.1.2.3 Displacement continuity equation

Substituting $f_1(\zeta, \tau)$ in (4.43) into the solution of (4.47), and applying the symmetries of $f_1(\zeta, \tau)$ and $\chi^*(\zeta, \tau)$, the solution (4.47) is:

$$\begin{aligned} \gamma_c^*(\zeta, \tau) = & 2 \sin \tilde{\beta} \cos \tilde{\beta} [-\tilde{Y}_{wl} + (\zeta - 1) \tan \beta] \\ & - \frac{4\zeta}{\pi} \chi^*(\zeta, \tau) \cdot \cos^2 \tilde{\beta} \{ (-\tau - \tan \beta) \cdot \int_{\zeta_0=b^-}^{b^+} \frac{1}{\chi^*(\zeta_0, \tau)(\zeta_0^2 - \zeta^2)} d\zeta_0 \\ & + \tan \beta \cdot \int_{\zeta_0=b^-}^{b^+} \frac{\zeta_0}{\chi^*(\zeta_0, \tau)(\zeta_0^2 - \zeta^2)} d\zeta_0 \} \end{aligned} \quad (4.52)$$

When $\zeta \rightarrow b^+$, there is a singularity in the kernel $\chi^*(\zeta, \tau)$. To separate the singularity, a partial fraction reduction identity from (Vorus 1996) is again used:

$$\frac{1}{\zeta_0^2 - \zeta^2} = -\frac{1}{b^{+2} - \zeta_0^2} \left(1 - \frac{b^{+2} - \zeta^2}{\zeta_0^2 - \zeta^2} \right) \quad (4.53)$$

Substituting Eq.(4.53) into Eq.(4.52):

$$\begin{aligned}
\gamma_c^*(\zeta, \tau) = & 2 \sin \tilde{\beta} \cos \tilde{\beta} [-\tilde{Y}_{wl} + (\zeta - 1) \tan \beta] \\
& - \frac{4\zeta}{\pi} \chi^*(\zeta, \tau) \cos^2 \tilde{\beta} \cdot \{ -(\tau + \tan \beta) \cdot [- \int_{\zeta_0=b^-}^{b^+} \frac{1}{\chi^*(\zeta_0, \tau)(b^{+2} - \zeta_0^2)} d\zeta_0] \\
& + (b^{+2} - \zeta^2) \int_{\zeta_0=b^-}^{b^+} \frac{1}{\chi^*(\zeta_0, \tau)(b^{+2} - \zeta_0^2)(\zeta_0^2 - \zeta^2)} d\zeta_0] \\
& + \tan \beta \cdot [- \int_{\zeta_0=b^-}^{b^+} \frac{\zeta_0}{\chi^*(\zeta_0, \tau)(b^{+2} - \zeta_0^2)} d\zeta_0 \\
& + (b^{+2} - \zeta^2) \int_{\zeta_0=b^-}^{b^+} \frac{\zeta_0}{\chi^*(\zeta_0, \tau)(b^{+2} - \zeta_0^2)(\zeta_0^2 - \zeta^2)} d\zeta_0] \}
\end{aligned} \tag{4.54}$$

As described in Chapter 3, the real flow physics requires a continuous body-free-surface contour at b^+ in CUW flow. Thus when $\zeta \rightarrow b^+$, the vortex strength $\gamma_c^*(\zeta, \tau)$ in Eq.(4.54) must be bounded (refer to (2.25)). This requirement results in the following displacement continuity condition:

$$0 = (\tilde{Y}_{wl} + \tan \beta) \cdot \int_{\zeta=b^-}^{b^+} \frac{d\zeta}{\chi^*(\zeta, \tau)(b^{+2} - \zeta^2)} - \tan \beta \int_{\zeta=b^-}^{b^+} \frac{\zeta}{\chi^*(\zeta, \tau)(b^{+2} - \zeta^2)} d\zeta \tag{4.55}$$

Define the followings relative to (4.55):

$$I_1 = \int_{\zeta=b^-}^{b^+} \frac{d\zeta}{\chi^*(\zeta, \tau)(b^{+2} - \zeta^2)} \tag{4.56}$$

$$I_2 = \int_{\zeta=b^-}^{b^+} \frac{\zeta}{\chi^*(\zeta, \tau)(b^{+2} - \zeta^2)} d\zeta \tag{4.57}$$

The displacement continuity condition is then expressed in terms of I_1 and I_2 as (refer to (3.44)),

$$0 = (\tilde{Y}_{wl} + \tan \beta) \cdot I_1 - \tan \beta \cdot I_2 \quad (4.58)$$

(4.58) provides one additional condition for solving the five unknowns in steady planing. Two additional conditions are now required.

Comparing the displacement continuity condition of (4.58) in the 2nd order model with the same condition in the 1st order model, (3.44), both have the same form, but the integrals I_1 and I_2 are functionally different. In the 1st order model, the I_1 and I_2 of (4.58) are in the Elliptic integral form; in the 2nd order model, the results are in Gauss' Hyper-geometric functions and Beta functions (refer to the numerical model in Chapter 5 for details).

4.1.3 Pressure continuity condition for steady planing

The pressure continuity condition of the 2nd order theory for steady planing is the same equation as in the 1st order theory. Therefore, we only list the main equations for solving the unknowns. The derivation process may refer to chapter 3.

At the outer jet-head z_b^+ , the pressure continuity condition is (refer to Eq. (3.54), (3.55) and Eq. (3.56)),

- In the chine un-wetted flow phase:

$$b_{\tau}^{+}(\tau) = \frac{V_s^2(s^+, \tau) - 1}{2V_s(s^+, \tau)} \quad \text{at } s = s^+ \quad (4.59)$$

- In the chine-wetted phase:

$$b_{\tau}^{+}(\tau) = \frac{1}{2}V_s(s^+, \tau) \quad \text{at } s = s^+ \quad (4.60)$$

where s^+ is the nondimensional outer jet-head defined in the catamaran coordinate transform in (3.48).

At the inner jet head z_b^- , since the flow at the keel z_k is always chine-wetted (Fig. 2.6), the pressure continuity condition thus is:

$$b_{\tau}^{-}(\tau) = \frac{1}{2}V_s(s^-, \tau) \quad \text{at } s = s^- \quad (4.61)$$

where s^- is the nondimensional inner jet-head defined in the catamaran coordinate transform in (3.48).

These are the same pressure continuity conditions as with the 1st order model.

On the free jet-head sheets of $s^- \leq s \leq 0$ and $1 \leq s \leq s^+$ (refer to Fig. 3.3), a constant pressure is required (refer to Fig. 2.6). To find the vortex sheet distributions required for applying (4.59) to (4.61), as in the 1st order model (refer to (3.57)), differentiate the pressure distribution (refer to Appendix C), on the free sheets. This gives the following Euler equation (same as (3.58)):

$$[V_s(s, \tau) - \frac{\partial z_c}{\partial \tau} s] \frac{\partial V_s}{\partial s} - (1 - z_c) \frac{\partial V_s}{\partial \tau}(s, \tau) = 0 \quad 1 \leq s \leq s^+ \quad (4.62)$$

In the region of $s^- \leq s \leq 0$, the Euler's (Burger's) equation is (refer to (3.59)),

$$[V_s(s, \tau) - \frac{\partial z_c}{\partial \tau} s] \frac{\partial V_s}{\partial s} - (1 - z_c) \frac{\partial V_s}{\partial \tau}(s, \tau) = 0 \quad s^- \leq s \leq 0 \quad (4.63)$$

Again, the two Euler equations in Eq. (4.62) and Eq. (4.63) required for the free vortex sheet distributions are the same form as those in 1st order model, refer to Eq. (3.58) and Eq. (3.59), and simply imply a constant particle velocity post-separation. The required numerical analysis is covered in Chapter 5.

In the 2nd order model, the pressure distribution formulation is the same as that in the 1st order model, refer to (3.61) and (3.62). In the 2nd order model, the pressure distribution computation on the contour is (details refer to Appendix C):

- **chine-wetted case**

$$\begin{aligned} C_p(s, \tau) = & 1 - V_s^2(s, \tau) + V_s^2(1, \tau) \\ & - 2 \frac{\partial z_c}{\partial \tau} \left[\int_1^s V_s(s_0, \tau) ds_0 + V_s(1, \tau) - s \cdot V_s(s, \tau) \right] \\ & + 2(1 - z_c) \int_1^s \frac{\partial V_s}{\partial \tau}(s_0, \tau) ds_0 \end{aligned} \quad 0 \leq s \leq 1 \quad (4.64)$$

- **chine un-wetted case**

$$\begin{aligned}
C_p(s, \tau) &= V_s^2(1, \tau) - V_s^2(s, \tau) \\
&\quad - 2 \frac{\partial z_c}{\partial \tau} \left[\int_1^s V_s(s_0, \tau) ds_0 + V_s(1, \tau) - s \cdot V_s(s, \tau) \right] \quad 0 \leq s \leq 1 \quad (4.65) \\
&\quad + 2(1 - z_c) \int_1^s \frac{\partial V_s}{\partial \tau}(s_0, \tau) ds_0
\end{aligned}$$

At this point five equations are available for solving for the five unknowns in the CUW case: $V_j^+(\tau)$, $V_j^-(\tau)$, $z_b^+(\tau)$, $z_b^-(\tau)$ and $z_c(\tau)$. They are:

- Two velocity continuity conditions when $z \rightarrow z_k$ and $z \rightarrow z_c^+$ in Eq. (4.26) and Eq. (4.27);
- Two pressure continuity conditions at $z = z_b^+(\tau)$, $z = z_b^-(\tau)$ in Eq. (4.59) and Eq. (4.61);
- One free-surface displacement continuity condition when $z \rightarrow z_b^+(\tau)$ in Eq. (4.58);

In the chine wetted CW case, since the jet separation point z_c^+ is known and fixed at the hard chine Z_{CH} , the displacement continuity condition is not needed. In this case, we have four equations and four unknowns:

- Two velocity continuity conditions at $z \rightarrow z_k$ and $z \rightarrow z_c^+$ in Eq. (4.26) and Eq. (4.27);
- Two pressure continuity conditions in Eq. (4.60) and Eq. (4.61)

to solve for the four unknowns: $V_j^+(\tau)$, $V_j^-(\tau)$, $z_b^+(\tau)$ and $z_b^-(\tau)$.

Therefore, the steady planing problem has a unique solution.

Next we will develop the 2nd order theory for catamaran seakeeping.

4.2 Second Order Nonlinear Sea-keeping Theory

In this chapter, we also develop the 2nd order seakeeping theory for the planing catamaran. As discussed in Chapter 3, the time variable t and the longitudinal variable x are independent in the seakeeping analysis. In the 2nd order seakeeping theory, at each time step, a complete x – flow problem is solved, just as it is in the 1st order case of the last chapter.

In the seakeeping model, at each time step, we have the same number of unknowns in the x – flow problem as in the steady planing problem. Thus we need the same number equations as in steady planing for a unique solution at each time step, as described in the section 3.2. The velocity continuity condition and the displacement continuity condition are the same as those in the steady planing problem. However, the pressure continuity condition in seakeeping is different from the condition in the steady planing since the pressure involves independent x and time variables.

4.2.1 Pressure distribution model

Following the derivation procedure in the 1st order model, we develop the pressure continuity conditions based on the unsteady Bernoulli equation in the seakeeping case.

4.2.1.1 Pressure continuity condition

In the seaway dynamics problem defined in Chapter 2, assuming the boat is advancing in waves with a constant forward speed U , Bernoulli's equation gives:

$$p + \frac{1}{2}\rho(V_n^2 + V_s^2) + \frac{1}{2}\rho V_x^2 + \rho\Phi_t = p_\infty + \frac{1}{2}\rho U^2 + \frac{1}{2}\rho V^2 + \rho\Phi_{\infty,t} \quad (4.66)$$

Define the streamwise flow perturbation velocity $u = \frac{\partial\phi}{\partial x}$. Thus the x -component of the relative velocity in the boat-fixed bow system $O - xyz$ will be:

$$V_x = U + u = U + \phi_x \quad (4.67)$$

In the catamaran coordinate system of Fig. 3.3 (refer to Fig. 3.4 for the longitudinal variable x definition), the pressure coefficient is of the following form (see (4.66)):

$$C_p(x, s; \tau) = V^2(x, \tau) - V_n^2(x, s, \tau) - V_s^2(x, s, \tau) - 2\left[\frac{\partial\phi(x, s; \tau)}{\partial\tau} + \frac{\partial\phi(x, s; \tau)}{\partial x}\right] - \left(\frac{\partial\phi(x, s; \tau)}{\partial x}\right)^2$$

$$0 \leq x \leq L(\tau), \quad 0 \leq s \leq s^+(x, \tau) \quad \text{or} \quad s^-(x, \tau) \leq s \leq 0 \quad (4.68)$$

where $L = L(\tau)$ is the wetted water line length at each time step.

Define the non-dimensional longitudinal variable $\xi(\tau)$ same as in the 1st order theory (refer to (3.64) and Fig. 3.5):

$$\xi(\tau) = \frac{x}{L(\tau)} \quad (4.69)$$

and the transverse non-dimensional variables ζ , $b^+(\xi, \tau)$, $b^-(\xi, \tau)$, $z_c^+(\xi, \tau)$ same as 1st order model in Eq. (3.65), furthermore in seakeeping the s coordinate will be (refer to (3.48)),

$$s(\xi, \tau) = \frac{\zeta - 1}{z_c(\xi, \tau) - 1}, \quad s^-(\xi, \tau) = \frac{b^- - 1}{z_c(\xi, \tau) - 1}, \quad s^+(\xi, \tau) = \frac{b^+ - 1}{z_c(\xi, \tau) - 1} \quad (4.70)$$

The pressure continuity conditions can be obtained in the same way as in the first order model. For the pressure continuity condition at the jet-head z_b^+ , starting from Eq.(3.66).

At the jet head z_b^+ , $C_p(x, s^+, \tau) = 0$ (see Fig. 2.6). (3.66) gives,

$$\begin{aligned} & V^2(\xi, \tau) - V_n^2(\xi, s^+, \tau) - V_s^2(\xi, s^+, \tau) \\ & + 2(z_c - 1)V_s(\xi, s^+, \tau) \left[\frac{\partial s^+}{\partial \tau} + \left(1 - x \frac{L_\tau}{L}\right) \frac{\partial s^+}{\partial x} \right] \\ & + 2[z_{c,\tau} + z_{c,x} \left(1 - x \frac{L_\tau}{L}\right)] s^+ \cdot V_s(\xi, s^+, \tau) \\ & = 0 \end{aligned} \quad (4.71)$$

Since $s^+(\xi, \tau) = \frac{b^+ - 1}{z_c(\xi, \tau) - 1}$ in (4.70), (4.71) becomes:

$$\begin{aligned} & V^2(\xi, \tau) - V_n^2(\xi, s^+, \tau) - V_s^2(\xi, s^+, \tau) \\ & - 2V_s(\xi, s^+, \tau) \left\{ \frac{\partial}{\partial \tau} + \left(1 - x \frac{L_\tau}{L}\right) \frac{\partial}{\partial x} \right\} [1 - b^+(\tau)] = 0 \end{aligned} \quad (4.72)$$

The jet head velocity can therefore be found from (4.72),

$$b_\tau^+ + \left(1 - x \frac{L_\tau}{L}\right) b_x^+ = \frac{V_s^2(\xi, s^+, \tau) + V_n^2(\xi, s^+, \tau) - V^2(\xi, \tau)}{2 \cdot V_s(\xi, s^+, \tau)} \quad \text{at } s = s^+ \quad (4.73)$$

where, according to the total time derivative definition in (3.68) and the axial variable transform (4.69), the total time derivative of the jet-head $b^+(\tau)$ is (see Fig. 3.5):

$$\frac{\partial b^+}{\partial \tau} [\xi(\tau), \tau] = \frac{\partial b^+}{\partial \tau} \Big|_{\xi=const} + \frac{\partial b^+}{\partial \xi} \frac{\partial \xi}{\partial \tau} = \frac{\partial b^+}{\partial \tau} \Big|_{\xi=const} - x \frac{L_\tau}{L} \frac{\partial b^+}{\partial x} \quad (4.74)$$

In the above, $b_\tau^+ = \frac{\partial b^+}{\partial \tau} \Big|_{\xi=fixed}$ is the temporal derivative term while the x – axial variable

ξ is fixed. b_τ^+ is the first term of the total time derivative in (4.74), which has not been considered in the 1st order model.

Recall that in the chine un-wetted case $V_n(\xi, s^+, \tau) = 0$ and in the chine wetted case $V_n(\xi, s^+, \tau) = V(\xi, \tau)$ (refer to Fig. 2.6) and $z_k(\xi) = 1$ in the $\zeta - \eta$ system. Thus from (4.73) the pressure continuity condition in 2nd order seakeeping model at $s = s^+$ is,

- In the chine un-wetted phase

$$b_\tau^+ + \left(1 - x \frac{L_\tau}{L}\right) b_x^+ = \frac{V_s^2(\xi, s^+, \tau) - V^2(\xi, \tau)}{2V_s(\xi, s^+, \tau)} \quad \text{at } s = s^+ \quad (4.75)$$

- In the chine wetted phase

$$b_\tau^+ + \left(1 - x \frac{L_\tau}{L}\right) b_x^+ = \frac{1}{2} V_s(\xi, s^+, \tau) \quad \text{at } s = s^+ \quad (4.76)$$

At the jet head z_b^- , applying the dynamic boundary condition $C_p(x, s^-, \tau) = 0$,

and using the coordinate transformation relation $s^-(\xi, \tau) = \frac{b^- - 1}{z_c(\xi, \tau) - 1}$ in (4.70), the jet

head velocity found at $s = s^-$ is,

$$b_\tau^- + \left(1 - x \frac{L_\tau}{L}\right) b_x^- = \frac{V_s^2(\xi, s^-, \tau) + V_n^2(\xi, s^-, \tau) - V^2(\xi, \tau)}{2V_s(\xi, s^-, \tau)} \quad \text{at } s = s^- \quad (4.77)$$

Since at the keel z_k , the flow is always in the chine-wetted phase (Fig. 2.6), $V_n(\xi, s^-, \tau) = V(\xi, \tau)$, thus we obtain the inner jet head pressure continuity condition at $s = s^-$:

$$b_\tau^- + (1 - x \frac{L_\tau}{L}) b_x^- = \frac{1}{2} V_s(\xi, s^-, \tau) \quad \text{at } s = s^- \quad (4.78)$$

Thus, as in the steady planing case, we have two pressure continuity conditions in either the chine un-wetted or chine-wetted flow phase.

Comparing Eq. (4.75), (4.76) and (4.78) with the pressure continuity condition of the 1st order model in Eq. (3.69) - Eq. (3.71), it is seen that the temporal derivative terms have been taken into account in the pressure continuity condition of the 2nd order theory.

4.2.1.2 Burger's equation and location of free vortices

For applying the pressure continuity conditions Eq. (4.75), (4.76) and (4.78) on the vortex sheets, the vortex sheet distribution must be specified. Differentiation of the pressure distribution in Eq.(4.68) gives:

$$\frac{\partial C_p}{\partial s}(x, s, \tau) = -2V_s(x, s, \tau) \frac{\partial V_s}{\partial s} - 2 \frac{\partial^2 \phi}{\partial \tau \partial s}(x, s, \tau) - 2 \frac{\partial^2 \phi}{\partial x \partial s}(x, s, \tau) - 2 \frac{\partial \phi}{\partial x} \cdot \frac{\partial^2 \phi}{\partial x \partial s}(x, s, \tau) = 0$$

$$0 \leq x \leq L(\tau), 1 \leq s \leq s^+(x, \tau) \text{ or } s^- \leq s \leq 0 \quad (4.79)$$

Substituting all derivative terms of (4.79), developed in Appendix D, back into (4.79), an Euler differential equation of the vortex sheet distribution is then derived that contains the temporal derivative terms discarded in the 1st order model; see (3.72) for comparison:

$$\begin{aligned} & \{ [V_s(\xi, s, \tau) - [\frac{\partial z_c}{\partial \tau} s + \frac{\partial z_c}{\partial x} s(1 - x \frac{L_\tau}{L})]] \} \frac{\partial V_s}{\partial s} \\ & - (1 - z_c) \frac{\partial V_s}{\partial \tau}(\xi, s, \tau) - (1 - z_c)(1 - x \frac{L_\tau}{L}) \frac{\partial V_s(\xi, s, \tau)}{\partial x} = 0 \end{aligned} \quad 1 \leq s \leq s^+ \quad (4.80)$$

Just as in the steady planing problem, this is an inviscid Euler's (Burger's) differential equation that governs the free vortex distribution, comparable with the Burger's equation in Eq.(4.62) for steady planing.

Comparison (4.80) with the Euler equation (3.72) of the 1st order model, confirms

that the temporal derivative term $\frac{\partial}{\partial \tau} \Big|_{\xi=fixed}$ has been included in the 2nd order model.

Similarly, in the region of $s^- \leq s \leq 0$, starting with the differentiation of the pressure distribution in Eq.(4.68), gives the inside Burger's equation for the inside free vortex sheet (refer to (3.73)),

$$\begin{aligned} & \{ [V_s(\xi, s, \tau) - [\frac{\partial z_c}{\partial \tau} s + \frac{\partial z_c}{\partial x} s(1 - x \frac{L_\tau}{L})]] \} \frac{\partial V_s}{\partial s} \\ & - (1 - z_c) \frac{\partial V_s}{\partial \tau}(\xi, s, \tau) - (1 - z_c)(1 - x \frac{L_\tau}{L}) \frac{\partial V_s(\xi, s, \tau)}{\partial x} = 0 \end{aligned} \quad s^- \leq s \leq 0 \quad (4.81)$$

Physically that the equations (4.80) and (4.81) are equivalent to the Euler equation:

$$\frac{DV_s}{D\tau} = \frac{\partial V_s}{\partial \tau} + \frac{\partial V_s}{\partial x} \frac{dx}{d\tau} + \frac{\partial V_s}{\partial s} \frac{ds}{d\tau} = 0 \quad (4.82)$$

Jet flows during impact are formed when free vortices are shed at the separation points z_c and z_k . Since the effects of viscosity and gravity are neglected, the free vortices continue advancing outward with the separation velocities. As discussed in Chapter 3, Eq. (4.80) and (4.81) state that there is no particle acceleration on the free vortex sheets separated at z_c^+ and z_k .

The solutions to (4.80), (4.81) can be developed in terms of the Galaeen transformation of the initial and boundary conditions (refer to Chapter 10 and Vorus 1993 for details) These solutions gives the particle positions at current time based on the previous time step information. Thus, the discretized motion of the free vortices can be calculated as time progresses, i.e., the location at time τ for the particle deposited at z_c onto the vortex sheet at time τ_0 , can be derived by using an approximate second order

algorithm of $\left. \frac{\partial}{\partial \tau} \right|_{\xi=const}$, (see Chapter 10 for details) as,

$$s(s', x; \tau) = \frac{V_s(x_0, s', \tau_0) \cdot [(x - x_0) + \frac{1}{2} \cdot \frac{L_\tau}{L} \cdot (x - x_0)^2] + s'[z_c(x_0; \tau_0) - 1]}{[z_c(x; \tau) - 1]}$$

$$1 \leq s' \leq s^+, \quad x \geq x_0 \quad (4.83)$$

The detailed mathematical model treating the free vortices movement can be found in Chapter 10.

4.2.1.3 Pressure distribution formulae

On the contour of the hull, the pressure distribution can be found from (4.68) (refer to Appendix D),

- **In the chine wetted case:**

$$\begin{aligned}
 C_p(x, s; \tau) &= V^2(x, \tau) - V_s^2(x, s, \tau) + V_s^2(\xi, 1, \tau) \\
 &+ 2(z_c - 1) \left\{ \int_{s(\xi, \tau)}^1 \left[\frac{\partial V_s}{\partial \tau}(\xi, s_0, \tau) + \left(1 - x \frac{L_\tau}{L}\right) \frac{\partial V_s(\xi, s_0, \tau)}{\partial x} \right] ds_0 \right\} \\
 &+ 2 \left[z_{c, \tau} + z_{c, x} \left(1 - x \frac{L_\tau}{L}\right) \right] \left[\int_{s(\xi, \tau)}^1 V_s(\xi, s_0, \tau) ds_0 + s \cdot V_s(\xi, s, \tau) - V_s(\xi, 1, \tau) \right] \\
 &0 \leq x \leq L(\tau), \quad 0 \leq s \leq 1 \quad (4.84)
 \end{aligned}$$

- **In the chine un-wetted case:**

$$\begin{aligned}
 C_p(x, s; \tau) &= V_s^2(x, 1, \tau) - V_s^2(x, s, \tau) \\
 &+ 2(z_c - 1) \left\{ \int_{s(\xi, \tau)}^1 \left[\frac{\partial V_s}{\partial \tau}(\xi, s_0, \tau) + \left(1 - x \frac{L_\tau}{L}\right) \frac{\partial V_s(\xi, s_0, \tau)}{\partial x} \right] ds_0 \right\} \\
 &+ 2 \left[z_{c, \tau} + z_{c, x} \left(1 - x \frac{L_\tau}{L}\right) \right] \left[\int_{s(\xi, \tau)}^1 V_s(\xi, s_0, \tau) ds_0 + s \cdot V_s(\xi, s, \tau) - V_s(\xi, 1, \tau) \right] \\
 &0 \leq x \leq L(\tau), \quad 0 \leq s \leq 1 \quad (4.85)
 \end{aligned}$$

Comparing with (3.74) and (3.75), Eq. (4.84) and (4.85) have taken the

$\frac{\partial}{\partial \tau} \Big|_{\xi=\text{fixed}}$ term into account

Therefore the pressure continuity conditions in (4.75), (4.76) and (4.78) together with the previous velocity continuity conditions in (4.26) and (4.27) and the displacement continuity condition (4.58) provide the necessary equations to solve for the unknowns in the sea-keeping case.

To proceed to obtain the time history of the solution, we need the wave model, the vessel motion model and the transient sectional impact velocity model, just as in the 1st order case.

4.2.2 Water wave model

The wave model in the 2nd order theory is the same as described in Chapter 3. For reducing the redundancy, we just cite the wave expressions here:

The non-dimensional regular wave is:

$$\zeta(x; \tau) = \zeta_a \sin[\Omega_e \tau + k(l(\tau) - x) + \theta_0] \quad (4.86)$$

For the random wave, according to the Jonswap spectrum given in (3.81) and (3.82),

$$\zeta(x; \tau) = \sum_{i=1}^N \zeta_i \sin[\Omega_{e,i} \tau + k_i(l(\tau) - x) + \theta_i] \quad (4.87)$$

For the definition of variables in (4.86) and (4.87) refer to Chapter 3.

4.2.3 Vessel motion model

Based on the Newton's second law, the boat motion (heave and pitch) in waves is described as:

$$\sum_k F_k = m\ddot{\eta}_3 \quad (4.88)$$

$$\sum_k M_{o,k} = J\ddot{\eta}_5 \quad (4.89)$$

where m is the mass of boat, F_k and $M_{o,k}$ are the external forces and moments. The inertia moment J is defined in (3.90).

Taking the coupling effect into account, the non-dimensional motion equations are:

$$m\ddot{\eta}_3 = C_{LT} - C_W - mx_{CG}\ddot{\eta}_5 \quad (4.90)$$

$$J\ddot{\eta}_5 = C_{MT} - C_W \times x_{CG} - mx_{CG}\ddot{\eta}_3 \quad (4.91)$$

where the force and moment C_W , C_{LT} , C_{MT} and x_{CG} refer to the definitions in Chapter 3.

Solving the above equations in the time domain, the heave and pitch time-history of the boat in seaway can be predicted by the numerical integration.

4.2.4 Boat impact velocity in waves

The wetted length $L(\tau)$ at any time can be found using the same condition (3.97) as in Chapter 3:

$$H_{T0} - \eta_3(t) = (\alpha_0 + \eta_5(t)) \cdot L(t) + y_k(0) - \zeta_w(L, t) \quad (4.92)$$

The transient draft at any section can be solved by the same equation (3.98):

$$Y_k(x, t) = (\alpha_0 + \eta_5) \cdot x + y_k(0) - y_k(x) + \zeta_w(L - x, t) - \zeta_w(L, t) \quad (4.93)$$

In seakeeping, at each time step a complete x - problem will be solved. The sectional impact velocity at each time will be needed to find the solution of the x - problem by using the slender body impact theory, refer to Fig. 6.1 of chapter 6 for the solution procedure. The section impact velocity in waves of the 2nd order theory is (refer to (3.105):

$$\begin{aligned} v_k(x, t) = & \alpha_0 - y'_{k0} \\ & - (y'_k(x) - y'_{k0}) + \eta_5(t) - \dot{\eta}_3(t) - \dot{\eta}_5 \cdot (1 - \xi)L(t) \\ & - (\alpha_0 + \eta_5(t)) \cdot (1 - \xi)\dot{L}(t) - y'_k(x)\xi \cdot \dot{L}(t) \\ & + \dot{\zeta}_w(L - x, t) + \zeta'_w(L - x, t)[1 - (1 - \xi)\dot{L}(t)] \end{aligned} \quad (4.94)$$

This chapter has systematically introduced the second order extension to the Vorus' first order nonlinear theory. The numerical models and the solution procedures for both theories will be given in following chapters.

CHAPTER 5

NUMERICAL MODELS

The first and second order theoretical models for planing catamarans have been described in previous chapters. These two formulations are solved by numerically executing the semi-analytic solutions developed. In this chapter, we concentrate on the descriptions of the numerical discretization models for both methods in the steady calm-water planing case. In next chapter, the time marching solution procedures for seakeeping are covered.

As shown in section 2.7 of Chapter 2 on steady planing, the non-dimensional variables \bar{x} and τ are identical (refer to (2.3)), so that the steady planing solution can be constructed directly from the time dependent impact solution. Thus the solution of steady planing must be numerically stepped forward in the impact time space from the initial condition at τ_0 in discrete steps to τ_i ($i=1, \dots, n$) in satisfying the three general continuity conditions on velocity, pressure, and the displacement (see Chapter 3 and 4).

We first review the numerical model of the 1st order theory, and then proceed to the 2nd order theory.

5.1 First Order Numerical Model

The system solution equations of the 1st order theory consist of the velocity Kutta conditions (3.14) and (3.15) (or equivalently (3.28) and (3.32)), the displacement continuity condition (3.44), and the pressure continuity conditions (3.54) to (3.56). The discrete formulations of these system equations for use in the numerical forward time integration in the impact-time space are as follows.

5.1.1 Numerical analysis of 1st order velocity continuity equations

Discretize the segment of the keel free vortex $\gamma_s^-(\zeta, \tau)$ sheet (refer to Fig. 2.6) in the region $b^- \leq \zeta \leq 1$ into $N_i^-(\tau)$ elements at each impact-time step τ_i , and the segment of the z_c^+ -side hull free vortex $\gamma_s^+(\zeta, \tau)$ sheet $z_c^+ \leq \zeta \leq b^+$ into $N_i^+(\tau)$ elements. Subscript i represents the impact-time step τ_i here.

In discrete notation, the velocity continuity conditions of (3.28) and (3.32) can be written as:

$$\begin{aligned}
 0 &= -z_c [E(k) - F(k)] \\
 &- \frac{1}{\pi} \frac{1 - z_c^2}{z_c} F(k) \sum_{j=1}^{N_i^+} \gamma_{s,j}^+(\tau) \int_{\zeta_j^+ - \varepsilon_j^+/2}^{\zeta_j^+ + \varepsilon_j^+/2} \frac{\zeta_0}{\zeta_0^2 - 1} d\zeta_0 \\
 &- \frac{1}{2} \sum_{j=1}^{N_i^-} \gamma_{s,j}^-(\tau) [1 - \Lambda_0(\varepsilon_{2,j}, k)] \int_{\zeta_j^- - \varepsilon_j^-/2}^{\zeta_j^- + \varepsilon_j^-/2} \sqrt{\frac{z_c^2 - \zeta_0^2}{1 - \zeta_0^2}} d\zeta_0 \\
 &- \frac{1}{2} \sum_{j=1}^{N_i^+} \gamma_{s,j}^+(\tau) [1 - \Lambda_0(\varepsilon_{3,j}, k)] \int_{\zeta_j^+ - \varepsilon_j^+/2}^{\zeta_j^+ + \varepsilon_j^+/2} \sqrt{\frac{\zeta_0^2 - z_c^2}{\zeta_0^2 - 1}} d\zeta_0
 \end{aligned}
 \quad \text{when } \zeta \rightarrow 1^+ \quad (5.1)$$

$$\begin{aligned}
0 &= -z_c [E(k) - \frac{1}{z_c^2} F(k)] \\
&- \frac{1}{\pi} \frac{1 - z_c^2}{z_c} F(k) \sum_{j=1}^{N_i^-} \gamma_{S,j}^-(\tau) \int_{\zeta_j^- - \varepsilon_j^- / 2}^{\zeta_j^- + \varepsilon_j^- / 2} \frac{\zeta_0}{z_c^2 - \zeta_0^2} d\zeta_0 \\
&- \frac{1}{2} \sum_{j=1}^{N_i^-} \gamma_{S,j}^-(\tau) [1 - \Lambda_0(\varepsilon_2 \setminus k)] \int_{\zeta_j^- - \varepsilon_j^- / 2}^{\zeta_j^- + \varepsilon_j^- / 2} \sqrt{\frac{1 - \zeta_0^2}{z_c^2 - \zeta_0^2}} d\zeta_0 \\
&- \frac{1}{2} \sum_{j=1}^{N_i^+} \gamma_{S,j}^+(\tau) [1 - \Lambda_0(\varepsilon_3 \setminus k)] \int_{\zeta_j^+ - \varepsilon_j^+ / 2}^{\zeta_j^+ + \varepsilon_j^+ / 2} \sqrt{\frac{\zeta_0^2 - 1}{\zeta_0^2 - z_c^2}} d\zeta_0
\end{aligned} \tag{5.2}$$

when $\zeta \rightarrow z_c^-$

where $F(k)$, $E(k)$ are the complete elliptic integrals of the first and second kind respectively (refer to Gradshteyn and Ryzhik, 1965), k , ε_2 , ε_3 , Λ_0 are all defined in Chapter 3 (refer to (3.23) - (3.27)).

In the above equations, ζ_j^- and ζ_j^+ ($j=1, \dots, N_i^-$ or N_i^+) represent the discrete node positions on the keel and the side hull free vortex sheets, respectively. ε_j^- and ε_j^+ stand for the numerical grid length on the keel and the side-hull sheet, respectively.

The semi-analytical form of the discrete integrals in the above equations can be found by the mathematical reduction (refer to Vorus 1996). The final semi-analytical forms are given below:

$$I_{11j} = \int_{\zeta_j^+ - \varepsilon_j^+ / 2}^{\zeta_j^+ + \varepsilon_j^+ / 2} \frac{\zeta_0}{\zeta_0^2 - 1} d\zeta_0 = \frac{1}{2} \ln(\zeta^2 - 1) \Big|_{\zeta_j^+ - \varepsilon_j^+ / 2}^{\zeta_j^+ + \varepsilon_j^+ / 2} = \ln \sqrt{\frac{(\zeta_j^+ + \varepsilon_j^+ / 2)^2 - 1}{(\zeta_j^+ - \varepsilon_j^+ / 2)^2 - 1}} \tag{5.3}$$

$$I_{13j} = \int_{\zeta_j^+ - \varepsilon_j^+ / 2}^{\zeta_j^+ + \varepsilon_j^+ / 2} \sqrt{\frac{\zeta_0^2 - z_c^2}{\zeta_0^2 - 1}} d\zeta_0 = \left\{ u \sqrt{\frac{u^2 - z_c^2}{u^2 - 1}} - z_c E(\mu, t) \right\}_{u^-}^{u^+} \tag{5.4}$$

$$I_{23j} = \int_{\zeta_j^+ - \varepsilon_j^+ / 2}^{\zeta_j^+ + \varepsilon_j^+ / 2} \sqrt{\frac{\zeta_0^2 - 1}{\zeta_0^2 - z_c^2}} d\zeta_0 = \left\{ \frac{z_c^2 - 1}{z_c} F(\mu, t) - z_c E(\mu, t) + u \sqrt{\frac{u^2 - z_c^2}{u^2 - 1}} \right\}_{u^-}^{u^+} \quad (5.5)$$

In the above expressions, $\mu = \arcsin \sqrt{\frac{u^2 - z_c^2}{u^2 - 1}}$, $u^- \leq u \leq u^+$, $u^+ = \zeta_j^+ + \varepsilon_j^+ / 2$,

$$u^- = \zeta_j^+ - \varepsilon_j^+ / 2, \quad t = \frac{1}{z_c}. \quad \text{And,}$$

$$I_{12j} = \int_{\zeta_j^- - \varepsilon_j^- / 2}^{\zeta_j^- + \varepsilon_j^- / 2} \sqrt{\frac{z_c^2 - \zeta_0^2}{1 - \zeta_0^2}} d\zeta_0 = z_c [E(\eta_j^+, t) - E(\eta_j^-, t)] \quad (5.6)$$

$$I_{21j} = \int_{\zeta_j^- - \varepsilon_j^- / 2}^{\zeta_j^- + \varepsilon_j^- / 2} \frac{\zeta_0}{z_c^2 - \zeta_0^2} d\zeta_0 = -\frac{1}{2} \ln(z_c^2 - \zeta^2) \Big|_{\zeta_j^- - \varepsilon_j^- / 2}^{\zeta_j^- + \varepsilon_j^- / 2} = -\ln \sqrt{\frac{z_c^2 - (\zeta_j^- + \varepsilon_j^- / 2)^2}{z_c^2 - (\zeta_j^- - \varepsilon_j^- / 2)^2}} \quad (5.7)$$

$$I_{22j} = \int_{\zeta_j^- - \varepsilon_j^- / 2}^{\zeta_j^- + \varepsilon_j^- / 2} \sqrt{\frac{1 - \zeta_0^2}{z_c^2 - \zeta_0^2}} d\zeta_0 = \left\{ z_c E(\eta, t) - \frac{z_c^2 - 1}{z_c} F(\eta, t) \right\}_{\lambda^-}^{\lambda^+} \quad (5.8)$$

In the above expressions, $\eta_j^+ = \arcsin(\zeta_j^- + \frac{\varepsilon_j^-}{2})$, $\eta_j^- = \arcsin(\zeta_j^- - \frac{\varepsilon_j^-}{2})$, $\eta = \arcsin(\lambda)$,

$$\lambda^- \leq \lambda \leq \lambda^+, \quad \lambda^+ = \zeta_j^- + \varepsilon_j^- / 2, \quad \lambda^- = \zeta_j^- - \varepsilon_j^- / 2, \quad t = \frac{1}{z_c}. \quad \text{Again } F(\eta, t), \quad E(\eta_j^+, t),$$

$E(\eta_j^-, t)$, $E(\mu, t)$ and $E(\eta, t)$ in above formula are the Elliptic integrals of the first kind and the second kind, respectively.

Substituting (5.3) - (5.8) into (5.1) and (5.2) to simplify the numerical expression of the velocity continuity equations, there results:

$$\begin{aligned}
0 &= -z_c[E(k) - F(k)] \\
&\quad - \frac{1}{\pi} \frac{1 - z_c^2}{z_c} F(k) \sum_{j=1}^{N_i^+} \gamma_{S,j}^+(\tau) \cdot I_{11j} \\
&\quad - \frac{1}{2} \sum_{j=1}^{N_i^-} \gamma_{S,j}^-(\tau) [1 - \Lambda_0(\varepsilon_{2,j}, k)] \cdot I_{12j} \\
&\quad - \frac{1}{2} \sum_{j=1}^{N_i^+} \gamma_{S,j}^+(\tau) [1 - \Lambda_0(\varepsilon_{3,j}, k)] \cdot I_{13j}
\end{aligned} \tag{5.9}$$

$$\begin{aligned}
0 &= -z_c[E(k) - \frac{1}{z_c^2} F(k)] \\
&\quad - \frac{1}{\pi} \frac{1 - z_c^2}{z_c} F(k) \sum_{j=1}^{N_i^-} \gamma_{S,j}^-(\tau) \cdot I_{21j} \\
&\quad - \frac{1}{2} \sum_{j=1}^{N_i^-} \gamma_{S,j}^-(\tau) [1 - \Lambda_0(\varepsilon_2 \setminus k)] \cdot I_{22j} \\
&\quad - \frac{1}{2} \sum_{j=1}^{N_i^+} \gamma_{S,j}^+(\tau) [1 - \Lambda_0(\varepsilon_3 \setminus k)] \cdot I_{23j}
\end{aligned} \tag{5.10}$$

Represent (5.9) and (5.10) in a compacted-matrix form,

$$z_c[E(k) - F(k)] = \sum_{j=1}^{N_i^-} \gamma_{S,j}^-(\tau) \times C_{j,11} + \sum_{j=1}^{N_i^+} \gamma_{S,j}^+(\tau) \times C_{j,12} \tag{5.11}$$

$$z_c[E(k) - \frac{1}{z_c^2} F(k)] = \sum_{j=1}^{N_i^-} \gamma_{S,j}^-(\tau) \times C_{j,21} + \sum_{j=1}^{N_i^+} \gamma_{S,j}^+(\tau) \times C_{j,22} \tag{5.12}$$

where the matrix coefficients are,

$$\begin{aligned}
C_{j,11} &= -\frac{1}{2} [1 - \Lambda_0(\varepsilon_{2,j}, k)] \times I_{12j} \\
&= -\frac{1}{2} [1 - \Lambda_0(\varepsilon_{2,j}, k)] \times z_c [E(\eta_j^+, t) - E(\eta_j^-, t)]
\end{aligned} \tag{5.13}$$

$$\begin{aligned}
C_{j,12} &= -\frac{1}{\pi} \frac{1-z_c^2}{z_c} F(k) \times I_{11j} - \frac{1}{2} [1 - \Lambda_0(\varepsilon_{3,j}, k)] \times I_{13j} \\
&= -\frac{1}{\pi} \frac{1-z_c^2}{z_c} F(k) \times \ln \sqrt{\frac{(\zeta_j^+ + \varepsilon_j^+ / 2)^2 - 1}{(\zeta_j^+ - \varepsilon_j^+ / 2)^2 - 1}} \\
&\quad - \frac{1}{2} [1 - \Lambda_0(\varepsilon_{3,j}, k)] \times \left\{ u \sqrt{\frac{u^2 - z_c^2}{u^2 - 1}} - z_c E(\mu, t) \right\}_{u^-}^{u^+}
\end{aligned} \tag{5.14}$$

$$\begin{aligned}
C_{j,21} &= -\frac{1}{\pi} \frac{1-z_c^2}{z_c} F(k) \times I_{21j} - \frac{1}{2} [1 - \Lambda_0(\varepsilon_2 \setminus k)] \times I_{22j} \\
&= \frac{1}{\pi} \frac{1-z_c^2}{z_c} F(k) \times \ln \sqrt{\frac{z_c^2 - (\zeta_j^- + \varepsilon_j^- / 2)^2}{z_c^2 - (\zeta_j^- - \varepsilon_j^- / 2)^2}} \\
&\quad - \frac{1}{2} [1 - \Lambda_0(\varepsilon_2 \setminus k)] \times \left\{ z_c E(\eta, t) - \frac{z_c^2 - 1}{z_c} F(\eta, t) \right\}_{u^-}^{u^+}
\end{aligned} \tag{5.15}$$

$$\begin{aligned}
C_{j,22} &= -\frac{1}{2} [1 - \Lambda_0(\varepsilon_3 \setminus k)] \times I_{23j} \\
&= -\frac{1}{2} [1 - \Lambda_0(\varepsilon_3 \setminus k)] \times \left\{ \frac{z_c^2 - 1}{z_c} F(\mu, t) - z_c E(\mu, t) + u \sqrt{\frac{u^2 - z_c^2}{u^2 - 1}} \right\}_{u^-}^{u^+}
\end{aligned} \tag{5.16}$$

with,

$$\varepsilon_{2,j} = \arcsin \left(z_c \sqrt{\frac{1 - \zeta_j^{-2}}{z_c^2 - \zeta_j^{-2}}} \right) \tag{5.17}$$

$$\varepsilon_{3,j} = \arcsin \sqrt{\frac{\zeta_j^{+2} - z_c^2}{\zeta_j^{+2} - 1}} \tag{5.18}$$

In the above expressions, η_j^+ , η_j^- , μ , u^+ , u^- , η , λ^+ , λ^- are defined as before.

The unknowns in (5.11) and (5.12) at any time step i are $\gamma_{S,N_i^-}^-(\tau_i)$ and $\gamma_{S,1}^+(\tau_i)$, which are the first separated elements at τ_i at the keel and at the side-hull jet separation points, respectively. Therefore we may separate the unknowns, and group the known terms together. The known terms are:

$$R_1 = z_c[E(k) - F(k)] - \sum_{j=1}^{N_i^- - 1} \gamma_{S,j}^-(\tau) \cdot C_{j,11} - \sum_{j=2}^{N_i^+} \gamma_{S,j}^+(\tau) \cdot C_{j,12} \quad (5.19)$$

$$R_2 = z_c[E(k) - \frac{1}{z_c} F(k)] - \sum_{j=1}^{N_i^- - 1} \gamma_{S,j}^-(\tau) \cdot C_{j,21} - \sum_{j=2}^{N_i^+} \gamma_{S,j}^+(\tau) \cdot C_{j,22} \quad (5.20)$$

The system equations are now reduced to the following:

$$\gamma_{S,N_i^-}^-(\tau) C_{N_i^-,11} + \gamma_{S,1}^+(\tau) \cdot C_{1,12} = R_1 \quad (5.21)$$

$$\gamma_{S,N_i^-}^-(\tau) C_{N_i^-,21} + \gamma_{S,1}^+(\tau) \cdot C_{1,22} = R_2 \quad (5.22)$$

Define the determinant,

$$\Delta = C_{N_i^-,11} \cdot C_{1,22} - C_{N_i^-,21} \cdot C_{1,12} \quad (5.23)$$

The solutions for the unknown γ 's are then:

$$\gamma_{S,N_i^-}^-(\tau_i) = \frac{R_1 \cdot C_{1,22} - R_2 \cdot C_{1,12}}{\Delta} \quad (5.24)$$

$$\gamma_{s,1}^+(\tau_i) = \frac{C_{N_i^-,11} \cdot R_2 - C_{N_i^-,21} \cdot R_1}{\Delta} \quad (5.25)$$

Therefore, based on the vortex distribution of the previous time steps, the vortex strength of the element shed at a new time step is solved by Eq.(5.24) and Eq.(5.25), which can be viewed as eliminating the unknown jet separation velocity $V_i^+(\tau)$, $V_i^-(\tau)$ (or $V_s(1,\tau)$, $V_s(0,\tau)$) in the s coordinate system of Fig. 3.3. It is based on the following relation of the line vortex strength $\gamma(\zeta, \tau)$ and the contour tangential velocity $V_s(\zeta, \tau)$ (refer to (4.3)):

$$V_s(\zeta, \tau) = -\frac{1}{2}\gamma(\zeta, \tau) + V(\tau) \sin \beta(\zeta, \tau) \quad (5.26)$$

5.1.2 Numerical model of 1st order displacement continuity condition

In the numerical model of the 1st order displacement continuity condition, CatSea has used a new coordinate transformation as shown in Fig. 5.1. In this R coordinate system, the transverse ζ – coordinate has been normalized by the keel side jet head coordinate b^- . The hull side jet head coordinate now is defined as $e = b^+/b^-$, the keel jet head now is at $R = 1$, the keel is at $1/b^-$, and the jet-head separation location is z_c/b^- . This R coordinate system is used specially for the derivation of the semi-analytic form of the integral transformation in the displacement continuity equation.

Fig. 5.1 shows the relationship of the ζ –, s – and R – coordinate transformations.

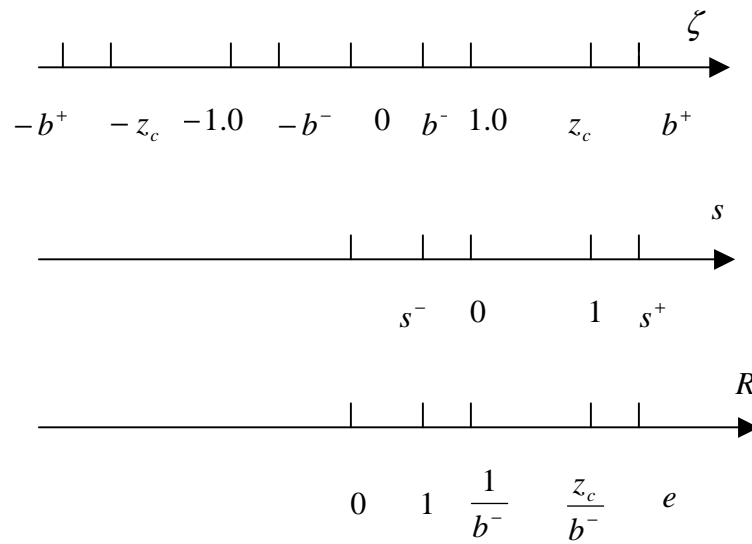


Fig. 5.1 R coordinate system

In this R – coordinate system, the displacement continuity condition will become (refer to (3.44)):

$$(\tilde{Y}_{wl} + \tan \beta) \cdot I_1 - b^- \cdot \tan \beta \cdot I_2 = 0 \quad (5.27)$$

where the integrals in (5.27) are as following,

$$I_1 = \int_{\zeta_0=1/b^-}^e \frac{1}{\chi^*(\zeta_0)(e^2 - \zeta_0^2)} d\zeta_0 \quad (5.28)$$

$$I_2 = \int_{\zeta_0=1/b^-}^e \frac{\zeta_0}{\chi^*(\zeta_0)(e^2 - \zeta_0^2)} d\zeta_0 \quad (5.29)$$

In another form, the displacement continuity condition in (5.27) can be written as:

$$\tilde{Y}_{wl} = \tan \beta \cdot \frac{(-I_1 + b^- I_2)}{I_1} \quad (5.30)$$

To calculate Eq. (5.30), the semi-analytical form of the integral terms I_1 and I_2 need to be developed. The kernel function in I_1 and I_2 is (refer to (3.42)):

$$\chi^*(\zeta) = \frac{1}{\sqrt{(\zeta^2 - (b^-)^2)((b^+)^2 - \zeta^2)}} \quad (5.31)$$

In the coordinate system of Fig. 5.1, the kernel function becomes,

$$\chi^*(\zeta_0) = \frac{1}{\sqrt{(\zeta_0^2 - 1)(e^2 - \zeta_0^2)}} \quad (5.32)$$

Substituting (5.32) into the integral I_1 in (5.28),

$$I_1 = \int_{\zeta_0=1/b^-}^e \sqrt{\frac{\zeta_0^2 - 1}{e^2 - \zeta_0^2}} d\zeta_0 \quad (5.33)$$

After careful integral transform and mathematical reduction, the easily calculated semi-analytical form of the integral I_1 can be found in an elliptic function form (refer to Gradshteyn and Ryzhik, 1965, p277.12):

$$I_1 = e \cdot E(\lambda, q) - \frac{1}{e} \cdot F(\lambda, q) \quad (5.34)$$

where $\lambda = \arcsin \sqrt{\frac{e^2 - (1/b^-)^2}{e^2 - 1}}$, $q = \frac{\sqrt{e^2 - 1}}{e}$, $E(\lambda, q)$ is the elliptic integral of the second kind, $F(\lambda, q)$ is the elliptic integral of the first kind.

Similarly substituting the kernel function in (5.32) into I_2 ,

$$I_2 = \int_{\zeta_0 = 1/b^-}^e \zeta_0 \cdot \sqrt{\frac{\zeta_0^2 - 1}{e^2 - \zeta_0^2}} d\zeta_0 \quad (5.35)$$

In I_2 , make a variable transformation, $t = \zeta_0^2$, then make the following variable transformations in order: $s = e^2 - t$, $s_1 = (b^-)^2 \cdot s$, $s_2 = \frac{s_1}{(b^+)^2 - 1}$, and $s_2 = \sin^2 \theta$. After

these step transformations, I_2 will have the following form:

$$I_2 = 2\alpha \int_0^{\pi/2} \sqrt{1 - \beta \sin^2 \theta} \cdot \cos \theta \cdot d\theta \quad (5.36)$$

where, $\alpha = \frac{1}{2} \cdot \frac{1}{(b^-)^2} \cdot \sqrt{(b^{+2} - 1)(b^{+2} - b^{-2})}$, $\beta = \frac{b^{+2} - 1}{b^{+2} - b^{-2}}$.

Then follows the integral in Gradshteyn and Ryzhik (1965, p158.3), an easy-calculated semi-analytical form of I_2 is found as:

$$\begin{aligned}
I_2 &= \int_{\zeta_0 = 1/b^-}^e \frac{\zeta_0}{\chi^*(\zeta_0)(e^2 - \zeta_0^2)} d\zeta_0 \\
&= \frac{1}{2} \cdot \frac{1}{(b^-)^2} \cdot [\sqrt{(b^{+2} - 1)(1 - b^{-2})} + (b^{+2} - b^{-2}) \arcsin \sqrt{\frac{b^{+2} - 1}{b^{+2} - b^{-2}}}]
\end{aligned} \tag{5.37}$$

5.1.3 Numerical model of 1st order pressure continuity condition

The relations that must be satisfied for zero pressure on the jet-head and free-surface are in (3.54), (3.55) and (3.56), with the vortex sheet distribution in (3.58) and (3.59).

With zero gravity, Euler's equations (3.58) and (3.59) require that for fluid particles flowing from the sectional contour, onto the free vortex sheet, and out the jet, the velocity of each particle stays constant at its separation values at $z_k(\tau')$ or $z_c(\tau')$ for all time $\tau > \tau'$ thereafter. The solution to (3.58) and (3.59) can be developed in terms of the Galaen transformation of the initial and boundary conditions (refer to Chapter 10 and Vorus 1996 for details).

In the s coordinate system in Fig. 3.3, at the hull jet-head region $1 \leq s \leq s^+(\tau)$, this solution gives the particle position on the free vortex sheet motion as \hat{s} , whose velocity is $V_s(\hat{s}, \tau)$, as :

$$\hat{s}(s', \tau) = \frac{V_s(s', \tau_0)(\tau - \tau_0) + s'[z_c(\tau_0) - 1]}{z_c(\tau) - 1} \quad 1 \leq s' \leq s^+(\tau_0), \tau \geq \tau_0 \tag{5.38}$$

$$\hat{s}(\tau, \tau') = \frac{V_s(1, \tau')(\tau - \tau') + [z_c(\tau') - 1]}{z_c(\tau) - 1} \quad \tau \geq \tau' \geq \tau_0 \tag{5.39}$$

where τ is current time stamp, $\hat{s}(s', \tau)$ and $\hat{s}(\tau, \tau')$ stand for the current particle position. τ_0 is the time at which the particle was shed, where $V_s(s', \tau_0)$ in $1 \leq s' \leq s^+(\tau_0)$ is known from the initial condition. τ' is a reference time at separation. For any $\tau' < \tau$, $V_s(1, \tau')$ (jet velocity at the separation point z_c) in (5.39), is always known from previous time step computations.

There are two important points to keep in mind. One is that at the current time step, with $\tau' = \tau$, $\hat{s}(\tau, \tau) = 1$, the jet velocity $V_s(1, \tau)$ is an unknown (refer to the discussion for the velocity continuity conditions in section 5.1.1). Another is that from the pressure continuity conditions in (3.54), (3.55) and (3.56), it is easy to see that the jet-head velocity is always less than the jet velocity of the particle at the jet-head position. That is, $s^+(\tau) \leq \hat{s}[s^+(\tau_0), \tau]$ for all $\tau \geq \tau_0$. This implies that the outward motion of the jet-head lags behind that of all the particles in the jet which have been overlaid with it at previous times.

Similarly, at the keel jet-head $s^- \leq s \leq 0$ in Fig. 3.3, the free vortex particle positions are:

$$\hat{s}(s', \tau) = \frac{V_s(s', \tau_0)(\tau - \tau_0)}{z_c(\tau) - 1} \quad s^-(\tau_0) \leq s' \leq 0, \tau \geq \tau_0 \quad (5.40)$$

$$\hat{s}(\tau, \tau') = \frac{V_s(0, \tau')(\tau - \tau')}{z_c(\tau) - 1} \quad \tau \geq \tau' \geq \tau_0 \quad (5.41)$$

where $V_s(0, \tau')$ is the jet velocity at the keel z_k .

At each current discrete time τ_i , the free vortex strength distribution has to be constructed as depicted in Fig. 5.2 (here, for example, is shown only the outboard jet-head region of $1 \leq s \leq s^+(\tau)$, refer to Vorus, 1996). This distribution is first constructed for all particle positions at $\tau_j = 0, 1, \dots, i-1$. The jet velocities $V_s(1, \tau_j)$, $j < i$ are known for all previous times. The particle position $\hat{s}(\tau_i, \tau_j)$, $j < i$ can be found from (5.39).

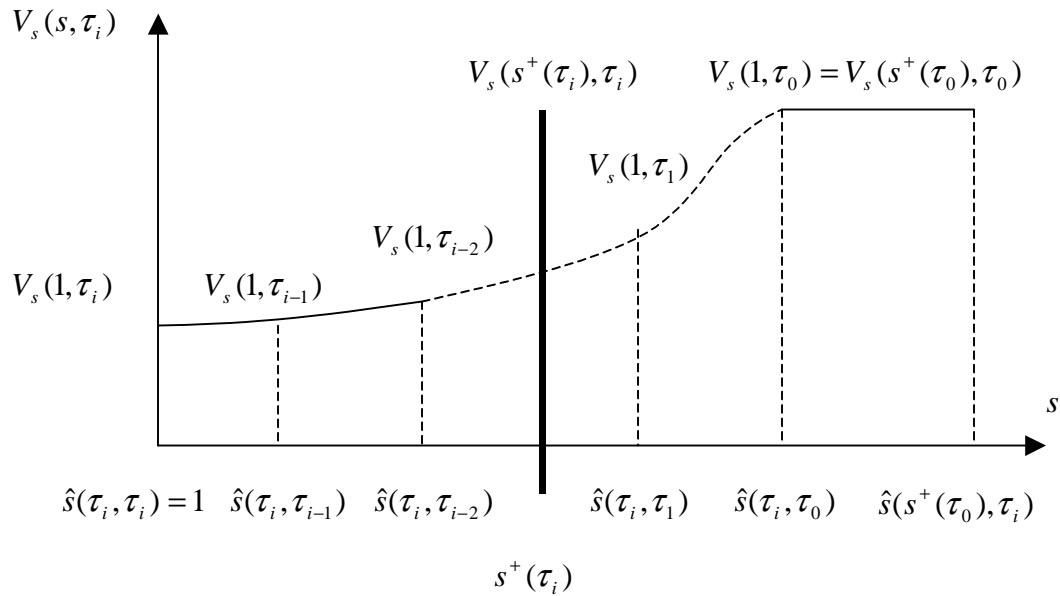


Fig. 5.2 Free vortex distribution

The jet-head free vortex sheet is then overlaid on the particle velocity distribution in Fig. 5.2 to determine the distribution of the sheet vortex strength at current time τ_i , exclusive of that at the separation point $\hat{s} = 1$. However, the jet-head offset $s^+(\tau_i)$ itself is an unknown at current time τ_i , and it must be determined by the iteration in satisfying the condition of Figure 5.2. The other unknown in Fig. 5.2 is the jet velocity $V_s(1, \tau_i)$; it

must be determined in conjunction with satisfying the velocity continuity condition in (5.25).

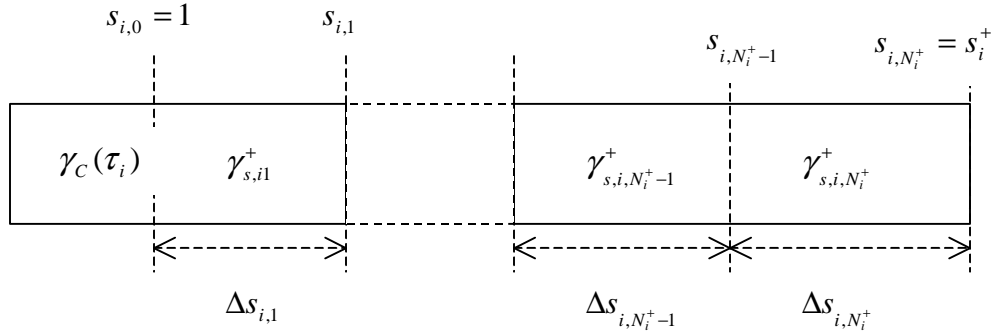


Fig. 5.3 Free vortex sheet discretization

The discretizing structure of the free vortex sheet can be conceptually constructed as in Fig. 5.3. In Fig. 5.3, for example, $\gamma_{s,ij}^+$, $j = 1, \dots, N_i^+$ are the piecewise constant free vortex strengths at the segments of length $\Delta s_{i,j}$, evaluated at the $s_{i,j}$ and averaged to apply at the segment midpoints. The $s_{i,j}$ coordinate are distributed along the free-sheet segment of Fig. 5.2 from $s_{i,0} = 1$ to $s_{i,N_i^+} = s^+(\tau_i)$. A new segment is added to the front of sheet in each time step (refer to Vorus 1996).

The pressure continuity condition in (3.54) and (3.55) then can be applied to the above free vortex sheet structure. For example, in the chine-unwetted phase, at the hull side, the jet head offset from,

$$b_{\tau}^+(\tau_i) = \frac{V_s^2(s^+(\tau_i), \tau_i) - 1}{2V_s(s^+(\tau_i), \tau_i)} \quad \text{at } s = s^+(\tau_i) \quad (5.42)$$

The essential unknowns in this case can be considered to be $V_s(1, \tau_i)$ and $\Delta s_{i,1}$ from Fig. 5.2 and Fig. 5.3, $\Delta s_{i,1}$ is the segment length added at $\zeta = z_c$ ($s = 1$) at the step τ_i . In any case, the pressure continuity numerical model, in conjunction with satisfying the velocity continuity conditions (and the displacement condition in the chine un-wetted flow phase) will be sufficient to determine these five unknowns $V_s(0, \tau_i)$, $V_s(1, \tau_i)$, $\Delta s_{i,1}^+$, $\Delta s_{i,N_i}^-$ and $z_{c\tau,i}$.

At the keel free vortex sheet in region $s^- \leq s \leq 0$, the numerical model description is the same as above, except at the keel z_k , the flow is always chine wetted, and the displacement continuity condition is not required.

5.1.4 Numerical model of the 1st order bounded vortex strength distribution

$\gamma_c(\zeta, \tau)$

The contour tangential velocity distribution $V_s(\zeta, \tau)$, $1 \leq \zeta \leq z_c(\tau)$ is determined by the associated contour bound vortex distribution $\gamma_c(\zeta, \tau)$ (refer to Fig. 2.6, and Eq. (5.26)). The numerical analysis of the bound vortex distribution $\gamma_c(\zeta, \tau)$ is as follows.

The $\gamma_c(\zeta, \tau)$ is given as (3.10):

$$\begin{aligned} \gamma_c(\zeta, \tau) = & \frac{4\zeta}{\pi} \chi(\zeta) \{V(\tau) [-\Lambda(\zeta)] \\ & + \frac{1}{\pi} \int_{b^-}^1 \gamma_s^-(\zeta_0, \tau) \frac{\zeta_0}{\zeta_0^2 - \zeta^2} d\zeta_0 [\Lambda^-(\zeta_0) - \Lambda(\zeta)] \\ & + \frac{1}{\pi} \int_{z_c}^{b^+} \gamma_s^+(\zeta_0, \tau) \frac{\zeta_0}{\zeta_0^2 - \zeta^2} d\zeta_0 [\Lambda^+(\zeta_0) - \Lambda(\zeta)] \} \end{aligned} \quad \text{on } 1 \leq \zeta \leq z_c \quad (3.10)$$

where $\Lambda(\zeta)$, $\Lambda^-(\zeta_0)$ and $\Lambda^+(\zeta_0)$ are the parameter integral terms defined in (3.11) to (3.13). These integral terms can be transformed into the semi-analytical forms as follows:

$$\Lambda(\zeta) = z_c E(k) - \frac{z_c}{\zeta^2} F(k) + \frac{\sqrt{(z_c^2 - \zeta^2)(\zeta^2 - 1)}}{\zeta} \{[E(k)F(\varepsilon_1 \setminus k) - F(k)E(\varepsilon_1 \setminus k)]\}$$

$$1 \leq \zeta \leq z_c \quad (5.43)$$

$$\Lambda^-(\zeta_0) = z_c [E(k) - F(k)] + \frac{\pi}{2\zeta_0} \sqrt{(z_c^2 - \zeta_0^2)(1 - \zeta_0^2)} [1 - \Lambda_0(\varepsilon_2 \setminus k)]$$

$$b^- \leq \zeta_0 \leq 1 \quad (5.44)$$

$$\Lambda^+(\zeta_0) = z_c E(k) - \frac{1}{z_c} F(k) - \frac{\pi}{2\zeta_0} \sqrt{(\zeta_0^2 - 1)(\zeta_0^2 - z_c^2)} [1 - \Lambda_0(\varepsilon_3 \setminus k)]$$

$$z_c \leq \zeta_0 \leq b^+ \quad (5.45)$$

where $F(k)$, $E(k)$ are the complete elliptic integrals of the first and second kinds, respectively, $F(\varepsilon \setminus k)$ and $E(\varepsilon \setminus k)$ are the incomplete elliptic integral of the first and second kinds, and,

$$\Lambda_0(\varepsilon \setminus k) = \frac{2}{\pi} \{F(k)E(\varepsilon \setminus k') - [F(k) - E(k)]F(\varepsilon \setminus k')\} \quad (5.46)$$

$$k = \sin \alpha = \sqrt{1 - \frac{1}{z_c^2}}, \quad k' = \cos \alpha = \frac{1}{z_c}, \quad \varepsilon_1 = \arcsin \frac{z_c}{z} \sqrt{\frac{z^2 - 1}{z_c^2 - 1}},$$

$$\varepsilon_2 = \arcsin(z_c \sqrt{\frac{1 - \zeta_0^2}{z_c^2 - \zeta_0^2}}), \quad \varepsilon_3 = \arcsin \sqrt{\frac{\zeta_0^2 - z_c^2}{\zeta_0^2 - 1}}.$$

With these integrals of $\Lambda(\zeta)$, $\Lambda^-(\zeta_0)$ and $\Lambda^+(\zeta_0)$ expressed in the semi-analytical forms of (5.43) to (5.46), the bounded vortex strength $\gamma_c(\zeta, \tau)$ can be numerically computed at each impact-time step.

At this point, we have outlined the numerical model of the 1st order solution. Next we move to the numerical model of the second order solution, with the same order of presentation.

5.2 Second Order Numerical Model

The numerical model for the 2nd order theory is very similar to that of the 1st order theory. However, the semi-analytic solutions are different, resulting in very different numerical analysis. In the 1st order theory, the solution formulation is expressed in terms of elliptic integrals. In the 2nd order theory the solution is in terms of hypergeometric function and Beta functions (see examples in (4.29) to (4.31)).

5.2.1 Numerical analysis of 2nd order velocity continuity equations

The Kutta conditions, via the kinematic boundary condition, provide two velocity continuity equations (Eq. (4.26) and Eq. (4.27)):

$$0 = \left\{ -\cos^2 \beta \cdot V(\tau) \cdot \Lambda(1) + \frac{1}{\pi} \int_{b^-}^1 \gamma_s^-(\zeta_0, \tau) \frac{\zeta_0}{\zeta_0^2 - 1} [\Lambda^-(\zeta_0) - \Lambda(1)] d\zeta_0 \right. \\ \left. + \frac{1}{\pi} \int_{z_c}^{b^+} \gamma_s^+(\zeta_0, \tau) \frac{\zeta_0}{\zeta_0^2 - 1} [\Lambda^+(\zeta_0) - \Lambda(1)] d\zeta_0 \right\} \quad \zeta \rightarrow 1^+ \quad (4.26)$$

$$\begin{aligned}
0 = & \{\cos^2 \beta \cdot V(\tau)[- \Lambda(z_c)] + \frac{1}{\pi} \int_{b^-}^1 \gamma_s^-(\zeta_0, \tau) \frac{\zeta_0}{\zeta_0^2 - z_c^2} [\Lambda^-(\zeta_0) - \Lambda(z_c)] d\zeta_0 \\
& + \frac{1}{\pi} \int_{z_c}^{b^+} \gamma_s^+(\zeta_0, \tau) \frac{\zeta_0}{\zeta_0^2 - z_c^2} [\Lambda^+(\zeta_0) - \Lambda(z_c)] d\zeta_0 \} \quad \zeta \rightarrow z_c^- \quad (4.27)
\end{aligned}$$

The fundamental integral terms $\Lambda(\zeta)$, $\Lambda^-(\zeta_0) - \Lambda(\zeta)$ and $\Lambda^+(\zeta_0) - \Lambda(\zeta)$ in Eq. (4.26) and Eq. (4.27) are derived in an analytical form developed in Appendix H, which consists of Beta functions and hypergeometric functions. The main results are listed here:

$$\begin{aligned}
\Lambda^-(\zeta_0) - \Lambda(\zeta) = & \frac{1}{2}(\zeta_0^2 - \zeta^2) \frac{1}{z_c} \cdot B\left(\frac{1}{2} - \frac{\tilde{\beta}}{\pi}, \frac{1}{2} + \frac{\tilde{\beta}}{\pi}\right) \cdot F\left(\frac{1}{2}, \frac{1}{2} - \frac{\tilde{\beta}}{\pi}; 1; \frac{z_c^2 - 1}{z_c^2}\right) \\
& - \frac{1}{2}(\zeta_0^2 - 1) \times \sum_{j=1}^N \frac{1}{\sqrt{t_j}} \cdot [\Lambda_{3,j}^+(\zeta_0) - \Lambda_{3,j+1}^+(\zeta_0)] \\
& + \frac{1}{2}(\zeta^2 - 1)(z_c^2 - \zeta^2) \times \sum_{j=1}^N \frac{1}{\sqrt{t_j}} \cdot \Delta I_{3,j}(\zeta) \\
& 1 \leq \zeta \leq z_c, \quad b^- \leq \zeta_0 \leq 1, \quad 1 < t_j < z_c^2 \quad (5.47)
\end{aligned}$$

$$\begin{aligned}
\Lambda^+(\zeta_0) - \Lambda(\zeta) = & \frac{1}{2}(\zeta_0^2 - \zeta^2) \frac{1}{z_c} \cdot B\left(\frac{1}{2} - \frac{\tilde{\beta}}{\pi}, \frac{1}{2} + \frac{\tilde{\beta}}{\pi}\right) \cdot F\left(\frac{1}{2}, \frac{1}{2} - \frac{\tilde{\beta}}{\pi}; 1; \frac{z_c^2 - 1}{z_c^2}\right) \\
& - \frac{1}{2}(z_c^2 - \zeta_0^2) \times \sum_{j=1}^N \frac{1}{\sqrt{t_j}} \cdot [\Lambda_{3,j+1}^-(\zeta_0) - \Lambda_{3,j}^-(\zeta_0)] \\
& + \frac{1}{2}(\zeta^2 - 1)(z_c^2 - \zeta^2) \times \sum_{j=1}^N \frac{1}{\sqrt{t_j}} \cdot \Delta I_{3,j}(\zeta) \\
& 1 \leq \zeta \leq z_c, \quad z_c \leq \zeta_0 \leq b^+, \quad 1 < t_j < z_c^2 \quad (5.48)
\end{aligned}$$

$$\begin{aligned}
\Lambda(\zeta) &= \frac{1}{2} z_c \cdot B\left(\frac{1}{2} - \frac{\tilde{\beta}}{\pi}, \frac{1}{2} + \frac{\tilde{\beta}}{\pi}\right) \cdot F\left(-\frac{1}{2}, \frac{1}{2} - \frac{\tilde{\beta}}{\pi}; 1; \frac{z_c^2 - 1}{z_c^2}\right) \\
&\quad + \frac{1}{2} (\zeta^2 - z_c^2 - 1) \frac{1}{z_c} \cdot B\left(\frac{1}{2} - \frac{\tilde{\beta}}{\pi}, \frac{1}{2} + \frac{\tilde{\beta}}{\pi}\right) \cdot F\left(\frac{1}{2}, \frac{1}{2} - \frac{\tilde{\beta}}{\pi}; 1; \frac{z_c^2 - 1}{z_c^2}\right) \\
&\quad - \frac{1}{2} (\zeta^2 - 1)(z_c^2 - \zeta^2) \times \sum_{j=1}^N \frac{1}{\sqrt{t_j}} \cdot \Delta I_{3,j}(\zeta)
\end{aligned}$$

$$1 \leq \zeta \leq z_c \quad (5.49)$$

where $B(\mu, \nu)$ and $F(\alpha, \beta; \gamma; z)$ are the Beta and Hypergeometric functions (refer to the section 8.38 and 9.10 of Gradshteyn and Ryzhik (1965)).

The domain of the integral $\Delta I_{3,j}(\zeta)$ in the above equations has different values according to the variation of the variable ζ (refer to (4.32) to (4.37)). To simplify the expression of the above equations define:

$$B_{11} = B\left(\frac{1}{2} - \frac{\tilde{\beta}}{\pi}, \frac{1}{2} + \frac{\tilde{\beta}}{\pi}\right) \quad (5.50)$$

$$F_{11} = F\left(-\frac{1}{2}, \frac{1}{2} - \frac{\tilde{\beta}}{\pi}; 1; \frac{z_c^2 - 1}{z_c^2}\right) \quad (5.51)$$

$$F_{12} = F\left(\frac{1}{2}, \frac{1}{2} - \frac{\tilde{\beta}}{\pi}; 1; \frac{z_c^2 - 1}{z_c^2}\right) \quad (5.52)$$

$$F_{21} = \sum_{j=1}^L \frac{1}{\sqrt{t_j}} \cdot (\Lambda_{3,j}^+ - \Lambda_{3,j+1}^+) \quad (5.53)$$

$$F_{22} = \sum_{j=1}^L \frac{1}{\sqrt{t_j}} \cdot (\Lambda_{3,j+1}^- - \Lambda_{3,j}^-) \quad (5.54)$$

Based on these notations, Eq.(5.47) to Eq.(5.49) can be expressed in the following

form:

$$\begin{aligned} \Lambda(\zeta) &= \frac{1}{2} z_c \cdot B_{11} \cdot F_{11} + \frac{1}{2} (\zeta^2 - z_c^2 - 1) \frac{1}{z_c} \cdot B_{11} \cdot F_{12} \\ &\quad - \frac{1}{2} (\zeta^2 - 1)(z_c^2 - \zeta^2) \times \sum_{j=1}^N \frac{1}{\sqrt{t_j}} \cdot \Delta I_{3,j}(\zeta) \end{aligned} \quad 1 \leq \zeta \leq z_c \quad (5.55)$$

$$\begin{aligned} \Lambda^-(\zeta_0) - \Lambda(\zeta) &= \frac{1}{2} (\zeta_0^2 - \zeta^2) \frac{1}{z_c} \cdot B_{11} \cdot F_{12} \\ &\quad - \frac{1}{2} (\zeta_0^2 - 1) \times F_{21}(\zeta_0) \\ &\quad + \frac{1}{2} (\zeta^2 - 1)(z_c^2 - \zeta^2) \times \sum_{j=1}^N \frac{1}{\sqrt{t_j}} \cdot \Delta I_{3,j}(\zeta) \end{aligned} \quad 1 \leq \zeta \leq z_c, b^- \leq \zeta_0 \leq 1, 1 < t_j < z_c^2 \quad (5.56)$$

$$\begin{aligned} \Lambda^+(\zeta_0) - \Lambda(\zeta) &= \frac{1}{2} (\zeta_0^2 - \zeta^2) \frac{1}{z_c} \cdot B_{11} \cdot F_{12} \\ &\quad - \frac{1}{2} (z_c^2 - \zeta_0^2) \times F_{22}(\zeta_0) \\ &\quad + \frac{1}{2} (\zeta^2 - 1)(z_c^2 - \zeta^2) \times \sum_{j=1}^N \frac{1}{\sqrt{t_j}} \cdot \Delta I_{3,j}(\zeta) \end{aligned} \quad 1 \leq \zeta \leq z_c, z_c \leq \zeta_0 \leq b^+, 1 < t_j < z_c^2 \quad (5.57)$$

Recall in Chapter 4, we have introduced that the solution domain for the kinematic boundary condition is $1 \leq \zeta \leq z_c$ (refer to Fig. 2.5), and there are two singular points at $\zeta = 1$ and $\zeta = z_c$. When $\zeta = 1$ or $\zeta = z_c$, where $\chi(\zeta) \rightarrow \infty$. Therefore, in the derivation of the velocity continuity conditions (refer to Eq. (4.26) and Eq. (4.27)), we set that $\zeta \rightarrow 1^+$, $\zeta \rightarrow (z_c)$ and require that the unbounded terms disappear.

For $\zeta \rightarrow 1^+$, in the numerical formula of the integral $\Delta I_{3,j}(\zeta)$, $\zeta^2 < t_j$, thus the case 2 formulation applies (refer to (4.34), (4.35) and (5.55)):

$$\begin{aligned}\Lambda(1) &= \frac{1}{2} z_c \cdot B_{11} \cdot F_{11} + \frac{1}{2} (-z_c^2) \frac{1}{z_c} \cdot B_{11} \cdot F_{12} \\ &= \frac{1}{2} z_c \cdot B_{11} \cdot [F_{11} - F_{12}]\end{aligned}\tag{5.58}$$

For $\zeta \rightarrow (z_c)$, in the numerical formula of the integral $\Delta I_{3,j}(\zeta)$, $\zeta^2 > t_{j+1}$, the case 1 formulation applies (refer to (5.55), (4.32) and (4.33)):

$$\begin{aligned}\Lambda(z_c) &= \frac{1}{2} z_c \cdot B_{11} \cdot F_{11} + \frac{1}{2} (-1) \frac{1}{z_c} \cdot B_{11} \cdot F_{12} \\ &= \frac{1}{2} B_{11} (z_c \cdot F_{11} - \frac{1}{z_c} \cdot F_{12})\end{aligned}\tag{5.59}$$

Therefore, from (5.56) and (5.57),

$$\Lambda^-(\zeta_0) - \Lambda(1) = \frac{1}{2} (\zeta_0^2 - 1) \frac{1}{z_c} \cdot B_{11} \cdot F_{12} - \frac{1}{2} (\zeta_0^2 - 1) \times F_{21}(\zeta_0) \quad b^- \leq \zeta_0 \leq 1 \tag{5.60}$$

$$\Lambda^-(\zeta_0) - \Lambda(z_c) = \frac{1}{2} (\zeta_0^2 - z_c^2) \frac{1}{z_c} \cdot B_{11} \cdot F_{12} - \frac{1}{2} (\zeta_0^2 - 1) \times F_{21}(\zeta_0) \quad b^- \leq \zeta_0 \leq 1 \tag{5.61}$$

$$\Lambda^+(\zeta_0) - \Lambda(1) = \frac{1}{2} (\zeta_0^2 - 1) \frac{1}{z_c} \cdot B_{11} \cdot F_{12} - \frac{1}{2} (z_c^2 - \zeta_0^2) \times F_{22}(\zeta_0) \quad z_c \leq \zeta_0 \leq b^+ \tag{5.62}$$

$$\Lambda^+(\zeta_0) - \Lambda(z_c) = \frac{1}{2} (\zeta_0^2 - z_c^2) \frac{1}{z_c} \cdot B_{11} \cdot F_{12} - \frac{1}{2} (z_c^2 - \zeta_0^2) \times F_{22}(\zeta_0) \quad z_c \leq \zeta_0 \leq b^+ \tag{5.63}$$

Substituting the above integral expressions into the velocity continuity equations in Eq.(4.26) and Eq.(4.27), the following system of equations is obtained:

$$\begin{aligned}
0 = & -\cos^2 \beta \cdot V(\tau) \cdot \frac{1}{2} z_c \cdot B_{11} \cdot [F_{11} - F_{12}] \\
& + \frac{1}{\pi} \cdot \frac{1}{2} \frac{1}{z_c} \cdot B_{11} \cdot F_{12} \cdot \int_{b^-}^1 \gamma_S^-(\zeta_0, \tau) \zeta_0 d\zeta_0 \\
& - \frac{1}{\pi} \cdot \frac{1}{2} \cdot \int_{b^-}^1 \gamma_S^-(\zeta_0, \tau) \zeta_0 \cdot F_{21}(\zeta_0) \cdot d\zeta_0 \quad \zeta \rightarrow 1^+ \quad (5.64) \\
& + \frac{1}{\pi} \cdot \frac{1}{2} \cdot \frac{1}{z_c} \cdot B_{11} \cdot F_{12} \cdot \int_{z_c}^{b^+} \gamma_S^+(\zeta_0, \tau) \zeta_0 d\zeta_0 \\
& + \frac{1}{\pi} \cdot \frac{1}{2} \cdot \int_{z_c}^{b^+} \gamma_S^+(\zeta_0, \tau) \frac{\zeta_0}{\zeta_0^2 - 1} (\zeta_0^2 - z_c^2) \cdot F_{22}(\zeta_0) d\zeta_0
\end{aligned}$$

$$\begin{aligned}
0 = & -\cos^2 \beta \cdot V(\tau) \cdot \frac{1}{2} \cdot B_{11} \cdot [z_c \cdot F_{11} - \frac{1}{z_c} \cdot F_{12}] \\
& + \frac{1}{\pi} \cdot \frac{1}{2} \frac{1}{z_c} \cdot B_{11} \cdot F_{12} \cdot \int_{b^-}^1 \gamma_S^-(\zeta_0, \tau) \zeta_0 d\zeta_0 \\
& - \frac{1}{\pi} \cdot \frac{1}{2} \cdot \int_{b^-}^1 \gamma_S^-(\zeta_0, \tau) \frac{\zeta_0}{\zeta_0^2 - z_c^2} (\zeta_0^2 - 1) \cdot F_{21}(\zeta_0) d\zeta_0 \quad \zeta \rightarrow z_c \quad (5.65) \\
& + \frac{1}{\pi} \cdot \frac{1}{2} \frac{1}{z_c} \cdot B_{11} \cdot F_{12} \cdot \int_{z_c}^{b^+} \gamma_S^+(\zeta_0, \tau) \zeta_0 d\zeta_0 \\
& + \frac{1}{\pi} \frac{1}{2} \cdot \int_{z_c}^{b^+} \gamma_S^+(\zeta_0, \tau) \zeta_0 \cdot F_{22}(\zeta_0) d\zeta_0
\end{aligned}$$

Discretization Eq.(5.64) and Eq. (5.65), the following two equations for satisfying the velocity continuity conditions results:

$$\begin{aligned}
& \cos^2 \beta \cdot V(\tau) \cdot \frac{1}{2} \cdot z_c \cdot B_{11} \cdot [F_{11} - F_{12}] = \\
& + \frac{1}{\pi} \cdot \frac{1}{2} \cdot \frac{1}{z_c} F_{12} \cdot B_{11} \cdot \sum_{j=1}^{N_j^-} \gamma_{S,j}^-(\tau) \cdot I_{11} - \frac{1}{\pi} \cdot \frac{1}{2} \cdot \sum_{j=1}^{N_j^-} \gamma_{S,j}^-(\tau) \cdot F_{21}(\zeta_j^-) \cdot I_{11} \\
& + \frac{1}{\pi} \cdot \frac{1}{2} \cdot \frac{1}{z_c} F_{12} \cdot B_{11} \cdot \sum_{j=1}^{N_j^+} \gamma_{S,j}^+(\tau) \cdot I_{21} + \frac{1}{\pi} \cdot \frac{1}{2} \cdot \sum_{j=1}^{N_j^+} \gamma_{S,j}^+(\tau) \cdot F_{22}(\zeta_j^+) \cdot [I_{21} - (z_c^2 - 1)I_{22}]
\end{aligned} \tag{5.66}$$

$$\begin{aligned}
& \cos^2 \beta \cdot V(\tau) \cdot \frac{1}{2} \cdot B_{11} [z_c \cdot F_{11} - \frac{1}{z_c} \cdot F_{12}] = \\
& + \frac{1}{\pi} \cdot \frac{1}{2} \cdot \frac{1}{z_c} F_{12} \cdot B_{11} \cdot \sum_{j=1}^{N_j^-} \gamma_{S,j}^-(\tau) \cdot I_{11} - \frac{1}{\pi} \cdot \frac{1}{2} \cdot \sum_{j=1}^{N_j^-} \gamma_{S,j}^-(\tau) \times F_{21}(\zeta_j^-) \cdot [I_{11} + (z_c^2 - 1) \cdot I_{12}] \\
& + \frac{1}{\pi} \cdot \frac{1}{2} \cdot \frac{1}{z_c} \cdot B_{11} \cdot F_{12} \cdot \sum_{j=1}^{N_j^+} \gamma_{S,j}^+(\tau) \cdot I_{21} + \frac{1}{\pi} \cdot \frac{1}{2} \cdot \sum_{j=1}^{N_j^+} \gamma_{S,j}^+(\tau) \times F_{22}(\zeta_j^+) \cdot I_{21}
\end{aligned} \tag{5.67}$$

where (referring to (5.3) to (5.8) for 1st order theory),

$$I_{11} = \int_{\zeta_j^- - \frac{\epsilon_j^-}{2}}^{\zeta_j^- + \frac{\epsilon_j^-}{2}} \zeta_0 d\zeta_0 = \frac{1}{2} [(\zeta_j^- + \frac{\epsilon_j^-}{2})^2 - (\zeta_j^- - \frac{\epsilon_j^-}{2})^2] \tag{5.68}$$

$$I_{12} = \int_{\zeta_j^- - \frac{\epsilon_j^-}{2}}^{\zeta_j^- + \frac{\epsilon_j^-}{2}} \frac{\zeta_0}{\zeta_0^2 - z_c^2} d\zeta_0 = \frac{1}{2} \ln(z_c^2 - \zeta^2) \Big|_{\zeta_j^- - \frac{\epsilon_j^-}{2}}^{\zeta_j^- + \frac{\epsilon_j^-}{2}} = \ln \sqrt{\frac{z_c^2 - (\zeta_j^- + \frac{\epsilon_j^-}{2})^2}{z_c^2 - (\zeta_j^- - \frac{\epsilon_j^-}{2})^2}} \tag{5.69}$$

$$I_{21} = \int_{\zeta_j^+ - \frac{\epsilon_j^+}{2}}^{\zeta_j^+ + \frac{\epsilon_j^+}{2}} \zeta_0 d\zeta_0 = \frac{1}{2} [(\zeta_j^+ + \frac{\epsilon_j^+}{2})^2 - (\zeta_j^+ - \frac{\epsilon_j^+}{2})^2] \tag{5.70}$$

$$I_{22} = \int_{\zeta_j^+ - \frac{\epsilon_j^+}{2}}^{\zeta_j^+ + \frac{\epsilon_j^+}{2}} \frac{\zeta_0}{\zeta_0^2 - 1} d\zeta_0 = \frac{1}{2} \ln(\zeta_0^2 - 1) \Big|_{\zeta_j^+ - \frac{\epsilon_j^+}{2}}^{\zeta_j^+ + \frac{\epsilon_j^+}{2}} = \ln \sqrt{\frac{(\zeta_j^+ + \frac{\epsilon_j^+}{2})^2 - 1}{(\zeta_j^+ - \frac{\epsilon_j^+}{2})^2 - 1}} \tag{5.71}$$

Define the following coefficients in the above equations to simplify the expressions (refer to (5.13) to (5.16) for 1st order theory):

$$C_j^{11} = \frac{1}{\pi} \cdot \frac{1}{2} \cdot \frac{1}{z_c} F_{12} \cdot B_{11} \cdot I_{11} - \frac{1}{\pi} \cdot \frac{1}{2} \cdot F_{21}(\zeta_j^-) \cdot I_{11} \quad (5.72)$$

$$C_j^{12} = \frac{1}{\pi} \cdot \frac{1}{2} \cdot \frac{1}{z_c} F_{12} \cdot B_{11} \cdot I_{21} + \frac{1}{\pi} \cdot \frac{1}{2} \cdot F_{22}(\zeta_j^+) [I_{21} - (z_c^2 - 1)I_{22}] \quad (5.73)$$

$$C_j^{21} = \frac{1}{\pi} \cdot \frac{1}{2} \cdot \frac{1}{z_c} F_{12} \cdot B_{11} \cdot I_{11} - \frac{1}{\pi} \cdot \frac{1}{2} \cdot F_{21}(\zeta_j^-) \cdot [I_{11} + (z_c^2 - 1) \cdot I_{12}] \quad (5.74)$$

$$C_j^{22} = \frac{1}{\pi} \cdot \frac{1}{2} \cdot \frac{1}{z_c} \cdot B_{11} \cdot F_{12} \cdot I_{21} + \frac{1}{\pi} \cdot \frac{1}{2} \cdot F_{22}(\zeta_j^+) \cdot I_{21} \quad (5.75)$$

Comparing the coefficients in (5.72) to (5.75) with the corresponding coefficients of (5.13) to (5.16) in 1st order numerical models, it is shown that these coefficients play the same roles in the numerical models, but with different numerical evaluations.

The two coupled equations are then expressed as follows (refer to (5.11) and (5.12)),

$$\cos^2 \beta \cdot V(\tau) \cdot \frac{1}{2} \cdot z_c \cdot B_{11} \cdot [F_{11} - F_{12}] = \sum_{j=1}^{N_i^-} \gamma_{s,j}^-(\tau) \cdot C_j^{11} + \sum_{j=1}^{N_i^+} \gamma_{s,j}^+(\tau) \cdot C_j^{12} \quad (5.76)$$

$$\cos^2 \beta \cdot V(\tau) \cdot \frac{1}{2} \cdot B_{11} [z_c \cdot F_{11} - \frac{1}{z_c} \cdot F_{12}] = \sum_{j=1}^{N_i^-} \gamma_{s,j}^-(\tau) \cdot C_j^{21} + \sum_{j=1}^{N_i^+} \gamma_{s,j}^+(\tau) C_j^{22} \quad (5.77)$$

The unknowns at any time step i will be $\gamma_{S,N_i^-}^- (\tau_i)$ and $\gamma_{S,1}^+ (\tau_i)$ as described in the 1st order solution. Separating the unknowns, and grouping the known terms together gives the corresponding equations of the 1st order solution ((5.19) and (5.20)):

$$R_1 = \cos^2 \beta \cdot V(\tau) \cdot \frac{1}{2} \cdot z_c \cdot B_{11} \cdot [F_{11} - F_{12}] - \sum_{j=1}^{N_i^- - 1} \gamma_{S,j}^- (\tau) \cdot C_j^{11} - \sum_{j=2}^{N_i^+} \gamma_{S,j}^+ (\tau) \cdot C_j^{12} \quad (5.78)$$

$$R_2 = \cos^2 \beta \cdot V(\tau) \cdot \frac{1}{2} \cdot B_{11} [z_c \cdot F_{11} - \frac{1}{z_c} \cdot F_{12}] - \sum_{j=1}^{N_i^- - 1} \gamma_{S,j}^- (\tau) \cdot C_j^{21} - \sum_{j=2}^{N_i^+} \gamma_{S,j}^+ (\tau) \cdot C_j^{22} \quad (5.79)$$

The system equations in the compact form for the 1st order solution are (refer to (5.21), (5.22)):

$$\gamma_{S,N_i^-}^- (\tau) C_{N_i^-}^{11} + \gamma_{S,1}^+ (\tau) \cdot C_1^{12} = R_1 \quad (5.80)$$

$$\gamma_{S,N_i^-}^- (\tau) C_{N_i^-}^{21} + \gamma_{S,1}^+ (\tau) \cdot C_1^{22} = R_2 \quad (5.81)$$

Proceeding as in the 1st order case, define the determinant from (5.80) and (5.81):

$$\Delta = C_{N_i^-}^{11} \cdot C_1^{22} - C_{N_i^-}^{21} \cdot C_1^{12} \quad (5.82)$$

The solutions of the unknowns are therefore again (refer to (5.24), (5.25)):

$$\gamma_{S,N_i^-}^- (\tau_i) = \frac{R_1 \cdot C_1^{22} - R_2 \cdot C_1^{12}}{\Delta} \quad (5.83)$$

$$\gamma_{s,1}^+(\tau_i) = \frac{C_{N_i^-}^{11} \cdot R_2 - C_{N_i^-}^{21} \cdot R_1}{\Delta} \quad (5.84)$$

Therefore, based on the velocity continuity conditions and the vortex distribution of the previous time step, the vortex element strengths shed at a new time are from Eq.(5.83) and Eq.(5.84).

Comparing the above numerical model of the velocity continuity conditions with the numerical model in the 1st order theory, it is seen that equations are of the identical final form, but the coefficients of the equations are different in detail.

5.2.2 Numerical model of displacement continuity equations

The displacement continuity equation derived in Eq. (4.58) is:

$$0 = (\tilde{Y}_{wl} + \tan \beta) \cdot I_1 - \tan \beta \cdot I_2 \quad (4.58)$$

The displacement continuity condition is readily computed numerically when the integral terms I_1 and I_2 are known. The semi-analytic form of the integrals I_1 and I_2 can be derived mathematically. For the variable transformation of the integral I_1 in (4.56), we first set the variable transformation $t = \zeta^2$, then define the new variable transformation $x = t - (b^-)^2$, and finally use the integral formula in Gradshteyn and Ryzhik (1965, p287, §3.197.8). The integral I_1 has the following analytical form; refer to Appendix B for details:

$$\begin{aligned}
I_1 &= \int_{\zeta=b^-}^{b^+} \frac{d\zeta}{\chi^*(\zeta)(b^{+2} - \zeta^2)} \\
&= \frac{1}{2} \frac{(b^+)^2 - (b^-)^2}{b^-} \cdot B\left(\frac{1}{2} - \frac{\tilde{\beta}}{\pi}, \frac{3}{2} + \frac{\tilde{\beta}}{\pi}\right) \cdot {}_2F_1\left(\frac{1}{2}; \frac{3}{2} + \frac{\tilde{\beta}}{\pi}; 2; -\frac{(b^+)^2 - (b^-)^2}{(b^-)^2}\right)
\end{aligned} \tag{5.85}$$

where $B\left(\frac{1}{2} - \frac{\tilde{\beta}}{\pi}, \frac{3}{2} + \frac{\tilde{\beta}}{\pi}\right)$ is the Beta function, and,

$${}_2F_1\left(\frac{1}{2}; \frac{3}{2} + \frac{\tilde{\beta}}{\pi}; 2; -\frac{(b^+)^2 - (b^-)^2}{(b^-)^2}\right) = F\left(\frac{1}{2}; \frac{3}{2} + \frac{\tilde{\beta}}{\pi}; 2; -\frac{(b^+)^2 - (b^-)^2}{(b^-)^2}\right) \quad \text{is Gauss'}$$

hypergeometric function.

Gradshteyn and Ryzhik (1965) provides an integral transformation for the hypergeometric function:

$$F(\alpha, \beta, \gamma; z) = (1-z)^{-\alpha} F\left(\alpha, \gamma - \beta, \gamma; \frac{z}{z-1}\right) \tag{5.86}$$

Applying Eq. (5.86) to (5.85), the integration I_1 has the following easily computable semi-analytical form:

$$I_1 = \frac{1}{2} \frac{b^{+2} - (b^-)^2}{b^+} \cdot B\left(\frac{1}{2} - \frac{\tilde{\beta}}{\pi}, \frac{3}{2} + \frac{\tilde{\beta}}{\pi}\right) \cdot F\left(\frac{1}{2}, \frac{1}{2} - \frac{\tilde{\beta}}{\pi}; 2; \frac{b^{+2} - (b^-)^2}{b^{+2}}\right) \tag{5.87}$$

Similarly the integral I_2 has the semi-analytical form (refer to Appendix B):

$$\begin{aligned}
I_2 &= \int_{\zeta=b^-}^{b^+} \frac{\zeta \cdot d\zeta}{\chi^*(\zeta)(b^{+2} - \zeta^2)} \\
&= \frac{1}{2}(b^{+2} - (b^-)^2) \cdot B\left(\frac{1}{2} - \frac{\tilde{\beta}}{\pi}, \frac{3}{2} + \frac{\tilde{\beta}}{\pi}\right)
\end{aligned} \tag{5.88}$$

Again, comparing the displacement conditions in the 2nd order model with that in the 1st order, it is shown that the displacement continuity equations are of the same form, but the expressions of the integrals I_1 and I_2 (refer to (5.34), (5.37) and (5.87), (5.88)) are functionally different.

5.2.3 Numerical model of pressure continuity equations

The pressure continuity equations are derived in Eq. (4.59), Eq. (4.60) and Eq. (4.61) for the steady planing problem. In steady planing, the numerical model of the pressure continuity conditions for the 2nd order theory is the same as that for the 1st order theory. To avoid redundancy, we just refer to the numerical model in the 1st order theory in the Section 5.1.3.

5.2.4 Numerical model of bound vortex distribution $\gamma_c(\zeta, \tau)$

The bound vortex distribution $\gamma_c(\zeta, \tau)$ representation in Eq.(4.20) has two terms: the normal component in Eq. (4.21) and the singular component in Eq. (4.22). Since the singularity has been removed from the singular component in Eq. (4.22) by the velocity

continuity requirements, we call the component in Eq. (4.22) the de-singular term from now on.

5.2.4.1 Computation of the $\gamma_{normal}(\zeta, \tau)$ term

Discretizing the integrals of the normal term in (4.21), the segment of the free jet region $b^- \leq \zeta_0 \leq 1$ is divided into $N_i^-(\tau)$ elements at different times τ_i as described in the Section 5.1.3. Similarly, the segment of the region of $z_c \leq \zeta_0 \leq b^+$ is divided into $N_i^+(\tau)$ elements.

Therefore, the normal term of the bound vortex will be:

$$\begin{aligned} \gamma_{C,normal}(\zeta, \tau) &= -2 \sin \tilde{\beta} \cos \tilde{\beta} \cos^2 \beta \cdot V(\tau) \\ &+ 2 \sin \tilde{\beta} \cos \tilde{\beta} \frac{1}{\pi} \cdot \sum_{i=1}^{N_i^-} 2V_s^-(i, \tau) J_{12}(\zeta_i^-, \zeta) \\ &+ 2 \sin \tilde{\beta} \cos \tilde{\beta} \frac{1}{\pi} \cdot \sum_{i=1}^{N_i^+} 2V_s^+(i, \tau) J_{22}(\zeta_i^+, \zeta) \end{aligned} \quad (5.89)$$

where $V_s^+(\zeta, \tau)$ and $V_s^-(\zeta, \tau)$ are the jet velocities, distributed on the free sheets according to Fig. 5.2 and Fig. 5.3, and the $J_{i,j}$ ($i, j = 1, 2$) coefficients are defined as the integrals appearing in (4.21):

$$J_{12} = \int_{\zeta_j^-}^{\zeta_{j+1}^-} \frac{\zeta_0}{\zeta_0^2 - \zeta^2} d\zeta_0 = - \int_{\zeta_j^-}^{\zeta_{j+1}^-} \frac{\zeta_0}{\zeta^2 - \zeta_0^2} d\zeta_0 = \ln \sqrt{\left| \frac{\zeta^2 - \zeta_{j+1}^{-2}}{\zeta^2 - \zeta_j^{-2}} \right|} \quad (5.90)$$

$$J_{22} = \int_{\zeta_j^+}^{\zeta_{j+1}^+} \frac{\zeta_0}{\zeta_0^2 - \zeta^2} d\zeta_0 = \frac{1}{2} \ln(\zeta_0^2 - \zeta^2) \Big|_{\zeta_j^+}^{\zeta_{j+1}^+} = \ln \sqrt{\frac{\zeta_{j+1}^{+2} - \zeta^2}{\zeta_j^{+2} - \zeta^2}} \quad (5.91)$$

5.2.4.2 Computation of the $\gamma_{de-singular}(\zeta, \tau)$ term

It is convenient to represent the de-singular term in (4.22) as the sum of three individual terms.

$$\gamma_{c,dis-singular}(\zeta, \tau) = \gamma_c^0(\zeta, \tau) + \gamma_c^-(\zeta, \tau) + \gamma_c^+(\zeta, \tau) \quad (5.92)$$

where

$$\gamma_c^0(\zeta, \tau) = \frac{4z}{\pi} \chi(\zeta) \cos^2 \tilde{\beta} \cdot \cos^2 \beta \cdot V(\tau) [-\Lambda(\zeta)] \quad (5.93)$$

$$\gamma_c^-(\zeta, \tau) = \frac{4\zeta}{\pi^2} \cos^2 \tilde{\beta} \cdot \chi(\zeta) \cdot \int_{b^-}^1 \gamma_s^-(\zeta_0, \tau) \frac{\zeta_0}{\zeta_0^2 - \zeta^2} d\zeta_0 [\Lambda^-(\zeta_0) - \Lambda(\zeta)] \quad (5.94)$$

$$\gamma_c^+(\zeta, \tau) = \frac{4\zeta}{\pi^2} \cos^2 \tilde{\beta} \cdot \chi(\zeta) \cdot \int_{z_c}^{b^+} \gamma_s^+(\zeta_0, \tau) \frac{\zeta_0}{\zeta_0^2 - \zeta^2} d\zeta_0 [\Lambda^+(\zeta_0) - \Lambda(\zeta)] \quad (5.95)$$

where the integral terms $\Lambda(\zeta)$, $\Lambda^-(\zeta_0) - \Lambda(\zeta)$ and $\Lambda^+(\zeta_0) - \Lambda(\zeta)$ are given in (5.47), (5.48) and (5.49).

The above integrals in (5.93), (5.94) and (5.95) can be analytically transformed to the following easily-computed forms in terms of standard special functions. The details are in Appendix E.

The $\gamma_c^0(\zeta, \tau)$ has following form:

$$\begin{aligned} \gamma_c^0(\zeta, \tau) = & -\frac{2\zeta}{\pi} \chi(\zeta) \cos^2 \tilde{\beta} \cdot \cos^2 \beta \cdot V(\tau) \cdot z_c \cdot B_{11} \cdot F_{11} \\ & -\frac{2\zeta}{\pi} \chi(\zeta) \cos^2 \tilde{\beta} \cdot \cos^2 \beta \cdot V(\tau) \cdot (\zeta^2 - z_c^2 - 1) \frac{1}{z_c} \cdot B_{11} \cdot F_{12} \\ & +\frac{2\zeta}{\pi} \chi(\zeta) \cos^2 \tilde{\beta} \cdot \cos^2 \beta \cdot V(\tau) \cdot (\zeta^2 - 1)(z_c^2 - \zeta^2) \times \sum_{j=1}^L \frac{1}{\sqrt{t_j}} \cdot \Delta I_{3,j}(\zeta) \end{aligned} \quad (5.96)$$

where B_{11} , F_{11} , F_{12} , $\Delta I_{3,j}$ defined in Section 5.2.1.

Substituting the definite integrals in Eq. (5.56) into the equation of $\gamma_c^-(\zeta, \tau)$, (5.94), yields the numerical formula of $\gamma_c^-(\zeta, \tau)$:

$$\begin{aligned} \gamma_c^-(\zeta, \tau) = & -\frac{2\zeta}{\pi^2} \cos^2 \tilde{\beta} \cdot \chi(\zeta) \cdot \frac{1}{z_c} \cdot B_{11} \cdot F_{12} \cdot \sum_{i=1}^{N_i^-(\tau)} 2 \cdot V_S^-(i, \tau) \cdot J_{11}(i) \\ & +\frac{2\zeta}{\pi^2} \cos^2 \tilde{\beta} \cdot \chi(\zeta) \cdot \sum_{i=1}^{N_i^-(\tau)} 2 \cdot V_S^-(i, \tau) \times F_{21}(\zeta_i^-) \cdot [J_{11}(i) + (z^2 - 1)J_{12}(i)] \\ & -\frac{2\zeta}{\pi^2} \cos^2 \tilde{\beta} \cdot \chi(\zeta) \cdot (\zeta^2 - 1)(z_c^2 - \zeta^2) \times \sum_{j=1}^L \frac{1}{\sqrt{t_j}} \cdot \Delta I_{3,j}(\zeta) \cdot \sum_{i=1}^{N_i^-(\tau)} 2 \cdot V_S^-(i, \tau) \cdot J_{12}(i) \end{aligned} \quad 1 \leq \zeta \leq z_c \quad (5.97)$$

where B_{11} , F_{12} , F_{21} and $\Delta I_{3,j}$ defined in Section 5.2.1, the integral J_{12} defined in (5.90)

and the integral J_{11} term is,

$$J_{11}(\zeta_i^-) = \int_{\zeta_i^-}^{\zeta_{i+1}^-} \zeta_0 d\zeta_0 = \frac{1}{2}[(\zeta_{i+1}^-)^2 - (\zeta_i^-)^2] \quad (5.98)$$

Similarly, numerically discretizing the equation of $\gamma_c^+(\zeta, \tau)$ in Eq. (5.95) yields

the numerical formula of $\gamma_c^+(\zeta, \tau)$:

$$\begin{aligned} \gamma_c^+(\zeta, \tau) = & -\frac{2\zeta}{\pi^2} \cos^2 \tilde{\beta} \cdot \chi(\zeta) \cdot \frac{1}{z_c} \cdot B_{11} \cdot F_{12} \cdot \sum_{i=1}^{N_i^+(\tau)} 2 \cdot V_S^+(i, \tau) \cdot J_{21}(i) \\ & + \frac{2\zeta}{\pi^2} \cos^2 \tilde{\beta} \cdot \chi(\zeta) \cdot \sum_{i=1}^{N_i^+(\tau)} 2 \cdot V_S^+(i, \tau) \times F_{22}(\zeta_i^+) \cdot [-J_{21}(i) + (z_c^2 - \zeta^2) J_{22}(i)] \\ & - \frac{2\zeta}{\pi^2} \cos^2 \tilde{\beta} \cdot \chi(\zeta) \cdot (\zeta^2 - 1)(z_c^2 - \zeta^2) \times \sum_{j=1}^L \frac{1}{\sqrt{t_j}} \cdot \Delta I_{3,j}(\zeta) \cdot \sum_{i=1}^{N_i^+(\tau)} 2 \cdot V_S^+(i, \tau) \cdot J_{22}(i) \end{aligned}$$

(5.99)

where B_{11} , F_{12} , F_{22} and $\Delta I_{3,j}$ are defined in Section 5.2.1, the integral J_{22} defined in

(5.91), and the integral J_{21} term is,

$$J_{21}(\zeta_i^+) = \int_{\zeta_i^+}^{\zeta_{i+1}^+} \zeta_0 d\zeta_0 = \frac{1}{2}[(\zeta_{i+1}^+)^2 - (\zeta_i^+)^2] \quad (5.100)$$

To this point, the most important formulations for the 1st and 2nd order in the steady planing have been given. The numerical model for dynamics in waves (seakeeping) uses the basic elements of the steady planing solution as an inner loop in the time integration (refer to discussion in section 3.2 of Chapter 3). The algorithm for the multi-step time marching for both the 1st and 2nd order seakeeping dynamics models is covered in the next chapter.

CHAPTER 6

TIME DOMAIN NUMERICAL SOLUTION

6.1 Solution Procedures

The time domain solution leading to a steady planning is also included as the case of zero wave height in the solution procedure for seaway dynamics. The dynamics solution has only the additional multi-time marching loops. Therefore, instead of explaining both, we concentrate on the solution procedure for seakeeping dynamics in this chapter, which uses the numerical procedures of the last chapter in $x -$ problem in the time marching steps. The solution procedure is the same for both the 1st and the 2nd order models, other than in details.

The data flow of the solution procedure is listed in the following "NewCat2-4" flow chart (see Fig. 6.1), which is the same as in the original 1st order CatSea2-4a code. The system solution is carried-out numerically in a time-marching, multiple-nested iteration of the semi-analytic solution formulae (see Chapter 5). Generally, the following steps are executed (refer to Fig. 6.1):

Step 1: Start at the time step loop $\tau = \tau_0$, where τ is the non-dimensional time, the time step index $IALL = 0, 1, 2, \dots, N_T$, N_T is the total time step number. At each time step, repeat the following steps (refer to the box 5 in Fig. 6.1).

Step 2: Start the vessel loop (the main body and the transverse steps); index $MHUL = 1, 2, 3, \dots, N_{HULL}$. For each hull/segment between any transverse steps, repeat the following steps and then go to Step 9 (refer to the box 7 in Fig. 6.1).

Step 3: Find the transient wetted length $L(\tau)$ or, $x_{\max}(\tau)$ at each time step (refer to the box 10 in Fig. 6.1). The numerical algorithm may refer to (3.97), (4.92) and Appendix I. This step is searching for the point where the sectional draft $Y_k(x_p, \tau) = 0$ (refer to Fig. 3.8); the correspondent vessel water line length will then be the wetted length $L(\tau) = x_p$.

Step 4: Set up the initial parameters or the initial condition of the entry section (see Vorus (1996) and refer to box 11 and 12 in Fig. 6.1).

Step 5: Set the x - section discretization along the length in the index $i = 1, 2, \dots, M$ (refer to the box 13 in Fig. 6.1). As described in Chapter 3 and Chapter 4, the x - problem is computed at each time step as in steady planing, but with the additional velocities and displacements associated with the craft motion and the sea waves. This uses the same time dependent impact solution; the numerical formulae have been given in Chapter 5.

Step 6: At each x - section, iterate to solve the system equations, (refer to Chapter 5 and the box 14 to box 18 in Fig. 6.1).

- Interpolate to get the geometry function values; for example, keel camber $y_k(x)$, average deadrise angle $\beta_0(x)$, etc., for the specified section $x = x_i$;

- Compute the incoming wave field in the seakeeping case (refer to (3.77), (3.79) and (4.86), (4.87) for details); for the dynamic evolution to steady planing from an arbitrary initial state the wave elevation will be set to zero;
- Calculate the sectional impact velocity $V(x,t)$ (refer to (3.105) and (4.94));
- Find the solutions for the chine-unwetted flow or the chine-wetted flow. In the chine-unwetted flow phase, iterate at each x_i to find the solution for $V_j^+(x)$, $V_j^-(x)$, $z_b^+(x)$, $z_b^-(x)$ and $z_c^+(x)$, (refer to (5.24), (5.25), (5.27), (3.54), (3.56) for the 1st order model and (5.83), (5.84), (4.58), (4.59), (4.61) for the 2nd order model). In the chine-wetted flow phase, iterate to find the solution for $V_j^+(x)$, $V_j^-(x)$, $z_b^+(x)$, $z_b^-(x)$ (refer to (5.24), (5.25), (3.55), (3.56) for the 1st order model and (5.83), (5.84), (4.60), (4.61) for the 2nd order model);
- Solve for the bound vortex distribution $\gamma_c(\zeta)$, $1 \leq \zeta \leq z_c$, refer to (3.10), (5.43), (5.44), (5.45) for the 1st order model and (5.89), (5.92) for the 2nd order model;
- Solve for the tangential velocity on the side-hull:

$$V_s(x; \zeta, \tau) = -\frac{1}{2} \gamma_c(\zeta, \tau) + V(x, \tau) \sin \beta(x, \zeta) \quad (6.1)$$

- Solve for the pressure distribution $C_p(\zeta)$ $1 \leq \zeta \leq z_c$. For the 1st order model, refer to (3.74), (3.75). For the 2nd order model, refer to (4.84), (4.85).
- Compute the sectional hydrodynamic lift and drag $C_L(x)$ and $C_D(x)$ coefficients, (refer to (3.86)).

Step 7: At each x – section, repeat Step 6. Then integrate total hydrodynamic lift force and drag forces along the vessel length appropriately to produce the x-y plane hydrodynamic forces and moments (refer to the box 19 in Fig. 6.1).

Step 8: Add the aerodynamic force and moment components and the hydrostatic force and moment components to the hydrodynamic components from step 7 (refer to the box 20, 21 in Fig. 6.1). The aero-dynamic forces have been predicted from a low-aspect-ratio wing model representing the cross-over structure connecting the catamaran demi-hulls.

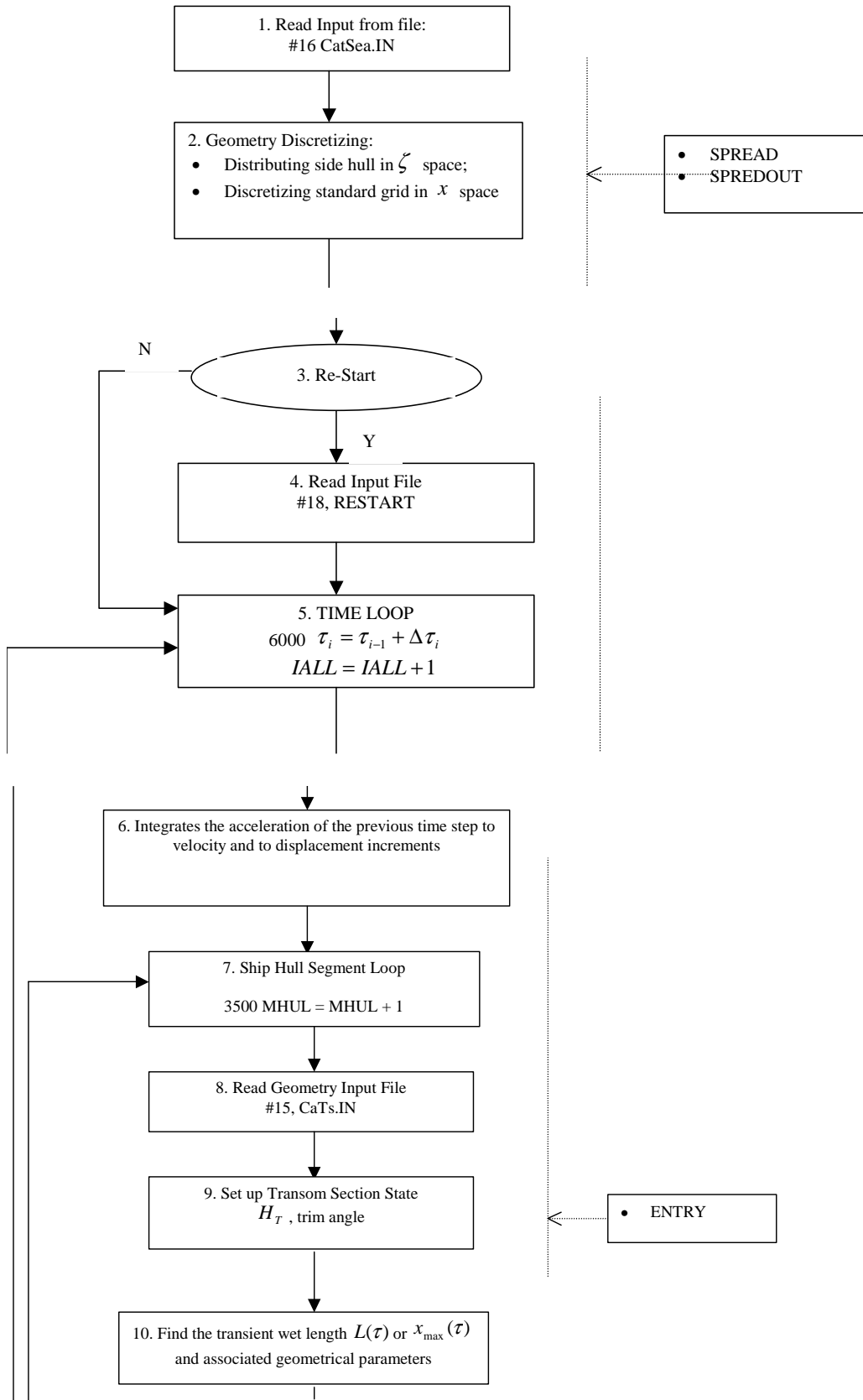
Step 9: Add the forces and moment components contributed by each hull segment separated by the transverse steps (refer to the box 20, 21 in Fig. 6.1).

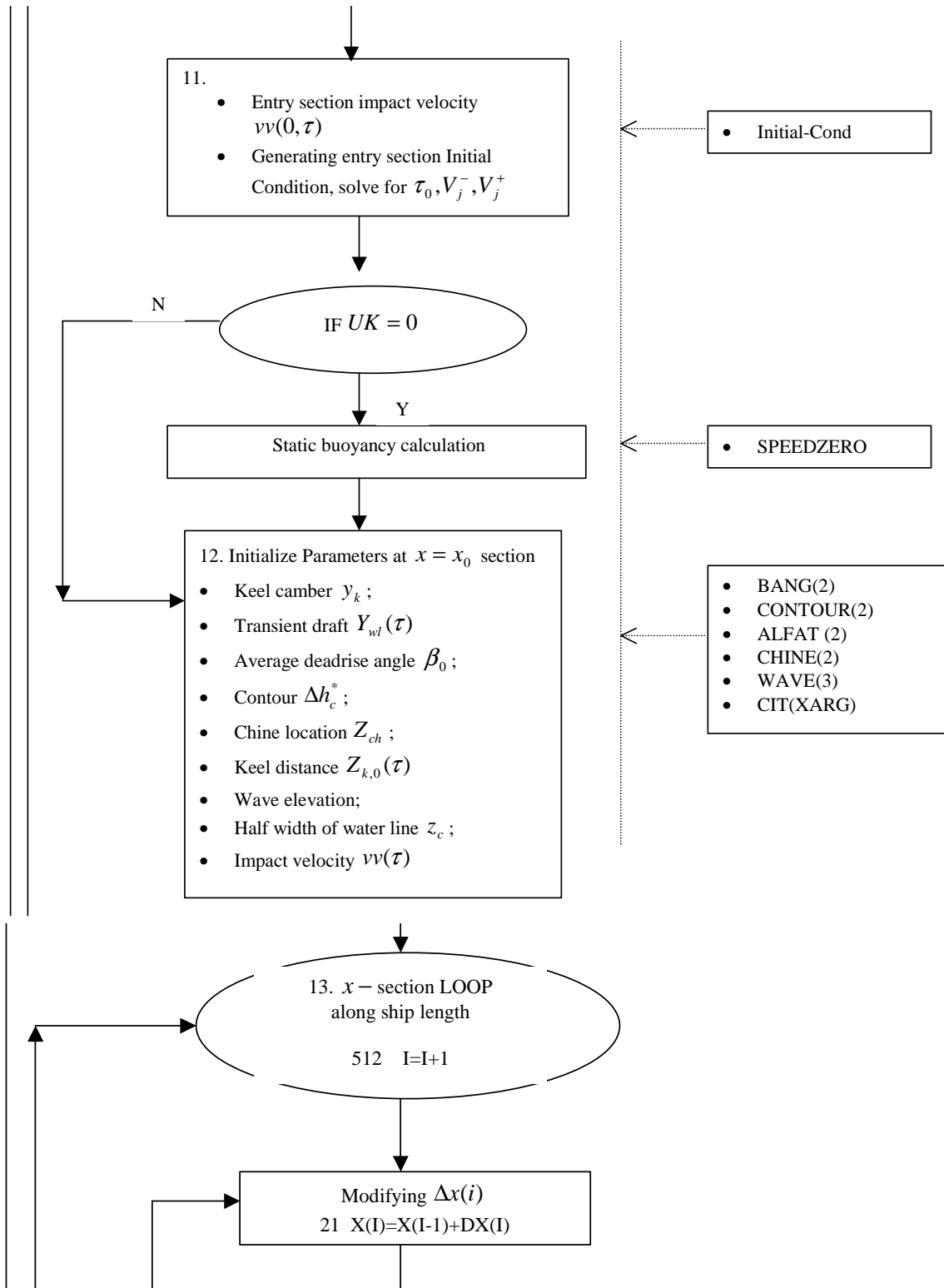
Step 10: Solve the two coupled motion equations (Newton's Law) to find the heave and the pitch accelerations $\ddot{\eta}_3(\tau)$, $\ddot{\eta}_5(\tau)$ (see the box 22 in Fig. 6.1 and refer to (3.93) and (3.94) for details).

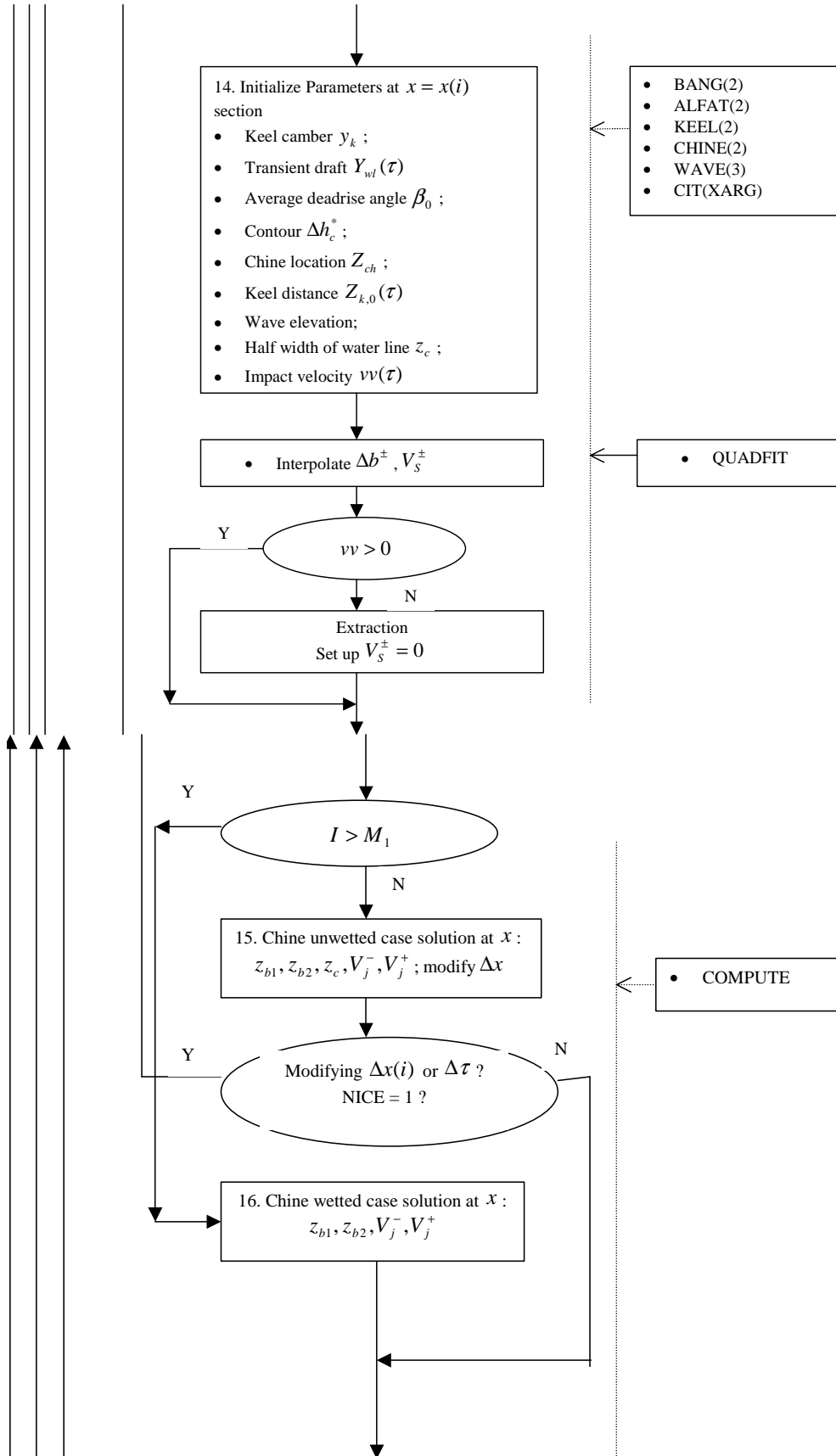
Step 11: Then perform double time integrations of the accelerations over the $\Delta\tau_i$ interval (refer to the box 6 in Fig. 6.1). The first time integral gives the new hull heave and pitch velocities $\dot{\eta}_3(\tau + \Delta\tau_i)$, $\dot{\eta}_5(\tau + \Delta\tau_i)$, which become components of the relative onset velocity distribution for the next time step (refer to (3.105), (4.94) and Appendix I). The second time integral gives the displacement $\eta_3(\tau + \Delta\tau_i)$ and $\eta_5(\tau + \Delta\tau_i)$ of the vessel in the wave system at $\tau = \tau_i$ for re-solving the x – problem at the new time, $\tau = \tau + \Delta\tau_i$; refer to (3.95), (4.93) and Appendix I. The artificial damping coefficient DEPS is involved in the two time integrals. The detail definition of the damping coefficient and its use in the time integrals is covered in Appendix I.

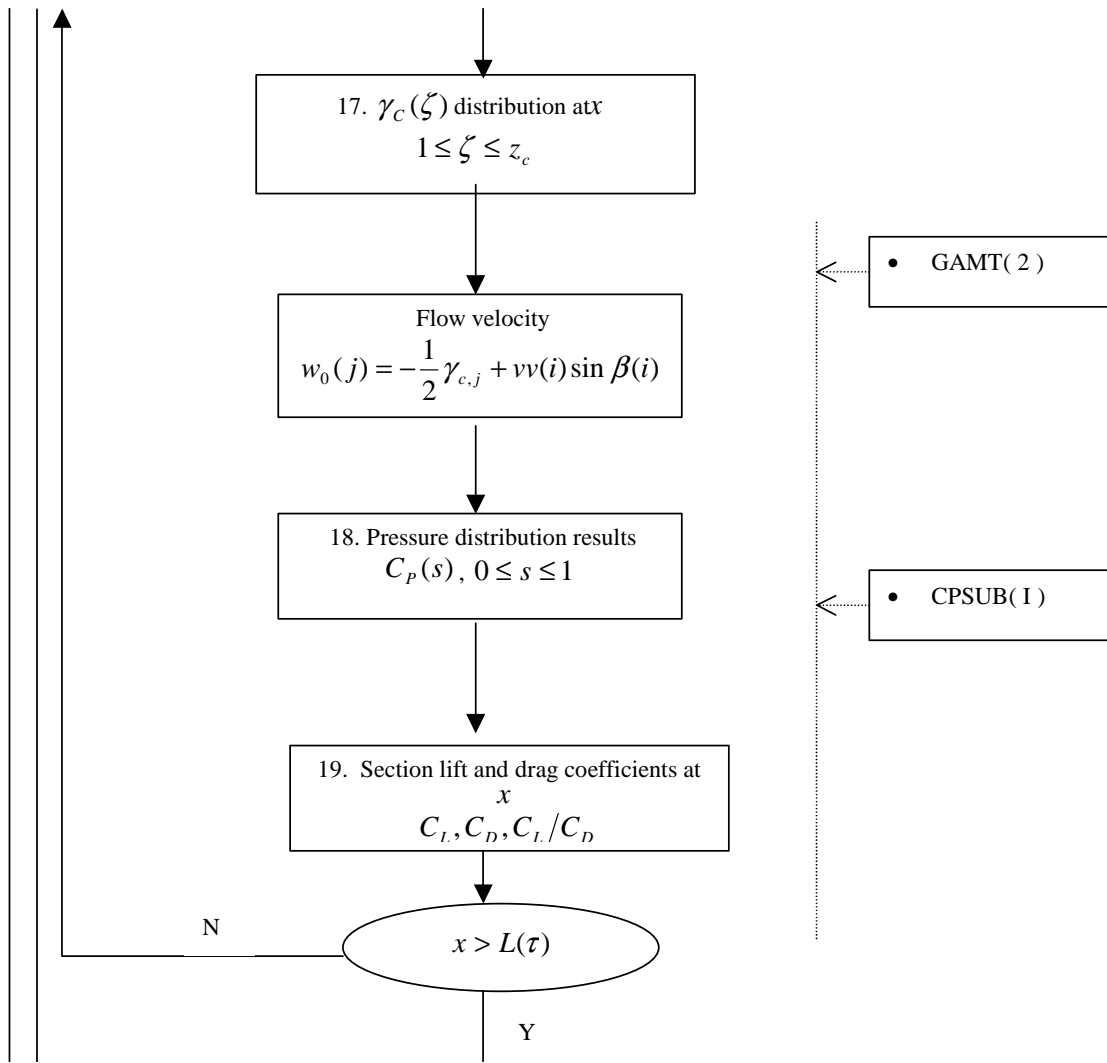
Step 12: Marching the time variable one step forward: $\tau = \tau + \Delta\tau_i$ (refer to the box 5 in Fig. 6.1), update the vessel to the new position. Go to Step 2.

Repeatedly executing these steps in a looping procedure gives the time history record of the motions of a planing catamaran in waves. The first step is always the calm water at $\tau_0 = 0$. The waves are then ramped-in according to (3.77) or (3.79).









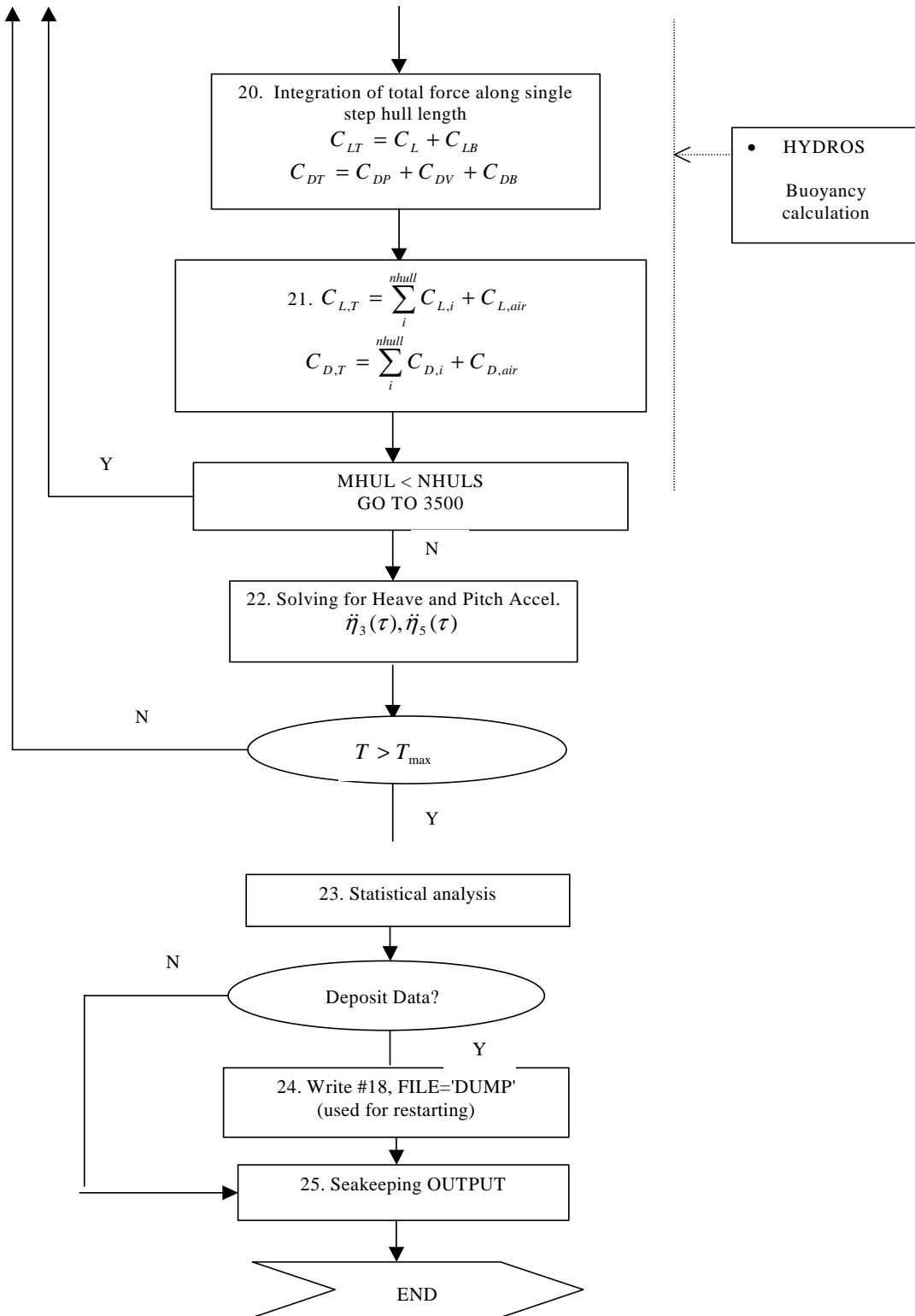


Fig. 6.1 "NewCat 2-4" flow chart

6.2 Non-Null and Null Hydrodynamics in the Impact or Extraction Phase

When a planing boat is running at sea, it undergoes relative motions with the wave system such that any section is either in an impact or extraction state. During the impact state, the sectional relative velocity $V(x,t) \geq 0$ (refer to (3.105)) is directed downward; the boat experiences positive hull surface pressure and upward lift. During the extraction phase, the sectional velocity gradient $dV/d\tau < 0$, and the hull section will at times be subjected to a downward suction force, such that the flow may detach depending on the magnitude of the negative gradient, and the direction and magnitude of $V(x,t)$.

As demonstrated in Vorus(1996), the fluid detachment process under extraction velocity gradients involves a very rapid "unzipping" on the hull contour from the outside in corresponding to $z_c(\tau)$ moving inward toward the keel and a jet velocity of zero. As a result, the surface pressure is reduced to zero very soon after the unzipping commences. The unzipping may commence at a positive impact velocity with a large enough negative gradient, but the threshold $V(x,t)$ will be near zero and decreasing if still positive. In the present theory, it is assumed that the unloading of the hull at any x – section occurs immediately as $V(x,t)$ passes through zero, and not before. Thus we assume that the extraction phase is a null hydrodynamic process; the sectional hydrodynamic pressure is taken as zero during extraction.

A numerical example of the null hydrodynamic process and the case where the jet velocity $V_j^+(\tau) = V_s(z_c, \tau) = 0$ is given in Fig. 15 and Fig. 16 of Vorus (1996) and its

discussion. There the flow field and the contour pressure distribution in a specified decreasing impact velocity case are plotted.

Based on Vorus' (1996) research results, a non-null hydrodynamics condition has been posted in the present seakeeping model as follows:

There are three conditions for non-null hydrodynamics at a section:

1) Section must be moving downward ($V(x,t) \geq 0$);

2) The zero pressure point, $z_c(\tau)$, must lie above the level of the instantaneous undisturbed free surface;

3) The jet velocity must be greater than zero, $V_j^+(\tau) = V_s(z_c, \tau) > 0$.

2) and 3) above are both evaluated by satisfying the velocity continuity condition (KC). Previous impact theory (Vorus 1996) showed that a $z_c(\tau)$ below the surface occurs when the jet velocity goes to zero; this is the unzipping case. There, the position of the inward advancing unzipping point $z_c(\tau)$ is the zero C_p point for the hydrodynamic pressure, which migrates to the keel very quickly, leaving zero dynamic pressure over the section, as discussed above. In consideration of hydrostatics, it is assumed, as a simplification, that the section pressure drops to zero immediately when conditions 1), 2), and 3) are not met, and gravity fills immediately to the level of the free surface (FS). Hydrostatic pressure is therefore assumed to still act.

6.3 Solution Procedures for CUW and CW Phases

The non-null solution for the x-section hydrodynamics is now addressed.

In the 2nd order algorithm, there are temporal derivative terms in the pressure continuity condition (refer to (4.75), (4.76) and (4.78), the pressure distribution (refer to (4.84) and (4.85)) and Euler's equation ((4.80) and (4.81)), which make the algorithms are complicate. For simplicity in the description of the algorithms in this section, only the 1st order algorithm and the 2nd order algorithm without considering the temporal derivative $\left. \frac{\partial}{\partial \tau} \right|_{\xi=const}$ terms, will be described here. The fully conditions will be treated later in chapter 10.

6.3.1 Solution procedure for CUW phase ($I < M_1$)

In the chine un-wetted (CUW) case, as developed in Chapter 5, there are five unknowns: $z_b^+, z_b^-, z_c^+, V_j^+, V_j^-$, and there are five equations: one displacement continuity equation (1-DC); two pressure conditions (2-PC); and two velocity continuity conditions (2-VC).

The data flow of the solution procedure for CUW is depicted in Fig. 6.2, which occurs when the contour section in the chine un-wetted flow (refer to the box 15 in Fig. 6.1 for the system solution procedure).

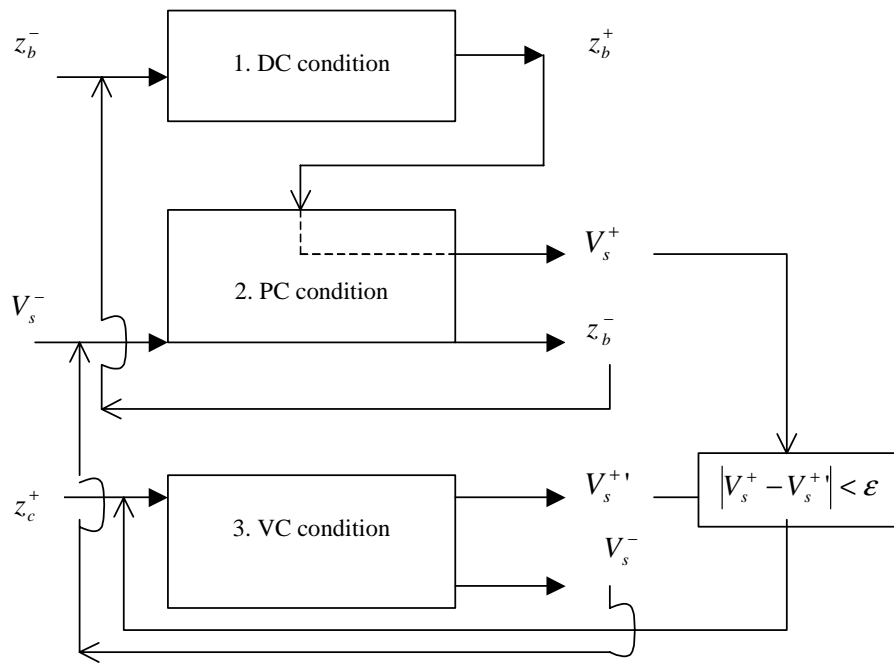


Fig. 6.2 Iteration procedure for the solution of CUW phase

The solution procedure follows as:

Step 1: Assume z_b^- and iterate to solve for z_b^+ (refer to the box 1 in Fig. 6.2) by requiring:

$$\left| \frac{Y_{wl} - \tilde{Y}_{wl}}{Y_{wl}} \right| < \epsilon \quad (6.2)$$

where the section draft $Y_{wl} = Y_k(\tau_i)$ (refer to (3.98)) corresponds with the waterline at time $\tau_i = \tau_{i-1} + \Delta\tau_i$, and \tilde{Y}_{wl} is an iteration of the local section draft from displacement continuity condition (refer to (3.44) and (4.58)). . In the 2nd order model,

$$\tilde{Y}_{wl} = \tan \beta \left(\frac{I_2}{I_1} - 1 \right) \quad (6.3)$$

where I_1 , I_2 are defined in (5.87) and (5.88) which involve the z_b^+ iterate sought.

Step 2: Using the z_b^+ obtained from the step 1, calculate $V_s(b^+, \tau)$ by the pressure continuity (PC) condition (refer to the box 2 in Fig. 6.2). From Eq. (4.75), in the chine un-wetted case the PC condition is:

$$b_\tau^+ + \left(1 - x \frac{L_\tau}{L}\right) b_x^+ = \frac{V_s^2(\xi, b^+, \tau) - V^2(\xi, \tau)}{2 \cdot V_s(\xi, b^+, \tau)} \quad (6.4)$$

Ignoring the term of b_τ^+ for now, as discussed, Eq.(6.4) becomes:

$$\left(1 - x \frac{L_\tau}{L}\right) b_x^+ = \frac{V_s^2(\xi, b^+, \tau) - V^2(\xi, \tau)}{2 \cdot V_s(\xi, b^+, \tau)} \quad (6.5)$$

Denote $B_\tau = \left(1 - x \frac{L_\tau}{L}\right) b_\tau^+$, $V_s^+ = V_s(\xi, b^+, \tau)$ and solve for the jet velocity from

the above equation (also refer to (3.69)):

$$V_s^+ = B_\tau + \sqrt{B_\tau^2 + V^2} \quad (6.6)$$

Add the stream component to the jet velocity:

$$V_s^+ = [B_\tau + \sqrt{B_\tau^2 + V^2}] + V \sin \beta(\tau) \quad (6.7)$$

Step 3: Assume V_s^- and solve for z_b^- by PC condition in Eq. (3.71), (4.78) (refer to the box 2 in Fig. 6.2), then return to step 1 for updating z_b^- . Iterate step 1 to step 3 to convergence.

Step 4: Assume z_c^+ , and with the results of z_b^+ , z_b^- , and calculate the V_s^+ , V_s^- by the velocity continuity (VC) condition (refer to the box 3 in Fig. 6.2 and (5.24), (5.25), (5.83), (5.84)). The iteration error criteria for the VC condition is:

$$\frac{|V_s^+ - V_s^{+'}|}{V_s^{+'}} < 0.001 \quad (6.8)$$

where $V_s^{+'}$ is the trial iterate value.

Then iterate z_c^+ for equality with V_s^+ from the step 2.

Step 5: Iterate V_s^- with the guessed value of V_s^- in step 3.

6.3.2 Solution procedure for CW phase ($I > M_1$)

In Chine Wetted (CW) case, as discussed in Chapter 2, the jet separation point z_c^+ is known and fixed at the chine z_{CH} , therefore there are four unknowns left:

$z_b^+, z_b^-, V_j^+, V_j^-$, and correspondently there are four equations: two pressure conditions (2-PC); and two velocity continuity conditions (2-VC).

The data flow of the solution procedure for CW is depicted in Fig. 6.3.

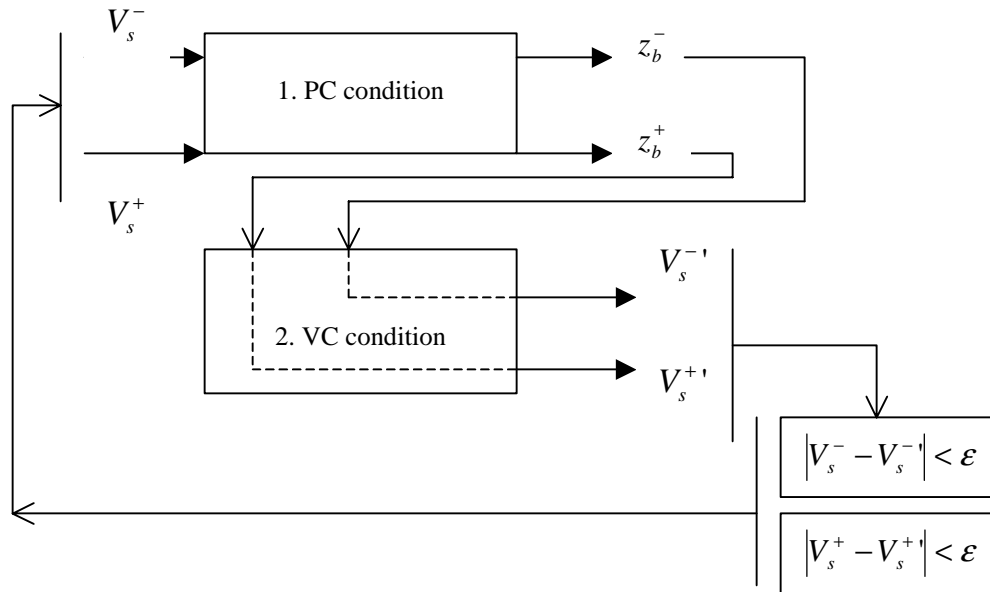


Fig. 6.3 Iteration procedure for the solution of CW phase

The solution procedure is:

Step 1: Assume V_s^+, V_s^- and solve for z_b^+, z_b^- by PC conditions (refer to the box 1 in Fig. 6.3 and (3.70), (3.71)).

Step 2: With the results of z_b^+, z_b^- from step 1, calculate V_s^+, V_s^- by VC conditions (refer to the box 2 in Fig. 6.3 and (5.83), (5.84)).

Step 3: Iterate V_s^+ , V_s^- obtained from the step 2 for equality with V_s^+ , V_s^- from the step 1. The iteration error criteria for V_s^+ is:

$$\left| \frac{V_s^+ - V_s^{+i}}{V_s^{+i}} \right| < 0.001 \quad (6.10)$$

Iterate z_b^- for equality with V_s^- from the step 1, the iteration error criteria for z_b^- is:

$$\left| \frac{z_b^- - z_b^{-i}}{z_b^-} \right| < 0.0001 \quad (6.11)$$

We have outlined the system solution procedure, the null hydrodynamics and the non-null hydrodynamics algorithm in this chapter. Till now, we have completed the instructions of the theoretical and numerical models of the catamaran hydrodynamics for the 1st order model and the 2nd order model. In next following chapters, we will give the numerical comparison of calculated results from the 1st order model and the 2nd order models.

CHAPTER 7

VALIDATION OF THE NUMERICAL ANALYSIS IN THE 2ND ORDER THEORY

Starting from this chapter, we begin to validate the numerical model for the 2nd order theory, and to compare the numerical prediction results of the 2nd order theory (refer to Chapter 4) with the results of the 1st order theory (refer to Chapter 3). The fundamental parameter integral terms $\Lambda(\zeta)$, $\Lambda^-(\zeta_0)$ and $\Lambda^+(\zeta_0)$ (in (3.11), (3.12) and (3.13) for 1st order model, in (4.23), (4.24) and (4.25) for 2nd order model) have played an important role in the derivation of the velocity continuity conditions (refer to Chapter 3 and 4). The numerical accuracy of the bound vortex distribution $\gamma_c(\zeta, \tau)$ has a key effect in the flow velocity field computation (refer to (4.3), (5.89), (5.92), (5.96), (5.97) and (5.99)). In this chapter, we give the results for the numerical models of the fundamental integrals and the bound vortex strength $\gamma_c(\zeta, \tau)$ of the 2nd order theory, relative to the 1st order. In the succeeding closing chapters, the comparisons of the numerical prediction results for the 1st and the 2nd order theories, in steady planing, in regular waves, and in random waves, are presented.

7.1 Three Fundamental Integrals

The three fundamental parameter integral terms $\Lambda(\zeta)$, $\Lambda^-(\zeta_0)$ and $\Lambda^+(\zeta_0)$ (refer to (3.11), (3.12), (3.13), (4.23), (4.24) and (4.25)) are in the same form, but defined in the different value domains. Each of them can be separated into three elemental integrals I_1 , $I_2(\zeta)$ and $I_3(\zeta)$ (refer to (3.16) and (4.28)). In following, the comparative study for the I_1 , $I_2(\zeta)$ and $I_3(\zeta)$ integrals in 1st order model with the 2nd order model is given.

7.1.1 Validation of the elemental integral I_1 and I_2

According to (4.29) and (4.30) (refer to the derivation in Appendix H), as presented in Chapter 5 by (5.49), I_1 and I_2 in the 2nd order model have the following semi-analytical forms:

$$I_1 = \frac{1}{2} z_c \cdot B\left(\frac{1}{2} - \frac{\tilde{\beta}}{\pi}, \frac{1}{2} + \frac{\tilde{\beta}}{\pi}\right) \cdot F\left(-\frac{1}{2}, \frac{1}{2} - \frac{\tilde{\beta}}{\pi}; 1; \frac{z_c^2 - 1}{z_c^2}\right) \quad (7.1)$$

$$I_2(\zeta) = \frac{1}{2} (\zeta^2 - z_c^2 - 1) \frac{1}{z_c} \cdot B\left(\frac{1}{2} - \frac{\tilde{\beta}}{\pi}, \frac{1}{2} + \frac{\tilde{\beta}}{\pi}\right) \cdot F\left(\frac{1}{2}, \frac{1}{2} - \frac{\tilde{\beta}}{\pi}; 1; \frac{z_c^2 - 1}{z_c^2}\right) \quad (7.2)$$

where the angle $\tilde{\beta}(\zeta, \tau)$ is defined in (4.12); the $B(x, y)$ is the Beta function, and $F(\alpha, \beta, \gamma; z)$ is Gauss' single variable hypergeometric function.

In the 1st order model, the integral I_1 and I_2 have different forms (refer to (3.17) and (3.18)).

$$I_1 = z_c E\left(\frac{\pi}{2}, \sqrt{1-1/z_c^2}\right) \quad (7.3)$$

$$I_2(\zeta) = (\zeta^2 - z_c^2 - 1) \cdot \frac{1}{z_c} F\left(\frac{\pi}{2}, \sqrt{1-1/z_c^2}\right) \quad (7.4)$$

where $F\left(\frac{\pi}{2}, k\right)$, $E\left(\frac{\pi}{2}, k\right)$ are the Elliptical integrals of the first kind and second kind respectively.

The kernel function $\chi(\zeta)$ as well as the elemental integral I_1 , $I_2(\zeta)$ in the 1st order model (refer to (3.17), (3.18) and (3.7)) is a special case of the kernel function and the elemental integrals in the 2nd order model (refer to (4.29), (4.30) and (4.16)). It is correspondent to the deadrise angle $\beta(z) = 0$ (and therefore, $\tilde{\beta}(z) = 0$) in the 2nd order model.

Therefore to verify the numerical accuracy of the formulae (7.1) and (7.2), a code has been developed to compute the numerical results in (7.3), (7.4) and the result in (7.1), (7.2) for the test case of deadrise angle $\beta(z) = 0$.

Fig. 7.1 shows the comparison of $I_1, I_2(\zeta)$ for the 1st and the 2nd order model for this special case ($\beta(z) = 0$). As is necessary, the results are numerically identical (refer to (7.1), (7.2), (7.3) and (7.4)). The deadrise angle was then increased to $\beta = 38$ degree. In this case, the results with the 1st order model stay the same since they are independent of β . However the results of the 2nd order model change since they are functions of β . Fig. 7.2 shows this comparison.

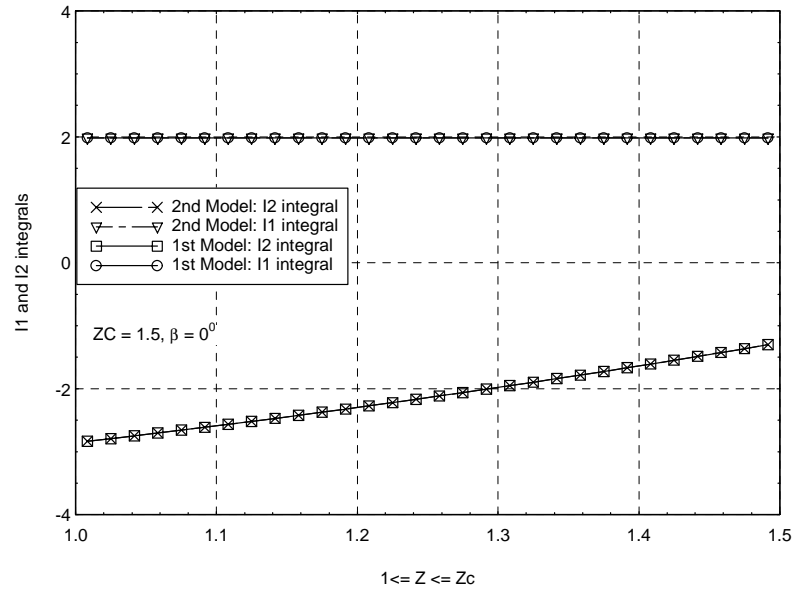


Fig. 7.1: Comparison of I1 & I2 integrals, $\beta = 0^\circ$

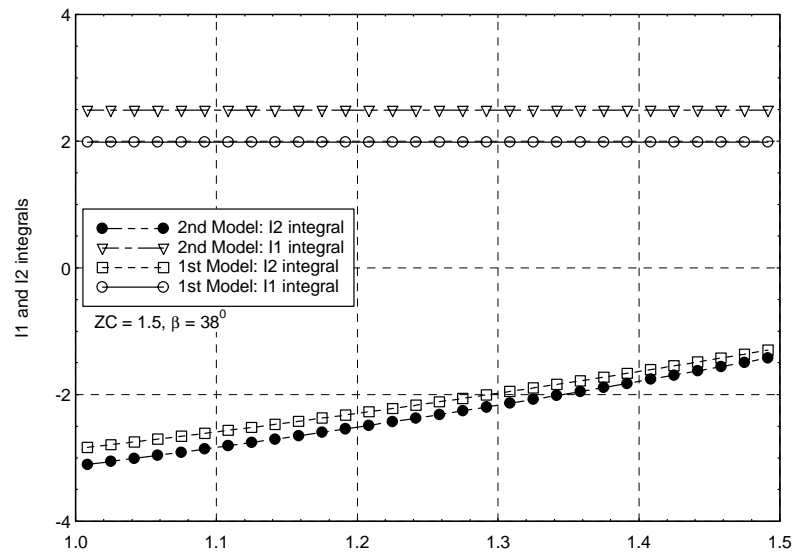


Fig. 7.2: Comparison of I1 & I2 integrals, $\beta = 38^\circ$

7.1.2 Numerical comparison and numerical accuracy of the $I_3(\zeta)$ integral

In the 1st order model, $\beta = 0$, therefore, the elemental integral $I_3(\zeta)$ of 1st order model in (3.19) has different formulations from the integral $I_3(\zeta)$ of 2nd order model in (4.31). For example, in 1st order model,

$$I_3(\zeta) = \frac{z_c^2 - \zeta^2}{z_c \zeta^2} \left\{ \Pi \left[\frac{\pi}{2}, \frac{\zeta^2(z_c^2 - 1)}{z_c^2(\zeta^2 - 1)}, \sqrt{1 - 1/z_c^2} \right] + (\zeta^2 - 1) F \left(\frac{\pi}{2}, \sqrt{1 - 1/z_c^2} \right) \right\}$$

$$1 \leq \zeta \leq z_c \quad (7.5)$$

where the parameter definitions in above formula may refer to chapter 3 and Appendix J.

In 2nd order model, since the $I_3(\zeta)$ integral can not be expressed in a direct semi-analytical form as it is in the 1st order model, it has been expressed in a discretized numerical integral form:

$$I_3(\zeta) = -\frac{1}{2}(\zeta^2 - 1)(z_c^2 - \zeta^2) \times \sum_{j=1}^N \frac{1}{\sqrt{t_j}} \cdot \Delta I_{3,j}(\zeta)$$

$$1 \leq \zeta \leq z_c \quad (7.6)$$

where the parameter definition in (7.6) refer to chapter 4.

In different value domains of the variable ζ , the integral $I_3(\zeta)$ has different computable semi-analytical forms (refer to (J.28), (J.42) and (J.52) in Appendix J for 1st order model, refer to (4.31), (4.32), (4.34), (4.36) and Appendix H for 2nd order model).

In the computation of the $I_3(\zeta)$ integral in (4.31), (4.32), (4.34) and (4.36) of the 2nd order model, there is an important parameter that needs to be determined. That is the number of the elements N used in the computation. Recall in the discretized $I_3(\zeta)$ integral in (4.31), (5.47), (5.48) and (5.49), the integral domain $z_c^2 - 1$ has been discretized into N elements. More elements, means higher accuracy, but also need more computer CPU time. Recall that in the seakeeping solution procedure (refer to Chapter 6), at every time step, a complete x – problem needs to be solved. Therefore the hull will be discretized into many segments (in our example, the main body is discretized into 80 segments, and 2 steps, with the sections after the steps discretized into 50 segments). Each segment must then be discretized into the transverse computation grids (above 60 ζ – axis sub-elements in our examples). At each computation grid ζ_i , it is necessary to calculate $I_3(\zeta_i)$ for the bound vortex strength $\gamma_c(\zeta_i, \tau)$, and also necessary to calculate $I_3(\zeta_i)$ when ζ_i is on the free vortex sheets for the velocity continuity conditions and for the vortex distributions. However, a large number of segments N for the $I_3(\zeta_i)$ computation would greatly slow down the computation speed, where N is the integral element number for the integral $I_3(\zeta_i)$ (refer to (7.6)). For the $I_3(\zeta)$ integral computation in the 1st order model, it does not need to discretize into N elements. It can calculate the $I_3(\zeta)$ integral value directly by the semi-analytical forms in (J.28), (J.42) and (J.52).

Comparing with the 1st order model, if assuming the CPU time needed by the 1st order model for $I_3(\zeta_i)$ computation as $O(1)$ (refer to (J.28), (J.42) and (J.52)) since it can calculate the integral value directly, then the CPU time for the 2nd order model would

be $O(N)$ (refer to (7.6)), with N being the number of segments. This $I_3(\zeta_i)$ computation is the main reason why the computation speed in 2nd order model appear to be so much slower than that in the 1st order model.

The following example demonstrates the relation of the accuracy and the computation speed for $I_3(\zeta_i)$ computation.

7.1.2.1 Deadrise angle $\beta = 0$ case

In the case of the deadrise angle $\beta = 0$, the formula in Eq. (J.28), (J.42) and (J.52) in the 1st order model are the established analytical evaluation of the integral $I_3(\zeta)$ in different value domains of the variable ζ . Thus to estimate the accuracy of the integral $I_3(\zeta)$ formula (4.31), (4.32), (4.34) and (4.36) in the 2nd order case, in the interest of debugging the code, the numerical results of the $I_3(\zeta)$ in the 2nd order model in $\beta = 0$ case have been compared with the results in the 1st order model. A code based on the mathematical models in (4.31), (4.32), (4.34) and (4.36) has been developed for the purpose of comparison.

Fig. 7.3 shows the comparison of $I_3(\zeta)$ in the region of $1 < \zeta < z_c$. In this example, the non-dimensional z_c is set to be 1.5. The segment number N in (7.6) is chosen to be $N = 3000$; the sensitivity to N is considered later. A good agreement is shown for the two different models. The difference in the two curves on Fig 7.3 represents numerical error, sine both formulations analytically produce the 1st order $I_3(\zeta)$ at $\beta = 0$.

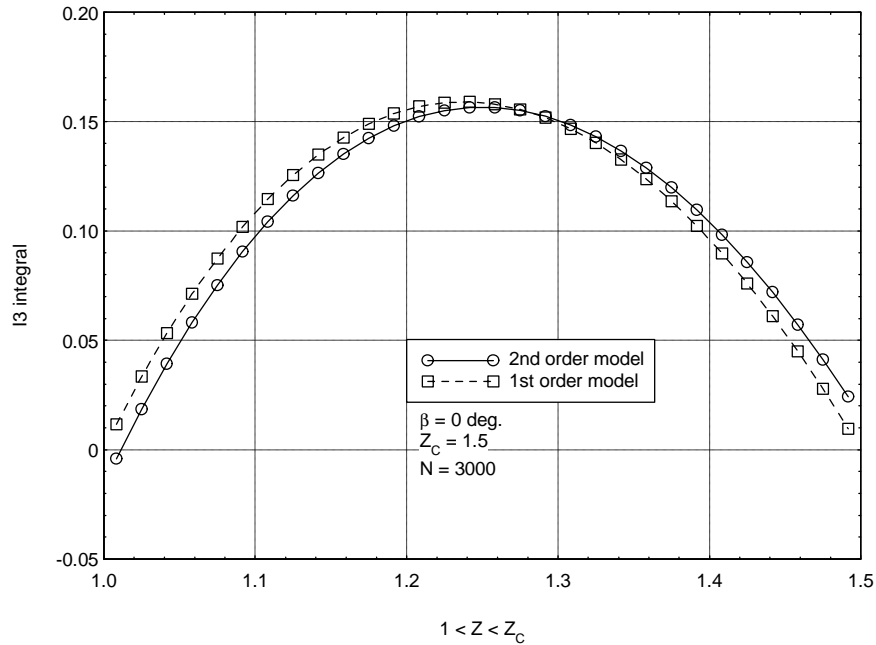


Fig. 7.3: I_3 integral in the domain: $1 < \zeta < z_c$, $\beta = 0$, $N = 3000$

Fig. 7.4 shows the comparison of $I_3(\zeta)$ in the region of $z_c < \zeta \leq b^+$. In this example, $z_c = 1.5$, $b^+ = 1.8$. These parameters were chosen from the computation result of CatSea2-4a. The element number in (7.6) is chosen to be $N = 3000$. A nearly perfect agreement for the two different theoretic models has been achieved. Similarly, Fig. 7.5 shows a very good agreement for the $I_3(\zeta)$ in the domain of $b^- \leq \zeta < 1$. Again, in (7.6) N is set to be 3000.

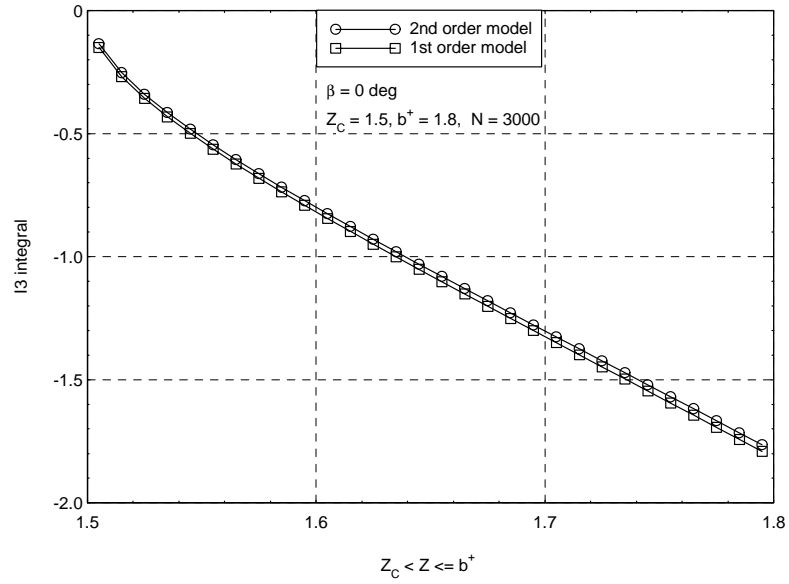


Fig. 7.4: I3 integral in the domain: $z_c < \zeta \leq b^+$, $\beta = 0$, $N = 3000$

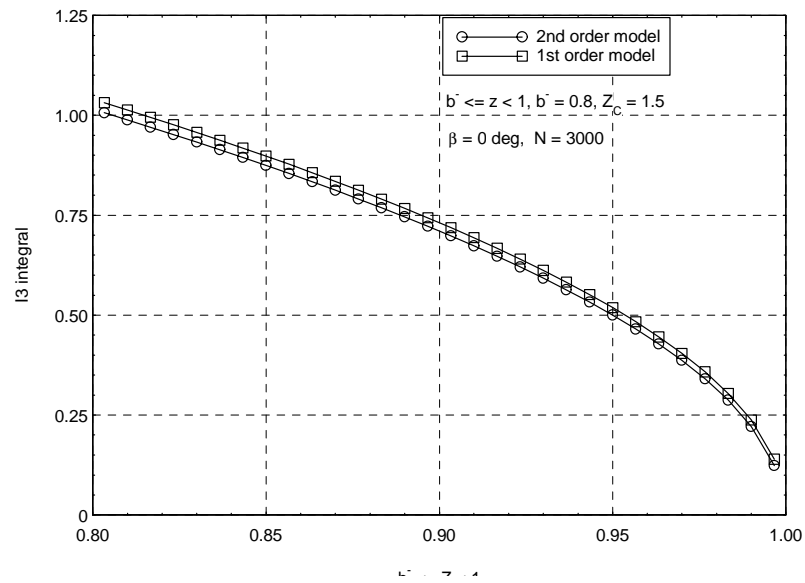


Fig. 7.5: I3 integral in the domain: $b^- \leq \zeta < 1$, $\beta = 0$, $N = 3000$

Fig. 7.3, Fig. 7.4 and Fig. 7.5 confirm that the algorithm for $I_3(\zeta)$ in 2nd order model is correct and that the new code for the $I_3(\zeta)$ computation is free of error. However, this accuracy is the accuracy when $N = 3000$.

Practically, if $N = 3000$ is chosen in the seakeeping computation, our PC-type computer may need to continually run several months to get results. For balancing the CPU time and with the necessary accuracy, at present examples, $N = 300$ is proposed in the seakeeping computation. However, with $N = 300$, the accuracy is much lower.

Fig. 7.6 shows the comparison of $I_3(\zeta)$ computation in the region of $1 < \zeta < z_c$ with $N = 300$. Comparing with Fig. 7.3, it is seen that the numerical results for the 2nd order model are off the analytical 1st order results, again at $\beta = 0$. Fig. 7.7 and Fig. 7.8 show the differences of numerical results in the region of $z_c < \zeta \leq b^+$ and $b^- \leq \zeta < 1$ respectively with $N = 300$. However, these differences may be acceptable at the present PC-type computer ability.

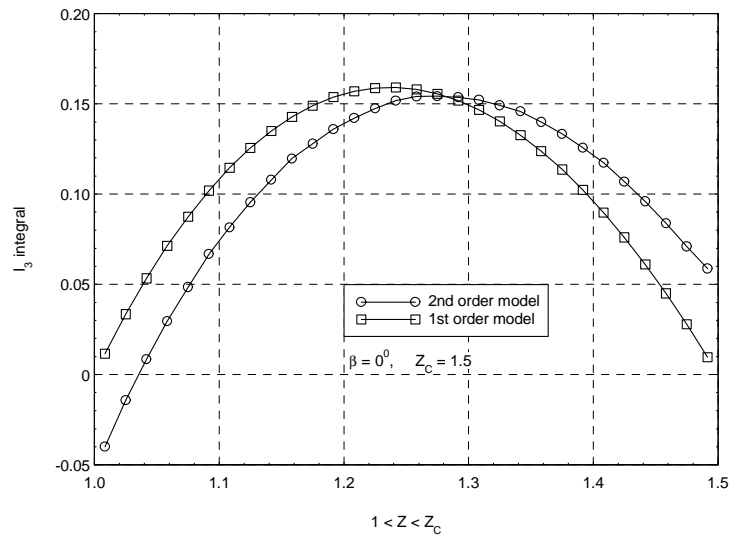


Fig. 7.6: Comparison of the I3 integral in the domain: $1 < \zeta < z_c$, $\beta = 0^0$, $N=300$

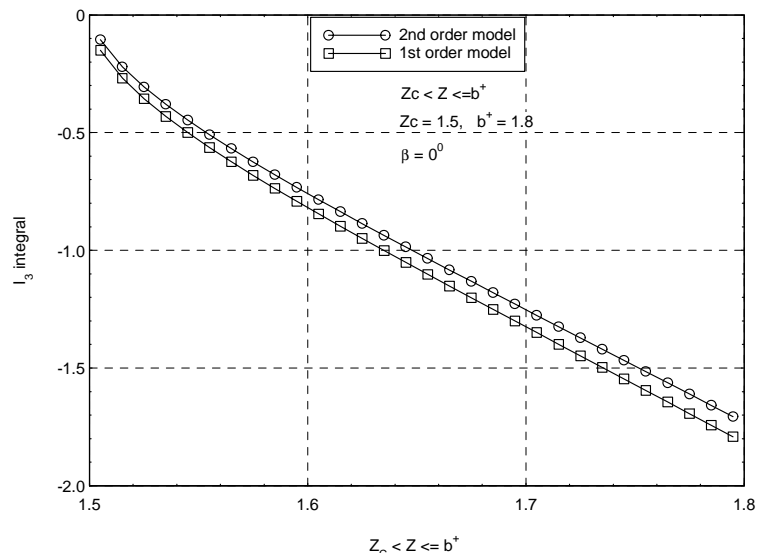


Fig. 7.7: Comparison of the I3 integral in the domain: $z_c < \zeta \leq b^+$, $\beta = 0^0$, $N=300$

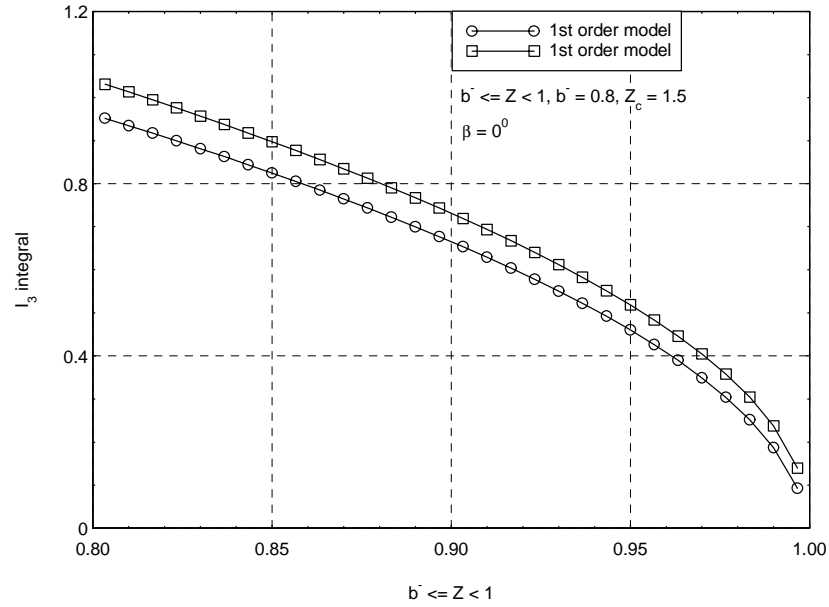


Fig. 7.8: Comparison of the I_3 integral in the domain: $b^- \leq \zeta < 1$, $\beta = 0^0$, $N=300$

7.1.2.2 Deadrise angle $\beta \neq 0$ case

The formulae of $I_3(\zeta)$ computation in the 2nd order model can take the $\beta \neq 0$ effect into account, but the 1st order model can not. Fig. 7.9 shows the comparison of the $I_3(\zeta)$ computation results for $\beta = 0$ and $\beta = 38^0$ case. It has a completely different trend for the results in the $\beta = 38^0$ case from the results at $\beta = 0$. Fig. 7.10 shows the family curves for the $I_3(\zeta)$ computation results for 2nd order model when the deadrise angle β changes, where $N = 300$.

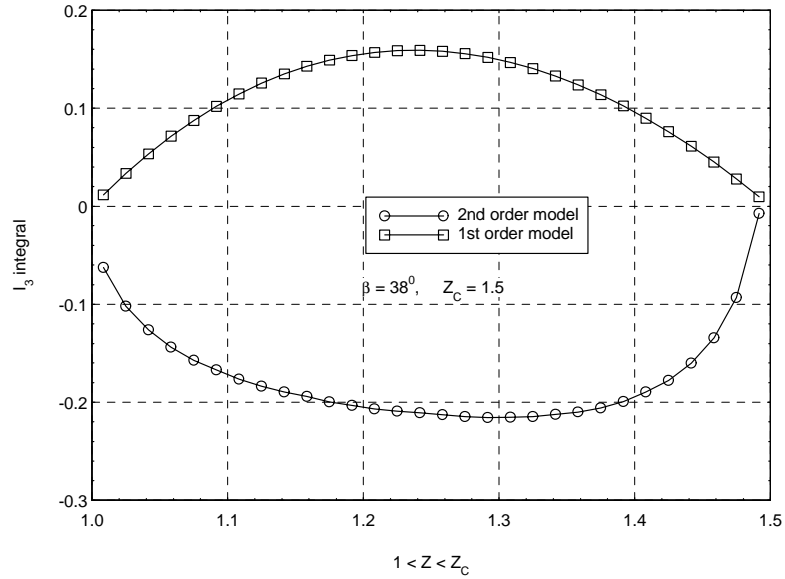


Fig. 7.9: I_3 integral in the domain: $1 < \zeta < z_c, \beta = 38^\circ, N=300$

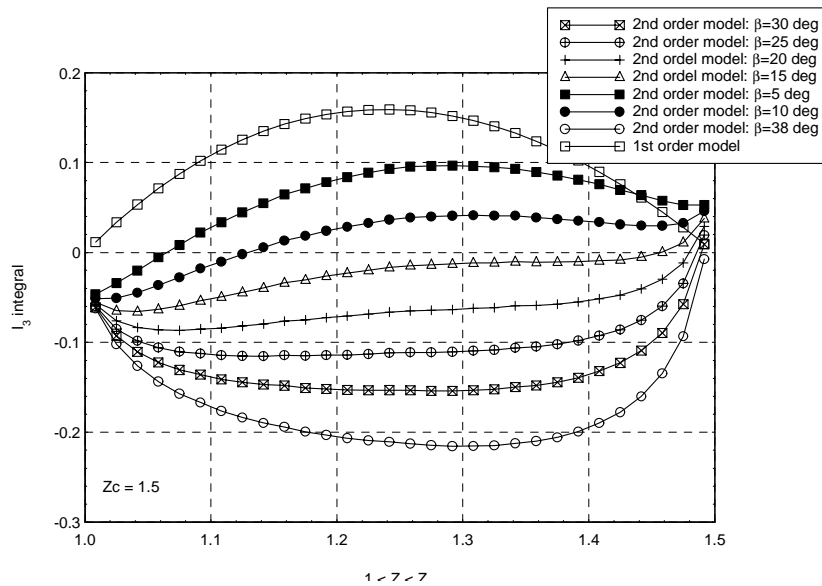


Fig. 7.10: β variation effect: I_3 integral in the domain: $1 < \zeta < z_c, N=300$

From the above research, the following conclusions may be drawn:

- The formulae of the $I_3(\zeta)$ computation in (4.31), (4.32), (4.34) and (4.36) in the 2nd order model are correct, so it can be used as an approximate numerical model;
- $I_3(\zeta)$ integral needs more segments, N , to achieve a high numerical accuracy. Small N , i.e., several hundreds, in the $I_3(\zeta)$ integral results in crude accuracy. However, more segments will greatly increase the computation time. A combination method for the segment numbers could be used. A numerical test shows that $N = 500$ could be used in the critical area (the area of steepest slope of the function), and a cell number $N = 300$ could be used for other areas to effectively speed up the computation.

7.2 Comparison of The Numerical Results For $\gamma_c(\zeta, \tau)$ Computation

The computation of the vortex strength $\gamma_c(\zeta, \tau)$ is a key issue for the craft computation. A run-time error problem in the $\gamma_c(z)$ computation was caused by the crude extrapolation in $I_3(\zeta)$ to the end of the interval where a small numerical error in removing the singular terms in satisfying the velocity continuity condition existed. When the numerical accuracy in the $I_3(\zeta)$ algorithm was refined, the run-time error problem in the $\gamma_c(z)$ computation was resolved.

The numerical model of $\gamma_c(\zeta, \tau)$ in the 1st order model is given in Chapter 5 (refer to (3.10), (5.43), (5.44) and (5.45)). The numerical model of $\gamma_c(\zeta, \tau)$ in the 2nd order is given in (5.89), (5.92), (5.96), (5.97) and (5.99).

A numerical comparison has been conducted for the $\gamma_c(\zeta, \tau)$ computation. The necessary input parameters are obtained from the output results of CatSea2-4a for the seakeeping case. Fig. 7.11 shows the comparison of the bounded vortex strength $\gamma_c(\zeta, \tau)$ computations in $\beta = 0$ case. At the end point, the vortex strengths for two methods are identical. At the other points, there exist some differences which may result from the difference in the mathematical models between the 1st order model and the second order model. Fig. 7.12 shows the effect of the variation of β in the 2nd order model. The bounded vortex strength $\gamma_c(\zeta, \tau)$ model in the 2nd order model can take the β variation effect into account.

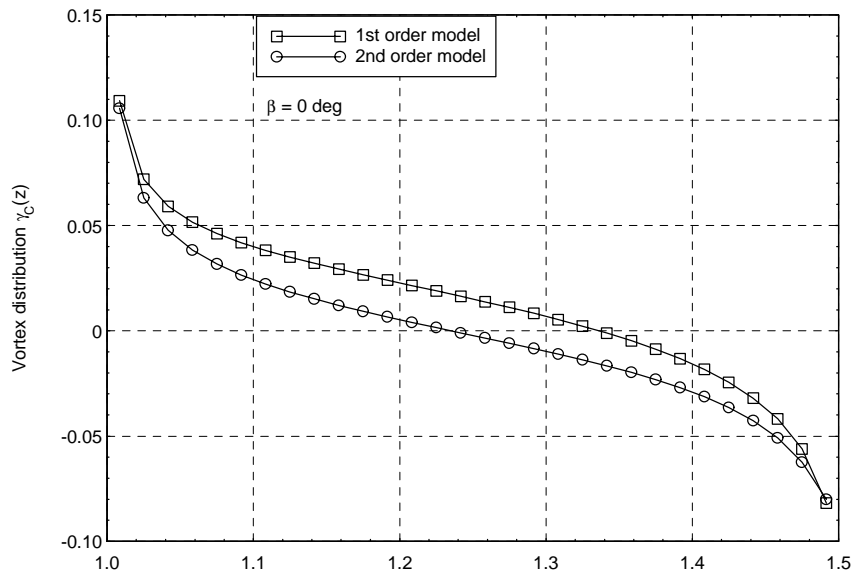


Fig. 7.11 Comparison of the vortex strength distribution $\gamma_c(\zeta)$ ($\beta = 0^0$)

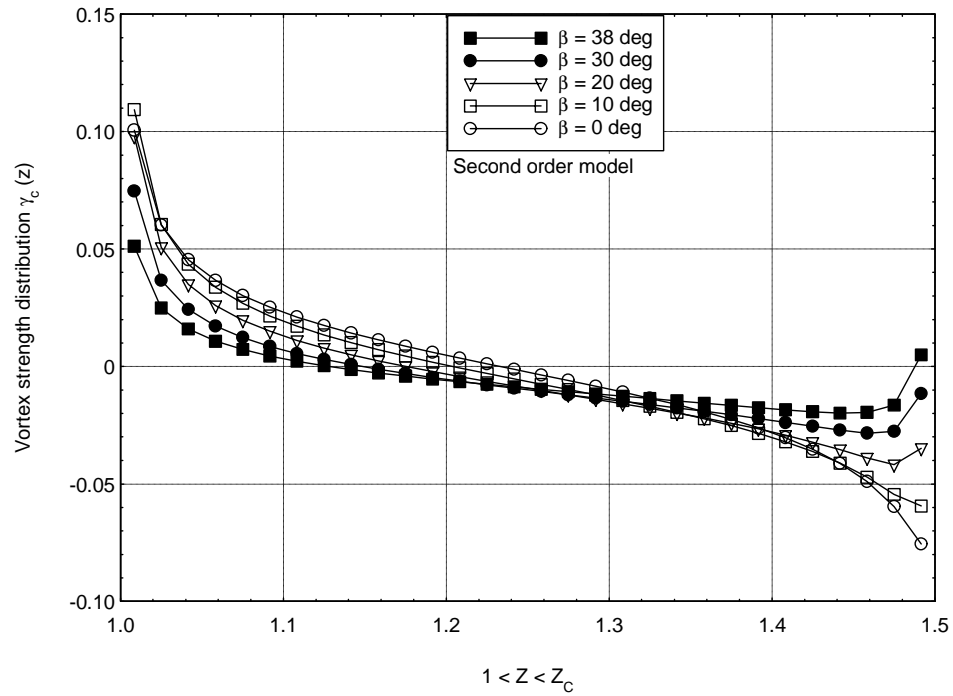


Fig. 7.12 Effect of the variation of β

From the above numerical comparison, the $\gamma_c(\zeta, \tau)$ computation accuracy in the 2nd order model is considered acceptable

In this chapter we have validated some important parts of the numerical model in the 2nd order theory. In next chapter, the numerical predictions for steady planing and comparisons between the 1st and 2nd order models are presented.

CHAPTER 8

NUMERICAL COMPARISONS FOR STEADY PLANING

8.1 30ft High-Speed Planing Catamaran With Steps

A tool for catamaran performance prediction has been developed according to the second order nonlinear theory of hydrodynamics for planing catamarans. The name of the software is NewCat (version 2-4a), the program flow charts for which are shown in Chapter 6.

We have applied this software to a planing catamaran that was developed by William Vorus and Larry DeCan. This high-speed catamaran has two transverse steps in the planning region of the hull.

Figs. 8.1 - 8.3 show the views of the Vorus-DeCan planning catamaran (the steps are not shown). Fig. 8.4 is the section view.

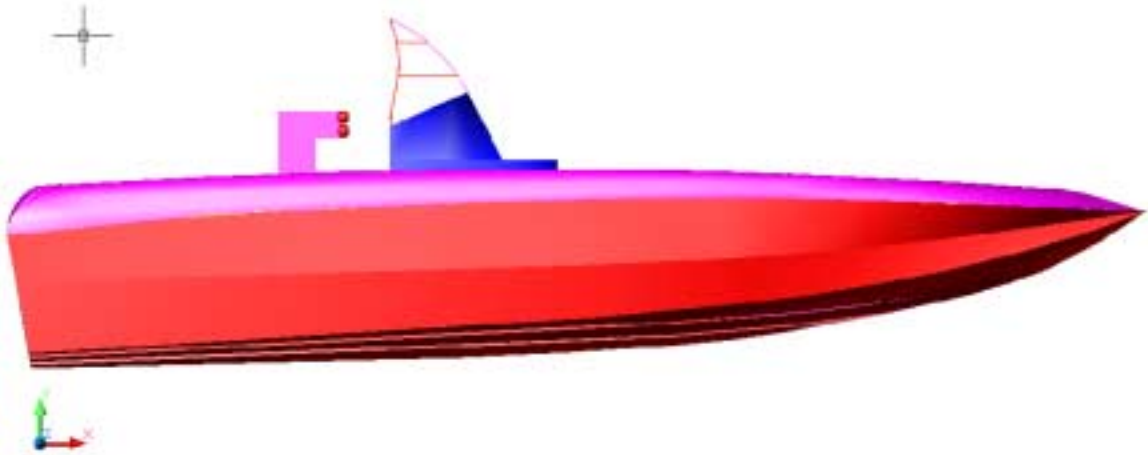


Figure 8.1 Stepped planing catamaran

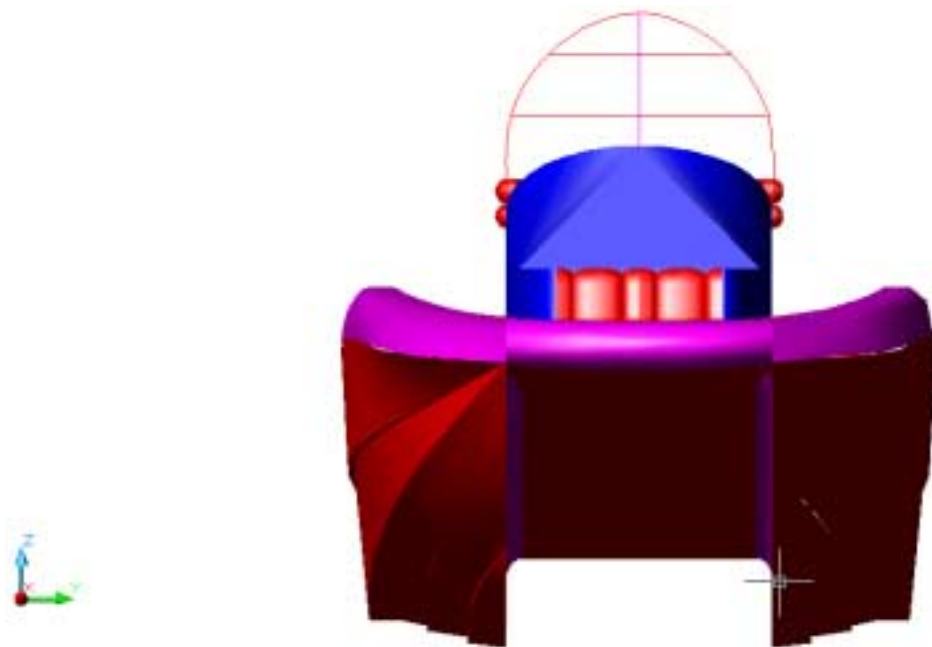


Figure 8.2 Stepped planing catamaran: bow end view

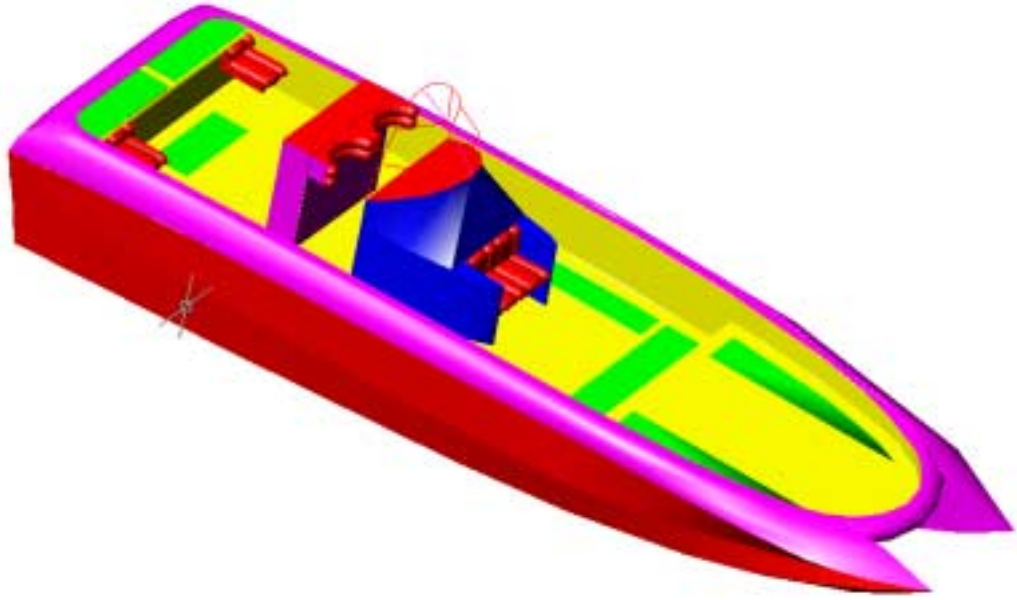


Figure 8.3 Stepped planing catamaran: top view

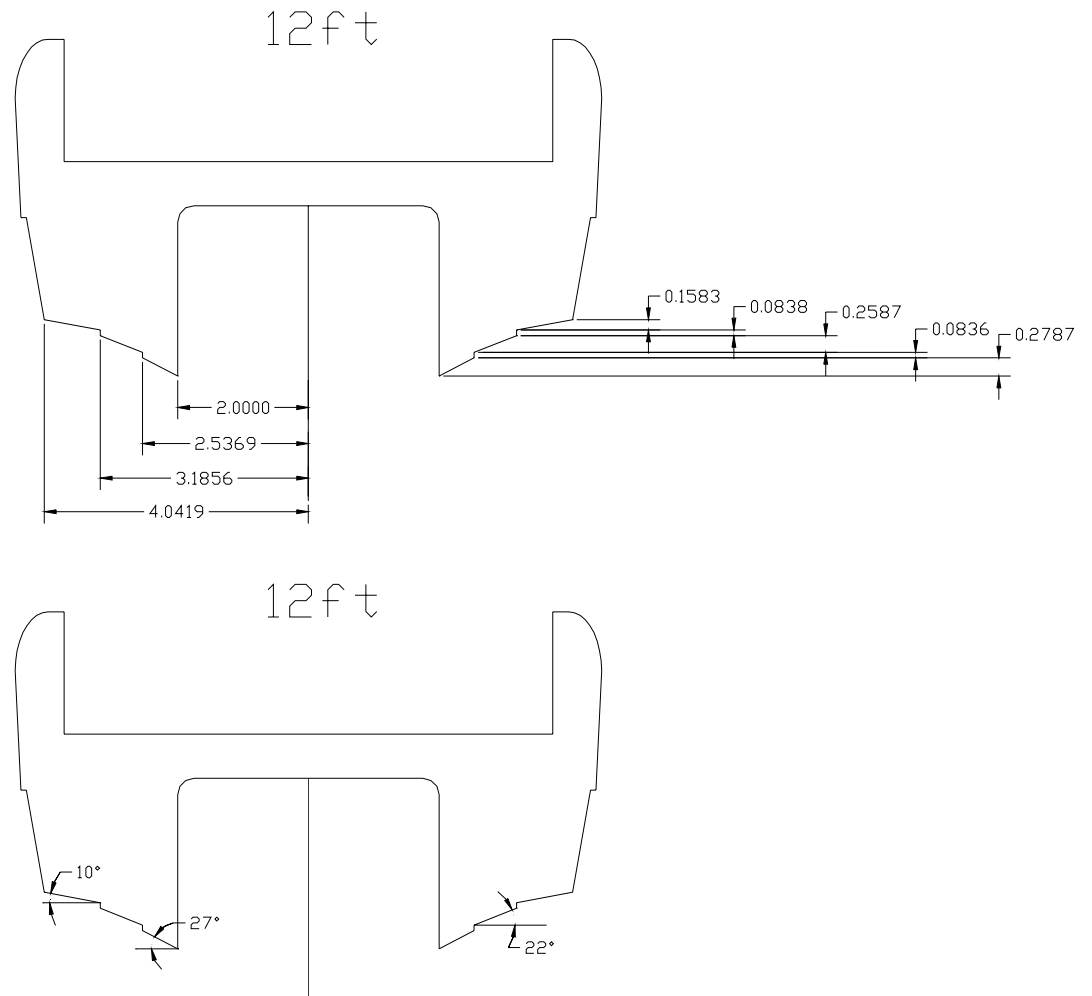


Figure 8.4 Cross section view at station #4 (12 ft forward of transom)

Fig. 8.5 to 8.7 are the longitudinal distributions, respectively, of deadrise angle $\beta(\bar{x}_i)$ (in degrees), chine offset $Z_{CH}(\bar{x}_i)$, and keel upset with the two steps. The XI – coordinate in these figures is the coordinate of the initial wetted length x_{\max} , it starts from bow to stern ($0 \rightarrow x_{\max}$). Because NewCat needs a high degree of accuracy in the computation, all geometric parameters used here are in the form of higher order continuous polynomials. Fig. 8.5 through Fig. 8.7 has shown the smooth geometric distributions. The geometry distributions plotted in Fig. 8.5 - Fig. 8.7 are the results of the first main hull and the subsequent two stepped hulls together. Fig. 8.7 also shows a ten-time amplified keel upset curve for zoom view.

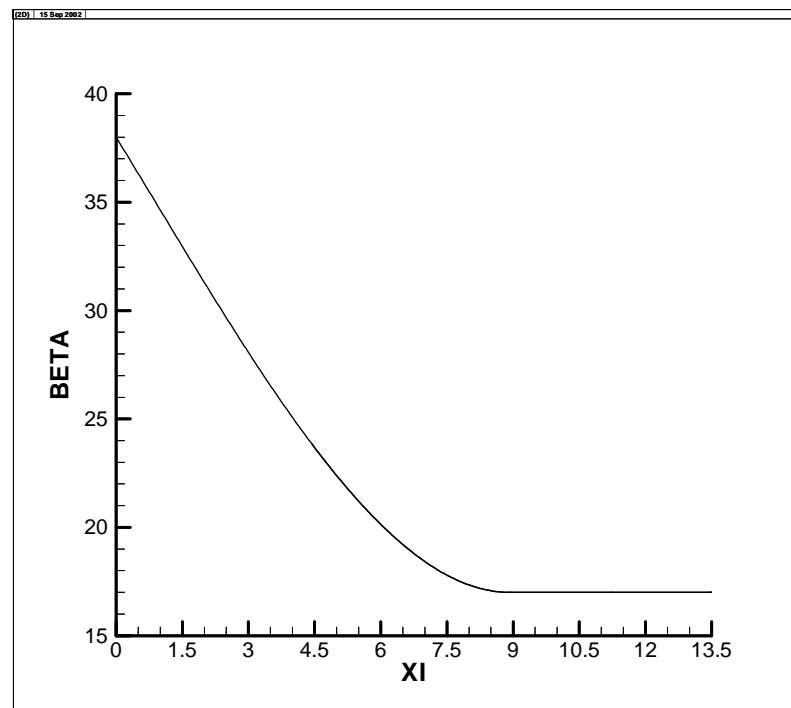


Fig. 8.5 Deadrise angle $\beta(\bar{x})$ distribution over the boat length (in degree)

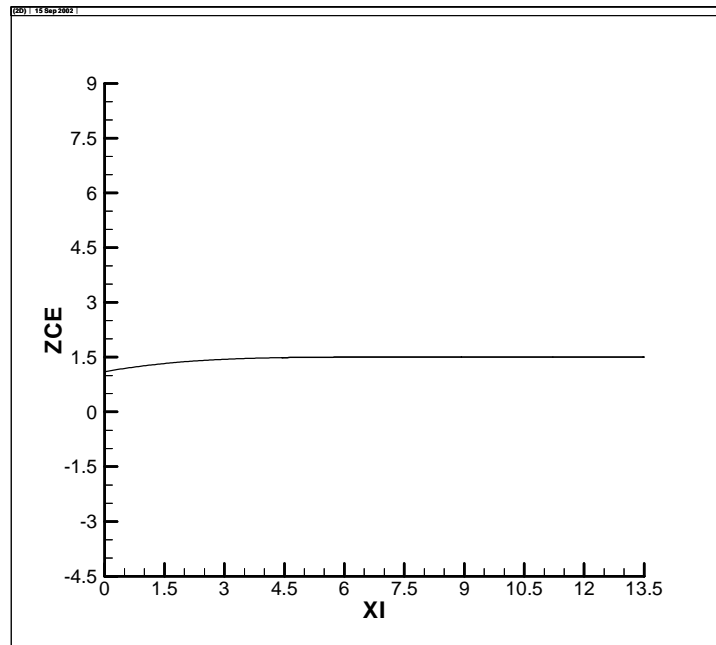


Fig. 8.6 The variation of chine $Z_{CH}(\bar{x})$ along the boat length

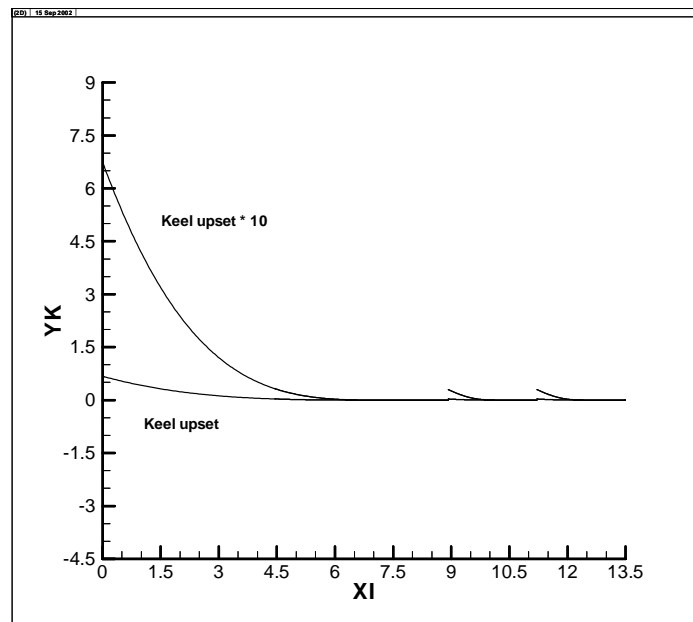


Fig. 8.7 Keel upset (2 steps)

The main geometric parameters of the Vorus-DeCan planing catamaran are listed in the Table 8.1, where,

Z_k : The dimensional keel offset measured from the center line, in FT;

Z_{CH} : The dimensionless chine offset;

W : The boat displacement, in lbs;

X_{mass} : The non-dimensional mass, $X_{mass} = W / (1/2 \rho g Z_k^3)$;

r_{cg} : The dimensionless gyration radius;

x_{cg} : The center of gravity measured from transom;

x_{step} : The non-dimensional distance from transom to step (refer to Fig. 8.7);

As an example, the input values to the codes for the main hull segment are listed in Table 8.2. The data for the two aft hull segments can be found in Appendix K.

Table 8.1 Geometric parameters of the Vorus-DeCan high speed stepped catamaran

Denomination	Symbol	Formulation	Units	Value
Keel offset	Z_k	Z_k	Ft	2.0
Chine offset	Z_{CH}	Z_{CH}	-	1.5
Weight	W	W	LBS	6000
Mass	XMASS	$X_{mass} = W / (1/2 \rho g Z_k^3)$	-	24.04
Radius gyration from transom	GYRAD	$r = \sqrt{r_{cg}^2 + x_{cg}^2} / Z_k$	-	6.33
Center of gravity from transom	XCG	x_{cg} / Z_k	-	5.0
Overall fitting length in computation	XLOA	$x_{LOA} = L / Z_k$	-	13.5
Max half-keel offset	ZKM	Z_{KM}	Meter/Ft	0.61/2.0
Fwd step location from transom	XLSTEP(1)	$x_{step,1} = L_{step,1} / Z_k$	-	4.58
Aft step location from transom	XLSTEP(2)	$x_{step,2} = L_{step,2} / Z_k$	-	2.29
Deadrise angle at transom	BET1	β_1	Degree	17.00

Table 8.2: Input geometry parameters of the main hull segment

Denomination	Symbol	Formulation	Units	Value
Keel upset at entry	YK0	$Y_{k,0}/Z_k$	-	0.675
Keel slope at entry	YK0P	$Y'_{k,0}$	-	-0.30
Keel curvature at entry	YK0PP	$Y''_{k,0}$	-	0.09
Keel upset at transom	YK1	$Y_{k,1}/Z_k$	-	-0.00
Keel slope at transom	YK1P	$Y'_{k,1}$	-	-0.00
Trial water line length	XMAX	x_{\max}/Z_k	-	8.92
Forward keel tangent point from transom	XLA	x_{LA}/Z_k	-	0.17
Aft keel tangent point from transom	XLC	x_{LC}/Z_k	-	0.00
Entry deadrise	BETA0	β_0	Degree	38.00

Slope of deadrise angle at entry	BETA0P	$\partial\beta_0/\partial x$	Deg. Per non-dim. distance	-3.33
Deadrise angle at transom	BETA1	β_1	Degree	17.00
Slope of deadrise angle at transom	BETA1P	$\partial\beta_1/\partial x$	Deg. Per non-dim. distance	-0.00
Forward deadrise angle tangent point from transom	XLAB	x_{LAB}/Z_k	-	0.00
Deadrise angle at keel at entry	BET11	β_{11}	Degree	38.00
Deadrise angle at chine at entry section	BET12	β_{12}	Degree	38.00
Deadrise angle at keel at transom	BET21	β_{21}	Degree	17.00
Deadrise angle at chine at transom	BET22	β_{22}	Degree	17.00
Keel offset at entry	ZK0	$Z_{k,0}/Z_k$	-	1.0
Slope of keel at entry	ZK0P	$Z'_{k,0} = \partial Z_k/\partial x$	-	0.0

Keel offset at transom	ZK1	$Z_{k,1}/Z_k$	-	1.0
Slope of keel at transom	ZK1P	$Z'_{k,1} = \partial Z_k / \partial x$	-	0.0
Chine offset at entry	ZCI0	$Z_{CH,0}/Z_k$	-	1.10
Slope of chine offset at entry	ZCI0P	$Z'_{CH,0} = \partial Z_{CH} / \partial x$	-	0.20
Max. chine offset	ZCIM	$Z_{CH,M}/Z_k$	-	1.50
Chine offset at transom	ZCI1	$Z_{CH,1}/Z_k$	-	1.50
Slope of chine offset at transom	ZCI1P	$Z'_{CH,1} = \partial Z_{CH} / \partial x$	-	0.00
Fwd tangent PT to ZCIM from transom	XLAC	x_{LAC}/Z_k	-	2.17
Aft tangent PT to ZCIM from transom	XLCC	x_{LCC}/Z_k	-	0.00

8.2 Steady Planing Computations

The case of steady planing corresponds to the $\tau = 0$ time step computation of the general seaway dynamics codes, NewCat or CatSea. However, the multi-time stepping computation is used to obtain the equilibrium trim and transom draft in steady planing. Integrating forward in time from an initial guessed trim and draft, the transient dies in time as the boat reaches an equilibrium steady planing. Once an equilibrium steady planing is established the seaway dynamics can commence. Thus, the multi-time step dynamic computation of NewCat and CatSea has been applied to find the equilibrium draft and trim angle. During this preliminary computation, the time step number was set at $IALL = 2000$, the non-dimension $\Delta\tau = 0.3$, so that the non-dimensional time length

$$T = \frac{Ut}{Z_k} = IALL \times \Delta\tau = 600 \text{ was used.}$$

In this steady planing computation, the forward speed is set as $U = 70$ knots. The fractional artificial damping coefficient used in this computation is set to be $\frac{C \times \Delta\tau}{m} = 0.5$. (This value, along with the $\Delta\tau = 0.3$, are significantly larger than used for the wave computations because of the slowly varying non-equilibrium calm-water case, and the fact that only the final equilibrium state is of interest). The initial draft and trim angle of the each hull segment for the equilibrium computation are shown in Table 8.3. In Table 8.3, the intermediate draft values are related to the transom draft by the rigid body trim rotation. The two principal unknowns are the transom draft of hull segment 3 and the trim angle.

Table 8.3: Initial transom draft and trim angle for the comparison computation

Denomination	Symbol	Formula	Initial Value
Transom draft at hull segment 1	HT	H_T/Z_k	0.1176
Transom draft at hull segment 2	HT	H_T/Z_k	0.1609
Transom draft at hull segment 3	HT	H_T/Z_k	0.2043
Trim angle (deg) at hull segment 1	TRIM	α_0	1.088
Trim angle (deg) at hull segment 2	TRIM	α_0	1.088
Trim angle (deg) at hull segment 3	TRIM	α_0	1.088

Define T as the maximum time of the computation. The computation reached steady state at the time $T = 300$. Fig. 8.8 shows the time histories of the transom draft and trim angle for 1st order model and 2nd order model. The transient state due to the non-equilibrium value assumed and its decay to achievement of steady planing state at around $T = 300$ is clearly shown. The computed value are unchanged to the time limit of $T = 600$.

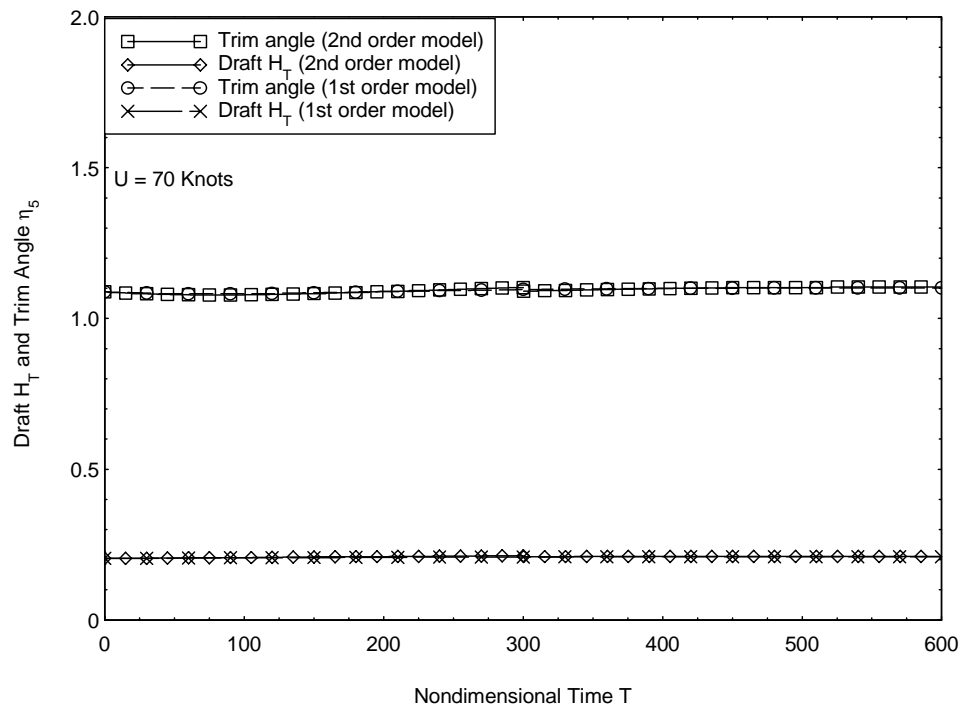


Fig. 8.8 Comparison of histories of draft and trim angle at transom

Table 8.4 lists the comparison values of the transom draft and trim angle at the steady planning state. The level of differences shown on Figure 8.8 and in Table 8.4 reflects the level of theoretical difference between the 1st and 2nd order models.

Table 8.4: Comparison of the transom draft and trim angle in steady planing

Denomination	Symbol	Formula	1 st Order Method	2 nd Order Method
Transom draft at hull 1	HT	H_T/Z_k	0.1214	0.1232
Transom draft at hull 2	HT	H_T/Z_k	0.1652	0.1672
Transom draft at hull 3	HT	H_T/Z_k	0.2091	0.2112
Trim angle (deg) at hull 1	TRIM	α_0	1.101	1.104
Trim angle (deg) at hull 2	TRIM	α_0	1.101	1.104
Trim angle (deg) at hull 3	TRIM	α_0	1.101	1.104

Table 8.5 shows the comparison of numerical results obtained from the two methods. The predicted lift and the center of lift are in a good agreement with the required design values. The lift produced by the planing hydrodynamics is in balance with the boat weight, and the lift force center is same as the gravity center, therefore the boat is running at a steady planing equilibrium. Then lift/drag ratios predicted by the two models are essentially the same, and are high values for a boat speed of 70 knots.

Table 8.5 Numerical comparison of two models in steady planing

Denomination	Symbol	Formula	1 st Order Method	2 nd Order Method
Required lift	CLT0	$W/(0.5\rho U^2 Z_k^2)$	0.11085820	0.11085820
Total lift	CL	$L/(0.5\rho U^2 Z_k^2)$	0.11091274	0.11123141
Total drag	CD	$D/(0.5\rho U^2 Z_k^2)$	0.02384798	0.02393888
Center of gravity required	XCG	x_{cg}/Z_k	5.00000000	5.00000000
Center of lift from transom	XBT	x_{CL}/Z_k	5.00001578	5.00093329
Lift-drag-ratio	XLOD	C_L/C_D	4.65082233	4.64647336

The following comparison and discussion are based on the results at the steady planing state. Figures 8.9 to 8.12 are computation results from the 2nd order nonlinear model. Again, the x - coordinate in these figures is the coordinate of the initial wetted length, it is from bow to stern. Fig. 8.9 is the sectional lift distribution over the hull length. In Fig. 8.9, each hull segment has its own contribution to the total lift distribution. The transverse steps restart a chine-unwetted flow, as evidenced by the large lift distributions off the steps. From Fig. 8.11, it is clearly shown that the jet velocity has a large jump across the steps. This large jet velocity results in the large sectional force peak

developed downstream of the steps (Fig. 8.9); refer to the $V_s^2(1, \tau)$ term in the pressure formulae of (4.84) and (4.85) in Chapter 4.

There is a singularity in the sectional force distribution at the chine-wetting point. This is due to the slope discontinuity of the hard-chine geometry. The sudden stop in z_c advancement when the chine is reached, results in an infinite velocity gradient, which is the reason for the negative suction pressure indicated on Figure 8.9. The forces are, of course, integrable.

Fig. 8.10 gives the plan view of the flow field geometry. It shows the jet-head offsets $z_b^+(x)$ and $z_b^-(x)$. Within this plot it is clearly evident that in the flow fields the aft two step hull segments are chine-unwetted. Without the steps, the flow of the first hull segment would develop into a chine-wetted flow, and the hull would continue to be chine-wetted from that point aft. As we expected, the steps are therefore seen to maintain the flow as chine-unwetted, which is desirable.

Fig. 8.12 is the running half-body plan. It shows the wetted and non-wetted hull contours, for all three hull segments, from the transom up to the forward end of the waterline.

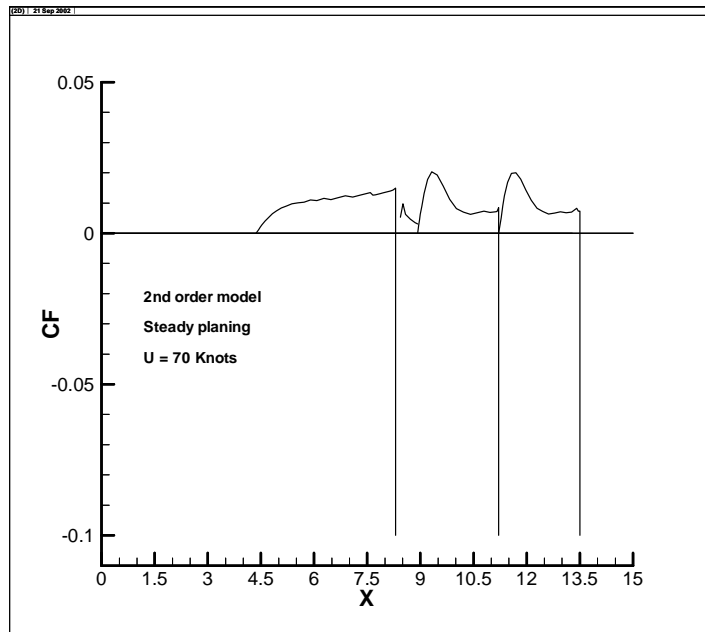


Fig. 8.9 Lift distribution over the boat length (Steady planing, 70 Knots)

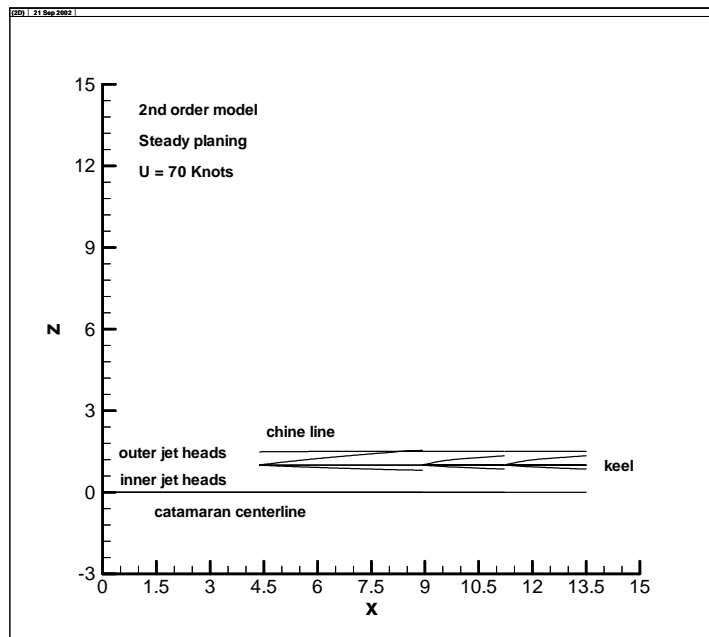


Fig. 8.10 Flow geometry in the plan view (70 knots)

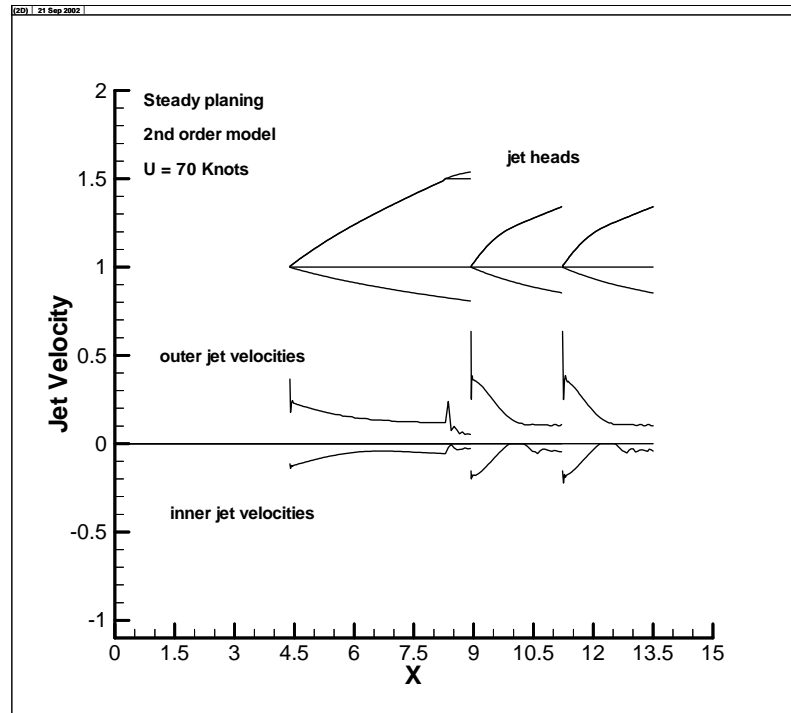


Fig. 8.11 Jet velocity distribution (Steady planing, 70 knots) (zoom view)

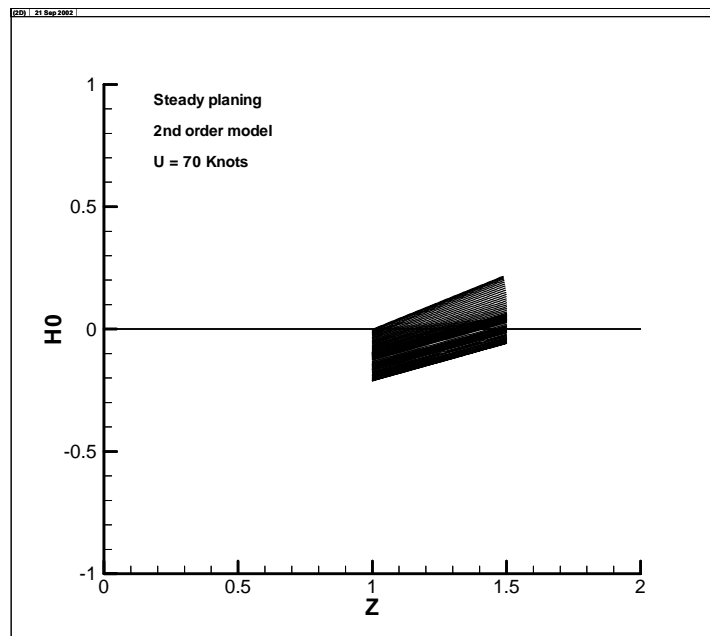


Fig. 8.12 Body plan (Steady planing, 70 Knots)

Fig. 8.13 to Fig. 8.15 show the comparison of the computation results of the 2nd order nonlinear model (NewCat 2-4a) with the 1st order nonlinear model (CatSea 2-4a) at the same steady planing. In general, the results of 2nd order model are in good agreement with the results of 1st order, excepting some local differences. Fig. 8.13 shows the comparison of the sectional lift distributions. The total lift results predicted by the two models, of course, have to be the same since the same boat weight was specified in the two equilibrium computations (ref. to Table 8.5). However, there are local differences when the details of the two computations are compared. Fig. 8.14 is the comparison of the jet head offsets in the plan view. The horizontal projection of the jet heads z_b^+ and z_b^- predicted by the 2nd order model are wider than that predicted by the 1st order model. Fig. 8.15 shows a longitudinal comparison of the jet velocity distributions. Again, the jet velocities predicted by the 2nd order model are larger than that by the 1st order model at the inside jet.

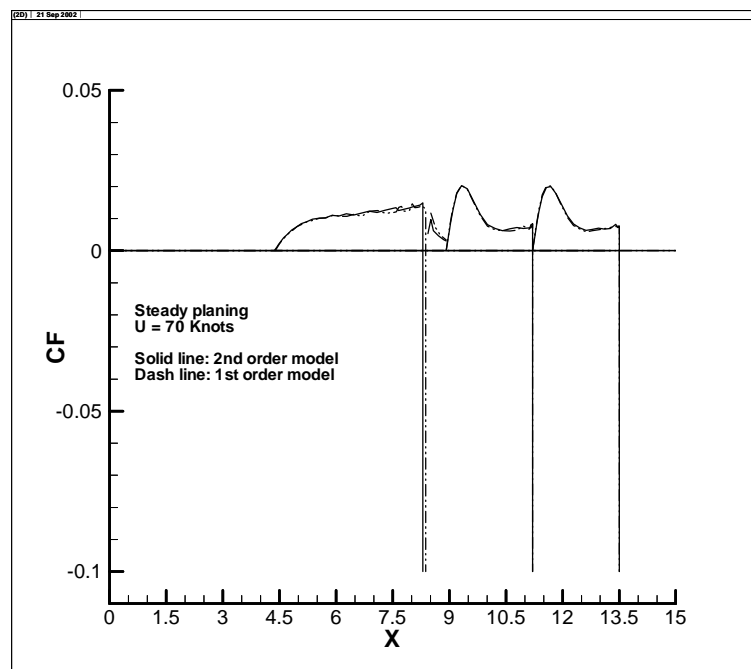


Fig. 8.13 Comparison of the sectional lift distributions in steady planing

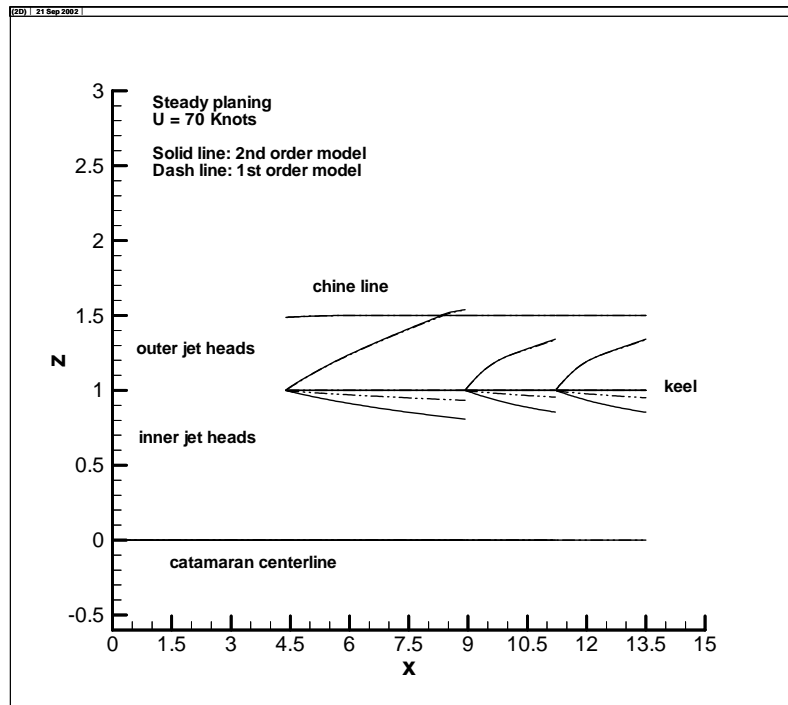


Fig. 8.14 Comparison of the horizontal projection of the jet heads (zoom view)

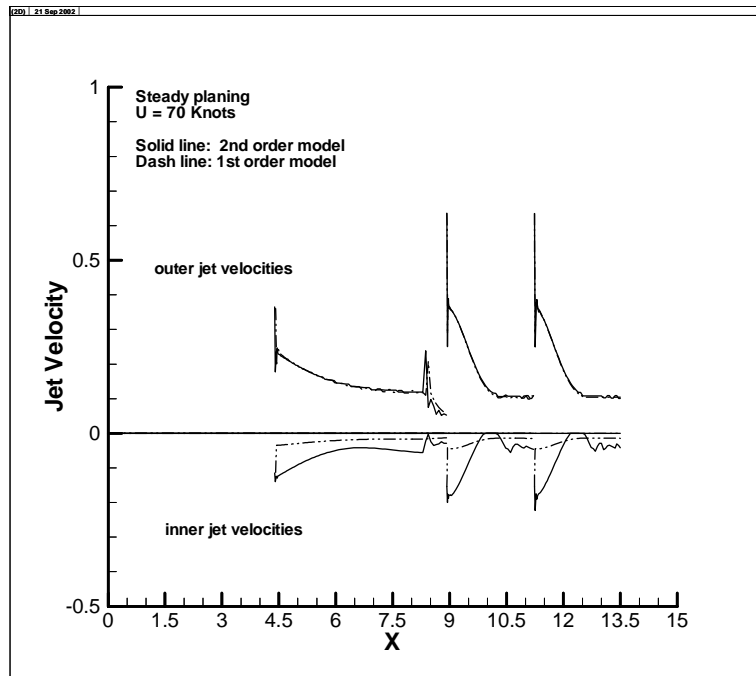


Fig. 8.15 Comparison of the jet velocity distribution along the boat length

Fig. 8.16 and Fig. 8.17 show a comparison of the pressure distribution in the main hull segments, CP is the pressure coefficient defined by (3.61), (3.62), (4.64) and (4.65). Fig. 8.18 and Fig. 8.19 show the comparison of the pressure distribution in the second hull segment, Fig. 8.20 and Fig. 8.21 show the comparison of the pressure distribution in the third hull segment. In these figures, the pressure distributions at the bow are much higher than that at the transom. Again, from these figures, it is found that the pressure at the two steps are much higher than at the main hull. The shape of the pressure distribution for the planing catamaran is, unlike the monohull (Vorus, 1996), close to a constant distribution, this appears to stem from the requirement for atmospheric pressure at the two jets. The pressure distributions appear to be almost discontinuous at each of the jets, but in fact they are not.

Generally speaking, the shape and the amplitude of resulting curves in the 2nd order model (NewCat) are very similar to the results in the 1st order model (CatSea), however, on the local details of the flow field and on the pressure distribution, there are some differences. The comparisons of results have established that the results of the 2nd order nonlinear model, for calm water planing, are compatible with the 1st order model, although the formulations have very clear differences.

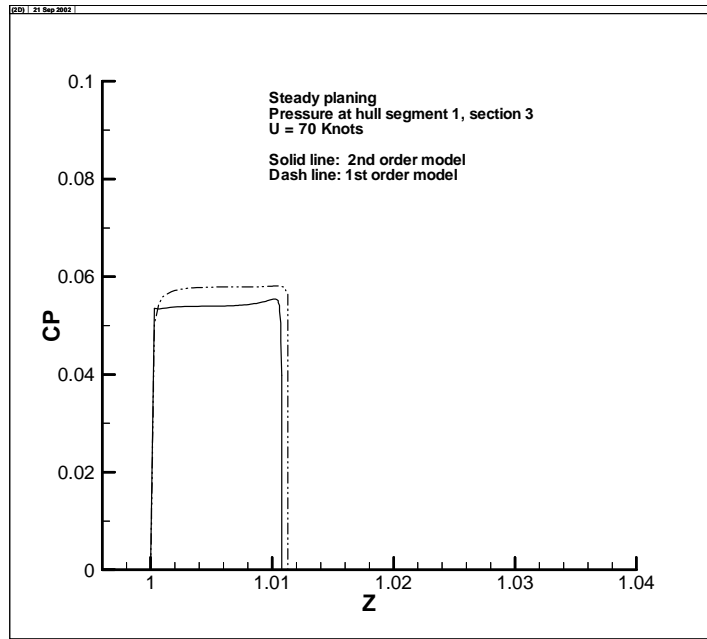


Fig. 8.16 Comparison of pressure distribution at hull segment 1, section 3

(from the entry $\bar{x}_i = 0.0681$ in 2nd order model, $\bar{x}_i = 0.067$ in 1st order model)

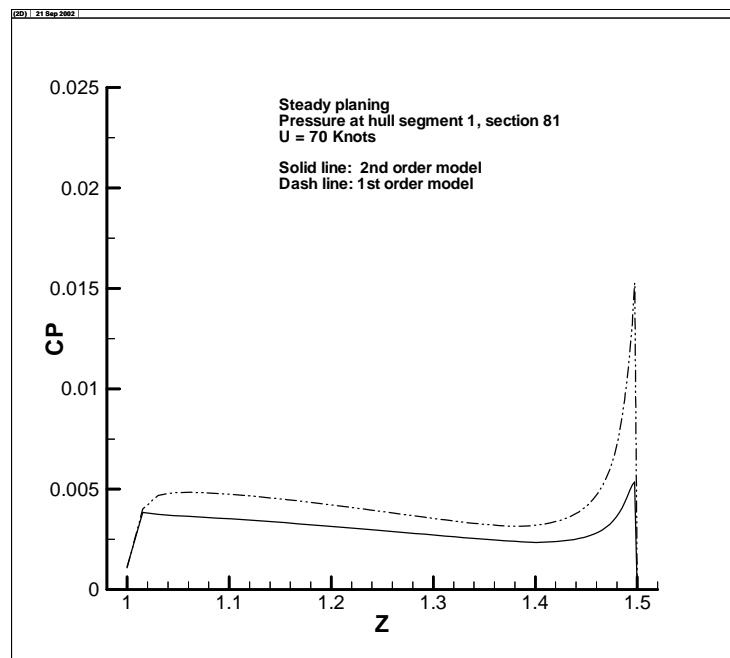


Fig. 8.17 Comparison of pressure distribution at hull segment 1, section 81

(from the entry $\bar{x}_i = 4.5552$ in 2nd order model, $\bar{x}_i = 4.4786$ in 1st order model)

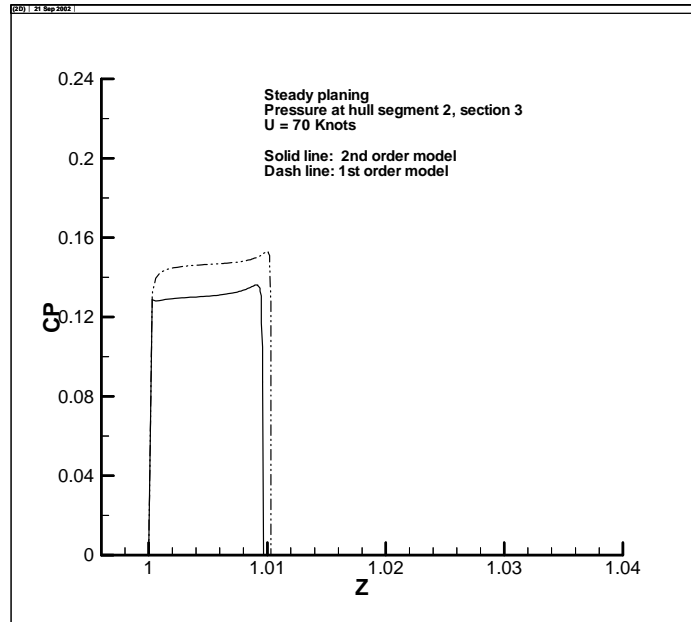


Fig. 8.18 Comparison of pressure distribution at hull segment 2, section 3

(from the forward step $\bar{x}_i = 0.034236$)

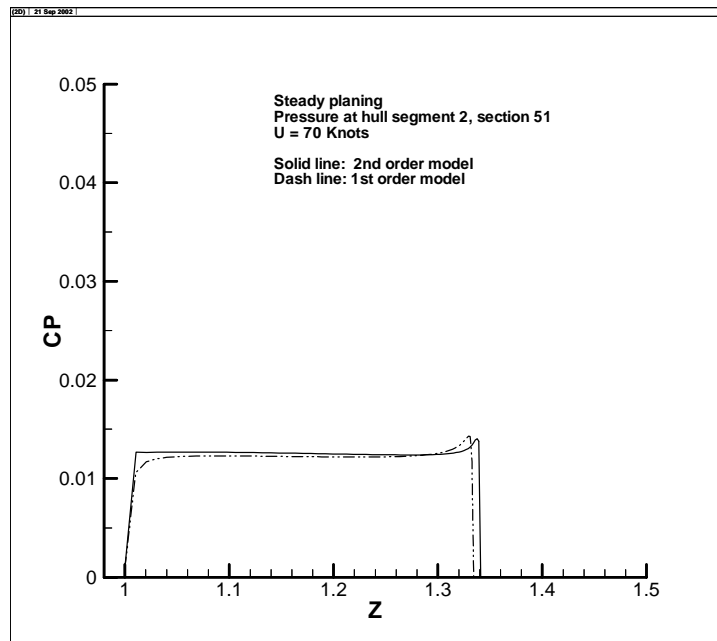


Fig. 8.19 Comparison of pressure distribution at hull segment 2, section 51

(from the forward step $\bar{x}_i = 2.29$)

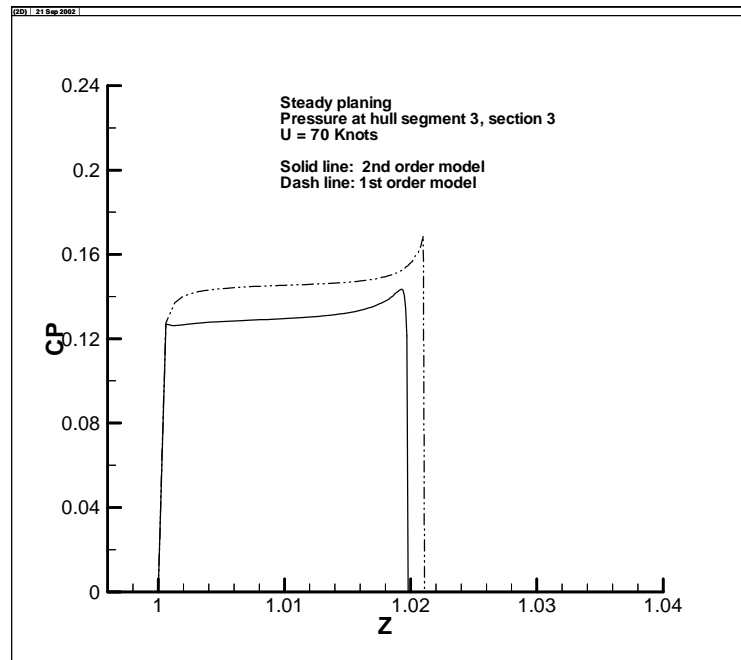


Fig. 8.20 Comparison of pressure distribution at hull segment 3, section 3
(from the aft step downstream $\bar{x}_i = 0.068242$)

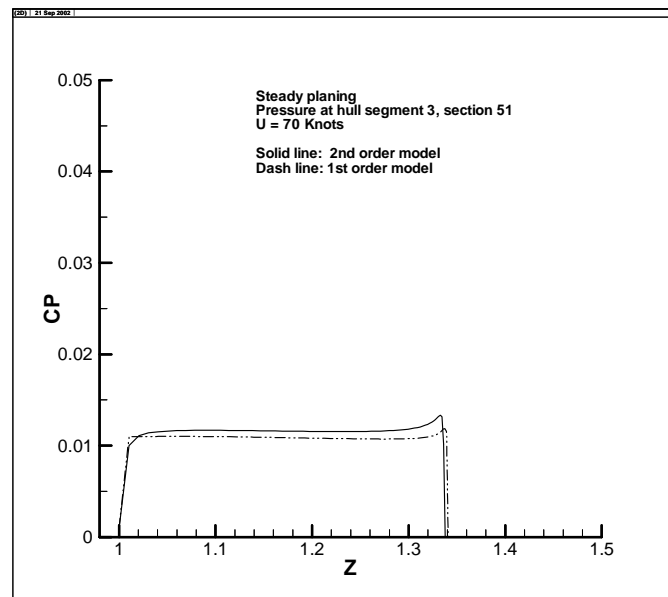


Fig. 8.21 Comparison of pressure distribution at hull segment 3, section 51
(from the aft step downstream $\bar{x}_i = 2.29$)

CHAPTER 9

HIGH SPEED CATAMARAN PLANING IN WAVES

At present, modern, high speed craft are usually not limited so much by structural strength requirements, but instead by the ability of the crew to survive the sometimes large impact accelerations associated with craft operation in the seaway. It has been noted that impact accelerations are sensitive to minor variations in the hull geometry. This is especially true where small changes in the deadrise angle can significantly reduce impact accelerations (Garner 2000). Therefore, the ability of the nonlinear model to correctly predict the high speed planing catamaran performance in a seaway is a focus of the present research.

As was described in Chapters 2 through 4, we solve the planing catamaran hydrodynamics problem in the time domain. The present nonlinear models (1st and 2nd order) predict the spatially varying pressure in time on the instantaneous wetted surface of the hull. This pressure is used to predict the nonlinear hydrodynamic force and moment on the planing hull. The impact accelerations are then computed from Newton's law in two degrees of freedoms. These accelerations are then integrated to compute the heave and pitch velocities and displacements. The new heave and pitch velocities and displacements, along with the ambient wave velocities and displacements along the hull, are used in the next time step as the initial conditions for that time step. This process is

repeated as time progresses. The histories of the heave and pitch motions, including accelerations at the bow, center of gravity, and stern, are thereby obtained.

9.1 Numerical Results of 2nd Order Model

The 2nd order design tool NewCat (2-4a) has been applied to the 30ft high speed stepped catamaran described in Chapter 8 for the regular wave cases.

In this computation example, we set up the forward speed $U = 70$ knots, same as that in the steady planing case. Time step number was set at $IALL = 12,500$, with an initial non-dimension time step increment $\Delta\tau = 0.02$. The non-dimensional time for the computation is therefore $T = 0.02 \times 12500 = 250$. It is 4.24 seconds in real dimensional time. The fractional artificial damping coefficient $\frac{C \times \Delta\tau}{m} = 0.1$. This is reduced from the Chapter 8 calm-water equilibrium calculation since the details of the time response is of interest here.

The programs (NewCat or CatSea) have a restart capability. The computation can be stopped after a specified number of time steps and a data DUMP file created at the stop. The DUMP file becomes the RESTART file on resumption of the computation with some possible adjustments in the input data such as the time step size or the convergence criteria, if necessary.

In this example, a non-dimensional regular, head wave of height $\frac{H_s}{z_k} = 0.50$ is used; this corresponds to a dimensional wave height of 1.0 ft. The wave length $\frac{\lambda}{z_k} = 60$,

and the initial wave phase angle $\theta_0 = 0^0$, corresponding to placement of a zero-wave amplitude at the at $\tau = 0$.

For the computation, the instantaneous wetted main hull segment was divided into 80 x -elements along its length, and the two instantaneous wetted sub-segment lengths were divided into 50 x - elements each.

Fig. 9.1 – Fig. 9.6 are the computation results of the 2nd order model. The 1st order model results will be listed in next section. Fig. 9.1 depicts the time histories of the regular sinusoidal wave elevations at the bow and at the transom, the bow displacement, the transom draft, the step drafts, and the pitch angle. From Fig. 9.1, it is evident that the pitch curve is not a simple harmonic response curve, and its phase shifted relative to the wave elevation at the bow. The drafts at the transom and steps are decreasing slightly over the time span of the computation. It can be noted from Figure 9.1 that the boat is rising in the regular wave system (decreasing draft and increasing bow elevation). As will be shown, this is due to the DC shift in the acceleration response (more up than down).

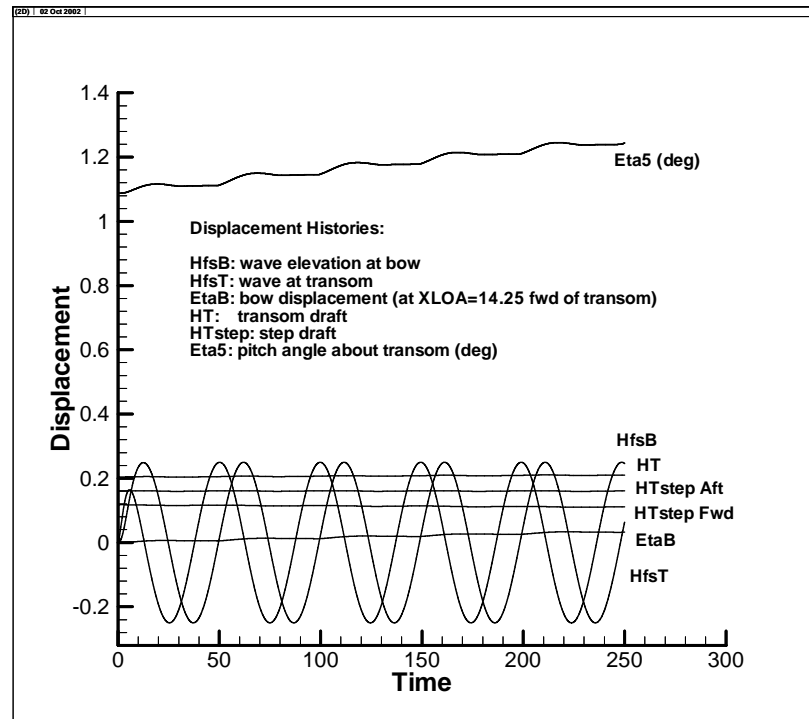


Fig. 9.1 Displacement histories (2nd order model)

Fig. 9.2 shows the predicted vertical acceleration, in g's, at the bow (solid line), at the center of gravity (dash line), and at the transom (dash-dot line). It is remarkable to observe the asymmetry of these curves. The positive upward acceleration peaks are much larger than the downward. Although the exciting wave is simple harmonic, the acceleration response is not, showing a strong non-linear, irregular characteristic. This non-linear behavior of the planing catamaran acceleration response demonstrates that the frequency response amplitude operator (RAO's) method is not valid for the computation of acceleration response, as in the typical small amplitude displacement-type ship case. Furthermore, the linear response superposition method is not applicable for predicting the acceleration response in the irregular seaway, i.e., a frequency domain solution method is not acceptable for predicting the response of the planing catamaran in waves.

Fig. 9.2 also shows that the boat is out of water at the wave trough region (refer to Fig. 9.3), the correspondent vertical acceleration at the transom is close to -1.0 g , which is the downward gravity acceleration. Therefore, when the boat re-contacts the wave surface, it experiences a large impact.

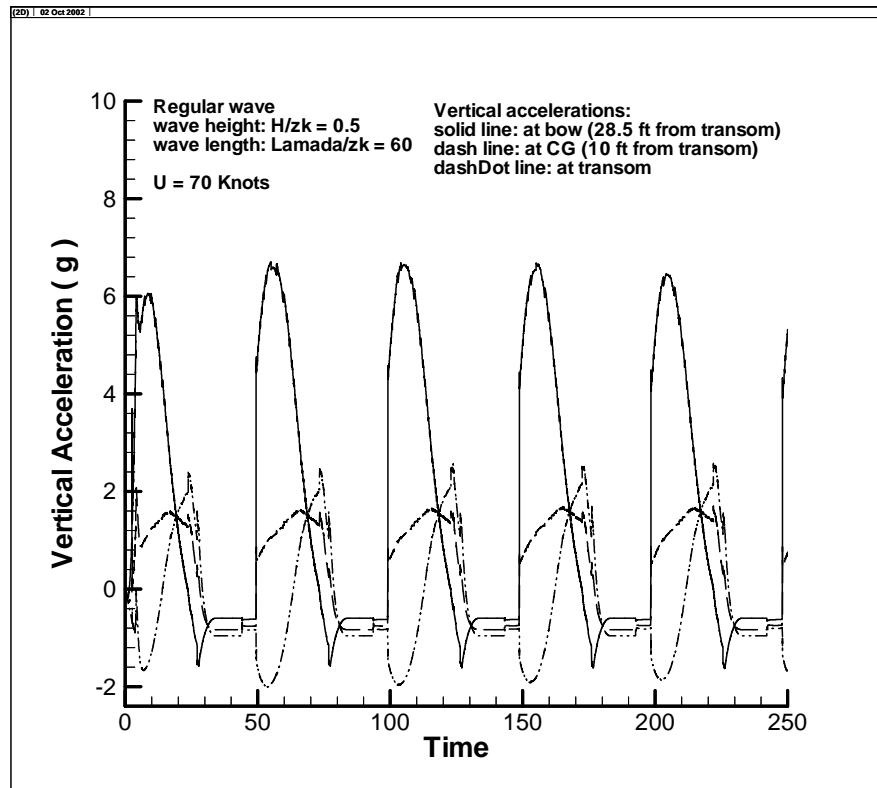


Fig. 9.2 Vertical accelerations (2nd order model)

Fig. 9.3 depicts the time histories of the wetted length (solid lines) and the chine-wetted length (dashed lines) for each of the three boat segments. Recall that the wetted water line length $L(\tau) = x_{\max}/Z_k$, is the distance from the each hull segment transom to its forward waterline-end (entry point) (refer to Fig. 3.8). The chine-wetted length $L_{cw}(\tau) = x_{cw}/Z_k$ is the distance to the point of chine-wetting from the each hull segment

transom. From these curves it is easy to see that the waterline length of the main hull changes with the period of the incoming waves; the waterlines of the sub-hull segments experience less change. The chine-wetted length of the sub-hull segments is zero most of the time, which implies that behind the steps the sub-hull segments remain fully chine-unwetted, which is the desired characteristic by design. The main hull has a chine-wetted length that varies with the boat and wave motions. By Fig 9.3, the main hull runs increasingly chine unwetted length with time. This is due to the rise of the boat relative to the wave system associated with the acceleration nonlinearity (cited with respect to Figures 9.1 and 9.2).

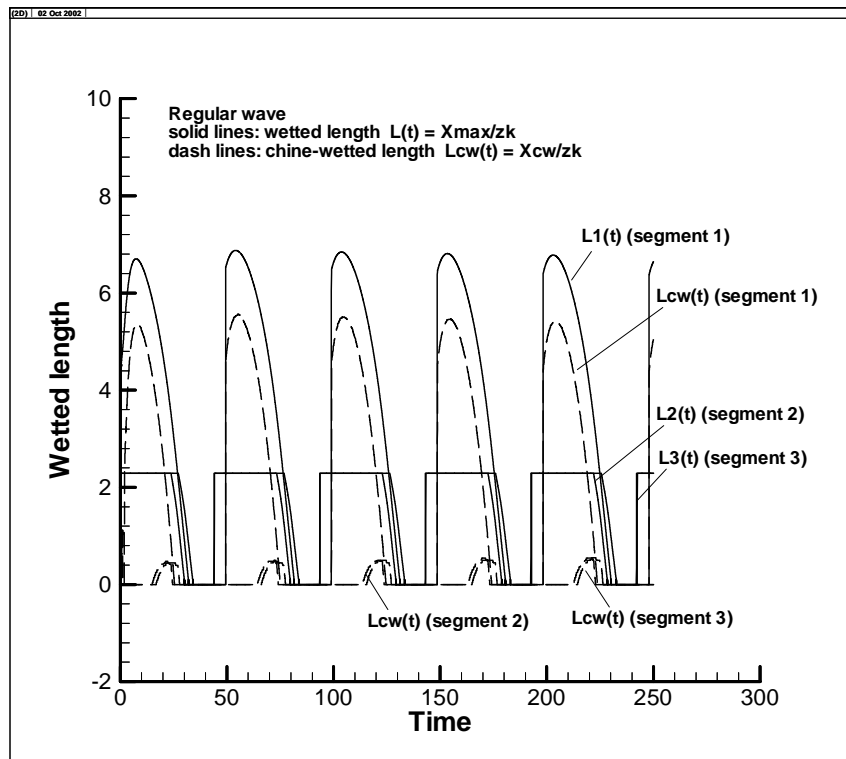


Fig. 9.3 Wetted length and chine wetted length (2nd order model)

Fig. 9.3 clearly shows the important behavior that the boat completely lifts clear of the water at the trough region of the incoming waves (refer to the waves in Fig. 9.1); the wetted lengths (water lines) for all three hull segments are zero in Fig. 9.3 during these periods.

The non-dimensional time $T = 250$ is the last step in our computation. The result of the flow field detail at $T = 250$ is shown here as an example. Fig. 9.4 shows the sectional lift distribution at the non-dimension time $T = 250$. It shows that the main lift at this time is contributed by the main hull segment. Fig. 9.5 represents the flow geometry in the plan view (at $T = 250$). It can be seen from Fig. 9.5, the two stepped hull segments are all chine-unwetted, which improves the lift characteristic of the boat, as explained previously. Fig. 9.6 depicts the jet velocity distribution at $T = 250$, the velocity has large peaks at the beginning of the steps, which is the same characteristic as demonstrated in the steady planing case, Chapter 8.

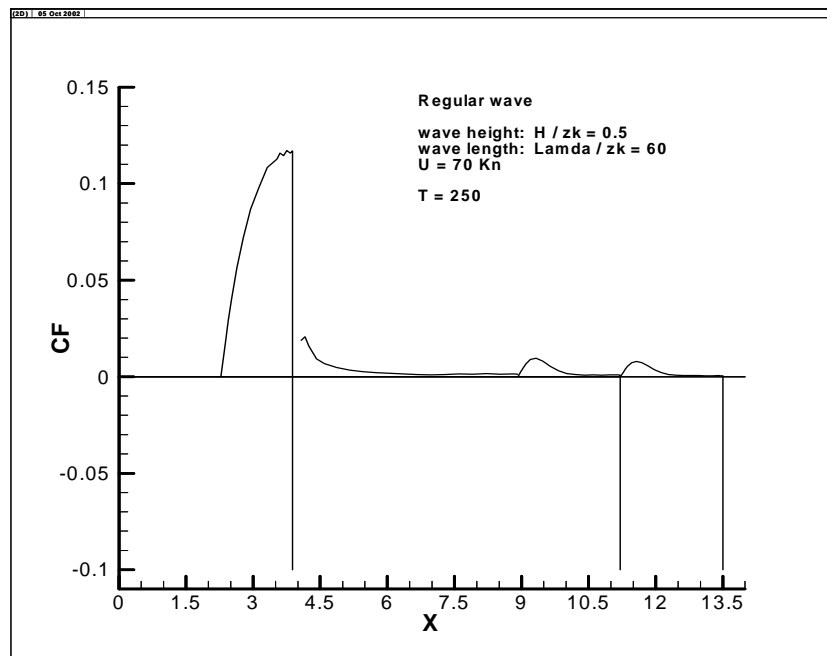


Fig. 9.4 The sectional lift distribution at $T = 250$

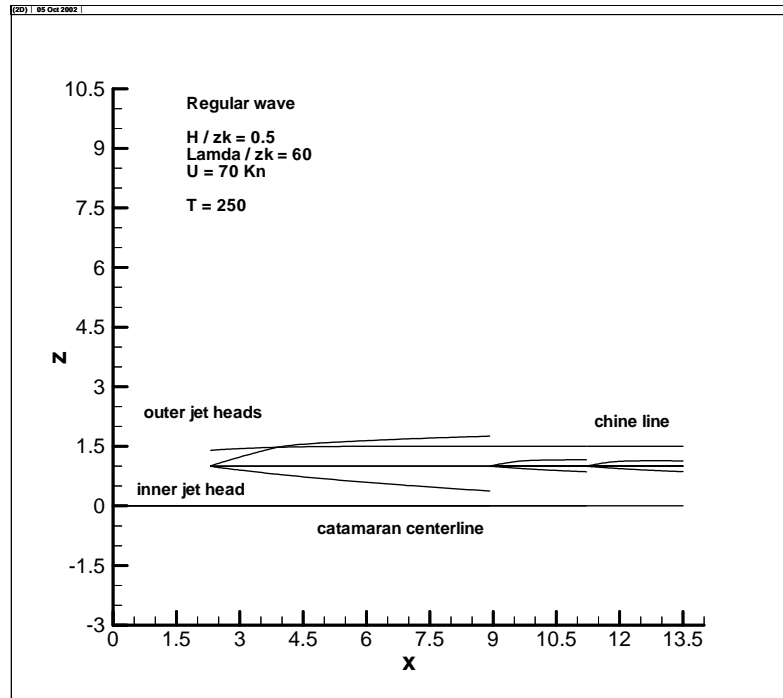


Fig. 9.5 Flow geometry in the plan view (at $T = 250$)

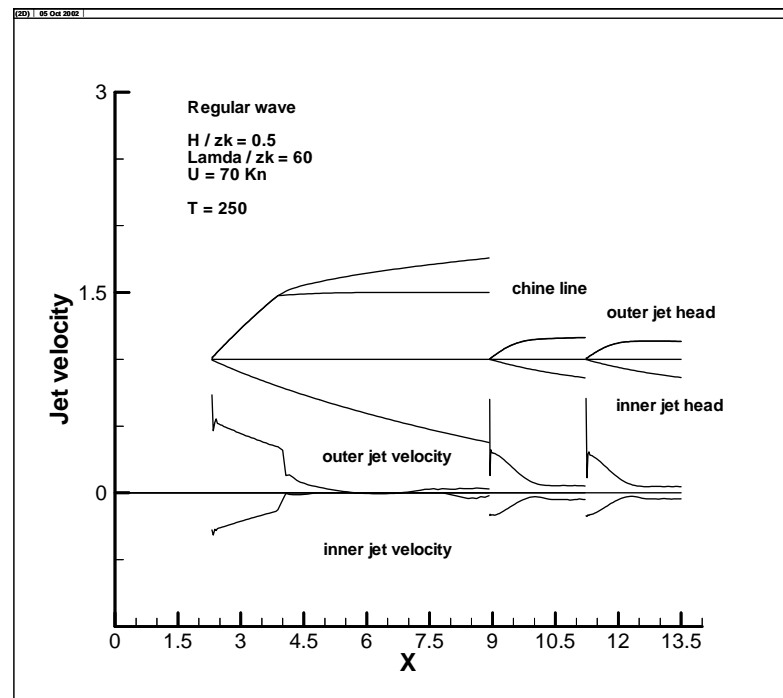


Fig. 9.6 Jet velocity distribution zoom view (at $T = 250$)

From this computation example, it is demonstrated that the present second order nonlinear model has the ability to predict the planing catamaran behavior in regular waves.

9.2 Comparisons For the Regular Wave Case

For comparison, the 1st order code CatSea2-4a has been applied to the same planning catamaran and the same regular waves.

Fig. 9.7 - Fig. 9.9 are the time histories of the waves, motions, vertical accelerations, the wetted lengths, which are the counterparts of Fig. 9.1 - Fig. 9.3.

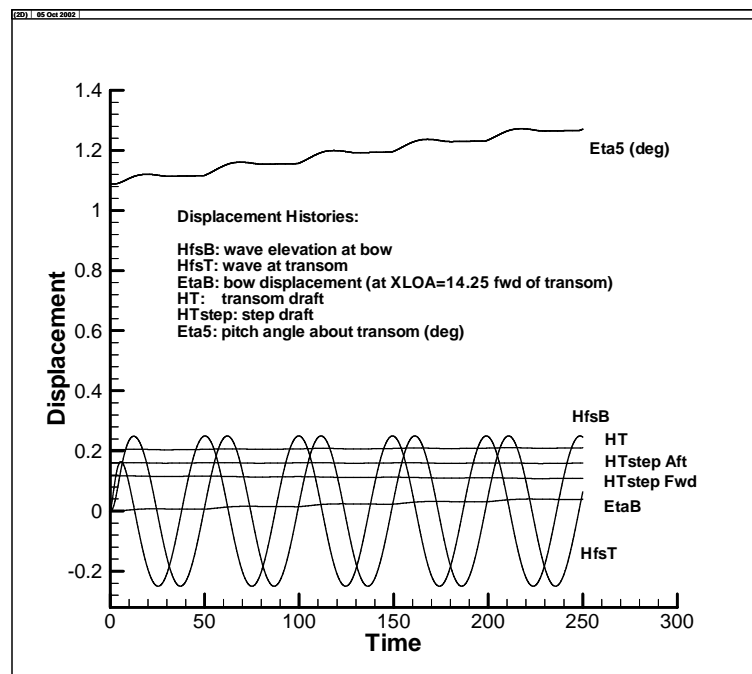


Fig. 9.7 Wave and motion histories from CatSea2-4a (1st order model)

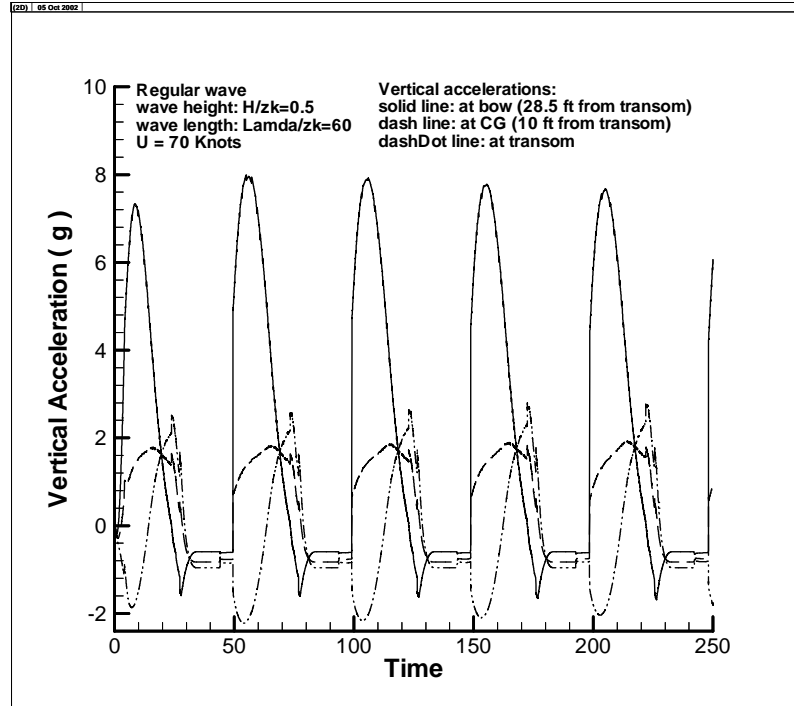


Fig. 9.8 Vertical accelerations from CatSea2-4a (1st order model)

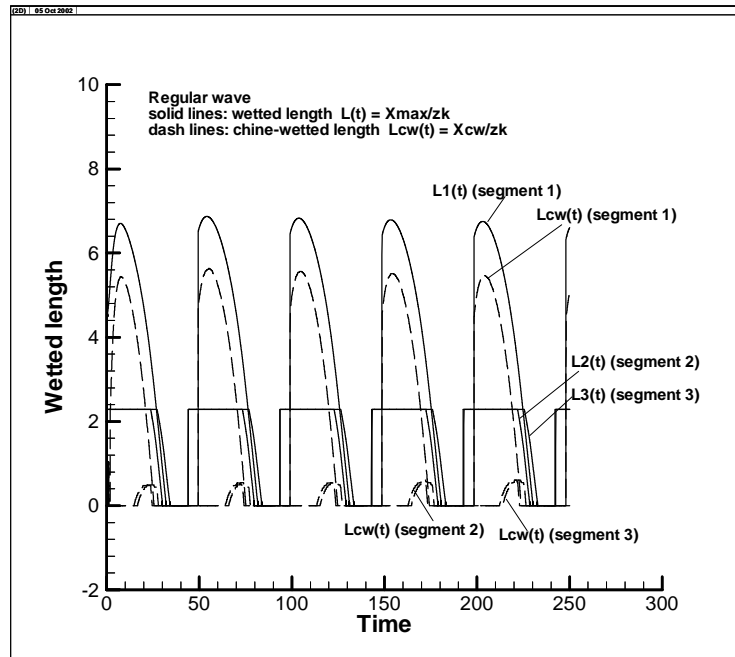


Fig. 9.9 Wetted lengths from CatSea2-4a (1st order model)

Comparing Fig. 9.7 – Fig. 9.9 in 1st order model with Fig. 9.1 – Fig. 9.3 in 2nd order model, it is evident that the two group figures are very similar, except for the local details. The local differences reflect the difference of the two different kind of theoretical models. The detail differences are shown in following figures.

Fig. 9.10 shows the comparison of the transom draft and the trim angle for the 1st and the 2nd order theories. In Fig. 9.10, the transom drafts are not actually identical, with greater differences in the trim angles. The predicted trim angle of the boat increases faster in the wave system by the 1st order theory. This mirrors the difference in the acceleration distributions predicted (refer to Fig. 9.11).

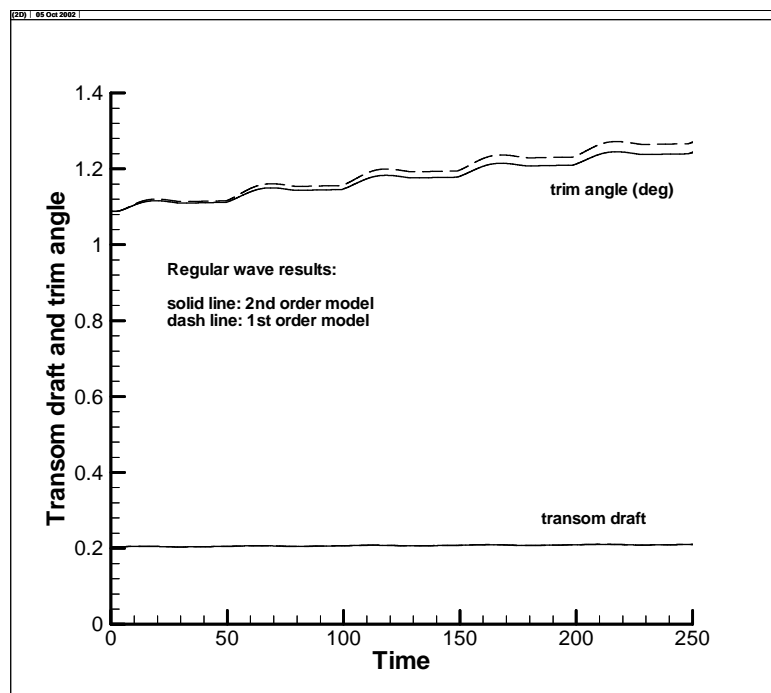


Fig. 9.10 Comparisons of trim angle and transom draft; 1st and 2nd order models

Fig. 9.11 – Fig. 9.13 shows the differences in the vertical accelerations. It is found that the 1st order model predicts much larger impact accelerations than the 2nd. Especially

at the bow region, the acceleration of 1st order model has a larger peak, which results in a larger trim angle as shown in Fig. 9.10.

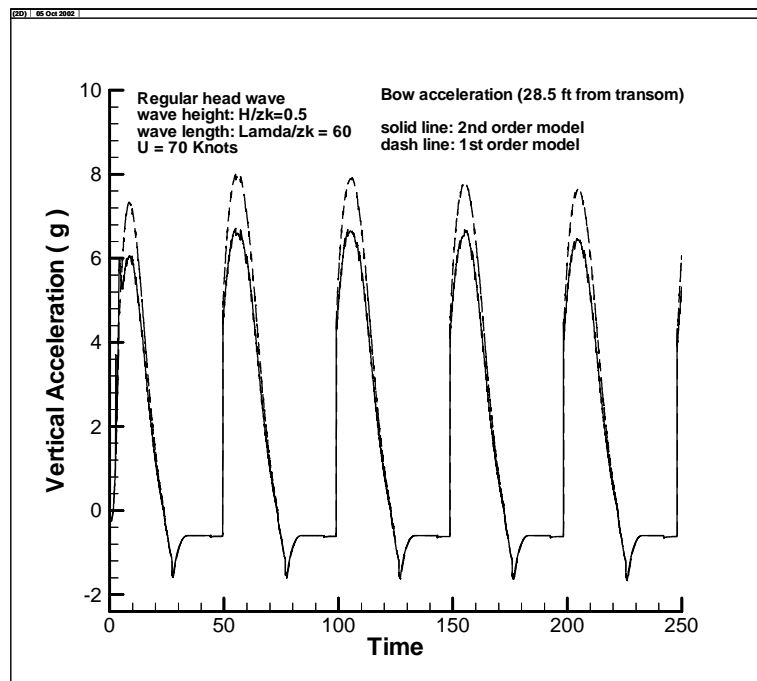


Fig. 9.11 Comparison of bow accelerations; 1st and 2nd order models

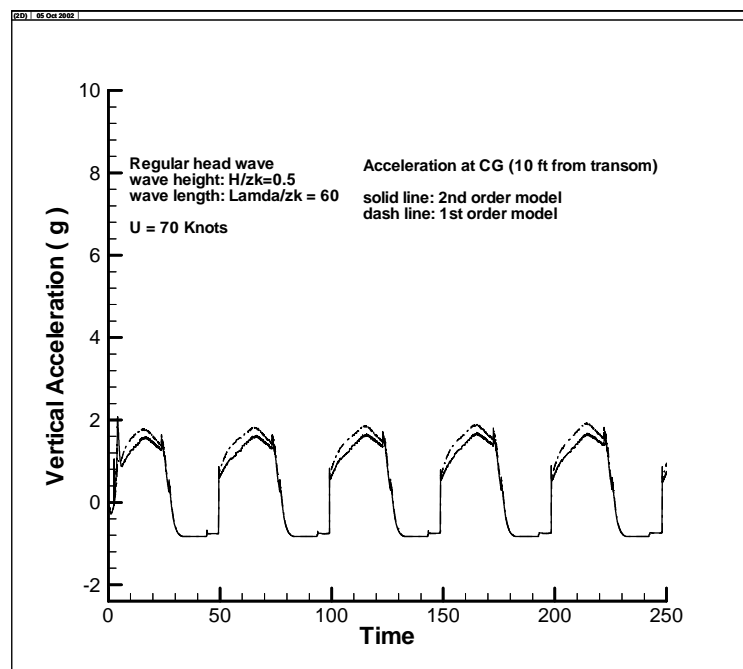


Fig. 9.12 Comparison of the vertical acceleration at CG; 1st and 2nd order models

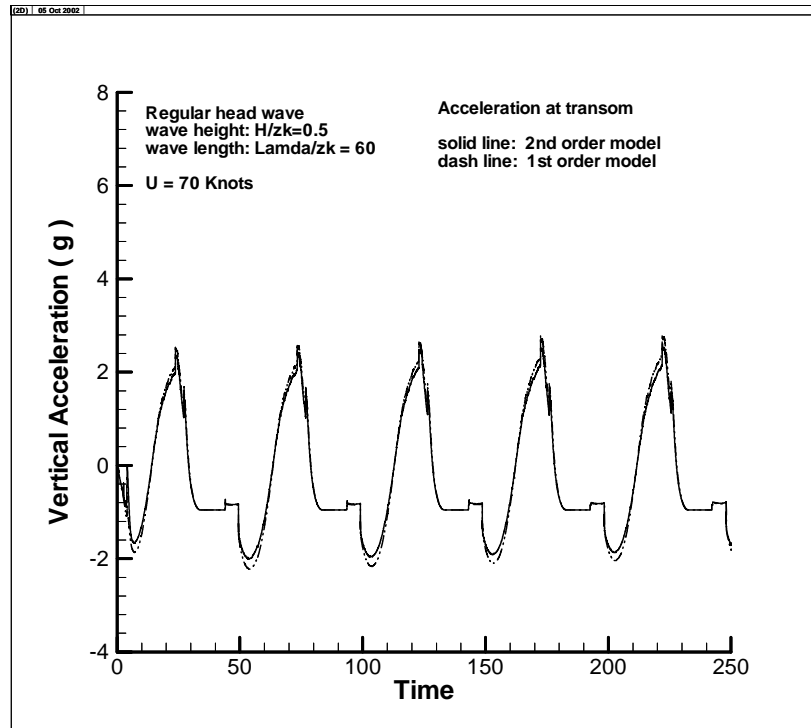


Fig. 9.13 Comparison of the vertical acceleration at transom; 1st and 2nd order models

Fig. 9.14 shows the comparison of the wetted length and the chine-wetted length for the main hull segment. The solid lines are the predicted results of the 2nd order model for the wetted length $L(\tau)$ and the chine-wetted length $L_{cw}(\tau)$, and the dash lines are the results of the 1st order model. Fig. 9.14 shows that the predicted $L(\tau)$ and $L_{cw}(\tau)$ are very close for both cases.

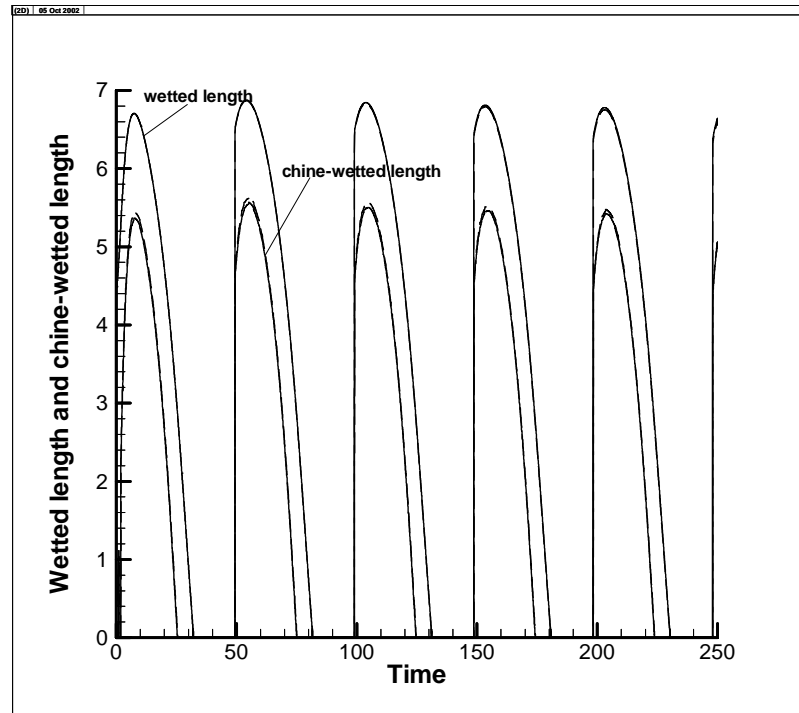


Fig. 9.14 Comparison of the wetted length and the chine-wetted length
for 1st and 2nd order models

Fig. 9.15 - Fig. 9.17 give the comparisons of the detail results of the two theories at the non-dimension time $T = 250$. Fig. 9.15 gives the comparison of the sectional lift distribution. The sectional lift by the 1st order model is larger than that predicted by the 2nd order model. This is again fully consistent with the higher accelerations (and higher trim angle) predicted by the 1st order. Fig. 9.16 depicts the difference in the jet-head streamline offsets in the two predictions. Both models predicted the chine-wetted condition of the first segment at the time displayed. However the outer jet-head streamline offset of 1st order model is wider than the results in the 2nd order model, and the inner jet-head streamline offset of the 1st order model is narrow than the results from the 2nd order model. Fig. 9.17 graphs the differences of the jet velocity distributions for

the two theories in zoom view. The jet velocity distribution of the 1st order model is higher in the outer jet-head region, and lower than the 2nd order model in the inner jet-head region, which is again completely consistent with the jet-head offset comparison in Fig. 9.16.

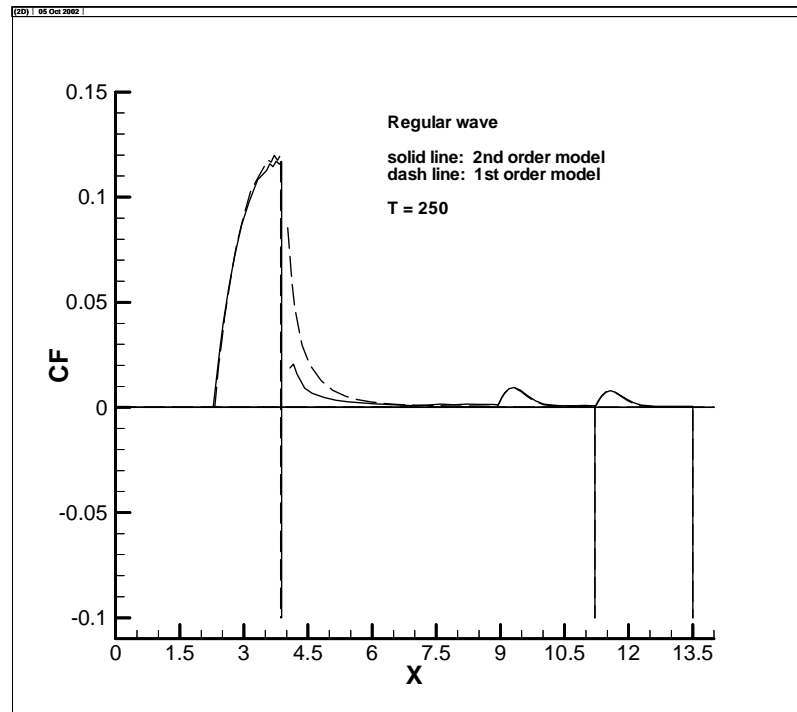


Fig. 9.15 Comparison of the sectional lift distribution at $T = 250$; 1st and 2nd order models

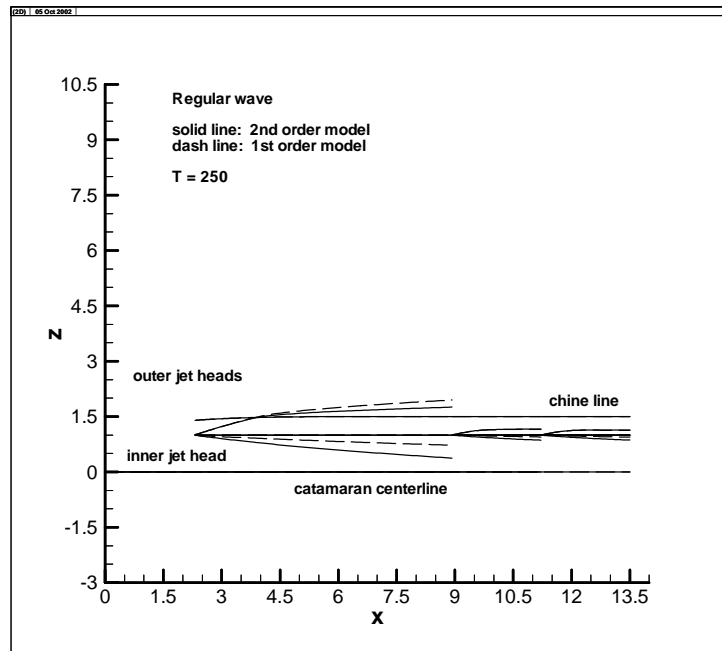


Fig. 9.16 Comparison of flow fields in a plan view at $T = 250$; 1st and 2nd order models

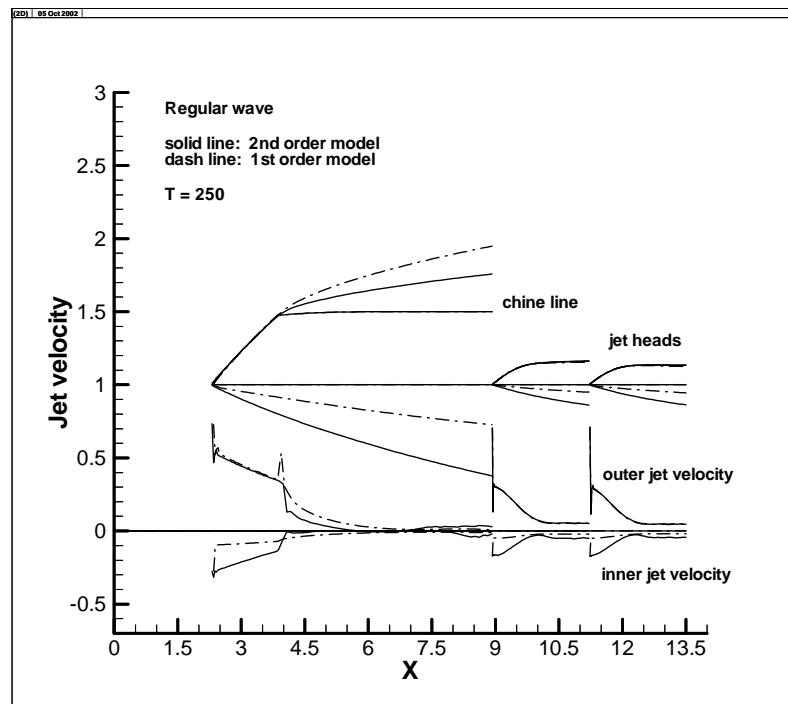


Fig. 9.17 Comparison of jet velocity distributions at $T = 250$ (zoom view)
for 1st and 2nd order models

Fig. 9.18 is the pressure distribution comparison at the section 3 of the main hull segment for both models. Again as displayed in Chapter 8, the pressure distribution of the 1st order model is higher than the pressure in the 2nd order model.

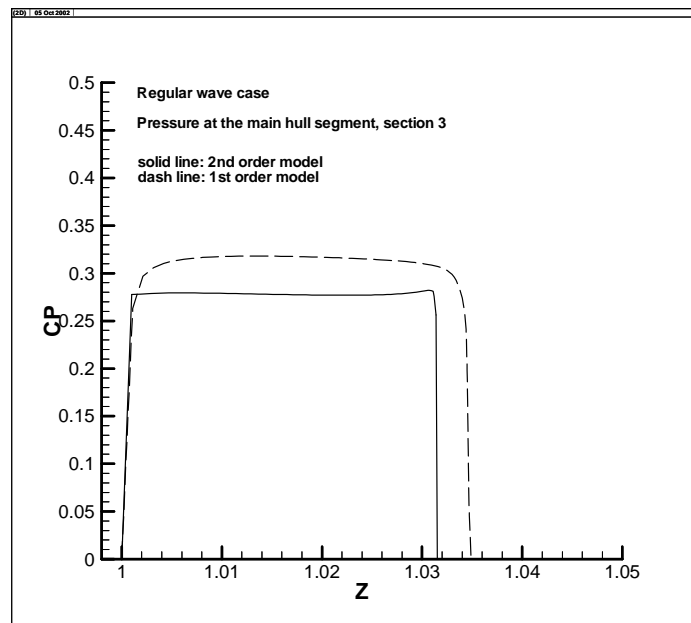


Fig. 9.18 Comparison of pressure distribution at hull segment 1, section 3 (from the entry

$\bar{x}_i = 0.099298$ in 2nd order model, $\bar{x}_i = 0.0098706$ in 1st order model)

On the basis of these comparisons, it is easily seen that the prediction of the 2nd order model in regular waves is comparable to the results of the 1st order model, which supports that the both the 1st and 2nd order models should be reliable as design tools.

9.3 Comparisons for the Random Wave Case

The 2nd order design tool NewCat (2-4a) has also been applied to the 30ft stepped planing catamaran for random wave cases.

The incoming wave is in the head-sea direction. The significant wave height is $H_{1/3} = 0.308$ m, and the natural wave peak period $T_p = \frac{2\pi}{\omega_0} = 4.188$ real seconds. A JONSWAP wave spectrum has been used here.

The computation parameters in this example are: the forward speed $U = 70$ knots, the time step number IALL = 10,000, the non-dimension time step increment $\Delta\tau = 0.02$. The total non-dimensional time for the computation is thus $T = 0.02 \times 10000 = 200$. It is 3.38 seconds of real time. The fractional artificial damping coefficient $\frac{C \times \Delta\tau}{m} = 0.1$ same as in the regular wave computation.

Fig. 9.19 shows the time histories of the wave elevations, the bow displacement, the transom draft, the step drafts, and the trim angle. Fig. 9.20 shows the vertical accelerations predicted by the 2nd order model. There are large acceleration peaks in the bow region due to the high speed impaction. Fig. 9.21 is the variation of the wetted water line lengths (solid lines) and the chine-wetted lengths (dashed lines). It is readily observed from Fig. 9.21 that the wetted water line of the main hull segment changes significantly, but the wetted water line of the aft stepped hull segment 3 changes insignificantly during the same time. From Fig. 9.21, the chine-wetted length of the main hull segment changes based on the wave action and the boat movement, but the chine-wetted length of the two stepped hull segments are zero at most time, which means that the main hull segment is often in chine-wetted flow phase and the two stepped hull segments are in chine-unwetted phase most of the time.

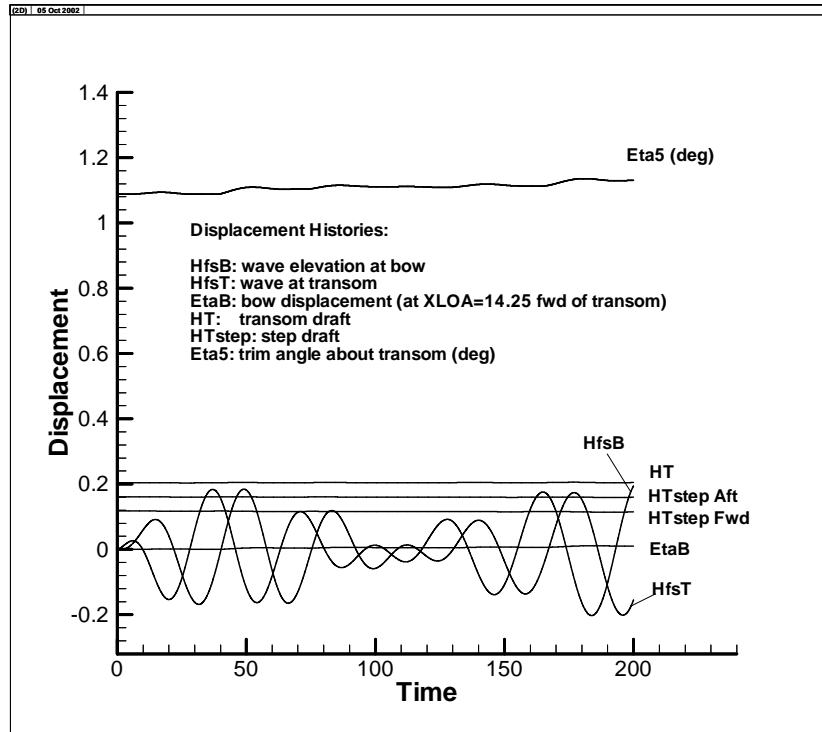


Fig. 9.19 Displacement histories predicted by the 2nd order model; irregular waves

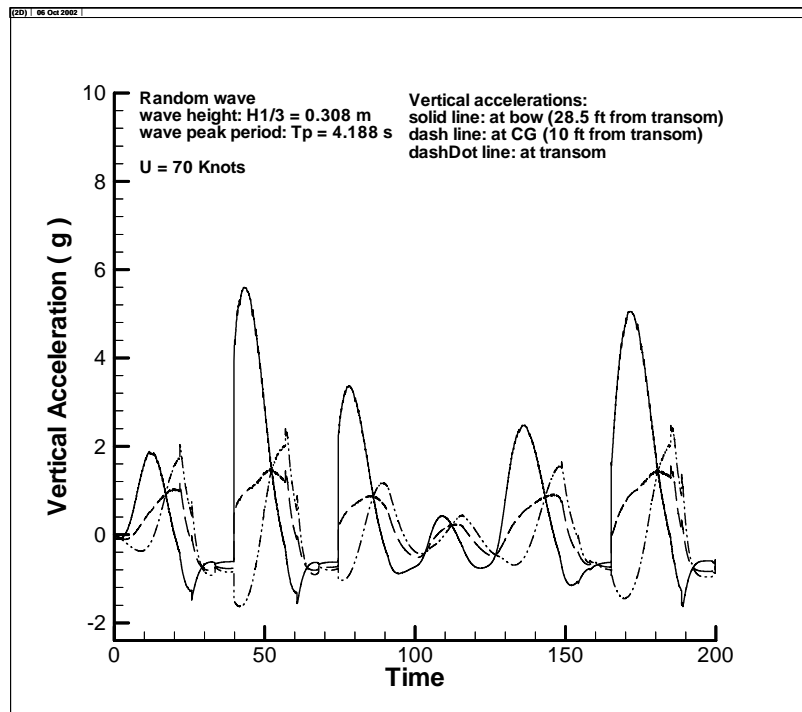


Fig. 9.20 Vertical accelerations predicted by the 2nd order model; irregular waves

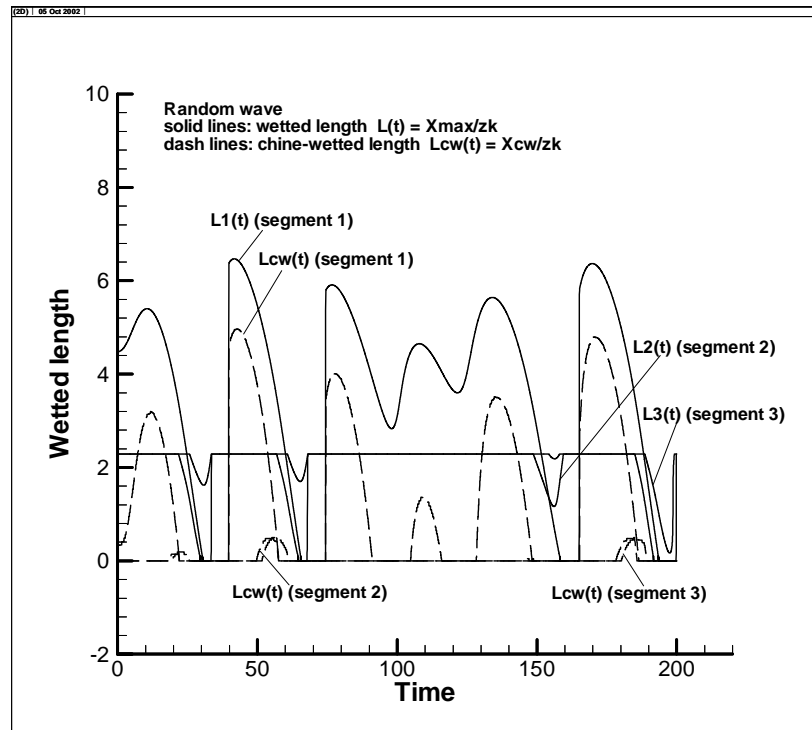


Fig. 21 Wetted water line lengths predicted by the 2nd order model; irregular waves

For comparison, the following figures (Fig. 9.22 – Fig. 9.24) depict the displacements, the vertical accelerations, the wetted water line lengths and the chine-wetted lengths predicted by the 1st order model (CatSea2-4). Comparing these figures with Fig. 9.19 – Fig. 9.21, it gives us a clear impression that the results predicted by the 1st and 2nd order models are close, although they are from very different theoretical formulations.

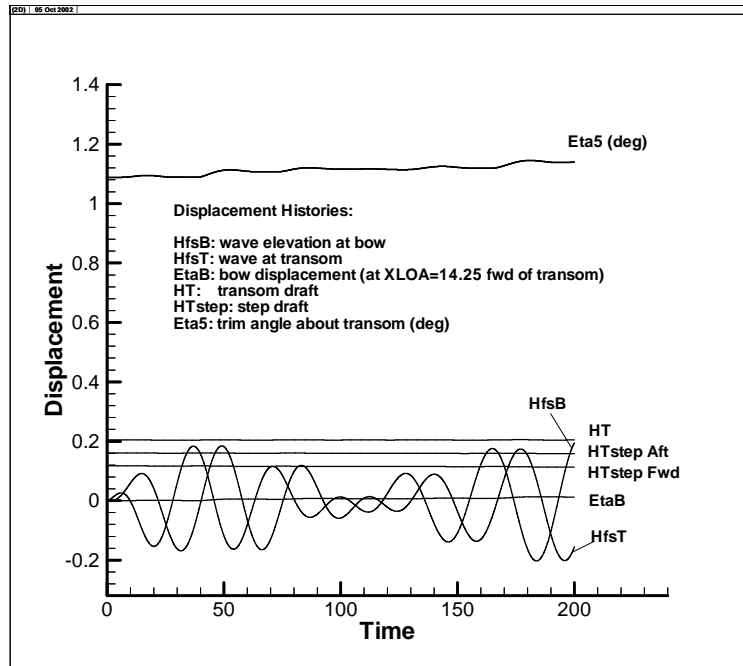


Fig. 9.22 Displacement histories predicted by the 1st order model; irregular waves

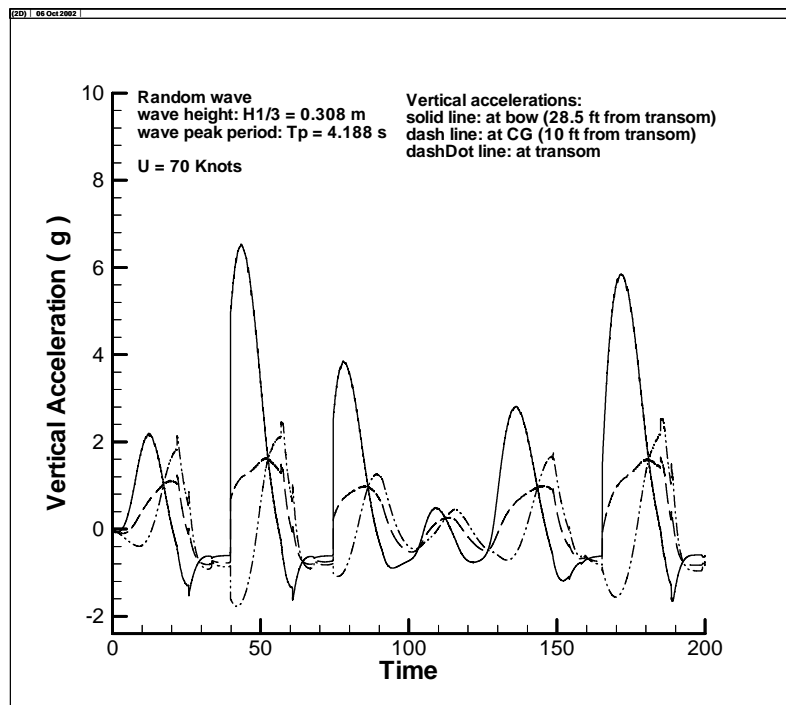


Fig. 9.23 Vertical accelerations predicted by the 1st order model; irregular waves

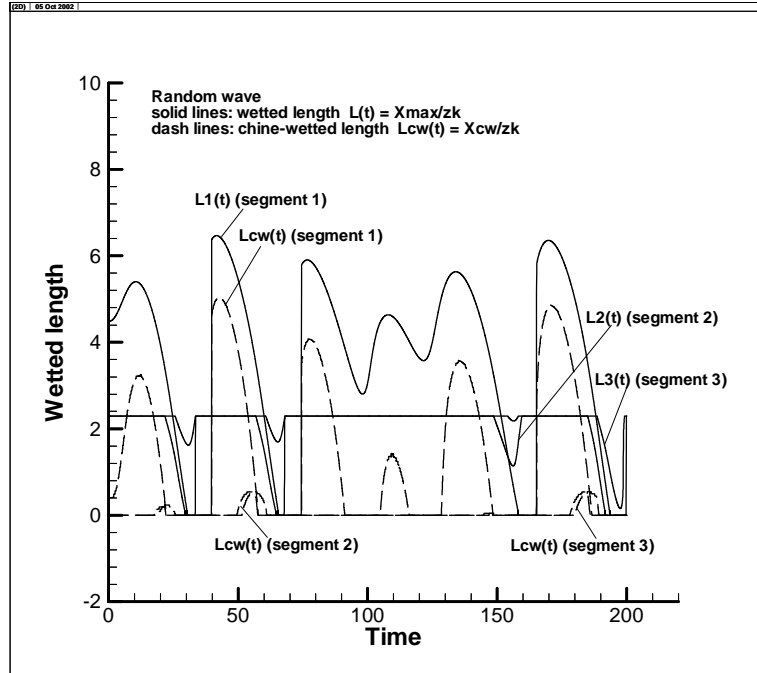


Fig. 24 Wetted water line lengths predicted by the 1st order model; irregular waves

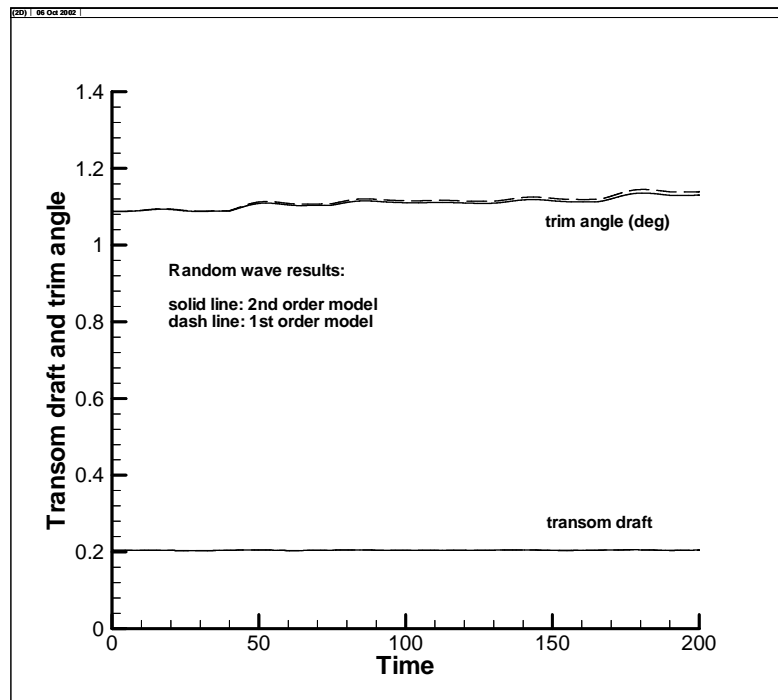


Fig. 9.25 Comparison of the trim angles and the transom drafts

Fig. 9.25 shows the difference of the trim angles and the transom drafts predicted by the 1st and 2nd order models. The differences are seen to be small.

Fig. 9.26 is the comparison of the sectional lift force distributions at $T = 200$. It demonstrates that the lift distributions are the same at this time. In Fig. 9.26, the main hull segment is out of water and therefore does not develop lift.

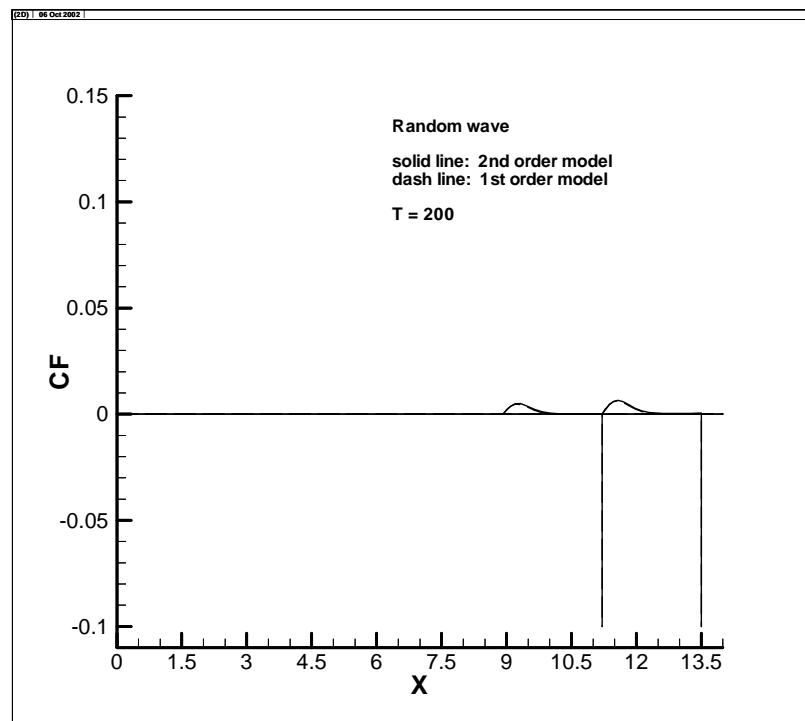


Fig. 9.26 Comparison of the sectional lift distributions

Fig. 9.27 – Fig. 9.29 demonstrates the differences between the vertical accelerations predicted by the different models for random waves. In 9.27, the bow acceleration predicted by the 1st order model is larger than the result predicted by the 2nd order model, which is consistent with the conclusion from the regular wave examples.

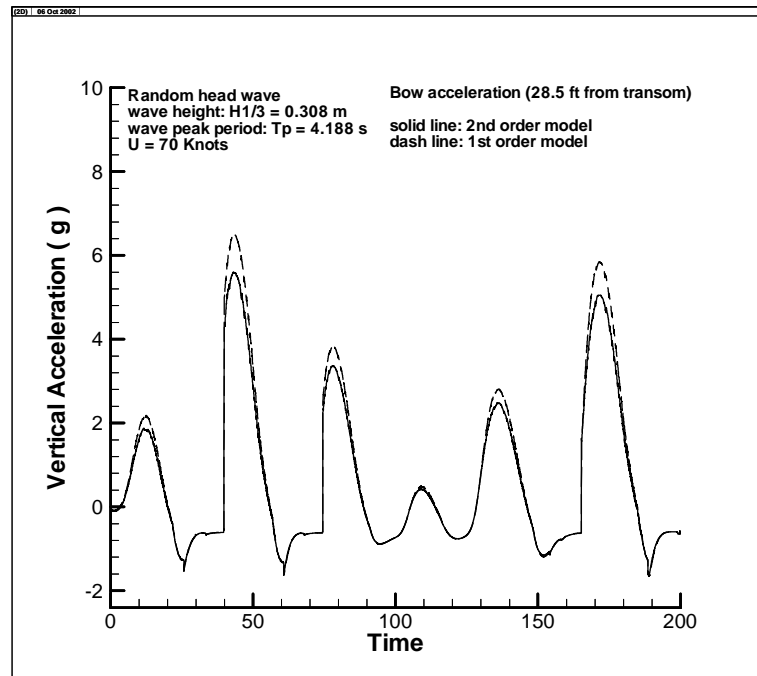


Fig. 9.27 Comparison of bow accelerations

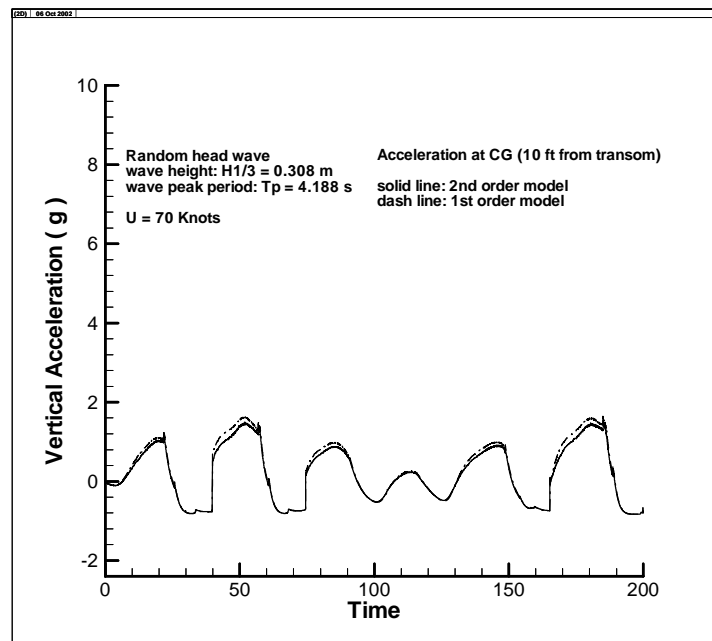


Fig. 28 Comparison of the accelerations at CG

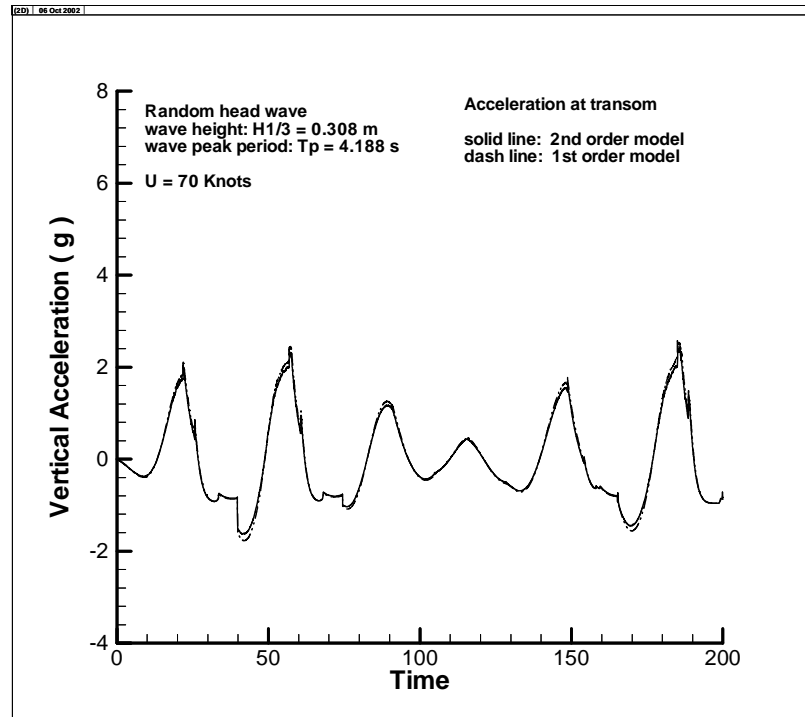


Fig. 9.29 Comparison of the accelerations at transom

Fig. 9.30 is the comparison of the jet-head streamline offsets in the two predictions. Fig. 9.31 shows the comparison of jet velocities. Fig. 9.32 shows the comparison of the wetted water line lengths and the chine-wetted lengths. The results predicted by the two theoretical models are relatively close, except for existing some differences at the inner jet head streamline offsets and at the inner jet velocities (refer to Fig. 9.31).

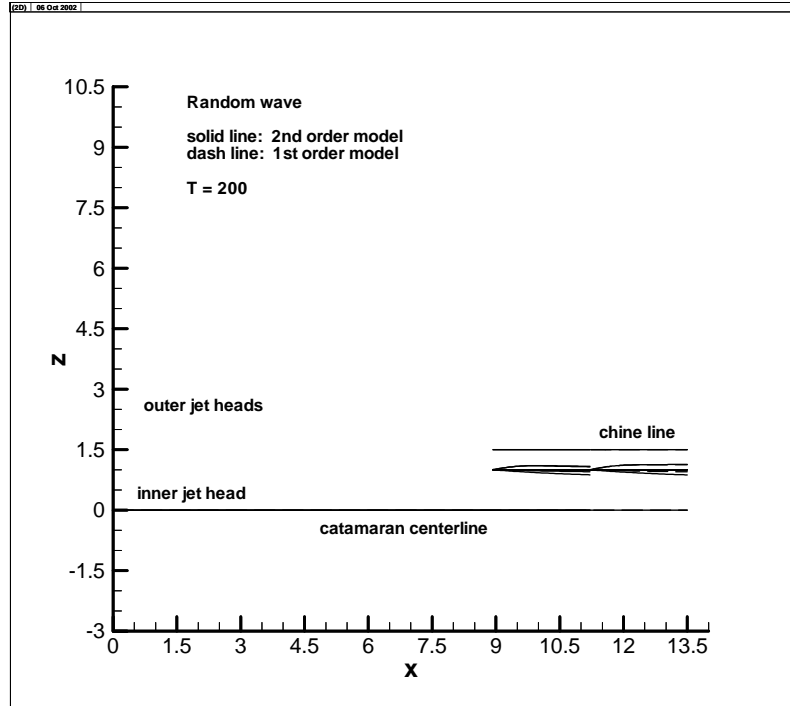


Fig. 9.30 Comparison of the jet-head streamline offsets

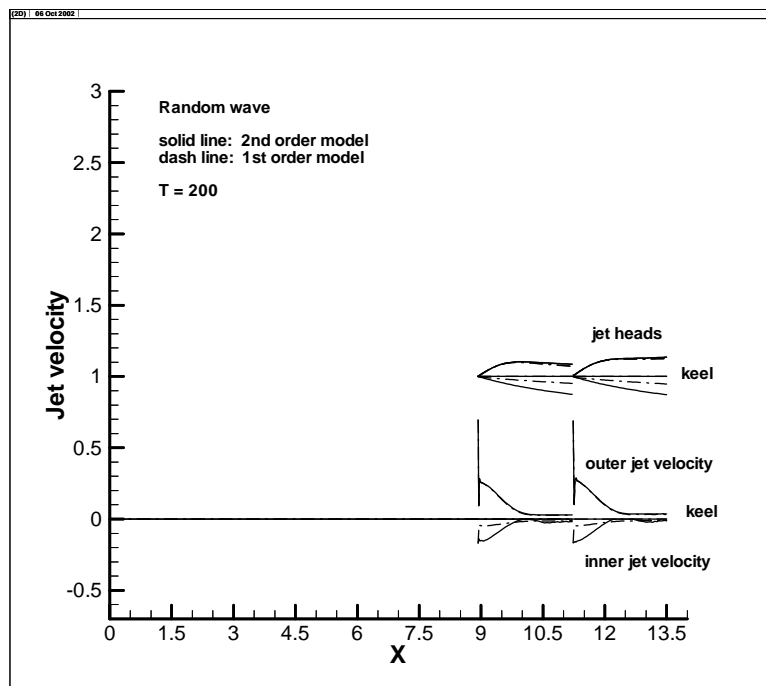


Fig. 9.31 Comparison of the jet velocities (zoom view)

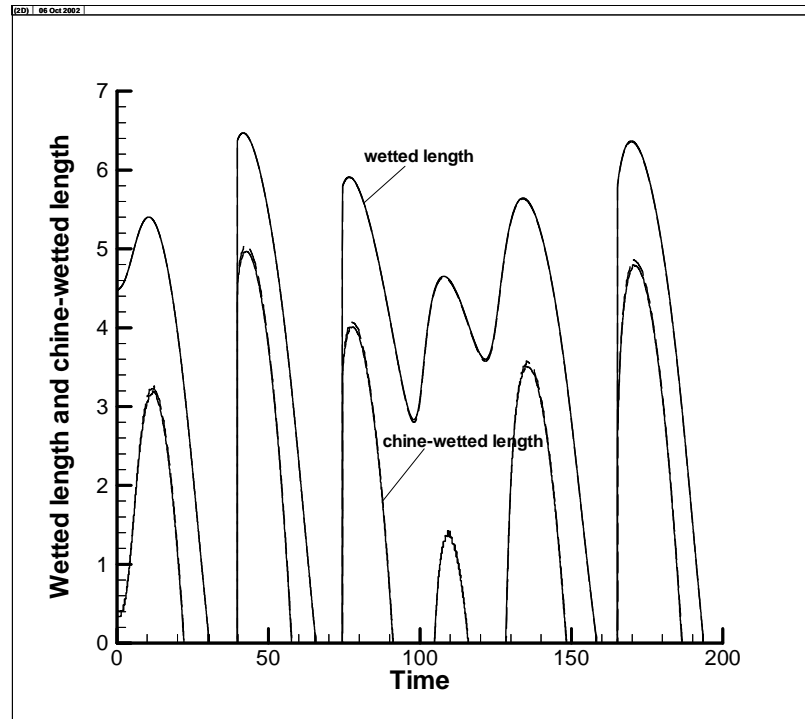


Fig. 9.32 Comparison of the water line lengths and the chine-wetted lengths

In this chapter, we have given the numerical comparison for the results predicted by the 1st and 2nd order models. From this comparison, we conclude that the predictions by the two models, in general, are close, but minor differences exist in some of the details. The 2nd order model has modified (reduced) the extreme values of the bow vertical impact accelerations.

So far, all predicted results given in this chapter are the results without considering the effect of the temporal derivative term $\left. \frac{\partial}{\partial \tau} \right|_{\xi=const}$, as discussed in Chapter

4, 5 and 6 in connection with equations (4.75), (4.76), (4.78), (4.80), (4.81), (4.84) and

(4.85). As discussed in Chapter 1, the $\left. \frac{\partial}{\partial \tau} \right|_{\xi=const}$ term calculation involves the

differentiation across the different time step, which very easily results in a numerical

singularity problem. How to deal with the $\frac{\partial}{\partial \tau} \Big|_{\xi=const}$ term appearing in (4.75), (4.76), (4.78), (4.80), (4.81), (4.84) and (4.85)? This is a complicated mathematical problem, which is the subject of the next (and last) chapter of this thesis.

CHAPTER 10

DISCUSSION ON PLANING DYNAMICS:

INFLUENCE OF THE TEMPORAL DERIVATIVE TERM $\left. \frac{\partial}{\partial \tau} \right|_{\xi=const}$

In the numerical model of the 2nd order theory, the pressure computation involves the calculation of the temporal $\frac{\partial \phi}{\partial \tau}(\xi, \tau)$ term. The formulation of $\frac{\partial \phi}{\partial \tau}(\xi, \tau)$ in the coordinate system of Fig. 3.5, and in the equations (3.66) and (3.67) has the following form:

$$\frac{\partial \phi}{\partial \tau}[\xi(\tau), \tau] = \left. \frac{\partial \phi}{\partial \tau} \right|_{\xi=const} + \frac{\partial \phi}{\partial \xi} \frac{\partial \xi}{\partial \tau} \Big|_{\tau=const} = \left. \frac{\partial \phi}{\partial \tau} \right|_{\xi=const} - x \frac{L_\tau}{L} \frac{\partial \phi}{\partial x} \quad (10.1)$$

where the non-dimensional x -variable is $\xi(\tau) = \frac{x}{L(\tau)}$, by (4.69), and $L(\tau)$ is the length of the instantaneous water line.

The second term in Eq.(10.1) has been included in the dynamic boundary condition calculation and in the pressure formula without difficulty. However, as discussed in Chapter 3, the first term requires differentiation across the time step, which is fraught with numerical difficulties. This is due especially to the non-smoothness of the

flow geometry in time at the chine wetting point, in which case the numerical time gradients become very large and usually result in run-time overflow.

As was said previously, the numerical results presented in Chapter 9 are the results excluding the $\left. \frac{\partial}{\partial \tau} \right|_{\xi=const}$ term in (10.1). In this chapter, we concentrate on

understanding the effects of the subject $\left. \frac{\partial}{\partial \tau} \right|_{\xi=const}$ terms that have not been included.

10.1 The Temporal Derivative Terms

The effect of the temporal derivatives of the potential $\phi(\xi, s, \tau)$ has been introduced into the 2nd order numerical model by following terms: $\phi(\xi, s, \tau)$, $\frac{\partial \phi(\xi, s, \tau)}{\partial \tau}$

and $\frac{\partial^2 \phi(\xi, s, \tau)}{\partial s \partial \tau}$ (refer to Chapter 4 and Appendix D). The expressions of these

derivatives are defined in Appendix D. We copy them here for clarity:

$$\phi(\xi, s, \tau) = -(z_c - 1) \int_{s(\xi; \tau)}^{s^+(\xi, \tau)} V_s(\xi, s_0, \tau) ds_0 \quad (10.2)$$

$$\begin{aligned}
-\frac{\partial \phi(\xi, s, \tau)}{\partial \tau} &= (z_c - 1) \left[\int_{s(\xi, \tau)}^{s^+(\xi, \tau)} \frac{\partial V_s}{\partial \tau}(\xi, s_0, \tau) ds_0 - x \frac{L_\tau}{L} \int_{s(\xi, \tau)}^{s^+(\xi, \tau)} \frac{\partial V_s}{\partial x}(x, s_0, \tau) ds_0 \right. \\
&\quad \left. + V_s(\xi, s^+, \tau) \frac{\partial s^+}{\partial \tau} - V_s(\xi, s^+, \tau) \frac{\partial s^+}{\partial x} \cdot x \frac{L_\tau}{L} \right] \\
&\quad + z_{c,\tau} \left[\int_{s(\xi, \tau)}^{s^+(\xi, \tau)} V_s(\xi, s_0, \tau) ds_0 + s \cdot V_s(\xi, s, \tau) \right] \\
&\quad - z_{c,x} \cdot x \frac{L_\tau}{L} \left[\int_{s(\xi, \tau)}^{s^+(\xi, \tau)} V_s(\xi, s_0, \tau) ds_0 + s \cdot V_s(\xi, s, \tau) \right]
\end{aligned}$$

(10.3)

$$\begin{aligned}
-\frac{\partial^2 \phi(\xi, s, \tau)}{\partial s \partial \tau} &= (1 - z_c) \left[\frac{\partial V_s}{\partial \tau}(\xi, s, \tau) - x \frac{L_\tau}{L} \frac{\partial V_s}{\partial x} \right] + z_{c,\tau} \cdot s \frac{\partial V_s}{\partial s} \\
&\quad - z_{c,x} \cdot x \frac{L_\tau}{L} \cdot \left[s \frac{\partial V_s}{\partial s} \right]
\end{aligned}$$

(10.4)

where the subscript denoting $\xi = const$ is to be considered as implied.

These temporal derivatives appeared in the pressure continuity equation (4.75), (4.76) and (4.78), in the pressure distribution computation formula (4.84) and (4.85) and in the Burger's equation of the free vortex distribution (4.80) and (4.81).

The final form of the temporal derivative terms in the pressure continuity conditions is as following (refer to (4.75), (4.76) and (4.78)):

- In chine un-wetted phase at s^+

$$b_\tau^+ + (1 - x \frac{L_\tau}{L}) b_x^+ = \frac{V_s^2(\xi, s^+, \tau) - V^2(\xi, \tau)}{2V_s(\xi, s^+, \tau)} \quad \text{at } s = s^+ \quad (10.5)$$

- In chine wetted phase at s^+ and s^-

$$b_{\tau}^+ + (1 - x \frac{L_{\tau}}{L}) b_x^+ = \frac{1}{2} V_s(\xi, s^+, \tau) \quad \text{at } s = s^+ \quad (10.6)$$

$$b_{\tau}^- + (1 - x \frac{L_{\tau}}{L}) b_x^- = \frac{1}{2} V_s(\xi, s^-, \tau) \quad \text{at } s = s^- \quad (10.7)$$

The final form of the temporal derivative terms in the pressure distribution formula is (refer to (4.84) and (4.85)),

- In chine un-wetted case, the pressure distribution is,

$$\begin{aligned} C_p(x, s; \tau) = & V^2(x, \tau) - V_s^2(x, s, \tau) + V_s^2(\xi, 1, \tau) \\ & + 2(z_c - 1) \left\{ \int_{s(\xi, \tau)}^1 \left[\frac{\partial V_s}{\partial \tau}(\xi, s_0, \tau) + (1 - x \frac{L_{\tau}}{L}) \frac{\partial V_s(\xi, s_0, \tau)}{\partial x} \right] ds_0 \right\} \\ & + 2[z_{c, \tau} + z_{c, x} (1 - x \frac{L_{\tau}}{L})] \left[\int_{s(\xi, \tau)}^1 V_s(\xi, s_0, \tau) ds_0 + s \cdot V_s(\xi, s, \tau) - V_s(\xi, 1, \tau) \right] \\ & - V^2(x, \tau) \end{aligned} \quad 0 \leq x \leq L(\tau), 0 \leq s \leq 1 \quad (10.8)$$

- In chine wetted case,

$$\begin{aligned}
C_p(x, s; \tau) &= V^2(x, \tau) - V_s^2(x, s, \tau) + V_s^2(\xi, 1, \tau) \\
&+ 2(z_c - 1) \left\{ \int_{s(\xi, \tau)}^1 \left[\frac{\partial V_s}{\partial \tau}(\xi, s_0, \tau) + (1 - x) \frac{L_\tau}{L} \frac{\partial V_s(\xi, s_0, \tau)}{\partial x} \right] ds_0 \right\} \\
&+ 2 \left[z_{c, \tau} + z_{c, x} \left(1 - x \frac{L_\tau}{L}\right) \right] \left[\int_{s(\xi, \tau)}^1 V_s(\xi, s_0, \tau) ds_0 + s \cdot V_s(\xi, s, \tau) - V_s(\xi, 1, \tau) \right] \\
&0 \leq x \leq L(\tau), \quad 0 \leq s \leq 1 \quad (10.9)
\end{aligned}$$

The temporal derivative terms in Euler's equation of the free vortex distribution (refer to (4.80) and (4.81)):

$$\begin{aligned}
\{ [V_s(\xi, s, \tau) - \left[\frac{\partial z_c}{\partial \tau} s + \frac{\partial z_c}{\partial x} s \left(1 - x \frac{L_\tau}{L}\right) \right]] \frac{\partial V_s}{\partial s} - (1 - z_c) \frac{\partial V_s}{\partial \tau}(\xi, s, \tau) - (1 - z_c) \left(1 - x \frac{L_\tau}{L}\right) \frac{\partial V_s(\xi, s, \tau)}{\partial x} = 0 \\
1 \leq s \leq s^+ \quad (10.10)
\end{aligned}$$

$$\begin{aligned}
\{ [V_s(\xi, s, \tau) - \left[\frac{\partial z_c}{\partial \tau} s + \frac{\partial z_c}{\partial x} s \left(1 - x \frac{L_\tau}{L}\right) \right]] \frac{\partial V_s}{\partial s} - (1 - z_c) \frac{\partial V_s}{\partial \tau}(\xi, s, \tau) - (1 - z_c) \left(1 - x \frac{L_\tau}{L}\right) \frac{\partial V_s(\xi, s, \tau)}{\partial x} = 0 \\
s^- \leq s \leq 0 \quad (10.11)
\end{aligned}$$

From Eq.(10.5) - Eq.(10.11), the time derivative terms that need to be dealt with

are: $\left. \frac{\partial z_c(\xi, \tau)}{\partial \tau} \right|_{\xi=const.}$, $\left. \frac{\partial b^+(\xi, \tau)}{\partial \tau} \right|_{\xi=const.}$, $\left. \frac{\partial b^-(\xi, \tau)}{\partial \tau} \right|_{\xi=const.}$ and $\left. \frac{\partial V_s}{\partial \tau}(\xi, s, \tau) \right|_{\xi=const.}$. All of

these terms represent the variations in the time domain while the space variable fixed.

10.2 The Computation of the Temporal Derivatives

To incorporate the above temporal derivative terms into the 2nd order numerical model, we first need to calculate these derivative terms. A simple Euler backward difference model was adopted here.

For the $\left. \frac{\partial z_c(\xi, \tau)}{\partial \tau} \right|_{\xi=const.}$, $\left. \frac{\partial b^+(\xi, \tau)}{\partial \tau} \right|_{\xi=const.}$, $\left. \frac{\partial b^-(\xi, \tau)}{\partial \tau} \right|_{\xi=const.}$ and

$\left. \frac{\partial V_s(\xi, s, \tau)}{\partial \tau} \right|_{\xi=const.}$ terms, the following backward difference form has been used:

$$\left(\frac{\partial u}{\partial \tau} \right)_i^n = \frac{u_i^n - u_i^{n-1}}{\Delta \tau} + o(\Delta \tau^2) \quad (10.12)$$

where n stands for the current time step, $n-1$ stands for the previous step, u represents z_c , b^- and b^+ , and i is the grid position in ξ – axis.

Representing the current time step as τ , the previous time step as $\tau - \Delta \tau$. Discretizing the nondimensional ξ – axis as the sectional computation grid. Denote the computational grid at time τ as $G(\tau)$, the computational grid at $\tau - \Delta \tau$ as $G(\tau - \Delta \tau)$. At every time step, before chine-wetted section, the computation grid is unchanged; after the chine-wetted section, the grid or section has to be adjusted. In (10.12), u_i^{n-1} is the variable value of $u(\tau - \Delta \tau)$ at the current time computation grid $G(\tau)$. The main difficulty to calculate Eq.(10.12) is that the variable $u_i^n = u_i(\tau)$ itself is an unknown,

where u_i^n is the variable value of $u(\tau)$ at the current time computation grid $G(\tau)$, for example the $b_i^-(\tau)$ and $b_i^+(\tau)$, at time step τ .

An interpolation algorithm has been used to find the u_i^{n-1} . The value pair $(G(\tau - \Delta\tau), u(\tau - \Delta\tau))$ has been reserved at the time step $\tau - \Delta\tau$ for the next time step computation, where $G(\tau - \Delta\tau)$ is the computation grid at time $\tau - \Delta\tau$. At the time step τ , the value of $u(\tau - \Delta\tau)$ at the current time computation grid $G(\tau)$ can be found by interpolation using the previous value pair $(G(\tau - \Delta\tau), u(\tau - \Delta\tau))$ (refer to Fig. 10.1 and Fig. 10.2).

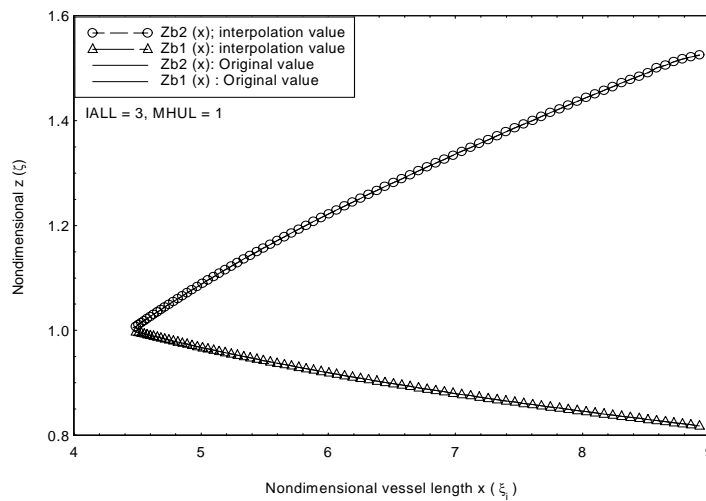


Fig. 10.1 z_b^- and z_b^+ interpolation accuracy of the main hull

Fig. 10.1 shows an example of the interpolated value of $z_b^-(\tau - \Delta\tau)$ and $z_b^+(\tau - \Delta\tau)$ at the main hull segment grid $G(\tau)$ at time τ . Fig. 10.2 shows the interpolated value of $z_c^+(\tau - \Delta\tau)$ at the main hull segment grid $G(\tau)$ at time τ . A high degree accuracy has been achieved in Fig. 10.1 and Fig. 10.2.

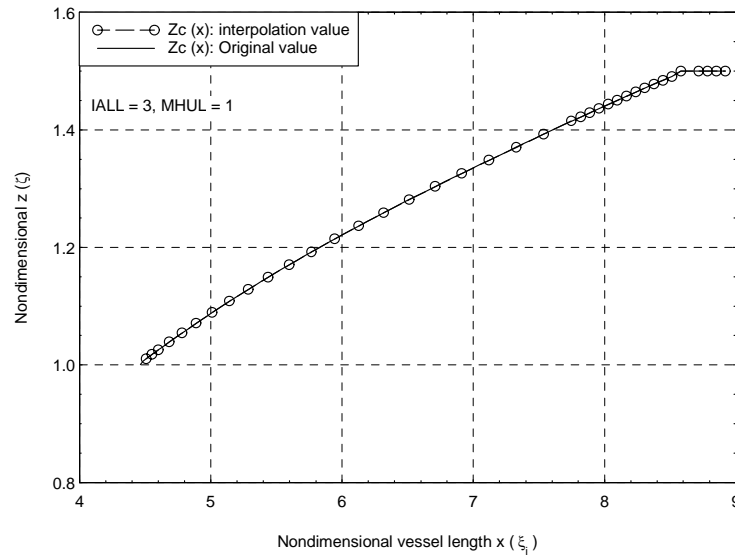


Fig. 10.2: z_c^+ interpolation accuracy of the main hull

To find the unknown $u_i^n = u_i(\tau)$ at time τ in (10.12), an iteration procedure has been adopted. Considering that b^- and b^+ in the current time step are unknowns themselves, the algorithm in the present numerical model uses the iteration method to find $\frac{\partial b^+(\xi, \tau)}{\partial \tau}$, $\frac{\partial b^-(\xi, \tau)}{\partial \tau}$ in the form of Eq. (10.12). At the first loop of the iteration, an

approximate value $\left. \frac{\partial b^+}{\partial \tau} \right|_{\xi=const}$, $\left. \frac{\partial b^-}{\partial \tau} \right|_{\xi=const}$ at the previous time step $\tau - \Delta \tau$ was used in

the pressure continuity conditions ((10.5), (10.6) and (10.7)) to replace $\left. \frac{\partial b^+}{\partial \tau} \right|_{\xi=const}$,

$\left. \frac{\partial b^-}{\partial \tau} \right|_{\xi=const}$ at the current time step τ . When the stable $b_i^-(\tau)$ and $b_i^+(\tau)$ terms have been

achieved, the $\left. \frac{\partial b^+}{\partial \tau} \right|_{\xi=const}$, $\left. \frac{\partial b^-}{\partial \tau} \right|_{\xi=const}$ terms in the pressure continuity condition (refer to

(4.75), (4.76) and (4.78)) have been updated. For the $\left. \frac{\partial z_c^+(\xi, \tau)}{\partial \tau} \right|_{\xi=const}$ and

$\left. \frac{\partial V_s}{\partial \tau}(\xi, s, \tau) \right|_{\xi=const}$ terms in the pressure distribution formula in (4.84) and (4.85), the

Euler difference, (10.12), can be executed directly without iteration, since the $z_c^+(\xi, \tau)$ and $V_s(\xi, s, \tau)$ terms have been obtained from the flow field solution of the current time

step before calculating the $\left. \frac{\partial z_c^+(\xi, \tau)}{\partial \tau} \right|_{\xi=const}$ and $\left. \frac{\partial V_s}{\partial \tau}(\xi, s, \tau) \right|_{\xi=const}$ terms (refer to Fig. 6.1

of Chapter 6).

Fig. 10.3 shows the difference of the $\left. \frac{\partial z_c^+}{\partial \tau} \right|_{\xi=const}$ term with the $\frac{\partial z_c^+}{\partial x}$ term at the

nondimensional time $\tau = 57.6$. The computational results are picked from the time marching computation at time step 2880 ($\Delta \tau = 0.02$). For easily comparing the effect of

the $\left. \frac{\partial}{\partial \tau} \right|_{\xi=const}$ term with the $\left. \frac{\partial}{\partial x} \right|_{\tau=const}$ term in the pressure distribution equations ((4.84) and

(4.85)), recall the transform in the nondimensional ξ – variable space, $\frac{\partial}{\partial x} = \frac{1}{L(\tau)} \cdot \frac{\partial}{\partial \xi}$,

we use the $\frac{\partial}{\partial \xi}$ term to calculate the $\frac{\partial}{\partial x}$ term. For comparison, the $z_c^+(\xi, \tau)$ value and the

$z_c^+(\xi, \tau - \Delta \tau)$ value at the current time step grid $G(\tau)$ also have been included in Fig.

10.3. In Fig. 10.3, the value of $\frac{\partial z_c^+}{\partial x}$ term is larger than the value of $\left. \frac{\partial z_c^+}{\partial \tau} \right|_{\xi=const}$ term, but

the $\left. \frac{\partial z_c^+}{\partial \tau} \right|_{\xi=const}$ term still can not be ignored (refer to (10.8) and (10.9)). There is a jump in the $\left. \frac{\partial z_c^+}{\partial \tau} \right|_{\xi=const}$ and the $\frac{\partial z_c^+}{\partial x}$ curves in Fig 10.3. This jump may result from the abrupt halt of $z_c^+(\xi, \tau)$ when the separation point $z_c^+(\xi, \tau)$ reaches the hard chine Z_{CH} (refer to the description of Chapter 2).

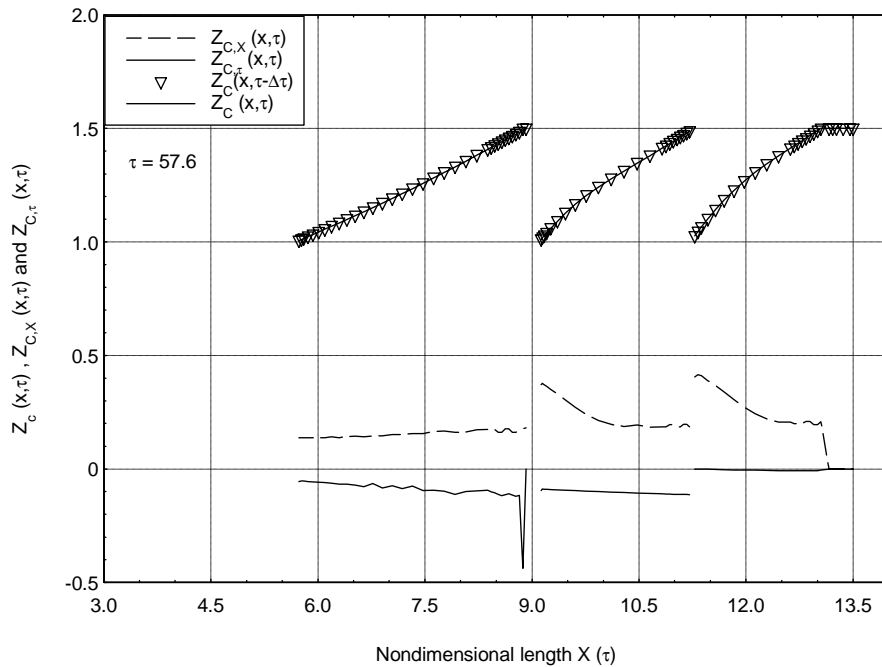


Fig. 10.3 The $\left. \frac{\partial z_c^+}{\partial \tau} \right|_{\xi=const}$ and the $\frac{\partial z_c^+}{\partial x}$ term at the time $\tau = 57.6$

Fig. 10.4 shows the difference of the $\left. \frac{\partial b^+}{\partial \tau} \right|_{\xi=const}$ term with the $(1 - x \frac{L_\tau}{L})b_x^+$ term at

the time $\tau = 57.6$. For comparison, the $b^+(\xi, \tau)$ value and the $b^+(\xi, \tau - \Delta\tau)$ value at the

current time step grid $G(\tau)$ have also been included. From Fig. 10.4, comparing with the

$\frac{\partial b^+}{\partial \tau} \Big|_{\xi=const}$ term, it is readily seen that the $(1 - x \frac{L_\tau}{L})b_x^+$ term is a dominant term.

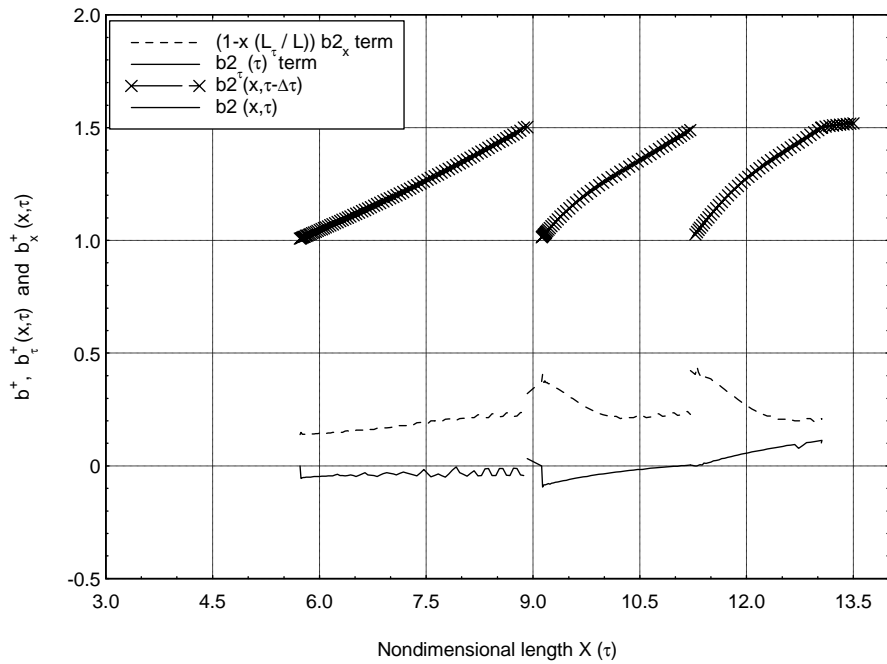


Fig. 10.4 The $\frac{\partial b^+}{\partial \tau} \Big|_{\xi=const}$ and the $(1 - x \frac{L_\tau}{L})b_x^+$ term at time $\tau = 57.6$

Fig. 10.5 shows the $\frac{\partial b^-}{\partial \tau} \Big|_{\xi=const}$ term at the time $\tau = 57.6$; the $b^-(\xi, \tau)$ term and

the $b^-(\xi, \tau - \Delta\tau)$ term are also included here.

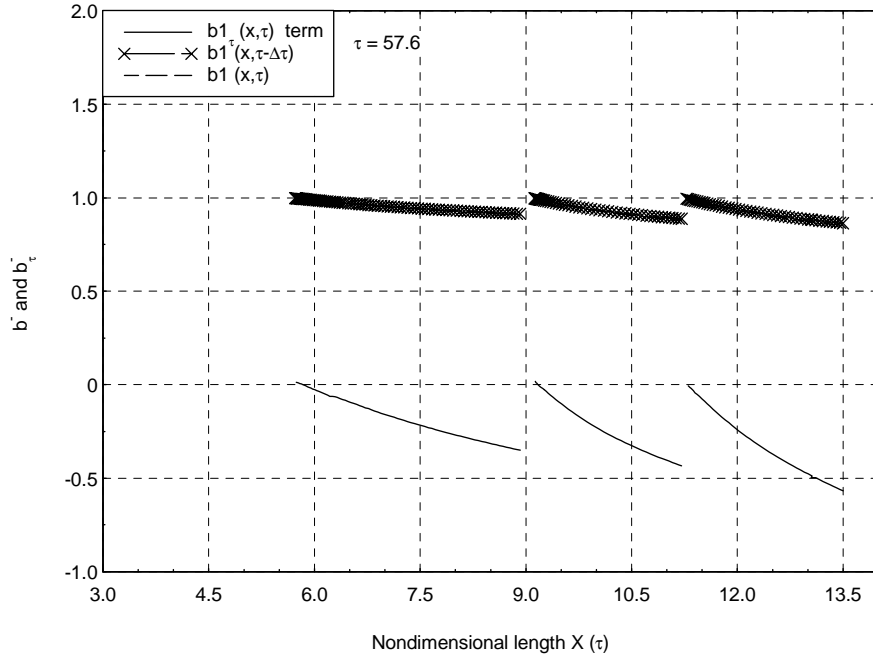


Fig. 10.5 The $\left. \frac{\partial b^-}{\partial \tau} \right|_{\xi=const}$ term at the time $\tau = 57.6$

Fig. 10.6 shows the difference of $\left. \frac{\partial V_s(\xi, \zeta, \tau)}{\partial \tau} \right|_{\xi=const}$ term and the $\frac{\partial V_s}{\partial x}(\xi, \zeta, \tau)$

term at the time $\tau = 57.6$, $\zeta = 1.12$ (recall $\zeta = \frac{z}{z_k}$ in (3.65)). The $V_s(\xi, \zeta, \tau)$ term and

the $V_s(\xi, \zeta, \tau - \Delta\tau)$ term are also included on the Fig. 10.6. Comparing with the

$\frac{\partial V_s}{\partial x}(\xi, \zeta, \tau)$ term, the $\left. \frac{\partial V_s(\xi, \zeta, \tau)}{\partial \tau} \right|_{\xi=const}$ term is a dominant, which means the

$\left. \frac{\partial V_s(\xi, \zeta, \tau)}{\partial \tau} \right|_{\xi=const}$ term can not be ignored in the computation of the pressure distribution

in (4.84) and (4.85).

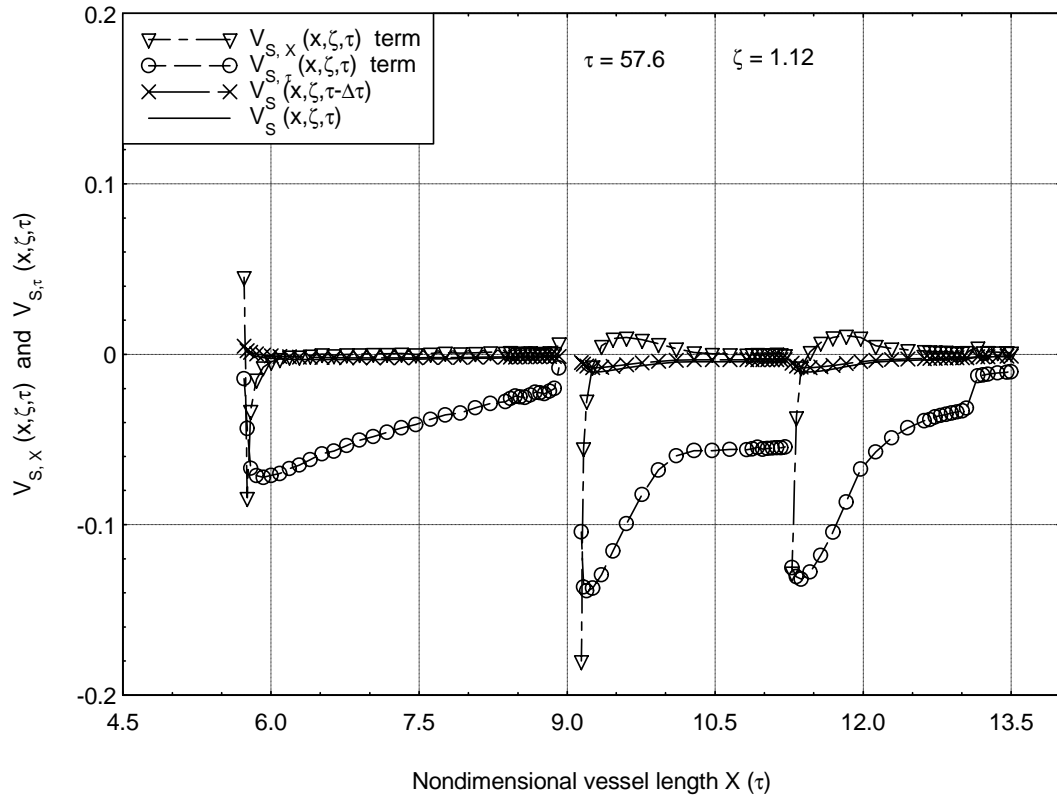


Fig. 10.6 The $\left. \frac{\partial V_s(\xi, \zeta, \tau)}{\partial \tau} \right|_{\xi=const}$ and the $\frac{\partial V_s}{\partial x}(\xi, \zeta, \tau)$ term at the time $\tau = 57.6$

From Fig. 10.3 – Fig. 10.6, the following conclusion may be drawn: Comparing

the values of the $\left. \frac{\partial z_c^+}{\partial \tau} \right|_{\xi=const}$ term and the $\left. \frac{\partial V_s(\xi, \zeta, \tau)}{\partial \tau} \right|_{\xi=const}$ term with the values of the

$\frac{\partial z_c^+}{\partial x}$ term and the $\frac{\partial V_s}{\partial x}(\xi, \zeta, \tau)$ term in the pressure distribution (4.84) and (4.85), it tells

us that the $\left. \frac{\partial z_c^+}{\partial \tau} \right|_{\xi=const}$ and the $\left. \frac{\partial V_s(\xi, \zeta, \tau)}{\partial \tau} \right|_{\xi=const}$ terms can not be neglected in the pressure

distribution computation (refer to (10.8) and (10.9)). Comparing the $\left. \frac{\partial b^+}{\partial \tau} \right|_{\xi=const}$ term and

the $(1-x\frac{L_\tau}{L})b_x^+$ term in Fig. 10.4, the $\frac{\partial b^+}{\partial \tau}\Big|_{\xi=const}$ term may can be neglected in the pressure continuity condition (refer to (10.5) and (10.7)) to simplify the flow field computation iteration.

10.3 Physical Explanation for Euler's Equation of the Free Vortex Distribution

The location of the free jet-head sheet must satisfy the Euler's equation in Eq.(10.10) and (10.11) (refer to (4.80) and (4.81)). Euler's equation (10.10) requires that when fluid particles flowing from the contour, onto the free vortex sheet, and out of the jet, the velocity of each particle stays constant at its separation value at $z_c(\tau_0)$, for all time $\tau > \tau_0$ thereafter.

Re-formatting Eq.(10.10) as,

$$\begin{aligned} \{ [V_s(\xi, s, \tau) - \left[\frac{\partial z_c}{\partial \tau} \Big|_{\xi=const.} s + \frac{\partial z_c}{\partial x} s(1-x\frac{L_\tau}{L}) \right]] \frac{\partial V_s}{\partial s} \\ + (z_c - 1) \left[\frac{\partial V_s(\xi, s, \tau)}{\partial \tau} \Big|_{\xi=const.} + (1-x\frac{L_\tau}{L}) \frac{\partial V_s(\xi, s, \tau)}{\partial x} \right] = 0 \end{aligned} \quad 1 \leq s \leq s^+ \quad (10.13)$$

Recall the transform: $\xi(\tau) = \frac{x}{L(\tau)}$, $\frac{\partial}{\partial \xi} = \frac{\partial}{\partial x} L(\tau)$, $\xi_\tau = -x\frac{L_\tau}{L^2} = -\xi\frac{L_\tau}{L}$ and (10.1), it

follows that,

$$\{ [V_s(\xi, s, \tau) - \left[\frac{\partial z_c}{\partial \tau} + \frac{\partial z_c}{\partial x} \right] \cdot s] \frac{\partial V_s}{\partial s} + (z_c - 1) \left[\frac{\partial V_s(\xi, s, \tau)}{\partial \tau} + \frac{\partial V_s(\xi, s, \tau)}{\partial x} \right] = 0 \quad 1 \leq s \leq s^+ \quad (10.14)$$

In the monohull planing hydrodynamics theory (Vorus 1996), the inviscid Burger's equation of the vortex distribution on the free jet-head sheet has the following form:

$$(V_s(\zeta, \tau) - \frac{dz_c}{d\tau} \cdot \zeta) \frac{\partial V_s}{\partial \zeta} + z_c \frac{dV_s(\zeta, \tau)}{d\tau} = 0 \quad 1 \leq \zeta \leq b(\tau) \quad (10.15)$$

Comparing with (10.15), it is easy to see that (10.14) is also a Burger's equation of a time and spatially variable stream that the vortex distribution of the free jet-head sheet must satisfy.

Eq. (10.14) states:

$$\frac{DV_s(\xi, s, \tau)}{D\tau} = 0 \quad (10.16)$$

Since in the vortex model, the effects of viscosity and gravity are neglected, the free vortices will continue advancing outward with the separation velocities. That is,

$$V_s(\xi, s, \tau) = \text{constant} \quad (10.17)$$

or,

$$V_s(\xi, s, \tau) = V_s(\xi_0, 1, \tau_0) \quad \text{on } s > 1, \text{ or } \zeta > z_c^+ \text{ when } \tau > \tau_0 \quad (10.18)$$

where $V_s(\xi_0, 1, \tau_0)$ is the jet velocity at the separation point z_c^+ ; τ_0 is the starting time that free vortex separated from the bound vortex sheet, onto the free jet-head vortex sheet, ξ_0 is the x – location of the separation on the vortex sheet, $s = 1$ is the z – location of the separation point z_c^+ on the vortex sheet.

As we stated in Chapter 2, in seaway dynamics problem (seakeeping), the flow field and the boat motion varies with the time. It is much more complicated than steady planing problem. Comparing the Euler equation of the seaway dynamics problem in (10.14) with the Euler equation of the steady planing problem in (10.15), it is evident that the solution space is a three-dimensional space $(x, z; t)$ (in dimension expression) in seaway dynamics, and the solution space is a two-dimensional space (x, z) in steady planing. The solution of the free vortex distribution from (10.14) will be a 3-D space curve, and the solution from (10.15) is a 2-D planar curve (Vorus 1996). The most important character is that, in seaway dynamics, the free vortex location development not only changes spatially but also temporally. In next section, we are going to develop the solution of the free vortex distribution from (10.14).

10.4 Free Vortex Location on the Sheet

The free vortex location on the sheet can be determined from the solution of Eq. (10.13). The solution to the non-linear Eq. (10.13) can be written in terms of the Galaan transformation of its initial and boundary conditions (This section is based on the development of Vorus 1993) as,

$$V_s[\bar{s}, \bar{\tau}; \bar{\xi}(\bar{x}, \bar{\tau})] = V_s(\sigma_1, 0, 0)H(\sigma_1) + V_s(0, \sigma_2, 0)H(\sigma_2) + V_s(0, 0, \sigma_3)H(\sigma_3) \quad (10.19)$$

where H is the Heaviside step-function, $\bar{s} = s - 1$, $\bar{\tau} = \tau - \tau_0$, $\bar{x} = x - x_0$ and σ_1 , σ_2 and σ_3 are three initially unknown functions of the form:

$$\sigma_i = \sigma_i[\bar{s}, \bar{\tau}; \bar{\xi}(\bar{x}, \bar{\tau}); V_s] \quad i = 1, 2, 3 \quad (10.20)$$

In view of the fact that the σ_1 , σ_2 and σ_3 are linearly independent, Eq.(10.19) may be simplified to:

$$V_s = V_s^*(\sigma_i[\bar{s}, \bar{\tau}; \bar{\xi}(\bar{x}, \bar{\tau})]) = V_{s,i}^* \quad i = 1, 2, 3 \quad (10.21)$$

where,

$$V_{s,1}^* = V_s(\sigma_1, 0, 0), \quad V_{s,2}^* = V_s(0, \sigma_2, 0) \text{ and } V_{s,3}^* = V_s(0, 0, \sigma_3) \quad (10.22)$$

and where $i = 1$ corresponds to the solution component in terms of the initial velocity distribution ($\tau = \tau_0$, $x = x_0$); $i = 2$ corresponds to the solution component in terms of the time distribution of velocity at the free-sheet separation point ($\zeta = z_c$, $x = x_0$); $i = 3$ corresponds to the solution component in terms of the initial velocity distribution along the boat length ($\zeta = z_c$, $\tau = \tau_0$).

Eq. (10.21) can be expressed in a general function form:

$$F(\bar{s}, \bar{\tau}, \bar{x}; V_s) = V_s - V_{s,i}^*[\sigma_i(\bar{s}, \bar{\tau}, \bar{x}; V_s)] = 0 \quad (10.23)$$

Differentiate Eq.(10.23) with respect to \bar{s} , $\bar{\tau}$ and \bar{x} to give,

$$\frac{\partial V_s}{\partial \bar{s}} = -\frac{\frac{\partial F}{\partial \bar{s}}}{\frac{\partial F}{\partial V_s}} = -\frac{-\frac{\partial V_{s,i}^*}{\partial \sigma_i} \cdot \frac{\partial \sigma_i}{\partial \bar{s}}}{1 - \frac{\partial V_{s,i}^*}{\partial \sigma_i} \cdot \frac{\partial \sigma_i}{\partial V_s}} \quad (10.24)$$

$$\frac{\partial V_s}{\partial \bar{\tau}} = -\frac{\frac{\partial F}{\partial \bar{\tau}}}{\frac{\partial F}{\partial V_s}} = -\frac{-\frac{\partial V_{s,i}^*}{\partial \sigma_i} \cdot \frac{\partial \sigma_i}{\partial \bar{\tau}}}{1 - \frac{\partial V_{s,i}^*}{\partial \sigma_i} \cdot \frac{\partial \sigma_i}{\partial V_s}} \quad (10.25)$$

$$\frac{\partial V_s}{\partial \bar{x}} = -\frac{\frac{\partial F}{\partial \bar{x}}}{\frac{\partial F}{\partial V_s}} = -\frac{-\frac{\partial V_{s,i}^*}{\partial \sigma_i} \cdot \frac{\partial \sigma_i}{\partial \bar{x}}}{1 - \frac{\partial V_{s,i}^*}{\partial \sigma_i} \cdot \frac{\partial \sigma_i}{\partial V_s}} \quad (10.26)$$

Substituting the above equations into Eq.(10.12) produces three equations to be solved independently for the three σ :

$$\begin{aligned} \{V_s(\bar{s}, \bar{\tau}; \bar{x}) - [\frac{\partial z_c}{\partial \bar{\tau}} \Big|_{\bar{\xi}=\text{const.}} \bar{s} + \frac{\partial z_c}{\partial \bar{x}} \bar{s}(1 - \bar{x} \frac{L_\tau}{L})]\} \frac{\partial \sigma_i}{\partial \bar{s}} \\ + (z_c - 1) [\frac{\partial \sigma_i}{\partial \bar{\tau}} \Big|_{\bar{\xi}=\text{const.}} + (1 - \bar{x} \frac{L_\tau}{L}) \frac{\partial \sigma_i}{\partial \bar{x}}] = 0 \end{aligned} \quad i = 1,2,3 \quad (10.27)$$

In Eq.(10.27), V_s is treated as a parameter, so that Eq.(10.27) is linear, and can be solved for σ_i .

Specifically, for $i = 1$,

$$V_s[\bar{s}, \bar{\tau}; \bar{\xi}(\bar{x}, \bar{\tau})] = V_{s,1}^* = V_s(\sigma_1, 0, 0) \quad (10.28)$$

At $\bar{\tau} = \tau - \tau_0 = 0$ and $\bar{x} = x - x_0 = 0$, $V_s(\bar{s}, 0, 0) = V_j \cdot H[s^+(0, 0) - s]$, where $1 \leq s \leq s^+$ (for the s coordinate, refer to Fig. 3.3 in Chapter 3), and V_j , $s^+(0, 0)$ are the solution at $\bar{\tau} = 0$, $\bar{x} = 0$.

Denote $\bar{s}' = \bar{s}$ in $0 \leq \bar{s} \leq s^+ - 1$ and set up $\sigma_1 = \bar{s}'$, thus,

$$V_s[\bar{s}, \bar{\tau}; \bar{x}] = V_s(\bar{s}', 0, 0) = V_j \quad (10.29)$$

Since we are interested in finding the location \bar{s} corresponding to \bar{s}' for $\tau > \tau_0$, in this interest, with σ_1 fixed at \bar{s}' , we have $\Delta\sigma_1 = 0$. Therefore,

$$\begin{aligned} \Delta\sigma_1 &= \frac{\partial\sigma_1}{\partial\bar{s}} \cdot \Delta\bar{s} + \frac{\partial\sigma_1}{\partial\bar{\tau}} \cdot \Delta\bar{\tau} + \frac{\partial\sigma_1}{\partial\bar{x}} \cdot \Delta\bar{x} \\ &= \frac{\partial\sigma_1}{\partial\bar{s}} \cdot \Delta\bar{s} + \left(\frac{\partial\sigma_1}{\partial\bar{\tau}} \Big|_{\xi=const.} - \bar{x} \frac{L_\tau}{L} \frac{\partial\sigma_1}{\partial\bar{x}} \right) \Delta\bar{\tau} + \frac{\partial\sigma_1}{\partial\bar{x}} \cdot \Delta\bar{x} \\ &= 0 \end{aligned} \quad (10.30)$$

At this stage, we have obtained two equations for σ_1 ((10.27) and (10.30)), but there are three σ_1 unknowns ($\frac{\partial \sigma_1}{\partial \bar{s}}, \frac{\partial \sigma_1}{\partial \bar{\tau}}, \frac{\partial \sigma_1}{\partial \bar{x}}$). To solve for \bar{s} which should satisfy the Euler's equation in (10.27), we need to make an assumption to reduce the number of unknowns for an approximate solution.

In following sections, we introduce three possible approximations that can be used to derive three different governing conditions to determine the free vortex locations.

10.4.1 Second order condition for the free vortex location

The first possible approximation: assuming $\frac{\partial}{\partial \bar{\tau}} \ll \frac{\partial}{\partial \bar{s}}, \frac{\partial}{\partial \bar{x}}$ in Eq.(10.30) and assuming $\frac{\partial}{\partial \bar{\tau}} \Big|_{\xi=const.}$ term is small in (10.27).

(10.30) is simplified to:

$$\Delta \sigma_1 \cong \frac{\partial \sigma_1}{\partial \bar{s}} \cdot \Delta \bar{s} + \frac{\partial \sigma_1}{\partial \bar{x}} \cdot \Delta \bar{x} = 0 \quad (10.31)$$

Eq.(10.31) yields that:

$$\frac{\Delta \bar{s}}{\Delta \bar{x}} = - \frac{\frac{\partial \sigma_1}{\partial \bar{x}}}{\frac{\partial \sigma_1}{\partial \bar{s}}} \quad (10.32)$$

In Eq.(10.27), assuming $\left. \frac{\partial}{\partial \bar{\tau}} \right|_{\xi=const.}$ term is small, and ignoring the $\left. \frac{\partial}{\partial \bar{\tau}} \right|_{\xi=const.}$ term,

the Euler's equation becomes:

$$\{V_s(\bar{s}',0,0) - [\frac{\partial z_c}{\partial \bar{x}} \bar{s}(1 - \bar{x} \frac{L_r}{L})]\} \frac{\partial \sigma_1}{\partial \bar{s}} + (z_c - 1)(1 - \bar{x} \frac{L_r}{L}) \cdot \frac{\partial \sigma_1}{\partial \bar{x}} = 0 \quad (10.33)$$

From Eq.(10.33), we have,

$$\frac{\frac{\partial \sigma_1}{\partial \bar{x}}}{\frac{\partial \sigma_1}{\partial \bar{s}}} = - \frac{V_s(\bar{s}',0,0) - \frac{\partial z_c}{\partial \bar{x}} \bar{s}(1 - \bar{x} \frac{L_r}{L})}{(z_c - 1)(1 - \bar{x} \frac{L_r}{L})} \quad (10.34)$$

Substituting Eq.(10.34) back into Eq.(10.32), we get the following relation:

$$\frac{\Delta \bar{s}}{\Delta \bar{x}} = \frac{V_s(\bar{s}',0,0) - \frac{\partial z_c}{\partial \bar{x}} \bar{s}(1 - \bar{x} \frac{L_r}{L})}{(z_c - 1)(1 - \bar{x} \frac{L_r}{L})} \quad (10.35)$$

or,

$$\frac{\Delta \bar{s}}{\Delta \bar{x}} = \frac{\frac{V_s(\bar{s}',0,0)}{(1 - \bar{x} \frac{L_r}{L})}}{(z_c - 1)} - \frac{\frac{\partial z_c}{\partial \bar{x}} \bar{s}}{(z_c - 1)} \quad (10.36)$$

$$\frac{d}{d\bar{x}}[\bar{s} \cdot (z_c - 1)] = \frac{V_s(\bar{s}', 0, 0)}{(1 - \bar{x} \frac{L_\tau}{L})} \quad (10.37)$$

Integration of above equation gives,

$$\bar{s} \cdot (z_c - 1) = -V_s(\bar{s}', 0, 0) \cdot \frac{L}{L_\tau} \ln(1 - \bar{x} \frac{L_\tau}{L}) + C \quad (10.38)$$

Using the initial condition, at $\bar{x} = x - x_0 = 0$, $\bar{\tau} = \tau - \tau_0 = 0$, $\bar{s} = \bar{s}'$, we find,

$$C = \bar{s}' [z_c(x_0, \tau_0) - 1] \quad (10.39)$$

Expanding $\ln(1 - \bar{x} \frac{L_\tau}{L})$ term with regards to the small parameter $\varepsilon = o(\bar{x} \frac{L_\tau}{L})$, we

have,

$$\ln(1 - \bar{x} \frac{L_\tau}{L}) \cong -[\bar{x} \frac{L_\tau}{L} + \frac{1}{2} (\bar{x} \frac{L_\tau}{L})^2] \quad (10.40)$$

Substituting the above equations back into Eq.(10.38), we have the following second order condition for determining the free vortex location:

$$s(s', x; \tau) = \frac{V_s(s', \tau_0, x_0) \cdot [(x - x_0) + \frac{1}{2} \cdot \frac{L_\tau}{L} \cdot (x - x_0)^2] + s' [z_c(x_0, \tau_0) - 1]}{[z_c(x, \tau) - 1]}$$

$$1 \leq s' \leq s^+, \quad x \geq x_0, \quad \tau \geq \tau_0 \quad (10.41)$$

10.4.2 First order condition for the free vortex location

The second possible approximation is: assuming $\frac{\partial}{\partial \bar{\tau}} \ll \frac{\partial}{\partial \bar{s}}, \frac{\partial}{\partial \bar{x}}$ in Eq.(10.30) and

in Eq.(10.27).

By ignoring the whole $\frac{\partial}{\partial \bar{\tau}}$ term in (10.27), the Euler's equation becomes:

$$\{V_s(\bar{s}, \bar{\tau}; \bar{x}) - \frac{\partial z_c}{\partial \bar{x}} \bar{s}\} \frac{\partial \sigma_i}{\partial \bar{s}} + (z_c - 1) \frac{\partial \sigma_i}{\partial \bar{x}} = 0 \quad i = 1, 2, 3 \quad (10.42)$$

Taking $i = 1$ as an example, we have,

$$\frac{\frac{\partial \sigma_1}{\partial \bar{x}}}{\frac{\partial \sigma_1}{\partial \bar{s}}} = - \frac{V_s(\bar{s}', 0, 0) - \frac{\partial z_c}{\partial \bar{x}} \bar{s}}{(z_c - 1)} \quad (10.43)$$

Substituting Eq.(10.43) into Eq.(10.32), we get the following relation:

$$\frac{\Delta \bar{s}}{\Delta \bar{x}} = \frac{V_s(\bar{s}', 0, 0) - \frac{\partial z_c}{\partial \bar{x}} \bar{s}}{(z_c - 1)} \quad (10.44)$$

and,

$$\frac{d}{d\bar{x}} [\bar{s} \cdot (z_c - 1)] = V_s(\bar{s}', 0, 0) \quad (10.45)$$

Integration of above equation, we get,

$$\bar{s} \cdot (z_c - 1) = V_s(\bar{s}', 0, 0) \cdot \bar{x} + C \quad (10.46)$$

Using the initial condition, at $\bar{x} = x - x_0 = 0$, $\bar{\tau} = \tau - \tau_0 = 0$, $\bar{s} = s'$, we find,

$$C = s' [z_c(x_0, \tau_0) - 1] \quad (10.47)$$

Substituting the above equations into Eq.(10.46), we have the following first order condition for the free vortex location:

$$s(s', x; \tau) = \frac{V_s(s', \tau_0, x_0) \cdot (x - x_0) + s' [z_c(x_0, \tau_0) - 1]}{[z_c(x, \tau) - 1]} \quad 1 \leq s' \leq s^+, \quad x \geq x_0, \quad \tau \geq \tau_0 \quad (10.48)$$

which is similar to the condition in the planing monohull hydrodynamic problem (Vorus, 1996).

10.4.3 An alternative of the first order condition for the free vortex location

The third possible approximation may be: assuming $\frac{\partial}{\partial \bar{x}} \ll \frac{\partial}{\partial \bar{s}}, \frac{\partial}{\partial \bar{\tau}}$ in Eq.(10.30)

and assuming $\frac{\partial}{\partial \bar{x}}$ term is small in Eq.(10.27).

By ignoring $\frac{\partial}{\partial \bar{x}}$ term, (10.30) becomes:

$$\Delta \sigma_1 \cong \frac{\partial \sigma_1}{\partial \bar{s}} \cdot \Delta \bar{s} + \frac{\partial \sigma_1}{\partial \bar{\tau}} \cdot \Delta \bar{\tau} = 0 \quad (10.49)$$

(10.49) yields that:

$$\frac{\Delta \bar{s}}{\Delta \bar{\tau}} = - \frac{\left. \frac{\partial \sigma_1}{\partial \bar{\tau}} \right|_{\xi=const.} - \bar{x} \frac{L_\tau}{L} \frac{\partial \sigma_1}{\partial \bar{x}}}{\frac{\partial \sigma_1}{\partial \bar{s}}} \quad (10.50)$$

In the Euler's equation of the (10.27), if we ignore the $\frac{\partial}{\partial \bar{x}}$ term, not the term

involving $\frac{\partial}{\partial \bar{\xi}} \frac{\partial \bar{\xi}}{\partial \bar{\tau}} = -\bar{x} \frac{L_\tau}{L} \frac{\partial}{\partial \bar{x}}$, the Euler's equation becomes:

$$\{V_s(\bar{s}, \bar{\tau}; \bar{x}) - \left[\frac{\partial z_c}{\partial \bar{\tau}} \Big|_{\xi=const.} \bar{s} - \bar{x} \frac{\partial z_c}{\partial \bar{x}} \frac{L_\tau}{L} \bar{s} \right] \} \frac{\partial \sigma_1}{\partial \bar{s}} + (z_c - 1) \left[\frac{\partial \sigma_1}{\partial \bar{\tau}} \Big|_{\xi=const.} - \bar{x} \frac{L_\tau}{L} \frac{\partial \sigma_1}{\partial \bar{x}} \right] = 0 \quad (10.51)$$

Therefore, from Eq.(10.51),

$$\frac{\frac{\partial \sigma_1}{\partial \bar{\tau}} \Big|_{\xi=const.} - \bar{x} \frac{L_\tau}{L} \frac{\partial \sigma_1}{\partial \bar{x}}}{\frac{\partial \sigma_1}{\partial \bar{s}}} = - \frac{V_s(\bar{s}', 0, 0) - \left[\frac{\partial z_c}{\partial \bar{\tau}} \Big|_{\xi=const.} \bar{s} - \bar{x} \frac{\partial z_c}{\partial \bar{x}} \frac{L_\tau}{L} \bar{s} \right]}{(z_c - 1)} \quad (10.52)$$

Combining (10.52) with (10.50), we have the following relation:

$$\frac{\Delta \bar{s}}{\Delta \bar{\tau}} = \frac{V_s(\bar{s}', 0, 0) - \left[\frac{\partial z_c}{\partial \bar{\tau}} \Big|_{\xi=const.} \bar{s} - \bar{x} \frac{\partial z_c}{\partial \bar{x}} \frac{L_\tau}{L} \bar{s} \right]}{(z_c - 1)} \quad (10.53)$$

and,

$$\frac{d}{d\bar{\tau}} [\bar{s} \cdot (z_c - 1)] = V_s(\bar{s}', 0, 0) \quad (10.54)$$

Integration of the above equation gives,

$$\bar{s} \cdot (z_c - 1) = V_s(\bar{s}', 0, 0) \cdot \bar{\tau} + C \quad (10.55)$$

Using the initial condition, at $\bar{\tau} = \tau - \tau_0 = 0$, $\bar{x} = x - x_0 = 0$, $\bar{s} = s'$, we find,

$$C = \bar{s}'[z_c(x_0, \tau_0) - 1] \quad (10.56)$$

Substituting the initial conditions into Eq.(10.55), we have the third possible form in the first order condition for the free vortex location:

$$s(s', x; \tau) = \frac{V_s(s', \tau_0, x_0) \cdot (\tau - \tau_0) + s'[z_c(\tau_0) - 1]}{[z_c(\tau) - 1]} \quad 1 \leq s' \leq s^+, \tau \geq \tau_0, \tau \geq \tau_0 \quad (10.57)$$

The solution of Eq. (10.27) for $i = 2,3$ can proceed similarly. The solution in the domain $s^- \leq s \leq 0$ could proceed same as in the domain $1 \leq s \leq s^+$.

So far, three possible solutions have been derived for the free vertex location under the three different possible approximations. The solution in (10.41) and (10.48) depend upon the relative distance between the current location and the separation point $(x - x_0)$, the solution in (10.57) depends upon the time interval between the current time and the initial separation time $(\tau - \tau_0)$. The conditions in (10.41) and (10.48) have given a reasonable free vortex distribution from the numerical examples, however the condition in (10.57) will give a divergent result as the time increasing. In the following numerical examples, the condition in (10.41) from the first approximation has been implemented in the numerical model.

10.5 Numerical Result Comparison

The temporal derivation terms: $\left. \frac{\partial z_c(\xi, \tau)}{\partial \tau} \right|_{\xi=const.}$, $\left. \frac{\partial b^+(\xi, \tau)}{\partial \tau} \right|_{\xi=const.}$, $\left. \frac{\partial b^-(\xi, \tau)}{\partial \tau} \right|_{\xi=const.}$

and $\left. \frac{\partial V_s}{\partial \tau}(\xi, s, \tau) \right|_{\xi=const.}$ in Eq.(10.5), (10.6), (10.7), (10.8),(10.9) (10.10), and (10.11) have

been incorporated into the present second order numerical model by using the described interpolation and difference algorithms, and the second order condition in (10.41) for the vortex location on the free jet-head sheet has been implemented in the numerical model. The modified software is named as NewCat (2-5).

The effect of these temporal derivation terms can be demonstrated by the comparison of the planing seakeeping results of the NewCat2-5 with the results of NewCat2-4, which is without these temporal derivation terms.

In this comparison, the Vorus-DeCan stepped catamaran has been used again. The input wave is a random wave in head sea. The significant wave height $H_{1/3} = 0.308$ m, the wave peak period $T_p = 4.188$ second. Again a JONSWAP wave spectrum has been used here. The forward speed has been chosen as $U = 70$ knots, the non-dimension time step $\Delta\tau = 0.02$, the artificial damping coefficient $DEPS = 0.1$, all same as in Chapter 9. The time duration in this example is $IALL = 3050$, the non-dimensional time length is 61.

Fig. 10.7 – 10.9 are the results of waves, displacements, vertical accelerations, wetted lengths from NewCat2-5. Fig. 10.7 shows the time histories of wave elevations, the displacement, the transom drafts and the trim angle, comparable to Fig. 9.19 in

Chapter 9. Fig. 10.8 is the vertical accelerations with these temporal derivation terms taken into account. Fig. 10.9 shows the wetted water line lengths and the chine-wetted lengths.

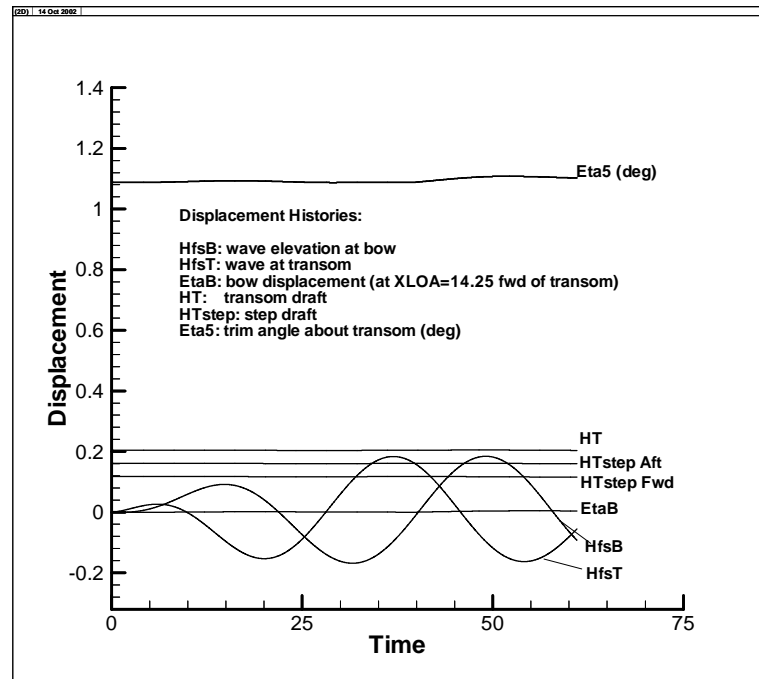


Fig. 10.7 Wave and motion histories from NewCat2-5

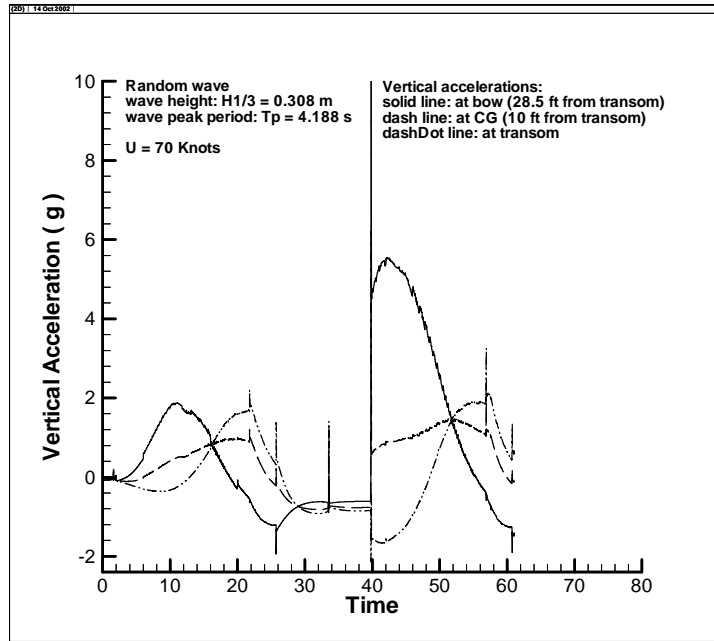


Fig. 10.8 Vertical accelerations from NewCat2-5

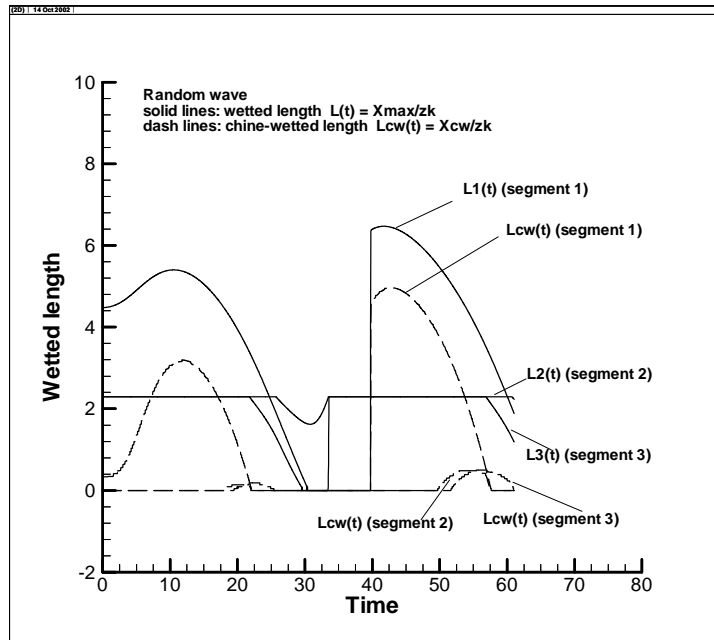


Fig. 10.9 Wetted lengths from NewCat2-5

Fig. 10.10 is the comparison of the vertical accelerations. The dashed line represents the result of the 2nd order model without considering the $\left. \frac{\partial}{\partial \tau} \right|_{\xi=const}$ terms (the software version is NewCat 2-4), marked as “the 2nd order kinematics model” for distinguishing from NewCat2-5. The solid line represents the results of the full 2nd order model with all the $\left. \frac{\partial}{\partial \tau} \right|_{\xi=const}$ terms implemented (the software version is NewCat 2-5), it marked as “the 2nd order dynamics model” based on the physical explanation. The free vortex location of (10.41) from the first approximation has been used in this example. It is easily seen that the results from the two models are close, however the dynamics model (NewCat 2-5) has produced much more spikes. Numerical tests show that these spikes may come from insufficient accuracy, since with these temporal derivation terms the numerical computation needs much higher numerical accuracy. Therefore a finer computation grids and more CPU time are required, which is difficult for present-PC type computer.

Fig. 10.11 shows the comparison of the trim angles. There is almost no difference for the two models.

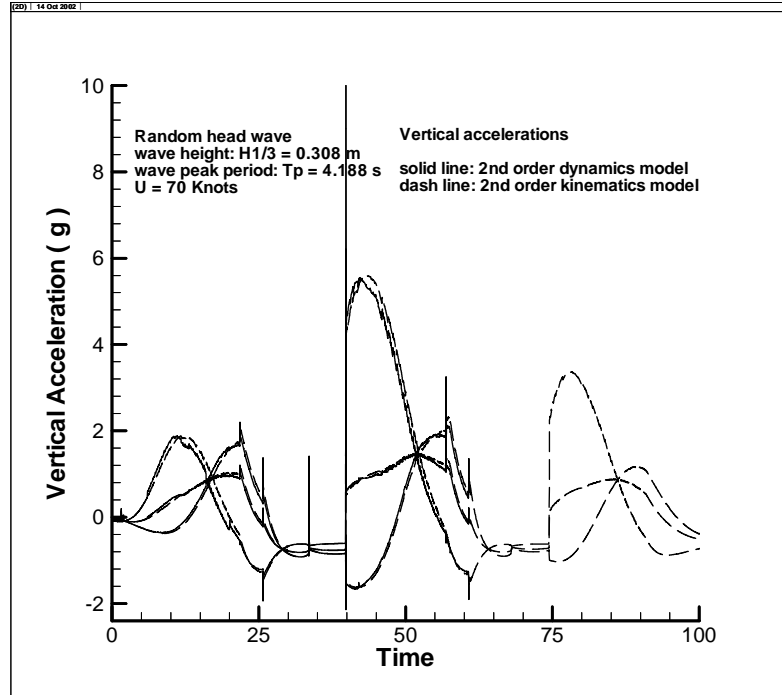


Fig. 10.10 Comparison of the vertical accelerations

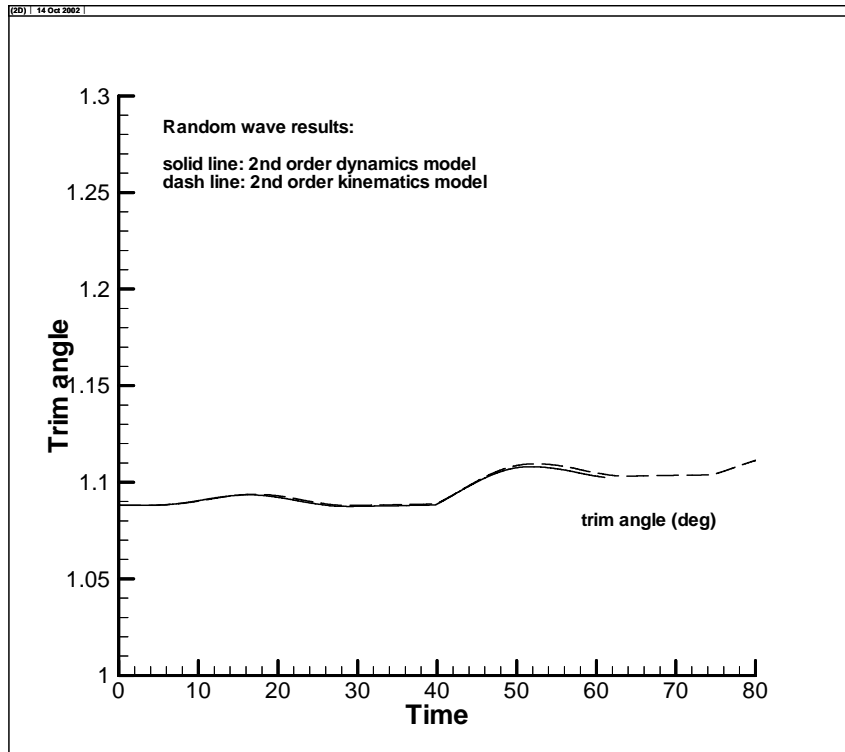


Fig. 10.11 Comparisons of trim angles

Fig. 10.12 is the comparison of the sectional lift distribution at the non-dimensional time $T = 42$. Fig. 10.13 is the comparison of the jet-head stream lines at $T=42$. Fig. 10.14 is the zoom view of the comparison of jet velocity distributions at $T = 42$. In Fig. 10.14, a local difference for the jet-head stream lines has been found. In general, these figures tell us that the solutions of the flow field and the lift are close, and that these temporal derivation terms do not have a large impact on the solutions. However it does increase the numerical complexity greatly.

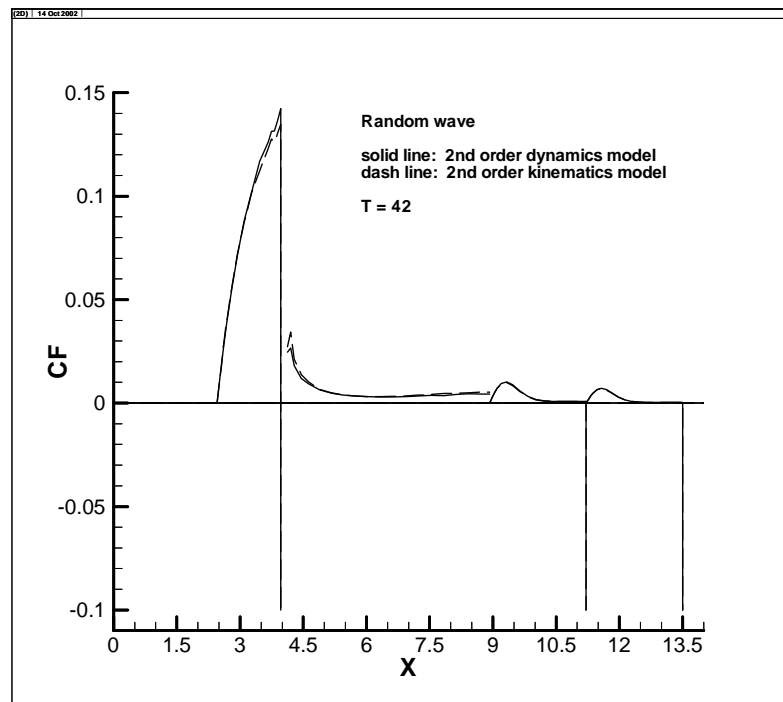


Fig. 10.12 Comparison of the sectional lift distribution at $T = 42$

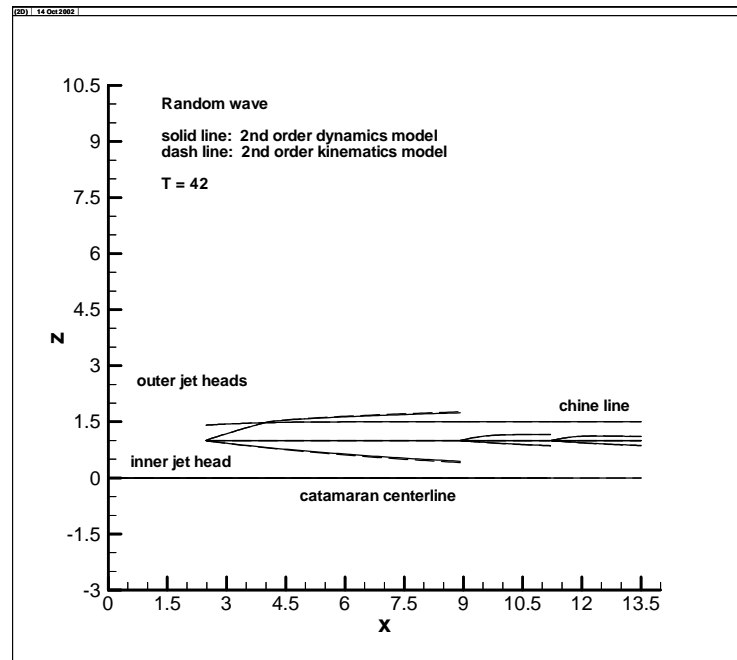
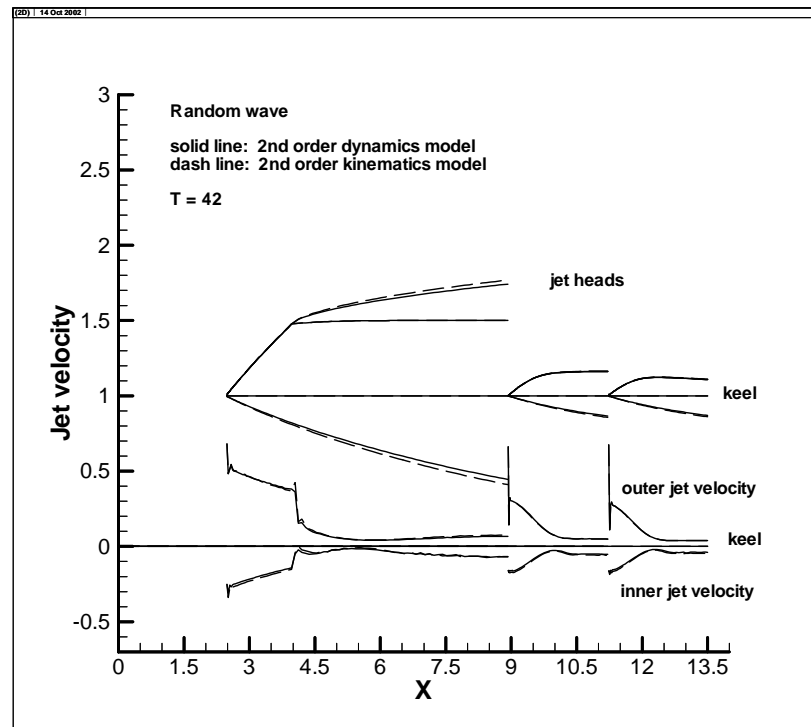
Fig. 10.13 Comparison of flow fields at $T = 42$ Fig. 10.14 Comparison of jet velocity distributions at $T = 42$ (zoom view)

Fig. 10.15 shows the comparison of pressure distribution at $T = 42$, at the section 22 of the main hull, the location of the section is from the entry $\bar{x}_i = 1.031$. There are some differences for the pressure distribution, since the $\left. \frac{\partial}{\partial \tau} \right|_{\xi=const}$ terms have been implemented in the pressure formula (refer to (10.8) and (10.9)).

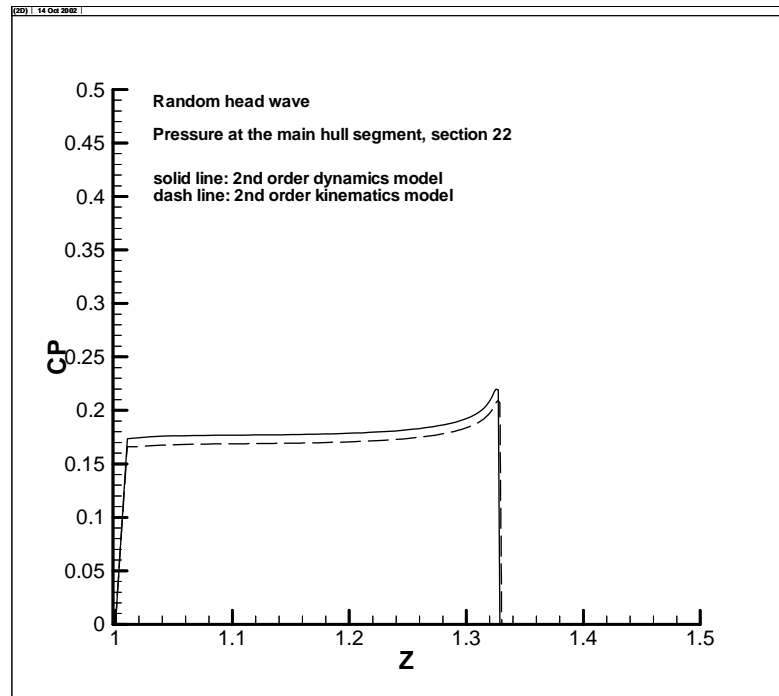


Fig. 10.15 Comparison of pressure distribution at main hull, section 22

(from the entry $\bar{x}_i = 1.031$, $T=42$)

From these comparisons, it is found that it is doable for numerically implementing all these temporal derivation terms in (10.5) – (10.11) into the program, and the effect of these temporal derivation terms on the final results is not large, however it will increase a great amount of the numerical complexity, especially for the iteration

loop of the jet-head $b^+(\xi, \tau)$, $b^-(\xi, \tau)$. At the x -location of the chine-wetted section, the jet-head $b^+(\xi, \tau)$ solution often has a numerical jump, since the chine-unwetted phase and the chine-wetted phase have difference iteration algorithms (refer to Fig. 6.2 and Fig. 6.3 in Chapter 6), this numerical jump will results in an larger $\left. \frac{\partial b^+(\xi, \tau)}{\partial \tau} \right|_{\xi=const.}$ value

which may cause the iteration to diverge.

Up till now, we have completed the introductions of the 2nd order model. Comparing the results of 2nd order kinematic model in Chapter 8 and 9 which without considering the effect of $\left. \frac{\partial}{\partial \tau} \right|_{\xi=const}$ terms, with the results from the 2nd order dynamic model in this chapter (with $\left. \frac{\partial}{\partial \tau} \right|_{\xi=const}$ terms), it seems that the impact of these

$\left. \frac{\partial}{\partial \tau} \right|_{\xi=const}$ terms on the final boat motions and on the accelerations may not be large, but

the $\left. \frac{\partial}{\partial \tau} \right|_{\xi=const}$ terms do make the problem behavior more complicated and difficult to solve. From the view of the practical engineering application, discarding the

$\left. \frac{\partial}{\partial \tau} \right|_{\xi=const}$ terms in the 2nd order model, it may be an acceptable approximation as the 1st

order model did.

CHAPTER 11

CONCLUSIONS AND SUGGESTIONS FOR FURTHER WORK

11.1 Summary and Conclusions

The present research is for relieving the initially implemented approximations on the catamaran planing hydrodynamics by the first order model, and further developing and extending the theory and application beyond that currently in use in CatSea. This has been achieved through a detail theoretical analysis, algorithm development, and careful coding.

The main achievements in this thesis, through the present research, are summarized as follows:

- This research has systematically introduced the current planing hydrodynamics theories (refer to Chapter 1), especially the Vorus' planing theory and analysis.
- The detail analysis and assumptions for the catamaran flow physics, and the boundary value problem definition, are given in Chapter 2.
- The first order nonlinear planing hydrodynamics theory for catamarans has been, for the first time, systematically reviewed and documented in this thesis (refer to Chapter 3). The material of the first order theory is from the unpublished manuscripts by William Vorus, and his planing catamaran design code CatSea.

- Through the present research, a new, complete nonlinear hydrodynamics theory for planing catamarans is developed, which relieves the major approximations and simplifications of the first order theory. This extended theory is referred to as the “second order nonlinear theory” (refer to Chapter 4).
- The detail numerical models and the correspondent solution procedures for the first order and the second order theory, for steady planing and for seakeeping, have been outlined in Chapter 5 and Chapter 6.
- The main numerical models (the fundamental integrals and the bound vortex distribution) in the second order theory have been validated in Chapter 7.
- A comparison of the numerical predictions by the second order theory and the predictions by the first order theory, in the steady planing example, is given in Chapter 8.
- A comparison of the numerical results, in both the regular and random wave cases, for both the first and second order theories, has been carried out. The details are in Chapter 9.
- A theoretical and numerical investigation on the effect of the temporal derivative terms $\frac{\partial}{\partial \tau} \Big|_{\xi=const}$ has been conducted in Chapter 10. The computation algorithm and the numerical comparison for the $\frac{\partial}{\partial \tau} \Big|_{\xi=const}$ effect have been presented.

The following conclusions are drawn with respect to the purpose of the present research:

- The new second order theory has relieved the major approximations and simplifications of the first order theory.

- The numerical comparison demonstrates that the first order theory has made a reasonable simplification for the kinematic boundary condition, which neglecting the higher order nonlinearity, make the problem easier to solve. This research finds that the software “CatSea” based on the first order theory is a practical design tool of the catamaran design for its fast computation speed, the robust run-time performance, and good accuracy.
- The research on the effect of the temporal derivative terms $\frac{\partial}{\partial \tau} \Big|_{\xi=const}$ indicate that it is possible to numerically implement all the temporal derivation terms into the code to run a full planing dynamics problem, however it will increase the numerical complexity extensively. It has been found that the effect of these temporal derivation terms on the final results is not large, thus the approximation made in the first order theory that, discarding all the $\frac{\partial}{\partial \tau} \Big|_{\xi=const}$ terms in CatSea, may be an acceptable algorithm for most engineering problems at present computer capability.
- The second order theory is a complete nonlinear theory, and it has the ability (like the first order) to include the detail hull geometry. For example, deadrise angle variation over craft length is fully considered; the software NewCat2-4 or NewCat2-5 based on the second order theory has the potential for a powerful design tool. The comparison of results demonstrate that the present second order nonlinear model has high accuracy and can be reliable for work with planing catamaran design on a high speed computer.

- The first order theory and the second order theory of the planing catamaran hydrodynamics have been fully and systematically documented in this thesis, which has provided a reliable foundation and very useful information for future research.

11.2 Suggestions to Further Works

- To provide a reliable design tool for planing catamaran design, further work should be undertaken to validate the accuracy of the present software. An experimental program is strongly recommended. A careful and detailed flow field measurement, including the vertical acceleration measurements, the measurements of the trim angle and the transom draft, the pressure distribution, and the jet-head streamlines and the jet velocities at different cross sections, should be carried out. With an available experimental data comparison, the present codes (CatSea and NewCat) can be validated and modified to become an important, valuable design tool, which will guide the planing craft designer to design good performing planing catamarans, free of empiricism.
- Further theoretical research on the solution of the exact Burger's equation (refer to (10.27)) in the dynamic boundary condition is recommended. A proper condition should be developed for constructing a three-equation system, including (10.27) and (10.30), to find a unique solution for the three unknowns $(\frac{\partial \sigma_1}{\partial \bar{s}}, \frac{\partial \sigma_1}{\partial \bar{\tau}}, \frac{\partial \sigma_1}{\partial \bar{x}})$ in (10.27) and (10.30). In this way, a solution in a form similar to (10.41) will be achieved to accurately define the instantaneous free vortex sheet location in the seaway dynamics problem.

REFERENCES

1. Abramowitz and Stegun (1964), Handbook of Mathematical Functions, National Bureau of Standards, U. S. Government Printing Office, Washington, D. C.
2. Akers, R., Collis, S., and Swanson, C., (2000), Motion Control in High Speed Craft, IBEX2000 Conference, Ft. Lauderdale, FL, February 2000.
3. Breslin, J. P., (2000), Chine-dry planning of slender hulls, Part I: A general theory applied to prismatic surfaces. January.
4. Clement, E. P. and Koelbel, J. G., Jr. (1992), Optimized designs for stepped planning monohulls and catamarans, Conference on Intersociety High Performance Marine Vehicles, Washington DC, June 24-27.
5. Cointe, R. (1989), Two-dimensional water-solid impact, ASME Journal of Offshore Mechanics and Arctic Engineering, 111, p.109 - 114.
6. Cointe, R. (1991), Free-surface flows close to a surface-piercing body, Mathematical Approaches in Hydrodynamics, Society for Industrial and Applied Mathematics, p.319 - 334.
7. Gradshteyn, I. S. and Ryzhik, I. M. (1965), Table Of Integrals, Series and Products, Academic Press, New York and London.

8. Garner, Matthew D., (2000), Validation of nonlinear time domain seakeeping code VsSea, Master Thesis, School of Naval Architecture and Marine Engineering, University of New Orleans.
9. Kim, D. J., Vorus, W. S., Troesch, A. W., Gollwitzer, R.M., Coupled Hydrodynamic Impact and Elastic Response, 21st ONR Symposium, Trondheim, Norway, June 1996.
10. Lai, C. and Troesch, A. W., (1995), Modeling issues related to the hydrodynamics of three dimensional steady planing, *Journal of Ship Research*, 39, 1.
11. Lai, C. and Troesch, A. W., (1996), A vortex lattice method of high speed planing, *International Journal for Numerical Method in Fluids*, 22, pp.495-513.
12. Lanczos, C., (1964), *SIAM Journal on Numerical Analysis*, ser. B, Vol. 1, pp. 86-96.
13. Muskhelishvili, N. I. (1958), *Singular Integral Equations*, Noordhoff International Publishing, Leyden.
14. Payne, P. R., (1995), *Boat 3D – A Time-Domain Computer program for Planing Craft*, Payne Associates, Stenensville, MD, 1990.
15. Payne, P. R., (1995), Contributions to planing theory. *Ocean Engineering*, 22, 257-309.
16. Royce, R.A., (1996), A Comparison of Empirical and Computational Planing Models, *Small Craft Marine Engineering, Resistance, and Propulsion Symposium*, Ann Arbor, Michigan, May.
17. Royce, R.A., and Vorus, W.S., (1998), Pressure Measurements on a Planing Craft and Comparisons with Calculation, 25th ATTC, Iowa City, IA, September.

18. Royce, R. A.(2001), 2-D theory extended to planing craft with experimental comparison, Ph. D. dissertation, Department of Naval Architecture and Marine Engineering, The University of Michigan.
19. Savander, B. R., (1997), Planing hull steady hydrodynamics. Ph. D. dissertation, Department of Naval Architecture and Marine Engineering, The University of Michigan.
20. Tricomi, F. G. (1957), Integral Equations, Interscience Publishers, Inc.
21. Troesch, A. W. and Kang, C. G., (1986), Hydrodynamic impact loads on three-dimensional bodies. 16th Symposium on naval hydrodynamics, University of California, Berkeley, July.
22. Troesch, A. W. and Kang, C. G., (1988), Evaluation of impact loads associated with flare slamming. SNAME 13th STAR Symposium, Pittsburgh, June.
23. Tulin, M. P., (1957), The theory of slender surfaces planning at high speeds, Schiffstechnik, 4.
24. von Karman, T. (1929), The impact of seaplane floats during landing, NACA TN 321, Washington, D.C., Oct.
25. Vorus, W.S., (1992), An Extended Slender Body Model for Planing Hull Hydrodynamics, SNAME GLGR Section Meeting, Cleveland, OH, January.
26. Vorus, W. S., (1993), Hydrodynamic impact and penetration of flat cylinders, research project report, project No. R/T-27, R/T-30, Grant No. NA89AA-D-SG083, April.
27. Vorus, W. S., (1994), Hydrodynamic impact and penetration of flat cylinders, in SNAME Great Lakes and Great Rivers Section Meeting, Cleveland, OH, January.

28. Vorus, W. S., (1996), A flat cylinder theory for vessel impact and steady planing resistance. *Journal of Ship Research*, vol. 40, no. 2, p.89-106.
29. Vorus, W. S., (1998), Shock reduction of planing boats. Gulf Coast Region Maritime Technology Center, 2nd Quarter Report, University of New Orleans.
30. Vorus, W. S., Shock Reduction of Planing Boats, GCRMTC Project 95-041A, Final Report, August 1999.
31. Vorus, W. S. and Royce, R. A., (2000), Shock Reduction of Planning Boats. *Ship Structures Symposium 2000*, Washington, D. C., June.
32. Wagner, H., (1932), Uber stoss-und gleitvorgange an der oberflache von flussigkeiten. *Zeitschrift für Angewandte Mathematik und Mechanik*, 12, 193, Aug.
33. Xu, L., Troesch, A. M. and Vorus, W. S., (1998), Asymmetric vessel impact and planing hydrodynamics. *Journal of Ship Research*, Vol. 42, No.3, pp.187-198, Sept..
34. Xu, L., Troesch, A. M. and Peterson, R., (1998), Asymmetric hydrodynamic impact and dynamic response of vessels. *OMAE '98*, Lisbon, Portugal, July 5-9.
35. Zarnick, E. E., (1978), A nonlinear mathematical model of motions of a planing boat in regular waves. *DTNSRDC Report 78/032*, Mar.
36. Zhao, R., and Faltinsen, O., (1993), Water entry of two-dimensional bodies, *Journal of Fluid Mechanics*, 246, p.593-612.
37. Zhao, R., Faltinsen, O. and Aarsnes, J. V., (1996), Water entry of arbitrary two-dimensional sections with and without flow separation. *21st Symposium on Naval Hydrodynamics*, Trondheim, Norway.
38. Zhao, R., Faltinsen, O. M. and Haslum, H. A., (1997), A simplified nonlinear analysis of a high-speed planing craft in calm water. *FAST '97*.

APPENDIX A
KINEMATIC BOUNDARY CONDITION
AND VELOCITY CONTINUITY CONDITION

A.1 Kinematic Boundary Condition On Body Contour

At the $y-z$ plane of the body-fixed system $O-xyz$, uses a 2-D coordinate system $\zeta-o_{keel}-\eta$ moving downward with the cross section as depicted in Fig. A.1. In Fig. A.1, $V_s(\zeta)$ and $V_n(\zeta)$ are the tangential and normal flow velocities on the body bottom contour, and $v(\zeta)$, $w(\zeta)$ are the perturbation velocities in the y and z directions, respectively.

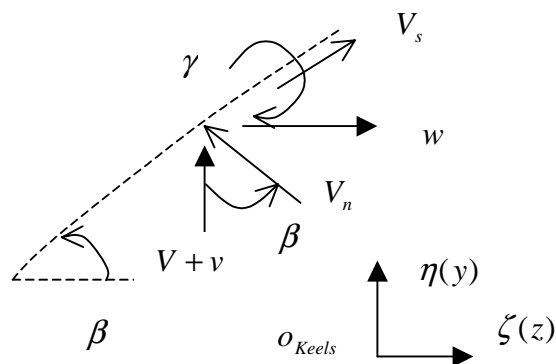


Fig. A.1 Kinematic boundary condition

The normal and tangential velocities, in terms of the perturbation velocities derived in Vorus (1996), can be expressed as (refer to Fig. A.1),

$$V_n = (V + v) \cos \beta(\zeta, \tau) - w \sin \beta(\zeta, \tau) \quad (\text{A.1})$$

$$V_s = (V + v) \sin \beta(\zeta, \tau) + w \cos \beta(\zeta, \tau) \quad (\text{A.2})$$

According to the physical model in Fig. 3.1, the jet velocity $V_s(\zeta)$ associated with a vortex strength $\gamma(\zeta, \tau)$ distribution can be described by the following relation:

$$V_s(\zeta, \tau) = -\frac{1}{2} \gamma(\zeta, \tau) + V(\tau) \sin \beta(\zeta, \tau) \quad (\text{A.3})$$

where $V(\tau) \sin \beta(\zeta, \tau)$ is the stream component.

In the downward moving coordinate system $\zeta - o_{keel} - \eta$ on the body boundary,

$$V_n(\zeta, \tau) = 0 \quad \text{for } 1 \leq \zeta \leq z_c \quad (\text{A.4})$$

To eliminate w from (A.1) and (A.2), multiply (A.1) by $\cos \beta(\zeta, \tau)$ and (A.2) by $\sin \beta(\zeta, \tau)$, then adding the two together with respect to (A.3) and (A.4), this process will give the following kinematic boundary condition on the hull contour (Vorus, 1996):

$$v(\zeta, \tau) + \frac{1}{2} \gamma(\zeta, \tau) \sin \beta(\zeta, \tau) = -V(\tau) \cos^2 \beta(\zeta, \tau) \quad \text{for } 1 \leq \zeta \leq z_c \quad (\text{A.5})$$

A.2 Integral Equation From the Kinematic Boundary Condition

Expressing the perturbation velocity $v(\zeta, \tau)$ in terms of $\gamma(\zeta, \tau)$ by the Biot-Savart law:

$$v(\zeta, \tau) = \frac{1}{2\pi} \int_{\zeta_0=-b^+}^{b^+} \frac{\gamma(\zeta_0, \tau)}{(\zeta_0 - \zeta)} d\zeta_0 \quad (\text{A.6})$$

Eliminating v in Eq.(A.5) using Eq.(A.6), we get the integral equation representing the kinematic boundary condition (KBC):

$$\frac{1}{2} \gamma(\zeta, \tau) \sin \beta(\zeta, \tau) + \frac{1}{2\pi} \int_{\zeta_0=-b^+}^{b^+} \frac{\gamma(\zeta_0, \tau)}{(\zeta_0 - \zeta)} d\zeta_0 = -V(\tau) \cos^2 \beta \quad \text{for } 1 \leq \zeta \leq z_c \quad (\text{A.7})$$

The integral on the whole computation domain can be separated as :

$$\int_{\zeta_0=-b^+}^{b^+} \frac{\gamma(\zeta_0, \tau)}{(\zeta_0 - \zeta)} d\zeta_0 = \left\{ \int_{-b^+}^{-z_c} + \int_{-z_c}^{-1.0} + \int_{-1.0}^{-b^-} \right\} \frac{\gamma(\zeta_0, \tau)}{(\zeta_0 - \zeta)} d\zeta_0 + \left\{ \int_{b^-}^{1.0} + \int_{1.0}^{z_c} + \int_{z_c}^{b^+} \right\} \frac{\gamma(\zeta_0, \tau)}{(\zeta_0 - \zeta)} d\zeta_0 \quad (\text{A.8})$$

Using the symmetry condition in ζ - axis:

$$\gamma(-\zeta, \tau) = -\gamma(\zeta, \tau) \quad (\text{A.9})$$

The first term in Eq.(A.8) becomes:

$$\frac{1}{2\pi} \int_{-b^+}^{-b^-} \frac{\gamma(\zeta_0, \tau)}{(\zeta_0 - \zeta)} d\zeta_0 = \frac{1}{2\pi} \int_{b^+}^{b^-} \frac{\gamma(-\zeta_0, \tau)}{(-\zeta_0 - \zeta)} (-d\zeta_0) = \frac{1}{2\pi} \int_{b^-}^{b^+} \frac{\gamma(\zeta_0, \tau)}{\zeta_0 + \zeta} d\zeta_0 \quad (\text{A.10})$$

Substituting Eq. (A.10) into Eq. (A.7),

$$\frac{1}{2} \gamma(\zeta, \tau) \sin \beta(\zeta, \tau) + \frac{1}{2\pi} \int_{b^-}^{b^+} \gamma(\zeta_0, \tau) \left[\frac{1}{\zeta_0 - \zeta} + \frac{1}{\zeta_0 + \zeta} \right] d\zeta_0 = -V(\tau) \cos^2 \beta(\zeta, \tau) \quad \text{on } 1 \leq \zeta \leq z_c \quad (\text{A.11})$$

The vortex is distributed on the axis is depicted in Fig. 2.6. The bounded vortex $\gamma(\zeta, \tau) = \gamma_c(\zeta, \tau)$ is over the hull segment $1 \leq \zeta \leq z_c$. The free vortex $\gamma(\zeta, \tau) = \gamma_s^+(\zeta, \tau)$ and $\gamma_s^-(\zeta, \tau)$ are over the free surface regions $z_c \leq \zeta \leq b^+(\tau)$, $b^- \leq \zeta \leq 1$ respectively.

Eq. (A.11) can be expressed in terms of the free-vortex sheet variable $\gamma_s(\zeta, \tau)$ as follows (Vorus, 1996):

$$\frac{1}{2} \gamma_c(\zeta, \tau) \sin \beta(\zeta, \tau) + \frac{1}{2\pi} \int_{-z_c}^{z_c} \frac{\gamma_c(\zeta_0, \tau)}{\zeta_0 - \zeta} d\zeta_0 = f(\zeta, \tau) \quad 1 \leq \zeta \leq z_c \quad (\text{A.12})$$

and, the region $-1 \leq \zeta_0 \leq 1$ in (A.12) is the free space between the demi-hulls (refer to Fig. 2.5).

$$\gamma_c(\zeta_0, \tau) = 0 \quad \text{on } -1 \leq \zeta_0 \leq 1 \quad (\text{A.13})$$

where:

$$f(\zeta, \tau) = -\cos^2 \beta \cdot V(\tau) - \frac{1}{\pi} \int_{b^-}^1 \gamma_s^-(\zeta_0, \tau) \frac{\zeta_0}{\zeta_0^2 - \zeta^2} d\zeta_0 - \frac{1}{\pi} \int_{z_c}^{b^+} \gamma_s^+(\zeta_0, \tau) \frac{\zeta_0}{\zeta_0^2 - \zeta^2} d\zeta_0 \quad (\text{A.14})$$

A.3 Solution to KBC Singular Integral Equation

Eq.(A.12) is the Carleman singular integration equation (Muskhelishvili 1958, Vorus 1996) ,

$$a(\zeta)\gamma_c(\zeta) - \lambda \int_{-1}^1 \frac{\gamma_c(s)}{s - \zeta} ds = f(\zeta) \quad \zeta \text{ on } L(\zeta) \quad (\text{A.15})$$

The solution domain L here includes two arcs of $-z_c \leq \zeta \leq -1$ and $1 \leq \zeta \leq z_c$.

Comparing Eq. (A.12), $a(\zeta)$ and λ are given respectively as:

$$a(\zeta) = \frac{1}{2} \sin \beta(\zeta, \tau) \quad (\text{A.16})$$

$$\lambda = -\frac{1}{2\pi} \quad (\text{A.17})$$

and $f(\zeta)$ is in Eq.(A.14).

Muskhelishvili(1958) or Tricomi(1957) give the general solution for the Carleman type singular integral equation. It takes the following form,

$$\gamma_c(\zeta) = \frac{a(\zeta)f(\zeta)}{a^2(\zeta) + (\lambda\pi)^2} + \frac{\lambda \cdot \chi(\zeta)}{\sqrt{a^2(\zeta) + (\lambda\pi)^2}} \int_{-1}^{*1} \frac{f(s)}{\chi(s)\sqrt{a^2(s) + (\lambda\pi)^2}} \frac{ds}{s - \zeta} \quad (\text{A.18})$$

Following the derivation of Vorus (1996), substituting Eq.(A.16) and (A.17) into Eq.(A.18), we have:

$$\gamma_c(\zeta, \tau) = \frac{2 \sin \beta f(\zeta)}{1 + \sin^2 \beta} - \frac{2 \cdot \chi(\zeta)}{\pi \sqrt{1 + \sin^2 \beta}} \int_{-z_c}^{z_c} \frac{f(s)}{\chi(s)\sqrt{1 + \sin^2 \beta}} \frac{ds}{s - \zeta} \quad (\text{A.19})$$

For convenience, define,

$$\sin \beta = \tan \tilde{\beta} \quad (\text{A.20})$$

thus,

$$1 + \sin^2 \beta = 1 + \tan^2 \tilde{\beta} = \frac{1}{\cos^2 \tilde{\beta}} \quad (\text{A.21})$$

Substituting above relations into Eq.(A.19) yields the solution of the line vortex strength distribution:

$$\gamma_c(\zeta, \tau) = 2 \sin \tilde{\beta} \cos \tilde{\beta} f(\zeta, \tau) - \frac{2 \cos \tilde{\beta} \cdot \chi(\zeta)}{\pi} \int_{-z_c}^{z_c} \frac{\cos \tilde{\beta} f(s)}{\chi(s)} \frac{ds}{s - \zeta}$$

on $1 \leq \zeta \leq z_c$ (A.22)

where

$$\tilde{\beta} = \tan^{-1}[\sin \beta(\zeta, \tau)] \quad (\text{A.23})$$

A.4 Kernel Function $\chi(\zeta)$

The kernel function solution development here closely follows for the mono-hull craft. From Muskhelishvili(1958) and Vorus (1996); the kernel function $\chi(\zeta)$ in Eq.(A.22) is:

$$\chi(\zeta) = P(\zeta) \cdot e^{\Gamma(\zeta)} \quad (\text{A.24})$$

where,

$$P(\zeta) = \prod_{m=1}^{2p} (\zeta - C_m)^{\lambda_m} \quad (\text{A.25})$$

$$\Gamma(\zeta) = \frac{1}{\pi} \sum_{k=1}^p \int_{L_k} \frac{\theta(t)}{t - \zeta} dt, \quad \theta(\zeta) = \arctan \frac{\lambda \pi}{(0, \pi) a(\zeta)} \quad (\text{A.26})$$

p in (A.25) and (A.26) is the number of arcs, with the end points at coordinates of C_m . The λ_m are integers which will be selected according to character of the $\chi(\zeta)$ function in each arc L_k , i.e., $-z_c \leq \zeta \leq -1$ and $1 \leq \zeta \leq z_c$ for present problem. Here $p = 2$, the respective $C_m = -z_c, -1.0, 1.0, z_c$. We may select the parameter λ_m to match the solution for the catamaran hull contour.

A kernel function for the type of integral in Eq.(A.22) is developed in Appendix F. It is different from the kernel function for the mono-hull (Vorus, 1996) for two singularity points located at the keel and z_c two points for the catamaran.

$$\chi(\zeta, \tau) = \frac{\kappa(\zeta, \tau)}{\sqrt{(\zeta^2 - 1)(z_c^2 - \zeta^2)}} \quad (\text{A.27})$$

where

$$\kappa(\zeta, \tau) = \prod_{j=1}^J \left| \frac{t_{j+1} + \zeta}{t_j + \zeta} \right|^{\frac{\beta_j(\tau)}{\pi}} \cdot \left| \frac{\zeta - t_{j+1}}{\zeta - t_j} \right|^{\frac{\beta_j(\tau)}{\pi}} \quad (\text{A.28})$$

The t_j and $\tilde{\beta}_j(\tau)$ are the end offsets and angles of the j th element (refer to Fig. 5 of Vorus(1996)). For deadrise contours $\beta(\zeta, \tau) = \beta(\tau)$ is constant in ζ , defining $\kappa(\zeta, \tau) = \kappa_0(\zeta, \tau)$ in this case:

$$\kappa_0(\zeta, \tau) = \left| \frac{z_c + \zeta}{1 + \zeta} \right|^{\frac{\tilde{\beta}(\tau)}{\pi}} \cdot \left| \frac{\zeta - z_c}{\zeta - 1} \right|^{\frac{\tilde{\beta}(\tau)}{\pi}} = \left(\frac{z_c^2 - \zeta^2}{\zeta^2 - 1} \right)^{\frac{\tilde{\beta}(\tau)}{\pi}} \quad (\text{A.29})$$

The kernel function then will be:

$$\chi(\zeta, \tau) = \frac{\kappa_0(\zeta, \tau)}{\sqrt{(\zeta^2 - 1)(z_c^2 - \zeta^2)}} = \frac{1}{\sqrt{(\zeta^2 - 1)(z_c^2 - \zeta^2)}} \cdot \left(\frac{z_c^2 - \zeta^2}{\zeta^2 - 1} \right)^{\frac{\tilde{\beta}(\tau)}{\pi}} \quad (\text{A.30})$$

A.5 Bounded Vortex $\gamma_c(\zeta, \tau)$

Expanding the equation (A.22) with respect to Eq.(A.13),

$$\begin{aligned} \gamma_c(\zeta, \tau) &= 2 \sin \tilde{\beta} \cos \tilde{\beta} f(\zeta, \tau) \\ &\quad - \frac{2}{\pi} \cos \tilde{\beta} \cdot \chi(\zeta, \tau) \left[\int_{\zeta_1 = -z_c}^{-1} \frac{f(\zeta_1, \tau) \cos \tilde{\beta}}{\chi(\zeta_1, \tau)} \frac{d\zeta_1}{(\zeta_1 - \zeta)} + \int_{\zeta_1 = 1}^{z_c} \frac{f(\zeta_1, \tau) \cos \tilde{\beta}}{\chi(\zeta_1, \tau)} \frac{d\zeta_1}{(\zeta_1 - \zeta)} \right] \end{aligned} \quad (\text{A.31})$$

Due to the symmetry of $\chi(\zeta, \tau)$ and $f(\zeta, \tau)$:

$$\chi(-\zeta, \tau) = \chi(\zeta, \tau) \quad (\text{A.32})$$

and

$$f(-\zeta, \tau) = f(\zeta, \tau) \quad (\text{A.33})$$

Thus the integral of first term in Eq.(A.31) will be,

$$\begin{aligned}
\int_{\zeta_1=-z_c}^{-1} \frac{f(\zeta_1, \tau) \cos \tilde{\beta}}{\chi(\zeta_1)} \frac{d\zeta_1}{(\zeta_1 - \zeta)} &= \int_{\zeta_1=z_c}^1 \frac{f(-\zeta_1, \tau) \cos \tilde{\beta}}{\chi(-\zeta_1)} \frac{d(-\zeta_1)}{(-\zeta_1 - \zeta)} \\
&= - \int_{\zeta_1=1}^{z_c} \frac{f(\zeta_1, \tau) \cos \tilde{\beta}}{\chi(\zeta_1)} \frac{d\zeta_1}{(\zeta_1 + \zeta)}
\end{aligned} \tag{A.34}$$

Substituting the above equation into Eq.(A.31) yields,

$$\begin{aligned}
\gamma_c(\zeta, \tau) &= 2 \sin \tilde{\beta} \cos \tilde{\beta} f(\zeta, \tau) \\
&\quad - \frac{2}{\pi} \cos \tilde{\beta} \cdot \chi(\zeta) \int_{\zeta_1=1}^{z_c} \frac{f(\zeta_1, \tau) \cos \tilde{\beta}}{\chi(\zeta_1)} \left[\frac{1}{(\zeta_1 - \zeta)} - \frac{1}{(\zeta_1 + \zeta)} \right] d\zeta_1 \\
&= 2 \sin \tilde{\beta} \cos \tilde{\beta} f(\zeta, \tau) \\
&\quad - \frac{4z}{\pi} \cos \tilde{\beta} \cdot \chi(\zeta) \int_{\zeta_1=1}^{z_c} \frac{f(\zeta_1, \tau) \cos \tilde{\beta}}{\chi(\zeta_1)} \frac{1}{(\zeta_1^2 - \zeta^2)} d\zeta_1
\end{aligned} \tag{A.35} \quad 1 \leq \zeta \leq z_c$$

Substituting $f(\zeta, \tau)$ into Eq.(A.35):

$$\begin{aligned}
\gamma_c(\zeta, \tau) &= -2 \sin \tilde{\beta} \cos \tilde{\beta} \cos^2 \beta \cdot V(\tau) \\
&\quad - 2 \sin \tilde{\beta} \cos \tilde{\beta} \frac{1}{\pi} \int_{b^-}^1 \gamma_s^-(\zeta_0, \tau) \frac{\zeta_0}{\zeta_0^2 - \zeta^2} d\zeta_0 \\
&\quad - 2 \sin \tilde{\beta} \cos \tilde{\beta} \frac{1}{\pi} \int_{z_c}^{b^+} \gamma_s^+(\zeta_0, \tau) \frac{\zeta_0}{\zeta_0^2 - \zeta^2} d\zeta_0 \\
&\quad + \frac{4z}{\pi} \cos \tilde{\beta} \cdot \chi(\zeta) [\cos^2 \beta \cdot V(\tau) \cdot \cos \tilde{\beta} \cdot \int_{\zeta_1=1}^{z_c} \frac{d\zeta_1}{\chi(\zeta_1)(\zeta_1^2 - \zeta^2)}] \\
&\quad + \frac{4z}{\pi} \cos \tilde{\beta} \cdot \chi(\zeta) \left[\frac{1}{\pi} \int_{b^-}^1 \gamma_s^-(\zeta_0, \tau) \cdot \zeta_0 \cdot \int_{\zeta_1=1}^{z_c} \frac{\cos \tilde{\beta} \cdot d\zeta_1}{\chi(\zeta_1)(\zeta_1^2 - \zeta^2)(\zeta_0^2 - \zeta_1^2)} \cdot d\zeta_0 \right] \\
&\quad + \frac{4z}{\pi} \cos \tilde{\beta} \cdot \chi(\zeta) \left[\frac{1}{\pi} \int_{z_c}^{b^+} \gamma_s^+(\zeta_0, \tau) \cdot \zeta_0 \cdot \int_{\zeta_1=1}^{z_c} \frac{\cos \tilde{\beta} \cdot d\zeta_1}{\chi(\zeta_1)(\zeta_1^2 - \zeta^2)(\zeta_0^2 - \zeta_1^2)} \cdot d\zeta_0 \right]
\end{aligned} \tag{A.36} \quad 1 \leq \zeta \leq z_c$$

According to the partial fraction reduction identity given by Vorus (1996):

$$\frac{1}{(\zeta_1^2 - \zeta^2)(\zeta_0^2 - \zeta_1^2)} = \frac{1}{\zeta_0^2 - \zeta^2} \left\{ \frac{1}{\zeta_0^2 - \zeta_1^2} + \frac{1}{\zeta_1^2 - \zeta^2} \right\} \quad (\text{A.37})$$

Thus, the inner integration in Eq.(A.36) becomes,

$$\begin{aligned} & \int_{\zeta_1=1}^{\zeta_c} \frac{d\zeta_1}{\chi(\zeta_1)(\zeta_1^2 - \zeta^2)(\zeta_0^2 - \zeta_1^2)} \\ &= \frac{1}{\zeta_0^2 - \zeta^2} \int_{\zeta_1=1}^{\zeta_c} \frac{d\zeta_1}{\chi(\zeta_1)} \left\{ \frac{1}{\zeta_0^2 - \zeta_1^2} + \frac{1}{\zeta_1^2 - \zeta^2} \right\} \\ &= \frac{1}{\zeta_0^2 - \zeta^2} \left\{ \int_{\zeta_1=1}^{\zeta_c} \frac{d\zeta_1}{\chi(\zeta_1)(\zeta_0^2 - \zeta_1^2)} - \int_{\zeta_1=1}^{\zeta_c} \frac{d\zeta_1}{\chi(\zeta_1)(\zeta^2 - \zeta_1^2)} \right\} \\ &= \frac{1}{\zeta_0^2 - \zeta^2} \{ \Lambda(\zeta_0) - \Lambda(\zeta) \} \end{aligned} \quad (\text{A.38})$$

where,

$$\Lambda(\zeta_0) = \int_{\zeta_1=1}^{\zeta_c} \frac{d\zeta_1}{\chi(\zeta_1)(\zeta_0^2 - \zeta_1^2)} \quad b^- \leq \zeta_0 \leq 1 \text{ or } z_c \leq \zeta_0 \leq b^+ \quad (\text{A.39})$$

$$\Lambda(\zeta) = \int_{\zeta_1=1}^{\zeta_c} \frac{d\zeta_1}{\chi(\zeta_1)(\zeta^2 - \zeta_1^2)} \quad 1 \leq \zeta \leq z_c \quad (\text{A.40})$$

Substituting Eq.(A.38) back into Eq.(A.36), we have the following expression for the bounded vortex $\gamma_c(\zeta)$:

$$\gamma_c(\zeta, \tau) = \gamma_{normal}(\zeta, \tau) + \gamma_{singular}(\zeta, \tau) \quad (\text{A.41})$$

where the normal component is the non-singular part of the solution:

$$\begin{aligned} \gamma_{c,normal}(\zeta, \tau) &= -2 \sin \tilde{\beta} \cos \tilde{\beta} \cos^2 \beta \cdot V(\tau) \\ &\quad - 2 \sin \tilde{\beta} \cos \tilde{\beta} \frac{1}{\pi} \int_{b^-}^1 \gamma_s^-(\zeta_0, \tau) \frac{\zeta_0}{\zeta_0^2 - \zeta^2} d\zeta_0 \\ &\quad - 2 \sin \tilde{\beta} \cos \tilde{\beta} \frac{1}{\pi} \int_{z_c}^{b^+} \gamma_s^+(\zeta_0, \tau) \frac{\zeta_0}{\zeta_0^2 - \zeta^2} d\zeta_0 \end{aligned} \quad (\text{A.42})$$

The singular term is the part with the singular kernel function $\chi(\zeta)$:

$$\begin{aligned} \gamma_{c,singular}(\zeta, \tau) &= \frac{4z}{\pi} \chi(\zeta, \tau) \cos \tilde{\beta} \{V(\tau) \cos^2 \beta \cos \tilde{\beta} \cdot [-\Lambda(\zeta)] \\ &\quad + \frac{1}{\pi} \cos \tilde{\beta} \int_{\zeta_0=b^-}^1 \gamma_s^-(\zeta_0, \tau) \frac{\zeta_0}{\zeta_0^2 - \zeta^2} d\zeta_0 [\Lambda^-(\zeta_0) - \Lambda(\zeta)] \\ &\quad + \frac{1}{\pi} \cos \tilde{\beta} \cdot \int_{\zeta_0=z_c}^{b^+} \gamma_s^+(\zeta_0, \tau) \frac{\zeta_0}{\zeta_0^2 - \zeta^2} d\zeta_0 [\Lambda^+(\zeta_0) - \Lambda(\zeta)]\} \end{aligned} \quad (\text{A.43})$$

where ζ is independent variable, ζ_1, ζ_0 are integration variables, and

$$\Lambda(\zeta) = \int_{\zeta_1=1}^{z_c} \frac{d\zeta_1}{\chi(\zeta_1)(\zeta^2 - \zeta_1^2)} \quad 1 \leq \zeta \leq z_c \quad (\text{A.44})$$

$$\Lambda^-(\zeta_0) = \int_{\zeta_1=1}^{z_c} \frac{d\zeta_1}{\chi(\zeta_1)(\zeta_0^2 - \zeta_1^2)} \quad b^- \leq \zeta_0 \leq 1 \quad (\text{A.45})$$

$$\Lambda^+(\zeta_0) = \int_{\zeta_1=1}^{\zeta_c} \frac{d\zeta_1}{\chi(\zeta_1)(\zeta_0^2 - \zeta_1^2)} \quad z_c \leq \zeta_0 \leq b^+ \quad (\text{A.46})$$

The numerical model for the bound vortex distribution $\gamma_c(\zeta, \tau)$ in Eq.(A.42) and Eq.(A.43) can be found in the Appendix E. Next we derive the velocity continuity condition based on the bound vortex distribution in Eq. (A.43).

A.6 Velocity Continuity or Vorticity Conservation Conditions

Equation (A.43) has singularity points in its solution domain at $\zeta = 1$ and $\zeta = z_c$.

When $\zeta \rightarrow 1$ and $\zeta \rightarrow z_c$, $\chi(\zeta) \rightarrow \infty$.

For non-singularization in Eq. (A.43) we use the following identities (Vorus, 1996):

$$\frac{1}{\zeta_0^2 - \zeta^2} = \frac{1}{\zeta_0^2 - 1} \left(1 + \frac{\zeta^2 - 1}{\zeta_0^2 - \zeta^2}\right) \quad \text{for } \zeta \rightarrow 1 \quad (\text{A.47})$$

$$\frac{1}{\zeta_0^2 - \zeta^2} = \frac{1}{\zeta_0^2 - z_c^2} \left(1 - \frac{z_c^2 - \zeta^2}{\zeta_0^2 - \zeta^2}\right) \quad \text{for } \zeta \rightarrow z_c \quad (\text{A.48})$$

When $\zeta \rightarrow 1^+$, use the identity in Eq.(A.47):

$$\begin{aligned}
\gamma_{c,\text{singular}}(\zeta, t) &= \frac{4\zeta}{\pi} \chi(\zeta) \cos \tilde{\beta} \\
&\quad \{ \cos^2 \beta \cos \tilde{\beta} \cdot [-\Lambda(\zeta)] \cdot V(\tau) \\
&\quad + \frac{1}{\pi} \cos \tilde{\beta} \int_{b^-}^1 \gamma_s^-(\zeta_0, \tau) \frac{\zeta_0}{\zeta_0^2 - 1} d\zeta_0 [\Lambda^-(\zeta_0) - \Lambda(\zeta)] \\
&\quad + (\zeta^2 - 1) \frac{1}{\pi} \cos \tilde{\beta} \int_{b^-}^1 \gamma_s^-(\zeta_0, \tau) \frac{\zeta_0}{(\zeta_0^2 - 1)(\zeta_0^2 - \zeta^2)} d\zeta_0 [\Lambda^-(\zeta_0) - \Lambda(\zeta)] \\
&\quad + \frac{1}{\pi} \cos \tilde{\beta} \cdot \int_{z_c}^{b^+} \gamma_s^+(\zeta_0, \tau) \frac{\zeta_0}{\zeta_0^2 - 1} d\zeta_0 [\Lambda^+(\zeta_0) - \Lambda(\zeta)] \\
&\quad + (\zeta^2 - 1) \frac{1}{\pi} \cos \tilde{\beta} \cdot \int_{z_c}^{b^+} \gamma_s^+(\zeta_0, \tau) \frac{\zeta_0}{(\zeta_0^2 - 1)(\zeta_0^2 - \zeta^2)} d\zeta_0 [\Lambda^+(\zeta_0) - \Lambda(\zeta)] \}
\end{aligned} \tag{A.49}$$

The requirement that γ_c be bounded results in the following velocity continuity equation (Kutta condition):

$$\begin{aligned}
0 &= \{ -\cos^2 \beta \cdot V(\tau) \cdot \Lambda(1) + \frac{1}{\pi} \int_{b^-}^1 \gamma_s^-(\zeta_0, \tau) \frac{\zeta_0}{\zeta_0^2 - 1} [\Lambda^-(\zeta_0) - \Lambda(1)] d\zeta_0 \\
&\quad + \frac{1}{\pi} \int_{z_c}^{b^+} \gamma_s^+(\zeta_0, \tau) \frac{\zeta_0}{\zeta_0^2 - 1} [\Lambda^+(\zeta_0) - \Lambda(1)] d\zeta_0 \} \\
&\hspace{25em} \zeta \rightarrow 1^+ \tag{A.50}
\end{aligned}$$

When $\zeta \rightarrow z_c^-$, use the identity in Eq.(A.48),

$$\begin{aligned}
\gamma_{c,\text{singular}}(\zeta) = & \frac{4\zeta}{\pi} \chi(\zeta) \cos \tilde{\beta} \\
& \{ \cos^2 \beta \cos \tilde{\beta} \cdot V(\tau) \cdot [-\Lambda(\zeta)] \\
& + \frac{1}{\pi} \cos \tilde{\beta} \cdot \int_{b^-}^1 \gamma_S^-(\zeta_0, \tau) \frac{\zeta_0}{\zeta_0^2 - z_c^2} [\Lambda^-(\zeta_0) - \Lambda(\zeta)] d\zeta_0 \\
& - \frac{1}{\pi} \cos \tilde{\beta} \cdot (z_c^2 - \zeta^2) \int_{b^-}^1 \gamma_S^-(\zeta_0, \tau) \frac{\zeta_0}{(\zeta_0^2 - z_c^2)(\zeta_0^2 - \zeta^2)} [\Lambda^-(\zeta_0) - \Lambda(\zeta)] d\zeta_0 \\
& + \frac{1}{\pi} \cos \tilde{\beta} \cdot \int_{z_c}^{b^+} \gamma_S^+(\zeta_0, \tau) \frac{\zeta_0}{\zeta_0^2 - z_c^2} [\Lambda^+(\zeta_0) - \Lambda(\zeta)] d\zeta_0 \\
& - \frac{1}{\pi} \cos \tilde{\beta} \cdot (z_c^2 - \zeta^2) \int_{z_c}^{b^+} \gamma_S^+(\zeta_0, \tau) \frac{\zeta_0}{(\zeta_0^2 - z_c^2)(\zeta_0^2 - \zeta^2)} [\Lambda^+(\zeta_0) - \Lambda(\zeta)] d\zeta_0 \}
\end{aligned} \tag{A.51}$$

The requirement that γ_c is bounded results in the following velocity continuity equation (Kutta condition), from (A.51):

$$\begin{aligned}
0 = & \{ \cos^2 \beta \cdot V(\tau) [-\Lambda(z_c)] + \frac{1}{\pi} \int_{b^-}^1 \gamma_S^-(\zeta_0, \tau) \frac{\zeta_0}{\zeta_0^2 - z_c^2} [\Lambda^-(\zeta_0) - \Lambda(z_c)] d\zeta_0 \\
& + \frac{1}{\pi} \int_{z_c}^{b^+} \gamma_S^+(\zeta_0, \tau) \frac{\zeta_0}{\zeta_0^2 - z_c^2} [\Lambda^+(\zeta_0) - \Lambda(z_c)] d\zeta_0 \} \\
& \zeta \rightarrow z_c^- \tag{A.52}
\end{aligned}$$

As was noted in Chapter 2, in the chine-unwetted flow phase, there are five unknowns: $V_j^+(\tau)$, $V_j^-(\tau)$, $z_b^+(\tau)$, $z_b^-(\tau)$, $z_c(\tau)$. The Kutta conditions of the kinematic boundary integral provide us with two velocity continuity equations (Eq.(A.50) and Eq. (A.52)).

APPENDIX B
DISPLACEMENT CONTINUITY CONDITION

In the chine un-wetted flow phase, the velocity continuity condition provides two equations of the five for solving five unknowns, the pressure continuity conditions provide another two equations. In this section, we develop the last necessary equation of the five based on the physics of a continuous body-free-surface contour at the jet-head b^+ in the chine un-wetted flow phase.

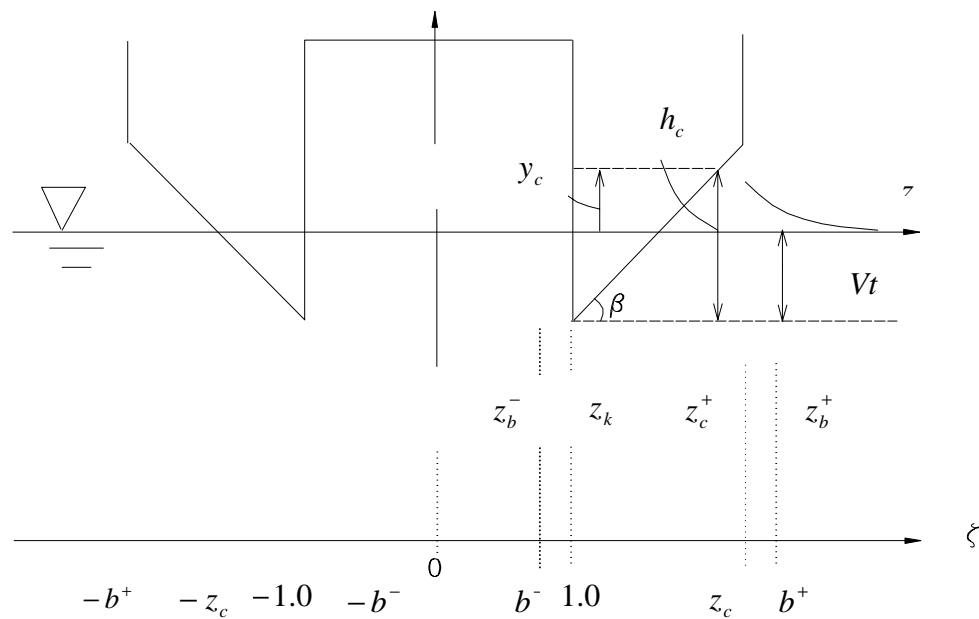


Fig. B.1 Displacement continuity condition model

B.1 Water Surface Elevation

In the time coordinate system $[0, t]$, in the chine-unwetted flow phase, the dimensional bottom contour $y_c(z, t)$ can be expressed as:

$$y_c(z, t) = h_c(z, t) - V(t) \cdot t \quad z_k \leq z \leq z_b^+ \quad (\text{B.1})$$

where V is the section impact velocity, the $V \cdot t$ term is, in fact, a transient draft, , and the water elevation above the keel is:

$$h_c(z, t) = \begin{cases} (z - z_k) \tan \beta & z_k \leq z \leq z_b^+(t) \\ 0 & z_b^-(t) \leq z < z_k \end{cases} \quad (\text{B.2})$$

The second branch of h_c is an approximation, assuming that the fluid surface is first order un-deflected, or the fluid separates at the keel.

Define the net vertical fluid velocity on the contour:

$$\frac{\partial y_c(z, t)}{\partial t} = -V(t) = v(z, t) + \frac{1}{2} \gamma(z, t) \sin \beta(z) \quad \text{on } z_k \leq z \leq z_b^+ \quad (\text{B.3})$$

Integration of the above equation gives the body contour:

$$\begin{aligned}
y_c(z, t) &= \int_{\tau=0}^t [v(z, \tau) + \frac{1}{2} \gamma(z, \tau) \sin \beta(z)] d\tau \\
&= v^*(z, t) + \frac{1}{2} \gamma^*(z, t) \sin \beta(z)
\end{aligned} \tag{B.4}$$

where:

$$v^*(z, t) = \int_{\tau=0}^t v(z, \tau) d\tau \quad \text{and} \quad \gamma^*(z, t) = \int_{\tau=0}^t \gamma(z, \tau) d\tau \tag{B.5}$$

Non-dimensionalize the transient draft variable $\tau = \frac{Vt}{Z_k}$ and the spatial variables

$\zeta = \frac{z}{z_k}$ and $\frac{y_c}{z_k}$. Substitute Eq.(B.4) into Eq.(B.1). The non-dimensional Eq.(B.1) now

becomes,

$$v^*(\zeta, \tau) + \frac{1}{2} \gamma^*(\zeta, \tau) \sin \beta(\zeta) = f(\zeta, \tau) \quad 1 \leq \zeta \leq b^+ \tag{B.6}$$

According to the above assumptions $f(\zeta, \tau)$ can be expanded into the domain:

$b^- \leq \zeta \leq b^+$ as:

$$f(\zeta, \tau) = \begin{cases} -\tau + \tilde{h}_c(\zeta, \tau) & 1 \leq \zeta \leq b^+(\tau) \\ -\tau & b^- \leq \zeta < 1 \end{cases} \tag{B.7}$$

where,

$$\tilde{h}_c(\zeta, \tau) = \begin{cases} (\zeta - 1) \tan \beta & 1 < \zeta \leq b^+(\tau) \\ 0 & b^-(\tau) \leq \zeta \leq 1 \end{cases} \quad (\text{B.8})$$

The vertical velocity time integral, $v^*(\zeta, \tau)$, is again expressible in terms of the time-integrated displacement vortex strength, $\gamma_c^*(\zeta, \tau)$, by the Biot-Savart law as in Eq.(A.6). Thus from (B.6),

$$\frac{1}{2} \gamma_c^*(\zeta, \tau) \sin \beta(\zeta) + \frac{1}{2\pi} \int_{-b^+}^{b^+} \gamma_c^*(\zeta_0, \tau) \frac{1}{\zeta_0 - \zeta} d\zeta_0 = f(\zeta, \tau) \quad 1 \leq \zeta \leq b^+ \quad (\text{B.9})$$

where,

$$\gamma_c^*(\zeta, \tau) = 0 \quad \text{on } -1 \leq \zeta \leq 1 \quad (\text{B.10})$$

Again Eq.(B.9) is the Carleman type of singular integration equation. Using the same transformation of Carleman type singular integral equation as in Appendix A, the solution to Eq.(B.9) is found in the following form (Vorus, 1996):

$$\gamma_c^*(\zeta, \tau) = 2 \sin \tilde{\beta} \cos \tilde{\beta} f(\zeta, \tau) - \frac{2 \cos \tilde{\beta} \cdot \chi^*(\zeta, \tau)}{\pi} \int_{-b^+}^{b^+} \frac{\cos \tilde{\beta} f(s)}{\chi^*(s, \tau) s - \zeta} ds$$

on $1 \leq \zeta \leq b^+$ (B.11)

where

$$\tilde{\beta} = \tan^{-1}[\sin \beta(\zeta)] \quad (\text{B.12})$$

B.2 Kernel Function $\chi^*(\zeta, \tau)$

The kernel function for the integral in Eq.(B.11) is developed in Appendix G. The difference from the kernel function $\chi(\zeta, \tau)$ is that the solution domain is now on the arcs of $-b^+ \leq \zeta \leq -b^-$ and $b^- \leq \zeta \leq b^+$. The respective $C_m = -b^+, -b^-, b^-, b^+$.

(1) In a general case, the kernel function will be in the form:

$$\chi^*(\zeta, \tau) = \frac{\kappa(\zeta, \tau)}{\sqrt{(\zeta^2 - (b^-)^2)((b^+)^2 - \zeta^2)}} \quad (\text{B.13})$$

where

$$\kappa(\zeta, \tau) = \prod_{j=1}^J \left| \frac{t_{j+1} + \zeta}{t_j + \zeta} \right|^{\frac{\beta_j(\tau)}{\pi}} \cdot \left| \frac{\zeta - t_{j+1}}{\zeta - t_j} \right|^{\frac{\beta_j(\tau)}{\pi}} \quad (\text{B.14})$$

The t_j and $\tilde{\beta}_j(\tau)$ are the end offsets and angles of the jth element.

(2) In the case of constant $\beta(\zeta, \tau) = \beta(\tau)$, the kernel function will be:

$$\chi^*(\zeta, \tau) = \frac{\kappa_0(\zeta, \tau)}{\sqrt{(\zeta^2 - (b^-)^2)((b^+)^2 - \zeta^2)}} = \frac{1}{\sqrt{(\zeta^2 - (b^-)^2)((b^+)^2 - \zeta^2)}} \cdot \left(\frac{(b^+)^2 - \zeta^2}{\zeta^2 - (b^-)^2} \right)^{\frac{\tilde{\beta}(\tau)}{\pi}} \quad (\text{B.15})$$

where

$$\kappa_0(\zeta, \tau) = \left| \frac{b^+ + \zeta}{b^- + \zeta} \right|^{\frac{\tilde{\beta}(\tau)}{\pi}} \cdot \left| \frac{b^+ - \zeta}{b^- - \zeta} \right|^{\frac{\tilde{\beta}(\tau)}{\pi}} = \left(\frac{(b^+)^2 - \zeta^2}{\zeta^2 - (b^-)^2} \right)^{\frac{\tilde{\beta}(\tau)}{\pi}} \quad (\text{B.16})$$

B.3 Displacement Continuity Equation

Expanding Eq.(B.11) with respect to Eq.(B.10) gives,

$$\gamma_c^*(\zeta, \tau) = 2 \sin \tilde{\beta} \cos \tilde{\beta} f(\zeta, \tau) - \frac{2}{\pi} \cos \tilde{\beta} \cdot \chi^*(\zeta, \tau) \left[\int_{\zeta_0=-b^+}^{-b^-} \frac{f(\zeta_0, \tau) \cos \tilde{\beta}}{\chi^*(\zeta_0, \tau)} \frac{d\zeta_0}{(\zeta_0 - \zeta)} + \int_{\zeta_0=b^-}^{b^+} \frac{f(\zeta_0, \tau) \cos \tilde{\beta}}{\chi^*(\zeta_0, \tau)} \frac{d\zeta_0}{(\zeta_0 - \zeta)} \right]$$

$$\text{on } -b^+ \leq \zeta \leq -1 \text{ and } 1 \leq \zeta \leq b^+ \quad (\text{B.17})$$

where ζ is independent non-dimensional variable.

Considering the following symmetries,

$$f(-\zeta, \tau) = f(\zeta, \tau) \quad (\text{B.18})$$

$$\chi^*(-\zeta, \tau) = \chi^*(\zeta, \tau) \quad (\text{B.19})$$

First term of the integral in Eq.(B.17) can be transformed into:

$$\int_{\zeta_0=-b^+}^{-b^-} \frac{f(\zeta_0, \tau)}{\chi(\zeta_0)} \frac{d\zeta_0}{(\zeta_0 - \zeta)} = \int_{\zeta_0=b^+}^{-b^-} \frac{f(-\zeta_0, \tau)}{\chi(-\zeta_0, \tau)} \frac{d(-\zeta_0)}{(-\zeta_0 - \zeta)} = - \int_{\zeta_0=b^-}^{b^+} \frac{f(\zeta_0, \tau)}{\chi(\zeta_0, \tau)} \frac{d\zeta_0}{(\zeta_0 + \zeta)} \quad (\text{B.20})$$

Substituting the above equation into Eq.(B.17) yields:

$$\begin{aligned} \gamma_c^*(\zeta, \tau) &= 2 \sin \tilde{\beta} \cos \tilde{\beta} f(\zeta, \tau) \\ &\quad - \frac{2}{\pi} \chi^*(\zeta, \tau) \cos \tilde{\beta} \int_{\zeta_1=b^-}^{b^+} \frac{f(\zeta_1, \tau) \cos \tilde{\beta}}{\chi^*(\zeta_1, \tau)} \left[\frac{1}{(\zeta_1 - \zeta)} - \frac{1}{(\zeta_1 + \zeta)} \right] d\zeta_1 \\ &= 2 \sin \tilde{\beta} \cos \tilde{\beta} f(\zeta, \tau) \\ &\quad - \frac{4\zeta}{\pi} \chi^*(\zeta, \tau) \cos \tilde{\beta} \int_{\zeta_1=b^-}^{b^+} \frac{f(\zeta_1, \tau) \cos \tilde{\beta}}{\chi^*(\zeta_1, \tau)} \frac{1}{(\zeta_1^2 - \zeta^2)} d\zeta_1 \end{aligned} \quad (\text{B.21})$$

Substituting $f(\zeta, \tau)$ into above equation, (B.21):

$$\begin{aligned} \gamma_c^*(\zeta, \tau) &= 2 \sin \tilde{\beta} \cos \tilde{\beta} [-\tau + (\zeta - 1) \tan \beta] \\ &\quad - \frac{4\zeta}{\pi} \chi^*(\zeta, \tau) \cos \tilde{\beta} \int_{\zeta_1=b^-}^{b^+} \frac{[-\tau + (\zeta_1 - 1) \tan \beta] \cos \tilde{\beta}}{\chi^*(\zeta_1, \tau)} \frac{1}{(\zeta_1^2 - \zeta^2)} d\zeta_1 \\ &= 2 \sin \tilde{\beta} \cos \tilde{\beta} [-\tau + (\zeta - 1) \tan \beta] \\ &\quad - \frac{4\zeta}{\pi} \chi^*(\zeta, \tau) \cos^2 \tilde{\beta} \times \\ &\quad \left\{ (-\tau - \tan \beta) \cdot \int_{\zeta_1=b^-}^{b^+} \frac{1}{\chi^*(\zeta_1, \tau)(\zeta_1^2 - \zeta^2)} d\zeta_1 + \tan \beta \cdot \int_{\zeta_1=b^-}^{b^+} \frac{\zeta_1}{\chi^*(\zeta_1, \tau)(\zeta_1^2 - \zeta^2)} d\zeta_1 \right\} \end{aligned} \quad (\text{B.22})$$

When $\zeta \rightarrow b^+$, there is a singularity in the kernel $\chi^*(\zeta, \tau)$. To eliminate the singularity, we express the term:

$$\frac{1}{\zeta_1^2 - \zeta^2} = -\frac{1}{b^{+2} - \zeta_1^2} \left(1 - \frac{b^{+2} - \zeta^2}{\zeta_1^2 - \zeta^2}\right) \quad (\text{B.23})$$

Substituting Eq.(B.23) into Eq.(B.22):

$$\begin{aligned} \gamma_c^*(\zeta, \tau) &= 2 \sin \tilde{\beta} \cos \tilde{\beta} [-\tau + (\zeta - 1) \tan \beta] \\ &\quad - \frac{4\zeta}{\pi} \chi^*(\zeta, \tau) \cos^2 \tilde{\beta} \cdot \{ -(\tau + \tan \beta) \cdot [- \int_{\zeta_1=b^-}^{b^+} \frac{1}{\chi^*(\zeta_1, \tau)(b^{+2} - \zeta_1^2)} d\zeta_1] \\ &\quad + (b^{+2} - \zeta^2) \int_{\zeta_1=b^-}^{b^+} \frac{1}{\chi^*(\zeta_1, \tau)(b^{+2} - \zeta_1^2)(\zeta_1^2 - \zeta^2)} d\zeta_1] \\ &\quad + \tan \beta \cdot [- \int_{\zeta_1=b^-}^{b^+} \frac{\zeta_1}{\chi^*(\zeta_1, \tau)(b^{+2} - \zeta_1^2)} d\zeta_1 \\ &\quad + (b^{+2} - \zeta^2) \int_{\zeta_1=b^-}^{b^+} \frac{\zeta_1}{\chi^*(\zeta_1, \tau)(b^{+2} - \zeta_1^2)(\zeta_1^2 - \zeta^2)} d\zeta_1] \} \end{aligned} \quad (\text{B.24})$$

When $\zeta \rightarrow b^+$, the vortex strength $\gamma_c^*(\zeta, \tau)$ must be bounded. This requirement results in the displacement continuity condition:

$$0 = (\tau + \tan \beta) \cdot \int_{\zeta_1=b^-}^{b^+} \frac{d\zeta_1}{\chi^*(\zeta_1, \tau)(b^{+2} - \zeta_1^2)} - \tan \beta \int_{\zeta_1=b^-}^{b^+} \frac{\zeta_1}{\chi^*(\zeta_1, \tau)(b^{+2} - \zeta_1^2)} d\zeta_1 \quad (\text{B.25})$$

Define the following notations:

$$I_1 = \int_{\zeta_1=b^-}^{b^+} \frac{d\zeta_1}{\chi^*(\zeta_1, \tau)(b^{+2} - \zeta_1^2)} \quad (\text{B.26})$$

$$I_2 = \int_{\zeta_1=b^-}^{b^+} \frac{\zeta_1}{\chi^*(\zeta_1, \tau)(b^{+2} - \zeta_1^2)} d\zeta_1 \quad (\text{B.27})$$

The displacement continuity condition then can be expressed in terms of I_1 and I_2 as:

$$0 = (\tau + \tan \beta) \cdot I_1 - \tan \beta \cdot I_2 \quad (\text{B.28})$$

(B.28) could be re-written in a transient draft form as in following (B.29), which provides an additional condition solving for the unknowns in the steady planing problem defined in Chapter 2.7 and a necessary equation for solving the seaway dynamics problem (seakeeping) at each time step.

$$\tau = \tan \beta \cdot \left[\frac{I_2}{I_1} - 1 \right] \quad (\text{B.29})$$

B.4 Integrals In Displacement Continuity Condition

The integrals in (B.29) can be transformed into an easy-calculated semi-analytical form.

B.4.1 Integral I_1

Substituting the kernel function in Eq.(B.15) into I_1 ,

$$\begin{aligned}
 I_1 &= \int_{\zeta_1=b^-}^{b^+} \frac{d\zeta_1}{\mathcal{X}^*(\zeta_1, \tau)(b^{+2} - \zeta_1^2)} \\
 &= \int_{\zeta_1=b^-}^{b^+} (\zeta_1^2 - b^{-2})^{\frac{1+\tilde{\beta}}{2}\pi} ((b^+)^2 - \zeta_1^2)^{-\frac{1-\tilde{\beta}}{2}\pi} d\zeta_1
 \end{aligned} \tag{B.30}$$

Defining variable transform $t = \zeta_1^2$ in Eq.(B.30), $d\zeta_1 = \frac{1}{2} \frac{dt}{\sqrt{t}}$,

$$I_1 = \frac{1}{2} \cdot \int_{t=b^{-2}}^{b^{+2}} t^{-\frac{1}{2}} (t - b^{-2})^{\frac{1+\tilde{\beta}}{2}\pi} (b^{+2} - t)^{-\frac{1-\tilde{\beta}}{2}\pi} dt \tag{B.31}$$

Define the transformation $x = t - (b^-)^2$, $dx = dt$. Then Eq.(B.31) becomes:

$$I_1 = \frac{1}{2} \cdot \int_{x=0}^{b^{+2}-b^{-2}} (x + b^{-2})^{-\frac{1}{2}} x^{\frac{1+\tilde{\beta}}{2}\pi} (b^{+2} - b^{-2} - x)^{-\frac{1-\tilde{\beta}}{2}\pi} dx \tag{B.32}$$

From Gradshteyn and Ryzhik (1965), p287, §3.197, Eq.(8):

$$\int_0^u x^{\nu-1} (x + \alpha)^\lambda (u - x)^{\mu-1} dx = \alpha^\lambda u^{\mu+\nu-1} B(\mu, \nu) \cdot {}_2F_1(-\lambda, \nu; \mu + \nu; -\frac{u}{\alpha}) \tag{B.33}$$

where $\left| \arg\left(\frac{u}{\alpha}\right) \right| < \pi$, $\operatorname{Re} \mu > 0$, $\operatorname{Re} \nu > 0$. Compare with Eq.(B.32) where,

$$\alpha = b^{-2}, u = b^{+2} - b^{-2}, \mu = 1 - \frac{1}{2} - \frac{\tilde{\beta}}{\pi} = \frac{1}{2} - \frac{\tilde{\beta}}{\pi}, \nu = \frac{3}{2} + \frac{\tilde{\beta}}{\pi}, \lambda = -\frac{1}{2}.$$

Thus:

$$\begin{aligned} I_1 &= \int_{\zeta_1=b^-}^{b^+} \frac{d\zeta_1}{\chi^*(\zeta_1, \tau)(b^{+2} - \zeta_1^2)} \\ &= \frac{1}{2} \frac{(b^+)^2 - (b^-)^2}{b^-} \cdot B\left(\frac{1}{2} - \frac{\tilde{\beta}}{\pi}, \frac{3}{2} + \frac{\tilde{\beta}}{\pi}\right) \cdot {}_2F_1\left(\frac{1}{2}; \frac{3}{2} + \frac{\tilde{\beta}}{\pi}; 2; -\frac{(b^+)^2 - (b^-)^2}{(b^-)^2}\right) \end{aligned} \quad (\text{B.34})$$

where $B(\mu, \nu)$ is the Beta function, and ${}_2F_1(\alpha, \beta; \gamma; z) = F(\alpha, \beta; \gamma; z)$ is Gauss' hypergeometric function.

Gradshteyn and Ryzhik (1965), P1043, §9.131, Eq.(1) provides an integral transform for the hypergeometric function:

$$F(\alpha, \beta, \gamma; z) = (1-z)^{-\alpha} F\left(\alpha, \gamma - \beta, \gamma; \frac{z}{z-1}\right) \quad (\text{B.35})$$

Compare with Eq.(B.34), the correspondent parameters are:

$$\gamma - \beta = 2 - \left(\frac{3}{2} + \frac{\tilde{\beta}}{\pi}\right) = \frac{1}{2} - \frac{\tilde{\beta}}{\pi}, \quad \frac{z}{z-1} = \frac{b^{+2} - b^{-2}}{b^{+2}} = 1 - \frac{b^{-2}}{b^{+2}}.$$

Therefore,

$$F_1\left(\frac{1}{2}; \frac{3}{2} + \frac{\tilde{\beta}}{\pi}; 2; -\frac{(b^+)^2 - (b^-)^2}{(b^-)^2}\right) = \frac{b^-}{b^+} F\left(\frac{1}{2}, \frac{1}{2} - \frac{\tilde{\beta}}{\pi}, 2; \frac{b^{+2} - b^{-2}}{b^{+2}}\right) \quad (\text{B.36})$$

Thus the integration I_1 will be,

$$I_1 = \frac{1}{2} \frac{b^{+2} - (b^-)^2}{b^+} \cdot B\left(\frac{1}{2} - \frac{\tilde{\beta}}{\pi}, \frac{3}{2} + \frac{\tilde{\beta}}{\pi}\right) \cdot F\left(\frac{1}{2}, \frac{1}{2} - \frac{\tilde{\beta}}{\pi}, 2; \frac{b^{+2} - (b^-)^2}{b^{+2}}\right) \quad (\text{B.37})$$

B.4.2 Integral I_2

Substituting the expression of $\chi^*(\zeta, \tau)$ into I_2 ,

$$\begin{aligned} I_2 &= \int_{\zeta_1=b^-}^{b^+} \frac{\zeta_1}{\chi^*(\zeta_1, \tau)(b^{+2} - \zeta_1^2)} d\zeta_1 \\ &= \int_{\zeta_1=b^-}^{b^+} (\zeta_1^2 - b^{-2})^{\frac{1}{2} + \frac{\tilde{\beta}}{\pi}} (b^{+2} - \zeta_1^2)^{-\frac{1}{2} - \frac{\tilde{\beta}}{\pi}} \zeta_1 d\zeta_1 \end{aligned} \quad (\text{B.38})$$

Defining variable transformation $t = \zeta_1^2$, $d\zeta_1 = \frac{1}{2} \frac{dt}{\sqrt{t}}$ in Eq.(B.38):

$$\begin{aligned} I_2 &= \int_{\zeta_1=b^-}^{b^+} (\zeta_1^2 - b^{-2})^{\frac{1}{2} + \frac{\tilde{\beta}}{\pi}} ((b^+)^2 - \zeta_1^2)^{-\frac{1}{2} - \frac{\tilde{\beta}}{\pi}} \zeta_1 d\zeta_1 \\ &= \frac{1}{2} \cdot \int_{t=b^{-2}}^{b^{+2}} (t - b^{-2})^{\frac{1}{2} + \frac{\tilde{\beta}}{\pi}} (b^{+2} - t)^{-\frac{1}{2} - \frac{\tilde{\beta}}{\pi}} dt \end{aligned} \quad (\text{B.39})$$

Again define the transformation $x = t - b^{-2}$, $dx = dt$. Then Eq.(B.39) becomes,

$$I_2 = \frac{1}{2} \cdot \int_{x=0}^{b^{+2}-b^{-2}} x^{\frac{1}{2}+\frac{\tilde{\beta}}{\pi}} (b^{+2} - b^{-2} - x)^{-\frac{1}{2}-\frac{\tilde{\beta}}{\pi}} dx \quad (\text{B.40})$$

From Gradshteyn and Ryzhik (1965), p284, §3.191, Eq.(1) :

$$\int_0^u x^{\nu-1} (u-x)^{\mu-1} dx = u^{\mu+\nu-1} B(\mu, \nu) \quad (\text{B.41})$$

where $\text{Re } \mu > 0$, $\text{Re } \nu > 0$. Compare with Eq.(B.40), where,

$$u = b^{+2} - b^{-2}, \quad \mu = 1 - \frac{1}{2} - \frac{\tilde{\beta}}{\pi} = \frac{1}{2} - \frac{\tilde{\beta}}{\pi}, \quad \nu = \frac{3}{2} + \frac{\tilde{\beta}}{\pi}.$$

Thus:

$$\begin{aligned} I_2 &= \int_{\zeta_1=b^-}^{b^+} \frac{\zeta_1 \cdot d\zeta_1}{\chi^*(\zeta_1, \tau)(b^{+2} - \zeta_1^2)} \\ &= \frac{1}{2} (b^{+2} - (b^-)^2) \cdot B\left(\frac{1}{2} - \frac{\tilde{\beta}}{\pi}, \frac{3}{2} + \frac{\tilde{\beta}}{\pi}\right) \end{aligned} \quad (\text{B.42})$$

where $B(\mu, \nu)$ is the Beta function.

In this appendix, a necessary condition: displacement continuity condition in (B.29) has been derived for solving the five unknowns in the chine-wetted flow phase.

APPENDIX C

PRESSURE CONTINUITY CONDITION FOR STEADY PLANING

C.1 Surface Pressure Distribution

As described in Chapter 2, the solution of the time-dependent impact problem can be used for the solution of steady planing (x -problem). This appendix develops the correspondent pressure distribution in steady planing in the impact (time) space.

Assuming the boat is advancing in with a constant forward speed U , the impact velocity V can be obtained from Eq. (2.19). Bernoulli's equation gives the dynamic boundary condition of the impact problem:

$$p + \frac{1}{2} \rho (V_n^2 + V_s^2) + \rho \varphi_t = p_\infty + \frac{1}{2} \rho V^2 \quad z_b^- \leq z \leq z_b^+ \quad (\text{C.1})$$

where the definition of V_n , V_s are given in Appendix A. With τ representing non-dimensional time and ζ representing non-dimensional z-distance, the non-dimensional pressure is,

$$C_p(\zeta, \tau) = \frac{p - p_\infty}{1/2 \rho V^2} = 1 - V_n^2 - V_s^2 - 2 \frac{\partial \phi}{\partial \tau}(\zeta, \tau) \quad b^- \leq \zeta \leq b^+ \quad (\text{C.2})$$

The relation of velocity potential $\phi(\zeta, \tau)$ with the velocity (V_n, V_s) is defined as,

$$\begin{cases} \frac{\partial \phi}{\partial n}(\zeta, \tau) = V_n(\zeta, \tau) \\ \frac{\partial \phi}{\partial \zeta}(\zeta, \tau) = V_s(\zeta, \tau) \end{cases} \quad (\text{C.3})$$

Define $\phi(b^+, \tau) = 0$ at the jet-head. Thus the potential is therefore defined in the region of $1 \leq \zeta \leq b^+$ as,

$$\phi(\zeta, \tau) = - \int_{\zeta}^{b^+(\tau)} V_s(\zeta_0, \tau) d\zeta_0 \quad 1 \leq \zeta \leq b^+ \quad (\text{C.4})$$

Define the following catamaran transform variables:

$$s(\tau) = \frac{\zeta - 1}{z_c(\tau) - 1}, \quad s^-(\tau) = \frac{b^- - 1}{z_c(\tau) - 1}, \quad s^+(\tau) = \frac{b^+ - 1}{z_c(\tau) - 1} \quad (\text{C.5})$$

By using these transforms, the solution domain will have a new coordinate system shown in Fig. 3.3. In this new coordinate system the potential is:

$$\phi(\zeta, \tau) = -(z_c - 1) \int_{s(\tau)}^{s^+(\tau)} V_s(s_0, \tau) ds_0 \quad (\text{C.6})$$

In the region of $0 \leq s \leq s^+$, the $\partial\phi/\partial\tau$ term will be,

$$\begin{aligned} -\frac{\partial\phi(s, \tau)}{\partial\tau} &= \frac{\partial z_c}{\partial\tau} \left[\int_{s(\tau)}^{s^+(\tau)} V_s(s_0, \tau) ds_0 + V_s(s, \tau) \cdot s \right] \\ &+ (z_c - 1) \left[V_s(s^+, \tau) \frac{ds^+}{d\tau} + \int_{s(\tau)}^{s^+(\tau)} \frac{\partial V_s}{\partial\tau}(s_0, \tau) ds_0 \right] \end{aligned} \quad 0 \leq s \leq s^+ \quad (\text{C.7})$$

where $\frac{ds(\tau)}{d\tau} = -\frac{s}{z_c(\tau) - 1} \cdot \frac{\partial z_c}{\partial\tau}$ has been used in the derivation. In the region of

$s^- \leq s \leq 0$, the similar form of $\partial\phi/\partial\tau$ is,

$$\begin{aligned} -\frac{\partial\phi(s, \tau)}{\partial\tau} &= \frac{\partial z_c}{\partial\tau} \left[\int_{s(\tau)}^{s^-(\tau)} V_s(s_0, \tau) ds_0 + V_s(s, \tau) \cdot s \right] \\ &+ (z_c - 1) \left[V_s(s^-, \tau) \frac{ds^-}{d\tau} + \int_{s(\tau)}^{s^-(\tau)} \frac{\partial V_s}{\partial\tau}(s_0, \tau) ds_0 \right] \end{aligned} \quad s^- \leq s \leq 0 \quad (\text{C.8})$$

Using the new variables, the pressure coefficient, (C.2), is,

$$C_p(s, \tau) = 1 - V_n^2 - V_s^2 - 2 \frac{\partial\phi}{\partial\tau}(s, \tau) \quad s^- \leq s \leq s^+ \quad (\text{C.9})$$

Substituting the $\partial\phi/\partial\tau$ term in Eq.(C.7) into the Eq.(C.9), we have the pressure distribution in the region of $0 \leq s \leq s^+$,

$$\begin{aligned}
C_p(s, \tau) &= 1 - V_n^2(s, \tau) - V_s^2(s, \tau) \\
&+ 2 \frac{\partial z_c}{\partial \tau} \left[\int_{s(\tau)}^{s^+(\tau)} V_s(s_0, \tau) ds_0 + V_s(s, \tau) \cdot s \right] \\
&+ 2(z_c - 1) \left[V_s(s^+, \tau) \frac{ds^+}{d\tau} + \int_{s(\tau)}^{s^+(\tau)} \frac{\partial V_s}{\partial \tau}(s_0, \tau) ds_0 \right]
\end{aligned} \quad 0 \leq s \leq s^+ \quad (\text{C.10})$$

Similarly, in the region $s^- \leq s \leq 0$,

$$\begin{aligned}
C_p(s, \tau) &= 1 - V_n^2(s, \tau) - V_s^2(s, \tau) \\
&+ 2 \frac{\partial z_c}{\partial \tau} \left[\int_{s(\tau)}^{s^-(\tau)} V_s(s_0, \tau) ds_0 + V_s(s, \tau) \cdot s \right] \\
&+ 2(z_c - 1) \left[V_s(s^-, \tau) \frac{ds^-}{d\tau} + \int_{s(\tau)}^{s^-(\tau)} \frac{\partial V_s}{\partial \tau}(s_0, \tau) ds_0 \right]
\end{aligned} \quad s^- \leq s \leq 0 \quad (\text{C.11})$$

C.2 Pressure Continuity Condition

At the jet head z_b^+ , the dynamic condition is $C_p(s^+, \tau) = 0$ (refer to Fig. 2.6).

Eq.(C.10) gives,

$$b_\tau^+(\tau) = \frac{V_s^2(s^+, \tau) + V_n^2(s^+, \tau) - 1}{2V_s(s^+, \tau)} \quad \text{at } s = s^+ \quad (\text{C.12})$$

Recall that in the chine un-wetted case $V_n(s^+, \tau) = 0$ and in the chine wetted case $V_n(s^+, \tau) = 1$ (Fig. 2.6), thus the pressure continuity condition at $s = s^+$ is,

- In the chine un-wetted phase

$$b_\tau^+(\tau) = \frac{V_s^2(s^+, \tau) - 1}{2V_s(s^+, \tau)} \quad \text{at } s = s^+ \quad (\text{C.13})$$

- In the chine wetted phase

$$b_\tau^+(\tau) = \frac{1}{2}V_s(s^+, \tau) \quad \text{at } s = s^+ \quad (\text{C.14})$$

Similarly, at the jet head z_b^- , $C_p(s^-, \tau) = 0$, Eq.(C.11) gives,

$$b_\tau^-(\tau) = \frac{V_s^2(s^-, \tau) + V_n^2(s^-, \tau) - 1}{2V_s(s^-, \tau)} \quad \text{at } s = s^- \quad (\text{C.15})$$

Recall that in Fig. 2.6 the keel at z_k is always in the chine-wetted phase, and

$V_n(s^-, \tau) = 1$, thus the pressure continuity condition at $s = s^-$ will be,

$$b_\tau^-(\tau) = \frac{1}{2}V_s(s^-, \tau) \quad \text{at } s = s^- \quad (\text{C.16})$$

Therefore we have two pressure continuity conditions in both the chine unwetted and chine wetted phases.

C.3 Euler's Equation

In the dynamic condition, $C_p(s, \tau) = 0$ in the regions of $s^- \leq s \leq 0$ and $1 \leq s \leq s^+$, differentiation of Eq. (C.9) gives,

$$\frac{\partial C_p}{\partial s}(s, \tau) = -2V_s(s, \tau) \frac{\partial V_s}{\partial s} - 2 \frac{\partial^2 \phi}{\partial \tau \partial s}(s, \tau) = 0 \quad 1 \leq s \leq s^+ \quad (\text{C.17})$$

Differentiation of Eq. (C.7) gives,

$$\begin{aligned} \frac{\partial^2 \phi(z, \tau)}{\partial s \partial \tau} &= -\left\{ \frac{\partial z_c}{\partial \tau} [-V_s(s, \tau) + V_s(s, \tau) + s \frac{\partial V_s}{\partial s}] - (z_c - 1) \frac{\partial V_s}{\partial \tau}(s, \tau) \right\} \\ &= -\left\{ \frac{\partial z_c}{\partial \tau} [s \frac{\partial V_s}{\partial s}] + (1 - z_c) \frac{\partial V_s}{\partial \tau}(s, \tau) \right\} \end{aligned} \quad 1 \leq s \leq s^+ \quad (\text{C.18})$$

Substituting (C.18) back into Eq.(C.17), an Euler equation results (refer to Vorus 1996):

$$[V_s(s, \tau) - \frac{\partial z_c}{\partial \tau} s] \frac{\partial V_s}{\partial s} - (1 - z_c) \frac{\partial V_s}{\partial \tau}(s, \tau) = 0 \quad 1 \leq s \leq s^+ \quad (\text{C.19})$$

This is the one-dimensional inviscid Burger's differential equation that the free vortex distribution on the jet-head sheet must satisfy.

Similarly, in the region of $s^- \leq s \leq 0$, the Burger's equation is ,

$$[V_s(s, \tau) - \frac{\partial z_c}{\partial \tau} s] \frac{\partial V_s}{\partial s} - (1 - z_c) \frac{\partial V_s}{\partial \tau}(s, \tau) = 0 \quad s^- \leq s \leq 0 \quad (\text{C.20})$$

C.4 Pressure Distribution Formulae

The pressure distribution on the hull contour $0 \leq s \leq 1$ can be obtained from Eq.(C.10). To find the pressure expression, first we need to deal with the $\frac{\partial V_s}{\partial \tau}$ term in (C.10). The expression of the velocity time derivative term can be found from Eq.(C.20),

$$\frac{\partial V_s}{\partial \tau}(s, \tau) = \frac{1}{1 - z_c} (V_s - \frac{\partial z_c}{\partial \tau} s) \frac{\partial V_s}{\partial s} \quad 1 \leq s \leq s^+ \quad (\text{C.21})$$

Re-formatting Eq.(C.10) yields,

$$\begin{aligned} C_p(s, \tau) = 1 - V_n^2 - V_s^2(s, \tau) + 2 \frac{\partial z_c}{\partial \tau} [- \int_{s^+(\tau)}^1 V_s(s_0, \tau) ds_0 - \int_1^s V_s(s_0, \tau) ds_0 + s \cdot V_s(s, \tau)] \\ + 2(1 - z_c) [\int_{s^+(\tau)}^1 \frac{\partial V_s}{\partial \tau}(s_0, \tau) ds_0 + \int_1^s \frac{\partial V_s}{\partial \tau}(s_0, \tau) ds_0 - V_s(s^+, \tau) \frac{ds^+}{d\tau}] \end{aligned}$$

$$0 \leq s \leq 1 \quad (\text{C.22})$$

Defining terms associated with the jet head as T,

$$T = -2 \frac{\partial z_c}{\partial \tau} \int_{s^+(\tau)}^1 V_s(s_0, \tau) ds_0 + 2(1 - z_c) \left[\int_{s^+(\tau)}^1 \frac{\partial V_s}{\partial \tau}(s_0, \tau) ds_0 - V_s(s^+, \tau) \frac{ds^+}{d\tau} \right] \quad (\text{C.23})$$

The pressure in (C.22) then can be written:

$$C_p(s, \tau) = 1 - V_n^2 - V_s^2(s, \tau) + 2 \frac{\partial z_c}{\partial \tau} \left[- \int_1^s V_s(s_0, \tau) ds_0 + s(z, \tau) V_s(s, \tau) \right] \quad 0 \leq s \leq 1 \quad (\text{C.24})$$

$$+ 2(1 - z_c) \int_1^s \frac{\partial V_s}{\partial \tau}(s_0, \tau) ds_0 + T$$

On the jet head $1 \leq s \leq s^+$, we substitute the $\frac{\partial V_s}{\partial \tau}$ term expression of Eq.(C.21) into

Eq.(C.23) to simplify the expression in T:

$$\int_{s^+(\tau)}^1 \frac{\partial V_s}{\partial \tau}(s_0, \tau) ds_0 = \frac{1}{1 - z_c} \left\{ \frac{1}{2} V_s^2(1, \tau) - \frac{1}{2} V_s^2(s^+, \tau) - \frac{\partial z_c}{\partial \tau} [V_s(1, \tau) - s^+ V_s(s^+, \tau) - \int_{s^+(\tau)}^1 V_s ds] \right\} \quad (\text{C.25})$$

Therefore, the T term in Eq.(C.23) can be expressed as:

$$T = V_s^2(1, \tau) - V_s^2(s^+, \tau) - 2 \frac{\partial z_c}{\partial \tau} V_s(1, \tau) + 2 \frac{\partial z_c}{\partial \tau} s^+ V_s(s^+, \tau) - 2(1 - z_c) V_s(s^+, \tau) \frac{ds^+}{d\tau} \quad (\text{C.26})$$

To find the pressure distribution on the hull contour $0 \leq s \leq 1$, substituting Eq.(C.26) back into the pressure expression in Eq.(C.24),

$$\begin{aligned}
C_p(s, \tau) = & 1 - V_n^2 - V_s^2(s, \tau) + 2 \frac{\partial z_c}{\partial \tau} \left[- \int_1^s V_s(s_0, \tau) ds_0 + s(z, \tau) V_s(s, \tau) \right] \\
& + 2(1 - z_c) \int_1^s \frac{\partial V_s}{\partial \tau}(s_0, \tau) ds_0 + V_s^2(1, \tau) \\
& - 2 \frac{\partial z_c}{\partial \tau} V_s(1, \tau) \\
& - V_s^2(s^+, \tau) + 2 \frac{\partial z_c}{\partial \tau} s^+ V_s(s^+, \tau) - 2(1 - z_c) V_s(s^+, \tau) \frac{ds^+}{d\tau}
\end{aligned} \tag{C.27}$$

The jet head terms in (C.27) can be simplified. Considering Eq.(C.10), in the regions of $1 \leq s \leq s^+$, with $C_p(s^+, \tau) = 0$ (Fig. 2.6) gives,

$$1 - V_n^2(s^+, \tau) - V_s^2(s^+, \tau) + 2 \frac{\partial z_c}{\partial \tau} s^+ V_s(s^+, \tau) - 2(1 - z_c) V_s(s^+, \tau) \frac{ds^+}{d\tau} = 0 \tag{C.28}$$

Substituting above equation into the pressure expression in Eq.(C.27) gives the pressure distribution:

$$\begin{aligned}
C_p(s, \tau) = & 1 - V_n^2 - V_s^2(s, \tau) + 2 \frac{\partial z_c}{\partial \tau} \left[- \int_1^s V_s(s_0, \tau) ds_0 + s \cdot V_s(s, \tau) \right] \\
& + 2(1 - z_c) \int_1^s \frac{\partial V_s}{\partial \tau}(s_0, \tau) ds_0 + V_s^2(1, \tau) - 2 \frac{\partial z_c}{\partial \tau} V_s(1, \tau) \\
& + V_n^2(s^+, \tau) - 1
\end{aligned} \tag{C.29}$$

- **In chine wetted case,** $V_n(s^+, \tau) = 1$

$$\begin{aligned}
 C_p(s, \tau) &= 1 - V_s^2(s, \tau) + V_s^2(1, \tau) \\
 &\quad - 2 \frac{\partial z_c}{\partial \tau} \left[\int_1^s V_s(s_0, \tau) ds_0 + V_s(1, \tau) - s \cdot V_s(s, \tau) \right] \quad 0 \leq s \leq 1 \quad (\text{C.30}) \\
 &\quad + 2(1 - z_c) \int_1^s \frac{\partial V_s}{\partial \tau}(s_0, \tau) ds_0
 \end{aligned}$$

- **In chine un-wetted case,** $V_n(s^+, \tau) = 0$, pressure distribution is,

$$\begin{aligned}
 C_p(s, \tau) &= V_s^2(1, \tau) - V_s^2(s, \tau) \\
 &\quad - 2 \frac{\partial z_c}{\partial \tau} \left[\int_1^s V_s(s_0, \tau) ds_0 + V_s(1, \tau) - s \cdot V_s(s, \tau) \right] \quad 0 \leq s \leq 1 \quad (\text{C.31}) \\
 &\quad + 2(1 - z_c) \int_1^s \frac{\partial V_s}{\partial \tau}(s_0, \tau) ds_0
 \end{aligned}$$

(C.30) and (C.31) are used to compute the pressure on the hull.

APPENDIX D

PRESSURE DISTRIBUTION AND EULER'S EQUATION IN SEAKEEPING

The pressure distribution in seakeeping is in the following form:

$$C_p(x, s; \tau) = V^2(x, \tau) - V_n^2(x, s, \tau) - V_s^2(x, s, \tau) - 2\left[\frac{\partial\phi(x, s; \tau)}{\partial\tau} + \frac{\partial\phi(x, s; \tau)}{\partial x}\right] - \left(\frac{\partial\phi(x, s; \tau)}{\partial x}\right)^2$$

$$0 \leq x \leq L(\tau), \quad 0 \leq s \leq s^+(x, \tau) \quad \text{or} \quad s^- \leq s \leq 0 \quad (\text{D.1})$$

The Euler's equation and the hull contour pressure distribution in seakeeping can be derived from (D.1).

D.1 Euler's Equation and Location of Free Vortices

The Euler's equation governing the free vortex distribution in seakeeping can be obtained from the differentiation of the pressure distribution equation (D.1). Considering the requirement of the dynamic boundary condition, $C_p = 0$ in the region of $1 \leq s \leq s^+(x, \tau)$ and $s^- \leq s \leq 0$ (Fig. 2.6), differentiation of the pressure distribution in Eq.(D.1) will give:

$$\begin{aligned} \frac{\partial C_P}{\partial s}(x, s, \tau) &= -2V_s(x, s, \tau) \frac{\partial V_s}{\partial s} - 2 \frac{\partial^2 \phi}{\partial \tau \partial s}(x, s, \tau) - 2 \frac{\partial^2 \phi}{\partial x \partial s}(x, s, \tau) - 2 \frac{\partial \phi}{\partial x} \cdot \frac{\partial^2 \phi}{\partial x \partial s}(x, s, \tau) \\ &= 0 \end{aligned}$$

$$0 \leq x \leq L(\tau), 1 \leq s \leq s^+(x, \tau) \text{ or } s^- \leq s \leq 0 \quad (\text{D.2})$$

The derivative terms in (D.2) can be found from the differentiation of potential.

Recall the potential definition in seakeeping:

$$\phi(\xi, s, \tau) = -z_k(\xi)(z_c - 1) \int_{s(\xi; \tau)}^{s^+(\xi, \tau)} V_s(\xi, s_0, \tau) ds_0 \quad 0 \leq s \leq s^+ \quad (\text{D.3})$$

where ξ is the non-dimensional x -coordinate, s is the non-dimensional z -coordinate, τ is the non-dimensional time.

Based on the potential definition in Eq.(D.3), the $\frac{\partial \phi}{\partial x}$ term in (D.1) has the

following form:

$$\begin{aligned} -\phi_x(\xi, s; \tau) &= z_k(\xi)(z_c - 1) \left[\int_{s(\xi; \tau)}^{s^+(\xi, \tau)} \frac{\partial V_s(\xi, s_0, \tau)}{\partial x} ds_0 + V_s(\xi, s^+, \tau) s_x^+ - V_s(\xi, s, \tau) s_x \right] \\ &\quad + [z_{k,x}(\xi)(z_c - 1)] \int_{s(\xi; \tau)}^{s^+(\xi, \tau)} V_s(\xi, s_0, \tau) ds_0 \\ &\quad + [z_k(\xi) z_{c,x}] \int_{s(\xi; \tau)}^{s^+(\xi, \tau)} V_s(\xi, s_0, \tau) ds_0 \end{aligned} \quad (\text{D.4})$$

Following the variable transformation in (4.70), $s_x = \frac{-(\zeta - 1)z_{c,x}}{[z_c(\zeta, \tau) - 1]^2} = -s \frac{z_{c,x}}{z_c(\zeta, \tau) - 1}$. The

$V_s \cdot s_x$ term in Eq.(D.4) becomes,

$$z_k(\xi)(z_c - 1)[-V_s(\xi, s, \tau)s_x] = [s \cdot z_k(\xi) \cdot z_{c,x}] \cdot V_s \quad (\text{D.5})$$

Substituting (D.5) back into (D.4) yields the ϕ_x term:

$$\begin{aligned} -\phi_x(\xi, s; \tau) &= z_k(\xi)(z_c - 1) \left[\int_{s(\xi; \tau)}^{s^+(\xi, \tau)} \frac{\partial V_s(\xi, s_0, \tau)}{\partial x} ds_0 + V_s(\xi, s^+, \tau)s_x^+ \right] \\ &\quad + z_{k,x}(\xi) [(z_c - 1) \int_{s(\xi; \tau)}^{s^+(\xi, \tau)} V_s(\xi, s_0, \tau) ds_0] \\ &\quad + z_k(\xi) z_{c,x} \left[\int_{s(\xi; \tau)}^{s^+(\xi, \tau)} V_s(\xi, s_0, \tau) ds_0 + s \cdot V_s(\xi, s; \tau) \right] \end{aligned} \quad (\text{D.6})$$

Similar to the derivation of the $\frac{\partial \phi}{\partial x}$ term, the $\frac{\partial \phi}{\partial \tau}$ term in (D.1) is:

$$\begin{aligned} -\frac{\partial \phi(\xi, s, \tau)}{\partial \tau} &= \frac{\partial}{\partial \tau} \left[z_k(z_c - 1) \int_{s(\xi; \tau)}^{s^+(\xi, \tau)} V_s(\xi, s_0, \tau) ds_0 \right] \\ &= z_k(z_c - 1) \left[\int_{s(\xi; \tau)}^{s^+(\xi, \tau)} \frac{\partial V_s}{\partial \tau}(\xi, s_0, \tau) ds_0 + \int_{s(\xi; \tau)}^{s^+(\xi, \tau)} \frac{\partial V_s}{\partial \xi} \cdot \frac{\partial \xi}{\partial \tau} ds_0 \right] \\ &\quad + z_k(z_c - 1) \left[V_s(\xi, s^+, \tau) \frac{ds^+}{d\tau} - V_s(\xi, s, \tau) \frac{ds}{d\tau} \right] \\ &\quad + z_k \left[\frac{\partial z_c}{\partial \tau} + \frac{\partial z_c}{\partial \xi} \frac{\partial \xi}{\partial \tau} \right] \int_{s(\xi; \tau)}^{s^+(\xi, \tau)} V_s(\xi, s_0, \tau) ds_0 \end{aligned} \quad (\text{D.7})$$

Following the definition of ξ in (4.69), $\frac{\partial}{\partial \xi} = \frac{\partial}{\partial x} L(\tau)$, $\xi_\tau = -x \frac{L_\tau}{L^2}$, therefore, the

derivative of the s – coordinates will be:

$$\begin{aligned}
 \frac{ds[\xi(\tau), \tau]}{d\tau} &= -\frac{(\zeta - 1)}{(z_c(\tau) - 1)^2} \left[\frac{\partial z_c}{\partial \tau} + \frac{\partial z_c}{\partial \xi} \frac{\partial \xi}{\partial \tau} \right] \\
 &= -\frac{(\zeta - 1)}{(z_c(\tau) - 1)^2} \left[\frac{\partial z_c}{\partial \tau} - \frac{\partial z_c}{\partial x} \cdot x \frac{L_\tau}{L} \right] \\
 &= -\frac{s}{z_c(\tau) - 1} \left[z_{c,\tau} - z_{c,x} \cdot x \frac{L_\tau}{L} \right]
 \end{aligned} \tag{D.8}$$

and,

$$\frac{ds^+[\xi(\tau), \tau]}{d\tau} = \frac{\partial s^+}{\partial \tau} + \frac{\partial s^+}{\partial \xi} \frac{\partial \xi}{\partial \tau} = \frac{\partial s^+}{\partial \tau} - \frac{\partial s^+}{\partial x} \cdot x \frac{L_\tau}{L} \tag{D.9}$$

Substituting (D.8) and (D.9) into Eq.(D.7) yields the ϕ_τ term:

$$\begin{aligned}
 -\frac{\partial \phi(\xi, s, \tau)}{\partial \tau} &= z_k(z_c - 1) \left[\int_{s(\xi, \tau)}^{s^+(\xi, \tau)} \frac{\partial V_s}{\partial \tau}(\xi, s_0, \tau) ds_0 - x \frac{L_\tau}{L} \int_{s(\xi, \tau)}^{s^+(\xi, \tau)} \frac{\partial V_s}{\partial x}(x, s_0, \tau) ds_0 \right. \\
 &\quad \left. + V_s(\xi, s^+, \tau) \frac{\partial s^+}{\partial \tau} - V_s(\xi, s^+, \tau) \frac{\partial s^+}{\partial x} \cdot x \frac{L_\tau}{L} \right] \\
 &\quad + z_k z_{c,\tau} \left[\int_{s(\xi, \tau)}^{s^+(\xi, \tau)} V_s(\xi, s_0, \tau) ds_0 + s \cdot V_s(\xi, s, \tau) \right] \\
 &\quad - z_k z_{c,x} \cdot x \frac{L_\tau}{L} \left[\int_{s(\xi, \tau)}^{s^+(\xi, \tau)} V_s(\xi, s_0, \tau) ds_0 + s \cdot V_s(\xi, s, \tau) \right]
 \end{aligned}$$

$$0 \leq s \leq s^+ \tag{D.10}$$

Second time differentiation of the ϕ_x term in (D.6) with respect to s gives,

$$\begin{aligned}
-\frac{\partial^2 \phi(x, s; \tau)}{\partial s \partial x} &= z_k(\xi)(z_c - 1) \left[-\frac{\partial V_s(\xi, s, \tau)}{\partial x} \right] \\
&+ z_{k,x}(\xi) [-(z_c - 1)V_s(\xi, s, \tau)] \\
&+ z_k(\xi) z_{c,x} [-V_s(\xi, s, \tau) + V_s(\xi, s; \tau) + s \frac{\partial V_s(\xi, s, \tau)}{\partial s}] \\
&= +z_k(\xi)(1 - z_c) \frac{\partial V_s(\xi, s, \tau)}{\partial x} \\
&+ z_{k,x}(\xi)(1 - z_c)V_s(\xi, s, \tau) \\
&+ z_k(\xi) z_{c,x} \cdot s \frac{\partial V_s(\xi, s, \tau)}{\partial s}
\end{aligned} \tag{D.11}$$

and differentiation of the ϕ_τ term in (D.10) with respect to s ,

$$\begin{aligned}
-\frac{\partial^2 \phi(\xi, s, \tau)}{\partial s \partial \tau} &= z_k(z_c - 1) \left[-\frac{\partial V_s(\xi, s, \tau)}{\partial \tau} + x \frac{L_\tau}{L} \frac{\partial V_s(\xi, s, \tau)}{\partial x} \right] \\
&+ z_k z_{c,\tau} [-V_s(\xi, s, \tau) + V_s(\xi, s, \tau) + s \frac{\partial V_s}{\partial s}] \\
&- z_k z_{c,x} \cdot x \frac{L_\tau}{L} \cdot [-V_s(\xi, s, \tau) + V_s(\xi, s, \tau) + s \frac{\partial V_s}{\partial s}] \\
&= z_k(1 - z_c) \left[\frac{\partial V_s}{\partial \tau}(\xi, s, \tau) - x \frac{L_\tau}{L} \frac{\partial V_s}{\partial x} \right] + z_k z_{c,\tau} \cdot s \frac{\partial V_s}{\partial s} \\
&- z_k z_{c,x} \cdot x \frac{L_\tau}{L} \cdot [s \frac{\partial V_s}{\partial s}]
\end{aligned} \tag{D.12}$$

summing up (D.11) and (D.12) terms yields,

$$\begin{aligned}
& -\frac{\partial^2 \phi}{\partial \tau \partial s}(x, s, \tau) - \frac{\partial^2 \phi}{\partial x \partial s}(x, s, \tau) = \\
& = z_k(\xi)(1 - z_c) \left[\frac{\partial V_s}{\partial \tau}(\xi, s, \tau) + \left(1 - x \frac{L_\tau}{L}\right) \frac{\partial V_s(\xi, s, \tau)}{\partial x} \right] \\
& + z_k(\xi) \left[z_{c,\tau} + z_{c,x} \left(1 - x \frac{L_\tau}{L}\right) \right] s \frac{\partial V_s(\xi, s, \tau)}{\partial s} \\
& + z_{k,x}(\xi)(1 - z_c) V_s(\xi, s, \tau)
\end{aligned} \tag{D.13}$$

Substituting above equation into Eq.(D.2), and recall that $z_k(\xi) = 1$ in ζ plane, therefore

the (D.2) becomes:

$$\begin{aligned}
& -V_s(\xi, s, \tau) \frac{\partial V_s}{\partial s} + (1 - z_c) \left[\frac{\partial V_s}{\partial \tau}(\xi, s, \tau) + \left(1 - x \frac{L_\tau}{L}\right) \frac{\partial V_s(\xi, s, \tau)}{\partial x} \right] \\
& + \left[z_{c,\tau} + z_{c,x} \left(1 - x \frac{L_\tau}{L}\right) \right] s \frac{\partial V_s(\xi, s, \tau)}{\partial s} + z_{k,x}(\xi)(1 - z_c) V_s(\xi, s, \tau) \\
& = \frac{\partial \phi}{\partial x} \cdot \frac{\partial^2 \phi}{\partial x \partial s}(x, s, \tau)
\end{aligned} \tag{D.14}$$

Simplifying, (D.14) takes the following form,

$$\begin{aligned}
& -V_s(\xi, s, \tau) \frac{\partial V_s}{\partial s} - (z_c - 1) \left[\frac{\partial V_s}{\partial \tau}(\xi, s, \tau) + \left(1 - x \frac{L_\tau}{L}\right) \frac{\partial V_s(\xi, s, \tau)}{\partial x} \right] \\
& + \left[z_{c,\tau} + z_{c,x} \left(1 - x \frac{L_\tau}{L}\right) \right] s \frac{\partial V_s(\xi, s, \tau)}{\partial s} = g(\xi, s, \tau)
\end{aligned} \tag{D.15}$$

where $g(\xi, s, \tau)$ is the right-hand-side terms in (D.15).

If we ignore the higher order $g(\xi, s, \tau)$ term in (D.15), and assuming the keel offset is constant in axial direction, thus $z_k(\xi) = 1$ and $z_{k,x}(\xi) = 0$, the Euler's equation in (D.15) is,

$$\begin{aligned} \{[V_s(\xi, s, \tau) - [\frac{\partial z_c}{\partial \tau} s + \frac{\partial z_c}{\partial x} s(1 - x \frac{L_\tau}{L})]] \frac{\partial V_s}{\partial s} - (1 - z_c) \frac{\partial V_s}{\partial \tau}(\xi, s, \tau) \\ - (1 - z_c)(1 - x \frac{L_\tau}{L}) \frac{\partial V_s(\xi, s, \tau)}{\partial x} = 0 \end{aligned} \quad 1 \leq s \leq s^+ \quad (\text{D.16})$$

This is an inviscid Burger's differential equation that the free vortex distribution at the free jet-head sheet must satisfy.

Similarly, in the region of $s^- \leq s \leq 0$ the Burger's equation is,

$$\begin{aligned} \{[V_s(\xi, s, \tau) - [\frac{\partial z_c}{\partial \tau} s + \frac{\partial z_c}{\partial x} s(1 - x \frac{L_\tau}{L})]] \frac{\partial V_s}{\partial s} - (1 - z_c) \frac{\partial V_s}{\partial \tau}(\xi, s, \tau) - (1 - z_c)(1 - x \frac{L_\tau}{L}) \frac{\partial V_s(\xi, s, \tau)}{\partial x} = 0 \end{aligned} \quad s^- \leq s \leq 0 \quad (\text{D.17})$$

D.2 Pressure Distribution Formulae

The hull contour pressure distribution in seakeeping can be found from (D.1). Substituting the $\partial\phi/\partial\tau$ and $\partial\phi/\partial x$ terms into the Eq.(D.1), we have the pressure distribution in the region of $0 \leq s \leq s^+$,

$$\begin{aligned}
C_p(\xi, s; \tau) = & V^2(\xi, \tau) - V_n^2(\xi, s, \tau) - V_s^2(\xi, s, \tau) \\
& + 2z_k(z_c - 1) \left\{ \int_{s(\xi; \tau)}^{s^+(\xi; \tau)} \left[\frac{\partial V_s}{\partial \tau}(\xi, s_0, \tau) + (1-x) \frac{L_\tau}{L} \frac{\partial V_s(\xi, s_0, \tau)}{\partial x} \right] ds_0 \right. \\
& + V_s(\xi, s^+, \tau) \left[\frac{\partial s^+}{\partial \tau} + (1-x) \frac{L_\tau}{L} \frac{\partial s^+}{\partial x} \right] \\
& + 2z_k z_{c, \tau} \left[\int_{s(\xi; \tau)}^{s^+(\xi; \tau)} V_s(\xi, s_0, \tau) ds_0 + s \cdot V_s(\xi, s, \tau) \right] \\
& + 2z_k(\xi) z_{c, x} \left[(1-x) \frac{L_\tau}{L} \int_{s(\xi; \tau)}^{s^+(\xi; \tau)} V_s(\xi, s_0, \tau) ds_0 + (1-x) \frac{L_\tau}{L} s \cdot V_s(\xi, s; \tau) \right] \\
& + 2z_{k, x}(\xi) [(z_c - 1) \int_{s(\xi; \tau)}^{s^+(\xi; \tau)} V_s(\xi, s_0, \tau) ds_0] \\
& - \left(\frac{\partial \phi(x, s; \tau)}{\partial x} \right)^2 \\
& 0 \leq x \leq L(\tau), \quad 0 \leq s \leq s^+(\xi, \tau) \quad (D.18)
\end{aligned}$$

On the contour of the ship hull $0 \leq s \leq 1$, the pressure distribution can be found by grouping terms in (D.18). As in Appendix C, collecting the relevant terms associated with the jet head in the region of $1 \leq s \leq s^+$ in Eq.(D.18) as T :

$$\begin{aligned}
T = & 2(z_c - 1) \left\{ \left(\int_1^{s^+(\xi; \tau)} \left[\frac{\partial V_s}{\partial \tau}(\xi, s_0, \tau) + (1-x) \frac{L_\tau}{L} \frac{\partial V_s(\xi, s_0, \tau)}{\partial x} \right] ds_0 \right. \right. \\
& + V_s(\xi, s^+, \tau) \left[\frac{\partial s^+}{\partial \tau} + (1-x) \frac{L_\tau}{L} \frac{\partial s^+}{\partial x} \right] \\
& + 2z_{c, \tau} \left[\int_1^{s^+(\xi; \tau)} V_s(\xi, s_0, \tau) ds_0 \right] + 2z_{c, x} \left[(1-x) \frac{L_\tau}{L} \int_1^{s^+(\xi; \tau)} V_s(\xi, s_0, \tau) ds_0 \right] \\
& + 2z_{k, x}(\xi) [(z_c - 1) \int_1^{s^+(\xi; \tau)} V_s(\xi, s_0, \tau) ds_0] \\
& \left. \right\} \quad (D.19)
\end{aligned}$$

the pressure thus can be written:

$$\begin{aligned}
C_p(\xi, s; \tau) = & V^2(\xi, \tau) - V_n^2(\xi, s, \tau) - V_s^2(\xi, s, \tau) \\
& + 2(z_c - 1) \left\{ \int_{s(\xi, \tau)}^1 \left[\frac{\partial V_s}{\partial \tau}(\xi, s_0, \tau) + \left(1 - x \frac{L_\tau}{L}\right) \frac{\partial V_s(\xi, s_0, \tau)}{\partial x} \right] ds_0 \right\} \\
& + 2[z_{c,\tau} + z_{c,x} \left(1 - x \frac{L_\tau}{L}\right)] \left[\int_{s(\xi, \tau)}^1 V_s(\xi, s_0, \tau) ds_0 + s \cdot V_s(\xi, s, \tau) \right] \\
& + 2z_{k,x}(\xi) [(z_c - 1) \int_{s(\xi, \tau)}^1 V_s(\xi, s_0, \tau) ds_0] \\
& - \left(\frac{\partial \phi(x, s; \tau)}{\partial x} \right)^2 + T
\end{aligned}$$

(D.20)

To simplify the expression of T term in (D.20), first we need to solve for the velocity time derivative term in T term of (D.19) from Eq.(D.16):

$$\left[\frac{\partial V_s}{\partial \tau}(\xi, s, \tau) + \left(1 - x \frac{L_\tau}{L}\right) \frac{\partial V_s(\xi, s, \tau)}{\partial x} \right] = \frac{1}{1 - z_c} \left\{ [V_s(\xi, s, \tau) - \left[\frac{\partial z_c}{\partial \tau} s + \frac{\partial z_c}{\partial x} s \left(1 - x \frac{L_\tau}{L}\right) \right]] \frac{\partial V_s}{\partial s} \right.$$

(D.21)

On the jet head $1 \leq s \leq s^+$, substitute the Burger's equation in Eq.(D.21) into Eq.(D.19) to simplify the integral expression in T term:

$$\begin{aligned}
& \int_1^{s^+(\xi, \tau)} \left[\frac{\partial V_s}{\partial \tau}(\xi, s_0, \tau) + (1-x) \frac{L_\tau}{L} \frac{\partial V_s(\xi, s_0, \tau)}{\partial x} \right] ds_0 \\
&= \frac{1}{1-z_c} \int_1^{s^+(\xi, \tau)} \left\{ V_s(\xi, s, \tau) - \left[\frac{\partial z_c}{\partial \tau} s + \frac{\partial z_c}{\partial x} s \left(1-x \frac{L_\tau}{L}\right) \right] \right\} \frac{\partial V_s}{\partial s} ds \\
&= \frac{1}{1-z_c} \left\{ \frac{1}{2} V_s^2(\xi, s^+, \tau) - \frac{1}{2} V_s^2(\xi, 1, \tau) \right. \\
&\quad \left. - \left[\frac{\partial z_c}{\partial \tau} + \frac{\partial z_c}{\partial x} \left(1-x \frac{L_\tau}{L}\right) \right] \left[s^+ V_s(\xi, s^+, \tau) - V_s \xi, 1, \tau \right] - \int_1^{s^+} V_s(\xi, s, \tau) ds \right\}
\end{aligned} \tag{D.22}$$

Substituting (D.22) back into T term in Eq.(D.19):

$$\begin{aligned}
T &= -V_s^2(\xi, s^+, \tau) + V_s^2(\xi, 1, \tau) \\
&\quad + 2 \left[\frac{\partial z_c}{\partial \tau} + \frac{\partial z_c}{\partial x} \left(1-x \frac{L_\tau}{L}\right) \right] \left[s^+ V_s(\xi, s^+, \tau) - V_s(\xi, 1, \tau) - \int_1^{s^+} V_s(\xi, s, \tau) ds \right] \\
&\quad - 2(1-z_c) V_s(\xi, s^+, \tau) \left[\frac{\partial s^+}{\partial \tau} + \left(1-x \frac{L_\tau}{L}\right) \frac{\partial s^+}{\partial x} \right] \\
&\quad + 2 \left[z_{c,\tau} + z_{c,x} \left(1-x \frac{L_\tau}{L}\right) \right] \left[\int_1^{s^+(\xi, \tau)} V_s(\xi, s_0, \tau) ds_0 \right] \\
&= -V_s^2(\xi, s^+, \tau) + V_s^2(\xi, 1, \tau) \\
&\quad + 2 \left[\frac{\partial z_c}{\partial \tau} + \frac{\partial z_c}{\partial x} \left(1-x \frac{L_\tau}{L}\right) \right] \left[s^+ V_s(\xi, s^+, \tau) - V_s(\xi, 1, \tau) \right] \\
&\quad - 2(1-z_c) V_s(\xi, s^+, \tau) \left[\frac{\partial s^+}{\partial \tau} + \left(1-x \frac{L_\tau}{L}\right) \frac{\partial s^+}{\partial x} \right]
\end{aligned} \tag{D.23}$$

Substituting (D.23) into Eq.(D.20) and ignoring the higher order $(\partial\phi/\partial x)^2$ term give a computable pressure distribution formula:

$$\begin{aligned}
C_p(\xi, s; \tau) &= V^2(\xi, \tau) - V_n^2(\xi, s, \tau) - V_s^2(\xi, s, \tau) \\
&+ 2(z_c - 1) \left\{ \int_{s(\xi, \tau)}^1 \left[\frac{\partial V_s}{\partial \tau}(\xi, s_0, \tau) + (1 - x \frac{L_\tau}{L}) \frac{\partial V_s(\xi, s_0, \tau)}{\partial x} \right] ds_0 \right\} \\
&+ 2[z_{c, \tau} + z_{c, x} (1 - x \frac{L_\tau}{L})] \left[\int_{s(\xi, \tau)}^1 V_s(\xi, s_0, \tau) ds_0 + s \cdot V_s(\xi, s, \tau) \right] \\
&- V_s^2(\xi, s^+, \tau) + V_s^2(\xi, 1, \tau) \\
&+ 2 \left[\frac{\partial z_c}{\partial \tau} + \frac{\partial z_c}{\partial x} (1 - x \frac{L_\tau}{L}) \right] [s^+ V_s(\xi, s^+, \tau) - V_s(\xi, 1, \tau)] \\
&- 2(1 - z_c) V_s(\xi, s^+, \tau) \left[\frac{\partial s^+}{\partial \tau} + (1 - x \frac{L_\tau}{L}) \frac{\partial s^+}{\partial x} \right] \\
&= V^2(x, \tau) - V_n^2(x, s, \tau) - V_s^2(x, s, \tau) + V_s^2(\xi, 1, \tau) \\
&+ 2(z_c - 1) \left\{ \int_{s(\xi, \tau)}^1 \left[\frac{\partial V_s}{\partial \tau}(\xi, s_0, \tau) + (1 - x \frac{L_\tau}{L}) \frac{\partial V_s(\xi, s_0, \tau)}{\partial x} \right] ds_0 \right\} \\
&+ 2[z_{c, \tau} + z_{c, x} (1 - x \frac{L_\tau}{L})] \left[\int_{s(\xi, \tau)}^1 V_s(\xi, s_0, \tau) ds_0 + s \cdot V_s(\xi, s, \tau) - V_s(\xi, 1, \tau) \right] \\
&- V_s^2(\xi, s^+, \tau) + 2 \left[\frac{\partial z_c}{\partial \tau} + \frac{\partial z_c}{\partial x} (1 - x \frac{L_\tau}{L}) \right] [s^+ V_s(\xi, s^+, \tau)] \\
&+ 2(z_c - 1) V_s(\xi, s^+, \tau) \left[\frac{\partial s^+}{\partial \tau} + (1 - x \frac{L_\tau}{L}) \frac{\partial s^+}{\partial x} \right]
\end{aligned} \tag{D.24}$$

Consider the fact that, at the jet head z_b^+ , $C_p(\xi, s^+, \tau) = 0$, which results in:

$$\begin{aligned}
&V^2(\xi, \tau) - V_n^2(\xi, s^+, \tau) - V_s^2(\xi, s^+, \tau) \\
&+ 2z_k(z_c - 1) V_s(\xi, s^+, \tau) \left[\frac{\partial s^+}{\partial \tau} + (1 - x \frac{L_\tau}{L}) \frac{\partial s^+}{\partial x} \right] \\
&+ 2z_k [z_{c, \tau} + z_{c, x} (1 - x \frac{L_\tau}{L})] s^+ \cdot V_s(\xi, s^+, \tau) \\
&= 0
\end{aligned} \tag{D.25}$$

Substituting (D.25) into (D.24), we have the following hull pressure expression:

$$\begin{aligned}
C_p(\xi, s; \tau) &= V^2(\xi, \tau) - V_n^2(\xi, s, \tau) - V_s^2(\xi, s, \tau) + V_s^2(\xi, 1, \tau) \\
&\quad + 2(z_c - 1) \left\{ \int_{s(\xi, \tau)}^1 \left[\frac{\partial V_s}{\partial \tau}(\xi, s_0, \tau) + \left(1 - x \frac{L_\tau}{L}\right) \frac{\partial V_s(\xi, s_0, \tau)}{\partial x} \right] ds_0 \right\} \\
&\quad + 2[z_{c,\tau} + z_{c,x} \left(1 - x \frac{L_\tau}{L}\right)] \left[\int_{s(\xi, \tau)}^1 V_s(\xi, s_0, \tau) ds_0 + s \cdot V_s(\xi, s, \tau) - V_s(\xi, 1, \tau) \right] \\
&\quad + V_n^2(\xi, s^+, \tau) - V^2(\xi, \tau)
\end{aligned}$$

$$0 \leq x \leq L(\tau), \quad 0 \leq s \leq 1 \quad (\text{D.26})$$

- **In the chine wetted case where** $V_n(\xi, s^+, \tau) = V(\xi, \tau)$:

$$\begin{aligned}
C_p(\xi, s; \tau) &= V^2(\xi, \tau) - V_s^2(\xi, s, \tau) + V_s^2(\xi, 1, \tau) \\
&\quad + 2(z_c - 1) \left\{ \int_{s(\xi, \tau)}^1 \left[\frac{\partial V_s}{\partial \tau}(\xi, s_0, \tau) + \left(1 - x \frac{L_\tau}{L}\right) \frac{\partial V_s(\xi, s_0, \tau)}{\partial x} \right] ds_0 \right\} \\
&\quad + 2[z_{c,\tau} + z_{c,x} \left(1 - x \frac{L_\tau}{L}\right)] \left[\int_{s(\xi, \tau)}^1 V_s(\xi, s_0, \tau) ds_0 + s \cdot V_s(\xi, s, \tau) - V_s(\xi, 1, \tau) \right]
\end{aligned}$$

$$0 \leq x \leq L(\tau), \quad 0 \leq s \leq 1 \quad (\text{D.27})$$

where on the contour, $V_n(\xi, s, \tau) = 0$ in $0 \leq S \leq 1$.

- **In the chine un-wetted case where** $V_n(s^+, \tau) = 0$:

$$\begin{aligned}
C_p(\xi, s; \tau) &= V_s^2(\xi, 1, \tau) - V_s^2(\xi, s, \tau) \\
&\quad + 2(z_c - 1) \left\{ \int_{s(\xi, \tau)}^1 \left[\frac{\partial V_s}{\partial \tau}(\xi, s_0, \tau) + \left(1 - x \frac{L_\tau}{L}\right) \frac{\partial V_s(\xi, s_0, \tau)}{\partial x} \right] ds_0 \right\} \\
&\quad + 2[z_{c,\tau} + z_{c,x} \left(1 - x \frac{L_\tau}{L}\right)] \left[\int_{s(\xi, \tau)}^1 V_s(\xi, s_0, \tau) ds_0 + s \cdot V_s(\xi, s, \tau) - V_s(\xi, 1, \tau) \right]
\end{aligned}$$

$$0 \leq x \leq L(\tau), \quad 0 \leq s \leq 1 \quad (\text{D.28})$$

(D.27) and (D.28) are the final forms for the pressure distribution on the surface contour.

APPENDIX E

COMPUTATION OF BOUND VORTEX DISTRIBUTION $\gamma_c(\zeta, \tau)$

The singular bounded vortex distribution representation derived in Eq.(4.20) has two terms:

$$\gamma_c(\zeta, \tau) = \gamma_{normal}(\zeta, \tau) + \gamma_{singular}(\zeta, \tau) \quad (E.1)$$

The normal component is derived at (5.89) and the singular term (refer to (4.22)) can be expressed as the sum of three individual terms as in (5.92).

$$\gamma_{c,singular}(\zeta, \tau) = \gamma_c^0(\zeta, \tau) + \gamma_c^-(\zeta, \tau) + \gamma_c^+(\zeta, \tau) \quad (E.2)$$

The following section gives the details of the derivations of the computational forms of the three terms in (E.2).

E.1 Computation of $\gamma_c^0(\zeta, \tau)$

Substitute the integral $\Lambda(\zeta)$ in (5.49) into the formula of $\gamma_c^0(\zeta, \tau)$ in (5.93):

$$\begin{aligned}
\gamma_c^0(\zeta, \tau) &= \frac{4z}{\pi} \chi(\zeta, \tau) \cos^2 \tilde{\beta} \cdot \cos^2 \beta \cdot V(\tau) [-\Lambda(\zeta)] \\
&= -\frac{4\zeta}{\pi} \chi(\zeta, \tau) \cos^2 \tilde{\beta} \cdot \cos^2 \beta \cdot V(\tau) \times \\
&\quad \left[\frac{1}{2} z_c \cdot B_{11} \cdot F_{11} + \frac{1}{2} (\zeta^2 - z_c^2 - 1) \frac{1}{z_c} \cdot B_{11} \cdot F_{12} \right. \\
&\quad \left. - \frac{1}{2} (\zeta^2 - 1)(z_c^2 - \zeta^2) \times \sum_{j=1}^L \frac{1}{\sqrt{t_j}} \cdot \Delta I_{3,j}(\zeta) \right] \\
&= -\frac{2\zeta}{\pi} \chi(\zeta, \tau) \cos^2 \tilde{\beta} \cdot \cos^2 \beta \cdot V(\tau) \cdot z_c \cdot B_{11} \cdot F_{11} \\
&\quad - \frac{2\zeta}{\pi} \chi(\zeta, \tau) \cos^2 \tilde{\beta} \cdot \cos^2 \beta \cdot V(\tau) \cdot (\zeta^2 - z_c^2 - 1) \frac{1}{z_c} \cdot B_{11} \cdot F_{12} \\
&\quad + \frac{2\zeta}{\pi} \chi(\zeta, \tau) \cos^2 \tilde{\beta} \cdot \cos^2 \beta \cdot V(\tau) \cdot (\zeta^2 - 1)(z_c^2 - \zeta^2) \times \sum_{j=1}^L \frac{1}{\sqrt{t_j}} \cdot \Delta I_{3,j}(\zeta)
\end{aligned}$$

$1 \leq \zeta \leq z_c$ (E.3)

where B_{11} , F_{11} and F_{12} defined in (5.50), (5.51) and (5.52) respectively, the numerical integral $\Delta I_{3,j}(\zeta)$ in the above equation defined in (4.32), (4.34) and (4.36) according to the variation of the variable ζ .

E.2 Computation of $\gamma_c^-(\zeta, \tau)$

Substitute the integral (5.47) into the expression of $\gamma_c^-(\zeta, \tau)$ in (5.94):

$$\begin{aligned}
\gamma_c^-(\zeta, \tau) &= \frac{4\zeta}{\pi^2} \cos^2 \tilde{\beta} \cdot \chi(\zeta, \tau) \cdot \int_{b^-}^1 \gamma_s^-(\zeta_0, \tau) \frac{\zeta_0}{\zeta_0^2 - \zeta^2} d\zeta_0 [\Lambda^-(\zeta_0) - \Lambda(\zeta)] \\
&= \frac{4\zeta}{\pi^2} \cos^2 \tilde{\beta} \cdot \chi(\zeta, \tau) \cdot \int_{b^-}^1 \gamma_s^-(\zeta_0, \tau) \frac{\zeta_0}{\zeta_0^2 - \zeta^2} d\zeta_0 \times \\
&\quad \left[\frac{1}{2} (\zeta_0^2 - \zeta^2) \frac{1}{z_c} \cdot B_{11} \cdot F_{12} - \frac{1}{2} (\zeta_0^2 - 1) \times F_{21}(\zeta_0) \right. \\
&\quad \left. + \frac{1}{2} (\zeta^2 - 1) (z_c^2 - \zeta^2) \times \sum_{j=1}^L \frac{1}{\sqrt{t_j}} \cdot \Delta I_{3,j}(\zeta) \right] \\
&= \frac{2\zeta}{\pi^2} \cos^2 \tilde{\beta} \cdot \chi(\zeta, \tau) \cdot \frac{1}{z_c} \cdot B_{11} \cdot F_{12} \cdot \int_{b^-}^1 \gamma_s^-(\zeta_0, \tau) \zeta_0 d\zeta_0 \\
&\quad - \frac{2\zeta}{\pi^2} \cos^2 \tilde{\beta} \cdot \chi(\zeta, \tau) \cdot \int_{b^-}^1 \gamma_s^-(\zeta_0, \tau) \frac{\zeta_0}{\zeta_0^2 - \zeta^2} (\zeta_0^2 - 1) \times F_{21}(\zeta_0) d\zeta_0 \\
&\quad + \frac{2\zeta}{\pi^2} \cos^2 \tilde{\beta} \cdot \chi(\zeta, \tau) \cdot (\zeta^2 - 1) (z_c^2 - \zeta^2) \\
&\quad \times \sum_{j=1}^L \frac{1}{\sqrt{t_j}} \cdot \Delta I_{3,j}(\zeta) \cdot \int_{b^-}^1 \gamma_s^-(\zeta_0, \tau) \frac{\zeta_0}{\zeta_0^2 - \zeta^2} d\zeta_0
\end{aligned}$$

$$1 \leq \zeta \leq z_c \quad (\text{E.4})$$

where F_{21} is defined in (5.53). Again, discretizing the above integrals:

$$\begin{aligned}
\gamma_c^-(\zeta, \tau) &= \frac{2\zeta}{\pi^2} \cos^2 \tilde{\beta} \cdot \chi(\zeta, \tau) \cdot \frac{1}{z_c} \cdot B_{11} \cdot F_{12} \cdot \sum_{i=1}^{N_i^-(\tau)} \gamma_{S,i}^-(\tau) \int_{\zeta_i^-}^{\zeta_{i+1}^-} \zeta_0 d\zeta_0 \\
&\quad - \frac{2\zeta}{\pi^2} \cos^2 \tilde{\beta} \cdot \chi(\zeta, \tau) \cdot \sum_{i=1}^{N_i^-(\tau)} \gamma_{S,i}^-(\tau) \times F_{21}(\zeta_i^-) \cdot \int_{\zeta_i^-}^{\zeta_{i+1}^-} \frac{\zeta_0}{\zeta_0^2 - \zeta^2} (\zeta_0^2 - 1) d\zeta_0 \\
&\quad + \frac{2\zeta}{\pi^2} \cos^2 \tilde{\beta} \cdot \chi(\zeta, \tau) \cdot (\zeta^2 - 1) (z_c^2 - \zeta^2) \\
&\quad \times \sum_{j=1}^L \frac{1}{\sqrt{t_j}} \cdot \Delta I_{3,j}(\zeta) \cdot \sum_{i=1}^{N_i^-(\tau)} \gamma_{S,i}^-(\tau) \cdot \int_{\zeta_i^-}^{\zeta_{i+1}^-} \frac{\zeta_0}{\zeta_0^2 - \zeta^2} d\zeta_0
\end{aligned}$$

$$1 \leq \zeta \leq z_c \quad (\text{E.5})$$

The integral in the second term in the above equation can be written in as follows:

$$\begin{aligned}
\int_{\zeta_i^-}^{\zeta_{i+1}^-} \frac{\zeta_0}{\zeta_0^2 - \zeta^2} (\zeta_0^2 - 1) d\zeta_0 &= \int_{\zeta_i^-}^{\zeta_{i+1}^-} \frac{\zeta_0}{\zeta_0^2 - \zeta^2} (\zeta_0^2 - \zeta^2 + \zeta^2 - 1) d\zeta_0 \\
&= \int_{\zeta_i^-}^{\zeta_{i+1}^-} \zeta_0 d\zeta_0 + (\zeta^2 - 1) \int_{\zeta_i^-}^{\zeta_{i+1}^-} \frac{\zeta_0}{\zeta_0^2 - \zeta^2} d\zeta_0 \\
&= J_{11}(\zeta_i^-) + (\zeta^2 - 1) \cdot J_{12}(\zeta_i^-)
\end{aligned} \tag{E.6}$$

where the integral $J_{12}(\zeta_i^-)$ defined in (5.90) and,

$$J_{11}(\zeta_i^-) = \int_{\zeta_i^-}^{\zeta_{i+1}^-} \zeta_0 d\zeta_0 = \frac{1}{2} [(\zeta_{i+1}^-)^2 - (\zeta_i^-)^2] \tag{E.7}$$

Substituting the above integral, (E.6), and the relation of the free vortex strength $\gamma_{s,i}^-(\tau)$

with the induced velocity $V_s^-(i, \tau)$ ($\gamma_{s,i}^-(\tau) = -2V_s^-(i, \tau)$) into (E.5) yields the numerical

formula of $\gamma_c^-(\zeta, \tau)$:

$$\begin{aligned}
\gamma_c^-(\zeta, \tau) &= -\frac{2\zeta}{\pi^2} \cos^2 \tilde{\beta} \cdot \chi(\zeta, \tau) \cdot \frac{1}{z_c} \cdot B_{11} \cdot F_{12} \cdot \sum_{i=1}^{N_i^-(\tau)} 2 \cdot V_s^-(i, \tau) \cdot J_{11}(i) \\
&\quad + \frac{2\zeta}{\pi^2} \cos^2 \tilde{\beta} \cdot \chi(\zeta, \tau) \cdot \sum_{i=1}^{N_i^-(\tau)} 2 \cdot V_s^-(i, \tau) \times F_{21}(\zeta_i^-) \cdot [J_{11}(i) + (z^2 - 1)J_{12}(i)] \\
&\quad - \frac{2\zeta}{\pi^2} \cos^2 \tilde{\beta} \cdot \chi(\zeta, \tau) \cdot (\zeta^2 - 1)(z_c^2 - \zeta^2) \\
&\quad \times \sum_{j=1}^L \frac{1}{\sqrt{t_j}} \cdot \Delta I_{3,j}(\zeta) \cdot \sum_{i=1}^{N_i^-(\tau)} 2 \cdot V_s^-(i, \tau) \cdot J_{12}(i)
\end{aligned}$$

$$1 \leq \zeta \leq z_c \tag{E.8}$$

E.3 Computation of $\gamma_c^+(\zeta, \tau)$

Substitute the integral, Eq.(5.48), into the expression of $\gamma_c^+(\zeta, \tau)$ in (5.95):

$$\begin{aligned}
\gamma_c^+(\zeta, \tau) &= \frac{4\zeta}{\pi^2} \cos^2 \tilde{\beta} \cdot \chi(\zeta, \tau) \cdot \int_{z_c}^{b^+} \gamma_S^+(\zeta_0, \tau) \frac{\zeta_0}{\zeta_0^2 - \zeta^2} d\zeta_0 [\Lambda^+(\zeta_0) - \Lambda(\zeta)] \\
&= \frac{4\zeta}{\pi^2} \cos^2 \tilde{\beta} \cdot \chi(\zeta, \tau) \cdot \int_{z_c}^{b^+} \gamma_S^+(\zeta_0, \tau) \frac{\zeta_0}{\zeta_0^2 - \zeta^2} d\zeta_0 \times \\
&\quad \left[\frac{1}{2} (\zeta_0^2 - \zeta^2) \frac{1}{z_c} \cdot B_{11} \cdot F_{12} - \frac{1}{2} (z_c^2 - \zeta_0^2) \times F_{22}(\zeta_0) \right. \\
&\quad \left. + \frac{1}{2} (\zeta^2 - 1)(z_c^2 - \zeta^2) \times \sum_{j=1}^L \frac{1}{\sqrt{t_j}} \cdot \Delta I_{3,j}(\zeta) \right] \\
&= \frac{2\zeta}{\pi^2} \cos^2 \tilde{\beta} \cdot \chi(\zeta, \tau) \cdot \frac{1}{z_c} \cdot B_{11} \cdot F_{12} \cdot \int_{z_c}^{b^+} \gamma_S^+(\zeta_0, \tau) \zeta_0 d\zeta_0 \\
&\quad - \frac{2\zeta}{\pi^2} \cos^2 \tilde{\beta} \cdot \chi(\zeta, \tau) \cdot \int_{z_c}^{b^+} \gamma_S^+(\zeta_0, \tau) \frac{\zeta_0}{\zeta_0^2 - \zeta^2} (z_c^2 - \zeta_0^2) \times F_{22}(\zeta_0) d\zeta_0 \\
&\quad + \frac{2\zeta}{\pi^2} \cos^2 \tilde{\beta} \cdot \chi(\zeta, \tau) \cdot (\zeta^2 - 1)(z_c^2 - \zeta^2) \\
&\quad \times \sum_{j=1}^L \frac{1}{\sqrt{t_j}} \cdot \Delta I_{3,j}(\zeta) \cdot \int_{z_c}^{b^+} \gamma_S^+(\zeta_0, \tau) \frac{\zeta_0}{\zeta_0^2 - \zeta^2} d\zeta_0
\end{aligned}$$

$1 \leq \zeta \leq z_c$ (E.9)

where F_{22} is defined in (5.54). Again, discretizing the above integrals:

$$\begin{aligned}
\gamma_c^+(\zeta, \tau) &= \frac{2\zeta}{\pi^2} \cos^2 \tilde{\beta} \cdot \chi(\zeta, \tau) \cdot \frac{1}{z_c} \cdot B_{11} \cdot F_{12} \cdot \sum_{i=1}^{N_i^+(\tau)} \gamma_{S,i}^+(\tau) \int_{\zeta_i^+}^{\zeta_{i+1}^+} \zeta_0 d\zeta_0 \\
&\quad - \frac{2\zeta}{\pi^2} \cos^2 \tilde{\beta} \cdot \chi(\zeta, \tau) \cdot \sum_{i=1}^{N_i^+(\tau)} \gamma_{S,i}^+(\tau) \times F_{22}(\zeta_i^+) \cdot \int_{\zeta_i^+}^{\zeta_{i+1}^+} \frac{\zeta_0}{\zeta_0^2 - \zeta^2} (z_c^2 - \zeta_0^2) d\zeta_0 \\
&\quad + \frac{2\zeta}{\pi^2} \cos^2 \tilde{\beta} \cdot \chi(\zeta, \tau) \cdot (\zeta^2 - 1)(z_c^2 - \zeta^2) \times \sum_{j=1}^L \frac{1}{\sqrt{t_j}} \cdot \Delta I_{3,j}(\zeta) \cdot \sum_{i=1}^{N_i^+(\tau)} \gamma_{S,i}^+(\tau) \cdot \int_{\zeta_i^+}^{\zeta_{i+1}^+} \frac{\zeta_0}{\zeta_0^2 - \zeta^2} d\zeta_0
\end{aligned}$$

$1 \leq \zeta \leq z_c$ (E.10)

The integral of the second term in the above equation can be written as:

$$\begin{aligned}
\int_{\zeta_i^+}^{\zeta_{i+1}^+} \frac{\zeta_0}{\zeta_0^2 - \zeta^2} (z_c^2 - \zeta_0^2) d\zeta_0 &= \int_{\zeta_i^+}^{\zeta_{i+1}^+} \frac{\zeta_0}{\zeta_0^2 - \zeta^2} (z_c^2 - \zeta^2 + \zeta^2 - \zeta_0^2) d\zeta_0 \\
&= - \int_{\zeta_i^+}^{\zeta_{i+1}^+} \zeta_0 d\zeta_0 + (z_c^2 - \zeta^2) \int_{\zeta_i^+}^{\zeta_{i+1}^+} \frac{\zeta_0}{\zeta_0^2 - \zeta^2} d\zeta_0 \\
&= -J_{21}(\zeta_i^+) + (z_c^2 - \zeta^2) \cdot J_{22}(\zeta_i^+)
\end{aligned} \tag{E.11}$$

where the integral $J_{22}(\zeta_i)$ defined in (5.91) and the integral $J_{21}(\zeta_i)$ is:

$$J_{21}(\zeta_i^+) = \int_{\zeta_i^+}^{\zeta_{i+1}^+} \zeta_0 d\zeta_0 = \frac{1}{2} [(\zeta_{i+1}^+)^2 - (\zeta_i^+)^2] \tag{E.12}$$

Again, substitute (E.12) and the relation of the free vortex strength $\gamma_{s,i}^+(\tau)$ with the induced velocity $V_s^+(i, \tau)$ ($\gamma_{s,i}^+(\tau) = -2V_s^+(i, \tau)$) into $\gamma_c^+(\zeta, \tau)$, Eq.(E.10). This yields the numerical formula of $\gamma_c^+(\zeta, \tau)$:

$$\begin{aligned}
\gamma_c^+(\zeta, \tau) &= -\frac{2\zeta}{\pi^2} \cos^2 \tilde{\beta} \cdot \chi(\zeta, \tau) \cdot \frac{1}{z_c} \cdot B_{11} \cdot F_{12} \cdot \sum_{i=1}^{N_i^+(\tau)} 2 \cdot V_s^+(i, \tau) \cdot J_{21}(i) \\
&\quad + \frac{2\zeta}{\pi^2} \cos^2 \tilde{\beta} \cdot \chi(\zeta, \tau) \cdot \sum_{i=1}^{N_i^+(\tau)} 2 \cdot V_s^+(i, \tau) \times F_{22}(\zeta_i^+) \cdot [-J_{21}(i) + (z_c^2 - \zeta^2) J_{22}(i)] \\
&\quad - \frac{2\zeta}{\pi^2} \cos^2 \tilde{\beta} \cdot \chi(\zeta, \tau) \cdot (\zeta^2 - 1)(z_c^2 - \zeta^2) \\
&\quad \times \sum_{j=1}^L \frac{1}{\sqrt{t_j}} \cdot \Delta I_{3,j}(\zeta) \cdot \sum_{i=1}^{N_i^+(\tau)} 2 \cdot V_s^+(i, \tau) \cdot J_{22}(i)
\end{aligned}$$

$$1 \leq \zeta \leq z_c \tag{E.13}$$

APPENDIX F
 KERNEL FUNCTION $\chi(\zeta)$

The solution procedure of the kernel function $\chi(\zeta)$ for the Carleman singular integral equation (refer to (4.8)) for the catamaran is similar to that for the monohull (Vorus 1996). The solution is developed here in slightly expanded detail over that presented by Vorus (1996).

The singular integral equation representing the kinematic boundary condition is:

$$\frac{1}{2} \gamma_c(\zeta, \tau) \sin \beta(\zeta, \tau) + \frac{1}{2\pi} \int_{-z_c}^{z_c} \frac{\gamma_c(\zeta_0, \tau)}{\zeta_0 - \zeta} d\zeta_0 = f(\zeta, \tau) \quad 1 \leq \zeta \leq z_c \quad (4.8)$$

where the parameters in (4.8) defined in Chapter 4.

From the definition of Muskhelishvili (1958), the kernel function for the solution of (4.8) has the following expression,

$$\chi(\zeta) = P(\zeta) \cdot e^{\Gamma(\zeta)} \quad (F.1)$$

where,

$$P(\zeta) = \prod_{m=1}^{2p} (\zeta - C_m)^{\lambda_m} \quad (\text{F.2})$$

$$\Gamma(\zeta) = \frac{1}{2\pi i} \int_L \frac{\log G(t) dt}{t - \zeta} \quad (\text{F.3})$$

The unknown function $G(t)$ and the definitions of the parameters in the above can be found from the solution procedure developed for the Carleman singular integral equation by Muskhelishvili(1958). The following derivation mainly follows Muskhelishvili(1958) and Tricomi(1957).

In a more general form than (4.8), the Carleman-type singular integral equation can be expressed as,

$$A(\zeta, \tau)\gamma_c(\zeta, \tau) + \frac{B(\zeta, \tau)}{\pi i} \int_L \frac{\gamma_c(\zeta_0, \tau)}{\zeta_0 - \zeta} d\zeta_0 = f(\zeta, \tau) \quad (\text{F.4})$$

where $A^2(\zeta, \tau) + B^2(\zeta, \tau) \neq 0$ everywhere on the integration path L . Introduce a sectionally analytic function,

$$\Phi(\zeta, t) = \frac{1}{2\pi i} \int_L \frac{\gamma_c(\zeta_0, \tau)}{\zeta_0 - \zeta} d\zeta_0 \quad (\text{F.5})$$

This function $\Phi(\zeta, t)$ vanishes at infinity. Following Tricomi's (1957) derivation, it can be proved that the analytic function $\Phi(\zeta, t)$ satisfies the following relations:

$$\Phi^+(\zeta, \tau) - \Phi^-(\zeta, \tau) = \gamma_c(\zeta, \tau) \quad (\text{F.6})$$

$$\Phi^+(\zeta, \tau) + \Phi^-(\zeta, \tau) = \frac{1}{\pi i} \int_L \frac{\gamma_c(\zeta_0, \tau)}{\zeta_0 - \zeta} d\zeta_0 \quad (\text{F.7})$$

Substituting (F.6) and (F.7) into (F.4) gives,

$$A(\zeta, \tau)[\Phi^+(\zeta, \tau) - \Phi^-(\zeta, \tau)] + B(\zeta, \tau)[\Phi^+(\zeta, \tau) + \Phi^-(\zeta, \tau)] = f(\zeta, \tau) \quad (\text{F.8})$$

Group the coefficients together:

$$[A(\zeta, \tau) + B(\zeta, \tau)]\Phi^+(\zeta, \tau) - [A(\zeta, \tau) - B(\zeta, \tau)]\Phi^-(\zeta, \tau) = f(\zeta, \tau) \quad (\text{F.9})$$

Solve for the boundary function $\Phi^+(\zeta, \tau)$ from the above equation to get:

$$\Phi^+(\zeta, \tau) = \frac{A(\zeta, \tau) - B(\zeta, \tau)}{A(\zeta, \tau) + B(\zeta, \tau)} \Phi^-(\zeta, \tau) + \frac{f(\zeta, \tau)}{A(\zeta, \tau) + B(\zeta, \tau)} \quad (\text{F.10})$$

Comparing (F.10) with the boundary condition in following equation of the non-homogeneous Hilbert problem in Muskhelishvili (1958),

$$\Phi^+(t) = G(t)\Phi^-(t) + g(t) \quad \text{on } L \quad (\text{F.11})$$

where $G(t)$ and $g(t)$ are the functions of the class H (the functions satisfy the Hölder condition, refer to Tricomi's (1957) and Muskhelishvili (1958)), given on L , and $G(t) \neq 0$ everywhere on L . Thus the unknown functions $G(t)$, $g(t)$ are of the following form:

$$G(\zeta, \tau) = \frac{A(\zeta, \tau) - B(\zeta, \tau)}{A(\zeta, \tau) + B(\zeta, \tau)} \quad (\text{F.12})$$

$$g(\zeta, \tau) = \frac{f(\zeta, \tau)}{A(\zeta, \tau) + B(\zeta, \tau)} \quad (\text{F.13})$$

The coefficients $A(\zeta, \tau)$ and $B(\zeta, \tau)$ then can be found by comparing (F.4) with the Carleman equation (4.8):

$$A(\zeta, \tau) = \frac{1}{2} \sin \beta(\zeta, \tau), \quad B(\zeta, \tau) = \frac{1}{2} \cdot i \quad (\text{F.14})$$

Substitute $A(\zeta, \tau)$ and $B(\zeta, \tau)$ into (F.12),

$$G(\zeta, \tau) = \frac{\sin \beta(\zeta, \tau) - i}{\sin \beta(\zeta, \tau) + i} \quad (\text{F.15})$$

Substitute the following complex identity into (F.15),

$$\sin \beta - i = \sqrt{1 + \sin^2 \beta} \cdot e^{i\theta} \quad (\text{F.16})$$

Therefore,

$$G(\zeta, \tau) = \frac{(\sin \beta - i)^2}{1 + \sin^2 \beta} = \frac{(\sqrt{1 + \sin^2 \beta})^2}{1 + \sin^2 \beta} e^{i2\theta} = e^{i2\theta} \quad (\text{F.17})$$

where the angle θ is,

$$\theta = \tan^{-1} \left[\frac{-1}{\sin \beta(\zeta, \tau)} \right] \quad (\text{F.18})$$

Using the transform defined in (A.20),

$$\sin \beta = \tan \tilde{\beta} \quad (\text{F.19})$$

At the X-Y axis intersection of Fig. F1, the θ -angles depicted in Fig. F.1 are,

$$\theta^\pm = \tan^{-1} \left[\frac{-1}{\pm \sin \beta(\zeta, \tau)} \right] = \tan^{-1} \left[\frac{-1}{\pm \tan \tilde{\beta}(\zeta, \tau)} \right] \quad (\text{F.20})$$

where the sign of $\pm \sin \beta(\zeta, \tau)$ comes from the two symmetric angles at the catamaran two sides respectively.

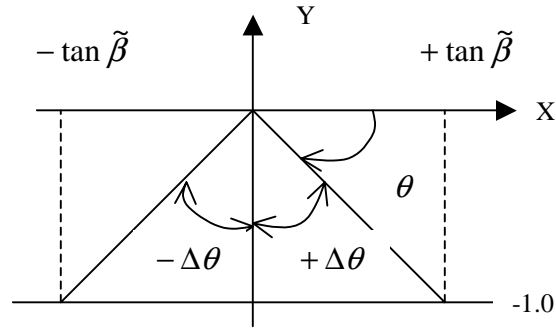


Fig. F.1: Phase angle definition

By Fig. F.1, the phase angle can be calculated as,

$$\theta^{\pm} = -\frac{\pi}{2} \pm \Delta\theta = -\frac{\pi}{2} \mp \text{atan}(\tan\tilde{\beta}) = -\frac{\pi}{2} \mp \tilde{\beta}(\zeta, \tau) \quad (\text{F.21})$$

Thus, the angle relation is:

$$\theta(\zeta) = \begin{cases} -\frac{\pi}{2} - \tilde{\beta}(\zeta) & -z_c \leq \zeta \leq -1 \\ -\frac{\pi}{2} + \tilde{\beta}(\zeta) & 1 \leq \zeta \leq z_c \end{cases} \quad (\text{F.22})$$

Substitute the $G(t)$ term in (F.17) into (F.3) to get,

$$\Gamma(\zeta) = \frac{1}{\pi} \sum_{k=1}^p \int_{L_k} \frac{\theta(t)}{t - \zeta} dt \quad (\text{F.23})$$

where p is the number of arcs, with the end points at coordinates of C_m . The λ_m are integers which will be selected according to character of the $\chi(\zeta)$ function in each arc L_k . For present problem, the arcs are $-z_c \leq \zeta \leq -1$ and $1 \leq \zeta \leq z_c$. Thus the number of arcs is 2, thereby $p = 2$. According to the correspondent end coordinates of the arcs, the respective C_m parameter in (F.2) may be chosen as $C_m = -z_c, -1, 0, 1, z_c$. Then from (F.2),

$$P(\zeta) = (1 + \zeta)^{\lambda_1} (z_c + \zeta)^{\lambda_2} (z_c - \zeta)^{\lambda_3} (\zeta - 1)^{\lambda_4} \quad (\text{F.24})$$

where the parameter set λ_m is selected to match the solution to the catamaran hull.

Expanding (F.23) according to (F.22),

$$\begin{aligned} \Gamma(\zeta) &= \frac{1}{\pi} \left[\int_{-z_c}^{-1} \frac{\theta^-(t) dt}{t - \zeta} + \int_1^{z_c} \frac{\theta^+(t) dt}{t - \zeta} \right] \\ &= -\frac{1}{2} \int_{-z_c}^{-1} \frac{dt}{t - \zeta} - \frac{1}{\pi} \int_{-z_c}^{-1} \frac{\tilde{\beta}(t) dt}{t - \zeta} - \frac{1}{2} \int_1^{z_c} \frac{dt}{t - \zeta} + \frac{1}{\pi} \int_1^{z_c} \frac{\tilde{\beta}(t) dt}{t - \zeta} \end{aligned} \quad (\text{F.25})$$

The integral in the third term of the above equation is changed into the following form,

$$\begin{aligned} \int_1^{z_c} \frac{dt}{t - \zeta} &= -\int_1^{\zeta - \varepsilon} \frac{dt}{\zeta - t} + \int_{\zeta + \varepsilon}^{z_c} \frac{dt}{t - \zeta} \\ &= \ln[\zeta - t]_1^{\zeta - \varepsilon} + \ln[t - \zeta]_{\zeta + \varepsilon}^{z_c} \\ &= \ln \varepsilon - \ln(\zeta - 1) + \ln(z_c - \zeta) - \ln \varepsilon \\ &= -\ln(\zeta - 1) + \ln(z_c - \zeta) \end{aligned} \quad (\text{F.26})$$

Substituting (F.26) into (F.25) produces,

$$\begin{aligned}
\Gamma(\zeta) &= -\frac{1}{2} \int_{-z_c}^{-1} \frac{dt}{t-\zeta} - \frac{1}{2} \int_1^{z_c} \frac{dt}{t-\zeta} - \frac{1}{\pi} \int_{-z_c}^{-1} \frac{\tilde{\beta}(t)dt}{t-\zeta} + \frac{1}{\pi} \int_1^{z_c} \frac{\tilde{\beta}(t)dt}{t-\zeta} \\
&= -\frac{1}{2} [\ln(-1-\zeta) - \ln(-z_c-\zeta) - \ln(\zeta-1) + \ln(z_c-\zeta)] - \frac{1}{\pi} \int_{-z_c}^{-1} \frac{\tilde{\beta}(t)dt}{t-\zeta} + \frac{1}{\pi} \int_1^{z_c} \frac{\tilde{\beta}(t)dt}{t-\zeta} \\
&= \ln \left[\frac{(\zeta-1) \cdot (-z_c-\zeta)}{(-1-\zeta)(z_c-\zeta)} \right]^{1/2} - \frac{1}{\pi} \int_{z_c}^1 \frac{\tilde{\beta}(-t)(-dt)}{-t-\zeta} + \frac{1}{\pi} \int_1^{z_c} \frac{\tilde{\beta}(t)dt}{t-\zeta} \\
&= \ln \left[\sqrt{\frac{(\zeta-1) \cdot (z_c+\zeta)}{(1+\zeta)(z_c-\zeta)}} \right] + \frac{1}{\pi} \int_1^{z_c} \frac{\tilde{\beta}(t)dt}{t+\zeta} + \frac{1}{\pi} \int_1^{z_c} \frac{\tilde{\beta}(t)dt}{t-\zeta}
\end{aligned} \tag{F.27}$$

To simplify the form of (F.27), we further reduce the last two integrals in (F.27).

Assuming $\beta(\zeta)$ is a piecewise constant,

$$\begin{aligned}
I &= \frac{1}{\pi} \int_1^{z_c} \frac{\tilde{\beta}(t)dt}{t+\zeta} + \frac{1}{\pi} \int_{z_1}^{z_c} \frac{\tilde{\beta}(t)dt}{t-\zeta} \\
&= \frac{1}{\pi} \sum_{j=1}^J \beta_j \int_{t_j}^{t_{j+1}} \frac{dt}{t+\zeta} + \frac{1}{\pi} \sum_{j=1}^J \beta_j \int_{t_j}^{t_{j+1}} \frac{dt}{t-\zeta}
\end{aligned} \tag{F.28}$$

The first term of (F.28) is,

$$\frac{1}{\pi} \sum_{j=1}^J \beta_j \int_{t_j}^{t_{j+1}} \frac{dt}{t+\zeta} = \frac{1}{\pi} \sum_{j=1}^J \beta_j \ln \frac{t_{j+1}+\zeta}{t_j+\zeta} \tag{F.29}$$

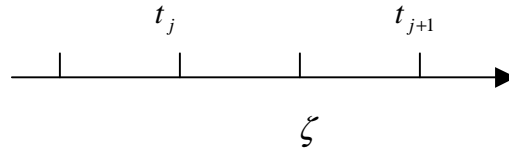


Fig. F.2: Singular Integration

According to Fig. F.2, the second integral term in Eq.(F.28) can be divided into two parts according to the parameter ζ ,

$$\begin{aligned}
\frac{1}{\pi} \sum_{j=1}^J \beta_j \int_{t_j}^{t_{j+1}} \frac{dt}{t-\zeta} &= -\frac{1}{\pi} \sum_{j=1}^{J_0} \beta_j \int_{t_j}^{t_{j+1}} \frac{dt}{\zeta-t} + \frac{1}{\pi} \sum_{j=J_0+1}^J \beta_j \int_{t_j}^{t_{j+1}} \frac{dt}{t-\zeta} \\
&= \frac{1}{\pi} \sum_{j=1}^{J_0} \beta_j \ln[\zeta-t]_{t_j}^{t_{j+1}} + \frac{1}{\pi} \sum_{j=J_0+1}^J \beta_j \ln[t-\zeta]_{t_j}^{t_{j+1}} \\
&= \frac{1}{\pi} \sum_{j=1}^{J_0} \beta_j [\ln(\zeta-t_{j+1}) - \ln(\zeta-t_j)] \\
&\quad + \frac{1}{\pi} \sum_{j=J_0+1}^J \beta_j [\ln(t_{j+1}-\zeta) - \ln(t_j-\zeta)] \\
&= \frac{1}{\pi} \sum_{j=1}^{J_0} \beta_j \ln \frac{\zeta-t_{j+1}}{\zeta-t_j} + \frac{1}{\pi} \sum_{j=J_0+1}^J \beta_j \ln \frac{t_{j+1}-\zeta}{t_j-\zeta} \\
&= \frac{1}{\pi} \sum_{j=1}^J \beta_j \ln \left| \frac{\zeta-t_{j+1}}{\zeta-t_j} \right|
\end{aligned} \tag{F.30}$$

Substituting above equations into (F.27), we get,

$$\begin{aligned}
\Gamma(\zeta) &= \ln\left[\sqrt{\frac{(\zeta-1)\cdot(z_c+\zeta)}{(1+\zeta)(z_c-\zeta)}}\right] + \frac{1}{\pi} \int_{z_1}^{z_c} \frac{\tilde{\beta}(t)dt}{t+\zeta} + \frac{1}{\pi} \int_{z_1}^{z_c} \frac{\tilde{\beta}(t)dt}{t-\zeta} \\
&= \ln\left[\sqrt{\frac{(\zeta-1)\cdot(z_c+\zeta)}{(1+\zeta)(z_c-\zeta)}}\right] + \frac{1}{\pi} \sum_{j=1}^J \beta_j \ln \frac{t_{j+1}+\zeta}{t_j+\zeta} + \frac{1}{\pi} \sum_{j=1}^J \beta_j \ln \left| \frac{\zeta-t_{j+1}}{\zeta-t_j} \right| \\
&= \ln\left[\sqrt{\frac{(\zeta-1)\cdot(z_c+\zeta)}{(1+\zeta)(z_c-\zeta)}}\right] + \frac{1}{\pi} \sum_{j=1}^J \beta_j \left[\ln \left| \frac{t_{j+1}+\zeta}{t_j+\zeta} \right| + \ln \left| \frac{\zeta-t_{j+1}}{\zeta-t_j} \right| \right] \\
&= \ln\left[\sqrt{\frac{(\zeta-1)\cdot(z_c+\zeta)}{(1+\zeta)(z_c-\zeta)}}\right] + \frac{1}{\pi} \sum_{j=1}^J \beta_j \ln \left[\left| \frac{t_{j+1}+\zeta}{t_j+\zeta} \right| \times \left| \frac{\zeta-t_{j+1}}{\zeta-t_j} \right| \right] \\
&= \ln\left[\sqrt{\frac{(\zeta-1)\cdot(z_c+\zeta)}{(1+\zeta)(z_c-\zeta)}}\right] + \sum_{j=1}^J \ln \left[\left| \frac{t_{j+1}+\zeta}{t_j+\zeta} \right|^{\frac{\beta_j}{\pi}} \times \left| \frac{\zeta-t_{j+1}}{\zeta-t_j} \right|^{\frac{\beta_j}{\pi}} \right] \\
&= \ln\left[\sqrt{\frac{(\zeta-1)\cdot(z_c+\zeta)}{(1+\zeta)(z_c-\zeta)}}\right] \times \prod_{j=1}^J \left| \frac{t_{j+1}+\zeta}{t_j+\zeta} \right|^{\frac{\beta_j}{\pi}} \cdot \left| \frac{\zeta-t_{j+1}}{\zeta-t_j} \right|^{\frac{\beta_j}{\pi}}
\end{aligned} \tag{F.31}$$

Now, according to the definition of the kernel function in (F.1), it is expressed as,

$$\begin{aligned}
\chi(\zeta) &= P(\zeta) \cdot e^{\Gamma(\zeta)} \\
&= (1+\zeta)^{\lambda_1} (z_c+\zeta)^{\lambda_2} (z_c-\zeta)^{\lambda_3} (\zeta-1)^{\lambda_4} \\
&\quad \times \sqrt{\frac{(\zeta-1)\cdot(z_c+\zeta)}{(1+\zeta)(z_c-\zeta)}} \times \prod_{j=1}^J \left| \frac{t_{j+1}+\zeta}{t_j+\zeta} \right|^{\frac{\beta_j}{\pi}} \cdot \left| \frac{\zeta-t_{j+1}}{\zeta-t_j} \right|^{\frac{\beta_j}{\pi}} \\
&= (1+\zeta)^{\lambda_1} (z_c+\zeta)^{\lambda_2} (z_c-\zeta)^{\lambda_3} (\zeta-1)^{\lambda_4} \times \kappa(\zeta) \sqrt{\frac{(\zeta-1)\cdot(z_c+\zeta)}{(1+\zeta)(z_c-\zeta)}}
\end{aligned} \tag{F.32}$$

where,

$$\kappa(\zeta) = \prod_{j=1}^J \left| \frac{t_{j+1}+\zeta}{t_j+\zeta} \right|^{\frac{\beta_j}{\pi}} \cdot \left| \frac{\zeta-t_{j+1}}{\zeta-t_j} \right|^{\frac{\beta_j}{\pi}} \tag{F.33}$$

β_j is the average value of $\tilde{\beta}(\zeta)$ over the j element. For the constant deadrise wedge contours, $\beta(\zeta)$ is constant. Denote $\kappa(\zeta) = \kappa_0(\zeta)$ in this case, which is,

$$\kappa_0(\zeta) = \left| \frac{z_c + \zeta}{1 + \zeta} \right|^{\frac{\beta}{\pi}} \cdot \left| \frac{\zeta - z_c}{\zeta - 1} \right|^{\frac{\beta}{\pi}} = \left| \frac{z_c + \zeta}{\zeta + 1} \right|^{\frac{\beta}{\pi}} \cdot \left| \frac{z_c - \zeta}{\zeta - 1} \right|^{\frac{\beta}{\pi}} = \left(\frac{z_c^2 - \zeta^2}{\zeta^2 - 1} \right)^{\frac{\beta}{\pi}} \quad (\text{F.34})$$

The choice of λ_m in (F.32) is for matching the solution of catamaran-type hull. This is accomplished by choosing $\lambda_1=0$, $\lambda_2=-1$, $\lambda_3=0$, $\lambda_4=-1$. Thus, the kernel function for the catamaran planing problem can be expressed as,

(1) In a general case $\beta = \beta(\zeta, \tau)$ (refer to (4.13)),

$$\begin{aligned} \chi(\zeta, \tau) &= \frac{1}{(z_c + \zeta)(\zeta - 1)} \kappa(\zeta, \tau) \sqrt{\frac{(\zeta - 1) \cdot (z_c + \zeta)}{(1 + \zeta)(z_c - \zeta)}} \\ &= \frac{\kappa(\zeta)}{\sqrt{(\zeta^2 - 1)(z_c^2 - \zeta^2)}} \end{aligned} \quad (\text{F.35})$$

(2) In the case of $\beta = \beta(\tau)$ constant in ζ (refer to (4.16)),

$$\chi(\zeta, \tau) = \frac{\kappa_0(\zeta, \tau)}{\sqrt{(\zeta^2 - 1)(z_c^2 - \zeta^2)}} = \frac{1}{\sqrt{(\zeta^2 - 1)(z_c^2 - \zeta^2)}} \cdot \left(\frac{z_c^2 - \zeta^2}{\zeta^2 - 1} \right)^{\frac{\beta(\tau)}{\pi}} \quad (\text{F.36})$$

APPENDIX G

KERNEL FUNCTION $\chi^*(\zeta)$

The construction procedure for the kernel function $\chi^*(\zeta)$ in the solution of the Carleman equation for the displacement vortex strength, (4.47), is, in general, the same as the procedure of $\chi(\zeta)$ in Appendix F. The difference of $\chi^*(\zeta)$ from $\chi(\zeta)$ in (4.13) is that its solution domain is now on the arcs of $-b^+ \leq \zeta \leq -b^-$ and $b^- \leq \zeta \leq b^+$.

The definition of the kernel function $\chi^*(\zeta)$ is same as in (F.1), (F.2) and (F.23):

$$\chi^*(\zeta) = P(\zeta) \cdot e^{\Gamma(\zeta)} \quad (\text{G.1})$$

where,

$$P(\zeta) = \prod_{m=1}^{2p} (\zeta - C_m)^{\lambda_m} \quad (\text{G.2})$$

$$\Gamma(\zeta) = \frac{1}{\pi} \sum_{k=1}^p \int_{L_k} \frac{\theta(t)}{t - \zeta} dt \quad (\text{G.3})$$

where $p = 2$ and the respective $C_m = -b^+, -b^-, b^-, b^+$. Then,

$$P(\zeta) = (\zeta + b^+)^{\lambda_1} (\zeta + b^-)^{\lambda_2} (\zeta - b^-)^{\lambda_3} (\zeta - b^+)^{\lambda_4} \quad (\text{G.4})$$

The angle relation in (F.22) now is:

$$\theta(\zeta) = \begin{cases} -\frac{\pi}{2} - \tilde{\beta}(\zeta) & -b^+ \leq \zeta \leq -b^- \\ -\frac{\pi}{2} + \tilde{\beta}(\zeta) & b^- \leq \zeta \leq b^+ \end{cases} \quad (\text{G.5})$$

Substituting (G.5) into (G.3) yields,

$$\begin{aligned} \Gamma(\zeta) &= \frac{1}{\pi} \left[\int_{-b^+}^{-b^-} \frac{\theta^-(t) dt}{t - \zeta} + \int_{b^-}^{b^+} \frac{\theta^+(t) dt}{t - \zeta} \right] \\ &= -\frac{1}{2} \int_{-b^+}^{-b^-} \frac{dt}{t - \zeta} - \frac{1}{\pi} \int_{-b^+}^{-b^-} \frac{\tilde{\beta}(t) dt}{t - \zeta} - \frac{1}{2} \int_{b^-}^{b^+} \frac{dt}{t - \zeta} + \frac{1}{\pi} \int_{b^-}^{b^+} \frac{\tilde{\beta}(t) dt}{t - \zeta} \end{aligned} \quad (\text{G.6})$$

Following the same derivation procedure as in Appendix F, we get the kernel function

$$\chi^*(\zeta),$$

$$\begin{aligned} \chi^*(\zeta) &= P(\zeta) \cdot e^{\Gamma(\zeta)} \\ &= (\zeta + b^+)^{\lambda_1} (\zeta + b^-)^{\lambda_2} (\zeta - b^-)^{\lambda_3} (\zeta - b^+)^{\lambda_4} \\ &\quad \times \sqrt{\frac{(\zeta - b^-) \cdot (b^+ + \zeta)}{(b^- + \zeta)(b^+ - \zeta)}} \times \prod_{j=1}^J \left| \frac{t_{j+1} + \zeta}{t_j + \zeta} \right|^{\frac{\beta_j}{\pi}} \cdot \left| \frac{\zeta - t_{j+1}}{\zeta - t_j} \right|^{\frac{\beta_j}{\pi}} \\ &= (\zeta + b^+)^{\lambda_1} (\zeta + b^-)^{\lambda_2} (\zeta - b^-)^{\lambda_3} (\zeta - b^+)^{\lambda_4} \times \kappa(\zeta) \sqrt{\frac{(\zeta - b^-) \cdot (b^+ + \zeta)}{(b^- + \zeta)(b^+ - \zeta)}} \end{aligned} \quad (\text{G.7})$$

where,

$$\kappa(\zeta) = \prod_{j=1}^J \left| \frac{t_{j+1} + \zeta}{t_j + \zeta} \right|^{\frac{\beta_j}{\pi}} \cdot \left| \frac{\zeta - t_{j+1}}{\zeta - t_j} \right|^{\frac{\beta_j}{\pi}} \quad (\text{G.8})$$

and β_j is the average value of $\tilde{\beta}(\zeta)$ over the j element. For the straight-bottom wedge contours, $\beta(\zeta)$ is constant. Denote $\kappa(\zeta) = \kappa_0(\zeta)$ in this case, giving,

$$\kappa_0(\zeta) = \left| \frac{b^+ + \zeta}{b^- + \zeta} \right|^{\frac{\tilde{\beta}}{\pi}} \cdot \left| \frac{b^+ - \zeta}{b^- - \zeta} \right|^{\frac{\tilde{\beta}}{\pi}} = \left| \frac{b^+ + \zeta}{\zeta + b^-} \right|^{\frac{\tilde{\beta}}{\pi}} \cdot \left| \frac{b^+ - \zeta}{\zeta - b^-} \right|^{\frac{\tilde{\beta}}{\pi}} = \left(\frac{(b^+)^2 - \zeta^2}{\zeta^2 - (b^-)^2} \right)^{\frac{\tilde{\beta}}{\pi}} \quad (\text{G.9})$$

The choice of λ_m in Eq.(G.7) is to match the solution for the catamaran hull. It is $\lambda_1 = -1$, $\lambda_2 = 0$, $\lambda_3 = -1$, $\lambda_4 = 0$. Thus the kernel function is,

(1) In the general case $\beta = \beta(\zeta, \tau)$ (refer to (4.48)),

$$\chi^*(\zeta) = \frac{\kappa(\zeta)}{\sqrt{(\zeta^2 - (b^-)^2)((b^+)^2 - \zeta^2)}} \quad (\text{G.10})$$

(2) In the case of constant $\beta = \beta(\tau)$ (refer to (4.50)),

$$\chi^*(\zeta) = \frac{1}{\sqrt{(\zeta^2 - (b^-)^2)((b^+)^2 - \zeta^2)}} \cdot \left(\frac{(b^+)^2 - \zeta^2}{\zeta^2 - (b^-)^2} \right)^{\frac{\tilde{\beta}(\tau)}{\pi}} \quad (\text{G.11})$$

APPENDIX H

FUNDAMENTAL INTEGRALS IN VELOCITY CONTINUITY FORMULATION

To develop a numerical model for the velocity continuity condition and the bound vortex distribution $\gamma_c(\zeta, \tau)$ computation, the fundamental singular integral terms in Eq.(4.23), (4.24) and (4.25) must be evaluated numerically. In this appendix, these integrals will be transformed into an easy numerical computation form by an analytic method.

H.1 Three Elemental Integrals

The three singular integrals in (4.23) – (4.25) are in the same form, but defined in different value domains. Therefore, it is convenient to derive the semi-analytical formulation according to the integral in (4.23), then to apply this derived formulae to the integrals in (4.24) and (4.25).

By (4.23),

$$\Lambda(\zeta) = \int_{\zeta_1=1}^{\zeta_c} \frac{d\zeta_1}{\chi(\zeta_1, \tau)(\zeta^2 - \zeta_1^2)} \quad 1 \leq \zeta \leq \zeta_c \quad (\text{H.1})$$

where the kernel function is (refer to (4.16)),

$$\chi(\zeta, \tau) = \frac{\kappa_0(\zeta, \tau)}{\sqrt{(\zeta^2 - 1)(z_c^2 - \zeta^2)}} \quad (\text{H.2})$$

and,

$$\kappa_0(\zeta, \tau) = \left(\frac{z_c^2 - \zeta^2}{\zeta^2 - 1} \right)^{\frac{\tilde{\beta}(\tau)}{\pi}} \quad (\text{H.3})$$

Thus,

$$\begin{aligned} \Lambda(\zeta) &= \int_{\zeta_1=1}^{z_c} \frac{\sqrt{(\zeta_1^2 - 1)(z_c^2 - \zeta_1^2)} d\zeta_1}{\kappa_0(\zeta_1) \cdot (\zeta^2 - \zeta_1^2)} \\ &= \int_{\zeta_1=1}^{z_c} \frac{1}{\kappa_0(\zeta_1) \cdot \sqrt{(\zeta_1^2 - 1)(z_c^2 - \zeta_1^2)}} \left[\frac{(\zeta_1^2 - 1)(z_c^2 - \zeta_1^2)}{(\zeta^2 - \zeta_1^2)} \right] d\zeta_1 \end{aligned} \quad (\text{H.4})$$

Introduce the identity:

$$\begin{aligned} \frac{\zeta_1^2 - 1}{\zeta^2 - \zeta_1^2} &= \frac{\zeta_1^2 + \zeta^2 - \zeta^2 - 1}{\zeta^2 - \zeta_1^2} = -1 + \frac{\zeta^2 - 1}{\zeta^2 - \zeta_1^2} \\ \frac{z_c^2 - \zeta_1^2}{\zeta^2 - \zeta_1^2} &= \frac{z_c^2 + \zeta^2 - \zeta^2 - \zeta_1^2}{\zeta^2 - \zeta_1^2} = 1 + \frac{z_c^2 - \zeta^2}{\zeta^2 - \zeta_1^2} \end{aligned} \quad (\text{H.5})$$

Substitute (H.5) into (H.4) to produce the result:

$$\begin{aligned}
\frac{(\zeta_1^2 - 1)(z_c^2 - \zeta_1^2)}{(\zeta^2 - \zeta_1^2)} &= (\zeta^2 - \zeta_1^2) \cdot \frac{(\zeta_1^2 - 1)(z_c^2 - \zeta_1^2)}{(\zeta^2 - \zeta_1^2)^2} \\
&= (\zeta^2 - \zeta_1^2) \cdot \left(-1 + \frac{\zeta^2 - 1}{\zeta^2 - \zeta_1^2}\right) \cdot \left(1 + \frac{z_c^2 - \zeta^2}{\zeta^2 - \zeta_1^2}\right) \\
&= (\zeta^2 - \zeta_1^2) \cdot \left[-1 + \frac{\zeta^2 - 1}{\zeta^2 - \zeta_1^2} - \frac{z_c^2 - \zeta^2}{\zeta^2 - \zeta_1^2} + \frac{\zeta^2 - 1}{\zeta^2 - \zeta_1^2} \cdot \frac{z_c^2 - \zeta^2}{\zeta^2 - \zeta_1^2}\right] \quad (\text{H.6}) \\
&= \zeta_1^2 - \zeta^2 + \zeta^2 - 1 - z_c^2 + \zeta^2 + \frac{(\zeta^2 - 1)(z_c^2 - \zeta^2)}{\zeta^2 - \zeta_1^2} \\
&= \zeta_1^2 + (\zeta^2 - z_c^2 - 1) + \frac{(\zeta^2 - 1)(z_c^2 - \zeta^2)}{\zeta^2 - \zeta_1^2}
\end{aligned}$$

Substituting Eq.(H.6) into Eq.(H.4) yields three elemental integrals,

$$\begin{aligned}
\Lambda(\zeta) &= \int_{\zeta_1=1}^{z_c} \frac{1}{\kappa_0(\zeta_1) \cdot \sqrt{(\zeta_1^2 - 1)(z_c^2 - \zeta_1^2)}} \left[\frac{(\zeta_1^2 - 1)(z_c^2 - \zeta_1^2)}{(\zeta^2 - \zeta_1^2)} \right] d\zeta_1 \\
&= \int_{\zeta_1=1}^{z_c} \frac{1}{\kappa_0(\zeta_1) \cdot \sqrt{(\zeta_1^2 - 1)(z_c^2 - \zeta_1^2)}} \left[\zeta_1^2 + (\zeta^2 - z_c^2 - 1) + \frac{(\zeta^2 - 1)(z_c^2 - \zeta^2)}{\zeta^2 - \zeta_1^2} \right] d\zeta_1 \\
&= I_1 + I_2(\zeta) + I_3(\zeta)
\end{aligned} \quad (\text{H.7})$$

The three elemental integrals are defined as (refer to (4.29), (4.30) and (4.31)),

$$\begin{aligned}
I_1 &= \int_{\zeta_1=1}^{z_c} \frac{\zeta_1^2}{\kappa_0(\zeta_1) \cdot \sqrt{(\zeta_1^2 - 1)(z_c^2 - \zeta_1^2)}} d\zeta_1 \\
&= \int_{\zeta_1=1}^{z_c} \zeta_1^2 (\zeta_1^2 - 1)^{-\frac{1}{2}} \pi^{\tilde{\beta}} (z_c^2 - \zeta_1^2)^{-\frac{1}{2}} \pi^{\tilde{\beta}} d\zeta_1
\end{aligned} \quad (\text{H.8})$$

$$\begin{aligned}
I_2(\zeta) &= (\zeta^2 - z_c^2 - 1) \cdot \int_{\zeta_1=1}^{z_c} \frac{1}{\kappa_0(\zeta_1) \cdot \sqrt{(\zeta_1^2 - 1)(z_c^2 - \zeta_1^2)}} d\zeta_1 \\
&= (\zeta^2 - z_c^2 - 1) \cdot \int_{\zeta_1=1}^{z_c} (\zeta_1^2 - 1)^{\frac{1}{2} + \frac{\tilde{\beta}}{\pi}} (z_c^2 - \zeta_1^2)^{\frac{1}{2} - \frac{\tilde{\beta}}{\pi}} d\zeta_1
\end{aligned} \tag{H.9}$$

$$\begin{aligned}
I_3(\zeta) &= (\zeta^2 - 1)(z_c^2 - \zeta^2) \cdot \int_{\zeta_1=1}^{z_c} \frac{1}{\kappa_0(\zeta_1^2) \cdot (\zeta^2 - \zeta_1^2) \sqrt{(\zeta_1^2 - 1)(z_c^2 - \zeta_1^2)}} d\zeta_1 \\
&= (\zeta^2 - 1)(z_c^2 - \zeta^2) \cdot \int_{\zeta_1=1}^{z_c} (\zeta^2 - \zeta_1^2)^{-1} (\zeta_1^2 - 1)^{\frac{1}{2} + \frac{\tilde{\beta}}{\pi}} (z_c^2 - \zeta_1^2)^{\frac{1}{2} - \frac{\tilde{\beta}}{\pi}} d\zeta_1
\end{aligned} \tag{H.10}$$

In following sections, we derive semi-analytical forms for the three elemental integrals.

H.2 Elemental Integral I_1

Define the variable transformation $t = \zeta_1^2$ in Eq.(H.8), with $d\zeta_1 = \frac{1}{2} \frac{dt}{\sqrt{t}}$. I_1

becomes:

$$I_1 = \frac{1}{2} \int_{t=1}^{z_c^2} t(t-1)^{\frac{1}{2} + \frac{\tilde{\beta}}{\pi}} (z_c^2 - t)^{\frac{1}{2} - \frac{\tilde{\beta}}{\pi}} \frac{1}{\sqrt{t}} dt = \frac{1}{2} \int_{t=1}^{z_c^2} t^{\frac{1}{2}} (t-1)^{\frac{1}{2} + \frac{\tilde{\beta}}{\pi}} (z_c^2 - t)^{\frac{1}{2} - \frac{\tilde{\beta}}{\pi}} dt \tag{H.11}$$

Again transform as $x = t - 1$, $t = x + 1$, $dx = dt$. Then Eq.(H.11) becomes,

$$\begin{aligned}
I_1 &= \frac{1}{2} \int_{t=1}^{z_c^2} t^{\frac{1}{2}} (t-1)^{\frac{1}{2} + \frac{\tilde{\beta}}{\pi}} (z_c^2 - t)^{\frac{1}{2} - \frac{\tilde{\beta}}{\pi}} dt \\
&= \frac{1}{2} \int_{x=0}^{z_c^2-1} (x+1)^{\frac{1}{2}} x^{\frac{1}{2} + \frac{\tilde{\beta}}{\pi}} (z_c^2 - 1 - x)^{\frac{1}{2} - \frac{\tilde{\beta}}{\pi}} dx
\end{aligned} \tag{H.12}$$

From Gradshteyn and Ryzhik (1965), p287, §3.197.8:

$$\int_0^u x^{\nu-1} (x + \alpha)^\lambda (u - x)^{\mu-1} dx = \alpha^\lambda u^{\mu+\nu-1} B(\mu, \nu) \cdot {}_2F_1(-\lambda, \nu; \mu + \nu; -\frac{u}{\alpha}) \quad (\text{H.13})$$

where $\left| \arg\left(\frac{u}{\alpha}\right) \right| < \pi$, $\operatorname{Re} \mu > 0$, $\operatorname{Re} \nu > 0$.

Comparing with (H.12),

$$\alpha = 1, u = z_c^2 - 1, \mu = 1 - \frac{1}{2} - \frac{\tilde{\beta}}{\pi} = \frac{1}{2} - \frac{\tilde{\beta}}{\pi}, \nu = \frac{1}{2} + \frac{\tilde{\beta}}{\pi}, \lambda = \frac{1}{2}.$$

Thus,

$$I_1 = \int_{\zeta_1=1}^{z_c} \frac{\zeta_1^2}{\kappa_0(\zeta_1) \cdot \sqrt{(\zeta_1^2 - 1)(z_c^2 - \zeta_1^2)}} d\zeta_1 = \frac{1}{2} B\left(\frac{1}{2} - \frac{\tilde{\beta}}{\pi}, \frac{1}{2} + \frac{\tilde{\beta}}{\pi}\right) \cdot {}_2F_1\left(-\frac{1}{2}, \frac{1}{2} + \frac{\tilde{\beta}}{\pi}; 1; 1 - z_c^2\right) \quad (\text{H.14})$$

The parameter $|1 - z_c^2|$ in (H.14) may be greater than 1, which results in a divergent hypergeometric series for $F(\alpha, \beta; \gamma; z)$. To obtain a convergent solution, use the transformation formulas in Gradshteyn and Ryzhik (1965), p1043, §9.131.1:

$$F(\alpha, \beta; \gamma; z) = (1 - z)^{-\alpha} F\left(\alpha, \gamma - \beta, \gamma; \frac{z}{z - 1}\right) \quad (\text{H.15})$$

Comparing with (H.14), $\alpha = -\frac{1}{2}$, $\beta = \frac{1}{2} + \frac{\tilde{\beta}}{\pi}$, $\gamma = 1$, $z = 1 - z_c^2$,

Therefore, in (H.15): $1 - z = 1 - 1 + z_c^2 = z_c^2$, $\frac{z}{z-1} = \frac{1 - z_c^2}{-z_c^2} = \frac{z_c^2 - 1}{z_c^2} < 1$,

$\gamma - \beta = 1 - \frac{1}{2} - \frac{\tilde{\beta}}{\pi} = \frac{1}{2} - \frac{\tilde{\beta}}{\pi}$, and,

$$F\left(-\frac{1}{2}, \frac{1}{2} + \frac{\tilde{\beta}}{\pi}; 1; 1 - z_c^2\right) = (z_c^2)^{\frac{1}{2}} \cdot F\left(-\frac{1}{2}, \frac{1}{2} - \frac{\tilde{\beta}}{\pi}; 1; \frac{z_c^2 - 1}{z_c^2}\right) = z_c \cdot F\left(-\frac{1}{2}, \frac{1}{2} - \frac{\tilde{\beta}}{\pi}; 1; \frac{z_c^2 - 1}{z_c^2}\right) \quad (\text{H.16})$$

The elemental integral I_1 therefore has the following semi-analytical form (see (7.1)):

$$\begin{aligned} I_1 &= \int_{\zeta_1=1}^{z_c} \frac{\zeta_1^2}{\kappa_0(\zeta_1) \cdot \sqrt{(\zeta_1^2 - 1)(z_c^2 - \zeta_1^2)}} d\zeta_1 = \frac{1}{2} B\left(\frac{1}{2} - \frac{\tilde{\beta}}{\pi}, \frac{1}{2} + \frac{\tilde{\beta}}{\pi}\right) \cdot {}_2F_1\left(-\frac{1}{2}, \frac{1}{2} + \frac{\tilde{\beta}}{\pi}; 1; 1 - z_c^2\right) \\ &= \frac{1}{2} z_c \cdot B\left(\frac{1}{2} - \frac{\tilde{\beta}}{\pi}, \frac{1}{2} + \frac{\tilde{\beta}}{\pi}\right) \cdot F\left(-\frac{1}{2}, \frac{1}{2} - \frac{\tilde{\beta}}{\pi}; 1; \frac{z_c^2 - 1}{z_c^2}\right) \end{aligned} \quad (\text{H.17})$$

H.3 Elemental Integral $I_2(\zeta)$

Define again the variable transformation $t = \zeta_1^2$ in (H.9), with $d\zeta_1 = \frac{1}{2} \frac{dt}{\sqrt{t}}$,

$$\begin{aligned}
I_2(\zeta) &= (\zeta^2 - z_c^2 - 1) \cdot \int_{\zeta_1=1}^{z_c} (\zeta_1^2 - 1)^{\frac{1}{2} + \frac{\tilde{\beta}}{\pi}} (z_c^2 - \zeta_1^2)^{\frac{1}{2} - \frac{\tilde{\beta}}{\pi}} d\zeta_1 \\
&= \frac{1}{2} (\zeta^2 - z_c^2 - 1) \cdot \int_{t=1}^{z_c^2} t^{\frac{1}{2}} (t-1)^{\frac{1}{2} + \frac{\tilde{\beta}}{\pi}} (z_c^2 - t)^{\frac{1}{2} - \frac{\tilde{\beta}}{\pi}} dt
\end{aligned} \tag{H.18}$$

Again define the second transform $x = t - 1$, with $dx = dt$. Then (H.18) becomes,

$$I_2(\zeta) = \frac{1}{2} (\zeta^2 - z_c^2 - 1) \cdot \int_{x=0}^{z_c^2-1} (x+1)^{\frac{1}{2}} x^{\frac{1}{2} + \frac{\tilde{\beta}}{\pi}} (z_c^2 - 1 - x)^{\frac{1}{2} - \frac{\tilde{\beta}}{\pi}} dx \tag{H.19}$$

From Gradshteyn and Ryzhik (1965), p287, §3.197.8 :

$$\int_0^u x^{\nu-1} (x+\alpha)^\lambda (u-x)^{\mu-1} dx = \alpha^\lambda u^{\mu+\nu-1} B(\mu, \nu) \cdot {}_2F_1(-\lambda, \nu; \mu + \nu; -\frac{u}{\alpha}) \tag{H.20}$$

where $\left| \arg\left(\frac{u}{\alpha}\right) \right| < \pi$, $\operatorname{Re} \mu > 0$, $\operatorname{Re} \nu > 0$.

Comparing with Eq.(H.19),

$$\alpha = 1, \quad u = z_c^2 - 1, \quad \mu = 1 - \frac{1}{2} - \frac{\tilde{\beta}}{\pi} = \frac{1}{2} - \frac{\tilde{\beta}}{\pi}, \quad \nu = \frac{1}{2} + \frac{\tilde{\beta}}{\pi}, \quad \lambda = -\frac{1}{2}.$$

Therefore:

$$\begin{aligned}
I_2(\zeta) &= (\zeta^2 - z_c^2 - 1) \cdot \int_{\zeta_1=1}^{z_c} \frac{1}{\kappa_0(\zeta_1) \cdot \sqrt{(\zeta_1^2 - 1)(z_c^2 - \zeta_1^2)}} d\zeta_1 \\
&= \frac{1}{2} (\zeta^2 - z_c^2 - 1) \cdot B\left(\frac{1}{2} - \frac{\tilde{\beta}}{\pi}, \frac{1}{2} + \frac{\tilde{\beta}}{\pi}\right) \cdot {}_2F_1\left(\frac{1}{2}, \frac{1}{2} + \frac{\tilde{\beta}}{\pi}; 1; 1 - z_c^2\right)
\end{aligned} \tag{H.21}$$

where $B(\mu, \nu)$ is the Beta function, and ${}_2F_1(\alpha, \beta; \gamma; z) = F(\alpha, \beta; \gamma; z)$ is Gauss' hypergeometric function, just as in the case of I_1 .

Again using the transformation formula (H.15), comparison with the parameters in (H.21)

gives: $\alpha = \frac{1}{2}$, $\beta = \frac{1}{2} + \frac{\tilde{\beta}}{\pi}$, $\gamma = 1$, $z = 1 - z_c^2$. Therefore, in (H.21): $1 - z = 1 - 1 + z_c^2 = z_c^2$,

$\frac{z}{z-1} = \frac{1 - z_c^2}{-z_c^2} = \frac{z_c^2 - 1}{z_c^2} < 1$, $\gamma - \beta = 1 - \frac{1}{2} - \frac{\tilde{\beta}}{\pi} = \frac{1}{2} - \frac{\tilde{\beta}}{\pi}$, and the hypergeometric function

in (H.21) becomes:

$$F\left(\frac{1}{2}, \frac{1}{2} + \frac{\tilde{\beta}}{\pi}; 1; 1 - z_c^2\right) = (z_c^2)^{-\frac{1}{2}} \cdot F\left(\frac{1}{2}, \frac{1}{2} - \frac{\tilde{\beta}}{\pi}; 1; \frac{z_c^2 - 1}{z_c^2}\right) = \frac{1}{z_c} \cdot F\left(\frac{1}{2}, \frac{1}{2} - \frac{\tilde{\beta}}{\pi}; 1; \frac{z_c^2 - 1}{z_c^2}\right) \quad (\text{H.22})$$

The elemental integral $I_2(\zeta)$ therefore has the following semi-analytical form (see (7.2)):

$$\begin{aligned} I_2(\zeta) &= (\zeta^2 - z_c^2 - 1) \cdot \int_{\zeta_1=1}^{\zeta_1=z_c} \frac{1}{\kappa_0(\zeta_1) \cdot \sqrt{(\zeta_1^2 - 1)(z_c^2 - \zeta_1^2)}} d\zeta_1 \\ &= \frac{1}{2} (\zeta^2 - z_c^2 - 1) \cdot B\left(\frac{1}{2} - \frac{\tilde{\beta}}{\pi}, \frac{1}{2} + \frac{\tilde{\beta}}{\pi}\right) \cdot {}_2F_1\left(\frac{1}{2}, \frac{1}{2} + \frac{\tilde{\beta}}{\pi}; 1; 1 - z_c^2\right) \\ &= \frac{1}{2} (\zeta^2 - z_c^2 - 1) \frac{1}{z_c} \cdot B\left(\frac{1}{2} - \frac{\tilde{\beta}}{\pi}, \frac{1}{2} + \frac{\tilde{\beta}}{\pi}\right) \cdot F\left(\frac{1}{2}, \frac{1}{2} - \frac{\tilde{\beta}}{\pi}; 1; \frac{z_c^2 - 1}{z_c^2}\right) \end{aligned} \quad (\text{H.23})$$

H.3 Elemental Integral $I_3(\zeta)$

For the elemental integral in (H.10), use the same variable transformation again:

$t = \zeta_1^2$ with $d\zeta_1 = \frac{1}{2} \frac{dt}{\sqrt{t}}$. The elemental integral I_3 becomes:

$$I_3(\zeta) = (\zeta^2 - 1)(z_c^2 - \zeta^2) \cdot \frac{1}{2} \int_{t=1}^{z_c^2} t^{\frac{1}{2}} (\zeta^2 - t)^{-1} (t-1)^{-\frac{1}{2} + \frac{\tilde{\beta}}{\pi}} (z_c^2 - t)^{-\frac{1}{2} - \frac{\tilde{\beta}}{\pi}} dt \quad (\text{H.24})$$

A convergent semi-analytical solution for the elemental integral $I_3(\zeta)$ in (H.24) can not be found analytically as for I_1 and $I_2(\zeta)$, but we can develop an approximate

solution for $I_3(\zeta)$ in a numerical form. Because the function $f(t) = \frac{1}{\sqrt{t}}$ in the integral

(H.24) is a slowly-variation function in the region of $1 \leq t \leq z_c^2$, let us assume that

$f(t) = \frac{1}{\sqrt{t}}$ is a piecewise constant function in this region. With this approximation, the

integral in (H.24) can be written in the following form (see Fig. H.1),

$$\begin{aligned} I_3(\zeta) &= (\zeta^2 - 1)(z_c^2 - \zeta^2) \cdot \frac{1}{2} \int_{t=1}^{z_c^2} t^{\frac{1}{2}} (\zeta^2 - t)^{-1} (t-1)^{-\frac{1}{2} + \frac{\tilde{\beta}}{\pi}} (z_c^2 - t)^{-\frac{1}{2} - \frac{\tilde{\beta}}{\pi}} dt \\ &= \frac{1}{2} (\zeta^2 - 1)(z_c^2 - \zeta^2) \times \sum_{j=1}^N \frac{1}{\sqrt{t_j}} \cdot \int_{t_j}^{t_{j+1}} \frac{(t-1)^{-\frac{1}{2} + \frac{\tilde{\beta}}{\pi}} (z_c^2 - t)^{-\frac{1}{2} - \frac{\tilde{\beta}}{\pi}}}{\zeta^2 - t} dt \\ &= -\frac{1}{2} (\zeta^2 - 1)(z_c^2 - \zeta^2) \times \sum_{j=1}^N \frac{1}{\sqrt{t_j}} \cdot \int_{t_j}^{t_{j+1}} \frac{(t-1)^{-\frac{1}{2} + \frac{\tilde{\beta}}{\pi}} (z_c^2 - t)^{-\frac{1}{2} - \frac{\tilde{\beta}}{\pi}}}{t - \zeta^2} dt \end{aligned} \quad (\text{H.25})$$

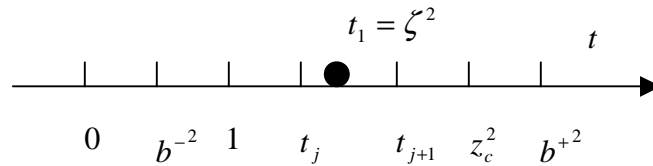


Fig. H.1: Integration elements

In Fig. H.1, $t_1 = \zeta^2$ is the parameter variable of the integral. Define the integral term in (H.25) to be:

$$\Delta I_{3,j}(\zeta) = \int_{t_j}^{t_{j+1}} \frac{(t-1)^{\frac{1}{2} + \frac{\tilde{\beta}}{\pi}} (z_c^2 - t)^{\frac{1}{2} - \frac{\tilde{\beta}}{\pi}}}{t - \zeta^2} dt \quad (\text{H.26})$$

The integral term $\Delta I_{3,j}(\zeta)$ can be computed in different domains of the variable ζ as follows.

Case 1: when $\zeta^2 > t_{j+1}$ (see 4.32)

Define:

$$I_{3,j}^-(\zeta^2) = \int_1^{t_j} \frac{(t-1)^{\frac{1}{2} + \frac{\tilde{\beta}}{\pi}} (z_c^2 - t)^{\frac{1}{2} - \frac{\tilde{\beta}}{\pi}}}{t - \zeta^2} dt \quad (\text{H.27})$$

Therefore,

$$\Delta I_{3,j} = I_{3,j+1}^- - I_{3,j}^- \quad (\text{H.28})$$

Case 2: when $\zeta^2 < t_j$ (see 4.34)

Define:

$$I_{3,j}^+(\zeta^2) = \int_{t_j}^{z_c^2} \frac{(t-1)^{-\frac{1+\tilde{\beta}}{2}\pi} (z_c^2-t)^{-\frac{1-\tilde{\beta}}{2}\pi}}{t-\zeta^2} dt \quad (\text{H.29})$$

Therefore,

$$\Delta I_{3,j} = I_{3,j}^+ - I_{3,j+1}^+ \quad (\text{H.30})$$

Case 3: when $t_j < \zeta^2 < t_{j+1}$

Define :

$$I_{3,0}(\zeta^2) = \int_1^{z_c^2} \frac{(t-1)^{-\frac{1+\tilde{\beta}}{2}\pi} (z_c^2-t)^{-\frac{1-\tilde{\beta}}{2}\pi}}{t-\zeta^2} dt \quad (\text{H.31})$$

Therefore,

$$\Delta I_{3,j} = I_{3,0} - I_{3,j}^- - I_{3,j+1}^+ \quad (\text{H.32})$$

At this point, we have a solution form for the integral I_3 . However, to calculate the terms in (H.27), (H.29) and (H.31), further development is needed to express the integrals in (H.27), (H.29) and (H.31) in terms of semi-analytical functions. The following sections: H3.1 – H3.3 present this development.

H.3.1 Integral $I_{3,0}(\zeta^2)$

For the integral in (H.31), use the definite integral formulas in Gradshteyn and Ryzhik (1965), p290, §3.228. (2):

$$\int_a^b \frac{(x-a)^{\nu-1} (b-x)^{-\nu}}{x-c} dx = -\frac{\pi(c-a)^{\nu-1}}{(b-c)^\nu} \operatorname{ctg}(\nu \cdot \pi) \quad \text{for } a < c < b \ [0 < \operatorname{Re} \nu < 1]$$

Comparing with (H.31), the parameters are: $a=1$, $\nu-1 = -\frac{1}{2} + \frac{\tilde{\beta}}{\pi} \rightarrow \nu = \frac{1}{2} + \frac{\tilde{\beta}}{\pi}$;

$b = z_c^2$, $-\nu = -\frac{1}{2} - \frac{\tilde{\beta}}{\pi} \rightarrow \nu = \frac{1}{2} + \frac{\tilde{\beta}}{\pi}$; $c = \zeta^2$, $1 < \zeta^2 < z_c^2$ which satisfies the condition

of $a < c < b$ [$0 < \operatorname{Re} \nu < 1$]. Therefore,

$$\begin{aligned} I_{3,0}(\zeta^2) &= \int_1^{z_c^2} \frac{(t-1)^{-\frac{1}{2} + \frac{\tilde{\beta}}{\pi}} (z_c^2 - t)^{-\frac{1}{2} - \frac{\tilde{\beta}}{\pi}}}{t - \zeta^2} dt \\ &= -\frac{\pi(\zeta^2 - 1)^{-\frac{1}{2} + \frac{\tilde{\beta}}{\pi}}}{(z_c^2 - \zeta^2)^{\frac{1}{2} + \frac{\tilde{\beta}}{\pi}}} \times \frac{1}{\tan(\frac{\pi}{2} + \tilde{\beta})} \end{aligned} \quad (\text{H.33})$$

Since $\tan(\frac{\pi}{2} + \tilde{\beta}) = -\cot \tilde{\beta}$,

$$I_{3,0}(\zeta^2) = \int_1^{z_c^2} \frac{(t-1)^{-\frac{1}{2} + \frac{\tilde{\beta}}{\pi}} (z_c^2 - t)^{-\frac{1}{2} - \frac{\tilde{\beta}}{\pi}}}{t - \zeta^2} dt = \frac{\pi(\zeta^2 - 1)^{-\frac{1}{2} + \frac{\tilde{\beta}}{\pi}}}{(z_c^2 - \zeta^2)^{\frac{1}{2} + \frac{\tilde{\beta}}{\pi}}} \times \tan \tilde{\beta} \quad 1 < \zeta < z_c \quad (\text{H.34})$$

H.3.2 Integral $I_{3,j}^-(\zeta^2)$

For the integral term in (H.27), defining the variable transformation $x = t - 1$, $t = x + 1$, with $dx = dt$. Then (H.27) becomes,

$$I_{3,j}^-(\zeta^2) = \int_{x=0}^{t_j-1} \frac{x^{\frac{1}{2} + \frac{\tilde{\beta}}{\pi}} (z_c^2 - 1 - x)^{\frac{1}{2} - \frac{\tilde{\beta}}{\pi}}}{x + 1 - \zeta^2} dx \quad (\text{H.35})$$

Define a second transformation:

$$y = \frac{x}{t_j - 1}, \quad x = (t_j - 1)y, \quad dx = (t_j - 1)dy, \quad x + 1 = 1 + (t_j - 1)y \quad (\text{H.36})$$

The above integral, (H.35), becomes,

$$\begin{aligned} I_{3,j}^-(\zeta^2) &= (t_j - 1)^{\frac{1}{2} + \frac{\tilde{\beta}}{\pi}} \cdot (t_j - 1) \cdot \int_{y=0}^1 \frac{y^{\frac{1}{2} + \frac{\tilde{\beta}}{\pi}} [z_c^2 - 1 - (t_j - 1)y]^{\frac{1}{2} - \frac{\tilde{\beta}}{\pi}}}{(t_j - 1)y - (\zeta^2 - 1)} dy \\ &= -(t_j - 1)^{\frac{1}{2} + \frac{\tilde{\beta}}{\pi}} \cdot (t_j - 1) \cdot (\zeta^2 - 1)^{-1} (z_c^2 - 1)^{\frac{1}{2} - \frac{\tilde{\beta}}{\pi}} \int_{y=0}^1 \frac{y^{\frac{1}{2} + \frac{\tilde{\beta}}{\pi}} [1 - \frac{(t_j - 1)}{z_c^2 - 1} y]^{\frac{1}{2} - \frac{\tilde{\beta}}{\pi}}}{1 - \frac{t_j - 1}{\zeta^2 - 1} y} dy \\ &= -\frac{(t_j - 1)^{\frac{1}{2} + \frac{\tilde{\beta}}{\pi}} \cdot (z_c^2 - 1)^{\frac{1}{2} - \frac{\tilde{\beta}}{\pi}}}{\zeta^2 - 1} \times \int_{y=0}^1 \frac{y^{\frac{1}{2} + \frac{\tilde{\beta}}{\pi}} [1 - \frac{(t_j - 1)}{z_c^2 - 1} y]^{\frac{1}{2} - \frac{\tilde{\beta}}{\pi}}}{1 - \frac{t_j - 1}{\zeta^2 - 1} y} dy \end{aligned} \quad (\text{H.37})$$

From Gradshteyn and Ryzhik (1965), p287, §3.211:

$$\int_0^1 x^{\lambda-1} (1-x)^{\mu-1} (1-ux)^{-\rho} (1-vx)^{-\sigma} dx = B(\mu, \lambda) F_1(\lambda, \rho, \sigma, \lambda + \mu; u, v) \quad (\text{H.38})$$

where $\text{Re } \mu > 0$, $\text{Re } \lambda > 0$.

Comparing with (H.37), the parameters are:

$$\lambda^- - 1 = -\frac{1}{2} + \frac{\tilde{\beta}}{\pi} \rightarrow \lambda^- = \frac{1}{2} + \frac{\tilde{\beta}}{\pi}; \quad \mu - 1 = 0 \rightarrow \mu = 1; \quad -\rho = -1 \rightarrow \rho = 1;$$

$$-\sigma = -\frac{1}{2} - \frac{\tilde{\beta}}{\pi} \rightarrow \sigma = \frac{1}{2} + \frac{\tilde{\beta}}{\pi} = \lambda^-; \quad u = \frac{t_j - 1}{\zeta^2 - 1}, \quad v = \frac{t_j - 1}{z_c^2 - 1}$$

The condition of $\text{Re } \lambda > 0$, $\text{Re } \mu > 0$ is satisfied. Therefore,

$$\begin{aligned} I_{3,j}^-(\zeta^2) &= -\frac{(t_j - 1)^{\frac{1}{2} + \frac{\tilde{\beta}}{\pi}} \cdot (z_c^2 - 1)^{-\frac{1}{2} - \frac{\tilde{\beta}}{\pi}}}{\zeta^2 - 1} \times \int_{y=0}^1 \frac{y^{\frac{1}{2} + \frac{\tilde{\beta}}{\pi}} [1 - \frac{(t_j - 1)}{z_c^2 - 1} y]^{\frac{1}{2} - \frac{\tilde{\beta}}{\pi}}}{1 - \frac{t_j - 1}{\zeta^2 - 1} y} dy \\ &= -\frac{(t_j - 1)^{\frac{1}{2} + \frac{\tilde{\beta}}{\pi}} \cdot (z_c^2 - 1)^{-\frac{1}{2} - \frac{\tilde{\beta}}{\pi}}}{\zeta^2 - 1} \times B(1, \lambda^-) \cdot F_1(\lambda^-, 1, \lambda^-, \lambda^- + 1, u, v) \end{aligned} \quad (\text{H.39})$$

where $B(\mu, \nu)$ is again the Beta function, and $F_1(\alpha, \beta; \beta', \gamma; x, y)$ is Hypergeometric function of two variables.

$$B(1, \lambda^-) = \frac{\Gamma(\lambda^-) \Gamma(1)}{\Gamma(\lambda^- + 1)} = \frac{\Gamma(\lambda^-)}{\lambda^- \Gamma(\lambda^-)} = \frac{1}{\lambda^-} \quad (\text{H.40})$$

From Gradshteyn and Ryzhik (1965), p1054, §9.182.1, the transformation of the Hypergeometric function of two variables to Gauss's hypergeometric function (of one variable) is the following formula,

$$F_1(\alpha, \beta, \beta', \beta + \beta'; x, y) = (1 - y)^{-\alpha} F(\alpha, \beta, \beta + \beta'; \frac{x - y}{1 - y}) \quad (\text{H.41})$$

Since,

$$\begin{aligned} 1 - y &= 1 - \frac{t_j - 1}{z_c^2 - 1} = \frac{z_c^2 - 1 - t_j + 1}{z_c^2 - 1} = \frac{z_c^2 - t_j}{z_c^2 - 1} \\ x - y &= \frac{t_j - 1}{\zeta^2 - 1} - \frac{t_j - 1}{z_c^2 - 1} = (t_j - 1) \left[\frac{1}{\zeta^2 - 1} - \frac{1}{z_c^2 - 1} \right] = (t_j - 1) \frac{z_c^2 - \zeta^2}{(\zeta^2 - 1)(z_c^2 - 1)} \\ \frac{x - y}{1 - y} &= (t_j - 1) \frac{z_c^2 - \zeta^2}{(\zeta^2 - 1)(z_c^2 - 1)} \cdot \frac{z_c^2 - 1}{z_c^2 - t_j} = \frac{t_j - 1}{\zeta^2 - 1} \cdot \frac{z_c^2 - \zeta^2}{z_c^2 - t_j} < 1 \end{aligned} \quad (\text{H.42})$$

Therefore, $\lambda^- = \frac{1}{2} + \frac{\tilde{\beta}}{\pi}$

$$F_1(\lambda^-, 1, \lambda^-, \lambda^- + 1, u, v) = \left(\frac{z_c^2 - t_j}{z_c^2 - 1} \right)^{-\left(\frac{1}{2} + \frac{\tilde{\beta}}{\pi}\right)} F\left(\frac{1}{2} + \frac{\tilde{\beta}}{\pi}, 1, \frac{3}{2} + \frac{\tilde{\beta}}{\pi}; \frac{t_j - 1}{\zeta^2 - 1} \cdot \frac{z_c^2 - \zeta^2}{z_c^2 - t_j}\right) \quad (\text{H.43})$$

Substituting the above equations into (H.39):

$$\begin{aligned}
I_{3,j}^-(\zeta^2) &= -\frac{(t_j-1)^{\frac{1}{2}+\frac{\tilde{\beta}}{\pi}} \cdot (z_c^2-1)^{-\frac{1}{2}-\frac{\tilde{\beta}}{\pi}}}{\zeta^2-1} \times \frac{1}{\lambda^-} \cdot \left(\frac{z_c^2-t_j}{z_c^2-1}\right)^{-\left(\frac{1}{2}+\frac{\tilde{\beta}}{\pi}\right)} \\
&\quad \times F\left(\frac{1}{2}+\frac{\tilde{\beta}}{\pi}, 1, \frac{3}{2}+\frac{\tilde{\beta}}{\pi}; \frac{t_j-1}{\zeta^2-1} \cdot \frac{z_c^2-\zeta^2}{z_c^2-t_j}\right) \\
&= -\frac{1}{\zeta^2-1} \frac{(t_j-1)^{\frac{1}{2}+\frac{\tilde{\beta}}{\pi}}}{(z_c^2-t_j)^{\frac{1}{2}+\frac{\tilde{\beta}}{\pi}}} \times \frac{1}{\lambda^-} \cdot F\left(\frac{1}{2}+\frac{\tilde{\beta}}{\pi}, 1, \frac{3}{2}+\frac{\tilde{\beta}}{\pi}; \frac{t_j-1}{\zeta^2-1} \cdot \frac{z_c^2-\zeta^2}{z_c^2-t_j}\right)
\end{aligned}$$

Therefore,

$$\begin{aligned}
I_{3,j}^-(\zeta^2) &= \int_1^{t_j} \frac{(t-1)^{\frac{1}{2}+\frac{\tilde{\beta}}{\pi}} (z_c^2-t)^{-\frac{1}{2}-\frac{\tilde{\beta}}{\pi}}}{t-\zeta^2} dt \\
&= -\frac{1}{\zeta^2-1} \frac{(t_j-1)^{\frac{1}{2}+\frac{\tilde{\beta}}{\pi}}}{(z_c^2-t_j)^{\frac{1}{2}+\frac{\tilde{\beta}}{\pi}}} \times \frac{1}{\lambda^-} \cdot F\left(\frac{1}{2}+\frac{\tilde{\beta}}{\pi}, 1, \frac{3}{2}+\frac{\tilde{\beta}}{\pi}; \frac{t_j-1}{\zeta^2-1} \cdot \frac{z_c^2-\zeta^2}{z_c^2-t_j}\right)
\end{aligned}$$

$\zeta^2 > t_{j+1}$ (H.44)

H.3.3 Integral $I_{3,j}^+(\zeta^2)$

For the integral in (H.29), define the variable transformation $x = z_c^2 - t$,

$t = z_c^2 - x$, with $dx = -dt$. Then (H.29) becomes,

$$\begin{aligned}
I_{3,j}^+(\zeta^2) &= -\int_{x=z_c^2-t_j}^0 \frac{x^{-\frac{1}{2}-\frac{\tilde{\beta}}{\pi}} (z_c^2-1-x)^{-\frac{1}{2}+\frac{\tilde{\beta}}{\pi}}}{z_c^2-\zeta^2-x} dx \\
&= \int_{x=0}^{z_c^2-t_j} \frac{x^{-\frac{1}{2}-\frac{\tilde{\beta}}{\pi}} (z_c^2-1-x)^{-\frac{1}{2}+\frac{\tilde{\beta}}{\pi}}}{z_c^2-\zeta^2-x} dx
\end{aligned}$$

(H.45)

Define another transformation,

$$y = \frac{x}{z_c^2 - t_j}, \quad x = (z_c^2 - t_j)y, \quad dx = (z_c^2 - t_j)dy, \quad (\text{H.46})$$

The above integral, (H.45), becomes,

$$\begin{aligned} I_{3,j}^+(\zeta^2) &= \int_{x=0}^{z_c^2 - t_j} \frac{x^{-\frac{1}{2} + \frac{\tilde{\beta}}{\pi}} (z_c^2 - 1 - x)^{-\frac{1}{2} + \frac{\tilde{\beta}}{\pi}}}{z_c^2 - \zeta^2 - x} dx \\ &= (z_c^2 - t_j)^{\frac{1}{2} + \frac{\tilde{\beta}}{\pi}} \cdot (z_c^2 - t_j) \cdot \int_{y=0}^1 \frac{y^{-\frac{1}{2} + \frac{\tilde{\beta}}{\pi}} [z_c^2 - 1 - (z_c^2 - t_j)y]^{-\frac{1}{2} + \frac{\tilde{\beta}}{\pi}}}{z_c^2 - \zeta^2 - (z_c^2 - t_j)y} dy \\ &= (z_c^2 - t_j)^{\frac{1}{2} + \frac{\tilde{\beta}}{\pi}} \cdot (z_c^2 - 1)^{\frac{1}{2} + \frac{\tilde{\beta}}{\pi}} \cdot (z_c^2 - \zeta^2)^{-1} \int_{y=0}^1 \frac{y^{-\frac{1}{2} + \frac{\tilde{\beta}}{\pi}} [1 - \frac{(z_c^2 - t_j)}{z_c^2 - 1} y]^{-\frac{1}{2} + \frac{\tilde{\beta}}{\pi}}}{1 - \frac{z_c^2 - t_j}{z_c^2 - \zeta^2} y} dy \\ &= \frac{1}{z_c^2 - \zeta^2} \cdot (z_c^2 - t_j)^{\frac{1}{2} + \frac{\tilde{\beta}}{\pi}} \cdot (z_c^2 - 1)^{\frac{1}{2} + \frac{\tilde{\beta}}{\pi}} \int_{y=0}^1 \frac{y^{-\frac{1}{2} + \frac{\tilde{\beta}}{\pi}} [1 - \frac{(z_c^2 - t_j)}{z_c^2 - 1} y]^{-\frac{1}{2} + \frac{\tilde{\beta}}{\pi}}}{1 - \frac{z_c^2 - t_j}{z_c^2 - \zeta^2} y} dy \end{aligned} \quad (\text{H.47})$$

From Gradshteyn and I. M. Ryzhik (1965), p287, §3.211:

$$\int_0^1 x^{\lambda-1} (1-x)^{\mu-1} (1-ux)^{-\rho} (1-vx)^{-\sigma} dx = B(\mu, \lambda) F_1(\lambda, \rho, \sigma, \lambda + \mu; u, v) \quad (\text{H.48})$$

where $\text{Re } \mu > 0$, $\text{Re } \lambda > 0$.

Compare with (H.47) with (H.48):

$$\lambda^+ - 1 = -\frac{1}{2} - \frac{\tilde{\beta}}{\pi} \rightarrow \lambda^+ = \frac{1}{2} - \frac{\tilde{\beta}}{\pi}; \quad \mu - 1 = 0 \rightarrow \mu = 1; \quad -\rho = -1 \rightarrow \rho = 1;$$

$$-\sigma = -\frac{1}{2} + \frac{\tilde{\beta}}{\pi} \rightarrow \sigma = \frac{1}{2} - \frac{\tilde{\beta}}{\pi} = \lambda^+; \quad u = \frac{z_c^2 - t_j}{z_c^2 - \zeta^2} < 1, \quad v = \frac{z_c^2 - t_j}{z_c^2 - 1} < 1$$

The condition of $\operatorname{Re} \lambda > 0$, $\operatorname{Re} \mu > 0$ satisfied. Therefore:

$$\begin{aligned} I_{3,j}^+(\zeta^2) &= \frac{1}{z_c^2 - \zeta^2} \cdot (z_c^2 - t_j)^{\frac{1}{2} \frac{\tilde{\beta}}{\pi}} \cdot (z_c^2 - 1)^{-\frac{1}{2} + \frac{\tilde{\beta}}{\pi}} \int_{y=0}^1 \frac{y^{\frac{1}{2} \frac{\tilde{\beta}}{\pi}} [1 - \frac{(z_c^2 - t_j)}{z_c^2 - 1} y]^{\frac{1}{2} + \frac{\tilde{\beta}}{\pi}}}{1 - \frac{z_c^2 - t_j}{z_c^2 - \zeta^2} y} dy \\ &= \frac{1}{z_c^2 - \zeta^2} \cdot (z_c^2 - t_j)^{\frac{1}{2} \frac{\tilde{\beta}}{\pi}} \cdot (z_c^2 - 1)^{-\frac{1}{2} + \frac{\tilde{\beta}}{\pi}} \times B(1, \lambda^+) \cdot F_1(\lambda^+, 1, \lambda^+, \lambda^+ + 1, u, v) \end{aligned}$$

(H.49)

where $B(\mu, \nu)$ is the Beta function, and $F_1(\alpha, \beta; \beta', \gamma; x, y)$ is Hypergeometric function of two variables. Again:

$$B(1, \lambda^+) = \frac{\Gamma(\lambda^+) \Gamma(1)}{\Gamma(\lambda^+ + 1)} = \frac{\Gamma(\lambda^+)}{\lambda^+ \Gamma(\lambda^+)} = \frac{1}{\lambda^+} \quad (\text{H.50})$$

Using the same integral transform as in (H.41), the parameters now are:

$$1 - y = 1 - \frac{z_c^2 - t_j}{z_c^2 - 1} = \frac{z_c^2 - 1 - z_c^2 + t_j}{z_c^2 - 1} = \frac{t_j - 1}{z_c^2 - 1}$$

$$\begin{aligned}
 x - y &= \frac{z_c^2 - t_j}{z_c^2 - \zeta^2} - \frac{z_c^2 - t_j}{z_c^2 - 1} = (z_c^2 - t_j) \left[\frac{1}{z_c^2 - \zeta^2} - \frac{1}{z_c^2 - 1} \right] = (z_c^2 - t_j) \frac{\zeta^2 - 1}{(z_c^2 - \zeta^2)(z_c^2 - 1)} \\
 \frac{x - y}{1 - y} &= (z_c^2 - t_j) \frac{\zeta^2 - 1}{(z_c^2 - \zeta^2)(z_c^2 - 1)} \cdot \frac{z_c^2 - 1}{t_j - 1} = \frac{z_c^2 - t_j}{z_c^2 - \zeta^2} \cdot \frac{\zeta^2 - 1}{t_j - 1} < 1
 \end{aligned} \tag{H.51}$$

and, $\lambda^+ = \frac{1}{2} - \frac{\tilde{\beta}}{\pi}$. Thus the hypergeometric function in (H.49) is,

$$F_1(\lambda^+, 1, \lambda^+, \lambda^+ + 1, u, v) = \left(\frac{t_j - 1}{z_c^2 - 1} \right)^{-\left(\frac{1}{2} - \frac{\tilde{\beta}}{\pi}\right)} F(\lambda^+, 1, \lambda^+ + 1; \frac{z_c^2 - t_j}{z_c^2 - z^2} \cdot \frac{\zeta^2 - 1}{t_j - 1}) \tag{H.52}$$

Substituting the above equations into (H.49), the integral $I_{3,j}^+(\zeta^2)$ is as follows:

$$\begin{aligned}
 I_{3,j}^+(\zeta^2) &= \frac{1}{z_c^2 - \zeta^2} \cdot (z_c^2 - t_j)^{\frac{1}{2} \frac{\tilde{\beta}}{\pi}} \cdot (z_c^2 - 1)^{-\frac{1}{2} + \frac{\tilde{\beta}}{\pi}} \times B(1, \lambda^+) \cdot F_1(\lambda^+, 1, \lambda^+, \lambda^+ + 1, u, v) \\
 &= \frac{1}{z_c^2 - \zeta^2} \cdot (z_c^2 - t_j)^{\frac{1}{2} \frac{\tilde{\beta}}{\pi}} \cdot (z_c^2 - 1)^{-\frac{1}{2} + \frac{\tilde{\beta}}{\pi}} \\
 &\quad \times \frac{1}{\lambda^+} \cdot \left(\frac{t_j - 1}{z_c^2 - 1} \right)^{-\left(\frac{1}{2} - \frac{\tilde{\beta}}{\pi}\right)} F(\lambda^+, 1, \lambda^+ + 1; \frac{z_c^2 - t_j}{z_c^2 - \zeta^2} \cdot \frac{\zeta^2 - 1}{t_j - 1}) \\
 &= \frac{1}{z_c^2 - \zeta^2} \cdot \frac{(z_c^2 - t_j)^{\frac{1}{2} \frac{\tilde{\beta}}{\pi}}}{(t_j - 1)^{\frac{1}{2} \frac{\tilde{\beta}}{\pi}}} \times \frac{1}{\lambda^+} \cdot F(\lambda^+, 1, \lambda^+ + 1; \frac{z_c^2 - t_j}{z_c^2 - \zeta^2} \cdot \frac{\zeta^2 - 1}{t_j - 1})
 \end{aligned}$$

Therefore,

$$\begin{aligned}
I_{3,j}^+(\zeta^2) &= \int_{t_j}^{z_c^2} \frac{(t-1)^{-\frac{1+\tilde{\beta}}{2}\pi} (z_c^2-t)^{-\frac{1-\tilde{\beta}}{2}\pi}}{t-\zeta^2} dt \\
&= \frac{1}{z_c^2-\zeta^2} \cdot \frac{(z_c^2-t_j)^{\frac{1-\tilde{\beta}}{2}\pi}}{(t_j-1)^{\frac{1+\tilde{\beta}}{2}\pi}} \times \frac{1}{\lambda^+} \cdot F(\lambda^+, 1, \lambda^++1; \frac{z_c^2-t_j}{z_c^2-\zeta^2}, \frac{\zeta^2-1}{t_j-1}) \\
&\qquad\qquad\qquad \zeta^2 < t_j \quad (\text{H.53})
\end{aligned}$$

At this point, all derivations required in the I_3 term computation, (H.10), have been completed. In next section, the final form of the fundamental integral $\Lambda(\zeta)$ will be given based on the above derivations.

H.4 Fundamental Integral $\Lambda(\zeta)$ in the Region of $1 \leq \zeta \leq z_c$

The integral $\Lambda(\zeta)$ can be expressed in terms of the above as,

$$\begin{aligned}
\Lambda(\zeta) &= \int_{\zeta_1=1}^{z_c} \frac{d\zeta_1}{\mathcal{X}(\zeta_1)(\zeta^2-\zeta_1^2)} \\
&= I_1 + I_2 + I_3 \\
&= \frac{1}{2} z_c \cdot B\left(\frac{1}{2} - \frac{\tilde{\beta}}{\pi}, \frac{1}{2} + \frac{\tilde{\beta}}{\pi}\right) \cdot F\left(-\frac{1}{2}, \frac{1}{2} - \frac{\tilde{\beta}}{\pi}; 1; \frac{z_c^2-1}{z_c^2}\right) \\
&\quad + \frac{1}{2} (\zeta^2 - z_c^2 - 1) \frac{1}{z_c} \cdot B\left(\frac{1}{2} - \frac{\tilde{\beta}}{\pi}, \frac{1}{2} + \frac{\tilde{\beta}}{\pi}\right) \cdot F\left(\frac{1}{2}, \frac{1}{2} - \frac{\tilde{\beta}}{\pi}; 1; \frac{z_c^2-1}{z_c^2}\right) \\
&\quad - \frac{1}{2} (\zeta^2 - 1)(z_c^2 - \zeta^2) \times \sum_{j=1}^L \frac{1}{\sqrt{t_j}} \cdot \Delta I_{3,j}(\zeta) \\
&\qquad\qquad\qquad 1 \leq \zeta \leq z_c \quad (\text{H.54})
\end{aligned}$$

with the $\Delta I_{3,j}(\zeta)$ term as:

- **Case 1:** $\zeta^2 > t_{j+1}$

$$\Delta I_{3,j} = I_{3,j+1}^- - I_{3,j}^- \quad (\text{H.55})$$

$$I_{3,j}^-(\zeta^2) = -\frac{1}{\zeta^2 - 1} \frac{(t_j - 1)^{\frac{1+\tilde{\beta}}{2}}}{(z_c^2 - t_j)^{\frac{1+\tilde{\beta}}{2}}} \times \frac{1}{\lambda^-} \cdot F\left(\frac{1}{2} + \frac{\tilde{\beta}}{\pi}, 1, \frac{3}{2} + \frac{\tilde{\beta}}{\pi}; \frac{t_j - 1}{\zeta^2 - 1} \cdot \frac{z_c^2 - \zeta^2}{z_c^2 - t_j}\right)$$

$$\zeta^2 > t_{j+1} \quad (\text{H.56})$$

- **Case 2:** $\zeta^2 < t_j$

$$\Delta I_{3,j} = I_{3,j}^+ - I_{3,j+1}^+ \quad (\text{H.57})$$

$$I_{3,j}^+(\zeta^2) = \frac{1}{z_c^2 - \zeta^2} \cdot \frac{(z_c^2 - t_j)^{\frac{1+\tilde{\beta}}{2}}}{(t_j - 1)^{\frac{1+\tilde{\beta}}{2}}} \times \frac{1}{\lambda^+} \cdot F\left(\lambda^+, 1, \lambda^+ + 1; \frac{z_c^2 - t_j}{z_c^2 - \zeta^2} \cdot \frac{\zeta^2 - 1}{t_j - 1}\right)$$

$$\zeta^2 < t_j \quad (\text{H.58})$$

- **Case 3:** $t_j < \zeta^2 < t_{j+1}$

$$\Delta I_{3,j} = I_{3,0} - I_{3,j}^- - I_{3,j+1}^+ \quad (\text{H.59})$$

$$I_{3,0}(\zeta^2) = \frac{\pi(\zeta^2 - 1)^{\frac{1+\tilde{\beta}}{2}}}{(z_c^2 - \zeta^2)^{\frac{1+\tilde{\beta}}{2}}} \times \tan \tilde{\beta} \quad 1 < \zeta < z_c \quad (\text{H.60})$$

As discussed at the beginning of this Appendix, the formulation in this section for $\Lambda(\zeta)$ can be applied to the formulation of the fundamental integrals in (4.24) and (4.25).

The next sections are the applications.

H.5 Fundamental Integral $\Lambda^-(\zeta_0)$ in the region of $b^- \leq \zeta_0 \leq 1$

Define,

$$\Lambda^-(\zeta_0) = \int_{\zeta_1=1}^{\zeta_c} \frac{d\zeta_1}{\chi(\zeta_1)(\zeta_0^2 - \zeta_1^2)} \quad b^- \leq \zeta_0 \leq 1 \quad (\text{H.61})$$

In the region of $b^- \leq \zeta_0 \leq 1$, the integral is,

$$\begin{aligned} \Lambda^-(\zeta_0) &= \int_{\zeta_1=1}^{\zeta_c} \frac{d\zeta_1}{\chi(\zeta_1)(\zeta_0^2 - \zeta_1^2)} \\ &= I_1 + I_2 + I_3 \\ &= \frac{1}{2} z_c \cdot B\left(\frac{1}{2} - \frac{\tilde{\beta}}{\pi}, \frac{1}{2} + \frac{\tilde{\beta}}{\pi}\right) \cdot F\left(-\frac{1}{2}, \frac{1}{2} - \frac{\tilde{\beta}}{\pi}; 1; \frac{z_c^2 - 1}{z_c}\right) \\ &\quad + \frac{1}{2} (\zeta_0^2 - z_c^2 - 1) \frac{1}{z_c} \cdot B\left(\frac{1}{2} - \frac{\tilde{\beta}}{\pi}, \frac{1}{2} + \frac{\tilde{\beta}}{\pi}\right) \cdot F\left(\frac{1}{2}, \frac{1}{2} - \frac{\tilde{\beta}}{\pi}; 1; \frac{z_c^2 - 1}{z_c}\right) \\ &\quad - \frac{1}{2} (\zeta_0^2 - 1)(z_c^2 - \zeta_0^2) \times \sum_{j=1}^L \frac{1}{\sqrt{t_j}} \cdot \Delta I_{3,j}(\zeta_0) \end{aligned}$$

$$b^- \leq \zeta_0 \leq 1, \quad 1 < t_j < z_c^2 \quad (\text{H.62})$$

where $\zeta_0^2 \leq 1 < t_j$. Apply the case 2 formulation,

$$\Delta I_{3,j} = I_{3,j}^+ - I_{3,j+1}^+ \quad (\text{H.63})$$

where

$$I_{3,j}^+(\zeta_0^2) = \frac{1}{z_c^2 - \zeta_0^2} \cdot \frac{(z_c^2 - t_j)^{\frac{1}{2} \frac{\tilde{\beta}}{\pi}}}{(t_j - 1)^{\frac{1}{2} \frac{\tilde{\beta}}{\pi}}} \times \frac{1}{\lambda^+} \cdot F(\lambda^+, 1, \lambda^+ + 1; \frac{z_c^2 - t_j}{z_c^2 - \zeta_0^2}, \frac{\zeta_0^2 - 1}{t_j - 1})$$

$$\zeta_0^2 \leq 1 < t_j, \quad 1 < t_j < z_c^2 \quad (\text{H.64})$$

Re-grouping,

$$\begin{aligned} \Lambda^-(\zeta_0) &= \int_{\zeta_1=1}^{z_c} \frac{d\zeta_1}{\mathcal{X}(\zeta_1)(\zeta_0^2 - \zeta_1^2)} \\ &= \frac{1}{2} z_c \cdot B\left(\frac{1}{2} - \frac{\tilde{\beta}}{\pi}, \frac{1}{2} + \frac{\tilde{\beta}}{\pi}\right) \cdot F\left(-\frac{1}{2}, \frac{1}{2} - \frac{\tilde{\beta}}{\pi}; 1; \frac{z_c^2 - 1}{z_c^2}\right) \\ &\quad + \frac{1}{2} (\zeta_0^2 - z_c^2 - 1) \frac{1}{z_c} \cdot B\left(\frac{1}{2} - \frac{\tilde{\beta}}{\pi}, \frac{1}{2} + \frac{\tilde{\beta}}{\pi}\right) \cdot F\left(\frac{1}{2}, \frac{1}{2} - \frac{\tilde{\beta}}{\pi}; 1; \frac{z_c^2 - 1}{z_c^2}\right) \\ &\quad - \frac{1}{2} (\zeta_0^2 - 1) \times \sum_{j=1}^L \frac{1}{\sqrt{t_j}} \cdot [\Lambda_{3,j}^+(\zeta_0) - \Lambda_{3,j+1}^+(\zeta_0)] \end{aligned}$$

$$b^- \leq \zeta_0 \leq 1, \quad 1 < t_j < z_c^2 \quad (\text{H.65})$$

where,

$$\Lambda_{3,j}^+(\zeta_0^2) = \frac{(z_c^2 - t_j)^{\frac{1}{2} \frac{\tilde{\beta}}{\pi}}}{(t_j - 1)^{\frac{1}{2} \frac{\tilde{\beta}}{\pi}}} \times \frac{1}{\lambda^+} \cdot F(\lambda^+, 1, \lambda^+ + 1; \frac{z_c^2 - t_j}{z_c^2 - \zeta_0^2}, \frac{\zeta_0^2 - 1}{t_j - 1})$$

$$\zeta_0^2 \leq 1 < t_j, \quad 1 < t_j < z_c^2 \quad (\text{H.66})$$

Therefore, the $\Lambda^-(\zeta_0) - \Lambda(\zeta)$ term in (4.26) and (4.27) of Chapter 4 will be,

$$\begin{aligned}
\Lambda^-(\zeta_0) - \Lambda(\zeta) &= \frac{1}{2} z_c \cdot B\left(\frac{1}{2} - \frac{\tilde{\beta}}{\pi}, \frac{1}{2} + \frac{\tilde{\beta}}{\pi}\right) \cdot F\left(-\frac{1}{2}, \frac{1}{2} - \frac{\tilde{\beta}}{\pi}; 1; \frac{z_c^2 - 1}{z_c^2}\right) \\
&+ \frac{1}{2} (\zeta_0^2 - z_c^2 - 1) \frac{1}{z_c} \cdot B\left(\frac{1}{2} - \frac{\tilde{\beta}}{\pi}, \frac{1}{2} + \frac{\tilde{\beta}}{\pi}\right) \cdot F\left(\frac{1}{2}, \frac{1}{2} - \frac{\tilde{\beta}}{\pi}; 1; \frac{z_c^2 - 1}{z_c^2}\right) \\
&- \frac{1}{2} (\zeta_0^2 - 1) \times \sum_{j=1}^L \frac{1}{\sqrt{t_j}} \cdot (\Lambda_{3,j}^+ - \Lambda_{3,j+1}^+) \\
&- \left\{ \frac{1}{2} z_c \cdot B\left(\frac{1}{2} - \frac{\tilde{\beta}}{\pi}, \frac{1}{2} + \frac{\tilde{\beta}}{\pi}\right) \cdot F\left(-\frac{1}{2}, \frac{1}{2} - \frac{\tilde{\beta}}{\pi}; 1; \frac{z_c^2 - 1}{z_c^2}\right) \right. \\
&+ \frac{1}{2} (\zeta^2 - z_c^2 - 1) \frac{1}{z_c} \cdot B\left(\frac{1}{2} - \frac{\tilde{\beta}}{\pi}, \frac{1}{2} + \frac{\tilde{\beta}}{\pi}\right) \cdot F\left(\frac{1}{2}, \frac{1}{2} - \frac{\tilde{\beta}}{\pi}; 1; \frac{z_c^2 - 1}{z_c^2}\right) \\
&- \left. \frac{1}{2} (\zeta^2 - 1)(z_c^2 - \zeta^2) \times \sum_{j=1}^L \frac{1}{\sqrt{t_j}} \cdot \Delta I_{3,j} \right\} \\
&= \frac{1}{2} (\zeta_0^2 - \zeta^2) \frac{1}{z_c} \cdot B\left(\frac{1}{2} - \frac{\tilde{\beta}}{\pi}, \frac{1}{2} + \frac{\tilde{\beta}}{\pi}\right) \cdot F\left(\frac{1}{2}, \frac{1}{2} - \frac{\tilde{\beta}}{\pi}; 1; \frac{z_c^2 - 1}{z_c^2}\right) \\
&- \frac{1}{2} (\zeta_0^2 - 1) \times \sum_{j=1}^L \frac{1}{\sqrt{t_j}} \cdot [\Lambda_{3,j}^+(\zeta_0) - \Lambda_{3,j+1}^+(\zeta_0)] \\
&+ \frac{1}{2} (\zeta^2 - 1)(z_c^2 - \zeta^2) \times \sum_{j=1}^L \frac{1}{\sqrt{t_j}} \cdot \Delta I_{3,j}(\zeta)
\end{aligned}$$

$$1 \leq \zeta \leq z_c, \quad b^- \leq \zeta_0 \leq 1, \quad \zeta_0^2 \leq 1 < t_j, \quad 1 < t_j < z_c^2 \quad (\text{H.67})$$

H.6 Fundamental integral $\Lambda^+(\zeta_0)$ in the region of $z_c \leq \zeta_0 \leq b^+$

Define,

$$\Lambda^+(\zeta_0) = \int_{\zeta_1=1}^{z_c} \frac{d\zeta_1}{\chi(\zeta)(\zeta_0^2 - \zeta_1^2)} \quad z_c \leq \zeta_0 \leq b^+ \quad (\text{H.68})$$

In the region of $z_c \leq \zeta_0 \leq b^+$, the integral is,

$$\begin{aligned}
\Lambda^+(\zeta_0) &= \int_{\zeta_1=1}^{\zeta_c} \frac{d\zeta_1}{\mathcal{X}(\zeta_1)(\zeta_0^2 - \zeta_1^2)} \\
&= I_1 + I_2 + I_3 \\
&= \frac{1}{2} z_c \cdot B\left(\frac{1}{2} - \frac{\tilde{\beta}}{\pi}, \frac{1}{2} + \frac{\tilde{\beta}}{\pi}\right) \cdot F\left(-\frac{1}{2}, \frac{1}{2} - \frac{\tilde{\beta}}{\pi}; 1; \frac{z_c^2 - 1}{z_c^2}\right) \\
&\quad + \frac{1}{2} (\zeta_0^2 - z_c^2 - 1) \frac{1}{z_c} \cdot B\left(\frac{1}{2} - \frac{\tilde{\beta}}{\pi}, \frac{1}{2} + \frac{\tilde{\beta}}{\pi}\right) \cdot F\left(\frac{1}{2}, \frac{1}{2} - \frac{\tilde{\beta}}{\pi}; 1; \frac{z_c^2 - 1}{z_c^2}\right) \\
&\quad - \frac{1}{2} (\zeta_0^2 - 1)(z_c^2 - \zeta_0^2) \times \sum_{j=1}^L \frac{1}{\sqrt{t_j}} \cdot \Delta I_{3,j}(\zeta_0)
\end{aligned}$$

$$z_c \leq \zeta_0 \leq b^+, \quad 1 < t_j < z_c^2 \quad (\text{H.69})$$

where $\zeta_0^2 \geq z_c^2 > t_{j+1}$. Apply the case 1 formulation,

$$\Delta I_{3,j} = I_{3,j+1}^- - I_{3,j}^- \quad (\text{H.70})$$

$$\begin{aligned}
I_{3,j}^-(\zeta_0^2) &= -\frac{1}{\zeta_0^2 - 1} \frac{(t_j - 1)^{\frac{1}{2} + \frac{\tilde{\beta}}{\pi}}}{(z_c^2 - t_j)^{\frac{1}{2} + \frac{\tilde{\beta}}{\pi}}} \times \frac{1}{\lambda^-} \cdot F\left(\frac{1}{2} + \frac{\tilde{\beta}}{\pi}, 1, \frac{3}{2} + \frac{\tilde{\beta}}{\pi}; \frac{t_j - 1}{\zeta_0^2 - 1}, \frac{z_c^2 - \zeta_0^2}{z_c^2 - t_j}\right)
\end{aligned}$$

$$\zeta_0^2 \geq z_c^2 > t_{j+1}, \quad 1 < t_j < z_c^2 \quad (\text{H.71})$$

Re-grouping,

$$\begin{aligned}
\Lambda^+(\zeta_0) &= \int_{\zeta=1}^{\zeta_c} \frac{d\zeta}{\mathcal{X}(\zeta)(\zeta_0^2 - \zeta^2)} \\
&= \frac{1}{2} z_c \cdot B\left(\frac{1}{2} - \frac{\tilde{\beta}}{\pi}, \frac{1}{2} + \frac{\tilde{\beta}}{\pi}\right) \cdot F\left(-\frac{1}{2}, \frac{1}{2} - \frac{\tilde{\beta}}{\pi}; 1; \frac{z_c^2 - 1}{z_c^2}\right) \\
&\quad + \frac{1}{2} (\zeta_0^2 - z_c^2 - 1) \frac{1}{z_c} \cdot B\left(\frac{1}{2} - \frac{\tilde{\beta}}{\pi}, \frac{1}{2} + \frac{\tilde{\beta}}{\pi}\right) \cdot F\left(\frac{1}{2}, \frac{1}{2} - \frac{\tilde{\beta}}{\pi}; 1; \frac{z_c^2 - 1}{z_c^2}\right) \\
&\quad - \frac{1}{2} (z_c^2 - \zeta_0^2) \times \sum_{j=1}^L \frac{1}{\sqrt{t_j}} \cdot (\Lambda_{3,j+1}^- - \Lambda_{3,j}^-)
\end{aligned}$$

$$z_c \leq \zeta_0 \leq b^+, \quad \zeta_0^2 \geq z_c^2 > t_j, \quad 1 < t_j < z_c^2 \quad (\text{H.72})$$

where,

$$\Lambda_{3,j}^-(\zeta_0^2) = -\frac{(t_j-1)^{\frac{1+\tilde{\beta}}{2}}}{(z_c^2-t_j)^{\frac{1+\tilde{\beta}}{2}}} \times \frac{1}{\lambda^-} \cdot F\left(\frac{1}{2} + \frac{\tilde{\beta}}{\pi}, 1, \frac{3}{2} + \frac{\tilde{\beta}}{\pi}; \frac{t_j-1}{\zeta_0^2-1} \cdot \frac{z_c^2-\zeta_0^2}{z_c^2-t_j}\right)$$

$$\zeta_0^2 \geq z_c^2 > t_{j+1}, 1 < t_j < z_c^2 \quad (\text{H.73})$$

Therefore, the $\Lambda^+(\zeta_0) - \Lambda(\zeta)$ term in (4.26) and (4.27) of Chapter 4 will be,

$$\begin{aligned} \Lambda^+(\zeta_0) - \Lambda(\zeta) &= \frac{1}{2} z_c \cdot B\left(\frac{1}{2} - \frac{\tilde{\beta}}{\pi}, \frac{1}{2} + \frac{\tilde{\beta}}{\pi}\right) \cdot F\left(-\frac{1}{2}, \frac{1}{2} - \frac{\tilde{\beta}}{\pi}; 1; \frac{z_c^2-1}{z_c^2}\right) \\ &\quad + \frac{1}{2} (\zeta_0^2 - z_c^2 - 1) \frac{1}{z_c} \cdot B\left(\frac{1}{2} - \frac{\tilde{\beta}}{\pi}, \frac{1}{2} + \frac{\tilde{\beta}}{\pi}\right) \cdot F\left(\frac{1}{2}, \frac{1}{2} - \frac{\tilde{\beta}}{\pi}; 1; \frac{z_c^2-1}{z_c^2}\right) \\ &\quad - \frac{1}{2} (z_c^2 - \zeta_0^2) \times \sum_{j=1}^L \frac{1}{\sqrt{t_j}} \cdot (\Lambda_{3,j+1}^- - \Lambda_{3,j}^-) \\ &\quad - \left\{ \frac{1}{2} z_c \cdot B\left(\frac{1}{2} - \frac{\tilde{\beta}}{\pi}, \frac{1}{2} + \frac{\tilde{\beta}}{\pi}\right) \cdot F\left(-\frac{1}{2}, \frac{1}{2} - \frac{\tilde{\beta}}{\pi}; 1; \frac{z_c^2-1}{z_c^2}\right) \right. \\ &\quad \left. + \frac{1}{2} (\zeta^2 - z_c^2 - 1) \frac{1}{z_c} \cdot B\left(\frac{1}{2} - \frac{\tilde{\beta}}{\pi}, \frac{1}{2} + \frac{\tilde{\beta}}{\pi}\right) \cdot F\left(\frac{1}{2}, \frac{1}{2} - \frac{\tilde{\beta}}{\pi}; 1; \frac{z_c^2-1}{z_c^2}\right) \right. \\ &\quad \left. - \frac{1}{2} (\zeta^2 - 1)(z_c^2 - \zeta^2) \times \sum_{j=1}^L \frac{1}{\sqrt{t_j}} \cdot \Delta I_{3,j} \right\} \\ &= \frac{1}{2} (\zeta_0^2 - \zeta^2) \frac{1}{z_c} \cdot B\left(\frac{1}{2} - \frac{\tilde{\beta}}{\pi}, \frac{1}{2} + \frac{\tilde{\beta}}{\pi}\right) \cdot F\left(\frac{1}{2}, \frac{1}{2} - \frac{\tilde{\beta}}{\pi}; 1; \frac{z_c^2-1}{z_c^2}\right) \\ &\quad - \frac{1}{2} (z_c^2 - \zeta_0^2) \times \sum_{j=1}^L \frac{1}{\sqrt{t_j}} \cdot [\Lambda_{3,j+1}^-(\zeta_0) - \Lambda_{3,j}^-(\zeta_0)] \\ &\quad + \frac{1}{2} (\zeta^2 - 1)(z_c^2 - \zeta^2) \times \sum_{j=1}^L \frac{1}{\sqrt{t_j}} \cdot \Delta I_{3,j}(\zeta) \end{aligned}$$

$$1 \leq \zeta \leq z_c, z_c \leq \zeta_0 \leq b^+, \zeta_0^2 \geq z_c^2 > t_j, 1 < t_j < z_c^2 \quad (\text{H.74})$$

The above formulae are used in the numerical computation of the velocity continuity condition and the bound vortex distribution $\gamma_c(\zeta, \tau)$.

APPENDIX I
TIME MARCHING ALGORITHM

I.1 Artificial Damping And Velocity Marching

For the purpose of developing the artificial damping concept, assume a simple mass-spring system, as depicted in Fig. I.1,

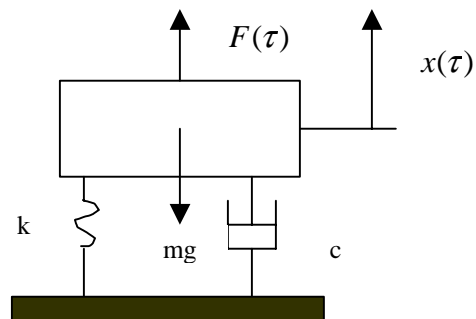


Fig. I.1 Artificial damping

The system equilibrium equation is,

$$m\ddot{x} + c\dot{x} = F(\tau) \quad (\text{I.1})$$

At the time τ_i , the system equation is,

$$m\ddot{x}_i + c\dot{x}_i = F(\tau_i) \quad (\text{I.2})$$

Thus, representing the acceleration in (I.2) by a backward difference in terms of the velocities at two successive times:

$$m \frac{\dot{x}_i - \dot{x}_{i-1}}{\Delta\tau} + c\dot{x}_i = F_i \quad (\text{I.3})$$

or,

$$\dot{x}_i - \dot{x}_{i-1} + \frac{c\Delta\tau}{m} \dot{x}_i = \frac{F_i \Delta\tau}{m} \quad (\text{I.4})$$

Therefore,

$$\dot{x}_i = \frac{\dot{x}_{i-1} + F_i \Delta\tau/m}{1 + \frac{c\Delta\tau}{m}} = \frac{\dot{x}_{i-1} + F_i \Delta\tau/m}{1 + C_{damp}} \quad (\text{I.5})$$

where $C_{damp} = \frac{c\Delta\tau}{m}$ is the effective damping coefficient, which set by the user input. In

steady planning case, a larger damping coefficient C_{damp} makes the computation more

rapidly settle to the stable time-independent state desired. The $\frac{F_i}{m}$ term is determined

from the average acceleration as follows:

$$\frac{F_i}{m} = \ddot{x}_i = \frac{1}{2}(\ddot{x}_i + \ddot{x}_{i-1}) \quad (\text{I.6})$$

Therefore, the velocity results at time τ_i can be obtained by integrating the acceleration results \ddot{x}_i which were directly from the coupled equations of motion.

I.2 Displacement Marching

Time marching of the vessel velocity and displacement is carried out according to following algorithms.

For the increments of the heave $\eta_3(\tau)$ and the pitch angle $\eta_5(\tau)$,

$$\Delta\eta_{3,i} = \frac{1}{2}(\Delta\dot{\eta}_{3,i} + \Delta\dot{\eta}_{3,i-1}) \times \Delta\tau \quad (\text{I.7})$$

where,

$$\Delta\dot{\eta}_{3,i} = \frac{1}{2} \frac{(\ddot{\eta}_{3,i} + \ddot{\eta}_{3,i-1}) \times \Delta\tau}{1 + C_{damp}} \quad (\text{I.8})$$

with C_{damp} developed in Eq. (I.5), and

$$\Delta\eta_{5,i} = \frac{1}{2}(\Delta\dot{\eta}_{5,i} + \Delta\dot{\eta}_{5,i-1}) \times \Delta\tau \quad (\text{I.9})$$

where

$$\Delta \dot{\eta}_{5,i} = \frac{1}{2} \frac{(\dot{\eta}_{5,i} + \dot{\eta}_{5,i-1}) \times \Delta \tau}{1 + C_{damp}} \quad (\text{I.10})$$

Thus, the displacements will be:

$$\eta_3(\tau_i) = \eta_3(\tau_i - 1) + \Delta \eta_3(\tau_i) \quad (\text{I.11})$$

$$\eta_5(\tau_i) = \eta_5(\tau_i - 1) + \Delta \eta_5(\tau_i) \quad (\text{I.12})$$

I.3 Algorithm to Determine The Transient Wetted Length

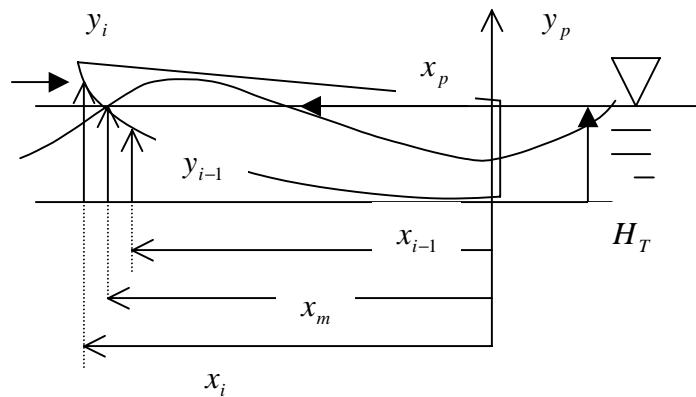


Fig. I.2 Determining wetted length

This algorithm is for the wetted length search outlined in (3.97) and (4.92) of Chapters 3 and 4,

In the transom coordinate system, the keel upsets (include the upsets due to trim angle and waves) are represented as x_i, y_i $i = 1, 2, \dots, n$. The transient wetted length can be found by comparing the transom draft H_T with the sectional transient keel upset $y_k(\tau)$ (see Fig. I.2).

Assuming $y_i > H_T$, $y_{i-1} < H_T$, it is desired to find the coordinate x_m which corresponds to the transient transom draft H_T , starting from the slope:

$$\frac{y_i - y_{i-1}}{x_i - x_{i-1}} = \frac{y_i - H_T}{x_i - x_m} \quad (\text{I.13})$$

From (I.13):

$$x_i - x_m = (y_i - H_T) \frac{x_i - x_{i-1}}{y_i - y_{i-1}} \quad (\text{I.14})$$

Thus, the entry position x_m is the required wetted length, from (I.14):

$$x_m = x_i - (y_i - H_T) \frac{x_i - x_{i-1}}{y_i - y_{i-1}} \quad (\text{I.15})$$

This algorithm is used in the following steps in the Subroutine ENTRY.

Step 1: Based on the last time step x_{\max} , discretize the vessel length x_{\max} into N sections. Interpolate the keel upset at every section, then modify by the displacement from trim angle and the wave elevation (refer to (3.97) and (4.92)).

Step 2: In the transom coordinate system, start from the transom section and move forward toward the bow, comparing with the transom draft H_T , to search for the entry intersection point (refer to (I.13)). This step mainly is for searching for the point where the transient draft $Y_k(x_p, \tau) = 0$ (refer to Fig. 3.8). The correspondent vessel length will be the wetted length $L(\tau) = x_p$.

APPENDIX J

FUNDAMENTAL INTEGRALS IN THE FIRST ORDER MODEL

The fundamental integrals in the vortex strength of the first order model are (3.11), (3.12) and (3.13). As in the 2nd order model, these three singular integrals are in the same form, but defined in different value domains. Each of the three integrals can be separated into three elemental integrals. In this Appendix, a more detail derivation for these semi-analytical evaluations is outlined.

J.1 Three Elemental Integrals

Define (refer to (3.11)),

$$\Lambda(\zeta) = \int_{\zeta_1=1}^{\zeta_c} \frac{d\zeta_1}{\chi(\zeta_1)(\zeta^2 - \zeta_1^2)} \quad 1 \leq \zeta \leq \zeta_c \quad (\text{J.1})$$

where the kernel function is (refer to (3.7)),

$$\chi(\zeta) = \frac{1}{\sqrt{(\zeta^2 - 1)(\zeta_c^2 - \zeta^2)}} \quad (\text{J.2})$$

Following the same procedure as in Appendix H, the integral in (J.1) can be separated into three simple elemental integrals as (refer to (3.16) and (H.7)):

$$\Lambda(\zeta) = I_1 + I_2(\zeta) + I_3(\zeta) \quad 1 \leq \zeta \leq z_c \quad (\text{J.3})$$

where (refer to (3.17), (3.18) and (3.19)),

$$I_1 = \int_{\zeta_1=1}^{z_c} \frac{\zeta_1^2}{\sqrt{(\zeta_1^2 - 1)(z_c^2 - \zeta_1^2)}} d\zeta_1 \quad (\text{J.4})$$

$$I_2(\zeta) = (\zeta^2 - z_c^2 - 1) \cdot \int_{\zeta_1=1}^{z_c} \frac{1}{\sqrt{(\zeta_1^2 - 1)(z_c^2 - \zeta_1^2)}} d\zeta_1 \quad (\text{J.5})$$

$$I_3(\zeta) = (\zeta^2 - 1)(z_c^2 - \zeta^2) \cdot \int_{\zeta_1=1}^{z_c} \frac{1}{(\zeta^2 - \zeta_1^2)\sqrt{(\zeta_1^2 - 1)(z_c^2 - \zeta_1^2)}} d\zeta_1 \quad (\text{J.6})$$

In following sections, semi-analytical forms for these three elemental integrals are developed.

J.2 Elemental Integral I_1

For the elemental integral I_1 of (J.4), transform the variable as $t = \zeta_1^2$; the integral I_1 becomes:

$$I_1 = \frac{1}{2} \int_{t=1}^{z_c^2} \frac{\sqrt{t}}{\sqrt{(t-1)(z_c^2-t)}} dt = \frac{1}{2} \int_{t=1}^{z_c^2} \sqrt{\frac{t}{(t-1)(z_c^2-t)}} dt \quad (\text{J.7})$$

From Gradshteyn and Ryzhik (1965, p233, §3.141.16):

$$\int_b^u \sqrt{\frac{x-c}{(a-x)(x-b)}} dx = 2\sqrt{a-c} E(\chi, p) - 2\sqrt{\frac{(a-u)(u-b)}{u-c}} \quad [a \geq u > b > c] \quad (\text{J.8})$$

$$\text{where } \chi = \arcsin \sqrt{\frac{(a-c)(u-b)}{(a-b)(u-c)}}, \quad p = \sqrt{\frac{a-b}{a-c}}.$$

Comparing (J.8) with (J.7), the parameters are: $a = u = z_c^2$, $b = 1$, $c = 0$, $\chi = \frac{\pi}{2}$,

$p = \sqrt{\frac{z_c^2-1}{z_c^2}} = \sqrt{1-\frac{1}{z_c^2}}$, Thus, the integral I_1 in (J.7) has the following semi-analytical

form:

$$\begin{aligned} I_1 &= \int_{\zeta_1=1}^{z_c} \frac{\zeta_1^2}{\sqrt{(\zeta_1^2-1)(z_c^2-\zeta_1^2)}} d\zeta_1 \\ &= \frac{1}{2} \times 2 \cdot z_c E\left(\frac{\pi}{2}, \sqrt{1-1/z_c^2}\right) \\ &= z_c E\left(\frac{\pi}{2}, \sqrt{1-1/z_c^2}\right) \end{aligned} \quad (\text{J.9})$$

where $E\left(\frac{\pi}{2}, \sqrt{1-1/z_c^2}\right)$ is the complete elliptic integral of the second kind.

J.3 Elemental Integral $I_2(\zeta)$

For the integral $I_2(\zeta)$ in (J.5), defining variable transformation $t = \zeta_1^2$,

$$\begin{aligned} I_2(\zeta) &= (\zeta^2 - z_c^2 - 1) \cdot \int_{\zeta_1=1}^{z_c} \frac{1}{\sqrt{(\zeta_1^2 - 1)(z_c^2 - \zeta_1^2)}} d\zeta_1 \\ &= \frac{1}{2} (\zeta^2 - z_c^2 - 1) \cdot \int_{t=1}^{z_c^2} \frac{1}{\sqrt{t(t-1)(z_c^2 - t)}} dt \end{aligned} \quad (\text{J.10})$$

From Gradshteyn and Ryzhik (1965, p219, §3.131.5):

$$\int_b^u \frac{dx}{\sqrt{(a-x)(x-b)(x-c)}} = \frac{2}{\sqrt{a-c}} F(\chi, p) \quad [a \geq u > b > c] \quad (\text{J.11})$$

$$\text{where } \chi = \arcsin \sqrt{\frac{(a-c)(u-b)}{(a-b)(u-c)}}, \quad p = \sqrt{\frac{a-b}{a-c}}.$$

Comparing (J.11) with (J.10), the parameters are: $a = u = z_c^2$, $b = 1$, $c = 0$, $\chi = \frac{\pi}{2}$,

$$p = \sqrt{\frac{z_c^2 - 1}{z_c^2}} = \sqrt{1 - \frac{1}{z_c^2}} = k, \text{ Thus, the integral } I_2 \text{ is,}$$

$$\begin{aligned} I_2(\zeta) &= \frac{1}{2} (\zeta^2 - z_c^2 - 1) \cdot \int_{t=1}^{z_c^2} \frac{1}{\sqrt{t(t-1)(z_c^2 - t)}} dt \\ &= (\zeta^2 - z_c^2 - 1) \cdot \frac{1}{z_c} F\left(\frac{\pi}{2}, k\right) \end{aligned} \quad (\text{J.12})$$

where $F(\frac{\pi}{2}, k)$ is the complete elliptic integral of the first kind.

J.4 Elemental Integral $I_3(1 < \zeta < z_c)$

For the integral $I_3(\zeta)$, from Gradshteyn and Ryzhik (1965, p251, §3.157. 9) :

$$\int_b^u \frac{dx}{(p-x^2)\sqrt{(a^2-x^2)(x^2-b^2)}} = \frac{1}{ap(p-b^2)} \left\{ b^2 \Pi(\chi, \frac{p(a^2-b^2)}{a^2(p-b^2)}, q) + (p-b^2)F(\chi, q) \right\} \quad [a \geq u > b > 0; p \neq b^2] \quad (\text{J.13})$$

$$\text{where } \chi = \arcsin \frac{a}{u} \sqrt{\frac{u^2-b^2}{a^2-b^2}}, \quad q = \frac{\sqrt{a^2-b^2}}{a}.$$

Comparing (J.13) with (J.6), these parameters are: $a^2 = u^2 = z_c^2$, $b^2 = 1$,

$$p = \zeta^2, \quad \chi = \frac{\pi}{2}, \quad q = \sqrt{\frac{z_c^2-1}{z_c^2}} = \sqrt{1 - \frac{1}{z_c^2}} = k.$$

Thus, the integral $I_3(\zeta)$ in (J.6) has the form:

$$\begin{aligned} I_3 &= (1-\zeta^2)(\zeta^2 - z_c^2) \cdot \frac{1}{z_c \zeta^2 (\zeta^2 - 1)} \left\{ \Pi\left[\frac{\pi}{2}, \frac{\zeta^2(z_c^2-1)}{z_c^2(\zeta^2-1)}, k\right] + (\zeta^2 - 1)F\left(\frac{\pi}{2}, k\right) \right\} \\ &= \frac{z_c^2 - \zeta^2}{z_c \zeta^2} \left\{ \Pi\left[\frac{\pi}{2}, \frac{\zeta^2(z_c^2-1)}{z_c^2(\zeta^2-1)}, k\right] + (\zeta^2 - 1)F\left(\frac{\pi}{2}, k\right) \right\} \end{aligned} \quad (\text{J.14})$$

where $\Pi(\phi, n, k)$ is the elliptic integral of the third kind.

The form elliptic integral of the third kind, $\Pi(\phi, n, k)$ in (J.14), is not in a semi-analytical form ready for the numerical computation. In the this section, further reductions of $\Pi(\phi, n, k)$ are accomplished.

Use the following identity (refer to (L.8)):

$$\Pi(n \setminus \alpha) = \Pi\left(n; \frac{1}{2} \pi \setminus \alpha\right) = \Pi\left[\frac{\pi}{2}, \frac{\zeta^2(z_c^2 - 1)}{z_c^2(\zeta^2 - 1)}, \sqrt{1 - \frac{1}{z_c^2}}\right] \quad 1 \leq \zeta \leq z_c \quad (\text{J.15})$$

According to the elliptic integral notation in Appendix L, and comparing with (J.14), the parameters in (J.15) are,

$$k = \sin \alpha = \sqrt{1 - \frac{1}{z_c^2}} \quad (\text{J.16})$$

$$n = \frac{\zeta^2(z_c^2 - 1)}{z_c^2(\zeta^2 - 1)} \quad 1 \leq \zeta \leq z_c \quad (\text{J.17})$$

In (J.17), when $\zeta \rightarrow 1^+$, $n \rightarrow +\infty$; $\zeta \rightarrow z_c^-$, $n \rightarrow 1$, which implies that,

$$n(\zeta) > 1 \quad 1 \leq \zeta \leq z_c \quad (\text{J.18})$$

According to the Case(ii) in Appendix L, when $n > 1$, the transformation in (L.13) can be applied:

$$N = \frac{\sin^2 \alpha}{n} = \left(1 - \frac{1}{z_c^2}\right) \frac{z_c^2(\zeta^2 - 1)}{\zeta^2(z_c^2 - 1)} = \frac{z_c^2 - 1}{z_c^2} \frac{z_c^2(\zeta^2 - 1)}{\zeta^2(z_c^2 - 1)} = \frac{(\zeta^2 - 1)}{\zeta^2} \quad (\text{J.19})$$

Since $\zeta > 1 \rightarrow N = 1 - \frac{1}{\zeta^2}$, and $n > 1 \rightarrow N = \frac{\sin^2 \alpha}{n} < \sin^2 \alpha$, the value domain for N

is:

$$0 < N < \sin^2 \alpha \quad (\text{J.20})$$

In this condition of (J.20), (L.14) in Appendix L will apply to the transform in (J.15):

$$\Pi(n \setminus \alpha) = F(\alpha) - \Pi(N \setminus \alpha) \quad (\text{J.21})$$

where α is defined in (J.16).

From (L.12) in Appendix L, in (J.21):

$$\Pi(N \setminus \alpha) = F(\alpha) + \delta_1 F(\alpha) Z(\varepsilon_1 \setminus \alpha) \quad (\text{J.22})$$

where,

$$\begin{aligned} \delta_1 &= [N(1-N)^{-1}(\sin^2 \alpha - N)^{-1}]^{1/2} \\ &= \sqrt{\frac{N}{1-N} \cdot \frac{1}{\sin^2 \alpha - N}} \end{aligned} \quad (\text{J.23})$$

Since,

$$\frac{N}{1-N} = \frac{(\zeta^2 - 1)}{\zeta^2} \times \frac{1}{1 - \frac{(\zeta^2 - 1)}{\zeta^2}} = \frac{(\zeta^2 - 1)}{\zeta^2} \times \frac{\zeta^2}{1} = \zeta^2 - 1,$$

$$\sin^2 \alpha - N = \frac{z_c^2 - 1}{z_c^2} - \frac{(\zeta^2 - 1)}{\zeta^2} = \frac{z_c^2 \zeta^2 - \zeta^2 - z_c^2 \zeta^2 + z_c^2}{z_c^2 \zeta^2} = \frac{z_c^2 - \zeta^2}{z_c^2 \zeta^2},$$

Thus, the parameter δ_1 is,

$$\delta_1 = \sqrt{\frac{N}{1-N} \cdot \frac{1}{\sin^2 \alpha - N}} = \sqrt{(\zeta^2 - 1) \cdot \frac{z_c^2 \zeta^2}{z_c^2 - \zeta^2}} = z_c \zeta \sqrt{\frac{\zeta^2 - 1}{z_c^2 - \zeta^2}} \quad (\text{J.24})$$

From (L.9) in Appendix L, ε_1 in (J.22) is:

$$\begin{aligned} \varepsilon_1 &= \arcsin(N / \sin^2 \alpha)^{\frac{1}{2}} \\ &= \arcsin \sqrt{\frac{N}{\sin^2 \alpha}} = \arcsin \sqrt{\frac{(\zeta^2 - 1)}{\zeta^2} \cdot \frac{z_c^2}{z_c^2 - 1}} = \arcsin \frac{z_c}{\zeta} \sqrt{\frac{\zeta^2 - 1}{z_c^2 - 1}} \end{aligned} \quad (\text{J.25})$$

From (L.11) in Appendix L,

$$Z(\varepsilon_1 \setminus \alpha) = E(\varepsilon_1 \setminus \alpha) - [E(\alpha) / F(\alpha)] F(\varepsilon_1 \setminus \alpha) \quad (\text{J.26})$$

Substituting all of the above into (J.21) yields the final form of the elliptic integral of the third kind, $\Pi(\phi, n, k)$, in (J.15):

$$\Pi(n \setminus \alpha) = z_c \zeta \sqrt{\frac{\zeta^2 - 1}{z_c^2 - \zeta^2}} [E(\alpha)F(\varepsilon_1 \setminus \alpha) - F(\alpha)E(\varepsilon_1 \setminus \alpha)] \quad (\text{J.27})$$

Substitute (J.27) back into (J.14) The final form of $I_3(\zeta)$ is then:

$$I_3 = \frac{\sqrt{(\zeta^2 - 1)(z_c^2 - \zeta^2)}}{z} [E(\alpha)F(\varepsilon_1 \setminus \alpha) - F(\alpha)E(\varepsilon_1 \setminus \alpha)] + \frac{z_c^2 - \zeta^2}{z_c \cdot \zeta^2} (\zeta^2 - 1) \cdot F(\alpha) \quad 1 < \zeta < z_c \quad (\text{J.28})$$

where $F(\alpha)$ and $E(\alpha)$ are the complete elliptic integrals of the first kind and the second kind respectively, $F(\varepsilon_1 \setminus \alpha)$ and $E(\varepsilon_1 \setminus \alpha)$ are the incomplete elliptic integrals of the first kind and the second kind respectively, with the angles $\alpha = \sin^{-1} \sqrt{1 - \frac{1}{z_c^2}}$, and

$\varepsilon_1 = \arcsin \frac{z_c}{\zeta} \cdot \sqrt{\frac{\zeta^2 - 1}{z_c^2 - 1}}$. During the derivation process, it is required that $\zeta \neq 1$ (refer to (J.13)).

The above derivation process for (3.11) is also applicable to the evaluation procedure for the integrals in (3.12) and (3.13). The semi-analytical form in (J.9) and (J.12) for the integral I_1 and I_2 are the same for the elemental integrals in (3.12) and (3.13), the only difference is for the elemental integral $I_3(\zeta)$ where the value domain is different. In next section, the semi-analytical form of $I_3(\zeta)$ in the different value domain is given.

J.5 Elemental Integral $I_3(b^- \leq \zeta < 1)$

In the value domain $b^- \leq \zeta < 1$, the elemental integral $I_3(\zeta)$ derived from (3.12) has the following form:

$$I_3(\zeta) = \frac{z_c^2 - \zeta^2}{z_c \zeta^2} \left\{ \Pi\left[\frac{\pi}{2}, \frac{\zeta^2(z_c^2 - 1)}{z_c^2(\zeta^2 - 1)}, k\right] + (\zeta^2 - 1)F\left(\frac{\pi}{2}, k\right) \right\} \quad (\text{J.29})$$

where the elliptic integral of the third kind, $\Pi(n \setminus \alpha)$, is defined as,

$$\Pi(n \setminus \alpha) = \Pi\left(n; \frac{1}{2} \pi \setminus \alpha\right) = \Pi\left[\frac{\pi}{2}, \frac{\zeta^2(z_c^2 - 1)}{z_c^2(\zeta^2 - 1)}, \sqrt{1 - \frac{1}{z_c^2}}\right] \quad b^- \leq \zeta < 1 \quad (\text{J.30})$$

In (J.30), $k = \sin \alpha = \sqrt{1 - \frac{1}{z_c^2}}$, $n = \frac{\zeta^2(z_c^2 - 1)}{z_c^2(\zeta^2 - 1)}$. when $\zeta \rightarrow 1^-$, $n \rightarrow -\infty$; $\zeta \rightarrow (b^-)$,

$n = \frac{(b^-)^2(z_c^2 - 1)}{z_c^2((b^-)^2 - 1)} < 0$, which implies the parameter n in (J.30) to be:

$$-\infty < n = \frac{\zeta^2(z_c^2 - 1)}{z_c^2(\zeta^2 - 1)} < 0 \quad b^- \leq \zeta < 1 \quad (\text{J.31})$$

With $n < 0$, the transform parameter N in (L.19) of Appendix L is:

$$N = \frac{\sin^2 \alpha - n}{1 - n} \quad (\text{J.32})$$

Since, $\sin^2 \alpha - n = -\frac{z_c^2 - 1}{z_c^2(\zeta^2 - 1)}$, $1 - n = \frac{\zeta^2 - z_c^2}{z_c^2(\zeta^2 - 1)}$, thus,

$$N = \frac{\sin^2 \alpha - n}{1 - n} = \frac{z_c^2 - 1}{z_c^2 - \zeta^2} \quad b^- \leq \zeta < 1 \quad (\text{J.33})$$

and, when $\zeta \rightarrow 1^-$, $N = \frac{z_c^2 - 1}{z_c^2 - (1^-)^2} < 1$; when $\zeta \rightarrow b^-$,

$$N = \frac{z_c^2 - 1}{z_c^2 - (b^-)^2} > \frac{z_c^2 - 1}{z_c^2} = \sin^2 \alpha. \text{ The value domain for the parameter } N \text{ thus is:}$$

$$\sin^2 \alpha < N < 1 \quad (\text{J.34})$$

In this condition, (L.40) in Appendix L applies to the transform for the elliptic integral of the third kind in (J.30):

$$\Pi(n \setminus \alpha) = \frac{-n \cdot \cos^2 \alpha}{(1 - n)(\sin^2 \alpha - n)} \cdot \Pi(N \setminus \alpha) + \frac{\sin^2 \alpha}{\sin^2 \alpha - n} \cdot F(\alpha) \quad (\text{J.35})$$

where $F(\alpha)$ is the complete elliptic function of the first kind, and

$$\cos^2 \alpha = 1 - \sin^2 \alpha = \left(\frac{1}{z_c}\right)^2.$$

From (L.18) of Appendix L, the third kind Elliptic function $\Pi(N \setminus \alpha)$ is,

$$\Pi(N \setminus \alpha) = F(\alpha) + \frac{1}{2} \pi \delta_2 [1 - \Lambda_0(\varepsilon_2 \setminus \alpha)] \quad (\text{J.36})$$

where,

$$\delta_2 = \sqrt{\frac{N}{1-N} \cdot \frac{1}{N - \sin^2 \alpha}} \quad (\text{J.37})$$

since $1 - N = \frac{1 - \zeta^2}{z_c^2 - \zeta^2}$, $N - \sin^2 \alpha = \frac{(z_c^2 - 1) \cdot \zeta^2}{(z_c^2 - \zeta^2) \cdot z_c^2}$, therefore,

$$\delta_2 = \sqrt{\frac{N}{1-N} \cdot \frac{1}{N - \sin^2 \alpha}} = \frac{z_c}{\zeta} \cdot \sqrt{\frac{z_c^2 - \zeta^2}{1 - \zeta^2}} \quad (\text{J.38})$$

and,

$$\varepsilon_2 = \arcsin \sqrt{\frac{1-N}{\cos^2 \alpha}} = \arcsin \left(z_c \cdot \sqrt{\frac{1-\zeta^2}{z_c^2 - \zeta^2}} \right) \quad (\text{J.39})$$

Substitute (J.38) and (J.39) into (J.36) to get the expression for $\Pi(N \setminus \alpha)$:

$$\Pi(N \setminus \alpha) = F(\alpha) + \frac{\pi}{2} \cdot \frac{z_c}{\zeta} \cdot \sqrt{\frac{z_c^2 - \zeta^2}{1 - \zeta^2}} \cdot [1 - \Lambda_0(\varepsilon_2 \setminus \alpha)] \quad (\text{J.40})$$

Substitute (J.40) back into (J.35):

$$\Pi(n \setminus \alpha) = (1 - \zeta^2) \left\{ F(\alpha) \cdot \frac{z_c^2}{z_c^2 - \zeta^2} + \frac{\pi}{2} \frac{z_c \times \zeta}{\sqrt{(z_c^2 - \zeta^2)(1 - \zeta^2)}} [1 - \Lambda_0(\varepsilon_2 \setminus \alpha)] \right\} \quad (\text{J.41})$$

Substituting (J.41) into (J.29), the final form of $I_3(\zeta)$ is:

$$I_3 = \frac{1 - \zeta^2}{z_c} F(\alpha) + \frac{\pi}{2} \frac{1}{\zeta} \sqrt{(1 - \zeta^2)(z_c^2 - \zeta^2)} [1 - \Lambda_0(\varepsilon_2 \setminus \alpha)] \quad b^- \leq \zeta < 1 \quad (\text{J.42})$$

where from (L.17) of appendix L,

$$\Lambda_0(\varepsilon_2 \setminus \alpha) = \frac{2}{\pi} \{ F(\alpha) E(\varepsilon_2 \setminus \alpha') - [F(\alpha) - E(\alpha)] F(\varepsilon_2 \setminus \alpha') \} \quad (\text{J.43})$$

The parameter ε_2 is defined in (J.39) and the parameter α' is:

$$\alpha' = 90^\circ - \alpha \quad (\text{J.44})$$

J.6 Elemental Integral $I_3(z_c \leq \zeta \leq b^+)$

In the value domain $z_c \leq \zeta \leq b^+$, the elemental integral $I_3(\zeta)$ derived from (3.13) has the following form:

$$I_3 = \frac{z_c^2 - \zeta^2}{z_c \zeta^2} \left\{ \Pi \left[\frac{\pi}{2}, \frac{\zeta^2(z_c^2 - 1)}{z_c^2(\zeta^2 - 1)}, k \right] + (\zeta^2 - 1) F \left(\frac{\pi}{2}, k \right) \right\} \quad z_c \leq \zeta \leq b^+ \quad (\text{J.45})$$

where the elliptic integral of the third kind, $\Pi(n \setminus \alpha)$, is defined as,

$$\Pi(n \setminus \alpha) = \Pi\left(n; \frac{1}{2} \pi \setminus \alpha\right) = \Pi\left[\frac{\pi}{2}, \frac{\zeta^2(z_c^2 - 1)}{z_c^2(\zeta^2 - 1)}, \sqrt{1 - \frac{1}{z_c^2}}\right] \quad z_c \leq \zeta \leq b^+ \quad (\text{J.46})$$

$$\text{In (J.46), } \sin \alpha = \sqrt{1 - \frac{1}{z_c^2}}, \quad n = \frac{\zeta^2(z_c^2 - 1)}{z_c^2(\zeta^2 - 1)}.$$

When $\zeta \rightarrow z_c$, $n = \frac{(z_c^2 - 1)}{z_c^2} \cdot \frac{z_c^2}{z_c^2 - 1} > \frac{(z_c^2 - 1)}{z_c^2} = \sin^2 \alpha$; when $\zeta \rightarrow b^+$,

$$\begin{aligned} n &= \frac{(b^+)^2(z_c^2 - 1)}{z_c^2((b^+)^2 - 1)} = \frac{(b^+)^2 z_c^2 - z_c^2 + z_c^2 - (b^+)^2}{z_c^2((b^+)^2 - 1)} = \frac{z_c^2((b^+)^2 - 1) - ((b^+)^2 - z_c^2)}{z_c^2((b^+)^2 - 1)} \\ &= 1 - \frac{(b^+)^2 - z_c^2}{z_c^2((b^+)^2 - 1)} < 1 \end{aligned}$$

which means the parameter n in (J.46) to be:

$$\sin^2 \alpha < n = \frac{\zeta^2(z_c^2 - 1)}{z_c^2(\zeta^2 - 1)} < 1 \quad z_c \leq \zeta \leq b^+ \quad (\text{J.47})$$

In this condition of (J.47), (L.18) in Appendix L can be applied to the elliptic integral of the third kind in (J.46):

$$\Pi(n \setminus \alpha) = F(\alpha) + \frac{1}{2} \pi \cdot \delta_3[1 - \Lambda_0(\varepsilon_3 \setminus \alpha)] \quad (\text{J.48})$$

where $F(\alpha)$ is the complete elliptic integral of the first kind, Λ_0 is defined in (J.43),

and,

$$\delta_3 = \sqrt{\frac{n}{1-n} \cdot \frac{1}{n - \sin^2 \alpha}} = z_c \cdot \zeta \cdot \sqrt{\frac{\zeta^2 - 1}{\zeta^2 - z_c^2}} \quad (\text{J.49})$$

and,

$$\varepsilon_3 = \arcsin \sqrt{\frac{1-n}{\cos^2 \alpha}} = \arcsin \sqrt{\frac{\zeta^2 - z_c^2}{\zeta^2 - 1}} \quad (\text{J.50})$$

Substitute (J.49) and (J.50) into (J.48) to give $\Pi(n \setminus \alpha)$:

$$\Pi(n \setminus \alpha) = F(\alpha) + \frac{\pi}{2} \cdot z_c \cdot \zeta \sqrt{\frac{\zeta^2 - 1}{\zeta^2 - z_c^2}} \cdot [1 - \Lambda_0(\varepsilon_3 \setminus \alpha)] \quad (\text{J.51})$$

This gives the final semi-analytical form for the integral $I_3(\zeta)$:

$$I_3 = \frac{z_c^2 - \zeta^2}{z_c} F(\alpha) - \frac{\pi}{2} \frac{1}{\zeta} \sqrt{(\zeta^2 - z_c^2)(\zeta^2 - 1)} [1 - \Lambda_0(\varepsilon_3 \setminus \alpha)] \quad z_c < \zeta \leq b^+ \quad (\text{J.52})$$

In this appendix, the semi-analytical forms for the fundamental integrals of (3.11), (3.12) and (3.13) in the first order model have been given.

APPENDIX K

INPUT FILES FOR THE REGULAR WAVE EXAMPLE

The input data for the CATSEA(2-4a) and NewCat(2-4a) of the design tools in the regular wave numerical computation have been listed in this appendix as an example. The physical explanation of the input data can be found in Chapter 8.

There are four input files for the catamaran with two transverse steps. The first input file "CATSEA.IN" is a control file which provides the global control data for the computation. The other three files are the local geometry data files which provide the detailed geometry parameters for three hulls, one for the main body hull, other two for each individual step hull.

K.1 Input File: CATSEA.IN

CATSEA.IN is the mater file which gives the global control data.

K.1.1 Input Data

1 1

Example-1: catamaran. ZK = 2 FT, 6000 LBS, 2 STEPS, 3 FT CHINE
60 .005 .03 2.

```
.001 .0001 .8 0 0
.02 24.04 6.33 5. 14.25 .0187 7.27 .01 .1 1 1 10001
1
10000
70. .61
2
2.29 2.29
.25 60. 0. 1
```

K.1.2 Read Statement in Fortran Code (CatSea2-4a or NewCat2-4a)

The following is the read statement in the code of CatSea2-4a and in NewCat2-4a.

```
OPEN(16,FILE='CATSEA.IN',STATUS='OLD')
READ (16,*) RESTART,DUMP
READ (16,2) (PROB(I),I=1,15)
READ (16,*) MMZ,DSPZ,SBARZ,RATZ
READ (16,*) CRIT(1),CRIT(2),FAC,KPRNT,KPLOT
READ (16,*) DTOS,XMASS,GYRAD,XCG,XLOA,CLA,XCA,CDA,DEPS,KODE,
KSTEP,MALL
READ (16,*) NPRNT
IF (NPRNT .NE. 0) READ (16,*) (IPRNT(I),I=1,NPRNT)
READ (16,*) UK,ZKM
IF (KSTEP .EQ. 0) GO TO 5998
READ (16,*) NSTEPS
READ (16,*) (XLSTEP(I),I=1,NSTEPS)
C DATA READ AND CONVERTED IN WAVE:
C
C KODE = 1: REGULAR WAVE;
C READ (16,*) AHTA,WAVL,PHASE,WAVES
C
C KODE = 2: IRREGULAR WAVE (JONSWAP Spectrum)
C READ (16,*) WMIN,W0,WMAX,GAM,NEW,WAVES
```

K.2 Input File: CATs1.IN

The CATs1.IN file is the local geometry data file for the first (main) hull segment.

K.2.1 Input Data

COBRA evaluations - 2 STEPs
 .1176 1.088
 1 1
 1.001 80 .005 .02 .015 .015 2 1
 .675 -.3 .09 -.0 -.0 8.92 .17 0.
 38. -3.33 17. 0. 0.
 38. 38. 17. 17.
 1. 0. 1. 0.
 1.1 0.2 1.5 1.5 0. 2.17 0.

K.2.2 Read Statement in Fortran Code (CatSea2-4a or NewCat2-4a)

The following is the read statement in the code of CatSea2-4a and in NewCat2-4a.

```

9000 IF (KSTEP .EQ. 0) OPEN(15,FILE='CATs.IN',STATUS='OLD')
      IF (KSTEP .NE. 0 .AND. MHUL .EQ. 1) OPEN(15,FILE='CATs1.IN',
      ,STATUS='OLD')
      IF (KSTEP .NE. 0 .AND. MHUL .EQ. 2) OPEN(15,FILE='CATs2.IN',
      ,STATUS='OLD')
      IF (KSTEP .NE. 0 .AND. MHUL .EQ. 3) OPEN(15,FILE='CATs3.IN',
      ,STATUS='OLD')
C
      READ(15,2) (PROB(I),I=1,15)
      READ (15,*) HT,TRIMD
      READ (15,*) NGAM,NSEC
      READ (15,*) ZC1,MM,DZMIN1,DELZ1,DZMIN2,DELZ2,KIT,NELE
      READ (15,*) YK0,YK0P,YK0PP,YK1,YK1P,XMAX,XLA,XLC
      READ (15,*) BETA0,BETA0P,BETA1,BETA1P,XLAB
      READ (15,*) BET11,BET12,BET21,BET22
      READ (15,*) ZK0,ZK0P,ZK1,ZK1P
      READ (15,*) ZCI0,ZCI0P,ZCIM,ZCI1,ZCI1P,XLAC,XLCC
      CLOSE(15)

```

K.3 Input File: CATs2.IN

The CATs2.IN file is the local geometry data file for the second hull segment (the hull segment after first step).

COBRA evaluations - 2 STEPs (segment 2)

```
.1609 1.088
1 1
1.001 50 .005 .04 .02 .02 2 1
.03 -.05 0. 0. 0. 2.29 .79 0.
17. 0. 17. 0. 0.
17. 17. 17. 17.
1. 0. 1. 0.
1.5 0. 1.5 1.5 0. 0. 0.
```

K.4 Input File: CATs3.IN

The CATs2.IN file is the local geometry data file for the third hull segment (the hull segment after the transverse second step).

COBRA evaluations - 2 STEPs (Segment 3)

```
.2043 1.088
1 1
1.002 50 .01 .04 .02 .02 2 1
.03 -.05 0. 0. 0. 2.29 .79 0.
17. 0. 17. 0. 0.
17. 17. 17. 17.
1. 0. 1. 0.
1.5 0. 1.5 1.5 0. 0. 0.
```

APPENDIX L
ELLIPTIC INTEGRALS

The following sections of this appendix are from Abramowitz and Stegun (1964) (Handbook of Mathematical Functions, National Bureau of Standards, U. S. Government Printing Office, Washington, D. C.). The material has been included here in the interest of independence of the presentation.

Defining $m = \sin^2 \alpha$, where m is the parameter, α is the modular angle, and,

$x = \sin \phi = \operatorname{sn} u$, $\cos \phi = \operatorname{cn} u$, the delta amplitude: $(1 - m \sin^2 \phi)^{\frac{1}{2}} = \operatorname{dn} u = \Delta(\phi)$,

the amplitude: $\phi = \arcsin(x) = \arcsin(\operatorname{sn} u) = \operatorname{am} u$.

- **Elliptical Integral of the First Kind**

$$\begin{aligned}
 F(\phi \setminus \alpha) = F(\phi \mid m) &= \int_0^{\phi} (1 - \sin^2 \alpha \sin^2 \theta)^{-\frac{1}{2}} d\theta \\
 &= \int_0^x [(1 - t^2)(1 - mt^2)]^{-\frac{1}{2}} dt \\
 &= \int_0^u dw = u
 \end{aligned} \tag{L.1}$$

- **Elliptical Integral of the Second Kind**

$$\begin{aligned}
 E(\phi \setminus \alpha) = E(u \mid m) &= \int_0^{\phi} (1 - \sin^2 \alpha \sin^2 \theta)^{\frac{1}{2}} d\theta \\
 &= \int_0^x (1 - t^2)^{-\frac{1}{2}} (1 - mt^2)^{\frac{1}{2}} dt
 \end{aligned} \tag{L.2}$$

- **Elliptical Integral of the Third Kind**

$$\Pi(n; \phi \setminus \alpha) = \int_0^{\phi} (1 - n \sin^2 \theta)^{-1} [1 - \sin^2 \alpha \sin^2 \theta]^{-\frac{1}{2}} d\theta \tag{L.3}$$

If $x = \text{sn}(u \mid m)$,

$$\Pi(n; u \mid m) = \int_0^x (1 - nt^2)^{-1} [(1 - t^2)(1 - mt^2)]^{-\frac{1}{2}} dt \tag{L.4}$$

Referred to above canonical forms of the elliptic integrals, they are said to be **complete** when the amplitude $\phi = \frac{\pi}{2}$ and so that $x = 1$. These complete integrals are designated as follows,

- **Complete Elliptical Integral of the First Kind**

Usually K and F are used to express the complete elliptic integral of the first kind.

$$K = [K(m)] = \int_0^1 [(1 - t^2)(1 - mt^2)]^{-1/2} dt = \int_0^{\pi/2} (1 - m \sin^2 \theta)^{-1/2} d\theta$$

$$K = F\left(\frac{1}{2}\pi \mid m\right) = F\left(\frac{1}{2}\pi \setminus \alpha\right) \quad (\text{L.5})$$

$$K' = [K(m_1)] = K(1-m) = \int_0^{\pi/2} (1 - m_1 \sin^2 \theta)^{-1/2} d\theta$$

$$K' = F\left(\frac{1}{2}\pi \mid m_1\right) = F\left(\frac{1}{2}\pi \setminus \frac{1}{2}\pi - \alpha\right)$$

$$m_1 = \sin^2(90^\circ - \alpha) = \cos^2 \alpha \quad (\text{L.6})$$

- **Complete Elliptical Integral of the Second Kind**

E is used to express the complete elliptic integral of the second kind.

$$E = E[K(m)] = \int_0^1 (1-t^2)^{-1/2} (1-mt^2)^{1/2} dt = \int_0^{\pi/2} (1-m \sin^2 \theta)^{1/2} d\theta$$

$$E = E[K(m)] = E(m) = E\left(\frac{1}{2}\pi \setminus \alpha\right) \quad (\text{L.7})$$

$$E' = E(m_1) = E(1-m) = \int_0^{\pi/2} (1 - m_1 \sin^2 \theta)^{-1/2} d\theta$$

$$E' = E[K(m_1)] = E(m_1) = E\left(\frac{1}{2}\pi \setminus \frac{1}{2}\pi - \alpha\right)$$

- **Complete Elliptical Integral of the Third Kind**

$\Pi(n \setminus \alpha)$ is used to express the complete elliptic integral of the third kind.

$$\Pi(n; \frac{1}{2}\pi \setminus \alpha) = \Pi(n \setminus \alpha) \quad (\text{L.8})$$

The following sections list the frequently referred cases for the complete integrals of the third kind.

- **Cases of the Complete Elliptic Integrals of the Third Kind**

Case (i): Hyperbolic Case $0 < n < \sin^2 \alpha$

Define:

$$\varepsilon = \arcsin(n / \sin^2 \alpha)^{\frac{1}{2}} \quad 0 \leq \varepsilon \leq \frac{1}{2}\pi \quad (\text{L.9})$$

$$\delta_1 = [n(1-n)^{-1}(\sin^2 \alpha - n)^{-1}]^{1/2} \quad (\text{L.10})$$

$$Z(\phi \setminus \alpha) = E(\phi \setminus \alpha) - (E / K)F(\phi \setminus \alpha) \quad (\text{L.11})$$

In this case, the elliptic integral of the third kind is,

$$\Pi(n \setminus \alpha) = K(\alpha) + \delta_1 K(\alpha) Z(\varepsilon \setminus \alpha) \quad (\text{L.12})$$

Case (ii): Hyperbolic Case $n > 1$

The $n > 1$ case can be reduced to the case $0 < N < \sin^2 \alpha$ by defining,

$$N = \frac{\sin^2 \alpha}{n} \quad (\text{L.13})$$

In this case, the elliptic integral of the third kind is,

$$\Pi(n \setminus \alpha) = K(\alpha) - \Pi(N \setminus \alpha) \quad (\text{L.14})$$

Case (iii): Circular Case $\sin^2 \alpha < n < 1$

Define:

$$\varepsilon = \arcsin[(1-n)/\cos^2 \alpha]^{\frac{1}{2}} \quad 0 \leq \varepsilon \leq \frac{1}{2}\pi \quad (\text{L.15})$$

$$\delta_2 = [n(1-n)^{-1}(n - \sin^2 \alpha)^{-1}]^{1/2} \quad (\text{L.16})$$

$$\begin{aligned} \Lambda_0(\phi \setminus \alpha) &= \frac{F(\phi \setminus 90^\circ - \alpha)}{K'(\alpha)} + \frac{2}{\pi} K(\alpha) Z(\phi \setminus 90^\circ - \alpha) \\ &= \frac{2}{\pi} \{K(\alpha) E(\phi \setminus 90^\circ - \alpha) - [K(\alpha) - E(\alpha)] F(\phi \setminus 90^\circ - \alpha)\} \end{aligned} \quad (\text{L.17})$$

In this case, the elliptic integral of the third kind is,

$$\Pi(n \setminus \alpha) = K(\alpha) + \frac{1}{2} \pi \delta_2 [1 - \Lambda_0(\varepsilon \setminus \alpha)] \quad (\text{L.18})$$

Case (iv): Circular Case $n < 0$

The $n < 0$ case can be reduced to the case $\sin^2 \alpha < n < 1$ by writing,

$$N = (\sin^2 \alpha - n)(1 - n)^{-1} \quad (\text{L.19})$$

In this case, the transform of the elliptic integral of the third kind is,

$$\Pi(n \setminus \alpha) = (-n \cos^2 \alpha)(1 - n)^{-1}(\sin^2 \alpha - n)^{-1} \Pi(N \setminus \alpha) + \sin^2 \alpha (\sin^2 \alpha - n)^{-1} K(\alpha) \quad (\text{L.20})$$

The above sections have listed the most useful elliptic integrals in the numerical computation for the 1st order model. In the numerical model, the third kind elliptic integrals, at most time, can not be calculated directly. In this case, it is very useful to use the above integral formulae based on the value domain of the integral parameters.

VITA

Zhengquan Zhou, born in China, AnHui. He received his Bachelor of Science degree from Harbin Engineering University of China, department of Naval Architecture and Ocean Engineering in 1982. He received his Master of Science degree in Applied Mechanics from China Research and Development Academy in 1985.

From 1986 to 1996, he worked as an engineer, senior engineer, research professor in China Ship Scientific Research Center (Wuxi, China). In 1997, he worked as a guest researcher in the Ship Hydrodynamics Department of Technology University of Delft, The Netherlands. In 1998, he worked as a researcher in the Offshore Research Department of Maritime Research Institute (MARIN), The Netherlands.

In August 1998, he enrolled in University of New Orleans as a Ph.D. candidate. From August 1998 to 2001, he was a graduate student and worked as a graduate research assistant at the University of New Orleans, School of Naval Architecture and Marine Engineering.

In May 2000, he received his Master of Science degree in Naval Architecture and Marine Engineering from University of New Orleans. In May 2002, he received his Master of Science degree in Computer Science from University of New Orleans.

From January 2002 to October 2002, he worked as a senior naval architect in Offshore Model Basin (Escondido, CA).

He is currently working in ABB Lummus Global Inc. (Houston, TX) as a senior naval architect.

DOCTORAL DISSERTATION REPORT

CANDIDATE: Zhengquan Zhou

MAJOR FIELD: Engineering and Applied Science

TITLE OF DISSERTATION: "A Theory and Analysis of Planing Catamaran in Calm and Rough Water"

APPROVED:




Major Professor & Co-Chair -
Dr. William S. Vorus




Robert C. Cashner, Dean of the Graduate School

EXAMINING COMMITTEE:



Dr. Kazim M. Akyuzlu



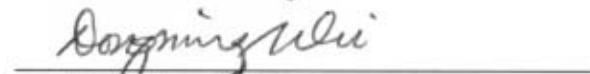
Dr. Jeffrey M. Falzarano



Dr. Martin Guillot



Dr. Russell E. Trahan



Dr. Dongming Wei

DATE OF EXAMINATION: March 28, 2003